

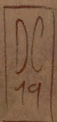


Daniel Vidal

EVOLUTION
of SAUROPOD DINOSAUR
POSTCRANIAL BIOMECHANICS

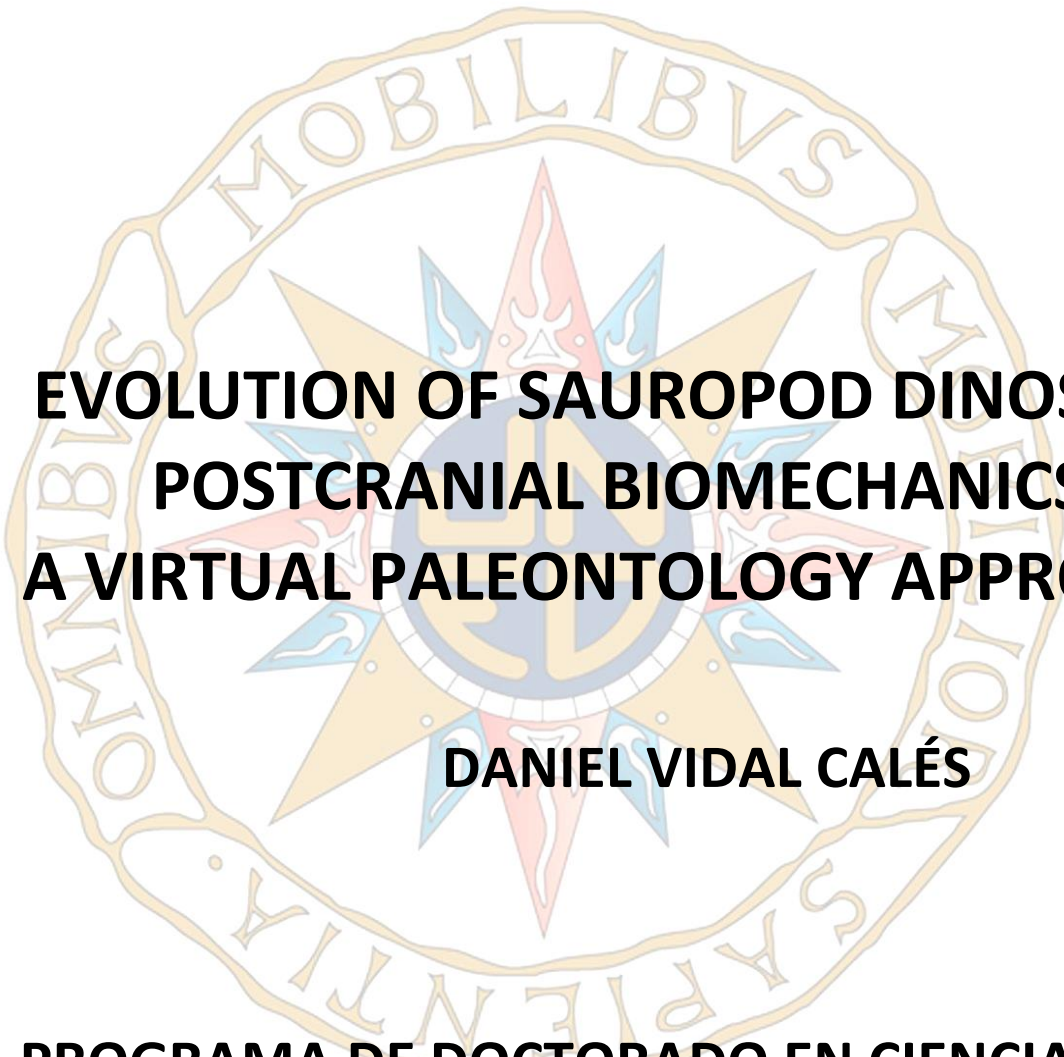
A virtual paleontology approach

Tesis doctoral • 2019



TESIS DOCTORAL

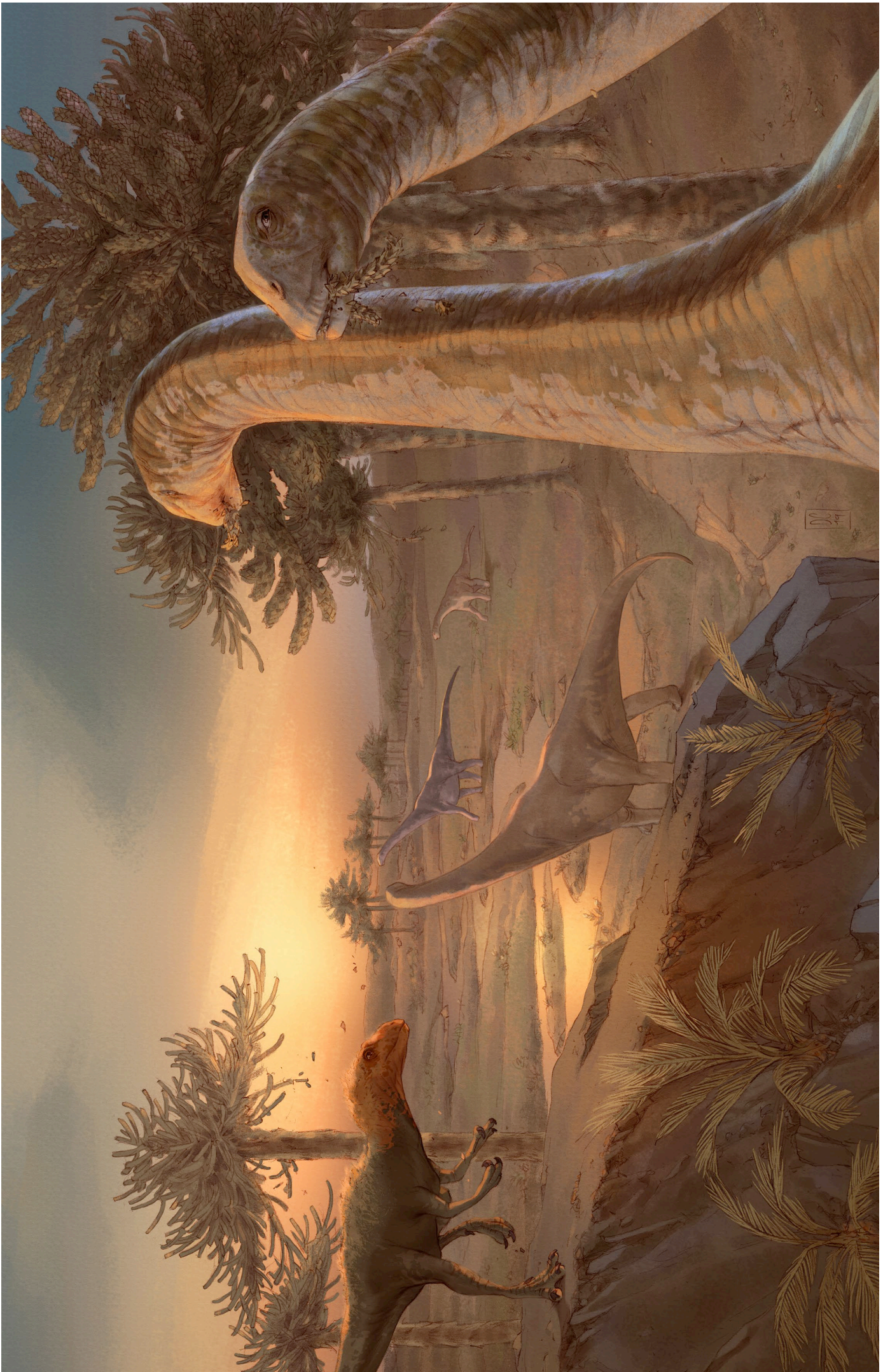
2019



EVOLUTION OF SAUROPOD DINOSAUR POSTCRANIAL BIOMECHANICS: A VIRTUAL PALEONTOLOGY APPROACH

DANIEL VIDAL CALÉS

PROGRAMA DE DOCTORADO EN CIENCIAS
FRANCISCO ORTEGA COLOMA
JOSÉ LUIS SANZ GARCÍA



Memoria presentada por **Daniel Vidal Calés** para optar al grado de Doctor en Ciencias por la Universidad Nacional de Educación a Distancia bajo la dirección del Dr. **Francisco Ortega Coloma** (Universidad Nacional de Educación a Distancia) y el Dr. **José Luis Sanz** (Universidad Autónoma de Madrid).

Fossil hunting is by far the most fascinating of all sports. It has some danger, enough to give it zest and probably about as much as in the average modern engineered big-game hunt, and the danger is wholly to the hunter. It has uncertainty and excitement and all the thrills of gambling with none of the vicious features. The hunter never knows what his bag may be, perhaps nothing, perhaps a creature never before seen by human eyes. It requires knowledge, skill, and some degree of hardihood. And its results are so much more important, more worthwhile, and more enduring than those of any other sport!

The fossil hunter does not kill, he resurrects.

George Gaylord Simpson, 1965

The magnitude of preparing one of this huge [sauropod] skeletons for public exhibition can be fully appreciated only by those who have passed through such an experience.

Charles W. Gilmore, 1932

Dinosaurs make us all humble.

Colin Trevorrow, 2018

ACKNOWLEDGEMENTS

“I didn’t think that far ahead”. That is this thesis reduced to a single sentence (and even more accurate and with fewer words than its sciency title!). It has a lot of possible interpretations: I didn’t think I would end up working with more specimens than when I started, I didn’t think I would end up being abroad for nearly 9 months, I didn’t think I would be rushing like mad to meet the deadline (ah, the optimism!). And, beyond all, I didn’t think I, a poorly focused student for the best part of 20 years, would have the focus and determination ever to try and pursue a doctoral degree. Thankfully, I’ve never ever been alone in this task, and there are plenty of people and institutions to thank for their help and support. It is quite an extensive list, and it is quite possible I am forgetting somebody (though I tried desperately to write down everybody who helped this thesis move forward).

First and foremost, thanks to the **Universidad Nacional de Educación a Distancia** (UNED) for granting me a predoctoral FPI contract (Ref. 0531174813 Y0SC001170) and two short-stay research grants for USA and Argentina. Thanks to **Render Area SL** for hiring me twice as a scientific advisor for 2015 DinoScience App and the 2016 Museo Nacional de Ciencias Naturales Ichthyosaur multimedia project (and thanks to my supervisors Francisco Ortega and José Luis Sanz for recommending me). Last, but far from least, a huge thank you to my parents **Carmela Calés** and **Miguel Ángel Vidal**. They financially supported my scientific activity prior to December 2016 by paying university tuition fees, conference travel expenses and hardware.

During these years, I have been kindly admitted to several vertebrate paleontological collections, without which I would have never been able to understand sauropod dinosaurs as well. Thanks to Paul Sereno, Tyler Keillor and Erin Fitzgerald (**University of Chicago**); Peter Makovicky and William Simpson (**Field Museum of Natural History**); Matthew Lamanna, Amy Heinrich, Joseph Sawchak, and David Berman (**Carnegie Museum of Natural History**); Amanda McGee, Michael Ryan and Ashley Hall (**Cleveland Museum of Natural History**); Daniel Brickman, Marilyn Fox and Jacques Gauthier (**Yale Peabody Museum**); Carl Mehling, Mark Norell and Ruth O’Leary (**American Museum of Natural History**); and Matthew Carrano (**Smithsonian United States National Museum of Natural History**); Rodolfo Coria, Ludmilla Coria and Guillermo Windholz (**Museo Carmen Funes**); Ignacio Cerda (Museo de Cinco Saltos); Ignacio Cerda, José Carlos and José Aravena (**Museo Provincial Carlos Ameghino**); Leonardo Filippi, Salvador Palomo, Joana Vanesa and Adrián (**Museo Argentino Urquiza**); Juan Canale (**Museo Ernesto Bachmann**); Diego Pol, Juliana Sterling, José Carballido, Eduardo Ruigomez and Norberto Pfeiffer (**Museo Paleontológico Egidio Feruglio**); Gabriel Casal and Marcelo Luna (**Universidad Nacional de la Patagonia San Juan Bosco**); Martín Ezcurra, Laura Chorno, Guillermo Aguirrezabala, Marcelo Miñana and Agustín Martinelli (**Museo Argentino de Ciencias Naturales Bernardino Rivadavia**), Pablo Ortiz and Rodrigo González (**Instituto Miguel Lillo**); Rafael Royo (**Fundación Conjunto-Paleontológico de Teruel Dinópolis**), Santiago Langreo (**Museo Paleontológico de Castilla La Mancha**) Ainara Aberasturi, José Manuel Marín and Ignacio Fierro (**Museo Paleontológico de Elche**).

Second, always two there are, no more, no less: a master and an apprentice. As the apprentice here, I’m extremely humbled to have had not one but two of the most compatible and best masters (aka thesis advisors) I could have ever hoped for. **José Luis Sanz (Pepelu)** has taught me plenty of things since I was an undergraduate student, but his teaching I treasure the most is the emphasis on the scientific method and epistemology. Knowing how the method works in its core is something I owe to you, and I believe it is one of the best lessons a young scientist can receive. Also, your knowledge of dinosaur movies and cinema in general has made me discover true jewels of the seventh art. Thank you, in Kaiju proportions of course. **Francisco Ortega (Patxi)** has had a different, yet equally important input in my education as a scientist with his constant reminding of the danger of *ad-hoc* hypotheses, always looking for the weakest points in my results and discussions and showing me how to work on different matters than just research, such as developing research projects and fieldwork logistics and techniques. You have been a terrific advisor, and you’ll always be in my memories like C-beams glittering in the dark near the Tannhäuser Gate. Thanks to both of you for taking me into this research group, giving me the freedom to propose the research I wanted to pursue, do it at my own pace yet always having time for solving all doubts that arose in this process.

Doing research on the Grupo de Biología Evolutiva (UNED) has introduced several great colleagues to my life who have transcended the professional world and have become great friends. **Fernando Escaso** has always been both extremely nice and helpful with anything related to research, fieldwork or bureaucracy, always willing to teach his vast experience in the most humble and optimistic way. **Adán Pérez**, who has the spirit of a puppy dog, the wisdom of his beloved turtles and the cultural versatility of a gentleman. It is always a pleasure doing research, digging, or playing board games and watching bad movies with you. **Iván Narváez (Chicho)** and his quick wit, endless B-movie and soccer knowledge and his impressive ability to tell any past anecdote 100x times funnier are dwarfed only by how willing to help he always is. **Elisabete (Beta) Malafaia** has a strong work ethic, which I admire, and has made me feel at home when I have been working in Portugal. I have awesome memories of digging with **Jose Miguel Gasulla**, one of my masters in fieldwork, who has been an exceptionally good host whenever I've been to Morella, in some of the best fieldwork campaigns I have ever had. Morella is a wonderful city on its own, but it is even more wonderful with people like you around. **Marcos Martín (Soriano)**, has been an awesome field and lab companion, as well as a terrific partner in crime in everything meme and pub related. I hope we make a lot more of "Atance Runs" in the "Vallekana Milenaria" in less than twelve parsecs, since fieldwork is always the best with you around. **Andrea Guerrero** has been a great lab, conference and dig buddy, who despite her silent contrasting with my usual loudness always has the precise input or touch needed to make anything the right amount of perfect. I can't believe you actually enjoy reviewing reference lists, I admire you. *Graciès per tot.*

I want to thank everybody in **Conservación GBE** for their terrific preparation and conservation skills, as well as for their friendship. I'll never forget that trip back from Burgos with **Fátima Marcos** in 2012 where she quit smoking. You've taught me since that trip lots of stuff about preparation and conservation of fossils and how to manipulate them. If I can be left alone in a museum collection, it is thanks to you. Thanks to **Irene Fernandez, Elena Zamora, Natalia Torres** and **Ana Santiandreu** for teaching me, and preparing fossil material I ended working with. I would also like to thank **Susana Bartolomé, Susana López** and **Marta Onrubia** that great 2016-17 season in the Bellas Artes classroom/prep-room, where I learned a lot of preparation and had tons after tons of fun. Some of my fondest memories come from those days.

I find difficult separating **Adrián Páramo** and **Ane De Celis** for this acknowledgement. Not only because their privileged minds for data analysis as well as for knowing the deep web and its contents better than any other paleontologist alive, but because they are always ready to help with their ability to understand all the big data issues my brain is totally unable to process. On a more personal note, Adrian, thank you for making our lives happier with the joy you share with your unmatched personality; Ane, thank you for being exactly opposite to me regarding being organized and always giving me the best advice, funny bird videos and *demigransia*. If I could say I've had a traveling sidekick, that would have to be **Pedro Mocho**, with whom I've been to more cities than with anybody else. I could also say that you have been a third supervisor to this thesis for sharing your knowledge, pictures and guidance regarding sauropods right away from the start. Not only I have learned a lot of science from you, but also about ideals and music. You are a great scientist, and a better friend. I believe I will never find a friend as wiseass, good-hearted, stoic, and loyal as **Alex Serrano**, who not only has reviewed plenty of this manuscript, but has always listened to all my far fetched occurrences, followed me in countless wild goose chases (scientific or not) and has helped me to keep my feet on the ground always. And as I always say, "hokey religions and ancient weapons are no match for a good *friend* at your side, kid".

This thesis would have been way different if the **DinoBuster** project had not existed and with two of my best mates on it. Because someone with a proficiency in the sport only matched by his love for science, nerd-stuff, life and his friends as **Francesc Gascó** means to me constant inspiration to be not only a better sportman, scientist and science communicator, but a better human being. Thanks for being like an older brother to me. Because somebody as **Carlos De Miguel**, whom I met begging for the paleontology class notes he took the year before and didn't think I was a lazy beggar and let me into his life. You have always been a strong support and a person I look up to when it comes to doing and communicating science or to drawing. Also, I cannot thank you enough for helping me getting back my confidence to become I biologist.

Finally, **Elena Cuesta**, through all these years you have become one of my best "work proximity associates" in the most ample of its possible acceptances, who has seen me at both my best and worst, and has always been there to help. You're a kind, intelligent, passionate, versatile, resourceful and fun human being who is capable of any goal you want to achieve... except maybe imitating accents. Thank you. For proofreading this manuscript, for your friendship and for whatever the future holds, which I'm sure in advance will be wonderful. I can't imagine a life where we didn't meet.

I would like to thank all non-paleo people at UNED, as you're also biologists and therefore worth mentioning... just kidding. Thanks **Charo, Óscar, Mónica, Lola** for the support and consideration these years and specially thanks to **Ana**, who has had to take care of me on more than one occasion (some more embarrassing than others) and for sharing our experience on doing very different thesis together at the end of the day.

However, there was a time when I did not yet belong to UNED, and I was a UAM student. I would not be here today without **Ángela Delgado Buscalioni**, who gave me my first little outreach project and helped me in my first steps into research and outreach, as well as always making me think in your always deep and interesting lectures. **Jesús Marugán** always was available to share his knowledge on geometric morphometrics, making understand the basics of such methodology easy for anybody. **Hugo Martín** was one of my first mentors regarding fossil preparation and was always ready to share his experience with enthusiasm in an extremely humble way I absolutely admire. **Candela Blanco** has been together with me since the beginning, in 2007, when we started our undergrad courses in Biology, and I am extremely happy that we have ended working the same field (only different Phyla, but still!). **Sandra Barrios** arrived later, her thesis literally was full of (fossil) crap (just kidding :)), and she proved everybody what a great job you can do with such small fossils. You really are a great scientist and friend, and I hope to keep seeing more of your work and of you. Finally, I want to thank **Francisco Poyato**, without whom I would not be writing these very words. When I took your paleontology lectures ten years ago, I was seriously considering quitting Biology and starting a degree outside of science. Thanks to your lectures, each more enticing than the previous, you made fully reconnect with biology and to crave for more and more paleontology and evolutionary biology knowledge. Thanks also to **Bea, Ioannis, Álvaro, Guille Navalón, Abel, Yayo**, and all the other great people I met in the first years at Las Hoyas. **Armando González** is one of the best teachers I have ever had. You made me love anthropology, a subject which never interested me before. So much that I took ALL other courses I could about physical anthropology I could. I learned a lot about human anatomy and evolution thanks to you. And, also, it is because of that I met **Daniel "Danilopithecus" García**, probably one of the best non-paleo buddies I have. It is always a joy hanging with you, *muchacho*, as I always learn something about our ancestors I didn't know before.

But not everyone I met at UAM was born lucky enough to be a paleo/anthropologist, and some people had to content with other areas of biology (just kidding :P), but their help as also been priceless. **Inés**, you have always been as resourceful as you are sensitive and intelligent. It is always a pleasure spending time with you, and I'm glad you're still into science. **Ana**, you are one of the smartest and most sensitive persons I know, and you're always supporting me when I need it. **Juampa**, the lord of butterflies, always a great person to be around with in fieldtrips or the UAM cantina. **Alejandro "Wushu"**, I will never forget the year you helped us train in that martial art. I have really come to love its beauty and it would not have been possible without you. Thank you also to **Judith, Gloria, Marta "caracoles", Pablo, Guille Prieto** for all the great moments.

It seems that when doing a PhD in paleontology, globetrotting is a prerequisite. Fortunately, I have been able to travel to do research, go to conferences and even scientific expeditions. I would like to thank **Peter Makovicky** and **Rodolfo Coria** for hosting my short stays at the Field Museum of Natural History (Chicago) and Museo Municipal Carmen Funes (Plaza Huincul) respectively. I want to thank **Matteo Fabbri, Jasmina Wiemann** and specially **Omar Regalado** for the great time during my stay in New Haven. Traveling alone is something I enjoy, but meeting great people like **Guillermo Windholz** makes traveling even better. Thank you for your hospitality and friendship when I was in Neuquén. Thanks also to **Mattia Baiano, Romina González, Mateo, Miriam Parada, Leo Filippi, Juan Canale, Eduardo Ruigomez, Guille Aguirrezabala, Marcelo Miñana, Mechis Fernández, Daniela, Agustín Martinelli, Jordi García**, for making my trip to Argentina so amazing.

I want to thank **Paul Sereno** for inviting me to two scientific expeditions to Niger, an opportunity not every graduate student can have and for which I am extremely grateful: it has been among the most intensive lessons in fieldwork I have yet received. Thanks to **Erin, Didier, Jordan, Chuck, Stephanie, Mohamed, Romain, Alexander, Matt, Minata, Bido, Nels, Lisa and Bob** for making the expedition so unique. I would also like to thank again **Stephanie Baumgart** for some last minute English proofreading.

I would like to thank everybody else who I have met during these years doing paleontology: **Angélica Torices**, always ready to help with anything. **Verónica Díez** has shown me the coolest places around Berlin, allowed me to "play" her banjo (I'm a guitar dude, sorry), taught me virtual paleontology techniques, reviewed

this manuscript and been a beautiful person always. **Ainara Aberasturi** always makes me feel at home when I'm visiting Elche, and is always trying to make the most of my time when I'm studying the collection there, even at the expense of her own personal time. I cannot be thankful enough for that. **Fernando Sanguino**, your passion is only equal to your love for everything theropod related. You deserve the best. It was a pleasure meeting **Aitziber Suárez** the first time in the 2015 dig at "El Atance", and it has been a greater pleasure getting to hang out and work together these years. *Eskerrik asko* for the printing tip, by the way. Thanks also to **Heinrich Mallison, Jeff Wilson, Mike D'Emic, Eloy Manzanero, Ina Díaz, Santiago Martín, Amparo Violero, Marco Ansón, Israel Sanchez, Mauricio Antón, Manuel Salesa, Oier Suárez, Miguel Moreno, Nicole Torres, Darío Estraviz, Leire Perales, Eduardo Puértolas, Jara Parrilla, Óscar Caballero, Mavi, Mireia Ferrer, Raúl San Juan, Carlos Aranzábal, Ana Lázaro, Álvaro Simarro, and María Ciudad Real.**

I want to thank **Diego Cobo** in particular. Not only are you a terrific artist with capital letters who has made lots of paleoartistic reconstructions for this thesis, its layout and its beautiful cover, but you are also an incredible friend. Thanks for showing me that a pig that doesn't fly is just a pig. I'm touched. I will always remember a conversation I had with **Dimitris Kioussis** in the summer of 2007, the year I began college. You were among the first to really show me science was not just a bunch of interesting trivia, but also a way to break the barrier of knowledge and expand it. Thanks to **Alejo Molinero** and **Eduardo Gómez**. It is hard to be a high school teacher, but you two really opened my mind back then to philosophy and biology, respectively. Thank you for feeding my curiosity during those years. **Javi, Manu** and **Miguel**, you guys have known me since we were little kids and with you, it is as if we had never grown up. **Natxo**, you're among the kindest human beings I have ever known. You have been there so many times for me I wish I could have always done the same. You're larger than life, but your kindness is even larger. **Sandy**, you know the drill: we may never see each other in months or years, but when we do it's as if time had never passed since the last time. I treasure our friendship, as much as I love your family (hi, Álvaro and Alex!).

Last but not least, I want to thank my family: **Nano, Igna, Marta, Alicia, Javier, Irene, Rosario** and **Mamá**, for understanding I never grew my dinosaur phase, and appreciate it. **Abu**, you always bought me dinosaur fanzines when I was little and probably listened to me as a little talking about dinosaurs more than I think I could ever do. You have earned Heaven just for that. I love you. **Pablo**, I know not mentioning you would hurt your heart (but as a cardiologist, you could have still cured yourself, haha), so I want to take this opportunity to tell you how much I admire you: while I'm driven, you're focused, while I'm chaotic, you're ordered, and while I'm bold, you're careful. I can't help but think I'd be a better person like you if I were like you. I love you. **Mom, Dad**, you're the first two persons to blame for this thesis: you always took me to the Museo Nacional de Ciencias Naturales to see the dinosaurs every Sunday, you let me see Jurassic Park and The Land Before Time way too many times and you fed my dino-mania without thinking of the consequences. I think this thesis may be its ultimate consequence, after more than 25 years of dino-mania. I cannot emphasize enough how thankful I am for having being raised in a home like ours, for stimulating my curiosity and never putting boundaries of any kind to it. This thesis is a product of the way I was raised, the way I am and the life choices I have made, all of them unthinkable without you.

And last, thanks to the Paleobiology Database, Wikipaleo, Sci-Hub and Ben Miller for supplying references and literature.



CONTENTS

CONTENTS

ABSTRACT

Resumen.....	3
Abstract.....	5

CHAPTER 1: INTRODUCTION

Introduction.....	9
Reviewed skeletal mounts.....	15
Case studies.....	16
Skeletal mounts as scientific tools.....	23
Criteria for scientific use of skeletal mounts.....	24
Hypotheses and objectives.....	26
Institutional abbreviations.....	28

CHAPTER 2: MATERIAL AND METHODS

Introduction.....	33
Material.....	35
Terminology.....	36
Methods.....	41

CHAPTER 3: A VIRTUAL SPINOPHOROSAURUS

Introduction.....	63
Systematic Paleontology.....	65
Assembling the virtual skeleton.....	66
<i>Spinophorosaurus</i> body plan.....	73
Osteological range of motion analyses.....	75
Reconstruction of the muscular system.....	83
Volumetric reconstructions and mass estimates.....	97
Discussion.....	97
Conclusions.....	113

CHAPTER 4: ONTOGENETIC SIMILARITIES BETWEEN GIRAFFE AND SAUROPOD NECK OSTEOLOGICAL MOBILITY

Introduction.....	119
Material.....	120
Methods.....	121
Results.....	126
Discussion.....	133
Conclusions.....	141

CHAPTER 5: THE EVOLUTION OF BIOMECHANICAL CAPABILITIES IN SAUROPODA

Introduction.....	147
Morphological characters with functional implications.....	147
Systematic paleontology of personally reviewed taxa.....	163
Phylogenetic analysis and character optimization.....	202
Discussion.....	205
Conclusions.....	208

CHAPTER 6: PRELIMINARY VIRTUAL PALEONTOLOGY APPROACH TO LO HUECO TITANOSAURS

Introduction.....	213
Material.....	215
Results.....	215
Discussion.....	220
Conclusions.....	225

CHAPTER 7: CONCLUSIONS

Conclusions.....	229
------------------	-----

REFERENCES

References.....	235
-----------------	-----



ABSTRACT

RESUMEN

Los dinosaurios saurópodos son los mayores vertebrados terrestres conocidos. Su característico plan corporal (cuadrúpedos de extremidades columnares con largos cuellos y colas) los hace únicos entre los vertebrados terrestres y es probablemente clave para comprender su evolución. Sin embargo, debido a lo fragmentario de su registro y la difícil manipulación de sus fósiles (frágiles, enormes y pesados en muchos casos), el conocimiento sobre su morfología funcional es aún muy limitado. Recientemente, el advenimiento de la tecnología 3D y su progresivo abaratamiento ha permitido abordar dicha cuestión con mejores medios de los que se contaba hasta hace pocos años.

El objetivo principal desarrollado en esta tesis doctoral ha sido generar, a partir del esqueleto excepcionalmente completo y bien preservado de *Spinophorosaurus nigerensis* (Jurásico de Níger), un modelo de un eusaurópodo basal mediante técnicas de paleontología virtual. Entre estas técnicas se cuentan (i) la reconstrucción de su plan corporal mediante articulación del esqueleto en un entorno virtual; (ii) el análisis del rango de movimiento de su esqueleto axial y apendicular; (iii) la reconstrucción de los orígenes e inserciones de los principales grupos musculares; y (iv) la estimación de las líneas de acción y volumen de esos músculos. Esta información se ha empleado para interpretar las capacidades funcionales de este saurópodo, para comparar los resultados con los obtenidos a partir de esqueletos virtuales de vertebrados actuales, y para abordar la interpretación morfofuncional de otros saurópodos que han podido ser digitalizados, con representantes de la mayor parte de los clados reconocidos en la actualidad.

Como resultado de estos análisis, se ha observado que el acuñaamiento del sacro tiene un papel principal para determinar la curvatura de la columna vertebral en la mayoría de los saurópodos, en concreto en todos los Eusauropoda (que agrupa a la mayoría de saurópodos conocidos). Esta comprobación supone la propuesta de cambios en las reconstrucciones esqueléticas y la reinterpretación de la orientación de la columna vertebral y la cintura pectoral en un gran número de dinosaurios saurópodos. Existe, por tanto, una repercusión directa sobre la interpretación de sus capacidades biomecánicas, algunas de las cuales evolucionaron en paralelo con el acuñaamiento del sacro como un módulo funcional relacionado con las estrategias de obtención de alimento. Algo similar ocurre con el módulo locomotor, en concreto con la cintura pélvica, el fémur y la serie caudal. A lo largo de la evolución de los saurópodos se produjo una reducción paulatina del tamaño de las estructuras que son correlatos osteológicos de la musculatura caudal y de la región pélvica posterior, mientras que la anterior aumentó su tamaño conforme la pelvis de los saurópodos fue ensanchándose. Este fenómeno es congruente con cambios en la locomoción hacia una menor propulsión por retracción del fémur. Ambos módulos, sin embargo, no evolucionaron de una forma súbita, sino en mosaico, como es común en otros módulos funcionales en Dinosauria.

Los resultados obtenidos al aplicar técnicas de paleontología virtual con vertebrados actuales ponen de manifiesto que es posible estimar correctamente sus posturas y rangos de movimiento sin necesidad de factores ajenos a la anatomía esquelética. Esta comprobación aporta robustez a las conclusiones obtenidas en los análisis con restos fósiles de saurópodos, aportando una vía de falsación independiente de las hipótesis construidas con restos fósiles para comprender sus capacidades biomecánicas.

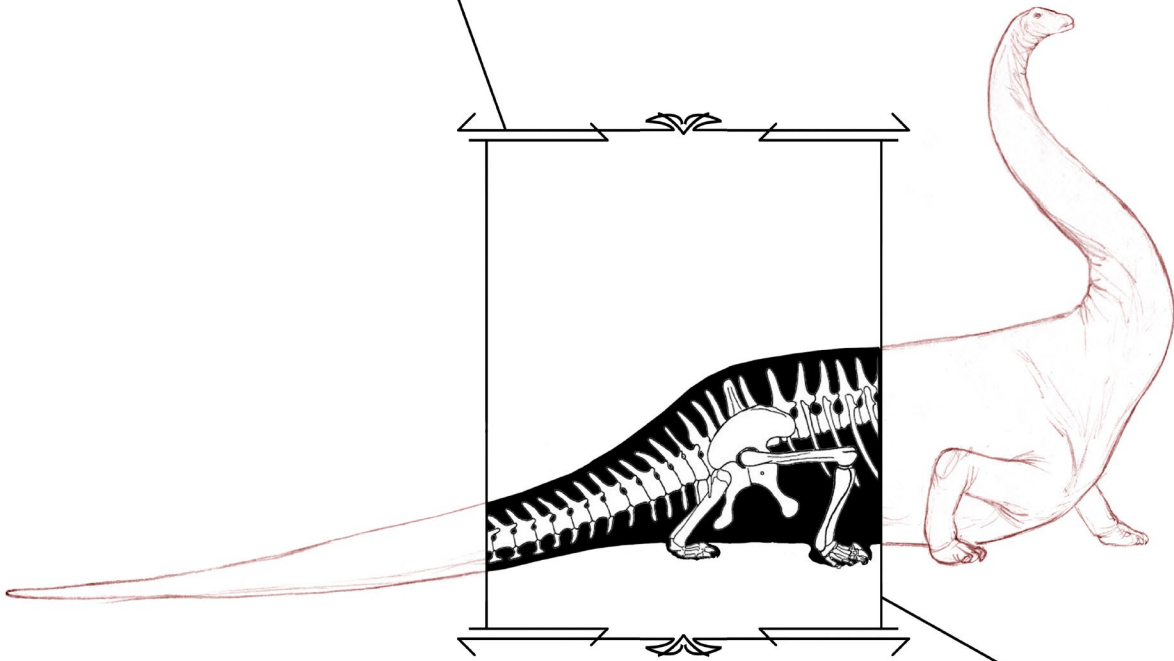
ABSTRACT

Sauropod dinosaurs are the largest known terrestrial vertebrates. Their characteristic body plan, quadrupeds with columnar limbs, long necks and tails, is unique among terrestrial vertebrates, and it is likely key to understanding their evolution. However, due to the fragmentary nature of the known fossil record and the difficult manipulation of their fossils (fragile, enormous and heavy in many cases), their functional morphology and motion capabilities are still relatively poorly known. Recently, the advent of 3D technology and its progressive cheapening has allowed studying the subject better than ever before.

The main goal developed in this PhD dissertation is to generate a virtual model for an early branching eusauropod using virtual paleontology techniques with the exceptionally complete and well-preserved holotypic skeleton of *Spinophorosaurus nigerensis* (Jurassic of Niger). Among these techniques are (i) reconstructing its body plan by articulating the skeleton in a virtual environment; (ii) assessing its osteological range of motion on axial and appendicular skeleton; (iii) reconstructing the origins and insertions of the principal muscle groups; and (iv) estimating muscle lines of action and volumes. The results have been used to assess the functional capabilities of this sauropod, to compare the same techniques applied to extant vertebrates, and to compare the results with virtual skeletons of more fragmentary sauropods representing most well established clades.

These analyses show that wedging of the sacrum has a key role in determining the osteologically induced curvature of the vertebral spine in all Eusauropoda (which includes most known sauropods). This finding changes the skeletal reconstructions and the interpretation of the body plan of a large number of sauropods. This has direct implications in the estimated biomechanical capabilities of these sauropods, some of them even evolving in covariation with the sacrum wedging as a functional module related to feeding strategies. Something similar occurs with the locomotor module, particularly with the pelvic girdle, femora and caudal vertebrae: throughout sauropod evolution, the osteological correlates for caudal, ischial and posterior iliac musculature become gradually more reduced while the anterior iliac musculature became more enlarged and the pelvis widened. This is explained by changes in locomotion toward less propulsion coming from femoral retraction. Both modules, however, did not evolve suddenly, but in mosaic, as is common with other functional modules in Dinosauria.

The result of applying virtual paleontology techniques to extant vertebrates reveal that these techniques can estimate correctly their actual posture and ranges of motion with no need for factors other than actual skeletal anatomy. This makes conclusions regarding sauropod taxa more robust, since it implies an independent line of evidence for testing the biomechanical capabilities of fossil vertebrates.



CHAPTER
• 1 •
INTRODUCTION

Introduction.....	9
Reviewed skeletal mounts.....	15
Case studies.....	16
Skeletal mounts as scientific tools.....	23
Criteria for scientific use of skeletal mounts.....	24
Hypotheses and objectives.....	26
Institutional abbreviations.....	28

1.1 INTRODUCTION

A brief history of early fossil skeletal mounts

Fossil skeletal mounts have been an ever-popular natural history museum attraction for more than two centuries. The first fossil skeleton ever given a Linnaean name (genus and species), *Megatherium americanum*, was also the first fossil skeleton used to erect a physical mount at the Royal Cabinet of Natural History in Madrid, Spain (now Museo Nacional de Ciencias Naturales; López Piñero, 1988). That mount was conducted by Valencian Juan Bautista Bru, and it was an experience crucial in the study of the fossil. Even the title of Bru's work revealed it: "Description of the skeleton in detail, following observations made while mounting and erecting it in the Royal Cabinet" (Bru, 1796). Bru mounted and described the skeleton following what Georges Cuvier would perfect as our modern comparative anatomy:

"for each bone of the skeleton under consideration, I have tried to keep not only the names given by anatomists to bones of the human body whenever I find any relation or similarity between the two, but also the names of the different parts"

Bru, 1796 as quoted in López Piñero, 1988

Bru also was very conservative in his approach when reconstructing missing bones:

"I did not want to supply them artificially, although I [at first] tried to, as it seemed to me that it would never be more than a figure based on conjecture"

Bru, 1796 as quoted in López Piñero, 1988

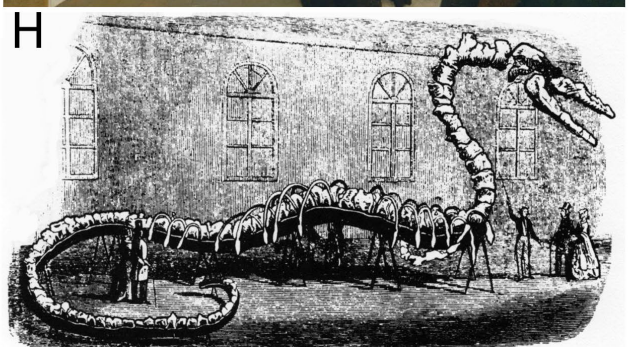
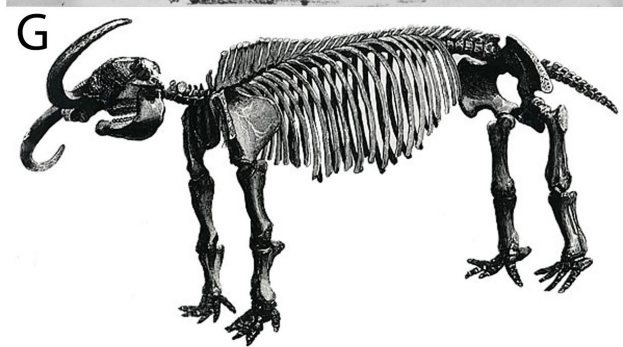
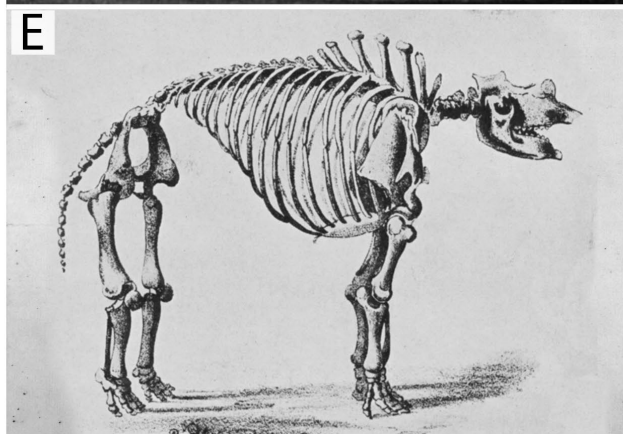
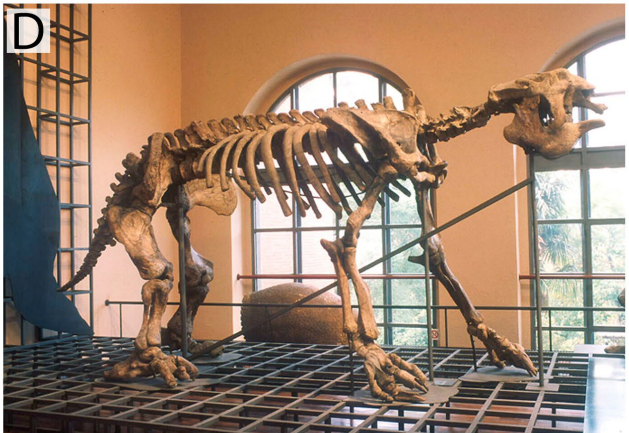
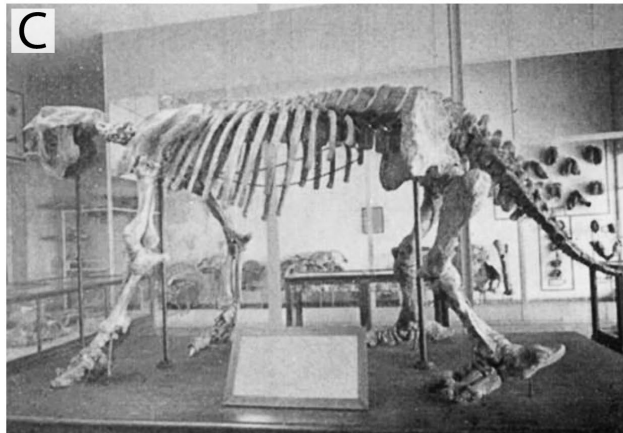
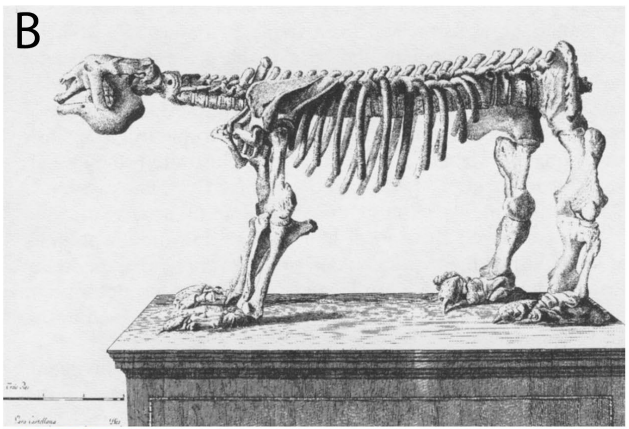
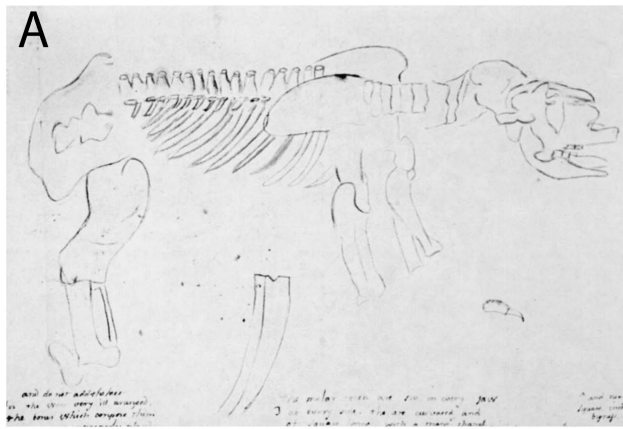
Bru's interpretation of the skeleton was not without mistakes (i.e. he misidentified the forelimb as the hindlimb; Cuvier, 1804), but it remains a work of great value and interest, considering the paradigm of natural sciences in the late XVIII century was very different from that of the XIX century, with evidence of extinction just being grasped by Cuvier and with evidence-based mechanisms for biological evolution not being written until decades later. The mount was on display at least from 1795 on (Bru, 1796; Garriga, 1796), and it has survived until present day with minor alterations (Fig. 1.1 A-D), even to the extent of maintaining Bru's errors (Boyd, 1958), despite being dismantled several times for moving between museum headquarters.

Around a decade later, in 1802 the mastodon *Mammuth americanus* was mounted in the Charles Peale's museum in Philadelphia, USA (Simpson, 1942; Carpenter, Madsen, & Lewis, 1994). Peale's mastodon mount was conceived with as much concern for scientific correctness as for its spectacle value, since a 50 cent fee was charged to the public for watching the specimen (Simpson, 1942). Unlike Bru's *Megatherium*, Peale's mastodon has not survived until present day (but it was partially depicted in the 1822 painting *The Artist in His Museum* as well as a 1855 lithograph, see Fig. 1.1 E, F). This mount was soon followed by more skeletal mounts in the USA, which were part of traveling exhibits by showman Albert Koch. Those included another mastodon informally named "Missourium" and an "*Hydrarchos*" archaeocete (Fig. 1.1 G,H), both composite skeletons of exaggerated size which were harshly criticized by academics of that time period because of their lack of scientific accuracy and forgery (Simpson, 1942). The nature of these mounts being more spectacular and practical than scientific is evidence that, very early on, skeletal mounts were already considered both as scientific tools (in the case of Bru's *Megatherium* and, to a lesser degree Peale's mastodon) as well as a popular attraction in which the artistic and/or craftsmanship approach (even forgery) was more important than scientific approaches.

This duality is evident in the first dinosaur ever mounted, *Hadrosaurus foulkii*. This mount was supervised by Joseph Leidy and performed by Benjamin Waterhouse Hawkins in 1868, in the Academy of Natural Sciences of Philadelphia (USA). The specimen used as the basis for the mount, the holotype of *Hadrosaurus*, is very fragmentary, so Waterhouse Hawkins had to fill in multiple parts of the skeleton with the then scarce knowledge of other dinosaurs: he gave the mount seven cervical vertebrae, a mammalian-like scapula but an iguana-like skull (Carpenter *et al.*, 1994), clearly a mixture of Gideon Mantell's and Richard Owen's interpretation of dinosaurs (Waterhouse Hawkins had worked under the former to sculpt the famous Crystal Palace dinosaurs). The mount, however, responded to an important scientific purpose: to showcase Leidy's finding regarding the stance of *Hadrosaurus*:

"the enormous disproportion between the fore and hind parts of the skeleton of Hadrosaurus has led me to suspect that this great herbivorous Lizard sustained itself in a semi-erect position on the huge hinder extremities and tail"

Leidy, 1865



This mount started the tradition of kangaroo-like mounts of bipedal dinosaurs, which would be carried on by Dollo when mounting *Iguanodon bernissartensis* (Carpenter *et al.*, 1994), where he actually disarticulated the complete tail at several points to reproduce the aforementioned kangaroo-like stance (Norman, 1980). Dollo nevertheless made several important observations when mounting the *Iguanodon*, particularly regarding its bird-like characteristics (Norman, 1980).

The preconceived notion of the “tripodal”, kangaroo-like stance of bipedal dinosaurs (either ornithopods or theropods) would continue during the XX century with the mounts performed at the American Museum of Natural History, the Smithsonian Museum of Natural History or the Carnegie Museum of Natural History. It would not be until the late 1960s and the early 1970s, during the paradigm shift of the *Dinosaur Renaissance* (Bakker, 1975, 1986), that the kangaroo model would be totally refuted by osteological evidence: the actual geometry of the skeleton as inferred from both articulated specimens and the articulation of individual vertebrae made the kangaroo stance impossible without disarticulating the tail in several points (Norman, 1980). Those of quadrupedal dinosaurs, among them sauropods, would follow a similar trend (Bakker, 1968, 1971; Coombs, 1975).

By the end of the XIX century and the beginning of the XX century, when the first sauropod dinosaur skeletons started being mounted, many decisions regarding the mounts were still preconceived notions from the researchers and craftsmen working on the mount, or those of other influential researchers. Just like the kangaroo-like stance, these notions would perpetuate for decades in several mounts and sauropod depictions and were debated in the scientific literature as well.

Sauropod paleobiology hypotheses and paradigm shifts before skeletal mounts

Sauropods are a clade of dinosaurs including all forms more related to *Saltasaurus loricatus* than to *Jingshanosaurus xiwaensis* and *Mussaurus patagonicus*, which includes the largest terrestrial animals known to date (Wilson, 2002; Upchurch, Barrett, & Dodson, 2004). They all share a very characteristic body plan: graviportal quadrupeds with long tails and necks, and a relatively small head. This makes their functional morphology particularly interesting, since it represents terrestrial life at the edge of its known limits on a bauplan unlike that of any living vertebrate, and therefore there has been lively discussion on that subject since the first remains were unearthed in the XIX century.

Richard Owen interpreted the first known remains of *Cetiosaurus* as belonging to a crocodile-like animal of aquatic habits with similitudes to cetacean vertebrae (Taylor, 2010), hence the name. *Pelorosaurus* was the first fossil of a sauropod (though back in the day it was not considered to be a dinosaur) recognized as terrestrial by Gideon Mantell in 1850, based on the medullary cavity in its long bones (Taylor, 2010). During the decade of 1870, however, the true nature of these animals started to emerge, as more complete remains were retrieved. Phillips described the lectotype of *Cetiosaurus oxoniensis* in 1871, based on a skeleton sufficiently complete to recognize *Cetiosaurus* as capable of terrestrial locomotion and an erect posture:

“the femur... seems to claim a movement of free stepping more parallel to the line of the body, and more approaching to the vertical than the sprawling gait of the crocodile”.

Phillipps, 1871

Phillips, however, interpreted *Cetiosaurus* as a marsh-loving or river-side animal (Phillips, 1871; Taylor, 2010).

Figure 1.1 (previous page) - Earliest historical skeletal mounts/reconstructions known.

A - The very first attempt at reconstructed what would be *Megatherium americanum* by Juan Bautista Bru in a letter to Thomas Jefferson dated 26 January 1789, modified from Boyd, 1958. **B** - An engraving of the original *Megatherium americanum* skeletal mount in the Royal Cabinet of Natural Sciences in Madrid by Juan Bautista Bru, published in José Garriga's monograph (Garriga, 1796). **C** - The skeletal mount of *Megatherium americanum* at the Museo Nacional de Ciencias Naturales, Madrid in 1958. Notice the mount has incorporated a tail which was absent on the original mount, likely added in the XIX century. Modified from Boyd, 1958. **D** - The skeletal mount of *Megatherium americanum* at the Museo Nacional de Ciencias Naturales, Madrid present day. Notice that while the supporting structure has been modified, the posture is the same as in 1958. **E** - The Peale Museum *Mammut americanum* mount, illustrated by John Warren in 1855. Modified from Simpson, 1942. **F** - Part of *The Artist at His Museum*, a self-portrait by Charles Peale in which part of the mastodon skeleton can be seen at the far right, partially hidden behind a curtain. Peale painted this to commemorate the day the mastodon skeleton was unveiled to the public. **G** - The composite mastodon informally called “Missorium” which was twice longer than the real mastodon. **H** - The composite archaeocete “*Hydrarchos*” skeletal mount, which was part of a touring exhibition and bore no resemblance to a real archaeocete.

The first sauropod dinosaur described in the USA was *Camarasaurus supremus* from the uppermost Morrison Formation outcrops at Canyon City, Colorado (USA). Edward Drinker Cope published a brief paper on it in 1877 based on some vertebrae (one cervical, three dorsals and four caudals) retrieved by O.W. Lucas (Cope, 1877a). It was followed up by a longer paper in early 1878 in which Cope, with more bones (including pelvis and femur) also sent by O.W. Lucas, could start to hypothesize on the habits of this dinosaur (Cope, 1878a).

“[*Camarasaurus*] was capable of and accustomed to progression on land is certain from the characters of the bones of the limbs and their supports above described”

Cope, 1878a

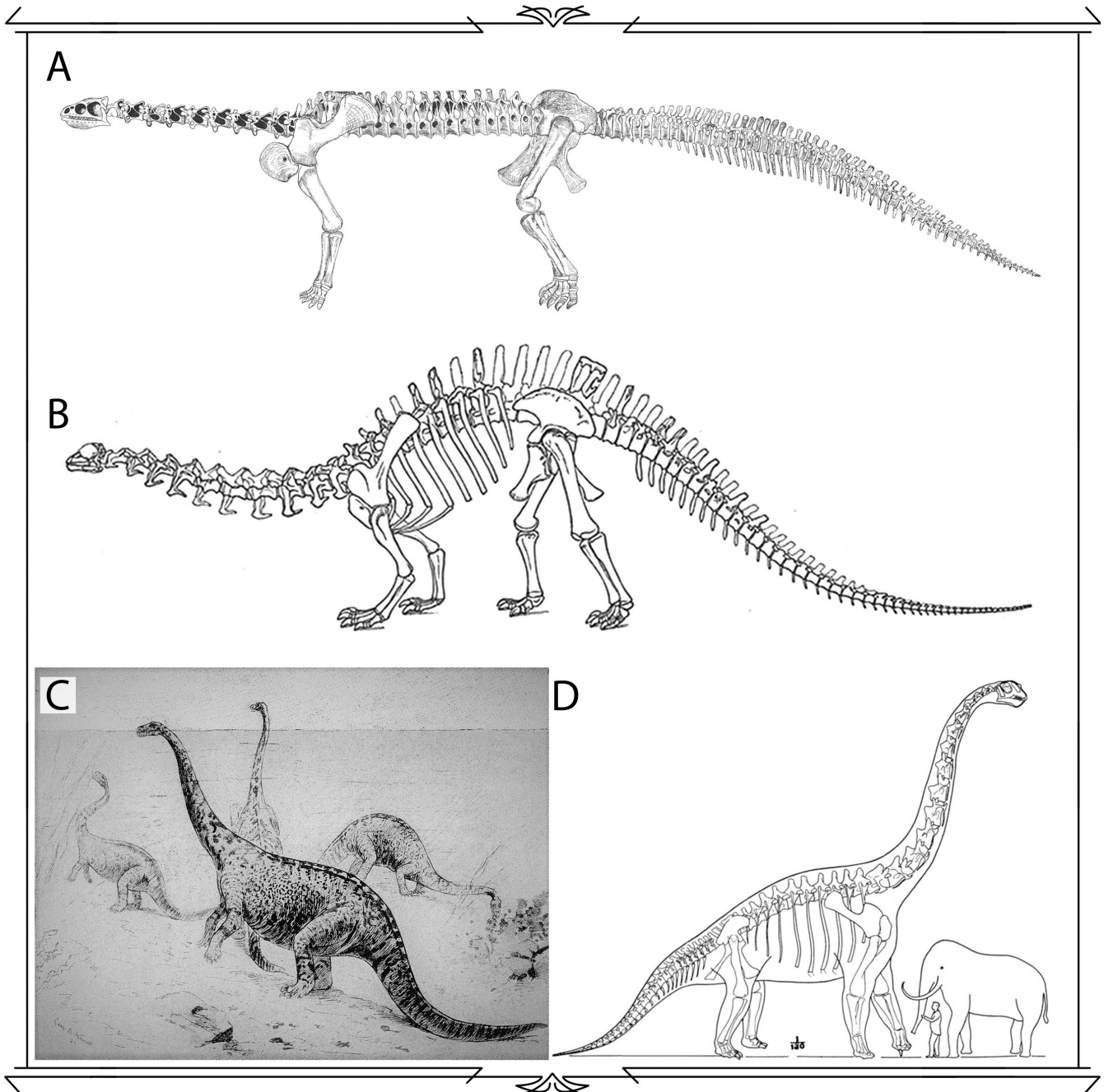


Figure 1.2 - Classic sauropod reconstructions.

A - The first skeletal reconstruction of a sauropod dinosaur, *Camarasaurus supremus* by John Adam Ryder, 1878. Ryder worked under the guidance of Edward Drinker Cope, who proposed a terrestrial lifestyle for *Camarasaurus* (Cope, 1878a) **B** - The second skeletal reconstruction of a sauropod dinosaur, *Brontosaurus excelsus* by Othniel Charles Marsh, 1883. Marsh proposed an amphibious lifestyle for *Brontosaurus* (Marsh, 1883). **C** - The first reconstruction of a sauropod dinosaur in an environment, *Amphicoelias altus* by Charles Robert Knight, 1897. Knight followed the hypothesis of a full aquatic lifestyle for *Amphicoelias* (Ballou, 1897). **D** - The first skeletal reconstruction of *Brachiosaurus altithorax* in 1915, with some elements (such as the scapula) after *Giraffatitan brancai* (back then *Brachiosaurus brancai*, which had just been discovered in Tanzania by the German expeditions). Notice the accuracy of the drawing, considering the limited amount of material it was based on.

The robust pillar-like femur, with an eccentric cross-section, and the hollow vertebrae, with buttresses and thin walls (Cope, 1877a) made Cope propose *Camarasaurus* as a terrestrial quadrupedal animal. In 1878, John Adam Ryder would depict the animal as a graviportal quadruped with a horizontal spine, in a 1:1 reconstruction which suffered from still having a lot of unprepared bones and the fact that it was intended for outreach. The reconstruction however can be superficially recognized as a sauropod (Fig. 1.2 A). William Ballou (1897) published an outreach article shortly after Cope's death, including a restoration of the second sauropod Cope described from Canyon City, *Amphicoelias altus* (Fig. 1.2 C). Both the text and the Charles Robert Knight restoration depict *Amphicoelias altus* as an obligatory aquatic animal unable to walk on land due to its weight and its slender femur, unlike *Camarasaurus supremus*, which had more robust limbs (Ballou, 1897). This is likely based on Cope's own suggestion, published only months after his hypothesis on terrestrial *Camarasaurus*, regarding the potential aquatic habits of a different species from Canyon City, *Amphicoelias fragillimus*, due its extremely large size and the architecture of the only vertebra retrieved (Cope, 1878b):

"the size of the vertebra is in direct proportion to the attenuation of its walls. This latter character, as seen in this and other species, resembles nothing so much as what is seen in deep sea fishes, as Alepidosaurus, etc. and suggests that these beasts may have walked in deep water and browsed on precipitous shores."

Cope, 1878b

Around the same time, Othniel Charles Marsh published the first sauropods from Como Bluff, Wyoming (USA). Among those, specimen YPM 1980 was the reasonably complete holotype of *Brontosaurus excelsus*, which Marsh used as a basis for the first scientifically published reconstruction of a sauropod dinosaur (Marsh, 1883). This reconstruction portrayed *Brontosaurus* in a quadrupedal, graviportal stance, dragging its tail and with an arched middle back, being its highest point (Fig. 1.2 B). Marsh considered the animal to have a flexible neck, to be stupid and slow moving due to its small head and slender neural cord, to have weighed more than 20 tons and to be of amphibious habits (Marsh, 1883). At the end of the XIX century, Henry Fairfield Osborn published *Diplodocus* sp. remains from the Bone Cabin Quarry in Wyoming, near Como Bluff (Osborn, 1899). While Osborn praised Marsh's effort as a pioneer work of great difficulty, he challenged some aspects of his *Brontosaurus* reconstruction. Among those, the arching of the back, according to Osborn, relegated the sacrum and pelvis to a subordinate functional importance, and made the tail an appendage of the body, instead of an important locomotor organ. He interpreted the tail to have three different functions: lever for balance, swimming propulsion and support when in tripod pose (Osborn, 1899).

"As in birds, the sacro-iliac junction is the center of power and of motion, and is of the most rigid character... Diplodocus gives us a new and different conception of the Cetiosaurs or Sauropoda, one which increases their ability as aquatic animals"

Osborn, 1899

Osborn's interpretation of *Diplodocus* challenged Marsh's claim of sauropods being slow moving and sluggish, but still considered sauropods to be amphibious, to drag their tails and to have a graviportal stance (Osborn, 1899)

Elmer Riggs published a first brief note on *Brachiosaurus altithorax* in 1903, a sauropod unlike any found before, in which the humerus was slightly longer than the femur (Riggs, 1903a). This, together with additional characters such as the first two caudal vertebrae, the extremely long dorsal ribs and the sacrum, made Riggs generate a very accurate hypothesis on his new taxon:

"Assuming that the lower fore-legs bones were proportionately long, we have to do with a creature whose shoulders were carried far above his hips and whose fore-legs played a more important part than the hind ones... the short spines and the slight processes of the anterior caudals show that the tail was much reduced both in size and in length"

Riggs, 1903

He even suggested arboreal food habits for *Brachiosaurus*, calling it "the giraffe among dinosaurs" (Riggs, 1903; Fig. 1.2 D), not too different from the skeletal mount Werner Janensch would erect thirty years later in Berlin of *Giraffatitan brancai*, then *Brachiosaurus brancai* (Janensch, 1950). In a subsequent paper, Riggs criticized the semi-aquatic or marsh-dwelling interpretation of sauropods, as he could not point out any evidence for aquatic adaptations (Riggs, 1904).

All in all, before the first complete skeletal mounts of sauropods were unveiled to the public, there was controversy regarding their habits, with three scenarios proposed: as fully terrestrial animals (Phillips, Cope,

Hatcher and Riggs), as fully aquatic animals (Ballou and Cope) or as amphibious animals (Marsh and Osborn). However, there was consensus on the posture of the limbs as erect and graviportal, the great flexibility of the neck and the dragging tails. The first skeletal mounts of these animals, which would present this consensus, were challenged in scientific circles, and the very same skeletal mounts were used to contrast the hypothesis regarding sauropod stance, mobility and functional capabilities.

This work presents a series of highlights on the impact of sauropod and sauropodomorph dinosaur skeletal mounts, on both hypotheses testing and perpetuating long-lasting misconceptions. Finally, some criteria which fossil mounts should meet to verify hypotheses are proposed.

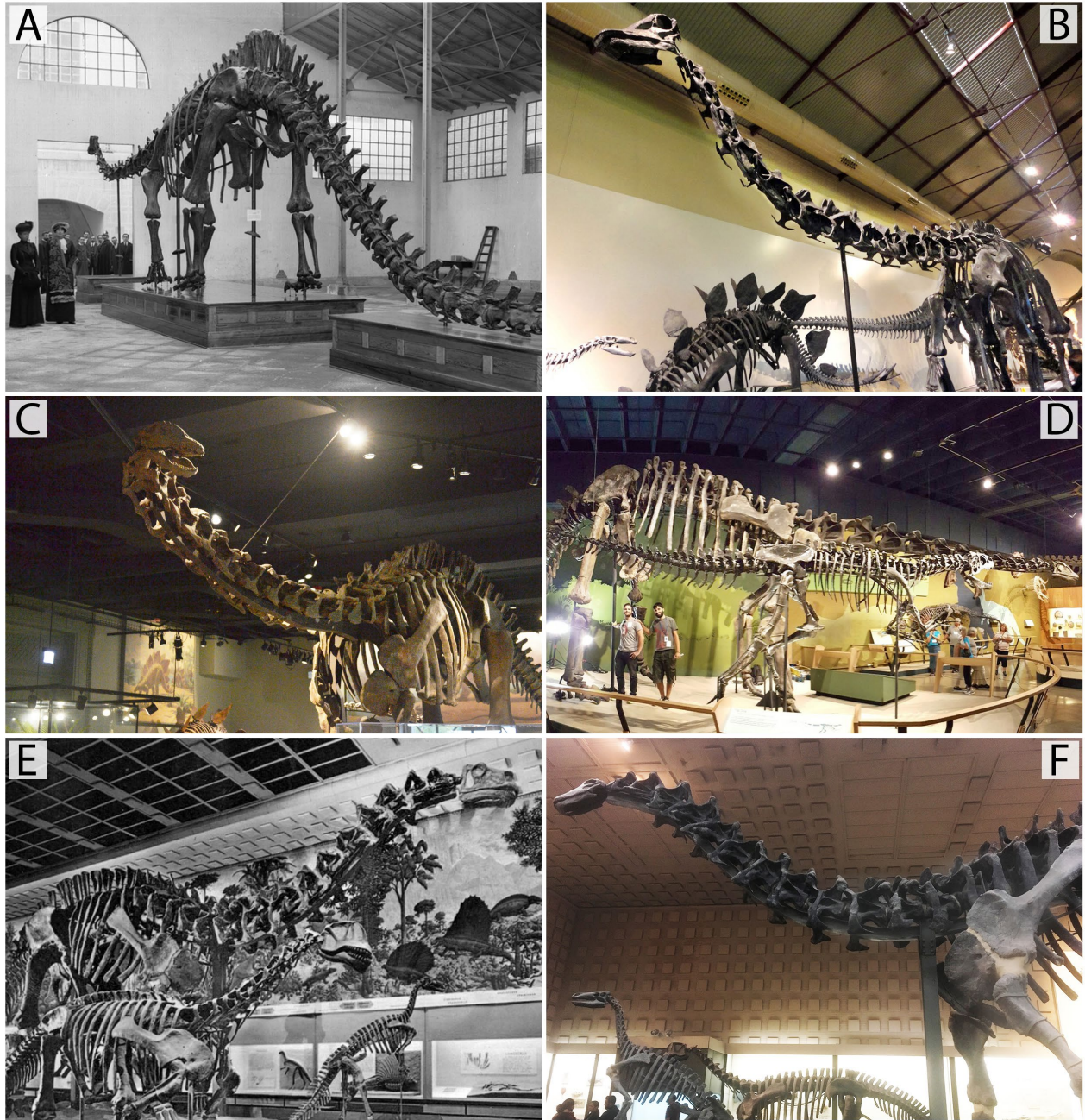


Figure 1.3 - Classic sauropod skeletal mounts reviewed.

A - The original *Diplodocus carnegie* mount at Madrid, Spain on the day it was revealed to the public. **B** - The same *Diplodocus* mount in the present day, where it has been ever since 1935 after moving in between exhibitions halls (Pérez García & Sánchez Chillón, 2009). **C** - Indeterminate diplodocid skeletal mount at the Field Museum of Natural History. **D** - *Haplocanthosaurus delfsi* skeletal mount at the Cleveland Museum of Natural History (behind the *Allosaurus* on the foreground). **E** - *Brontosaurus excelsus* skeletal mount at the Yale Peabody Museum with its original sculpted skull. **F** - The same *Brontosaurus* mount in the present day in the same hall at the Yale Peabody Museum. Notice the only change between the old and new mount is the updated skull, now a cast of *Apatosaurus*.

1.2 REVIEWED SKELETAL MOUNTS

In order to analyze the scientific impact of the skeletal mounts of sauropod dinosaurs, a combination of bibliography revision and firsthand inspection of sauropod mounts has been carried on. The analysis of these skeletons consisted on assessing the reliability of the mounts regarding the articulation of their vertebrae. Disarticulated or sculpted elements (i.e. not casts) were considered to be unreliable (Carpenter *et al.*, 1994).

The mounted sauropodomorphs reviewed firsthand were (Fig. 1.3):

- 1. The Carnegie Museum *Diplodocus carnegie*** (Fig. 1.3 A,B): The first copy of this composite skeleton was unveiled in London in 1905, and the original bones were mounted in Pittsburgh in 1907 (Rea, 2004). The mount was composed mainly of two individuals from Sheep Creek Quarry, Wyoming (CM 84 and CM 94), with additional elements stemming from other skeletons of compatible size, most notably the preorbital region of the skull, the forelimbs (a cast from a Bone Cabin Quarry AMNH specimen which turned out to be *Camarasaurus*) and the tail, which is composed of vertebrae from CM 84, CM 94, CM 307 and the chevrons of an AMNH specimen from Bone Cabin Quarry. Although the original skeleton at Pittsburgh was remounted in 2007 when the Carnegie Museum renovated its vertebrate paleontology halls, many of the casts still retain the original mount (Pérez García & Sánchez Chillón, 2009). The original skeleton at Pittsburgh (remounted) and the cast at Museo Nacional de Ciencias Naturales, Madrid (original) were inspected firsthand, together with photographic archives.
- 2. The Field Museum of Natural History indeterminate *Diplodocid*** (Fig. 1.3 C): This mount was unveiled with only the tail, pelvis, legs, dorsal vertebrae and ribs in 1908 and it was not until 1958 that the pectoral girdle, forelimb, neck and head would be added. This was due to the fact that specimen FMNH P 25112 from Fruita, Colorado, was missing the anterior region of the body. Missing parts would be subsequently added from a second specimen from near Green River, Utah. Although the halls of FMNH have been renovated several times, the only change to this mount has been replacing the *Camarasaurus*-like skull for a more accurate cast of an *Apatosaurus* skull, so it preserves its original dragging tail. Originally considered to be *Apatosaurus*, recent analyses have found it to be an indeterminate diplodocid (Tschopp, Mateus, & Benson, 2015).
- 3. The Yale Peabody Museum *Brontosaurus excelsus*** (Fig. 1.3 E,F): Despite being the first specimen used to create a skeletal reconstruction of a sauropod dinosaur under a scientific criterion, the holotype YPM 1980 would not be mounted until 1929, since the Peabody museum did not have an adequate exhibition facility to house something as big as a mounted sauropod until 1925 (Conniff, 2016). While this mount only used the remains of YPM 1980, it incorporated a lot of missing bones sculpted in plaster, with all of them painted in a similar hue, making it difficult to assess what is fossil and what is sculpted bone. The original mount has survived to this day, with the exception of the original sculpted skull, which was substituted in the 1980s for a more accurate cast of *Apatosaurus*.
- 4. The Carnegie Museum juvenile *Camarasaurus lentus***: One of the most complete specimens of a sauropod dinosaur ever retrieved, CM 11338 was mounted on a wall recreating its field position. All mounted bones are originals except the head and hyoids, which are deposited in the collection facility of Carnegie Museum. While unfortunately the original field pose was corrected when exhibition was prepared (the hyperextended tail, sternal plates and left limbs were positioned in an aesthetic way), the original pose is documented in photographs and the right side and presacral column remain embedded in the original matrix (Gilmore, 1925).
- 5. The Cleveland Museum of Natural History *Haplocanthosaurus delfsi*** (Fig. 1.3 D): This is one of the last classically mounted sauropods, erected before the *Dinosaur Renaissance* of the 1970s. Therefore, it still has all preconceived notions of sauropod anatomy (dragging tail, arched back...). The specimen was found by Edwin Delfs when he was a high school student on a field trip. It was subsequently excavated by an amateur team, deposited in the CMNH and mounted by preparators of the AMNH (McIntosh & Williams, 1988). It was not until the 1980s that it was studied by John S. McIntosh, finding it to be a new species of the genus *Haplocanthosaurus*, *H. delfsi* (McIntosh & Williams, 1988). The specimen preserves 12 caudal vertebrae, sacrum and most dorsal vertebrae with no interruptions in the sequence, the anteriormost four cervical

vertebrae, a complete hindlimb, pelvis and incomplete scapulocoracoid. The missing bones were sculpted after those of other sauropods (McIntosh & Williams, 1988). The classic mount has survived until present day.

1.3 CASE STUDIES

The case of the sprawling Diplodocus: first scientific use of skeletal mounts

Philanthropist Andrew Carnegie funded the excavation and preparation of two fairly complete specimens of *Diplodocus* from Sheep Creek Quarry (specimens CM 84 and CM 94). John Bell Hatcher described the taxon in an extensive monograph by in 1901, in which he stated that both Carnegie Museum specimens were different enough from Marsh's *Diplodocus longus* YPM and USNM specimens (Hatcher, 1901). Therefore, he erected *D. carnegie* in honor of his patron, to whom a reconstruction of the skeleton was gifted. Carnegie displayed this reconstruction on his Castle at Skibo (Scotland), where King Edward VII would be captivated by it during a visit in 1902 (Rea, 2004). The king asked Carnegie whether he could provide the British National Museum with another dinosaur, and Carnegie transmitted the king's petition to William Holland, the director of Carnegie Museum. Holland remembered his patron that complete specimens were rare and finding another would be difficult, and proposed instead to create a high quality replica in plaster (Rea, 2004).

The Carnegie preparators began working on the copy with help from Italian artisans hired specifically for the task of molding the bones (Rea, 2004). After a preliminary mount in Pittsburgh, the *Diplodocus carnegie* replica was unveiled in London in 1905 (Holland, 1905, 1906; Rea, 2004). Soon, Carnegie would also gift several plaster casts of this skeleton to institutions worldwide, providing access to a complete dinosaur skeleton to many scientists and museum visitors all around the world for the first time in History (Rea, 2004). The process of mounting these replicas taught Hatcher and Holland several unknown facts regarding *Diplodocus* anatomy, including the head forming an angle with the neck in an avian fashion, instead of emerging straight as in crocodiles (Holland, 1906). They mounted the *Diplodocus* skeletons following established consensus regarding sauropod stance: the tail was dragging and the limbs were pillar-like erect (Fig. 1.3 A,B).

Despite sauropod skeletal reconstructions existing as drawings as far back as 1877 (by John Adam Ryder, Fig. 1.2 A), and a consensus existed on them being graviportal quadrupeds, it was the mounted cast of *Diplodocus* which would spark the most controversy. Some North American (Hay, 1908, 1910) and European scientists (Tornier, 1909) proposed that since *Diplodocus* was a reptile, it should sprawl, like modern reptiles do. Hay criticized using the straight femora of sauropods as a criterion for an erect stance of the limbs, arguing that sprawling animals like *Sphenodon* have straight femora (Hay, 1908). He also considered the great masses estimated at the time for sauropods (more than 20 tons for *Brontosaurus*; Marsh, 1883) was a strong argument against a mammal-like carriage. In agreement with the phylogenetic context of dinosaurs in the early 20th century, Hay questioned why would sauropods evolve a mammal-like stance if they had evolved from ancestors which walked in a crocodile-like manner (although now we know sauropods inherited their erect gait from bipedal ancestors; Sereno, 1999).

He proposed that *Diplodocus* was an amphibious animal which could swim with considerable ease while crawling on land would be a laborious effort (Hay, 1908). Hay published a second paper in 1910, accompanied by an illustration by Mary Mason Mitchel entitled *The form and attitudes of Diplodocus* in which the sprawling posture and ecology of *Diplodocus* was depicted as Hay thought them to be (Hay, 1910). This paper included a more detailed discussion of his proposal, including figures used to cast doubt on the digitigrady of sauropod feet and the erect, graviportal position of the femur. Hay noted the scarring on the epiphyses of sauropod long bones indicated extensive cartilage caps, and reconstructed that of *Diplodocus* following those of lacertilians (Hay, 1910). Gustav Tornier agreed with the hypothesis of Hay, and he provided a skeletal reconstruction of a sprawling *Diplodocus* (Tornier, 1909). His reconstruction depicts a vertical scapula, with the humerus retracted, the femur protracted and both the knee and elbow flexed at more than 90° (Fig. 1.4 A).

All evidence supporting the sprawling sauropod hypothesis was refuted by Holland, who had supervised most Carnegie Museum *Diplodocus* replicas. He wrote an equally elegant and sarcastic response to the hypotheses of Hay and Tornier (Holland, 1910): he performed an experiment with a cast of *Diplodocus* at the Carnegie Museum which was being prepared for mounting at St. Petersburg. Holland articulated the bone

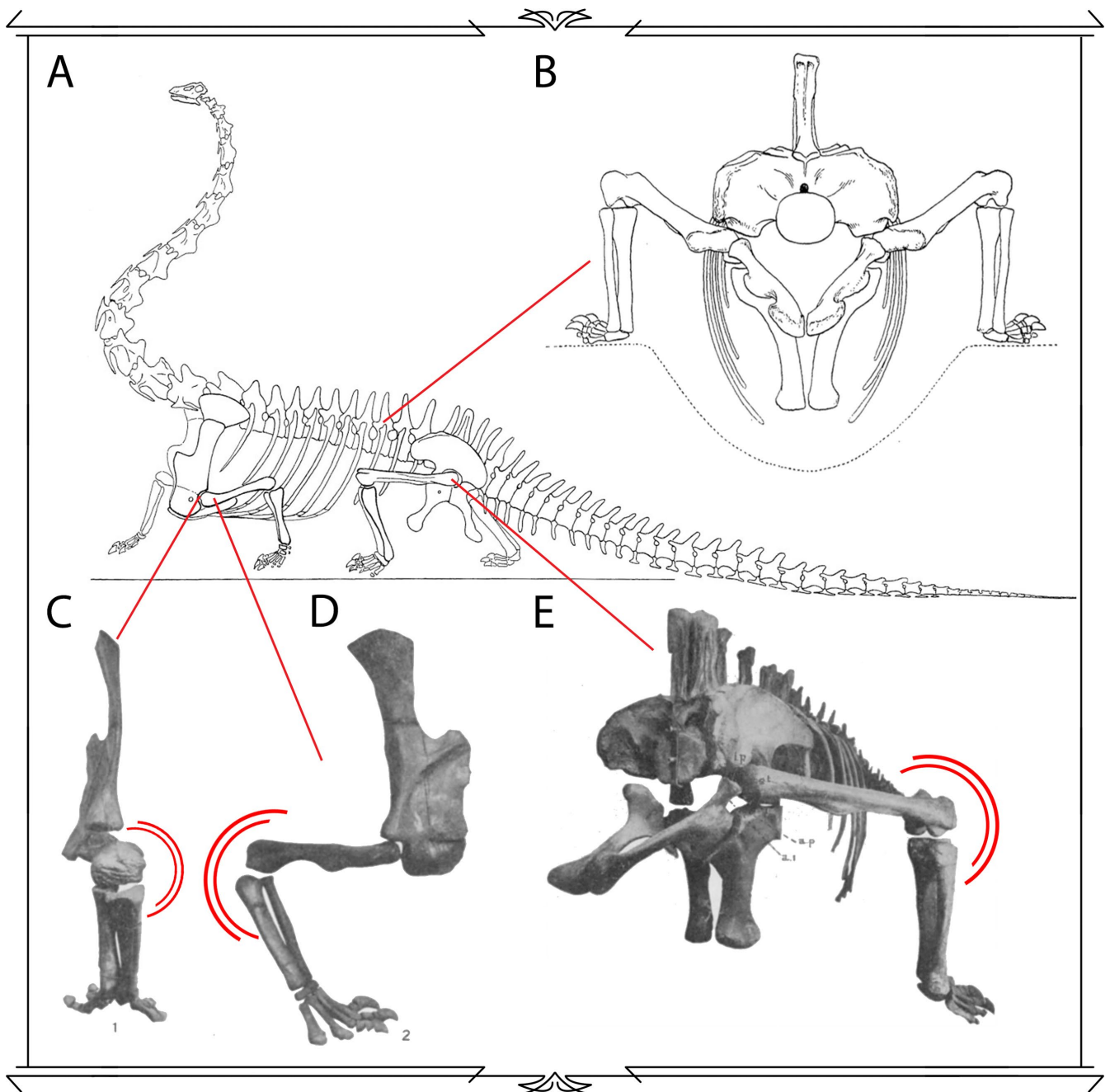


Figure 1.4 - Using a physical skeletal mount to evaluate the stance of sauropods.

A - The stance of *Diplodocus carnegie* as conceived by Tornier (1909), with arrows pointing at the main issues which were refuted by Holland. **B** - The ribcage of *Diplodocus* (and all known sauropods) is deep, much taller than wide, since their ribs are very long and straight compared with those of crocodiles or lacertilians. If *Diplodocus* were to adopt the posture proposed by Tornier, the ribcage would reach the ground before the animal could sprawl, as can be seen in posterior view. **C, D** - In order to adopt the sprawling posture, the elbow of the physical skeleton of *Diplodocus* is dislocated, in posterior (C) and -lateral (D) views. **E** - In order to adopt the sprawling posture, the knee of the physical skeleton of *Diplodocus* is dislocated, in postero-lateral view. **B-D** modified from Holland, 1910.

replicas to achieve the pose claimed by Hay and drawn by Tornier. In doing so, he found that such a posture was anatomically impossible (Fig. 1.4 B-E):

1. The femur would not fit the acetabulum in the pose suggested by Hay, since the transverse diameter of the proximal end of the femur is longer than the acetabulum diameter.
2. The tibia and fibula would be disarticulated from their respective condyles from the femur in order to achieve the 90° flexion depicted in Tornier's reconstruction (Fig. 1.4 E).
3. The lines of action of most hindlimb muscles would be inefficient, even to the point of not being functional at all.
4. The deep ribcage of *Diplodocus*, unlike the round ribcage of lizards or crocodilians, would

reach the ground before the animal would sprawl with their knees and elbows at 90° flexion. Holland used this last conclusion to ridicule with bitter sarcasm the work of Hay and Tornier, hinting that, in order to move around sprawling, sauropods would have needed special previously dug trenches to do so (Fig. 1.4 B).

The conclusions of Holland's experiment with the *Diplodocus carnegie* cast were compatible with a subsequent fossil find of another sauropod, the nearly complete *Camarasaurus lentus* CM 11338 from Dinosaur National Monument. This specimen preserved both its right fore and hindlimbs articulated with their respective girdles (Gilmore, 1925). In his description of the specimen, Gilmore also noticed that the diameter of the acetabulum (175 mm) was much smaller than the greatest length of the proximal epiphysis of the femur (220 mm). In his opinion, that fact alone "absolutely disposes of the proposed articulation of the femur suggested by Hay" (Gilmore, 1925). When mounting *Diplodocus* sp. specimen USNM 10865, Gilmore also remarked that the sprawling pose would involve anatomical impossibilities, although he did not detail them (Gilmore, 1932). Further evidence from fossilized sauropod trackways were compatible as well with Holland's conclusions, since all trackways attributed to sauropods (of both the narrow- or wide-gauge type) showed the trackmakers stepped very close to the midline of the animal, indicating an erect stance for sauropods. However, although the composite nature of the *Diplodocus* skeletal mount was explicitly stated in academic publication (Holland, 1906), the actual mount and exhibition did not explicitly state it.

"there ought to be a decided difference between the color of the bone and that of the plaster... the visitor has a right to know whether he is gazing at real bone or at plaster, and the reasons therefore. Moreover, it is futile and mischievous to attempt to hide the nature of the restoring materials"

Hay, 1909

Despite the Carnegie Museum *Diplodocus* failing at explicitly revealing its composite nature to visitors, it allowed Holland to prove that skeletal mounts could be effectively used to test gait and posture hypotheses for extinct vertebrates, his results later vindicated by further fossil finds. Holland nevertheless noted that performing experiments with 1:1 fossil replicas was still an arduous task, and pointed out that few could perform such analyses without risking the casts (Holland, 1910).

The case of the tail-dragging sauropods: the hazards of preconceived notions

As mentioned earlier, Joseph Leidy and his crew erected the first dinosaur mount in History, *Hadrosaurus foulki*, with a dragging tail and kangaroo-like stance (Carpenter *et al.*, 1994). Most dinosaur mounts and reconstructions for a century would be depicted with dragging tails. Sauropods were not an exception to this rule, except John Adam Ryder's first restoration of *Camarasaurus supremus* (which was largely speculative, Fig. 1.2 A). All restorations of sauropod dinosaurs (skeletal as well as paleoartistic reconstructions) depicted them with dragging tails (Marsh, 1883; Ballou, 1897; Osborn, 1899; Hatcher, 1901; Tornier, 1909; Hay, 1910; Matthew, 1915), and as such were incorporated into the first sauropod mounts: all were mounted with dragging tails (Fig. 1.3). A close inspection of those classic mounts reveals that many tail vertebrae were dislocated in order to produce the smooth curve to drag the tail. Dislocated vertebrae were found in:

- 1. The Carnegie Museum *Diplodocus carnegie*:** While the original fossil mount in Pittsburgh has been remounted with all its caudal vertebrae articulated, the cast specimen from MNCN maintains the dragging tail despite having being remounted at least once (Pérez García & Sánchez Chillón, 2009). To make the tail assume such a posture, caudal vertebrae 5, 6, 7, 8 and 10 had to be disarticulated (Fig. 1.5 A). This has been corrected in most remounts of this specimen, including the original skeleton at Carnegie Museum (Fig. 1.5 B).
- 2. The Field Museum of Natural History indeterminate diplodocid:** This mount still has a dragging tail, although it is a smoother ventriflexion than that in the MNCN *Diplodocus*. In order to achieve the posture, caudal vertebrae 2 and 3 were strongly disarticulated. Additional caudal vertebrae were not in proper articulation, but this appears to be a problem in their preparation.
- 3. The Yale Peabody Museum *Brontosaurus excelsus*:** This is the only sauropod with a dragging tail in which all the caudal vertebrae are articulated. Ventriflexion occurs smoothly from caudal vertebra 6 to caudal vertebra 10 (Fig. 1.6 B). However, since extensive restoration of this skeleton took place, with bone and repaired parts/sculpture being painted with

the same hue (Tschopp *et al.*, 2015), it is difficult to differentiate real fossil bone from bone sculpted in plaster. Until this skeleton is disassembled, stabilized and re-prepared, it will not be possible to assess how much of its curvature was artificially created and how much is caused by the morphology of the vertebrae.

- 4. The Cleveland Museum of Natural History *Haplocanthosaurus delphi*:** The tail of this mount has a very abrupt ventriflexion, since caudal vertebrae 1, 2, 3, 4 and 5 are completely disarticulated (Fig. 1.6 A).

The preconceived notion that sauropods “should” drag their tails likely comes from observations of living crocodiles when performing *high walk*. Since it was present in most reconstructions of sauropods prior to 1905, it is conceivable that the steel armatures which would support the bones were designed *a priori* with the intention of dragging the tail, and the bones had to be disarticulated to match the pre-existing supporting structure. This might explain why the skeletal reconstruction of the AMNH partial *Diplodocus longus* with a dragging tail (Osborn, 1899) did not match the mounted specimen, which did not have an dragging tail (page 70 in Dingus, 1995). Holland also mentioned that long-tailed reptiles usually carry their tails elevated, and casted his doubts on the dragging tail of *Diplodocus* in his rebuttal of the Hay/Tornier hypothesis of sprawling *Diplodocus* (Holland, 1910). However, Holland’s doubts did not transpire into the following mounts of *Diplodocus carnegie*, as all of them dragged their tails.

Charles Gilmore was the main critic of the dragging tails of sauropod dinosaurs and the first to write about noticing the dislocations in caudal vertebrae needed to achieve the pose. In his description of the juvenile *Camarasaurus lentus* CM 11338, he stated the mount been reconstructed with an elevated proximal tail (Gilmore, 1925). He claimed the same was true for the Carnegie Museum *Apatosaurus louisae* mounted in 1915 in Pittsburgh, and that the elevated tail was a product of the actual articulation of the bones (Gilmore, 1925). Gilmore found further evidence for this when mounting a specimen of *Diplodocus* sp. (USNM 10865) from the Dinosaur National Monument at the Smithsonian Institution. The skeleton individual bones were articulated in pairs and measurements on how they did were taken before creating the steel supports for the skeleton (Gilmore, 1932). This revealed Gilmore aspects of the anatomy of *Diplodocus* previously unknown. When articulating the caudal vertebrae together, the tail was not dragging as abruptly as in the *Diplodocus carnegie* mount at the Carnegie Museum (Gilmore, 1932). Gilmore noticed that articulating all the vertebrae, as well as the wedged V shaped centrum of caudal vertebra 3 of USNM 10865 made the tail deflect horizontally from the sacrum and being carried out far out before beginning to be dragged. Despite this argument being so compelling, it would be largely ignored until the *Dinosaur Renaissance*, when it was deemed that sauropods never (Bakker, 1968) or only on rare occasion (Coombs, 1975) dragged their tails.

Gilmore also noticed that not only the caudal vertebrae did not ventrally diverge from the sacrum, but also

“the presacrals in our specimen have a decided upward arcuation of the column beginning with the vertebrae in front of the sacrum... when the tenth dorsal vertebra is in position the lower half is inclined backward, which brings the forward leaning spine into a nearly vertical position and thus the spines are evenly spaced, whereas in both the Carnegie Museum an American Museum specimens there are wide gaps between the sacrodorsal and the first free dorsal in front of it”.

Gilmore, 1932

Classic mounts and their remounted versions also have disarticulated presacral vertebrae:

- 1. The Carnegie Museum *Diplodocus carnegie*:** Despite having been remounted, there are two disarticulated presacral vertebrae on the mount from original fossils at the Carnegie Museum: dorsal vertebrae 10 is disarticulated from the sacrum, as well as cervical vertebra 14 from cervical 15 (Fig. 1.7 A, B). The mounted *Diplodocus* at Senckenberg Museum of Natural History at Frankfurt, Germany, does not have dorsal vertebra 10 disarticulated, and its dorsal spine is less horizontal and more rampant, the same that happened to USNM 10865 *Diplodocus* (Gilmore, 1932). It is likely that articulating the Carnegie Museum last dorsal with the sacrum will render a similar dorsally sloping presacral column. The original mount from MNCN has more disarticulated presacral vertebrae in addition to those disarticulated the remounted skeleton, among them the first two dorsal vertebrae (Fig. 1.7 A).
- 2. The Yale Peabody Museum *Brontosaurus excelsus*:** As with the caudal vertebrae, extensive restoration took place on the presacrals (Tschopp *et al.*, 2015), so it is not possible to ascertain if the vertebrae were actually disarticulated in order to achieve the pose of the presacrals.

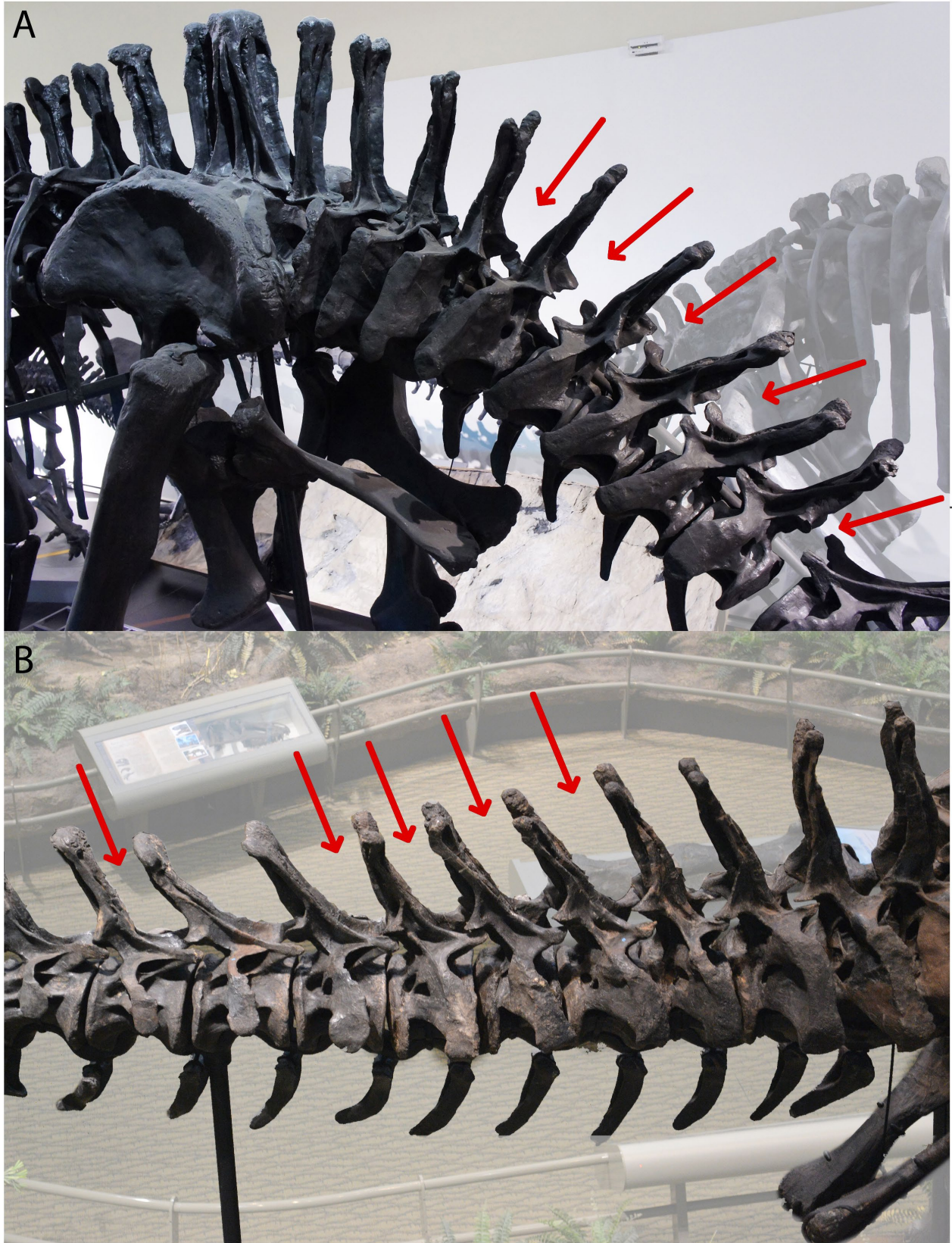


Figure 1.5 - The tail of *Diplodocus carnegie* CM 84.

A - The original skeletal mount of a cast of *Diplodocus carnegie* at Museo Nacional de Ciencias Naturales in Madrid, where caudal vertebrae 5, 6, 7, 8 and 10 are disarticulated in order to ventriflex the tail (red arrows). **B** - The remounted original skeleton of CM 84 at the Carnegie Museum in Pittsburgh, where the originally disarticulated vertebrae have been articulated (red arrows).

3. **The Cleveland Museum of Natural History *Haplocanthosaurus delfsi*:** There are plenty of dorsal vertebrae disarticulated on this specimen, creating a ventrally deflected presacral spine. The last dorsal vertebra is disarticulated from the sacrum, with a great angulation, which creates a V shaped inter-vertebral space (Fig. 1.7 C). Other dorsal vertebrae are ventrally flexed to the limit (but remain in relative articulation). If the last dorsal were articulated with the sacrum, the presacral spine would likely rise above the horizontal, with more dorsal deflection, similar to the Senckenberg Museum of Natural History *Diplodocus* or UNSM 10865 *Diplodocus* (Gilmore, 1932).

Eventually, while many of the old mounts were updated, the disarticulated caudal vertebrae were fixed (Dingus, 1995) and new skeletons were mounted following the modern criterion (Carpenter *et al.*, 1994), in which articulating the complete series of caudal vertebrae render a completely horizontal tail (Fig. 1.5 B). However, as already indicated, the presacral series of many sauropod mounts still have dislocated vertebrae, creating artificial curvatures on the axial skeleton based on preconceived notions (Fig. 1.7). Such preconceived notions when mounting skeletons and devising skeletal reconstructions have made researchers interpret in the past sauropod functional morphology under an opinion-based paradigm. Hence, sauropod skeletal geometry should be revised to evaluate the foundations of our present understanding of sauropod functional morphology and paleobiology.

The case of the quadrupedal Plateosaurus: the advent of virtual paleontology

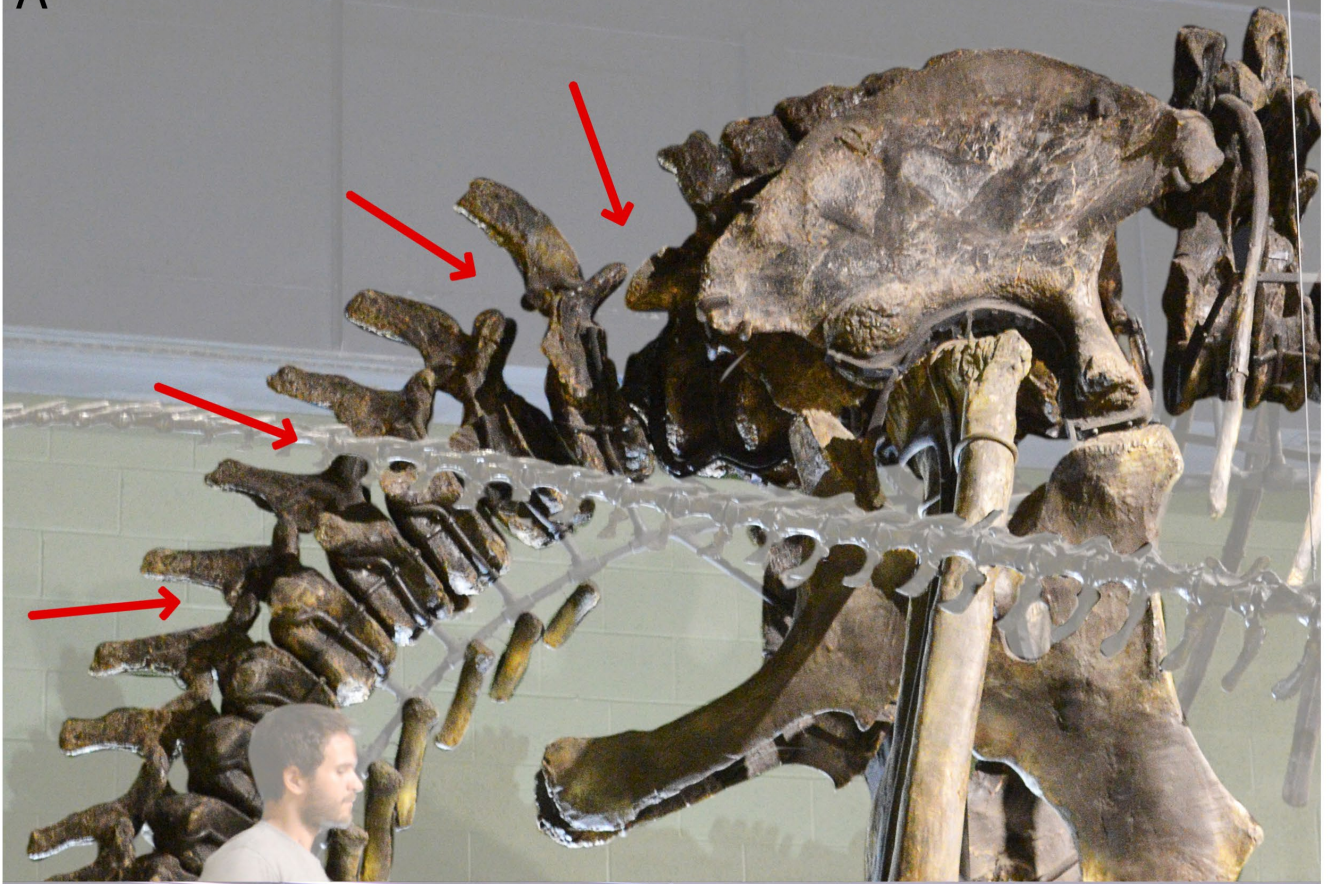
While there is little doubt that sauropods were quadrupeds, there has been more controversy on the quadrupedal capabilities of “prosauropods”, a paraphyletic group of taxa more related to Sauropoda than to other Dinosauria. Since dinosaurs are known to have diverged from a bipedal last common ancestor (Sereno, 1999), and the evolutionary transition from a biped with grasping hands to a graviportal quadrupedal sauropod is a subject of great interest, “prosauropods” have been thoroughly studied.

Plateosaurus is one of the best-known “prosauropods”, with a large number of nearly complete specimens known since the XIX century (i.e. Young, 1947; Langer *et al.*, 1999; Galton, Van Heerden, & Yates, 2005; Mallison, 2010b). Despite these many skeletons known, many interpretations were proposed regarding its locomotion and stance: a lumbering quadruped, a cursorial biped, cursorial biped dragging its tail or a galloping quadruped (Mallison, 2007). The most spread hypothesis was that *Plateosaurus* was a facultative quadruped: quadruped and biped at once. Despite this, many skeletal mounts and paleoart depicted *Plateosaurus* as a strict quadruped for decades.

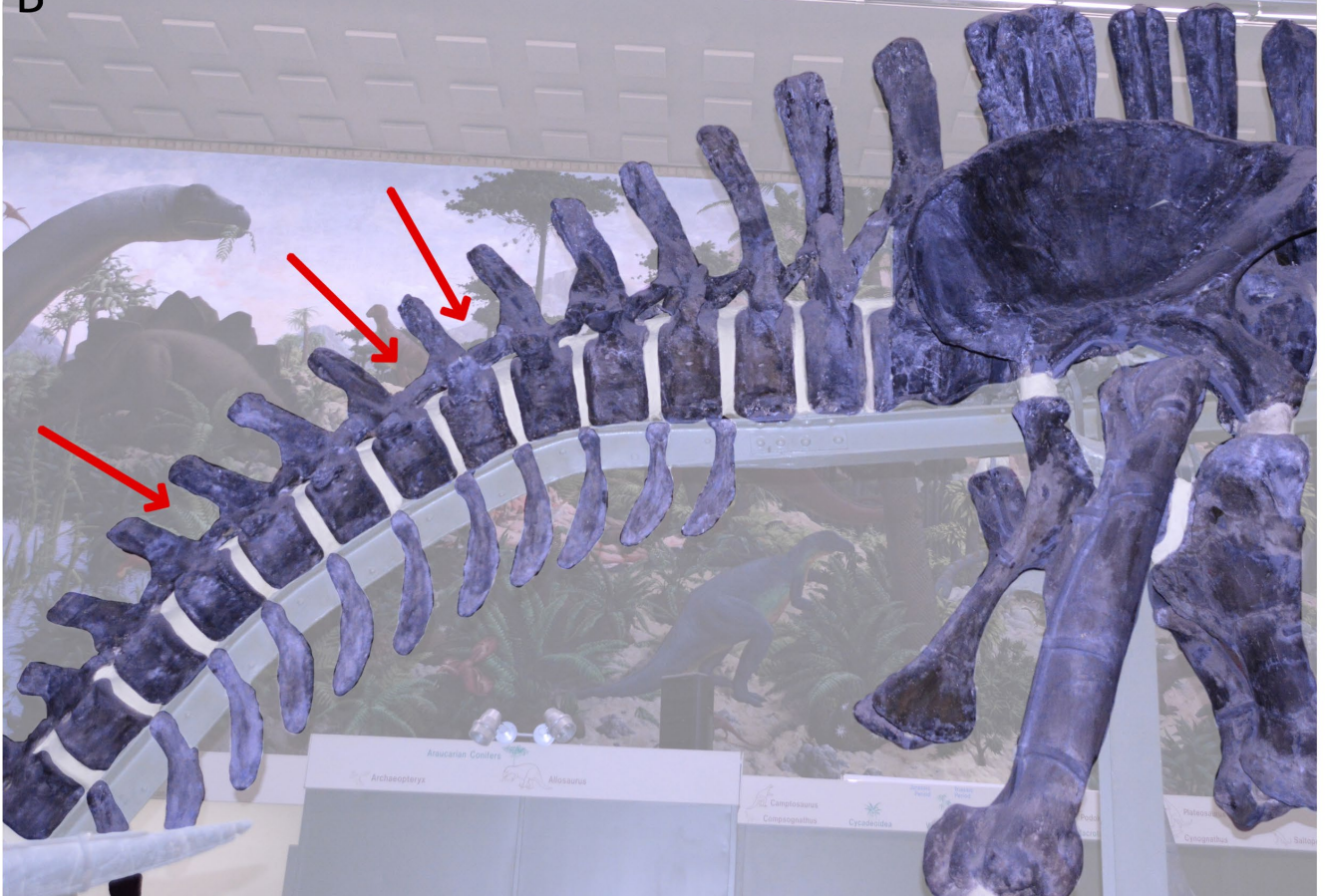
Mallison nevertheless employed Computer Aided Design/Computer Aided Engineering (CAD/CAE) software to refute all the hypotheses regarding the locomotion of *Plateosaurus* but one: a biped with grasping hands which could not run with an aerial phase (Mallison, 2010a,b). He did so by using the 3D scanned skeleton mostly of a single specimen of *Plateosaurus* (GPIT1, some elements of GPIT2), performing a rigorous articulation of the skeleton in maximum articulation, range of motion analyses, mass estimation and walking gait kinematic analysis. While the *Plateosaurus* reconstruction by Mallison was not the first virtual dinosaur skeleton (the USNM composite *Triceratops* known as “Hatcher” scanned by Chapman, Andersen, & Sabo (1999) was the first), it was the first complete virtual skeleton stemming from a single individual. This allowed to reduce the uncertainty of many aspects of the fossil mount: proportions, articulation, and range of motion all represented the possibilities of a single individual.

Mallison also was among the first to delineate a protocol for assembling and experimenting with virtual skeletons minimizing preconceived notions, in a reproducible way and using the actual morphology of the bones (Mallison, 2007, 2010b). Virtual skeletons would be assembled in osteologically neutral pose (ONP, maximum articular overlap; Stevens & Parrish, 1999; Stevens, 2002, 2013; Dzemeski & Christian, 2007; Mallison, 2010b; Christian *et al.*, 2013). In doing so, he made sure he was producing a posture based on the actual morphology of the bones (Mallison, 2010b; Stevens, 2013) and not just on a random criterion (i.e. articulating the bones perpendicularly). He also did it with only a pair of bones visible at a time: one static while the other was posed in ONP. Once the pair was in articulation, the static element would be hidden and the last added element would remain visible but static when adding the following bone (Mallison, 2007, 2010b). The whole skeleton was assembled this way several times, in different directions (anterior to posterior and vice-versa, distal to proximal and vice-versa), and if the obtained neutral posture was always the same, it was deemed positive (Mallison, 2010b,c). Doing this, it was ensured that preconceived notions were minimized. Finally,

A



B



when performing the range of motion analyses, in absence of osteological stops the limit of motion was set to be disarticulations: the bones had to remain in articulation for a posture to be considered possible. All this revealed that it was impossible for *Plateosaurus* to be a quadruped, since the forelimb was too short to allow its hands to reach the ground, not even walking as a plantigrade (Mallison, 2007, 2010a,b). It also set a repeatable standard to follow when assembling and analyzing fossil skeletons.

1.4 SKELETAL MOUNTS AS SCIENTIFIC TOOLS

Ever since the dawn of vertebrate paleontology, voices have raised against mounting fossil skeletons. As noted above, Albert Koch's "Missourium" mount in particular was partially forged and was criticized by the academics of the day, most notably Richard Owen. They thought these mounted skeletons casted doubt on the science of paleontology. The criticism of mounted vertebrate skeletons continued into the first decades of the XX century. However, early XX century researchers were supervising the skeletal mounts of the museums they worked for, so criticism usually stemmed from researchers from other institutions, as well as scientists among different institutions.

In modern paleontology, there are criticisms against mounting both original fossils and cast skeletons. The main arguments against mounting original fossil skeletons come from a curatorial point of view: fluctuating conditions of temperature, humidity and vibrations in exhibition halls may damage unique specimens in the long term, sometimes permanently, as well as making them harder to access for scientific study (Horner & Lessem, 1993). This has led to many museums retiring specimens from exhibit due the damage suffered after decades of exhibition and to mount casts of those specimens instead (Dingus, 1995).

Mounting cast specimens is not been free of criticism in the present day either: bones may be mounted in unrealistic ways or following preconceived ideas, therefore spreading notions about the animals which are not grounded at all on scientific evidence (Horner & Lessem, 1993; Dingus, 1995), not too different from what Hay wrote almost a century ago (Hay, 1909). This criticism comes from a change in the trends regarding the way skeletons are posed in exhibitions, that has shifted from the static poses of the early XX century to a more dynamic and life-like reconstructions (Carpenter *et al.*, 1994). However, the same issues are being used to criticize dynamic than static mounts: incorrectly articulated bones, poor workmanship, hiding whether the mounts are composites or sculpted and, as a combination of the three previous issues, unrealistic/unnatural postures (Hay, 1909; Gilmore, 1932; Horner & Lessem, 1993; Carpenter *et al.*, 1994; Dingus, 1995). Meeting these criteria are regarded today as requirements for skeletal mounts to be rigorous, and of scientific value (Carpenter *et al.*, 1994; Stevens, 2002, 2013; Mallison, 2007, 2010b).

The advent of virtual paleontology, with prize-reduction and simplification of digitalization techniques (Mallison & Wings, 2014) is allowing a more widespread use of skeletal mounts as scientific tools. A virtual environment, unlike using physical models, allows assembling a number of bones only limited by computation power without the need for supports. Also, virtual skeletal mounts using high resolution scans of the actual fossils (Mallison, 2010b,c; Ibrahim *et al.*, 2014; Lacovara *et al.*, 2014) allow creating mounts faithful to the original skeletons, in contrast with building virtual models manually from pictures or drawings of specimens (Stevens & Parrish, 1999; Stevens, 2002) which is not only time consuming, but also leading to huge differences in shape between the model and the real fossil bones (Mallison, 2007).

However, virtual mounts also may replicate all problems of physical mounts:

1. Mounting virtual skeletons using bones manually modeled from pictures or drawings of fossils may accumulate errors derived from preconceived notions present in photographs or drawings, as happened with skeletal reconstructions of *Plateosaurus* (Mallison, 2007, 2010b).
2. Virtual skeletons may also disarticulate bones, creating postures which require disarticulated bones (which also help in spreading preconceived notions).

Figure 1.6 (previous page) - The dragging tails of *Haplocanthosaurus* and *Brontosaurus*.

A - The Cleveland Museum of Natural History original mount of *Haplocanthosaurus delfsi*, with caudal vertebrae 1, 2, 4 and 6 disarticulated in order to ventriflex the tail (red arrows). **B** - The Yale Peabody Museum of Natural History original mount of *Brontosaurus excelsus* YPM 1980, where no disarticulation is apparent (probably due to the extensive reconstruction applied to the original fossils (Tschopp *et al.*, 2015)), but there are some inflexion points where the tail ventriflexes (red arrows).

3. Mounting virtual composite skeletons may render chimaeras, as could be the case for the virtual *Spinosaurus aegyptiacus* (Ibrahim *et al.*, 2014) if some of the bones used in its construction belong to *Sigilmassaurus* or a yet unnamed spinosaur (Evers *et al.*, 2015).

Given that virtual mounts are likely to be more widespread for scientific use in the future (since it is at once cheaper and easier to mount and remount it as many times as needed), combining all lessons learned from the pioneers of fossil mount with the possibilities of virtual environments, such is the possibility of working with a pair of bones at a time, may ensure accuracy of results of functional morphology, biomechanics or paleobiology derived from studying fossil skeletons.

1.5 CRITERIA FOR SCIENTIFIC USE OF SKELETAL MOUNTS

This review of historic and contemporary sauropodomorph skeletal mounts reveals that they have been used to refute hypotheses and to spread false preconceived notions as well. Nevertheless, they can be valid scientific tools if appropriate, rigorous protocols are employed. These criteria should be met to use skeletal mounts (virtual or physical) as scientific tools:

1. **Work with complete skeletons when possible:** since some studies on isolated regions of the skeleton have been overridden by further research incorporating full skeletons. Full mounts created from very partial skeletons with lots of missing data should always be treated as less supported hypotheses than those created from complete or nearly complete specimens.
2. **Use the most complete individual available as the basis for a mount.** If remains of other individuals have to be used to complete the mount, it should always be acknowledged.
3. **If the mount is a composite, it should be explicitly stated.** If a mount is using real fossils, panels and figures may indicate which bones come from which specimen using a color-code. Cast and virtual skeletal mounts can easily use this color coding on the actual bones.
4. **Always keep the bones articulated.** Keeping the bones articulated will be definitive evidence that the skeleton allowed the pose (although soft tissues might have affected it further), hence minimizing speculation.
5. **Diminish preconceived notions.** Something more easily done using digital technology, as skeletons can be assembled with only two bones visible at once. By doing so, the neutral articulation and the positions achieved in range of motion analyses will be more a product of their own anatomy than any preconceived notions.

Figure 1.7 (next page) - Disarticulated presacral vertebrae on sauropod skeletal mounts.

A - The original skeletal mount of a cast of *Diplodocus carnegie* at Museo Nacional de Ciencias Naturales in Madrid, where some of the cervical and dorsal vertebrae are disarticulated (red arrows), making the neck slope ventrally. **B** - The remounted original skeleton of CM 84 at the Carnegie Museum in Pittsburgh, where dorsal vertebra 10 is completely disarticulated from the sacrum (red arrow), which makes presacral vertebrae to be horizontal instead of rampant (Gilmore, 1932). **C** - The Cleveland Museum of Natural History original mount of *Haplocanthosaurus delfsi*, with the last dorsal vertebra completely disarticulated from the sacrum, with other dorsal vertebrae also disarticulated (red arrows), making presacral vertebrae to emerge horizontally.

A



B



C



1.7 HYPOTHESES AND OBJECTIVES

The main objective of the project behind this PhD thesis is to generate virtual models for an early branching sauropod using the exceptionally well-preserved fossil remains of *Spinophorosaurus nigerensis* (Middle? Jurassic of Niger), and use it as a foundation to understand the evolution of the postcranial biomechanical capabilities of Sauropoda. Since multiple specimens representing multiple sauropod clades (and some non-sauropod sauropodomorphs and theropods, as outgroups) could be visited and digitized, the information obtained with the virtual skeleton of *Spinophorosaurus* could be compared and further expanded. This allows to gain a better understanding of how variation among the characters affected functional morphology of different taxa.

To organize all the work, three blocks have been devised. The first block focuses on analyzing the body plan and functional capabilities of a sample of sauropods representing most of the well-established clades, to understand differences and similitudes in posture, range of motion, myology and biomechanics between the different taxa analyzed. A second block focuses on finding which osteological characters (both those already used in morphological analyses and new characters) had a direct impact in the functional capabilities studied in the first block, how these were distributed in sauropod phylogeny and whether they had a direct impact on cladogram topologies. A third block focuses on applying the conclusions of previous blocks to the titanosaur sauropods from Lo Hueco fossil site, to test how many functional morphotypes exist in said fossil locality.

The following hypotheses and objectives are the focus of each block.

BLOCK 1: Body plan and biomechanical capabilities in Sauropoda

Hypothesis 1: Sauropod skeletal mounts and reconstructions still have a great amount of preconceived notions, with drastic differences from their osteologically induced curvatures on the axial skeleton.

Hypothesis 2: the geometry of fossil vertebrae does not allow predicting accurately the amount of inter-vertebral space.

Hypothesis 3: some postures attained by live, extant vertebrates, cannot be accurately reconstructed just with osteological range of motion analyses.

Hypothesis 4: juveniles of Sauropoda have axial skeleton ranges of motion more similar to the adult forms of more basal sauropodomorphs than their own adult forms.

Hypothesis 5: more elongated cervical vertebrae imply not only longer necks, but a larger feeding envelope.

Hypothesis 6: more elongated zygapophyseal facets allow greater intervertebral deflection.

Hypothesis 7: sacra are the main keystone in sauropod axial skeleton geometry, its angulation a reliable indicator for hind/forelimb proportions.

To test these hypotheses, the following objectives have been carried out:

Objective 1: Obtain virtual skeletons of sauropod specimens representing all major well-established clades, digitizing their bones to minimize errors between the models and the fossil counterparts.

Objective 2: Evaluate osteological range of motion on the virtual skeletons.

Objective 3: Estimate mass, volume, and lines of action of the main muscle groups using the Extant Phylogenetic Bracketing (EPB) on virtual skeletons.

Objective 4: Compare the results from previous objective ontogenetically (where possible) and phylogenetically.

BLOCK 2: Evolution of Sauropoda body plan and biomechanics

Hypothesis 1: a wedged sacrum is only present in sauropods with long forelimbs.

Hypothesis 2: some appendicular and axial osteological characters evolved as a functional module early in sauropod evolution, resulting in an enlargement on the vertical component of the feeding envelope.

Hypothesis 3: the caudofemoral musculature function shifts from the primitive femoral retractor to derived femur adductor in sauropods with wide gauge stance.

Hypothesis 4: the reduction of the osteological correlates for the origin of the caudofemoral musculature is related with the appearance of wide gauge stance and walking.

Hypothesis 5: characters with strong functional implications on the same functional module derived at different rates, in a stepwise mosaic-evolution.

To test these hypotheses, the following objectives have been carried out:

Objective 1: To look for osteological correlates for functional capabilities (in the literature as well as new characters) which will allow inferring functional morphology in taxa known from less complete remains.

Objective 2: To determine to which degree the different character states affect their particular function/s.

Objective 3: Modify an already published sauropod phylogenetic data matrix to incorporate all the taxa studied and the new characters.

Objective 4: Create a second matrix with only the functional characters established in Objective 2 to perform a cluster analysis to find potential functional modules.

BLOCK 3: Ecology of "Lo Hueco" titanosaurs from biomechanical evidence

Hypothesis 1: The Lo Hueco fossil site includes at least 3 titanosaur sauropod morphotypes with a great degree of neck/trunk/tail and forelimb/hindlimb proportions.

Hypothesis 2: The different morphotypes of Lo Hueco titanosaurs have marked differences on their locomotor dynamics.

Hypothesis 3: Morphotypes of Lo Hueco titanosaurs with dermal armor have osteological characteristics which sets them apart from unarmored morphotypes.

Hypothesis 4: Given the dorsal armor acts as a limit to range of motion, morphotypes of Lo Hueco titanosaurs with dermal armor would have a greater range of motion (without the armor) than unarmored morphotypes.

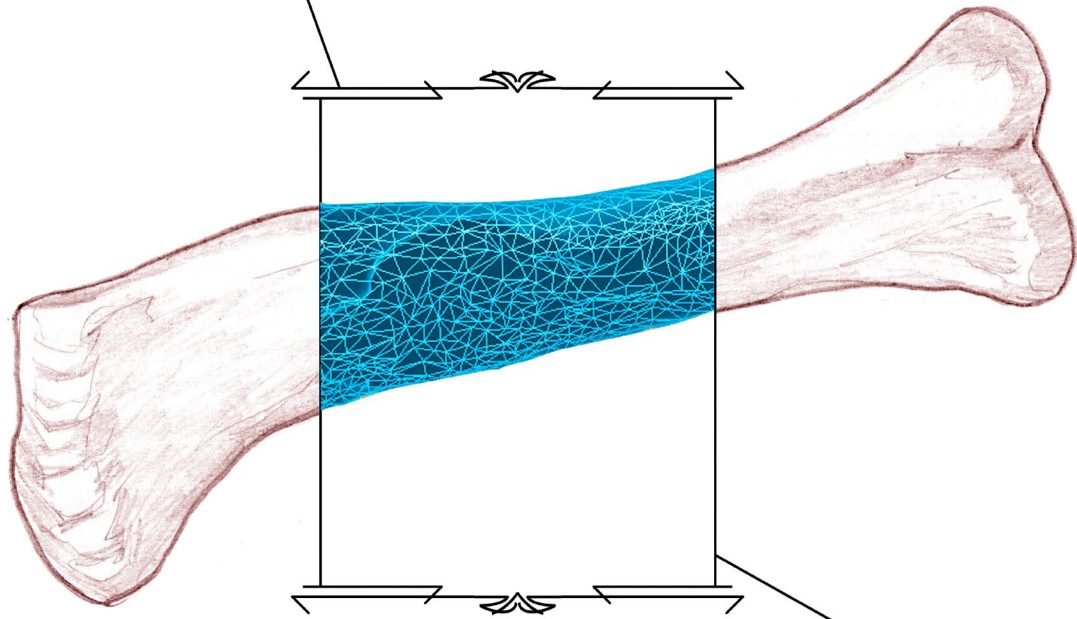
To test these hypotheses, the following objectives have been carried out:

Objective 1: To compare the functional analyses in the available skeletons of titanosaurs from Lo Hueco with previous paleoneurological, morphometric and odontological analyses.

Objective 2: To establish a correspondence between previously established morphotypes/taxa and functional capabilities.

1.8 INSTITUTIONAL ABBREVIATIONS

AMNH (American Museum of Natural History - New York, USA), **BYU** (Bingham Young University - Provo, Utah, USA), **CM** (Carnegie Museum of Natural History - Pittsburgh, Pennsylvania, USA), **CMNH** (Cleveland Museum of Natural History - Cleveland, Ohio, USA), **DINO** (Dinosaur National Monument - Vernal, Utah, USA), **DMNH** (Denver Museum of Natural History - Denver, Colorado, USA), **FCPT-D** (Fundación Conjunto Paleontológico de Teruel, Dinópolis - Teruel, Aragón, Spain), **FMNH** (Field Museum of Natural History - Chicago, Illinois, USA), **GCP-CV** (Grupo Cultural Paleontológico de Elche, Fundación Cidarís - Elche, Alicante, Spain), **GPIT** (Institut für Geowissenschaften, Eberhardt–Karls–Universität Tübingen - Tübingen, Germany) **IVPP** (Institute of Paleontology and Paleoanthropology - Beijing, China), **MACN** (Museo Argentino de Ciencias Naturales - Buenos Aires, Argentina), **MAU** (Museo Municipal Argentino Urquiza - Rincón de los Sauces, Neuquén, Argentina), **MB** (Humboldt Museum für Naturkunde - Berlin, Germany), **MCF** (Museo Municipal Carmen Funes - Plaza Huinacul, Neuquén, Argentina), **MCS** (Museo Municipal de Cinco Saltos - Cinco Saltos, Río Negro, Argentina), **ML** (Museu da Lourinhã - Lourinhã, Portugal), **MNN** (Musée National du Niger Boubou Hama - Niamey, Niger), **MPCA** (Museo Provincial Carlos Ameghino - Cipolletti, Río Negro, Argentina), **MPEF** (Museo Paleontológico Egidio Feruglio - Trelew, Chubut, Argentina), **MOR** (Museum Of the Rockies - Bozeman, USA), **MUCP** (Museo de la Universidad Nacional del Comahue - Neuquén, Argentina), **MUPA** (Museo Paleontológico de Castilla-La Mancha - Cuenca, Castilla-La Mancha, Spain), **MMCH** (Museo Municipal Ernesto Bachmann - El Chocón, Neuquén, Argentina), **MNCN** (Museo Nacional de Ciencias Naturales - Madrid, Spain), **OMNH** (Sam Noble Oklahoma Museum of Natural History - Norman, Oklahoma, USA), **OUMNH** (Oxford University Museum of Natural History - Oxford, England, UK), **PVL** (Fundación Miguel Lillo, Universidad Nacional de Tucumán - San Miguel de Tucumán, Tucumán, Argentina), **SMNS** (Stuttgart Museum für Naturkunde - Stuttgart, Germany), **USNM** (Smithsonian Institution National Museum of Natural History - Washington D.C., USA), **YPM** (Yale Peabody Museum of Natural History - Yale University, New Haven, Connecticut, USA), **ZDM** (Zigong Dinosaur Museum - Zigong, Sichuan, China).



CHAPTER
• 2 •

MATERIAL AND METHODS

Introduction.....	33
Material.....	35
Terminology.....	36
Methods.....	41

2.1 INTRODUCTION

Extinct vertebrate skeletal mounts have been assembled early in History, as soon as complete fossil skeletons were unearthed. The first fossil skeletal mount ever erected was that of *Megatherium americanum*, after the studies of Juan Bautista Bru in 1789 (López Piñero 1988; Chapter 1). Dinosaur skeletal mounts arrived almost a century after, with the publication of *Hadrosaurus foulki* in 1858 and the skeletal mount conceived by Joseph Leidy and Benjamin Waterhouse Hawkins in 1868. However, it was the skeletal mount and casts of *Diplodocus carnegii* distributed worldwide by Andrew Carnegie (Holland 1910) when dinosaur skeletal mounts began to include a very high percentage of known skeletal elements from the same species.

Dinosaur skeletal mounts are key to some research areas, specifically biomechanics, where studies on locomotion (Hutchinson and Garcia 2002; Hutchinson et al. 2005; Mallison 2010a; Reiss and Mallison 2014), body weight (Mallison 2010a; Hutchinson et al. 2011; Bates et al. 2016), feeding strategies (Stevens and Parrish 1999; Stevens 2013) or functional morphology (Xing et al. 2009; Mallison 2010b, 2011) depend on a precise knowledge of the skeletal proportions and their spatial arrangement.

Dinosaur fossil skeletons rarely are found complete. Sauropod dinosaurs particularly have a great preservational bias against their bones due their large sizes and fragility, as most of the skeleton was pneumatized (Wedel 2003a, 2003b). The majority of sauropod skeletal mounts are composites of multiple

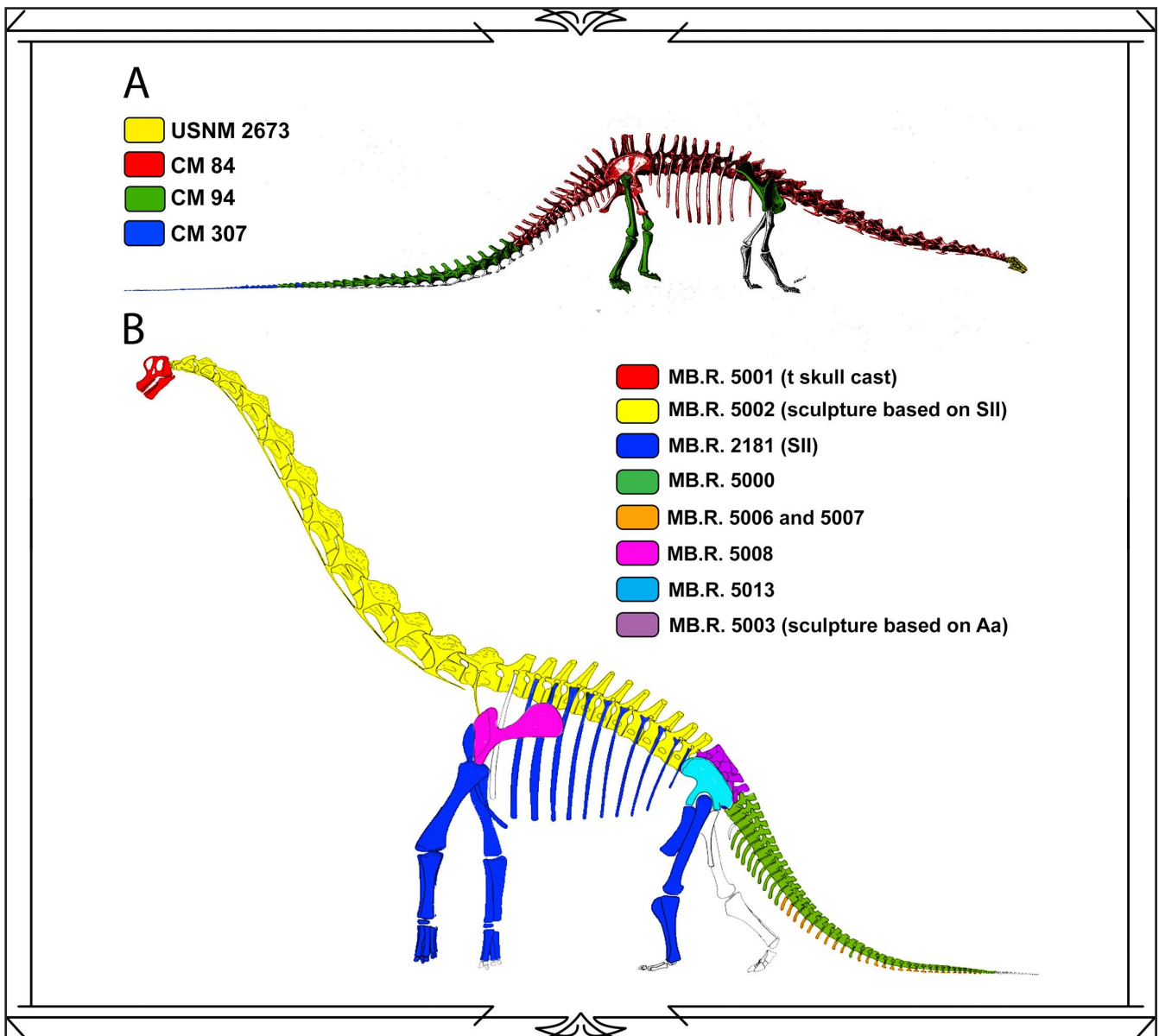


Figure 2.1 - Classical skeleton mounts of sauropod dinosaurs.

A - *Diplodocus carnegii* restoration from the mount at Carnegie Museum of Natural History (Pittsburg, USA) modified from (Hatcher, 1901). **B** - *Giraffatitan brancai* reconstruction from the mount at Museum für Naturkunde (Berlin, Germany) modified from (Janensch, 1950). The different colored bones belong to different individuals.

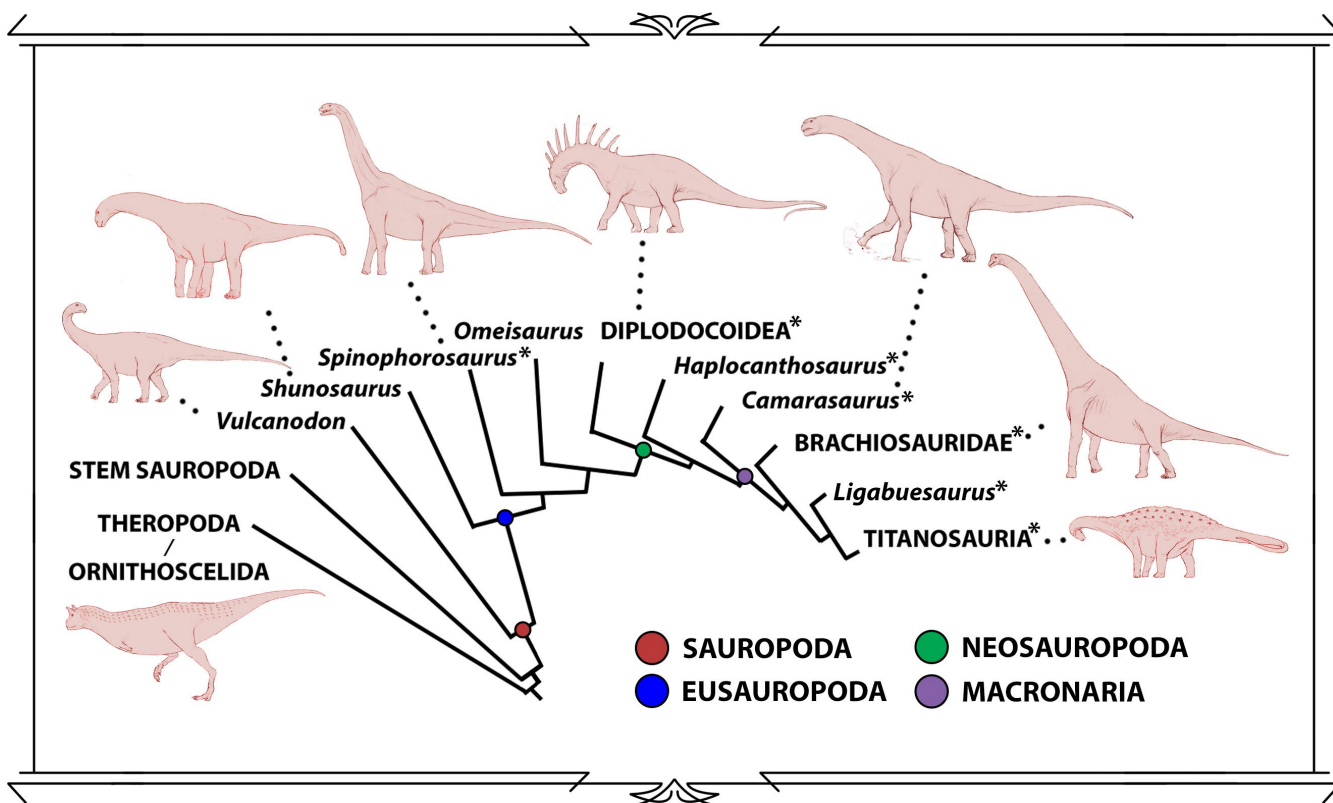


Figure 2.2 - Simplified phylogeny of sauropod dinosaurs modified from Wilson & Sereno (1998) with taxa studied with virtual paleontology techniques on this thesis highlighted with an asterisk (*).

Dinosaur reconstructions by Diego Cobo.

specimens or incorporate some sculpted elements based upon real fossils or closely related species (Fig. 2.1). Traditionally, overlapping specimens of similar sizes (Hatcher 1901; Fig. 2.1 A) or scaled-up or down specimens of different sizes (Janensch 1950; Fig. 2.1 B) were used to create the mounts. However, many taxa are known from multi-specimen bonebeds with a high size disparity. Thus, the skeletal proportions of such taxa have been known only through rigorous skeletal drawings (Paul and Chase 1989).

Recent years have seen tremendous advances concerning Virtual Paleontology. As defined by Sutton et al. (2014), "Virtual Paleontology is the study of fossils through interactive digital visualizations, or virtual fossils. This approach involves the use of cutting edge imaging and computer technologies (...)", e.g. computer-aided scanning and digitization techniques, digital visualization and computational analyses (see Lautenschlager, 2016; and references therein). As stated by Mallison and Wings (2014) these virtual fossils or "models allow archiving, analyzing, and visualizing specimens that would otherwise be difficult or impossible to access, and can protect delicate specimens from handling". In addition, "X-ray computed tomography (CT) and digital visualization can facilitate the non-destructive extraction of fossil specimens from rocks or the reconstruction of soft-tissue structures from fossils" (Lautenschlager, 2016; and references herein).

Thanks to Virtual Paleontology, numerous research areas can overcome many of the disadvantages of physical methods, and benefit from the use of three-dimensional digitization of specimens, like geometric morphometric and finite-element analyses (e.g. Arbour & Currie 2012), virtual dissection and sectioning (e.g. Klinkhamer et al. 2017), studying the inner cavities of bones (Witmer & Ridgely, 2008), ichnology (e.g. Breithaupt et al. 2004) and biomechanics (Sellers *et al.*, 2013; Bates *et al.*, 2016; Klinkhamer *et al.*, 2018, 2019). Given all the currently available virtual paleontology resources and tools, generating virtual skeletal reconstructions comes at once with lots of advantages and caveats. The principal advantages are the possibilities of mounting a skeleton as many times as needed in a safe environment for the original fossils, fixing taphonomic deformation of elements or filling missing elements scaling up or down differently sized specimens. The main caveat, however, resides in generating reconstructions too far-fetched or even forged, as has happened with physical skeletal mounts.

To assure the virtual skeletons of this thesis cope with the best possible standards, a thorough methodology to elaborate a 3D reconstruction of a fossil sauropod skeleton is elaborated upon, both using a nearly complete specimen and elaborating a composite skeleton using different sized specimens.

2.2 MATERIAL

The experimentation subjects for this thesis were virtual skeletons of sauropod dinosaurs including representatives of most presently known clades (Fig. 2.2), obtained by performing surface scans on the actual preserved fossils. The raw scans of the fossils were digitally prepared following a protocol described in 2.4 (Methods). The main skeletons digitized are summarized in Table 2.1. However, many additional partial skeletons were digitized and used for comparative purposes (summarized on Table S1).

In order to compare the results of neck range of motion analyses with an extant, long-necked analogue, two skeletons of *Giraffa camelopardalis* were borrowed from two different institutions: a complete CT-scanned newborn specimen (TMM M-16050) from Morphosource.org by Duke University and a complete neck and the first thoracic vertebra of an adult specimen (no number AMNH, courtesy of Kent Stevens).

Also, the neck and skull of *Carnotaurus sastrei* MACN-CH-894 (also digitized using photogrammetry) and high resolution 3D meshes of *Tyrannosaurus rex* MOR-555 and *Plateosaurus engelhardti* GPIT-1 publicly available (courtesy by the Smithsonian Institution and the University of Tübingen respectively) were used for outgroup comparison purposes.

Taxon	Specimen(s)	Clade	Age	n° digitized bones
<i>Spinophorosaurus</i>	GCP-CV-4229 GCP-CV-BB NMB-1968-R	Eusauropoda	Baj-Bath ?	134
<i>Patagosaurus</i>	PVL 4017 MACN-CH-935 MACN-CH-936 MACN-CH-1192	Eusauropoda	Toa-Baj	53
<i>Haplocanthosaurus</i>	CM 572 CM 789	Eusauropoda	Kim_Tit	85
Rebbachisauridae indet.	MMCh-PV-49	Rebbachisauridae	Cen	26
<i>Amargasaurus</i>	MACN-N-15	Dicraeosauridae	Bar	36
<i>Brachytrachelopan</i>	MPEF-PV-1716	Dicraeosauridae	Oxf-Tit	21
<i>Camarasaurus</i>	AMNH 5761 YPM 1901 YPM 1905 CM 11338 CM 584	Macronaria	Kim-Tit	442
<i>Brachiosaurus</i>	FMNH-P-25107	Titanosauriformes	Kim	14
<i>Tastavinsaurus</i>	FCPT-D-MPZ-99/9	Titanosauriformes	Bar	74
<i>Ligabuesaurus</i>	MCF-PVPH-233 MCF-PVPH-261	Somphospondily	Apt-Alb	32
<i>Epachthosaurus</i>	UNPSJB-PV-920	Titanosauria	Cen-Tur	77
<i>Overosaurus</i>	MAU-Pv-CO-439	Aeolosaurini	Cam	48
<i>Neuquensaurus</i>	MCS-5	Saltasaurini	Cam-Maa	37

Table 2.1 - The principal sauropod dinosaurs studied on this thesis with virtual paleontology.

Taxa ordered according to the least inclusive clade they belong to. Colors according to the International Commission of Stratigraphy for the Mesozoic (Cohen *et al.*, 2013): Dark Blue = Middle Jurassic. Light Blue = Upper Jurassic. Dark Green = Lower Cretaceous. Light Green = Upper Cretaceous.

2.3 TERMINOLOGY

The terminology of this thesis follows that of previous authors, although some minor adjustments have been made to narrow the precision of the terms employed. The implications of the different definitions given to some terms are further discussed in order to remain as precise as possible:

Browsing height: there have been four categories described for interpreting the height at which sauropod dinosaurs fed, namely:

Ground-level browsing: feeding at ground level (Serenio *et al.*, 2007).

Low browsing: feeding with the head below shoulder height / cervicodorsal transition height (Christian *et al.*, 2013).

Medium-height browsing: feeding with the head kept between shoulder height and half neck length above the shoulders, about 30° (Christian *et al.*, 2013).

High browsing: feeding with the neck more inclined than 30° (Christian *et al.*, 2013).

Comment: Most of these categories have quite arbitrary limits, and most are not mutually exclusive, since a high browser (e.g. *Giraffa*) can browse lower than its shoulder height. These terms refer to the capabilities of an organism, not to their actual role in an ecosystem (a small sized organism may be able to browse with the neck more inclined more than 30° but won't physically reach the higher vegetation canopy). Therefore, these terms should be used as descriptive on the physical capabilities of fossil organisms rather than on their behavior or ecological role.

Cartilaginous Neutral Pose (CNP): the term was coined by Taylor (2014) for “the pose found when intervertebral cartilage [that separates the centra of adjacent vertebrae] is included”. Since the amount of inter-vertebral space cannot be certainly known for most fossil vertebrate taxa, true CNP will likely remain unknown for most taxa or always based on estimates.

Cervicalization: the term is usually employed as the incorporation of dorsal vertebrae into the neck (Mateus, Maidment, & Christiansen, 2009) while maintaining the same number of presacral vertebrae as ancestors without cervicalized dorsals. **The first dorsal vertebra acquires the characters of a cervical vertebra** (i.e. centra as long as tall or longer than tall, prezygapophyses projected anteriorly to the anterior face of the centrum, longer prezygapophyseal facets). Those characters enable it to become functionally part of the neck. Cervicalization is a complex process with several homeotic genes involved, and not all the characters may appear at once (Gunji & Endo, 2016). Therefore, when anteriormost dorsal vertebrae have both cervical and dorsal characters in mosaic fashion, the term **partial cervicalization** is employed herein.

Elongation Index (EI): it was devised by Upchurch (1995) as a way to quantify the elongation of a vertebral centrum, “the length of a vertebral centrum divided by the width across its caudal face”. Wilson & Sereno (1998) used the height of the centrum instead of the width, and Wedel, Cifelli, & Sanders (2000a,b) used the latter definition with the former name “elongation index”. Since taphonomic deformation can drastically alter the shape of a vertebral centrum, using width or height may render different values for the same vertebra, Chure *et al.* (2010) coined “aEI” to the “scale [of] centrum length to the average of centrum height and width (aEI) to avoid confusing changes in centrum elongation with those in cross-sectional shape as well as to account for deformation”, which is the index followed in this publication.

Evolutionary Innovation vs Evolutionary novelty: Erwin (2015, 2017) differentiates evolutionary innovation from evolutionary novelty. An evolutionary novelty is when a newly individuated character or feature of an organism not present in an ancestral species appears but does not necessarily have an impact in diversity or disparity of the lineage on which it appears. An evolutionary innovation is when whether a newly individuated character appears or a previously present feature derives into a new character state and it has a noticeable impact of the diversity or disparity of the lineage.

Neutral Bone Only Posture (NBOP): Paul (2017) coined this term for the definition of “neutral deflection” given by Stevens & Parrish (2005), including zygapophyseal alignment and vertebral centra alignment criteria (contra ONP, which would only account for the zygapophyseal alignment criterion, see below). The definition of Steven and Parrish is exhaustive and complete: “Posture of an intervertebral joint defined by the full articulation of the zygapophyseal facets, with platycoelous

vertebral centra surfaces or the rims of cotyle-condyle (procoelous or opisthocoelous) articulations parallel". ONP may or may not coincide with NBOP (Fig 2.3 A,B).

Osteologically Induced Curvature (OIC): Stevens (2013) defines it as "the curvature of a vertebral column in ONP, as distinguished from curvature induced by joint deflection".

Osteologically Neutral Pose (ONP):

General definition: Maximum alignment of articular surfaces.

Synonyms: neutral pose (Stevens & Parrish, 1999), neutral deflection (Stevens, 2002; Stevens & Parrish, 2005), zygapophyseal alignment (Christian & Dzemski, 2007), optimal fit, best fit (Christian *et al.*, 2013) neutral articulation (Paul, 2017).

Specific definitions: This term is common in literature from the last decades to present, and seeks to find the pose achieved by the maximum osteological articulation of a skeleton. However, the precise definitions vary slightly depending upon the anatomical region referred (axial and appendicular definitions necessarily vary) and sometimes authors have given slightly different definitions and different names to the same concept, rendering its usage a bit imprecise. Despite this, there appears to be an underlying consensus about its usage as the maximum overlap of articular surfaces. More specific and exhaustive definitions for the different types of bones can be given after reviewing previous works:

Intervertebral ONP: Stevens and Parrish first used the concept just as "neutral pose" in their 1999 landmark paper, defining it as "wherein the paired articular facets of the postzygapophyses of each vertebra were centered over the facets of the prezygapophyses of its caudally adjacent counterparts" (Stevens & Parrish, 1999).

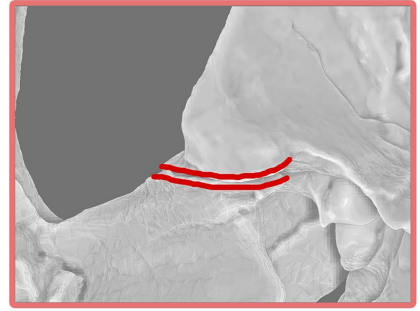
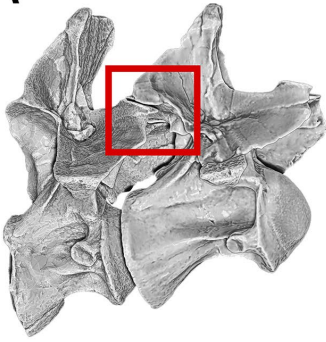
Their study centered on the axial skeleton and the zygapophyseal facets in particular, and therefore this first definition was in accordance with the variables that these authors explored. Nevertheless, it is the most extensively used definition for osteological neutral pose of the axial skeleton, with the same general concept used a few years later by Stevens: (as neutral deflection) "the zygapophyses [were] centered post above prezygapophyses" (Stevens, 2002) and (as osteological neutral pose) "centering the associated pre- and postzygapophyses" (Stevens, 2013). Other authors have also used the maximum zygapophyseal facets overlap as the criterion defining ONP. Dzemski & Christian (2007) positioned "the centres of the facets of the postzygapophyses above the centres of the prezygapophyses of the caudally adjacent vertebrae" in extant vertebrates. Taylor, Wedel, & Naish (2009) used "maximum overlap between the zygapophyses", as well as Mallison (2010a,b) "maximal overlap of the zygapophyses".

Some authors have also implemented different criteria of the vertebral centra in their definitions of ONP as well as the maximum overlap of the zygapophyses. Christian *et al.* (2013) considered ONP "bringing post and prezygapophyses of adjacent vertebrae into contact, so that the joint between the centra was articulated and the joint facets of pre and postzygapophyses were centered above each other". Stevens & Parrish (2005) used a more precise criterion for the articulation of centra, coining neutral deflection as "defined geometrically by the alignment of the zygapophyses and by nulling the deflection at the central articulation. Pre and postzygapophyses are centered within their range of dorsoventral travel when the two vertebrae are in their undeflected state. Simultaneously, the central facets will be in a neutral or undeflected state. For platycoelous vertebrae, the two planar articular surfaces are parallel when undeflected. Determining neutral position for opisthocoelous vertebrae requires closer scrutiny of the margins of the central articulation. The synovial capsule surrounding the condyle-cotyle exhibits circumferential attachment scars. These ridges are parallel when the joint is undeflected".

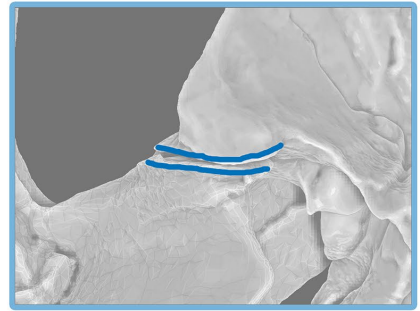
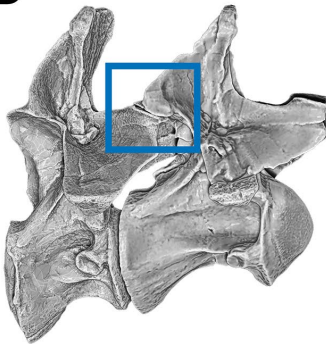
Carabajal, Carballido, & Currie (2014) used the same concept in their work, "when the zygapophyses of successive vertebrae are aligned and the deflection at the central articulation is minimal". Paul (2017) would coin the term "Neutral Bone Only Posture" for the pose in which "the zygapophyses are in full, 100% overlapping articulation and the centra rims are parallel to one another".

There is an important caveat when trying to align the zygapophyses and set the centra rims parallel when using physical or virtual three dimensional vertebrae, which has been

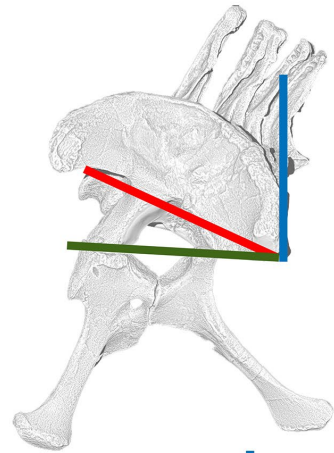
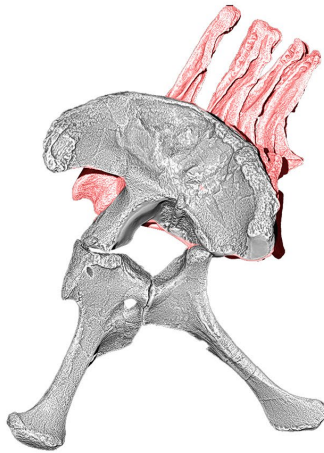
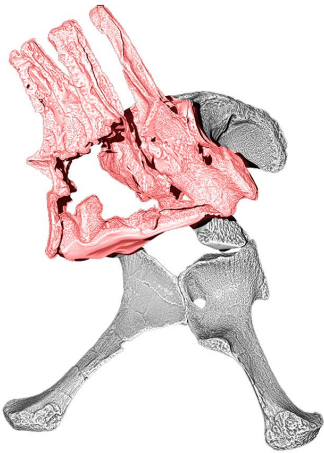
A



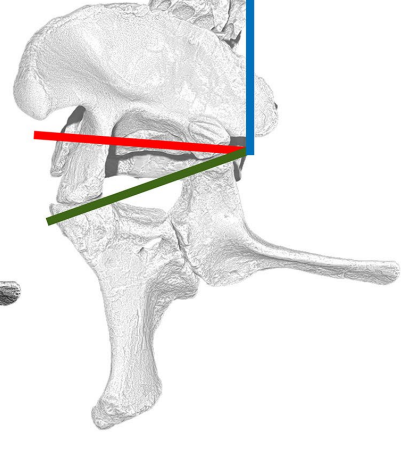
B



C



D



encountered through this work with opisthocoelous sauropod dinosaurs (Fig. 2.3 A) as well as with platycoelous modern human vertebrae (Riesco, García-Martínez, & Bastir, 2018). When the zygapophyses are in 100% overlap (in all three dimensions, lateral-medial, antero-posterior and dorso-ventral planes) the centra rims are not parallel in most cases (Fig. 2.3 B). Studies on intervertebral cartilage have revealed that its thickness may vary between different species, between individuals of the same species, particularly thorough ontogeny (Taylor & Wedel, 2013a) or even within a single individual, depending on the region of the axial skeleton (Taylor & Wedel, 2013a). The zygapophyseal capsules, however, are not thicker than a flat sheet covering (Taylor & Wedel, 2013a), albeit enlarging the actual area of the articular facet outline, see below Range of Motion (Taylor, 2014).

The preferred usage of the term ONP should refer only to the zygapophyseal joints, given (i) the discrepancy between zygapophyseal and centra alignments which sometimes makes impossible to align both at once, (ii) the more widespread use of the maximal zygapophyseal overlap criterion alone without the parallel centra criterion, and (iii) the fact that intervertebral soft tissue thickness is more variable than zygapophyseal capsule thickness. The term “Neutral Bone Only Posture” coined by Paul should be used to include the centra rim criterion.

Therefore, we propose the following definition for axial skeleton ONP in order to summarize exhaustively all previous definitions: *Posture of an intervertebral joint defined by the full articulation of the zygapophyseal facets, with complete overlap of the facet surfaces in all three anatomical planes (antero-posterior, lateral-medial, dorso-ventral; Fig 2.3 A).*

Appendicular joints ONP: The only definition stems from Reiss and Mallison’s work on the hand of *Plateosaurus*, where they defined it as “*the position in which the long axes of two bones articulating with each other are approximately parallel to each other in lateral view*”. (Reiss & Mallison, 2014)

Finally, osteologically neutral pose should be always taken explicitly as a consensual “standard” for comparing the intrinsic deflection of joints between different specimens and subsequent biomechanical analyses. Using the same “standard” starting point, independent results from different researchers working on different specimens are therefore more easily comparable than when different starting points are used. However, the pitfall of taking morphofunctional and/or behavioral conclusions out of ONP alone must be avoided. ONP can be the source for morphofunctional and/or behavioral hypotheses that will have to be tested with additional evidence, but not the sole criterion for drawing conclusions on paleobiological hypotheses.

Osteological Stops: Stevens (2013) defines them as “*contact between vertebrae that limits angular deflection at a vertebral joint and provides load-bearing bracing against disarticulation*”. The term can be used in a broader sense for *any bone to bone contact which prevents further displacement of any given bone in the direction in which both bones collide*. The osteological stop may coincide with an *in vivo* stop (when soft tissue in the area of bone-bone contact would not be very extensive) or, more likely, may indicate that *in vivo*, extensive soft tissues might have stopped motion way before bones might have contacted.

Retroverted pelvis: This term was coined by Paul (1998) to describe a phenomenon first reported in the pelvis of *Cathetosaurus lewisii* (Jensen, 1988), and later found to be widespread among other camarasaurids. This condition was described by Jensen as “*Iliac rotated around a transverse acetabular axis, lowering the anterior iliac processes approximately 0-20 degrees, ventrally, below the axis of the vertebral column*” (Jensen, 1988). He also suggested it conferred *Cathetosaurus* mechanical advantages for bipedality. McIntosh et al (McIntosh et al., 1996) would later refer to this condition as “*the longitudinal axis of the ilium has been rotated counterclockwise by about 20°*”

Figure 2.3 (previous page) - Terminology 1

A - 3D model of first dorsal and last cervical vertebrae of *Spinophorosaurus nigerensis* in Osteological Neutral Pose (ONP, lateral view), showing the full zygapophyseal overlap in detail. Notice the central rims are not completely parallel. **B** - First dorsal and last cervical vertebrae of *S. nigerensis* in Neutral Bone Only Posture (NBOP, lateral view). Notice how despite the central rims being parallel, the zygapophyses are not in 100% overlap as when they are in ONP. **C** - 3D model of sacrum and pelvis of *Diplodocus carnegii* (CM 94) right lateral and left lateral views (left and middle). **D** - 3D model of sacrum and pelvis of *Camarasaurus supremus* (AMNH 5761) in right lateral and left lateral views (left and middle). Notice how despite both having wedged sacra, the pelvis of *Diplodocus* is not retroverted, whereas the pelvis of *Camarasaurus* is. For C and D: blue = last sacral centra at 90°; red = sacricostal yoke; green: plane defined by ischial and pubic peduncles of the ilium. Fossils not to scale.

about a transverse axis through the acetabulum” and suggest that not only other *Camarasaurus* specimens, but also other sauropods might have a similar condition.

Paul coined the term retroverted pelvis/hips (Paul, 1998) citing Jensen (1988) for the definition and used it in subsequent works, giving a new, different take redefining retroverted pelvis as “in which the dorsal series slopes dorsally relative to the horizontal axis of the entire pelvis” and adding “in some sauropods such as brachiosaurs pelvic retroversion results in the dorsal series sloping strongly up and forwards while the pelvis and tail remain horizontal relative to the ground, in other sauropods such as camarasaurus the dorsal-sacral-caudal series remains horizontal to the ground while the pelvis is rotated relative to the latter” (Paul, 2017).

This latter redefinition of the term incorporates the wedging of the sacrum and its influence on the geometry of the axial skeleton. However, pelvic retroversion is a condition caused by the morphology of the ilia (particularly the pubic pedicle and the angle it forms with the antero-posterior axis of the ilium blade) and the orientation of the sacricostal yoke, independent from the wedging of the sacral vertebrae (Fig. 2.3 C, D). Therefore, we think the definition of “retroverted pelvis” is a character independent from the wedging of the sacrum, and it should specifically refer to the condition originally reported by Jensen and McIntosh: Anteroventral rotation of about 20° of the ilium respect to the antero-posterior axis of the sacral vertebrae centra (Fig. 2.3D contra Fig. 2.3C).

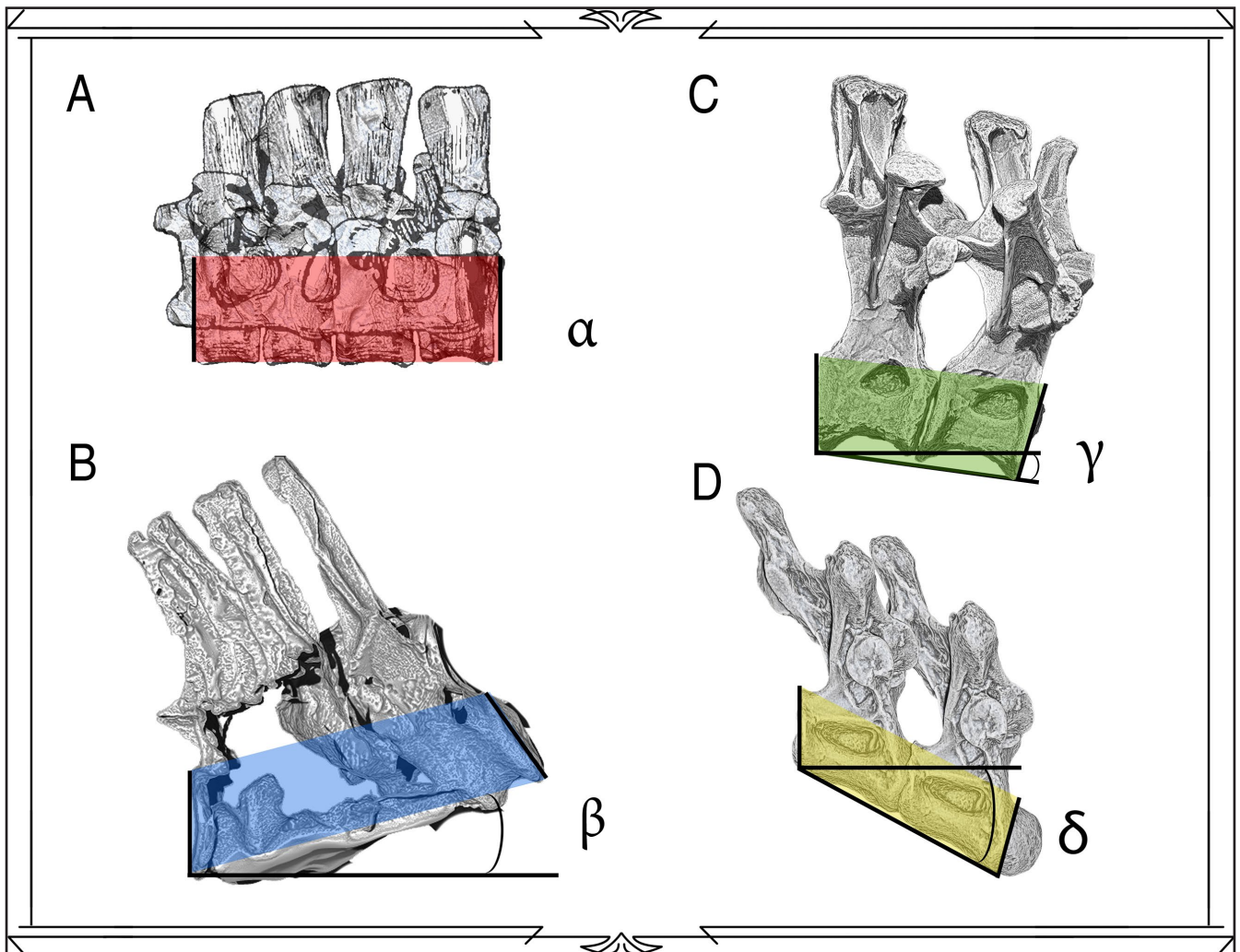


Figure 2.4 - Terminology 2.

A - Sacrum of *Kotasaurus* 26/S1Y/76 in left view, showing no wedging at all. **B** - 3D model of sacrum from *Diplodocus carnegii* (CM 94) in right view, showing acute wedging (when the adjacent vertebrae form an acute angle). **C** - 3D model of two middle dorsal vertebrae of *Haplocanthosaurus priscus* (CM 572) in right view, showing obtuse wedging. **D** - 3D model of two middle dorsal vertebrae of *Neuquensaurus australis* (MCS-5) in right view, showing obtuse wedging due to the trapezoidal shape of the centra. Fossils not to scale.

Wedged Vertebrae: The term describes *marked trapezoidal shape in the centrum of a platycoelous vertebrae in lateral view or in the rims of a condyle-cotyle (procoelous or opisthocoelous) centrum type*. If the wedging makes the ventral rim of the centrum longer than the dorsal rim, the adjacent vertebrae will form an acute angle with it in ONP (Fig. 2.4 B), while a wedging with the ventral rim of the centrum shorter than the dorsal rim will create an obtuse angle between the adjacent vertebrae in ONP (Fig. 2.4 C,D)

2.4 METHODS

In order to generate a virtual skeleton suitable for scientific use, that is, repeatable and refutable, a series of steps were carried out (Fig. 2.5).

STEP 1: digitizing the fossils

Scanning. The majority of dinosaur skeletons digitized for this thesis were scanned by means of photogrammetry. This technique consists basically in taking a series of overlapping pictures surrounding the specimen (Fig. 2.6 A). Photogrammetry has been used to digitize both dinosaur bones and tracksites, and it is described in detail with very useful tips by Breithaupt, Matthews, & Noble, (2003), Matthews, Noble, & Breithaupt, (2006), Falkingham (2012) and Mallison & Wings (2014). The methodology employed follows mainly that published by Mallison and Wings (2014), because they use photogrammetry on fossil bones, and their methodology is focused on the software Agisoft Photoscan Professional (www.agisoft.ru), the one also used on this research. A few points will be commented to clarify the exact protocol followed for this study.

All pictures were taken with monochrome backgrounds (black most of the times) in order to mask them, making the processing faster in the computer. As one side of the specimen cannot be photographed (given the specimen is resting upon it while taking the first photo set), at least a second photo set had to be taken changing the resting side of the specimen so that the area not visible in the first set could be photographed, resulting in the full surface digitized. Photogrammetry is scale-less, so at least one physical scale was incorporated in each scan, so the model could be scaled *a posteriori* during the computer processing stages.

Once taken, the pictures were processed on the computer, in the software Agisoft Photoscan Professional 1.3 (www.agisoft.ru). The software finds homologous points between the overlapping pictures, creating a point cloud from which a 3D polygon mesh with photorealistic texture can be created (Fig. 2.6). The monochrome backgrounds were masked using the magic wand tool and the "Add Selection" option (Photo>Add Selection). In order to process the pictures, the "one chunk method" described by Mallison and Wings (2014) was carried out whenever possible. It consists of processing all the pictures taken (all photo sets) at once. Whenever it did not work out well, the "two chunk" method was employed. It consists of processing each photo set on a different chunk in Photoscan, aligning them separately in a posterior stage. This alignment can be done automatically through points or manually, placing at least three markers on landmarks on both sets. On either method, for the "Align Photos" stage (Workflow>Align Photos...) the accuracy was always set to high and pair preselection was set to generic. When the alignment under those settings was not satisfactory, pair preselection was disabled.

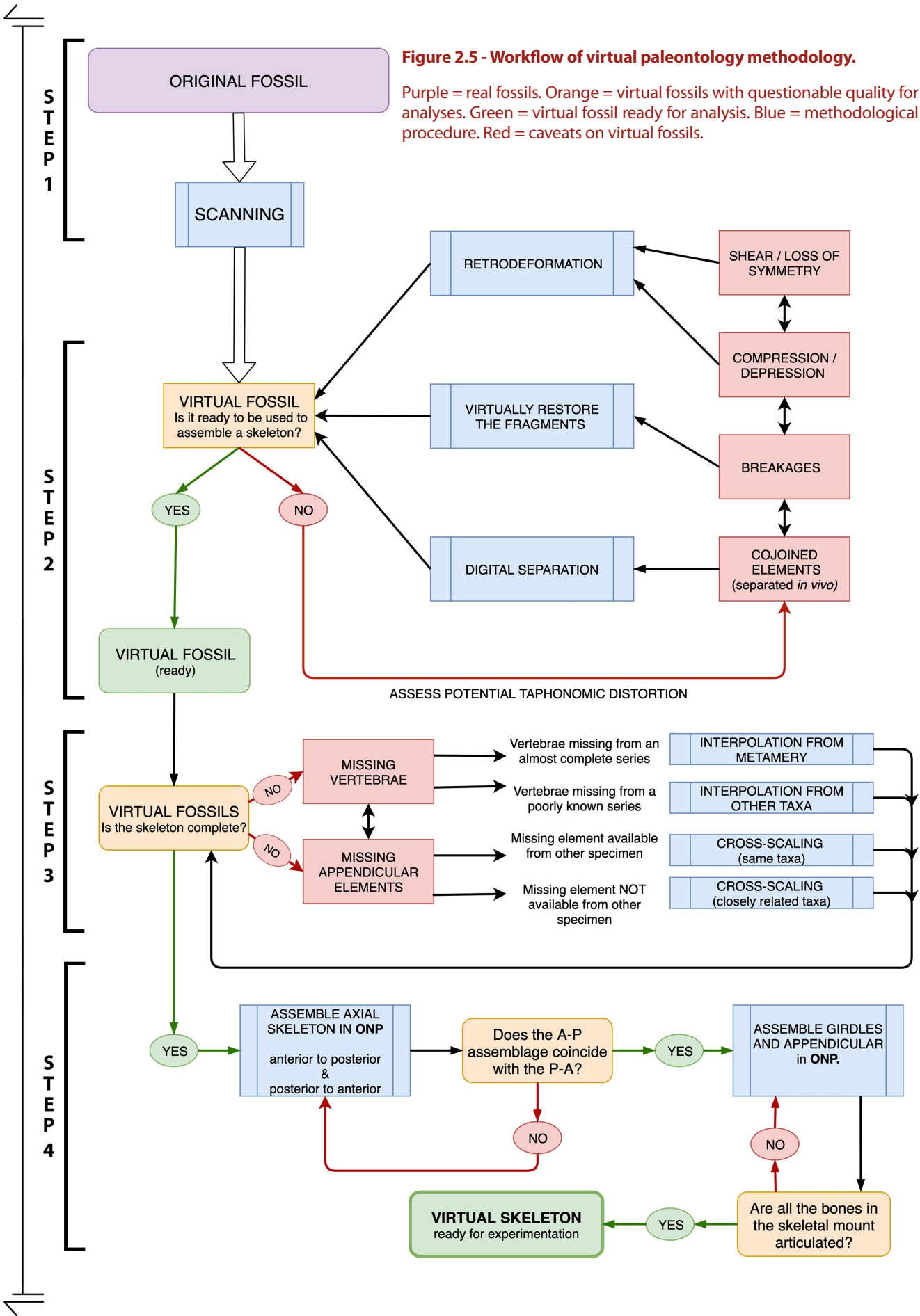
The sparse point cloud was cleaned up a bit using the free-form selection tool as well as with "Gradual selection" (Edit>Gradual Selection...), deleting at least a third of the original point number, making the dense cloud calculation much faster without losing resolution.

For the "Dense cloud" stage (Workflow>Dense Cloud...), accuracy was set mostly on Medium, but in some cases High was employed for a higher resolution. With masks, there are not many undesired points retrieved (points from the surroundings of the specimen, not part of the specimen itself, such as the scale bars) in the dense cloud. However, when such points were present, the free form selection tool was employed to delete them.

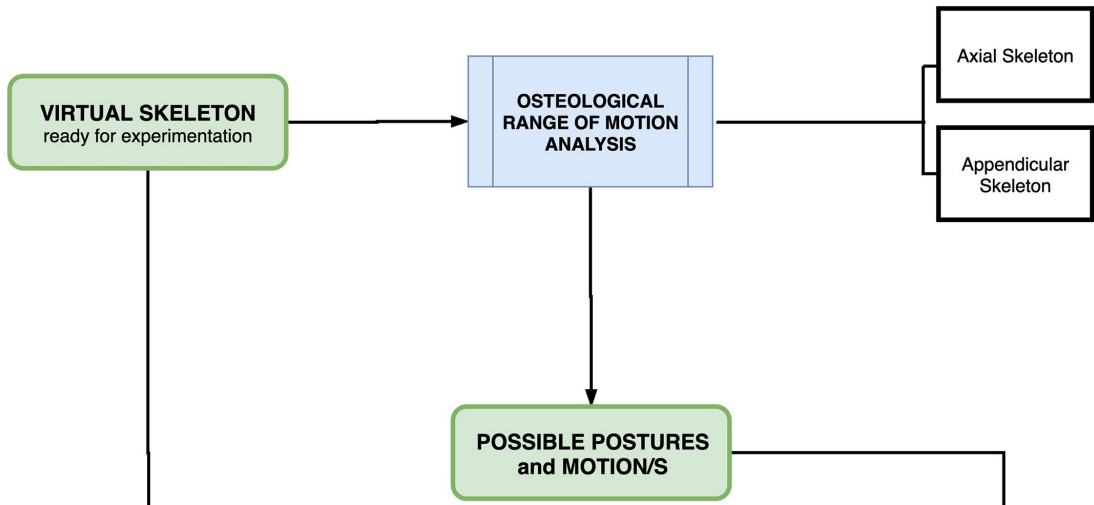
For the "Build mesh" stage (Workflow>Build Mesh...) a polygon count between half a million and million and a half was selected, depending on the complexity of geometry of the fossil (the more complex, the higher resolution the final mesh would have). When building the texture, default settings were employed. Right before the first stage of post-processing, if needed, a mesh decimation (reducing the number of polygons) was carried out (Tools>Mesh>Mesh Decimation).

Figure 2.5 - Workflow of virtual paleontology methodology.

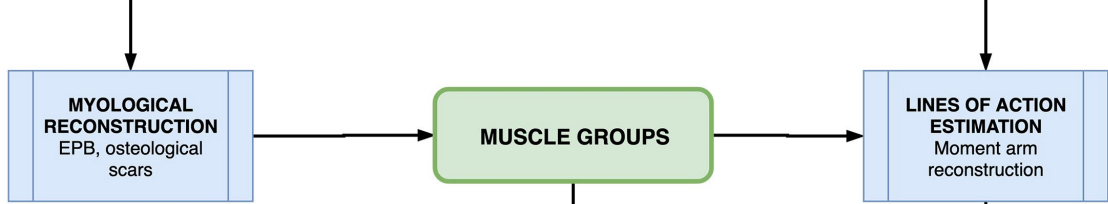
Purple = real fossils. Orange = virtual fossils with questionable quality for analyses. Green = virtual fossil ready for analysis. Blue = methodological procedure. Red = caveats on virtual fossils.



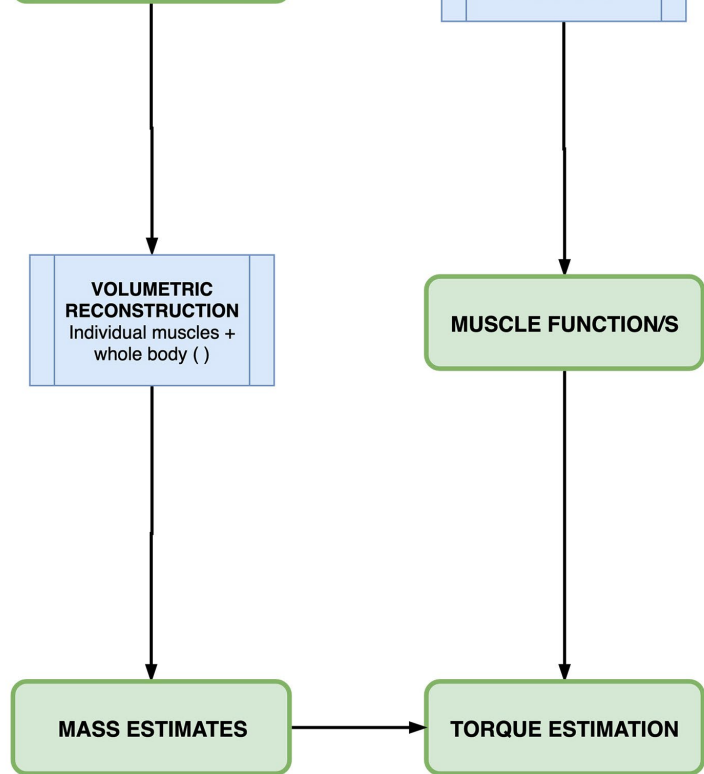
STEP 5



STEP 6



STEP 7



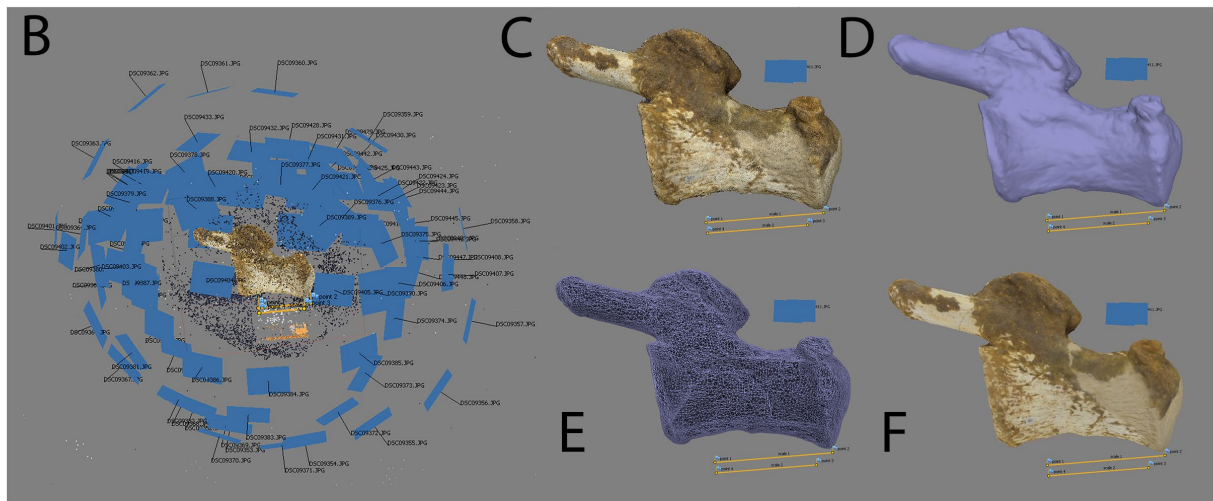
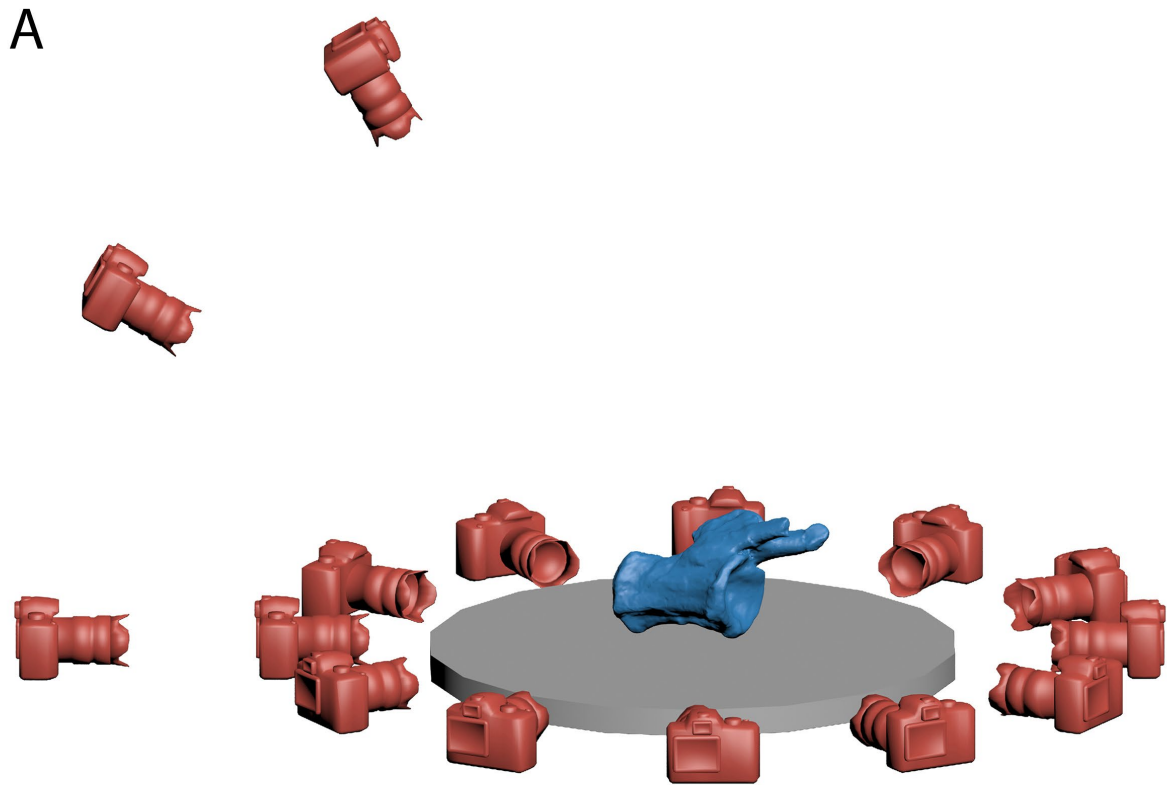


Figure 2.6 - Digitalization by photogrammetry.

A - Schematic photogrammetry protocol used to digitize the skeletons of all sauropods in this thesis, with *Lirainosaurus astibiae* middle caudal vertebra MCNA 1812 as example. **B** - Sparse point cloud of vertebrae MCNA 1812 as rendered by Agisoft Photoscan with the inferred position of the cameras (blue squares). **C** - Dense point cloud. **D** - Polygon mesh before decimation. **E** - Polygon mesh after decimation to 50.000 polygons. **F** - Polygon mesh with photorealistic texture.

For those bones collected in multiple good-fitting fragments not put back together after preparation when the scans were performed, a virtual alignment technique was devised for Photoscan. This technique consisted in digitizing the fragments while fitting them manually first, creating a rough 3D model termed “aligner” on a separate “chunk”. Then, separate 3D models of the different parts were digitized separately on different chunks. Finally, the alignment option from the software (Workflow>Align Chunks..) was used to align the separate fragments with the “aligner”. This way, fitting the different fragments together to create the complete bone would take less man-time (although it took a larger computation-time) and with a fraction of mm error in the alignments.

The resulting meshes were exported in OBJ format, scaled in millimeters as unit of measure to postprocess them.

STEP 2: post processing of virtual bones

Post-processing I - Retrodeformation. Taphonomic processes often result in both plastic deformation and/or breakages of bones. Quite often, a lot of anatomical information is lost due to these processes and, when just distorted, makes its interpretation difficult (Lautenschlager 2016). When considering biomechanics and range of motion analyses, taphonomic distortion can make articulation of specimens difficult or even impossible. Hence the need for retrodeforming some fossils.

Automatic retrodeformation landmark-based methods have been developed, in an attempt to minimize subjective interpretation of the process. These methods are mostly based on the principles of symmetry, using different algorithms in which landmark symmetry is used to retrodeform the mesh. However, the results obtained in experiments with manually deformed extant bones revealed automatic retrodeformation techniques retrieved different results for the same bone model, depending on the initial deformation condition (Tschopp et al., 2013). Thus, obtaining a reconstructed *in vivo* bone model from a fossil bone will always be a hypothesis, and not a definitive, established fact. Also, several problems may arise when applying landmark-based methods on fossil vertebrae:

- i) Fossils may break as an outcome of fossil diagenetic processes, rendering some landmarks useless.
- ii) Unlike skulls, vertebrae are completely metameric and, in many cases, part of a morphological cline without abrupt changes in shape.

Given that biomechanical range of motion analyses require articulating the bones and that landmark-based methods may produce different results depending on the type and amount of initial deformation, the resulting vertebrae may not fit together when articulating after retrodeformation.

Given these caveats, a different approach has been taken here. We propose following the same protocol for all fossils but taking into account the visible signs of deformation for their reconstruction, instead of applying the exact same criteria for all fossils, as the taphonomic processes that affected each fossil are unique (Cambra, 2006). This way, although retrodeformed models will remain hypotheses, they will be based upon the visible marks of the taphonomic processes and the morphology of preceding and following vertebrae on the series. Such retrodeformation has to be conducted manually, but based upon the most robust criteria available, in order to minimize subjective interpretation. The proposed retrodeformation criteria employed in reconstructing a vertebral series are the following, and all of them carried on Pixologic ZBrush 4R7 software (<http://pixologic.com>):

- 1) Use the least deformed element of the series as a starting point:
 - (i) Arrange the elements in their respective anatomical positions (see 2.4.4).
 - (ii) Determine which element of the series was the least deformed, that is, the more symmetrical, less compressed/depressed and fragmented vertebra.
 - (iii) This element will be the first to be retrodeformed, and will be the comparison point thereafter.
- 2) Restoring symmetry by applying plastic retrodeformation in the distorted axis whenever deformation was non-symmetrical using the "Transpose" brush with the "Move" mode (Fig. 2.7 A). Whenever using the "Transpose" brush, the axis of the brush was always placed perpendicular to the plane requiring deformation in order to avoid deforming accidentally the mesh in the other two axes. This was first applied on the comparison vertebra.
- 3) Fix non-plastic asymmetrical breakages and deformation (Fig. 2.7 B). In order to fix the breakage, all the bone but the broken area was masked using the brush "Mask". This way, only the broken region would be affected by further repositioning procedures. Then, the "Transpose" brush in "Move" and/or "Rotation" modes were employed to properly align the broken area into its original pre-breakage position. The following criteria are followed when restoring these breakages, from least to most speculative:
 - (i) Restore the breakage copying the counterlateral non-distorted/broken element.
 - (ii) If only one of the elements is present, restoration is based upon the same element on the closest, non-distorted homologous element on the vertebral series.
 - (iii) If the homologous element is missing and/or is distorted in the closest vertebrae but the

element has fracture lines, the element is restored by aligning the broken parts as it would be done physically, by separating and repositioning them virtually (Lautenschlager, 2016).

- 4) Fix Compression (lateral) and/or Depression (dorso-ventral) distortions. The amount of retrodeformation to be applied for these kinds of distortion is subject of controversy (Arbour & Currie, 2012; Tschopp *et al.*, 2013; Lautenschlager, 2016). Unlike plastic distortion in which the original symmetry of the bone is lost and thus the amount of distortion can be measured to a certain degree, compression and depression may be idiosyncratic to the original bones and just enhanced by taphonomic processes. Several criteria have been developed in order to apply the right amount of retrodeformation, such as the roundness of the orbit for skulls (Arbour & Currie, 2012). However, given that the vertebrae neural canal can vary in shape not just among species but within the same vertebral series as well (see Figs. 6 and 7 in Taylor, 2015)

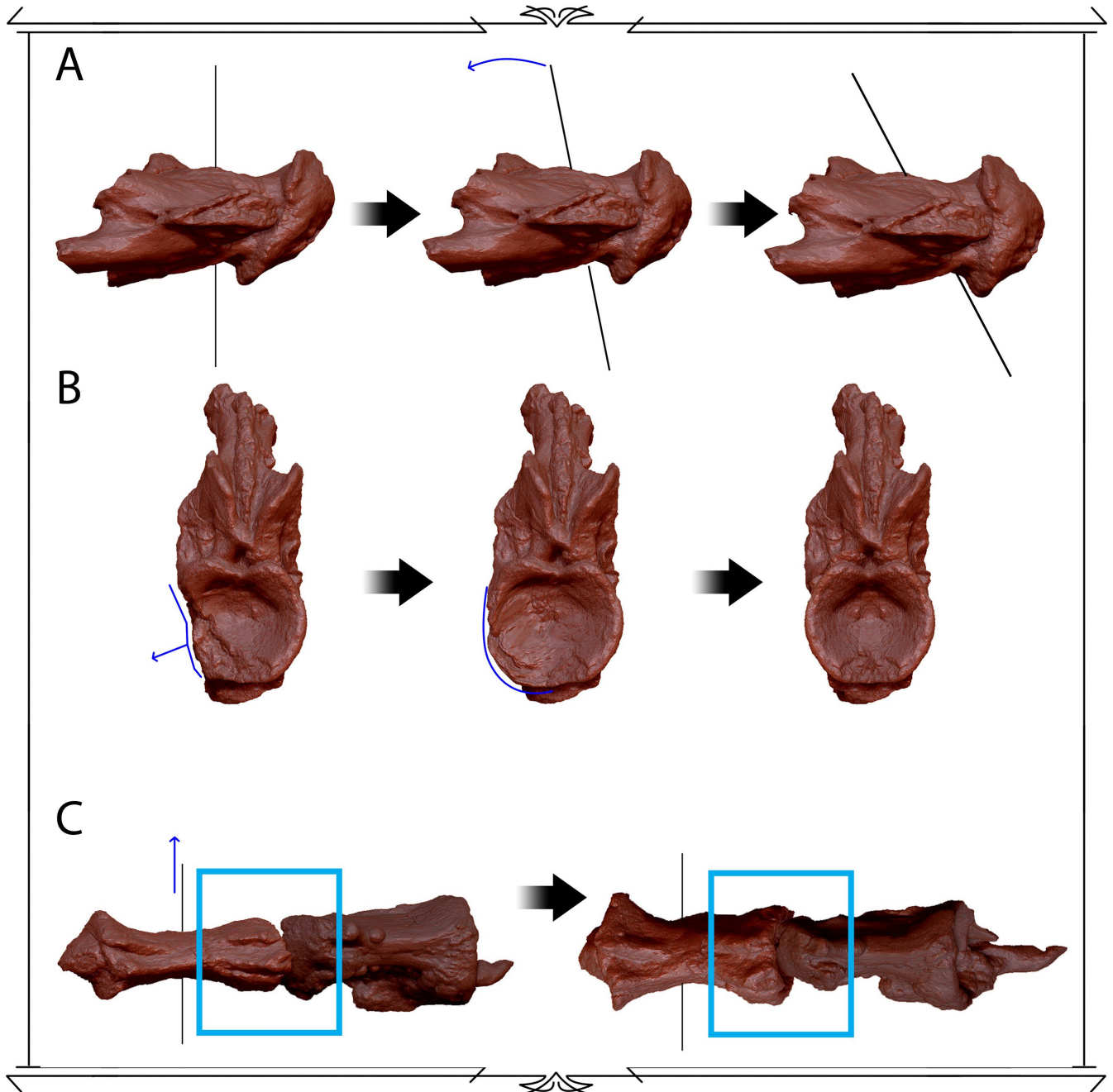


Figure 2.7 - Retrodeformation techniques applied to fossil vertebrae.

A - Correcting asymmetrical deformation of *Lirainosaurus* caudal vertebra MCNA 13338 in dorsal view. Left corresponds to the unaltered fossil, middle to the intermediate stage, right after applying retrodeformation. **B** - Correcting non-symmetric breakages on the centrum of *Lirainosaurus* caudal vertebra MCNA 7458 in anterior view. Left corresponds to the unaltered fossil, middle to a manual retrodeformation approach and right to a mirror technique. **C** - Correcting symmetrical deformation of *Lirainosaurus* caudal vertebra MCNA 7457. Left corresponds to the unaltered fossil, right after applying retrodeformation. The blue square marks the condyle-cotyle centra, which would not fit before retrodeformation. Black lines represent the axis to which retrodeformation was applied. Blue arrows indicate the direction of retrodeformation in all the examples.

its shape cannot be used as criterion. As a compromise solution for range of motion analyses, elements which cannot articulate due to deformation can be retrodeformed until they articulate in osteological neutral pose with each other. This approach was taken always retrodeforming the most compressed/depressed element, and its use should always be acknowledged. It was achieved using the Transpose brush in Move mode and always starting with the vertebrae immediately preceding and following the comparison vertebra (Fig. 2.7 C).

Post-Processing 2 - Preparing bones for analysis. This step mainly consists of separating elements that have been joined during fossilization but which would be separated *in vivo*, such as fragments of preceding vertebrae, ribs and/or haemal arches which have been moved away from their anatomical positions (Fig. 2.8). These elements were all deleted and separated in ZBrush 4R6, masking the region to be preserved and then using the "Trim Lasso" brush to delete the region. The newly exposed areas were sculpted using the visible surfaces on adjacent vertebrae as reference, only adding additional geometry when there was direct evidence (e.g. laminae broken by crushing against another bone fragment).

Some skeletal elements which would have not been permanently fixed in life (co-adjacent vertebrae would have been mobile in life, chevrons and ribs would be independent from their respective vertebrae, etc.) have become so due to fossilization processes, rendering further physical preparation to separate them hazardous to the integrity of the fossils.

To digitally separate those elements on ZBrush, each mesh was duplicated (once per each part meant to be separated) and then sliced to separate the parts, thus generating a separate mesh for each virtual bone desired. After separation, non-visible surfaces (i.e., medial side of prezygapophyseal rami or ribs) were sculpted. The surfaces were reconstructed, ranging from more accurate to less, based on:

- (i) The actual geometry of the bone when the missing area was very small.
- (ii) The most proximal anterior and/or posterior accessible preserved elements, on single metameric elements (vertebrae and chevrons).
- (iii) The counterlateral bone in paired elements (ribs, girdles and limbs).
- (iv) Overlapping elements on other referred specimens.
- (v) Overlapping elements from close relatives.

STEP 3: reconstructing missing elements

Vertebral series. In order to create a hypothetical vertebral sequence, other complete vertebral sequences stemming from the same individual need to be used as a comparison. In the case of a continuous vertebral series with a single missing or damaged element or two (i.e. *Spinophorosaurus nigerensis* GCP-CV-4229 or *Camarasaurus grandis* YPM 1901), the task is simple and reliable. If the element is damaged, missing parts can be restored following the retrodeformation protocol in step 2. If the element is too damaged, the missing element can be reconstructed as the intermediate morphology of the preceding and following element in the series (Fig. 2.9 A-C). This can be sculpted manually or interpolating landmark and sliding semi-landmark positions using geometric morphometry (García-Martínez, Vidal, & Ortega, 2018).

In the most complex cases, such as an individual only with few elements from the vertebral series and plenty of isolated referred vertebrae, the approximation has to be more cautious (i.e. *Lirainosaurus astibiae*, an Upper Cretaceous Iberian titanosaur sauropod with an individual represented by 4 associated caudal vertebrae and a lot of missing elements). An ideal scenario would be to compare the vertebrae from *Lirainosaurus* with those from its closest basal and derived relatives. However, titanosaurian phylogeny is still far from resolved (Wilson 2006) and the phylogenetic position of *Lirainosaurus* is not robust. In order to sort the caudal vertebrae of *Lirainosaurus* (or, for that matter, any titanosaur within the phylogenetic bracket proposed), we chose to use published metric data from the following taxa with complete caudal series: *Andesaurus* (Mannion and Calvo 2011), *Alamosaurus* (Gilmore 1946), *Baurutitan* (Kellner et al. 2005), *Dreadnoughtus* (Lacovara et al. 2014), *Malawisaurus* (Gomani 2005) and *Opisthocoelicaudia* (Borsuk-bialynicka 1977). Although complete or almost

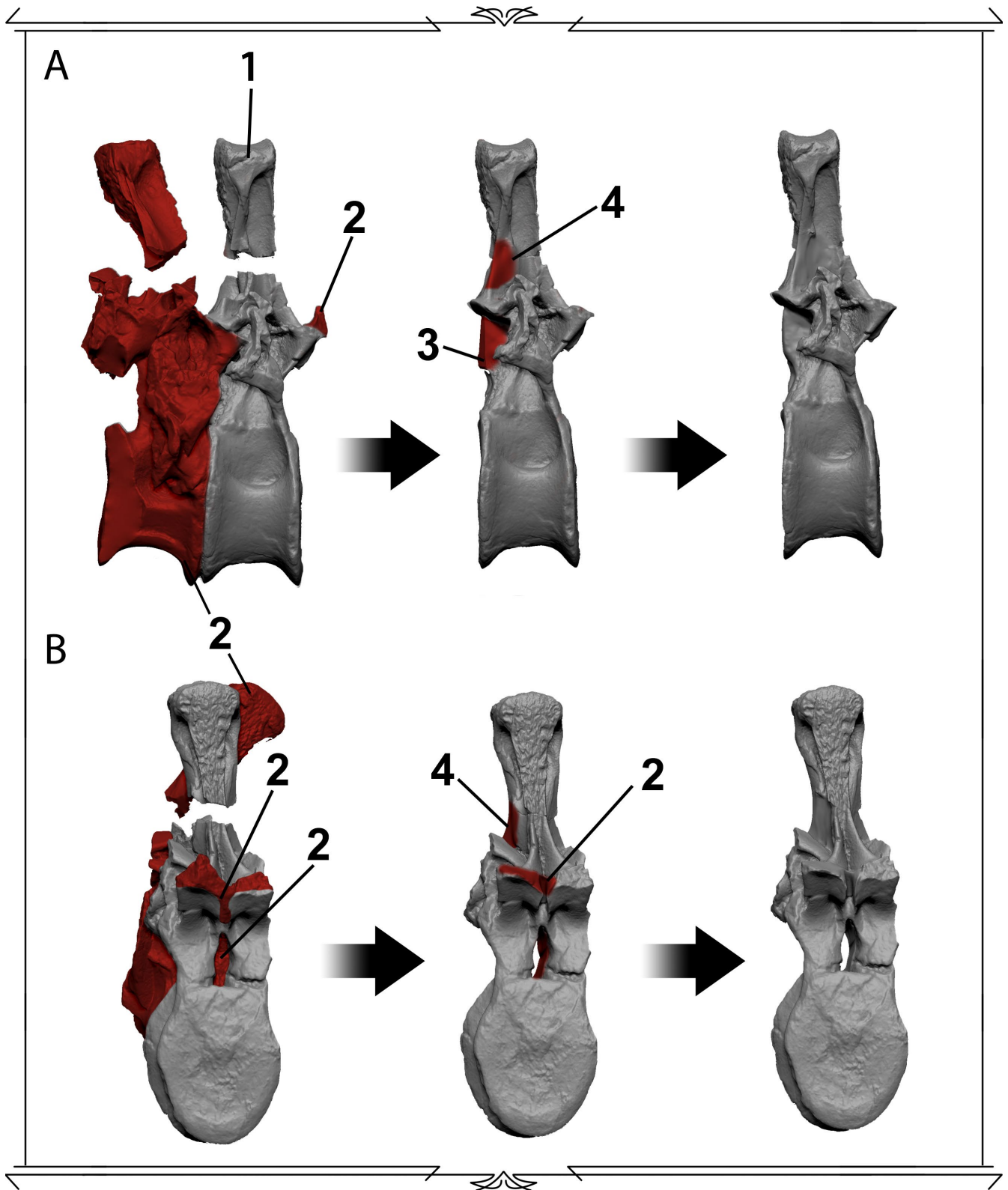


Figure 2.8 - Preparing bones for the virtual assemblage.

Spinophorosaurus nigerensis holotype GCP-CV-4229 dorsal and sacral vertebrae used as example. **A** - Lateral view. **B** - Anterior View. **1** = Broken elements have been put together. **2** = Bones or bone fragments which would not have been physically stuck have been separated. **3** = Elements hidden by those fragments or bones have been sculpted joining the visible parts in the real fossil. **4** = Broken elements have been restored by joining their non-broken parts. Left corresponds to the actual fossils before retrodeformation and the elements which have been modified in red. Middle shows the areas which have been restored in red. Right corresponds with the finished model.

complete, these caudal sequences often include damaged elements with regions of the neural arch missing. The better preserved regions are usually the vertebral centra, and their proportions are known to change through the caudal series, with slight differences between different sauropod clades (Myhrvold & Currie, 1999). As it was unknown whether centra proportions varied greatly among different titanosaurian taxa, we used a centrum

height/centrum length ratio to measure their basic shape. As titanosaurian caudals are procoelous, the anterior centrum height was chosen. We plotted the values obtained against the position in the series (Fig. 2.9 D). Then, we calculated the ratio values for *Lirainosaurus* caudal vertebrae and compared them with the ratios from other titanosaurs. As all studied titanosaurs represent a wide phylogenetic bracket yet their centra proportions vary very similarly along the caudal series (with the exception of the proximal caudals of *Andesaurus*, the basalmost titanosaur), *Lirainosaurus* vertebrae were assigned a position in a hypothetical sequence based on their centra proportions (Fig. 2.9 E). These positions were allowed to have an error of ± 1 . Outliers in the plot were interpreted as a result of drastic taphonomic deformation, although general morphology indicated such position was likely.

Appendicular elements. In order to reconstruct missing appendicular bones, the approach was a combination of scaling known elements and phylogenetic interpolation for unknown elements. Since appendicular elements maintain similar proportions in different ontogenetic stages at least in *Camarasaurus* (see Table 3.1), cross scaling between similarly sized specimens of the same taxa could be used for estimating missing bones. Also, the proportions of closely related taxa were applied when no appendicular element was known for a given taxon, as the best possible estimate.

These estimates therefore consider no abrupt changes in limb proportions relative to closely related sauropods: it is a more parsimonious hypothesis than assuming proportionately longer or shorter appendicular elements.

STEP 4: assembling a virtual skeleton

All virtual skeletons were assembled in ZBrush 4R6 in osteological neutral pose (ONP).

Axial skeleton. Axial elements were assembled following the protocol of Mallison (2010a) in which the spine was split into different sectors (caudal, sacral, dorsal and cervical) and each sector was assembled separately. The assemblage was performed from anteriormost element to posteriormost and vice versa. All sectors were articulated in pairs (only two elements visible at once, one remained static while the other was articulated in ONP) in order to minimize preconceived notions on axial skeleton geometry. If both skeletal assemblages (anterior to posterior and vice versa) had the same Osteologically Induced Curvature (OIC, *sensu* Stevens, 2013) the osteological neutral pose for that sector was considered positive. Available dorsal and cervical ribs were articulated with their tubercula and capitula in maximum articulation with diapophyses and parapophyses respectively.

A final, complete assemblage was done following Carpenter *et al.* (1994) using the conventional sequence for mounting a physical skeleton: (i) sacrum and pelvis; (ii) caudal vertebrae; (iii) presacral vertebrae and ribs; (iv) limbs; (v) skull; (vi) chevrons.

The sacrum was situated so that the first caudal vertebra was parallel to the horizontal plane, and from there, sectors were articulated again by pairs. By positioning the first caudal with its neural canal at roughly 0° deflection allowed to have a reference point to measure axial skeleton deflection, analogous to an origin of coordinates. This enables to contrast the results with the assemblages obtained following the protocol of Mallison (devised for mounting virtual specimens).

Girdles and appendicular skeleton. There have been some controversies on whether the pectoral girdle of sauropods would articulate in an “avian” fashion (McIntosh, 1990; Upchurch *et al.*, 2004), that is, with the longest axis of the scapula sub-horizontal; or in a “crocodilian” fashion, that is, with the longest axis of the scapula sub-vertical. All evidence which seemed to point to a subhorizontal scapula has been recently questioned or refuted (Remes, 2007; Schwarz, Frey, & Meyer, 2007a; Tschopp & Mateus, 2013), and a subvertical placement of the scapula (between 60°-70°) is favored based upon osteological (Schwarz *et al.*, 2007a; Tschopp & Mateus, 2013) and myological evidence (Remes, 2007). The pectoral girdle in sauropods has been thus reconstructed with a sub-vertical scapula, the coracoid antero-ventral to the ribcage and most of the scapular head more anterior to the ribcage, since is the only possible position which allows:

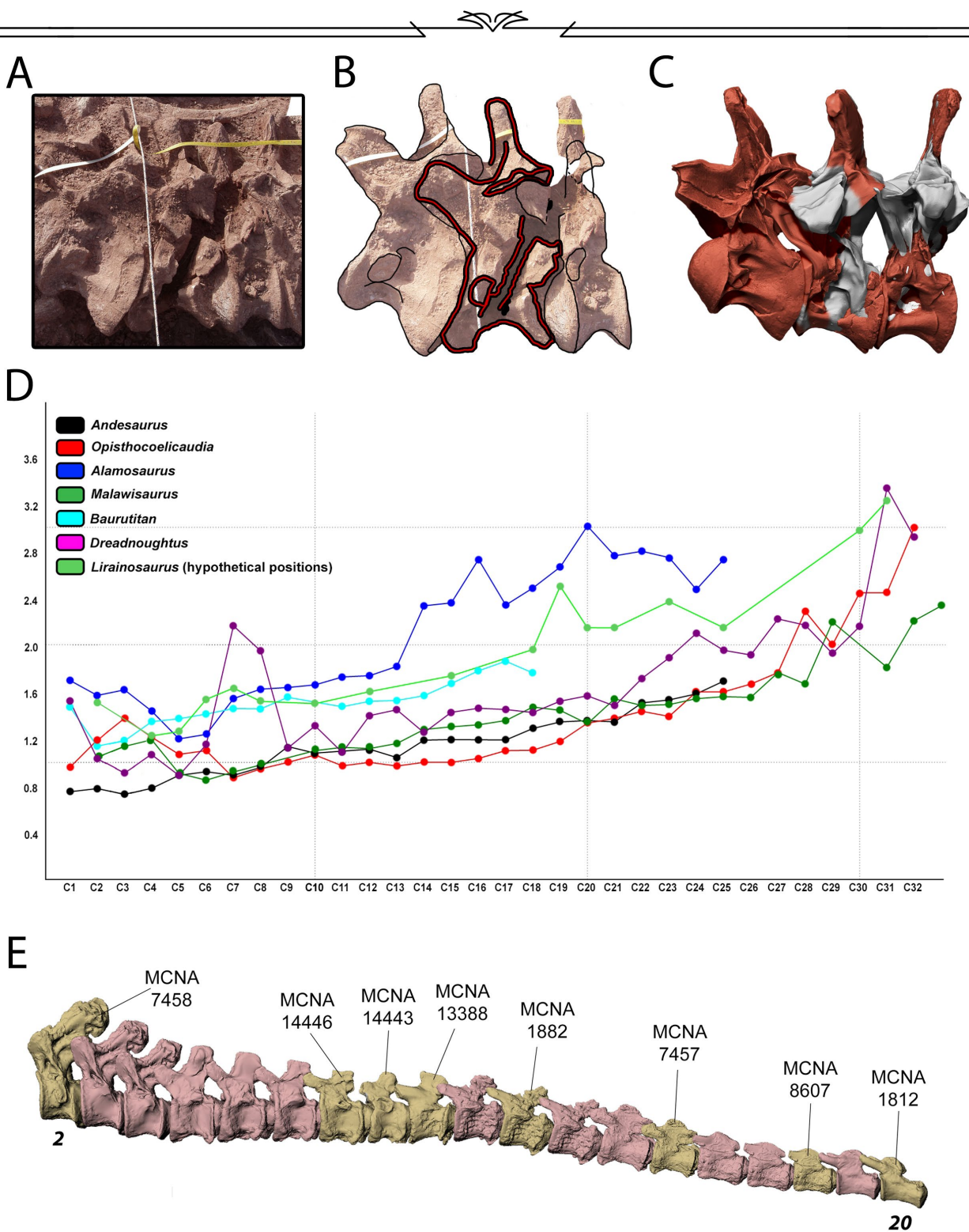


Figure 2.9 - Reconstructing missing or damaged elements in a vertebral series.

A - Cervicodorsal transition of *Spinophorosaurus nigerensis* holotype as it was found in the field. Notice the large fault affecting large portions of the second dorsal vertebra that, however, maintained its original shape and spine direction. **B** - Traced outlines of the three vertebrae. **C** - 3D model of the cervico-dorsal transition, with original digitized fossil bone in red and digitally restored bone in light gray. **D** - Titanosaur caudal vertebrae centrum proportions. X-axis corresponds to caudal vertebra number. Y-axis corresponds to the centrum length/anterior centrum height ratio values. The hypothetical position of *Lirainosaurus* caudal vertebrae has been estimated so the values followed a similar pattern to that of titanosaurs more derived than *Andesaurus*. **E** - The hypothetical, reconstructed tail of *Lirainosaurus astibiae* in right view, in osteological neutral pose, with the actual fossils in yellow and the hypothetical vertebrae in pink.

(i) To keep the scapulocoracoids articulated with the clavicles and interclavicle (Tschopp & Mateus, 2013) and fit within the ribcage.

(ii) To not have the ribcage become an osteological stop for humerus retraction.

(iii) To have functional cingulo-axial and humeral musculature lines (Remes, 2007; Hohn-Schulte, 2010), particularly for *M. serratus (superficialis and profundus)*, *M. sternocoracoideus*, *M. scapulohumeralis*, *M. subcoracoscapularis* and *M. deltoideus scapularis*.

(iv) To place the costo-coracoideal articulation subparallel to the distal ribs axis as is the case of all extant non-mammalian tetrapods (Schwarz *et al.*, 2007a).

(v) To leave room dorsal to the distal expansion for the cartilaginous suprascapula, which would be the insertion point for *M. rhomboideus* (Remes, 2007; Hohn-Schulte, 2010).

The completeness of the pectoral girdle and anterior dorsal ribs of the holotype *Spinophorosaurus nigerensis* in particular served as an excellent example to test different configurations with the inclinations of the scapulae and the connection of them with the other bones from the pectoral girdle and with the dorsal ribs (see Chapter 3.2).

As for the pelvic girdle, the sacrum and preserved ilium suffered from compression as the rest of the axial skeleton, but the pubes and ischia were not heavily distorted. By articulating both pubes and ischia, the distance of the left and right articulation with the ilia helped in reconstructing a model close to the original width of the pelvis. The pelvis is narrow, and therefore the hind limbs articulate so that the hind feet can step over the midline of the dinosaur, as would be expected for an early branching non-neosauropod eusauropod (Carrano, 2005).

The appendicular skeleton was articulated in ONP, with the articular surfaces in maximum overlap.

Physical model articulation. Taking advantage of rapid prototyping, a scaled 1:4 and 1:8 scale model of the neck of *Spinophorosaurus nigerensis* was used to test the results from the virtual reconstruction and range of motion analyses. The models were printed in an Ultimaker 2 Extended printer, using thermoplastic Polylactic Acid (PLA), which can recreate surfaces with great accuracy. Physical scaled models have advantages and disadvantages next to the virtual models, but the most important advantage, however, is that the 3D printed model has the physical properties a virtual 3D model lacks, and hence osteological stops can be grasped in a way impossible in the virtual environment.

The 1:8 scale model was glued together with hot melted adhesive using the ONP criterion by fully articulating the pre- and postzygapophyses. The resulting model is very similar to the OIC achieved in the virtual environment, with only minor differences, not affecting the overall pose. The 1:4 model was employed to test the range of motion results. A 1:12 scale model of the hindlimb was also prototyped in order to assess the articulation of the tibia and fibula, and the articulation of both with the astragalus and femur.

STEP 5: range of motion analyses

While there are standards for comparing neutral postures (See CNP, ONP, OIC, NBOP, etc.) there are no standards defined yet for range of motion analyses: maximum articular excursions follow different criteria for different authors. Also, since some authors have employed either the real fossils, 1:1 scale casted replicas, virtual fossils or scaled down 3D printed replicas the results may slightly vary. Until more standardized criteria are established, range of motion analyses will necessarily need to be compared in relative terms, rather than absolute.

There has been a little controversy on how much pre- and postzygapophyseal articular facets can deflect before they effectively disarticulate. Early studies found the zygapophyseal safety factor (minimal overlap of the facets before there is too much strain on the zygapophyseal articular capsules *sensu* Stevens (2013) to be at around 50% of overlap (Stevens & Parrish, 1999). Nevertheless, observations on extant organisms such as crocodiles (Stevens & Parrish, 2005) or birds (Mallison, 2010b) have shown that alive extant animals can attain postures with barely any overlap between their zygapophyseal facets. Moreover, extant birds have zygapophyseal facets enlarged by a soft tissue capsule, which can increase the osteological facet up to 12.5% (Taylor & Wedel, 2013a). Knowing this, it could be argued that *in vivo* zygapophyseal facets were larger than

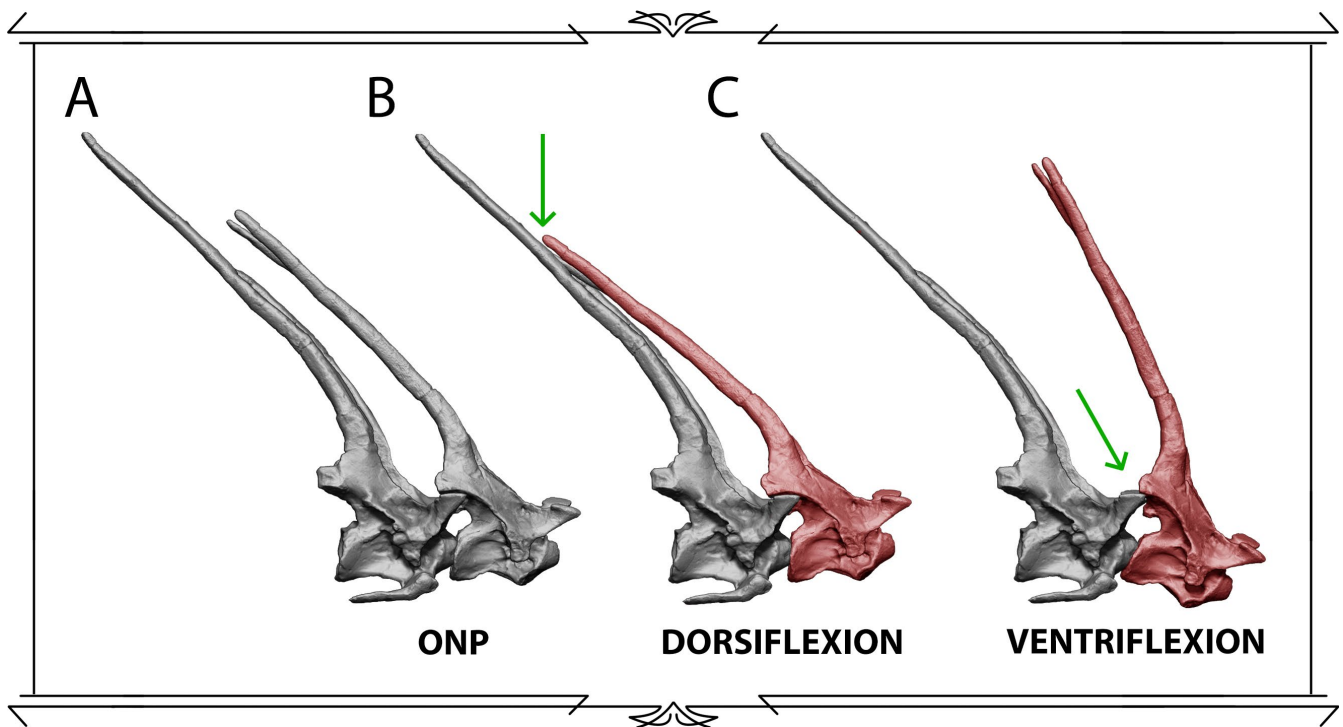


Figure 2.10 - Limits on osteological range of motion analyses, *Amargasaurus cazau* as case study.

A - Cervical vertebrae 4 and 5 in osteologically neutral pose (ONP), full zygapophyseal overlap. **B** - Osteological stop as the limit for dorsiflexion, with the elongated neural spines colliding way before the zygapophyseal facets are disarticulated. **C** - Disarticulation of the zygapophyseal facets as limit of ventriflexion.

their osteological counterparts, as the soft tissues did not fossilize. However, there is not a reliable way to estimate how much soft tissue is missing from the zygapophyses yet, and that soft tissue might have been variable between species and even among individuals from the same species.

All in all, it was decided to follow the protocols of Mallison, in which vertebrae were deflected until only a minimum overlap of the facets was retained, that is, just before they disarticulated (Fig. 2.10 C). That way, accounting for a larger facet *in vivo*, the range of motion is underestimated rather than overestimated (in accordance with what happens in present day archosaurs). The center of rotation was the anteriormost part of the cotyle of the posterior vertebra when the articulation was opisthocoelus and at midheight of the posterior centrum face in platycoelous articulations. This would prevent the misalignment of the neural canals, in order to avoid adopting poses that would put stress on the spinal cord (Heinrich Mallison pers. comm. 2016).

In lateral flexion, zygapophyseal overlap was retained in three different ways: (i) maintaining one zygapophyseal pair in full articulation and deflecting the other pair anteriorly, (ii) maintaining one zygapophyseal pair in full articulation and deflecting the other pair posteriorly, and (iii) deflecting one zygapophyseal pair posteriorly and the other pair anteriorly (as seen in Mallison (Mallison, 2010b) figure 3A), which would be the maximum range of motion before disarticulation. Both (i) and (ii) rendered similar range of motion at all intervertebral joints, so all figures depicting lateral range of motion of the neck depict (i) and (iii).

Criteria like the maximum dorso-ventral flexion employed by Christian *et al.* (2013) are less conservative and precise when it comes to comparing the ranges of motion of different taxa. According to Christian *et al.* (2013), it is in accordance with the results on the maximal dorsal excursion obtained for extant vertebrates with long necks. However, since the osteological stop may not happen in all taxa (Stevens, 2013), unlike zygapophyseal disarticulation, the criterion is therefore less useful when it comes to comparative analyses.

To measure the angles between two individual vertebrae, we used the angulation between the same landmark between two consecutive vertebrae: the posteriormost and ventralmost point of the vertebral centrum in lateral view for dorso-ventral ROM, and the right prezygapophyses in dorsal view for lateral ROM. These were later contrasted against a different method: drawing straight lines parallel to the main axis of the vertebral centrum in lateral (dorso-ventral ROM) or the neural spines in dorsal view (lateral ROM) and measuring the angle they make, which was the same measured between landmarks in all cases.

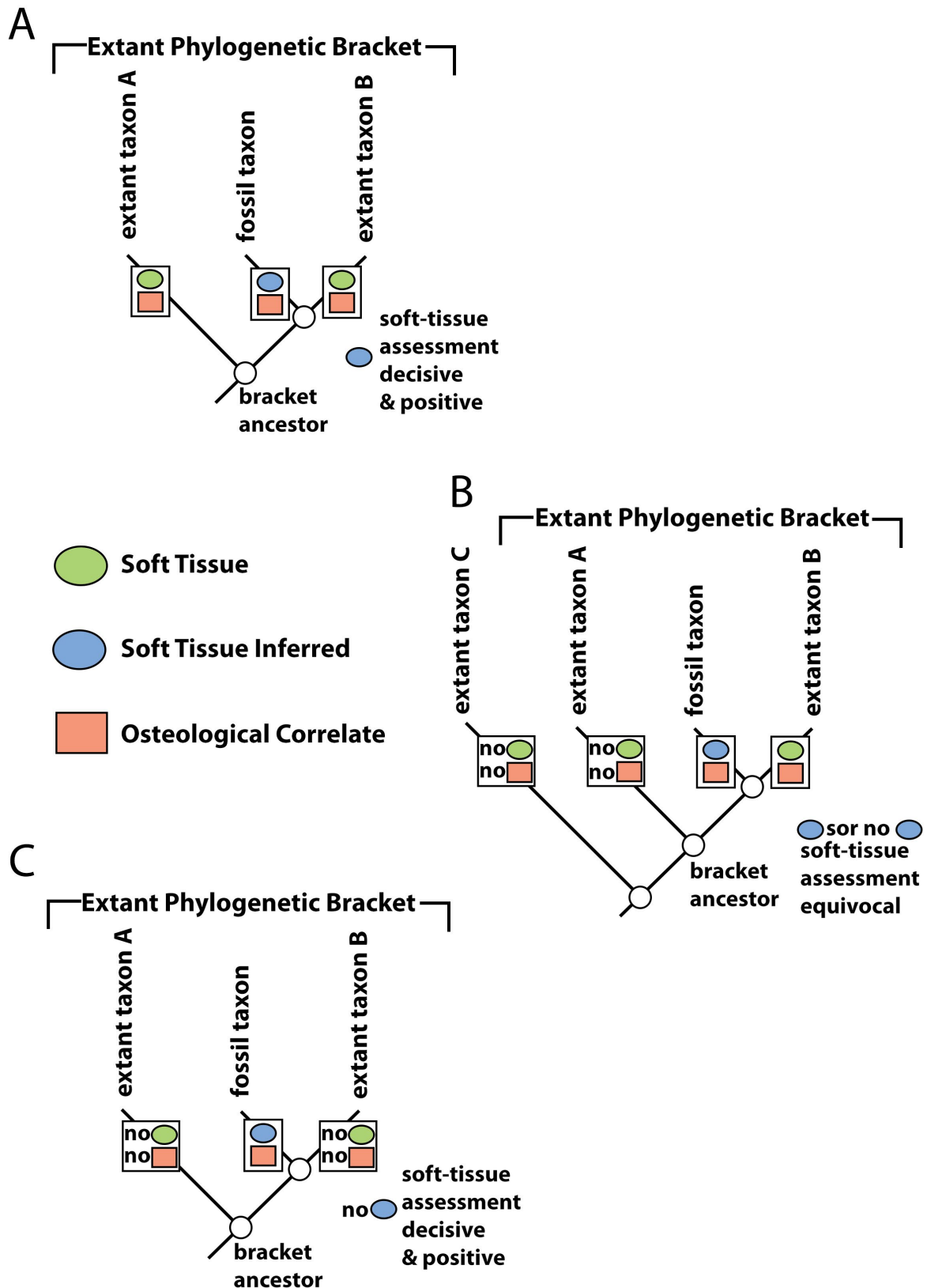


Figure 2.11 - Extant Phylogenetic Bracket (EPB) applied to muscle reconstruction.

A - Level I inference: both extant taxa making the EPB possess the soft-tissue attribute and associated osteological correlate which is also present in the fossil taxon. This leads to a decisive positive assessment of the outgroup node. **B** - Level II inference: only one of the extant taxa making the EPB has the soft tissue, leading to an equivocal assessment of the outgroup node. **C** - Level III inference: neither component of the EPB has the soft tissue, leading to a decisive negative assessment. In B and C, inference of the soft tissue in the fossil taxon may be justified if there is compelling evidence. Modified from Fig. 2.5 from Witmer (1995).

STEP 6: muscle reconstruction

In order to reconstruct the musculature of extinct vertebrates, two main lines of evidence have been followed: muscle insertion scars on the fossil bones (to assess the presence of a muscle) and phylogenetic inference (to identify which muscle present in extant taxa that scar corresponds to).

The main phylogenetic inference method for soft tissue reconstruction is called Extant Phylogenetic Bracketing (EPB), devised by Bryant & Russell (1992), and named and further developed by Witmer (1995). It basically consists in establishing the presence or absence of a particular soft tissue in the extant taxa that constitute the phylogenetic bracket of our extinct taxon of interest (that is, an extant earlier branching taxon and a more deeply nested extant taxon). There are 3 main levels of inference, with 3 additional sublevels (if there are no osteological correlates for the soft tissue of interest). The levels of inference have been summarized in figure 2.11.

There have been plenty of studies of postcranial muscle inference in dinosaurs, both axial (Wedel & Sanders, 2002; Schwarz, Frey, & Meyer, 2007b; Snively & Russell, 2007a; Schwarz-Wings, 2009; Mallison, 2010a; Persons & Currie, 2010; Hutchinson *et al.*, 2011) and appendicular (Carrano & Hutchinson, 2002; Hutchinson & Garcia, 2002; Otero, 2010; Grillo & Azevedo, 2011; Ibiricu, Lamanna, & Lacovara, 2014; Ibiricu, Martínez, & Casal, 2018; Klinkhamer *et al.*, 2018). Since the great majority of inferences have been well supported with these studies, the inferred muscles of those studies are used here as well, with the exception of those muscles for which there are controversies. The presence or absence of controversial muscles has been discussed.

STEP 7: volumetric reconstruction and physical properties

Volumetric reconstruction from virtual skeletons stems of the classic method of using Archimede's principle with submerged dinosaur scale models to estimate their body mass (Colbert, 1962; Alexander, 1989). Since the scale models could accumulate a lot of propagating errors, virtual skeletons provide a representation using scans of the actual bones with errors smaller than 0.1 mm, making a lot of errors regarding proportions to be minimized. There have been several ways to create volumetric reconstructions of the whole body of an extinct animal. By far, the most popular is the convex hull method, which creates a mesh of basic geometric shapes which contains the virtual skeleton just to its boundaries using mathematical integration (Bates *et al.*, 2016). The main advantage of this method is its repeatability, as it is based on a mathematical equation, which can be applied equally to all the models. However, the method is known also making underestimates, and therefore making all further research based on these mass estimates underestimate the physical capabilities of extinct animals (Mallison, Pittman, & Schwarz, 2015).

A different method to estimate body volume is using Non-Uniform Rational B-Splines (NURBS) with 2D ellipses (Bates *et al.*, 2009; Mallison, 2010a, 2011a; Hutchinson *et al.*, 2011). The method consists in creating 2D curves for sections of the body of an animal in different points (like it would be done in a CT-Scan). The ellipses are then used to create a 3D object by extrapolating the points between each ellipse. From this 3D object, a 3D polygon mesh can be created. The resulting mesh has the same scale the virtual skeleton had, and can be used to calculate volume and cross-section areas, and all physical parameters that can be derived from those two variables (i.e. mass, torques...). This method was favored in this thesis (Fig. 2.12 A-D) over the convex hull method, as although the models are more time-consuming, they are more realistic (Mallison *et al.*, 2015).

In order to make the ellipses, these were drawn in McNeel Associates Rhinoceros 5.1 (<https://www.rhino3d.com>), using the "Control Point Curve" tool. Once the ellipses were all traced over the virtual skeleton (Fig. 2.12 E-G), the "One rail sweep" option was used to make a NURBS out of the ellipses (Fig. 2.12 H). The resulting 3D object was meshed (right click > create mesh) and exported as a Wavefront OBJ. The mesh was loaded onto the freeware Meshlab, where its volume and its center of mass were measured (Filters > Quality, Measure and computation > Compute Geometric Measures). The NURBS method was also used to reconstruct tail musculature on some sauropod taxa, as there is pretty detailed data on their cross-sections in extant archosaurs (Mallison *et al.*, 2015; Klinkhamer *et al.*, 2017). While the origin and insertions are fairly well known, but there are no good proxies to have a precise estimate of the actual cross-section of most muscles in extant taxa yet, a crocodile tail was used as a model for sauropods. This is justified on the fact that it is better to have rougher estimates than to predict such reconstruction with too much precision that does not correlate with the data (Mallison *et al.*, 2015).

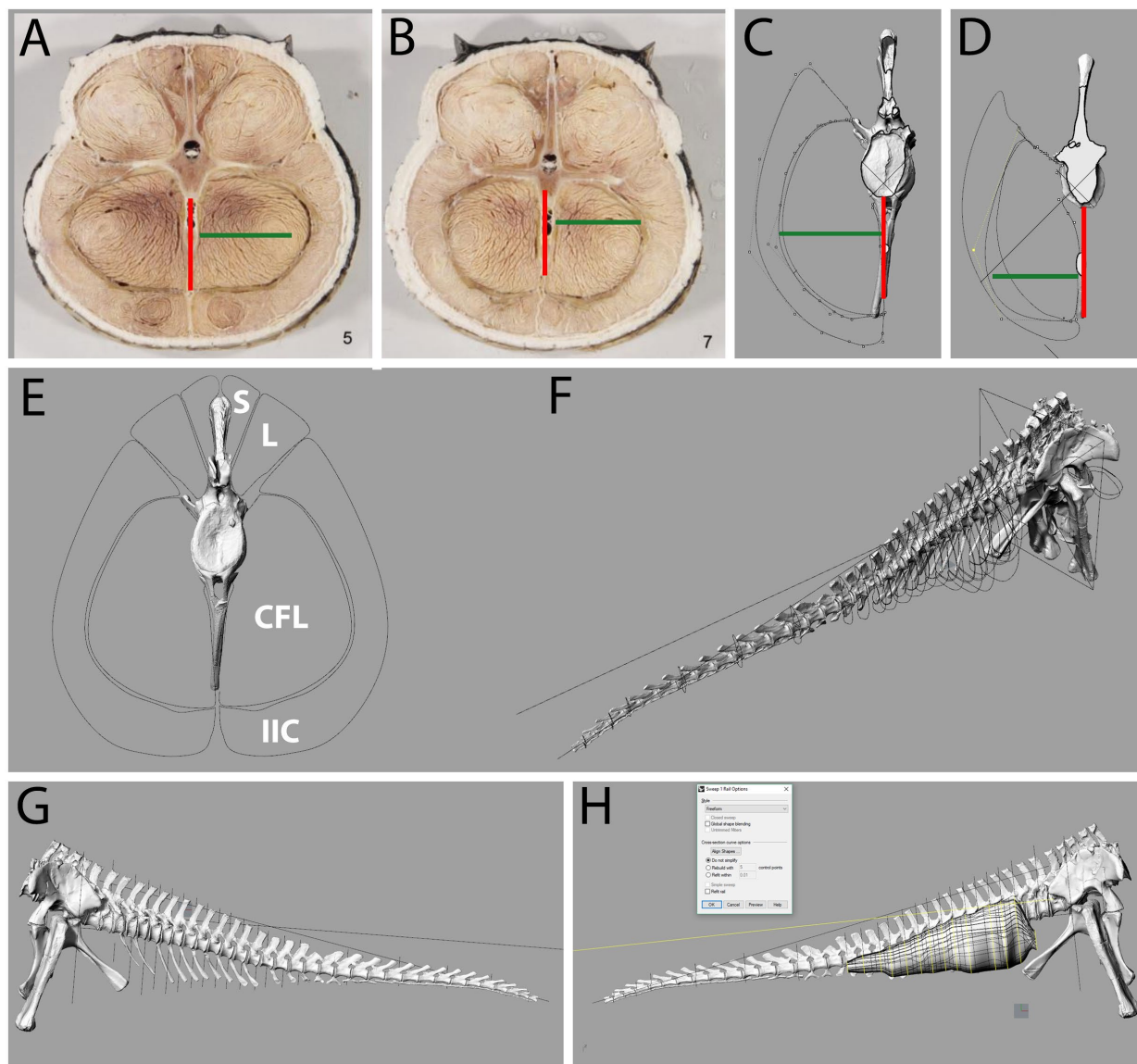


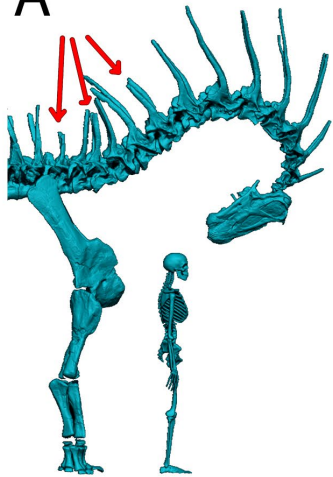
Figure 2.12 - Volumetric reconstruction of muscles with NURBS.

A - Cross-section of an *Alligator mississippiensis* tail at the base, showing the major muscle groups. **B** - Cross-section of the same tail in a more posterior position. **C** - Virtual reconstruction process of the cross-section of the *Spinophorosaurus nigerensis* tail at caudal vertebra 4. **D** - Virtual reconstruction process of the cross-section of the *Spinophorosaurus nigerensis* tail at caudal vertebra 9. **E** - Finished reconstructed outlines for caudal musculature section at caudal vertebra 4 in *Spinophorosaurus nigerensis*. **F** - Complete tail of *Spinophorosaurus nigerensis* in posterodorso-lateral view with all cross-sections and rails of the right side visible before generating the volumetric reconstruction with NURBS. **G** - Complete tail of *Spinophorosaurus nigerensis* in lateral view with all cross-sections of the right side visible before generating the volumetric reconstruction with NURBS. **H** - Complete tail of *Spinophorosaurus nigerensis* in lateral view with the volume of *M. caudofemoralis longus* generated after applying NURBS. Red bars in A-D indicate chevron length, and green bars in A-D indicate CFL maximum width. S = *Mm. spinalis*. L = *Mm. longissimus*. CFL = *M. caudofemoralis longus*. IIC = *Mm. ilio-ischiocaudalis*. A and B modified from Mallison *et al.* (2015).

In order to gain some insight into the potential function of some muscles, the 3D models of the estimated muscles were used to roughly estimate their torques. First, the lines of action of muscles were estimated as a vector drawing a straight line between the origins and insertions. The lever arm for any given joint was estimated to be the distance between the center of rotation and the insertion of the muscle. With the line of action for the muscle force and the lever arm, moment arm is calculated as the perpendicular distance from the center of rotation to the line of action of a force (see Fig. 3.21).

Torque, the capacity of a force (muscle) to generate rotation on a lever (joint), is dependent on three variables: (i) moment arm, (ii) the angle of application of force (which also influences moment arm length) and (iii) amount of force. Since the amount of force a muscle can generate is directly related with its physiological cross-section (Snively & Russell, 2007a; Persons & Currie, 2010), this variable was used as a proxy for iii.

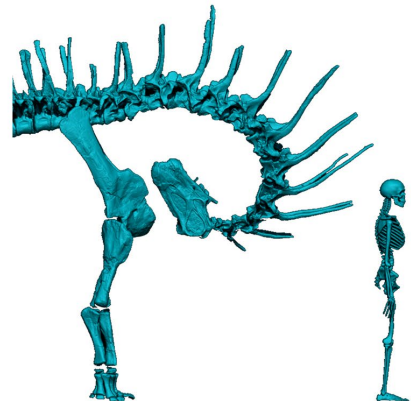
A



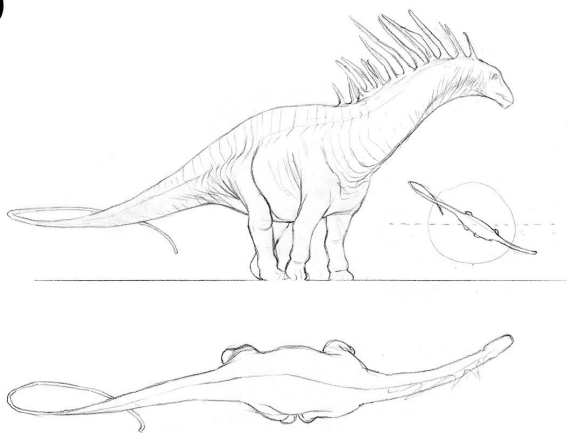
B



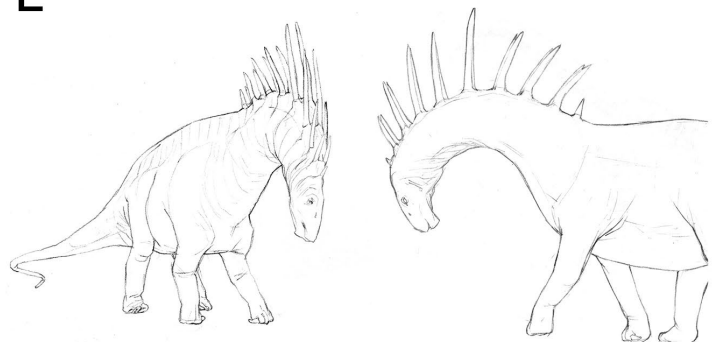
C



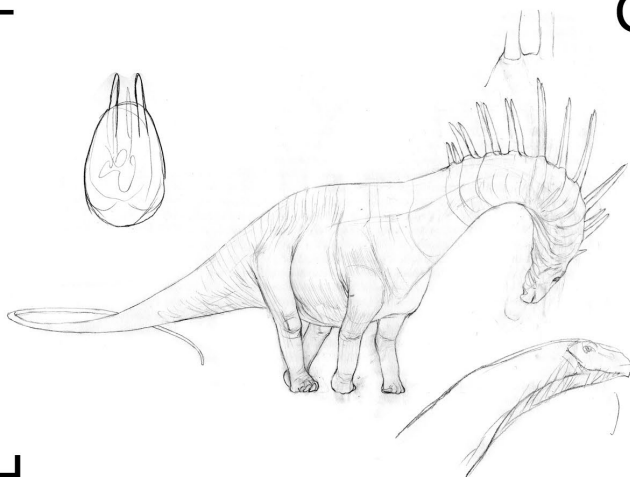
D



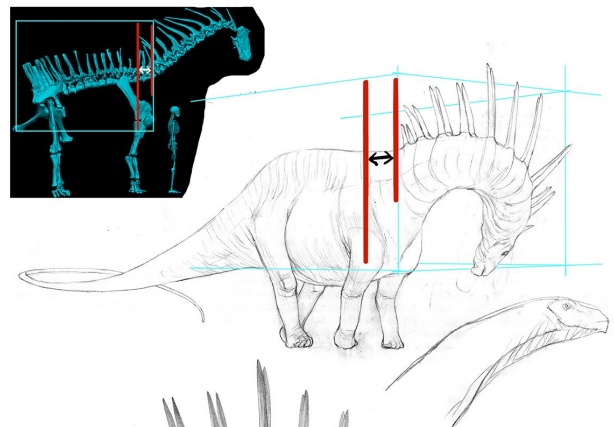
E



F



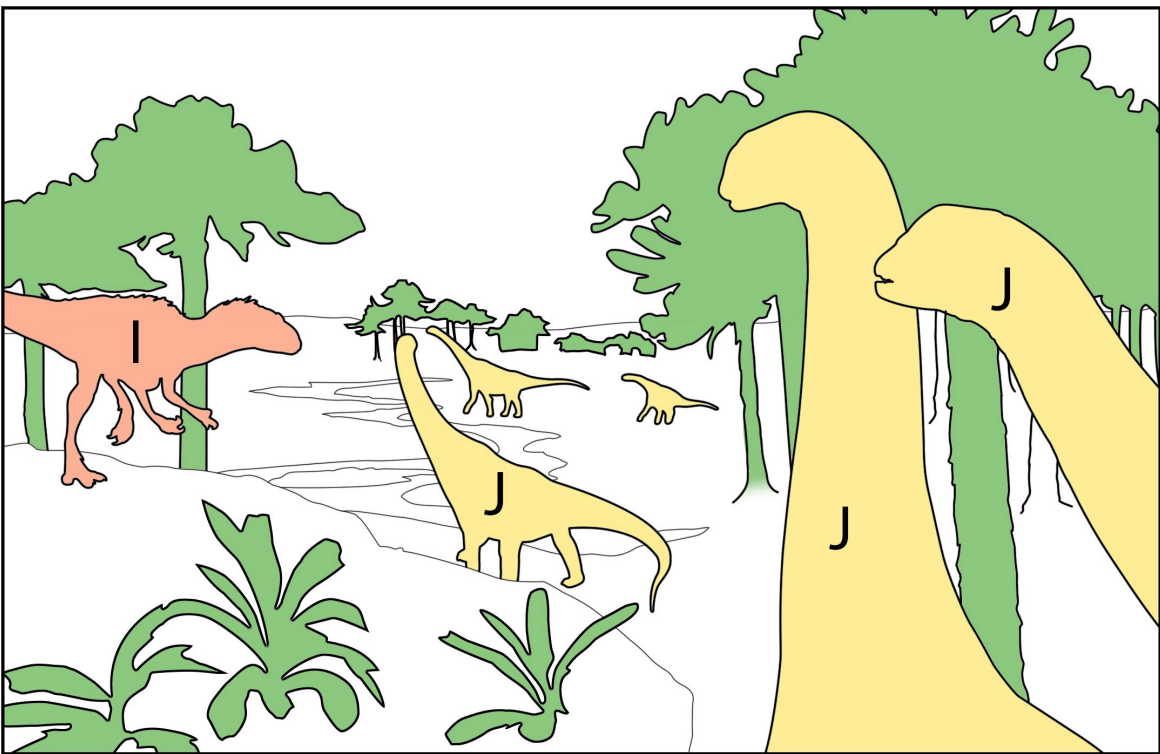
G



H



I



J

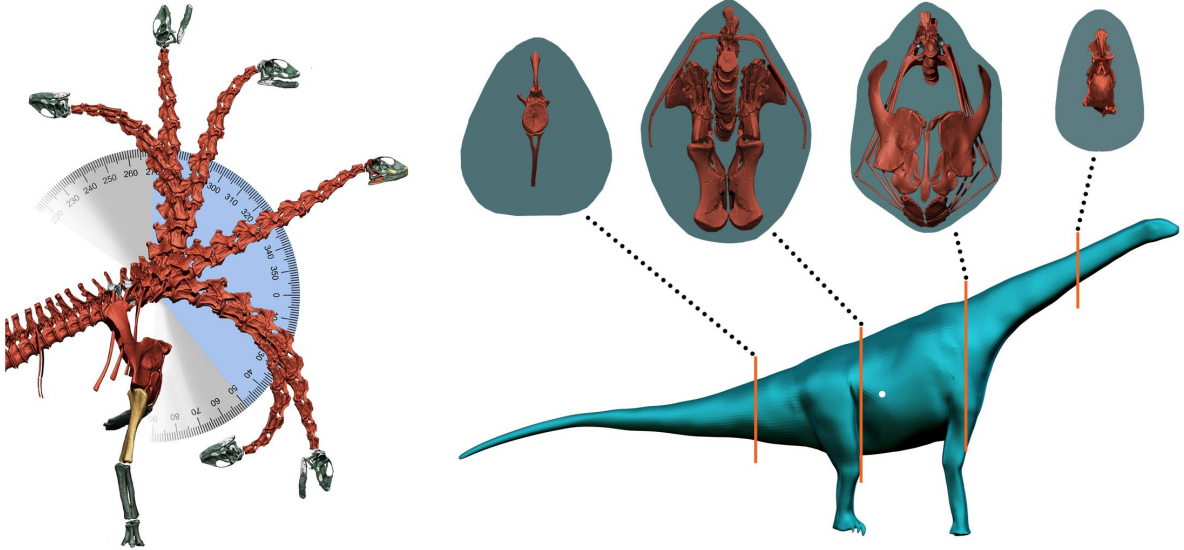


Figure 2.13 (previous page) - Stages of a paleoartistic reconstruction.

A - Virtual skeleton of *Amargasaurus cazau* with hypothetical display pose dorsiflexing posterior cervicals and ventrifleflexing middle and anterior cervicals. Red arrows point at broken neural spines. **B** - Virtual skeleton of *Amargasaurus* with neck posed in alter posture (sensu Taylor, Wedel and Naish (2009)). **C** - Virtual skeleton of *Amargasaurus* with hypothetical display pose dorsiflexing posterior cervicals and middle and anterior cervicals in osteologically neutral pose. **D** - Initial sketch in 3/4 perspective with neck in alert pose. **E** - Sketches in 3/4 and lateral view exploring possible display postures within the osteological range of motion. **F** - Sketch in 3/4 with the selected neck position for hypothetical display posture, with details on neck cross-section and skull-neck transition. **G** - Sketch correcting the proportions of the previous drawing. **H** - Final detailed drawing, with 170 cm human scale. **I** - Theropod teeth found associated with the holotype of *Spinophorosaurus nigerensis* tentatively assigned to a dinosaur close to *Afrovenator*. **J** - Simplified outlines of elements from the paleontological restoration of the L'Irhazer plain. **K** - Range of motion and postures of the neck of *Spinophorosaurus* and volumetric reconstruction used to reconstruct the dinosaur in the restoration. Drawings by Diego Cobo.

Phylogenetic analysis

Many characters employed in data matrices for phylogenetic analyses may include potential functional implications in areas surveyed in this thesis, such as range of motion, muscle inference or function. In order to evaluate the impact of sauropod postcranial biomechanics in phylogenetic analyses (Chapter 5), the matrix and dataset of Carballido *et al.* (2017) were used as a case study, as it includes almost all the sauropods from Table 2.1.

The postcranial characters were reviewed, and those with potential functional implications were discussed under the information obtained from the study of *Spinophorosaurus* in Chapters 3 and 4. If functional characters were not in Carballido *et al.*'s dataset but were considered to be potentially phylogenetically informative, they were incorporated into the dataset. Since "El Chocón Rebbachisauridae" was not in the dataset, it was coded as well. *Spinophorosaurus nigerensis* is currently regarded as a member of Eusauropoda, rather than a earlier branching sauropod as first described. However, it is being redescribed and the discussion of its precise phylogenetic position beyond its situation as a non-neosauropod eusauropod is beyond the scope of this thesis.

Finally, two analyses of the matrix were performed in *Tree analysis using New Technology* or TNT (Goloboff, Farris, & Nixon, 2008), courtesy of the Willi Henig Society. First, the original, unmodified matrix was analysed to replicate the original result. Once the result had been duplicated, the modified matrix with all the original characters and new characters was analyzed. The analyses were all performed using the exact settings from (Carballido *et al.*, 2017): a heuristic tree search consisted of 10.000 replicates of Wagner trees (with random additionsequence of taxa) followed by ten rounds of tree bisection-reconstruction (TBR) branch swapping.

Paleoartistic restoration

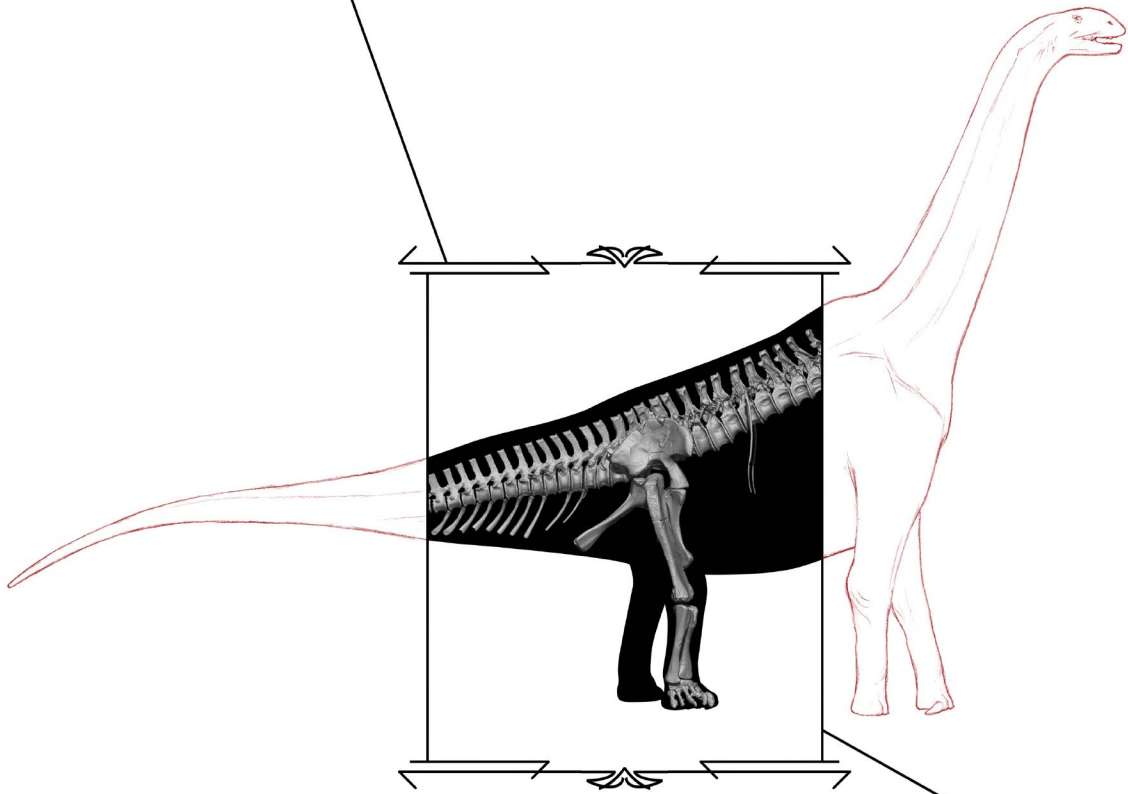
Paleoart can be considered "*any original artistic manifestation that attempt to reconstruct o depict prehistoric life according to the current knowledge and scientific evidence at the moment of creating the artwork*" (Ansón, Hernández Fernández, & Saura Ramos, 2015). Since the amount of body plan, range of motion and myological evidence obtained during the development of this thesis has a large impact in the life appearance of some sauropods, it was decided to work together with paleoartist Diego Cobo in order to incorporate said evidence into several artistic restorations. The followed steps were the same summarized by Antón & Sanchez, (2004) and Ansón & Hernández Fernández (2013): (i) reconstruction of the skeleton, (ii) reconstruction of soft tissue, (iii) reconstruction of locomotion and behavior, and (iv) integration of the reconstructed animals into an environmental and ecological setting (Fig. 2.13).

Since the first three steps largely overlap with steps 4, 5 and 6 of the methodology aforementioned, most of the information was readily available to work with the artist in preparing the reconstructions. Special attention was paid to highlight physical characteristics of the animals inherent to their anatomical proportions and/or skeletal reconstructions. Only some reconstructions have incorporated particular behavioral hypotheses.

Regarding the last step, since the reconstructions serve an illustrative purpose to incorporate all evidence derived from the results of this thesis, the environmental setting was limited to a few, minimalistic details to

some of the sauropods reconstructed. Also, a 170 cm human character was added to each reconstruction for scale purposes (Fig. 2.13 H).

The only exception to this rule has been the artwork for the cover of this thesis: an attempt at reconstructing the environment which produced the fossils of *Spinophorosaurus nigerensis*, in what today is known as L'Irhazer plain, close to the city of Agadez (Niger). Since studies of the flora of the L'Irhazer plain are very scarce (limited to the presence of fossilized wood, sometimes large trunks), vegetation was reconstructed using information from the Middle and Upper Jurassic flora of Gondwana, particularly Argentina. A flooding plain with recognizable Cheirolepidaceae, Cycadaceae and Pteridophyta vegetation was chosen as the paleoenvironment. Given that at least four individuals of *Spinophorosaurus* of different sizes were buried in similar degree of articulation in close proximity (Remes *et al.*, 2009; D. Vidal personal visit to L'Homme Blanc fossil site in 2018), a herd of the animals was depicted walking through the plain. Theropod teeth referable to a taxon closely related to *Afrovenator abakensis* were found closely associated with the skeleton of the holotype (Fig. 2.13 I; Serrano-Martínez *et al.*, 2016), so a juvenile Megalosauroida indet. was incorporated into the reconstruction to depict the complete faunal assemblage known from L'Homme Blanc site as of 2019.



CHAPTER
 . 3 .

A VIRTUAL SPINOPHOROSAURUS:

**OSTEOLOGICAL, MYOLOGICAL, VOLUMETRIC RECONSTRUCTION, AND EVIDENCE
 OF AN EVOLUTIONARY INNOVATION**

Introduction.....	63
Systematic Paleontology.....	65
Assembling the virtual skeleton.....	66
<i>Spinophorosaurus</i> body plan.....	73
Osteological range of motion analyses.....	75
Reconstruction of the muscular system.....	83
Volumetric reconstructions and mass estimates.....	97
Discussion.....	97
Conclusions.....	113

3.1 INTRODUCTION

Sauropods were the earliest large herbivorous dinosaurs, with an unparalleled disparity in body size, since their Late Triassic origin until their demise at the end of the Cretaceous (Sander *et al.*, 2011). Their quadrupedal, long-necked, long-tailed body plan remained fixed during their evolution, although both relatively shorter necks (Rauhut *et al.*, 2005; Sereno *et al.*, 2007) and extremely long necks (Jensen, 1985; Wedel *et al.*, 2000b; Christian *et al.*, 2013; Taylor & Wedel, 2016) appeared on several different clades of sauropods. This characteristic body plan had a direct impact on the feeding efficiency of these animals (Sander *et al.*, 2011; Sander, 2013): different feeding adaptations regarding this body plan were likely key in their evolutionary history (Sander, 2013). However, whether these adaptations allowed, or not, high browsing capabilities has been the subject of a lively debate (Stevens & Parrish, 1999, 2005; Christian, 2002, 2010; Christian & Dzemski, 2007; Taylor *et al.*, 2009; Stevens, 2013).

Previous studies on sauropod feeding capabilities based on their postcrania have focused mostly on neck posture and range of motion (Martin, 1987; Martin, Martin-Rolland, & Frey, 1998; Stevens & Parrish, 1999, 2005; Christian & Dzemski, 2007; Christian, 2010; Christian *et al.*, 2013). Evidence from neutral articulation of the bones and computerized analyses suggested straighter, less flexible necks (Martin, 1987; Stevens & Parrish, 1999; Stevens, 2013), with some authors suggesting most sauropods could barely raise the neck above shoulder height (Martin, 1987; Stevens & Parrish, 1999). However, evidence stemming from comparisons with extant relatives and analyses on inter-vertebral stress suggested elevated, more flexible and curved necks (Christian, 2002, 2010; Christian & Dzemski, 2007; Dzemski & Christian, 2007; Taylor *et al.*, 2009). More recent studies have revealed the relationship between sauropod neck posture and feeding habits is more complex than previously thought (Stevens, 2013; Taylor, 2015): forelimb/hindlimb proportions (Stevens & Parrish, 2005) or scapula orientation and position probably had a strong role in browsing capabilities also (Schwarz *et al.*, 2007a; Stevens, 2013). Unfortunately, the fragmentary nature of the known sauropod fossil record has been a large caveat in understanding how the axial skeleton, girdles and limbs vary within sauropod dinosaurs, making the study of their functional morphology complex.

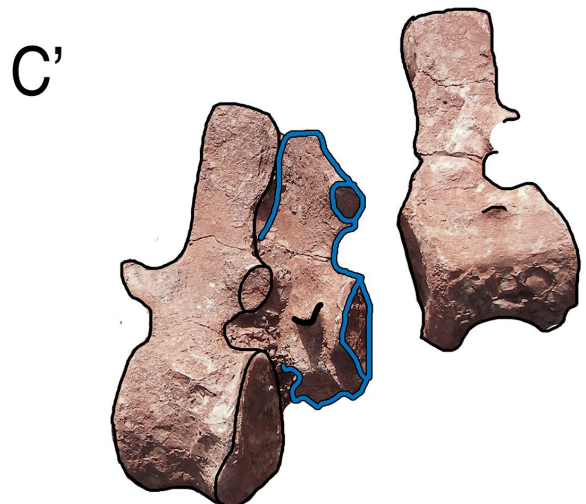
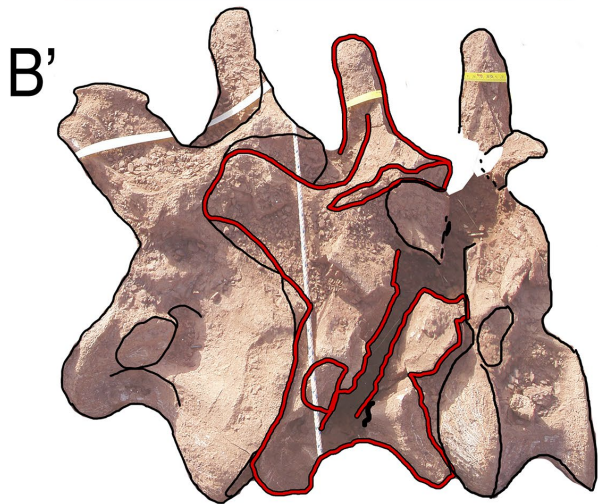
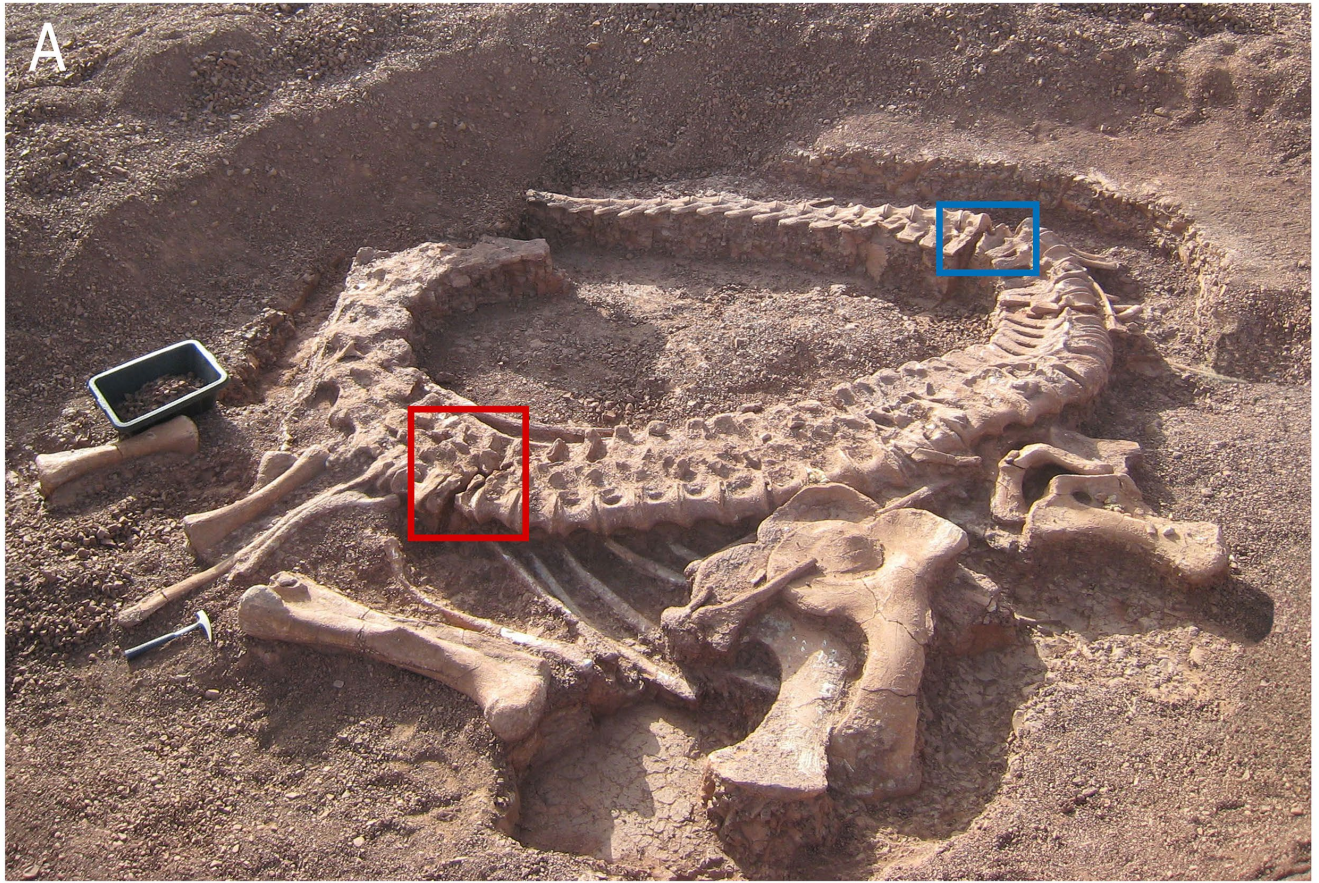
In 2007, the holotypic specimen of *Spinophorosaurus nigerensis* was unearthed from the Middle Jurassic of Niger (Remes *et al.*, 2009; Mocho *et al.*, 2013), being one of the most complete single specimens retrieved among basally branching eusauropods. *Spinophorosaurus nigerensis*, an early branching Eusauropod sauropod from the Middle Jurassic of Niger (Remes *et al.*, 2009; Mocho *et al.*, 2013), is one of the few sauropods known with a virtually complete and well-preserved neck (only missing the atlas). The exceptional preservation and completeness of this specimen has enabled to generate a virtual skeletal mount with less uncertainty than previous attempts. This accurate model has been used to reconstruct a “neutral” pose based on its osteology, with which the following analyses have been performed: osteological range of motion, myological reconstruction, muscle line of action estimation and volumetric reconstruction (see Chapter 2 for methods).

The obtained results were used to test the following hypotheses:

- (i) the body plan of the virtual *Spinophorosaurus* is similar to the reconstruction attempted in Remes *et al.* (2009);
- (ii) *Spinophorosaurus* was capable of high browsing, with greater range of motion than previously recognized in sauropods;
- (iii) the caudal musculature of *Spinophorosaurus* was more developed than that of Neosauropods;
- (iv) the overlapping chevrons at the distalmost preserved tail of *Spinophorosaurus* created an osteological stop which precludes motion in that sector of the tail;
- (v) the virtual skeleton of *Spinophorosaurus* can be used to refute poses previously proposed as habitual for sauropod dinosaurs.

Figure 3.1(next page) - *Spinophorosaurus nigerensis* holotype field quarry context.

A - General in situ situation of the holotype of *Spinophorosaurus nigerensis* during its excavation in “L’Homme Blanc” quarry at Azenak (Niger). **B** - Detail of the cervico-dorsal transition, damaged by a micro-fault, with the vertebrae outlined below in B'. **C** - Detail of caudal vertebra 15, damaged by the same micro-fault, with the vertebrae outlined below in C'.



3.2 SYSTEMATIC PALEONTOLOGY

Dinosauria Owen 1842 *sensu* Baron *et al.* 2017

Sauropodomorpha Huene 1932 *sensu* Sereno 2005

Sauropoda Marsh 1878 *sensu* Sereno 2005

Eusauropoda Upchurch 1995 *sensu* Sereno 2005

Spinophorosaurus nigerensis **Remes *et al.* 2009**

Holotype. GCP-CV-4229 / NMB-1699-R nearly complete specimen consisting of a partial skull (a braincase, postorbital, squamosal, quadrate, pterygoid, surangular), an almost uninterrupted axial sequence from the second cervical vertebra (axis) to the 31st caudal vertebra (60 vertebrae overall), all right-side ribs and most of the left ones and most chevrons, only missing those articulating with CdV4 and CdV13. The pectoral girdle is almost entirely represented, only missing one coracoid and the sternal plates (if they were ossified). No elements from the forelimb were retrieved. The pelvic girdle is almost completely represented, but some elements are damaged, as most of the left ilium and the distal left ischium. Only the right femur, tibia, fibula and astragalus were retrieved. The axial skeleton was found articulated, with girdles and limbs partially scattered

Paratype. NMB-1698-R partial skull and incomplete postcranial skeleton. Additional elements not preserved in the holotype individual include the premaxilla, maxilla, lacrimal, dentary, angular (most fragmentary), a complete set of right dorsal ribs, the humerus, and an isolated pedal phalanx. The identical morphology of the overlapping elements (postorbital, squamosal, pterygoid, surangular, teeth, axial skeleton, scapula) and the proximity of both skeletons in the same stratigraphical level (see below) justify their referral to the same species.

Referred specimens. GCP-CV-BB-15 A likely juvenile specimen, it preserves an almost complete cervical series from the axis to the first dorsal vertebra, two dorsal centra (one anterior and one middle), a mid dorsal neural arch and several cervical and dorsal ribs fragments. It shares most (but not all) of the diagnostic characters of *Spinophorosaurus* (Páramo & Ortega, 2012) and is currently under description by Adrián Páramo.

Locality and horizon. All specimens were collected in an area north of the Rural Community of Aderbissinat (Thirozerine Dept., Agadez Region, Republic of Niger), stratigraphically below the outcrops of the Tegama Group in the “Falaise de Tiguidit”. Holotype and paratype were found in the same level of this layer, about 15 meters laterally apart from each other on the upper unit (Remes *et al.*, 2009). The age of this horizon is not well-established, but it is likely to range from Middle to Upper Jurassic (Rauhut & López-Arbarello, 2009; Remes *et al.*, 2009).

Diagnosis. Modified after (Remes *et al.*, 2009). Autapomorphies marked with an asterisk (*). A small pineal foramen that opens dorsally between the contralateral frontals, not parietals*; laterally oriented basal tubera*; cervical vertebrae with U-shaped recess between centrum and interpostzygapophyseal lamina (tpol) in lateral view*; spinodiapophyseal laminae (spdl) restricted to sacral vertebrae; apex of proximal and middle caudal neural spines saddle-shaped*; bifurcated distal chevrons transformed into overlapping rod-like horizontal elements whose cranial and caudal projections contact at the level of the middle part of the vertebral centra*; kidney-shaped coracoid*; ossified clavicles and interclavicle; femur shaft with large foramen on its caudal side, lateral to the fourth trochanter*.

Personal description/remarks. Some axial skeleton elements of the holotype (GCP-CV-4229/NMB-1699-R) where damaged by micro-faults, but their relative position was not very distorted. The general outline was preserved faithfully on the second dorsal (Fig. 3.1 B) and a little more damaged in the case of the 15th caudal vertebra (Fig 3.1 C), but with enough detail to allow a digital reconstruction minimizing speculation (see below 3.3). It is possibly a subadult specimen, as it has unfused arches and centra in most vertebrae and sutures still visible in those vertebrae with fused centra and arches and is smaller than the paratype (which has ossified vertebrae and is histologically an adult, see below) (Fronimos & Wilson, 2017). However, since neurocentral suture fusion may not be the most reliable indicative of ontogenetic state (Brochu, 1996; Irmis, 2007), its subadult status must be considered tentative and to be tested by histological sampling in the future. However, thorough this paper both “subadult” and “holotype” will refer to this specimen.

The paratype specimen (NMB-1698-R) preserves fewer elements than the holotype, among them six cervical vertebrae, four with remarkably well-preserved pre- and postzygapophyses. It is not a fully grown adult, but appears to be in a more advanced stage in its ontogeny than the holotype, since most bones are larger than the same bones on the holotype, the neurocentral sutures are closed and not visible, but the cervical ribs and scapula and coracoid are unfused. Recent histological analyses have found it not only to be an adult, but also to have survived an osteological tumor-like pathology which caused radial fibrolamellar bone (Jentgen-Ceschino, Stein, & Fisher, 2019).

The likely juvenile specimen (GCP-CV-BB-15) has one cervical vertebra (CV6) very damaged. The neurocentral sutures are open, the centra are less elongated than on the holotype and paratype and the vertebrae are a quarter the size of the holotype. The third specimen was found *ex-situ* in the surface, but with most elements articulated and no duplicity in vertebrae, so it can be considered a single specimen. The lithology of the matrix containing this specimen is identical to both holotype and paratype, and the absence of relief and being found near the upper unit close to both specimens likely means that it stems from the same horizon.

3.3 ASSEMBLING THE VIRTUAL SKELETON

The postcranial skeleton of the holotype specimen is nearly complete, and thus the assemblage of the axial skeleton, girdles and hindlimb (except for most of the pes) could be carried out with less uncertainty than skeletons assembled from bones stemming from multiple individuals. Only a few elements had to be interpolated, with estimated proportions and size-based (see above and table 3.1) were articulated unmodified, and no further size or proportion adjustments were needed. The majority of fossil bones are very well-preserved, with only a few elements having shear deformation altering bilateral symmetry.

Axial skeleton

As described in Chapter 2, the axial skeleton was assembled in osteologically neutral pose (ONP) in ZBrush 4R6, with only one pair of vertebral elements visible at one to minimize preconceived notions. The osteologically induced curvature (OIC) of the axial skeleton is as follows (Fig. 3.2):

- I) Cervical vertebrae articulate almost straight, but with a slight sigmoidal dorsal deflection. The posterior half of the neck (CV12-CV6) describes a very straight yet slightly dorsally sloping posture, while the anterior half is more dorsally deflected at the CV6-CV5 and particularly CV5-CV4 joints than preceding joints. Finally, a ventral deflection occurs at cervical vertebrae CV3 and the axis. It is therefore, though slightly different, in accordance with previous results on sauropodomorph neck ONPs such as *Plateosaurus* (Mallison, 2010b), *Mamenchisaurus* (Christian *et al.*, 2013), *Diplodocus*, *Apatosaurus*, *Camarasaurus* or *Giraffatitan* (Stevens, 2013). The condyles fit deeply in the cotyles, so there is no evidence of strong inter-vertebral space on this specimen.
- II) Dorsal vertebrae articulate as a straight line dorsally deflected about 5° due to the slight acute wedging of the posteriormost two dorsal vertebrae. There is no evidence of an arched dorsal series often reconstructed for other sauropods. This is due all the centra from DV11 to DV1 have their rims subparallel, and therefore there are no obtuse wedged vertebrae which can cause the back to be arched. The anteriormost ribs (1st to 3rd) are particularly straight, as are in other known sauropods such as *Overosaurus* (Coria *et al.*, 2013; Chaper 5). When the ribs are totally articulated with the diapophyses and parapophyses, the shape of the anterior region of the ribcage is bell shaped in anterior view (Fig. 3.3 A). The anterior ribs are posteriorly directed in lateral view. The only mid or posterior fossil rib yet prepared and available for digitization is the 10th dorsal rib, which would not have articulated with the sternum, makes a ribcage more barrel-shaped by the 10th dorsal vertebra (Fig. 3.3 C). The 10th dorsal rib points also posteriorly, but at a much lesser angle than dorsal ribs 1-3.
- III) Caudal vertebrae also describe a sigmoid curvature, more pronounced than that of the neck. A slight ventral deflection of CdV1-12, more pronounced at the anterior half, changing gradually to a very slightly dorsally deflected region from CdV13-27, to gradually shift again to a slight ventral deflection until the last preserved vertebrae. This ventral deflection is

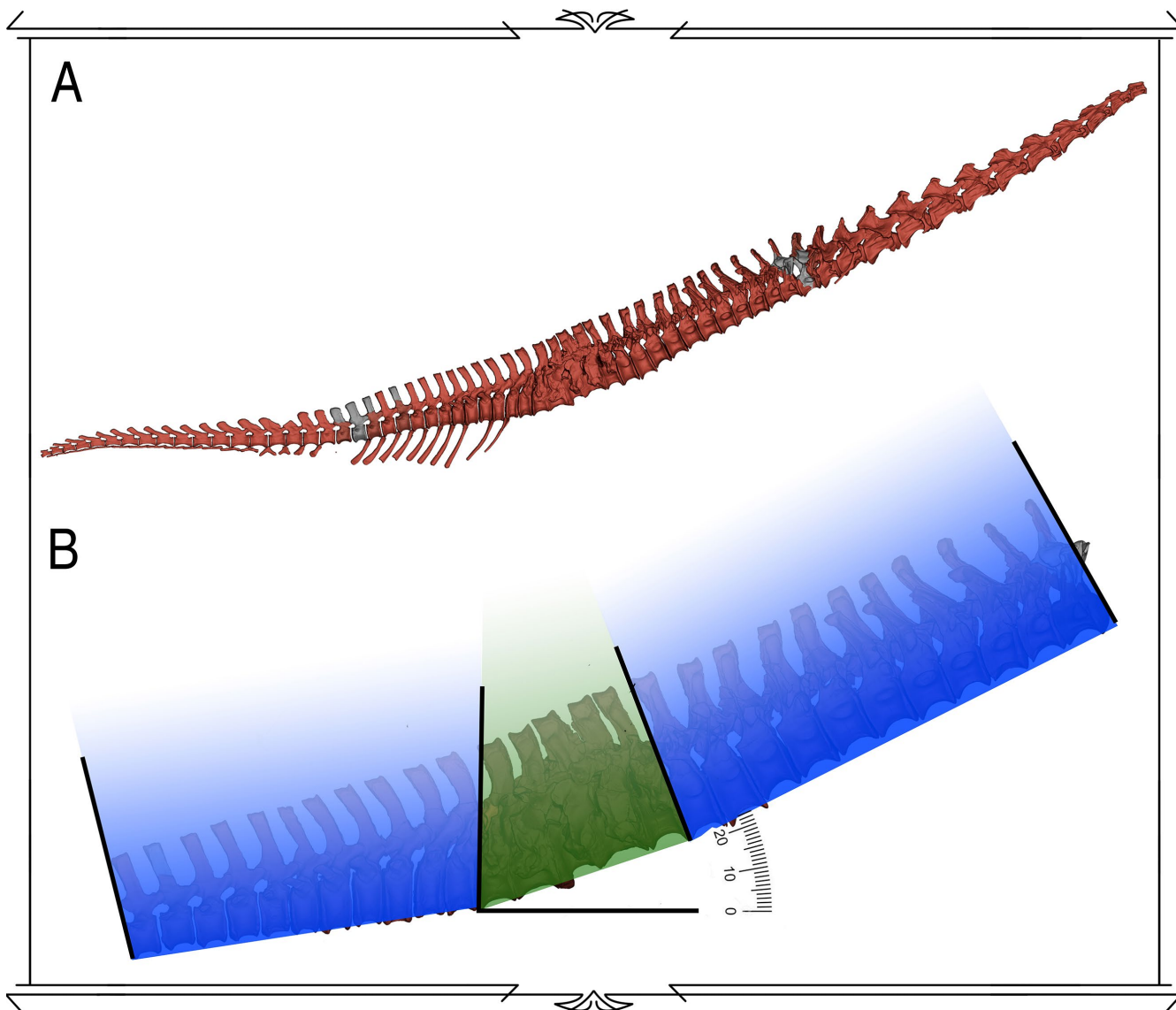


Figure 3.2 - Virtual articulation of *Spinophorosaurus nigerensis* vertebral column.

A - Osteologically induced curvature of the vertebral column of *Spinophorosaurus nigerensis* in lateral view. Red = bones from holotypic specimen. Gray = reconstructed bone based on closely, non-damaged preserved elements from the same individual. **B** - Detail on the sacrum of *S. nigerensis*, showing how it makes deflect the dorsal vertebrae 20° from the first caudal vertebra in lateral view.

very slight, and most of the distal-most preserved caudal vertebrae articulate in an almost straight line, with the bifurcated chevrons overlapping. These chevrons overlap from CdV21 until CdV29, making that segment to articulate almost straight. Field evidence reveals the posterior region of the chevron overlaps laterally the following chevron, which is situated medially to the preceding chevron. The chevrons in CdV30 do not overlap with those on CdV29. All in all, CdV32 just deflects 5° ventrally from CdV1 due to the sigmoidal curvature of the tail.

- IV) The wedged sacrum makes DV13 deflect 20° dorsally from CdV1 (Fig 3.2 B). Therefore, the overall spine articulates with a subhorizontal tail and a dorsally sloping presacral column, with the skull deflecting 30° from the first caudal.

Scapular Girdle

The controversies regarding the placement of the pectoral girdle in the sauropod ribcage has been summarized on Chapter 2. Overall, the most likely hypothesis consists of a subvertical scapula with the scapular head anterior to the ribcage and the coracoids antero-ventral to the ribcage (Fig. 3.4 A). The completeness of

Taxa	Sc Length	H Length	F Length	F/H Ratio	Sacrum Angle
<i>Spinophorosaurus nigerensis</i> GCP-CV-4229	1243	1014*	1215	1.20	20.1
<i>Shunosaurus lii</i> ZDM T5402	902	670	1200	1.79	14.7
<i>Mamenchisaurus youngi</i> ZDM0083	1190	825	1160	1.40	15.8
<i>Omeisaurus tianfuensis</i> ZDM T5704	1330	1040	1280	1.23	18.5
<i>Jobaria tiguidensis</i> MNN TIG4	?	1040*	1800	1.73	15.0
<i>Dicraeosaurus hansemanni</i> MB.R.4886	?	620 *	1220	1.96 *	11.0
<i>Diplodocus carnegii.</i> CM94	1240	?	1542	?	16.0
<i>Apatosaurus louisae</i> CM3018	1640	1150	1785	1.55	15.5
<i>Brontosaurus excelsus</i> YPM 1980	?	1114	1910	1,72	15.0
<i>Tehuelchesaurus benitezii</i> MPEF-PV-1125	1801	1183	1550	1.31	20?
<i>Camarasaurus grandis</i> YPM 1901	1.155	856	1172	1.37	17.5
<i>Brachiosaurus altithorax</i> FMNH P25107	?	2042	2025	0.99	28.8
<i>Giraffatitan brancai</i> MB.R 2181 (formerly SII)	1930	2130	1990 *	0.93	25.0
<i>Dreadnoughtus schrani</i> MPM PV 1156	1772	1600	1910	1,19	21.1
<i>Opisthocoelicaudia skarzynskii</i> ZPAL MgD1/48	1180	1000	1395	1,39	14.1
<i>Kotasaurus yamanpalliensis</i>	?	*770	1130	1,46 *	3.7
<i>Melanorosaurus readi</i> NM QR1551	489	450	638	1,41	1.0
<i>Lufengosaurus huenei</i> IVPP 15	?	335	560	1.67	5.4
<i>Jingshanosaurus xinwaensis</i> LFGT-ZLJ0113	?	470	850	1.80	1.5
<i>Yunnanosaurus huangi</i> IVPP V20	305	231	435	1,88	2.1

Table 3.1. Length measurements and ratios of different sauropod taxa, with specimen number indicated.

Asterisk (*) indicates estimated measurements scaled from other specimens of the same species (see Supplementary Material). The sacrum angle and F/H ratio are plotted in the XY graphic on Figure 2B. All lengths in mm. Angles in degrees. Sc = scapula, H = humerus, F = femur.

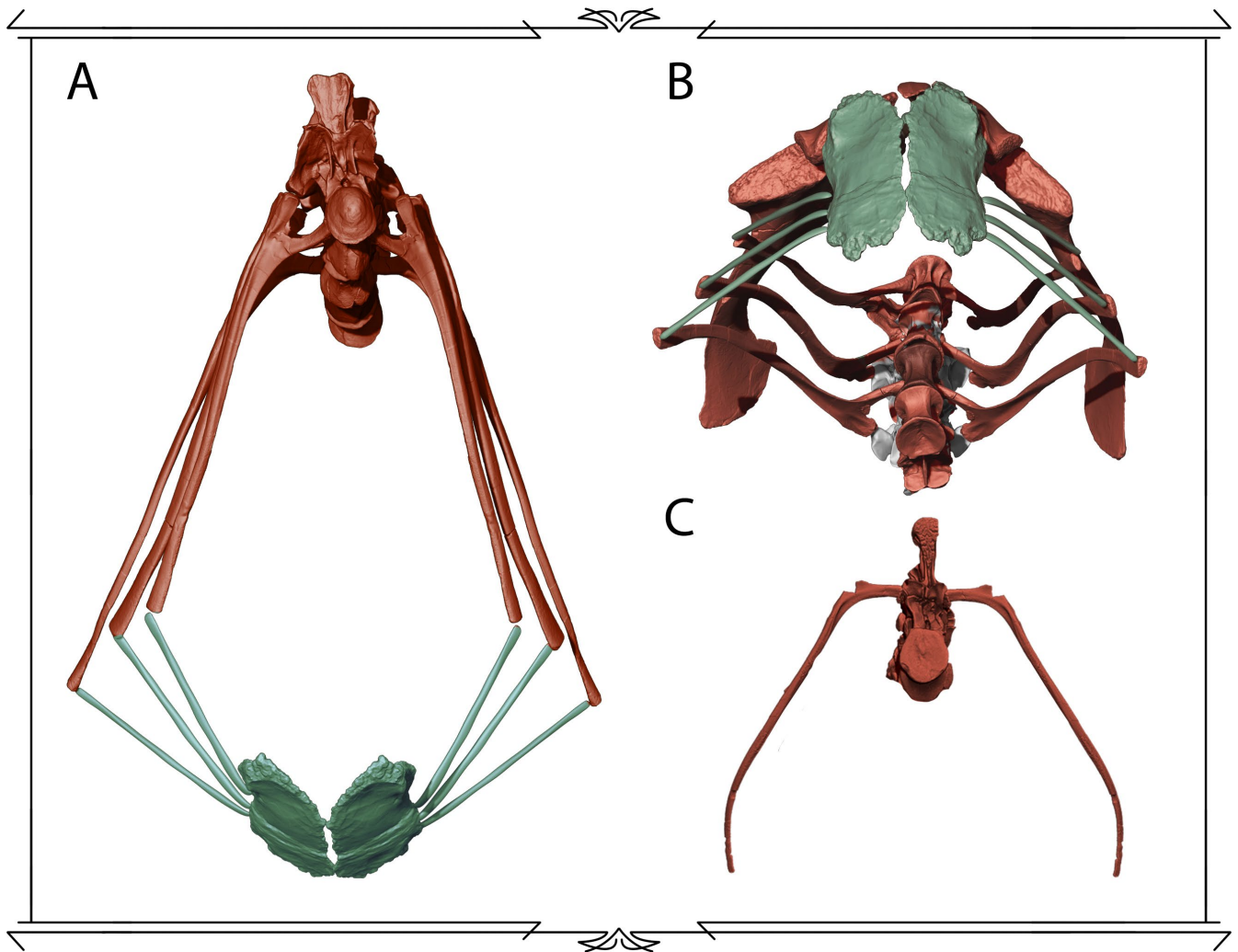


Figure 3.3 - Virtual reconstruction of the ribcage of *Spinophorosaurus nigerensis*.

A - Ribcage in anterior view, at dorsal vertebra 1 level. Red = bones from holotypic specimen. Blue = Sternal plates and sternal ribs, after those of other sauropods (Filla & Redman, 1994; Tschopp & Mateus, 2013) clavicles and sternal ribs are known in a variety of reptilians, including dinosaurs. In sauropods, however, the identity of these bones is controversial. The peculiar shapes of these bones complicate their identification, which led to various differing interpretations in the past. Here we describe different elements from the chest region of diplodocids, found near Shell, Wyoming, USA. Five morphotypes are easily distinguishable: (A. **B** - Ribcage and pectoral girdle in ventral view, showing the glenoid cavity free of rib or sternal ribs, making humeral articulation possible. Gray = reconstructed bone based on closely non-damaged preserved elements from the same individual. **C** - Ribcage in anterior view, at dorsal vertebra 10 level.

the pectoral girdle and anterior dorsal ribs of *Spinophorosaurus nigerensis*, however, allowed testing different configurations to see which were possible:

Hypotheses for pectoral girdle-axial skeleton configurations were rejected if: i) the pectoral girdle would not fit the ribcage, ii) the pectoral girdle elements had to be disarticulated, iii) the lines of actions for cingulo-axial and humeral muscles were non-functional, iv) the humerus could not be correctly articulated in the glenoid.

A subhorizontal placement of the scapula impedes articulating the clavicles and interclavicle with the acromia and coracoids respectively, as the ribcage makes separating the scapulocoracoids necessary to pose the girdle this way (Fig. 3.4 B). It also creates inefficient lines of action for some muscles, such as the *M. deltoideus scapularis* (Remes, 2007).

The subvertical scapula of the 2009 reconstruction, which has the acromia at the same height as the ventral edge of the dorsal vertebrae centra, also impedes articulating the pectoral girdle (Fig. 3.4 C). Also, since the length of the anteriormost two dorsal ribs reconstructed in 2009 was 25% shorter than the actual first two dorsal ribs of the *Spinophorosaurus* holotype, the glenoid would be situated more dorsal than the distal dorsal ribs (Fig. 3.4 C). This impedes to articulate the humerus in a columnar, graviportal way and also creates an osteological stop for retracting the humerus. Also, placing the scapular head in articulation with the dorsal ribs creates an osteological stop for *M. subcoracoscapularis pars scapularis*, which has its origin on the acromial region, on the medial side (Remes, 2007; Hohn-Schulte, 2010).

Only subvertical scapulae with the coracoid and the scapular head antero-ventral to the ribcage allows:

- i. To correctly articulate the clavicles and interclavicles to the condition present in non-mammalian tetrapods (clavicles to acromia, both with interclavicle, interclavicle with coracoids and sternum (Tschopp & Mateus, 2013).
- ii. To place the sternal plates parallel to the distal tips of the anterior dorsal ribs, so that they both can articulate with the sternal ribs as in extant archosaurs and lepidosaurs (Schwarz *et al.*, 2007a).
- iii. To have room for a cartilaginous suprascapula with an homologous muscular and ligament attachment to the neural spines as in extant archosaurs (Remes, 2007; Schwarz *et al.*, 2007a).
- iv. To articulate the forelimb so that the front feet step at the same medio-lateral distance from the sagittal plane of the skeleton than the hind feet, over the midline. Just as the ichnological evidence shows is the case narrow-gauge sauropod track-makers (Carrano, 2005), since the pelvis of *Spinophorosaurus* is narrow and the feet of the reconstructed skeleton step over the midline.

It is the only position which the osteological, myological and ichnological evidence would not refute.

Pelvic Girdle.

As for the pelvic girdle, the sacrum and preserved ilium suffered from compression as the rest of the axial skeleton, but the pubes and ischia were not heavily distorted. By articulating both pubes and ischia, the distance of the left and right articulation with the ilia helped in reconstructing a model close to the original width of the pelvis. The pelvis is narrow, and therefore the hind limbs articulate so that the hind feet can step over the midline of the dinosaur, as would be expected for an early branching non-neosauropod eusauropod (Carrano, 2005).

Appendicular Skeleton

In order to reconstruct missing bones from the holotype specimen, the approach was a combination of scaling known elements in the paratype and phylogenetic interpolation for elements unknown in both specimens.

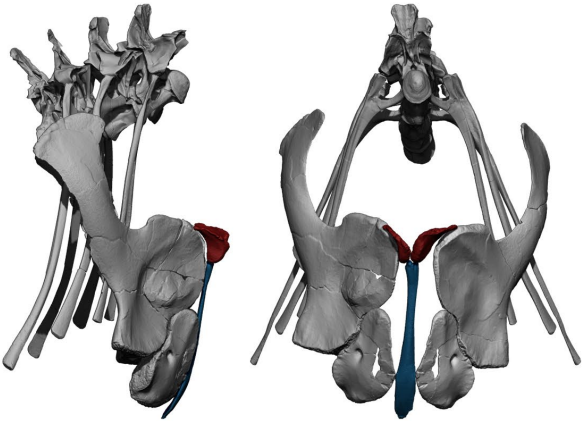
The forelimb is completely unknown in the holotype specimen of *Spinophorosaurus nigerensis*. The paratype, however, preserved both humerus and scapula. Since the scapulae of both holotype and paratype are complete and the greatest scapula length to greatest humerus length ratio appears to be characteristic at the genus level (Table 3.2), even maintaining similar proportions in different ontogenetic stages at least in *Camarasaurus* (Table 3.2), the holotype was assumed to have had the same humerus to scapula ratio as the paratype (Fig. 3.4 E)

For both antebrachium bones (ulna and radius) are unknown in both specimens. In order to estimate how large they might have been, proportions between humerus and ulna were calculated for sauropod

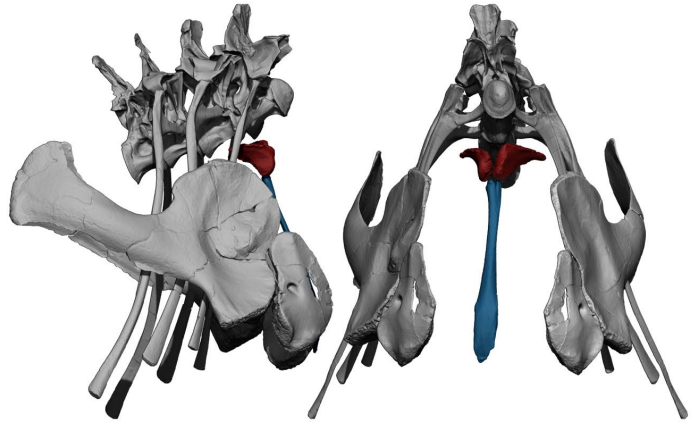
Figure 3.4 (next page) - Girdle and limbs articulation in *Spinophorosaurus nigerensis*.

A - Virtual pectoral girdle as mounted for the virtual reconstruction in lateral (left) and anterior (right) view. The coracoids and scapulae are in articulation with the clavicles and interclavicle, the scapular head and coracoid anteroventral to the ribcage and the longest axis of the scapula with a subvertical inclination. **B** - Traditional reconstruction for sauropod pectoral girdle, in lateral (left) and anterior (right) view. The longest axis of the scapula is subhorizontal. This posture is impossible to attain without disarticulating the scapula and coracoids from the clavicles and interclavicle and is therefore not supported according to present evidence. **C** - Pectoral girdle positioned as in the reconstruction by Remes *et al.* (2009) in lateral (left) and anterior (right) view. The original 2009 reconstruction underestimated the actual length of the ribs, which would occupy the glenoid, making humeral articulation impossible. Also, by articulating the girdle more dorsally, the shape of the ribcage does not allow articulating scapulae and coracoids with clavicles and interclavicle. This position is not supported with present evidence. **D** - Pelvic girdle and sacrum in lateral (left) and medial (right) view. The pelvis is oriented with a mesopubic condition present in all sauropods (Rasskin-Gutman & Buscalioni, 2001), showing the coalesced, wedged sacrum causes a change in the axial skeleton curvature due to its morphology. **E** - Comparative measurements of the scapulae of holotype and paratype used to estimate humerus size for the holotypic specimen. Measurements in mm.

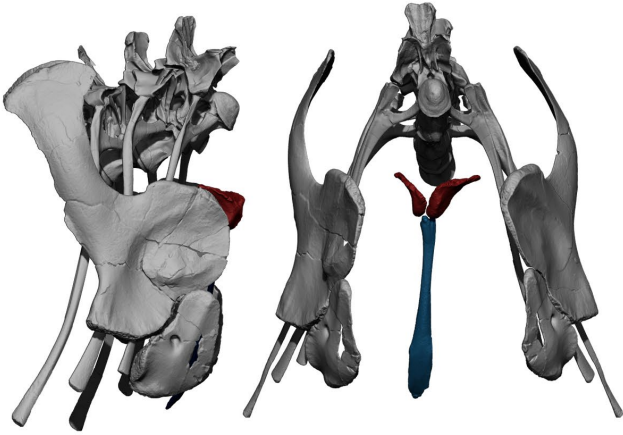
A



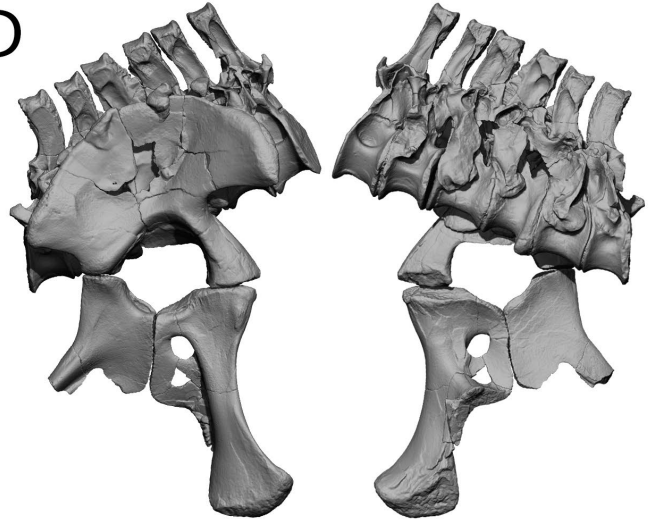
B



C



D



E

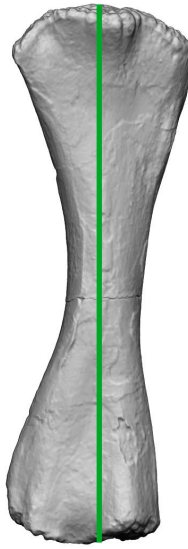
X = 1007



Y = 1243



X' = 1121



Y' = 1374



HOLOTYPE GCP-CV-4229

PARATYPE NMB-19668-R

Species	H/Sc	U/H	Mc/U	F/H
<i>Spinophorosaurus nigeriensis</i> NMB-1968-R	0.816	?	?	1.19*
<i>Shunosaurus lii</i> ZDM T5402	0.74	0.7	0.36	1.79
<i>Patagosaurus fariasi</i> MACN-CH 932 (juvenile)	0.83	0.74	?	?
<i>Cetiosaurus oxoniensis</i> OUMNH lectotype	0.91	0.73	?	1.28
<i>Cetiosauriscus stewarti</i> NHMUK R3078	?	0.80 **	?	1.44
<i>Klamelisaurus gobiensis</i> IVVP # V9492	0.70	0.65	?	1.30
<i>Omeisaurus tianfuensis</i> ZDM T5704	0.71-0.78	0.8	0.3	1.21-1.23
<i>Omeisaurus jiaoi</i> ZDM 5050	0.71	0.76	?	1.20
<i>Mamenchisaurus youngii</i> ZDM 0083	0.69	0.69	0.39	1,40
<i>Ferganasaurus verzilini</i> PIN-N-3042	?	0.71	0.35	1.21
<i>Turiasaurus riodevensis</i> CPT-1195 to CPT-1210	?	0.7	0.34	?
<i>Mierasaurus bobyongi</i> UMNH VP.26004	?	?	0.44	?
<i>Dicraeosaurus hansemanni</i> MB.R.4886	?	0.66	?	1.96 *
<i>Amargasaurus cazau</i> MACN-N-15	0.68	0.67	?	1.52
<i>Apatosaurus louisae</i> CM 3018	0.7	0.74	0.33	1.55
<i>Diplodocus</i> sp. USNM 10865	0.87	0.73	?	1,58
<i>Giraffatitan brancai</i> MB.R 2181 (formerly SII)	1.10	0.61	0.48	0.93*
<i>Brachiosaurus altithorax</i> FMNH P25107	?	?	?	0.99
<i>Tehuelchesaurus benitezii</i> MPEF-PV-1125	0.65	0.67	?	1.31
<i>Camarasaurus grandis</i> YPM 1901/1905 (subadults)	0.74	0.77	0,43	1,37
<i>Camarasaurus lentus</i> CM 11338 (juvenile)	0.73	0.74	0.42	1.36
<i>Catethosaurus lewisii</i> BYU 9047	?	0.76	0.41	?
<i>Epachthosaurus sciutto</i> UNPSJB-PV-920	?	0.69	0.52	
<i>Dreadnoughtus schrani</i> MPM PV 1156	0.91	0.63	?	1.19
<i>Opisthocoelicaudia skarzynskii</i> ZPAL MgD1/48	0.84	0.78-0.67	0.4	1.39

Table 3.2. Limb bone length ratios in several sauropod dinosaurs

One asterisk (*) indicates when ratios are estimated from bones stemming from different but similarly sized specimens. Two asterisks (**) indicate dubious measurements due to restoration not allowing to appreciate the actual length of the bone. Sc = Scapula. H = Humerus. U = Ulna. Mc = Longest Metacarpal.

specimens that preserved all the elements (Table 3.2). The most parsimonious estimates for greatest ulna length to greatest humerus length ratio range from 0.7 to 0.8. That estimate for *Spinophorosaurus* implies the proportions between the ulna relative to the humerus were the same as in its closest relatives, non-neosauropod eusauropods which preserve forelimbs from a single specimen (Table 3.2). Metacarpal length was established the same way, scaling the longest metacarpal with the ulna (Table 3.2). The most parsimonious estimates for greatest metacarpal length to greatest ulna length ratio for *S. nigeriensis* range from 0.35 to 0.39.

The estimated possible lengths for the ulna, radius and longest metacarpal are in Table 3.3, but on the skeletal reconstruction the exact values (the minimum length needed for the hand to reach the ground) were a 748 mm ulna and a 278 mm longest metacarpal. Both values are closer to the shorter end of the spectrum of the

estimated lengths (Table 3.3). These estimates therefore consider no abrupt changes in forelimb proportions occurred in *Spinophorosaurus* relative to closely related sauropods: it is a more parsimonious hypothesis than assuming a proportionately longer or shorter forearm and/or hand.

Regarding the feet, the astragalus from the holotype specimen is the only foot element preserved in *Spinophorosaurus*. Since most eusauropod feet phalanges are fairly similar, a generic pes (minus the astragalus) based upon *Turiasaurus* (Royo-Torres, Cobos, & Alcalá, 2006), *Shunosaurus* (Zhang, 1988), *Cetiosauriscus* (Woodward, 1905), and *Ferganasaurus* (Alifanov & Averianov, 2003) was used as a placeholder.

Once missing appendicular skeleton elements were obtained, it was articulated in ONP with the scapular and pelvic girdles, then posed in a fast walking gait for the figures. The length of the speculative ulna and longest metacarpal of the virtual model are 748 mm and 278 mm, respectively, both values within the inferior ranges of estimated length for those bones (Table 3.2)

Element	Length (Paratype)	Length (Holotype)
Longest metacarpal	275-350**	248-316**
Ulna	785-897**	710-810**
Humerus	1121	1014*
Scapula	1374	1243

Table 3.3. Limb and pectoral girdle measurements and estimations in *Spinophorosaurus nigerensis* specimens

Estimated measurements are indicated with an asterisk (*) when based upon another specimen of *Spinophorosaurus nigerensis*, and two asterisks (**) when they are based upon other sauropod relatives (see “Reconstruction of missing elements” above). Measurements in millimeters.

3.4 SPINOPHOROSAURUS BODY PLAN

Mounting the digital skeleton has revealed that *Spinophorosaurus* had tall shoulders and an elevated neck well above shoulder level when in OIC (Fig. 3.5). The resulting body plan, analogous to that of the more extremely verticalized brachiosaurid sauropods, is the result of two main skeletal characters:

- (i) An elongated forelimb, the humerus being longer relative to the scapula and femur than those of most other sauropods, and the scapula being slightly longer than the femur (Table 3.1).
- (ii) An acute wedged sacrum and posteriormost dorsal vertebrae, which deflect the presacral vertebrae dorsally in neutral articulation (Fig. 3.5).

Given the position of the pelvis in Sauropoda, with an antero-posteriorly projected ilium and a mesopubic and opisthoischial condition (Rasskin-Gutman & Buscalioni, 2001), which allows the femur to be upright and graviportal, the coalesced sacrum is situated so that the posterior face of the last sacral centrum is sub-vertical. This makes the tail sub-horizontal and the presacral series to slope antero-dorsally.

This way, when the last dorsal vertebra articulates with the sacrum, it deflects 20° from the centrum of the first caudal vertebra in lateral view (Fig. 3.2 B). In addition, the slightly wedged centra of the two last dorsal vertebrae (Fig. 3.5 B) deflect the dorsal series further, making the first dorsal vertebra deflect 5° from the last dorsal centrum (overall 25° from the first caudal). The cervical series is almost straight, but with a slight sigmoidal dorsal deflection, with the axis deflecting 5° from the first dorsal vertebra (overall 30° from the first caudal), a little different from the straight and slightly ventrally deflected posture previously described for other sauropods (Stevens & Parrish, 1999, 2005). When using the lateral semicircular canals (LSCs) of the inner ear (Knoll *et al.*, 2012) to reconstruct the position of the skull, it forms an angle of 10° with the neck, compatible with the non-deflected, osteologically induced curvature of the presacral vertebrae (Fig. 3.5).

When all scapular girdle bones remain in articulation and are situated in the ribcage following the results of independent studies on osteological, myological and phylogenetic bracketing evidence, the scapular girdle is mounted with: sub-vertical scapulae, coracoid antero-ventral to ribcage, scapular head anterior to the ribcage and glenoid a bit ventral to the distal anterior dorsal ribs. This allows for an upright articulation of the humerus, as is known to be the condition for sauropods. The distal humerus to floor distance is 1.11 m.

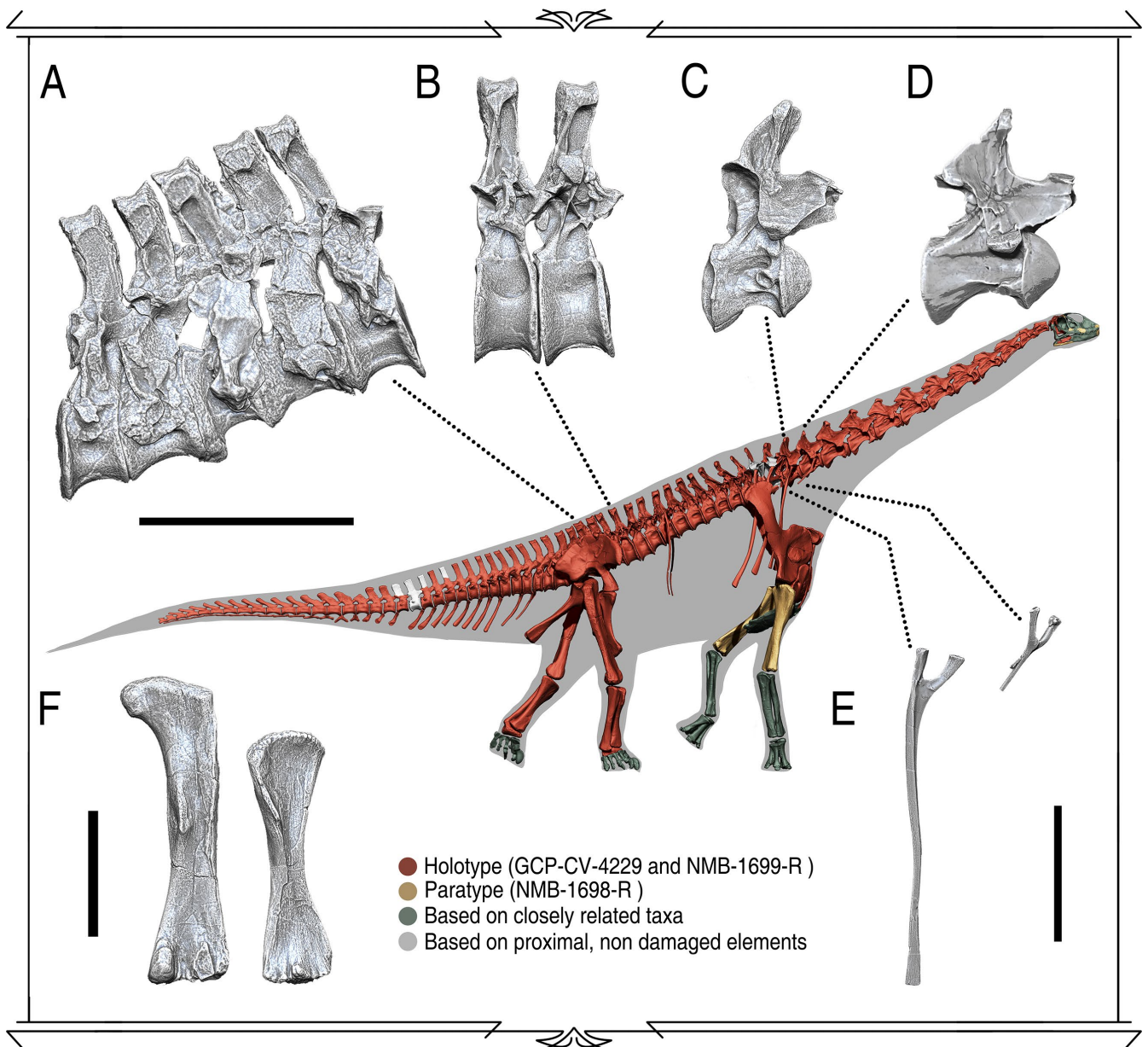


Figure 3.5 - Virtual skeletal reconstruction and high browsing adaptations in *Spinophorosaurus nigerensis*.

Skeletal reconstruction in osteologically neutral pose with bones color-coded according to their provenance, with the holotype in red, paratype in yellow, and bones inferred from close relatives in green. Gray indicates reconstructed bone. **A** - Sacrum, showing the 20° angle wedging. **B** - 12th and 13th dorsal vertebrae, showing a slight acute wedging. **C** - Partially cervicalized 1st dorsal vertebra. **D** - 12th Cervical Vertebra. **E** - First dorsal and last cervical ribs. **F** - Humerus and femur, to scale. Scales A-F = 500 mm.

The forearm and hand are not yet known in any *Spinophorosaurus* specimen. However, the aforementioned distance implies a forearm (0.748 m ulna) and hand (0.278 m metacarpal III + 0.06 m carpals) with similar proportions relative to the humerus to those of individuals of closely related non-neosauropod Eusauropoda (Table 3.2). These reconstructed forearm and hand are, therefore, more parsimonious than assuming a proportionately longer or shorter forearm and/or hand.

Summing up, the osteologically induced curvature of the presacral column of *Spinophorosaurus* makes its skull deflect 30° dorsally from the first caudal vertebra in osteologically neutral posture, with the snout situated at about 5 m above the ground, more than twice as high as the shoulder and acetabulum, at 2.15 m, very different from previous reconstructions (Fig. 3.6).

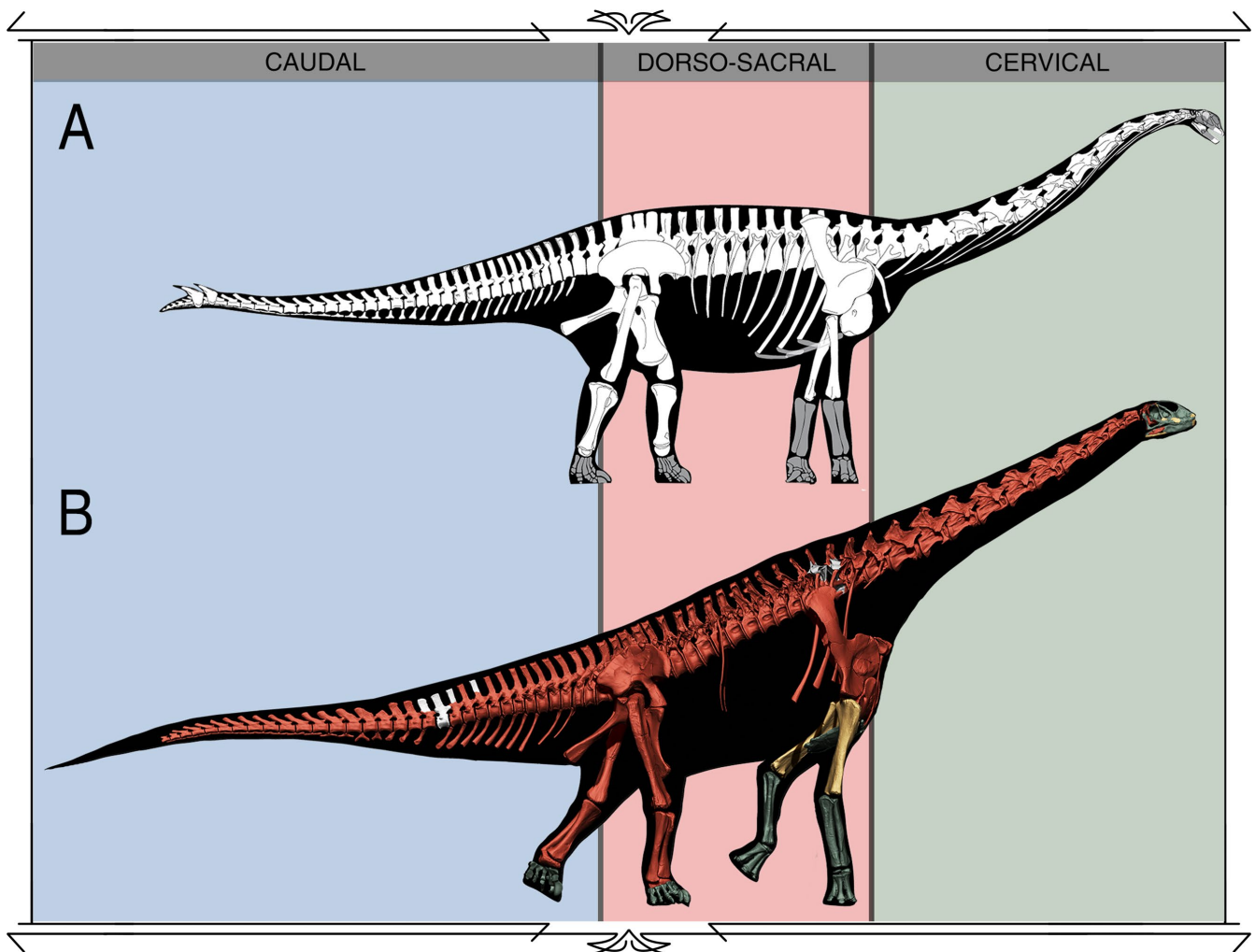


Figure 3.6 - Skeletal reconstructions of *Spinophorosaurus nigerensis*.

A - Original skeletal reconstruction of *Spinophorosaurus* first published in 2009, modified from the original publication (Remes *et al.*; 2009) **B** - Virtual skeletal reconstruction of *Spinophorosaurus*. All the skeletal reconstructions have been scaled to the same dorso-sacral sector length (between the last sacral vertebra and the first dorsal vertebra). Previous reconstruction lacked information on precise sacrum morphology, hence the radically different osteologically induced curvatures of the presacral vertebrae. Other bones that differ between the 2009 reconstruction and actual fossils (as further preparation has been carried out) are the ilium, the first 3 dorsal ribs, the cervicodorsal transition and the anterior caudal vertebrae.

3.5 OSTEOLOGICAL RANGE OF MOTION ANALYSES

Osteological range of motion (ROM) is the first line of evidence regarding the motion capabilities of an extinct vertebrate, being the easiest way to refute a posture or motion (Mallison, 2007, 2010b). ROM only refers to the osteological capabilities of an extinct vertebrate, with further evidence required to assess the paleobiology of an extinct taxon.

Cervical Vertebrae

The osteological ROM of the holotype *Spinophorosaurus* can be better estimated in the antero-posterior axis in all joints, since the medial portion of the prezygapophyses is obscured in most vertebrae, as they could not be separated from the preceding vertebra during preparation. The lateral range of motion is more dubious, so the only considered postures were those in which the portion of the prezygapophyses overlapped was not extrapolated and was visible in the actual fossil.

The neck of *Spinophorosaurus* has 12 moderately elongated cervical vertebrae (largest average Elongation Index, aEI = 3.63, see Terminology in Chapter 2 for more details) with two features increasing range of motion

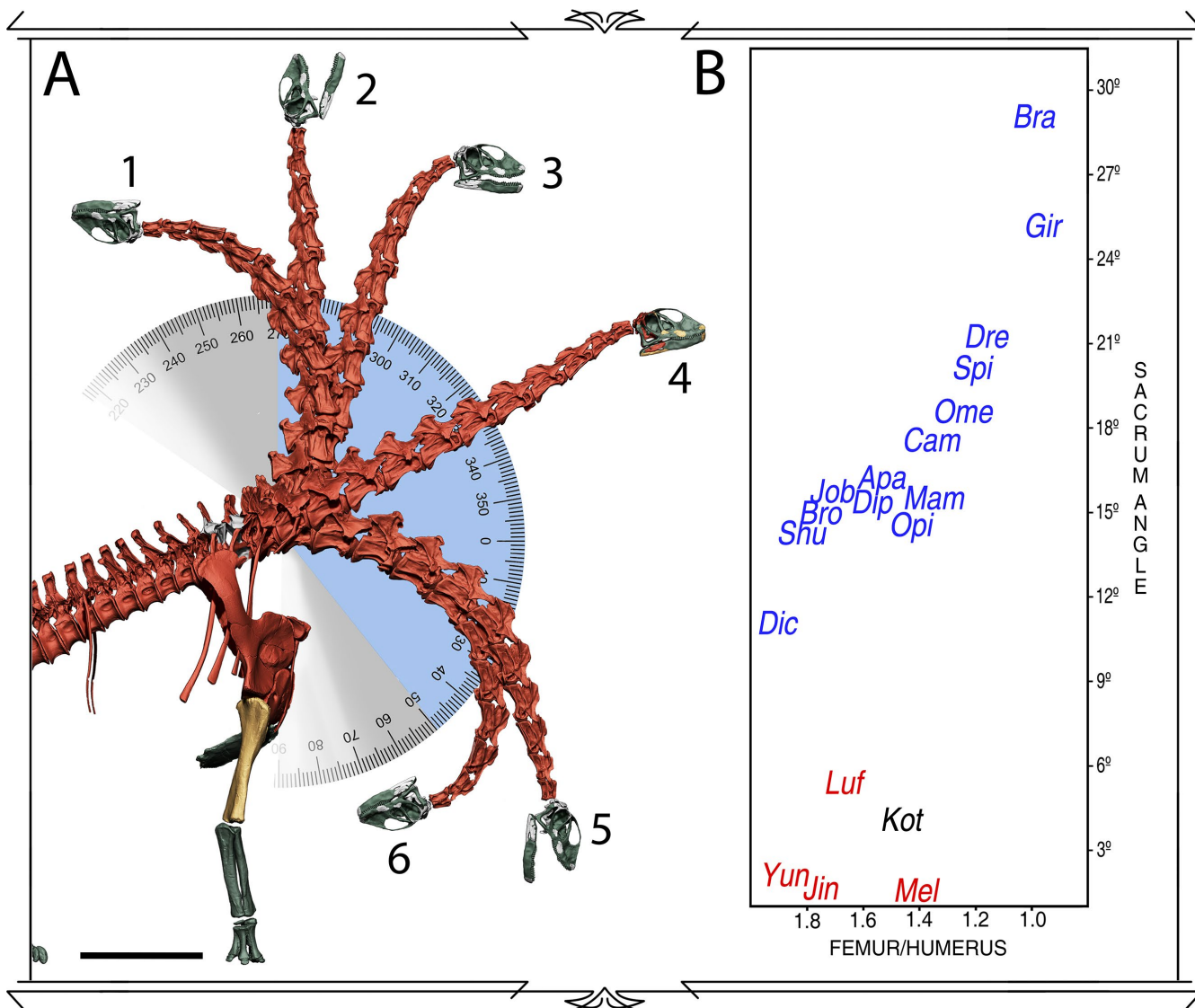


Figure 3.7 - The verticalization of the feeding envelope of *Spinophorosaurus nigerensis*.

A - Increased neck range of motion in *Spinophorosaurus* in the dorso-ventral plane, with the first dorsal as the vertex and the 0° marking the ground. Poses shown: (1) maximum dorsiflexion; (2) highest vertical reach of the head (7.16 m from the ground), with the neck 90° deflected; (3) alert pose *sensu* Taylor *et al.* (2009); (4) osteological neutral pose *sensu* Stevens (2013); (5) lowest vertical reach of the head (0.72 m from the ground at 0°), with the head as close to the ground without flexing the appendicular elements; (6) maximum ventriflextion. Blue indicates the arc described between maximum and minimum head heights. Gray indicates the arc described between maximum dorsiflexion and ventriflextion. **B** - Bivariate plot comparing femur/humerus proportion with sacrum angle. The proportion of humerus and femur are compared as a ratio of humerus maximum length / femur maximum length. Sacrum angle measures the angle the presacral vertebral series are deflected from the caudal series by sacrum geometry in osteologically neutral pose. Measurements and taxa on Table 3.1. Scale = 1000 mm.

in the dorso-ventral plane. The prezygapophyseal facets on the cervical vertebrae are particularly antero-posteriorly elongated next to those of other sauropod cervical vertebrae. These elongated articulation facets provide a greater range of motion per joint than in other sauropods in comparable joint positions (Fig. 3.7).

Cervical vertebra 12 has all traits expected of a cervical, including a short and small cervical rib, but while the first dorsal vertebra of *Spinophorosaurus* shows a tendency to cervicalization, it already bears a dorsal rib (Fig 3.5 E). This vertebra is more elongated than any of the other dorsal vertebrae and its centrum has a trapezoidal shape in lateral view (its anterior condyle is more dorsally located than the cotyle). Also, the prezygapophyseal rami are anteriorly projected, the prezygapophyseal facets have the same elongation present in the preceding cervical vertebra and the ventral keel is very pronounced. Most of these characters are missing in the second dorsal vertebra (Table 3.4). This partial cervicalization makes the first dorsal vertebra a functional cervico-dorsal vertebra, sharing many convergences with the cervicalized first thoracic vertebra of giraffes: longer than wide prezygapophyseal facets, a ventral keel in the centrum or a centrum length intermediate between that of the preceding cervical and the following dorsal vertebra (Table 3.4). Despite having a dorsal rib, the cervicothoracic vertebra of giraffes has a greater range of motion than any of the other thoracic vertebrae, but more reduced

Character	DV 2	DV 1	Last Cervical	Penultimate cervical
1 - Length of vertebral centrum	Giraffa: Short	Giraffa: Intermediate	Giraffa: Long	Giraffa: Long
	Spino: Short	Spino: Intermediate	Spino: Long	Spino: Long
2 - Posterior centrum morphology:	Giraffa: Flat	Giraffa: Flat	Giraffa: Concave	Giraffa: Concave
	Spino: Concave	Spino: Concave	Spino: Concave	Spino: Concave
3 - Prezygapophyseal rami	Giraffa: Reduced	Giraffa: Small	Giraffa: Long	Giraffa: Long
	Spino: Small	Spino: Small	Spino: Long	Spino: Long
4 - Prezygapophyseal facets	Giraffa: Wider	Giraffa: Longer	Giraffa: Longer	Giraffa: Longer
	Spino: Wider	Spino: Longer	Spino: Longer	Spino: Longer
5 - Neural Spine Length	Giraffa: Large	Giraffa: Intermediate	Giraffa: Short	Giraffa: Short
	Spino: Intermediate	Spino: Intermediate	Spino: Short	Spino: Short
6 - Ventral Keel	Giraffa: Absent	Giraffa: Present	Giraffa: Present	Giraffa: Present
	Spino: ?	Spino: Present	Spino: Present	Spino: Present

Table 3.4. Comparison of the cervico-dorsal boundary between *Giraffa* and *Spinophorosaurus*.

Character states are as follows, for the following characters: 1) Short refers to centra that are taller than long. Long refers to centra that are longer than tall. Intermediate refers to square or close to square centra. 4) Wider refers to prezygapophyseal facets that are wider than long. Longer refers to prezygapophyseal facets that are longer than wide. 5) Large refers to the neural spine being as tall or taller than the vertebral centrum. Short refers to the neural spine being shorter than half the centrum height. Spino = *Spinophorosaurus nigerensis*; Giraffa = *Giraffa camelopardalis*.

than the other cervical vertebrae. This situation is also present in *Spinophorosaurus*, in which the first dorsal vertebra has an amount of osteological mobility greater than that of the following dorsal vertebrae but smaller than that of the preceding cervical vertebra (Table 3.5). This is particularly noticeable on its first dorsal vertebra and, to a lesser degree, on the second and third because their prezygapophyseal facets and centra are shorter than on the first dorsal.

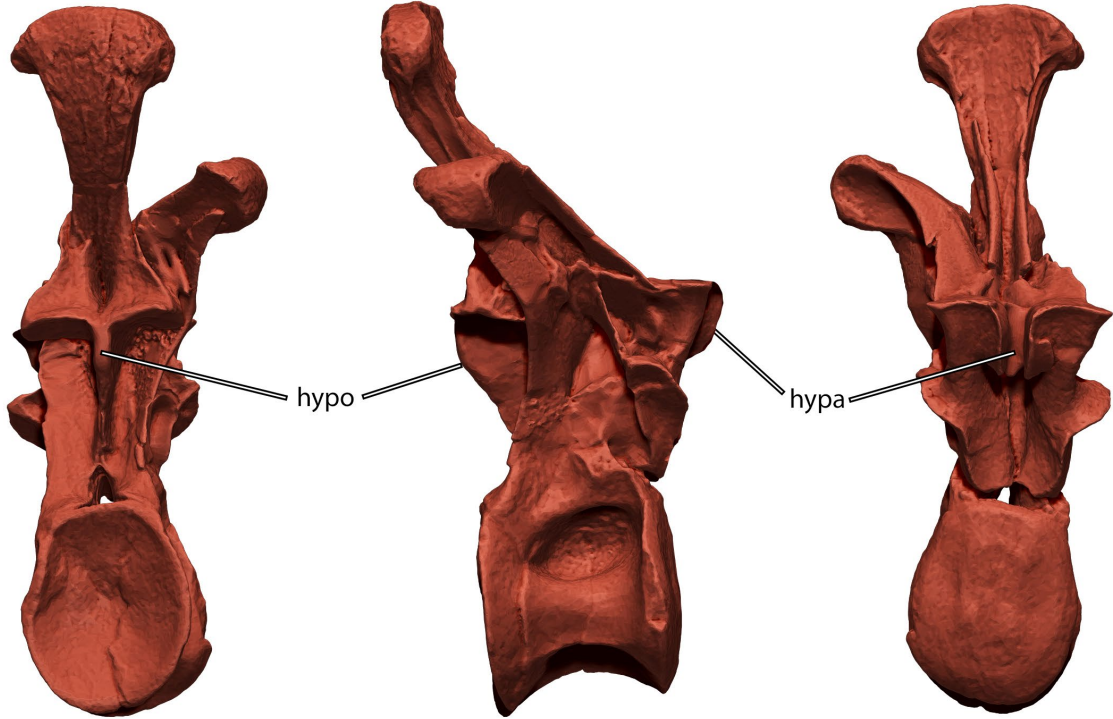
The range of motion of the neck alone (without deflecting the first dorsal from ONP) allows placing it vertical, with the skull antero-posterior axis perpendicular to the ground without disarticulation (Fig. 3.7.2). The inner ear semicircular canals are relatively very large and slender. This has been related with the perception of angular accelerations of the head of animals, predicting a highly flexible neck for *Spinophorosaurus*, corroborated at least in the dorso-ventral plane by our range of motion analysis (Fig. 3.7).

	DV 3	DV 2	DV 1	LCV	PCV
<i>Okapia</i>	3	4	3	9	17.5
<i>Giraffa</i>	5	4	14	25-27	25-28
<i>Plateosaurus</i>	4	4	8	10	10
<i>Spinophorosaurus</i>	*7	*9	17	27	28

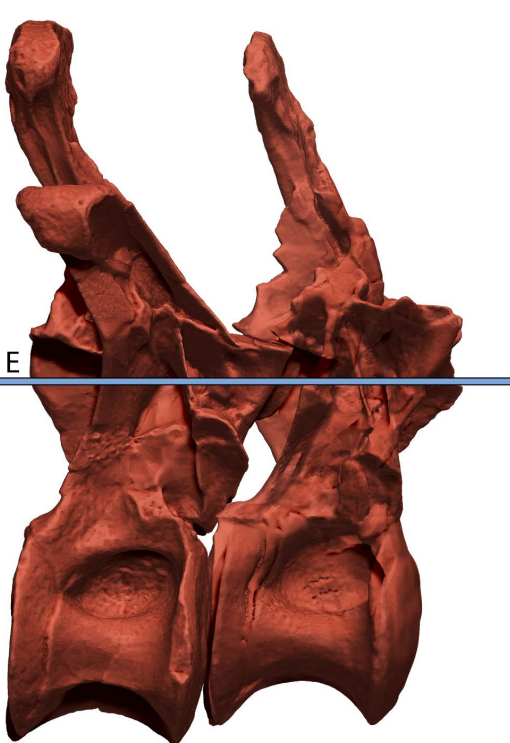
Table 3.5. Dorso-ventral range of motion values at the cervico-dorsal boundary for *Spinophorosaurus*, *Plateosaurus*, *Okapia* and *Giraffa*.

Range of motion measured as degrees between maximum dorsiflexion and ventriflexion in the referred vertebra. DV = dorsal vertebra; LCV = Last Cervical Vertebra; PCV = Penultimate Cervical Vertebra. *Asterisk indicates estimated measurements based on field pose (dorsiflexion) and osteological stop of ribs (ventriflexion). Data from *Okapia johnstoni* and *Giraffa camelopardalis* from Gunji & Endo (2016). Data from *Plateosaurus engelhardti* from Mallison (2010b)

A



B



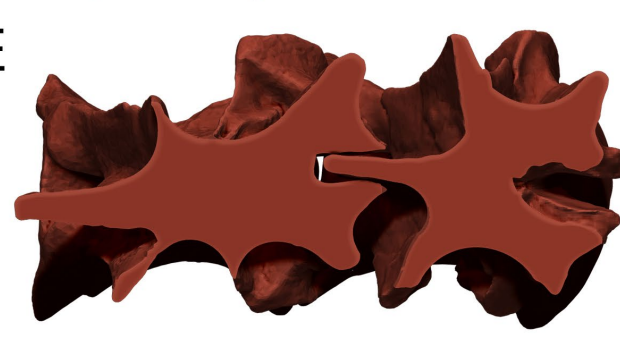
C



D



E



Dorsal Vertebrae

All dorsal vertebrae from DV2 to DV13 in *Spinophorosaurus* have hyposphene-hypantrum articulations. Unlike in many sauropods, where this articulation has a wedged morphology in posterior view, ventrally widened with two strong ridges, in *Spinophorosaurus* it does not expand ventrally to form the wedge (Fig. 3.8 A), being only a thickened, rhomboidal medial intrapostzygapophyseal lamina (Wilson, 1999; Apesteguia, 2005), similar to that of *Barapasaurus* (Jain *et al.*, 1979; Apesteguia, 2005). This kind of articulation creates an osteological stop, which completely impedes any lateral motion in all dorsal vertebrae that have it (Fig. 3.8 E), from DV13 to DV3 at least (its presence on the second dorsal vertebra cannot be assessed at present). Dorsiflexion and ventriflexion are possible to a certain extent, particularly on anteriormost dorsals (Fig. 3.8 C). As the pedicels grow taller the more posterior the dorsal, the center of rotation and the articulation facets (pre-postzygapophyses) become further apart, making the zygapophyses disarticulate with less degrees of flexion. Overall, the trunk of *Spinophorosaurus* is very stiff on its posterior and middle regions, as is in most non-titanosaur sauropods.

Caudal Vertebrae

The osteological ROM can be assessed fairly well in all the tail of *Spinophorosaurus*, both in the antero-posterior and lateral planes. Although the pre- and postzygapophyses of distal caudal vertebrae do not articulate, the forked distal chevrons overlap from caudal CdV-21 until CdV-29 at mid-centra, limiting the range of motion.

The first 20 caudal vertebrae, vertebrae pairs may deflect for up to 20° per joint before osteological stop due to neural spines colliding in dorsiflexion. It is likely that soft tissue (muscle and ligaments) would not allow such drastic dorsiflexion in life, since it might have put excessive stress on intervertebral discs (Zahari *et al.*, 2017). The opisthotonic posture, in which the fossil was found, can be achieved by deflecting each pair of vertebrae 5° (Fig. 3.9 A,C). In lateral flexion, each vertebra pair may deflect up to a 8°-10°. This limit is due the orientation of the pre- and postzygapophyses, which are sub-parallel to the neural spine axis, which hinders torsion and, to a lesser degree, lateral flexion (Mallison *et al.*, 2015). Ventriflexion is limited by osteological stop from the rather long chevrons, which collide with less than 5° of deflection per joint (Fig. 3.9 A).

The range of motion is limited in the dorso-ventral plane in the distal region of the tail, where the forked chevrons overlap. This is due the orientation of the surfaces in which the chevrons overlap (which are flattened, hence they may be termed inter-chevron facets). These facets are inclined around 30°, which makes them closer to horizontal than vertical (Fig. 3.9 B). While sub-horizontal pre- and postzygapophyses are known to allow great dorso-ventral excursion, this is not true for the chevrons. While pre-postzygapophyses are situated close to the center of rotation of vertebrae (centra-centra articulation), the inter-chevron facets are located at mid centrum, the furthest possible from the center of rotation (Fig. 3.9 B). Chevrons articulate with their respective vertebrae at the posteriormost region of the centrum, on the chevron articulation facets. When vertebrae deflect from ONP, the chevron moves with the respective vertebra. The osteological stop is inevitable in dorso-ventral plane as the inter-chevron facets overlapping at mid-centrum work as locking bolts in the same way as in a door with latches (Fig. 3.9 B).

Lateral motion in the distal tail with overlapping chevrons is possible only with some torsion per joint (Fig. 3.9 D). Since the inter-chevron facets are closer to horizontal, but not completely horizontal, lateral motion alone is not possible as the chevrons act as locking bolts as well. With a slight torsion of 6° per joint, each pair of vertebrae may deflect up to 10°. Torsion is more likely to happen in this region

Figure 3.8 (previous page)- Range of motion restriction from the hyposphene-hypantrum complex in *Spinophorosaurus nigerensis*.

A - Dorsal vertebra 4 in posterior (left), lateral (middle) and anterior (right) view, with hyposphene and hypantrum highlighted. **B** - Dorsal vertebra 3 and 4 in osteologically neutral pose, lateral view. **C** - Maximum ventriflexion of dorsal vertebra 3, not affected by hyposphene-hypantrum complex (rib not considered for this example), lateral view. **D** - Section of dorsal vertebrae 3 and 4 at hyposphene-hypantrum height in osteologically neutral pose. **E** - Section of dorsal vertebrae 3 and 4 at hyposphene-hypantrum height in maximum lateral flexion, in which the hyposphene-hypantrum create an osteological stop which barely allows any motion. hypo = Hyposphene. hypa = Hypantrum.

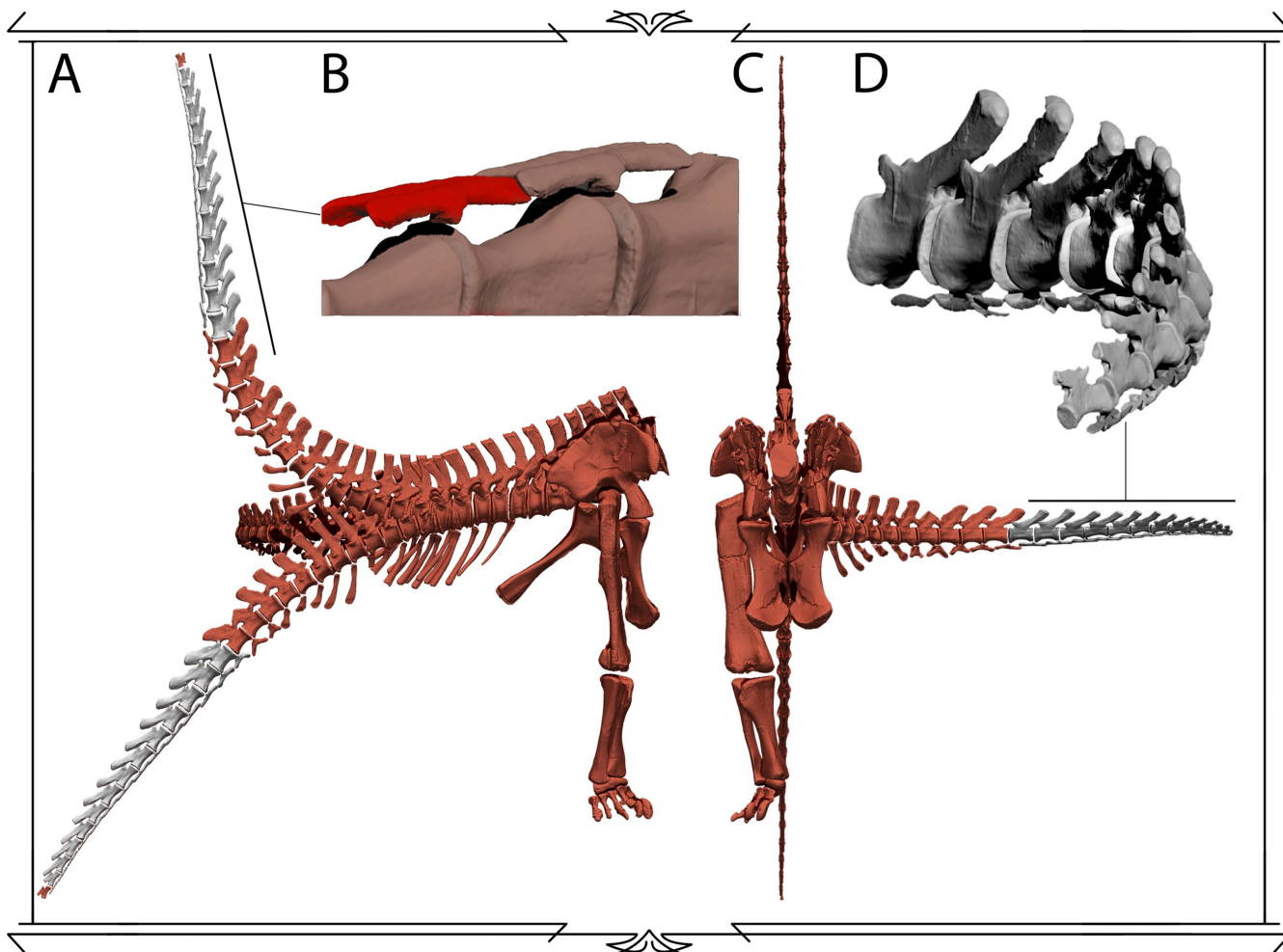


Figure 3.9 - Range of motion in the tail of *Spinophorosaurus nigerensis*.

A - Maximum estimated tail dorsiflexion in lateral view. Distalmost tail region, in gray, is unable to ventriflex or dorsiflex due to an osteological stop from the overlapping chevrons. **B** - Detail on middle-distal caudal vertebrae in ventro-lateral view, showing the overlapping chevrons and the osteological stop produced in ventriflexion. **C** - Maximum estimated tail dorsiflexion and lateral flexion in anterior view. **D** - Detail on distal tail lateral flexion, which can only be performed with a slight inter-vertebral torsion.

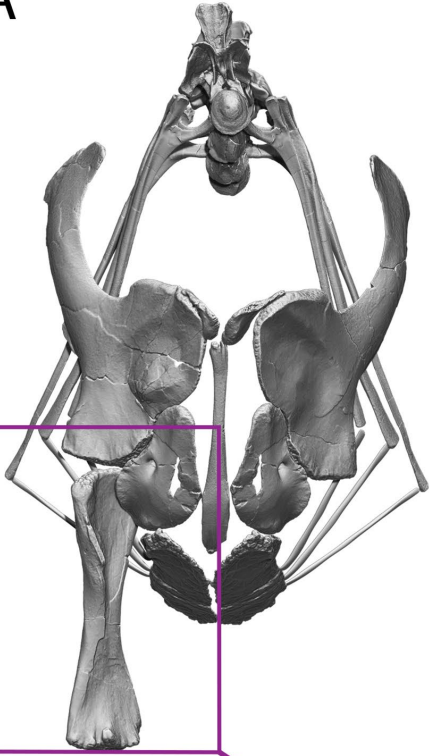
of the tail, as the zygapophyses do not contact, just as in extant crocodiles (Mallison *et al.*, 2015).

Overall, dorsiflexion would have been limited by soft tissue rather than by osteological stop or disarticulation except in the distal region of the tail, where chevrons overlap. Ventriflexion is limited to 5° per joint due to osteological stop from the long chevrons colliding and less than 1° per joint the distal region of the tail, where chevrons overlap. Despite these osteological stops, the tail can reach the ground by ventriflexion (Fig. 3.9 A). Lateral flexion is limited to up to 10° per vertebra pair due to the sub-vertical zygapophyses in caudals anterior to CdV-21, and due to the overlapping in the distal region of the tail, where torsion is needed to hinder this osteological stop. Despite this, a mere deflection of 5° per joint will allow a curve of 90° from ONP (Fig. 3.9 C).

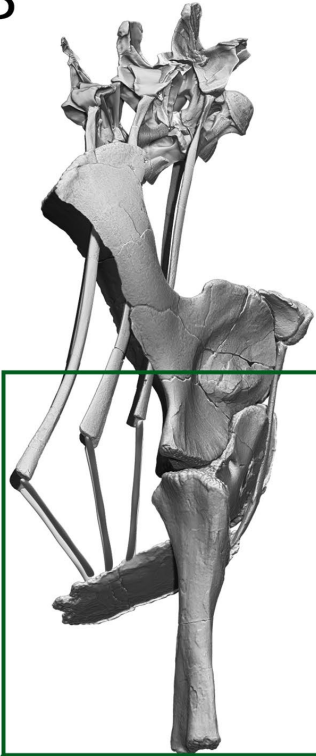
Appendicular skeleton

The humerus is the only articulation in which range of motion can be measured in the forelimb of *Spinophorosaurus*. In order to determine osteological stops, sternal ribs and sternal plates were modelled after those of other sauropods (Filla & Redman, 1994; Tschopp & Mateus, 2012). They were not retrieved or they may not have been ossified in *Spinophorosaurus*, but phylogenetic bracketing implies they must have been present (Fig. 3.3 B; Tschopp & Mateus, 2013). In the latero-medial plane, adduction is limited by osteological stop from the sternal plates. The humerus can only adduct a few degrees from ONP before the osteological stop (Fig. 3.10 D). Abduction is limited by disarticulation, with the humeral head disarticulating from the glenoid after 30° of abduction from ONP (Fig. 3.10 D). In the antero-posterior plane, both protraction and retraction are limited. Protraction is limited by disarticulation, as the humeral head disarticulated from the glenoid cavity

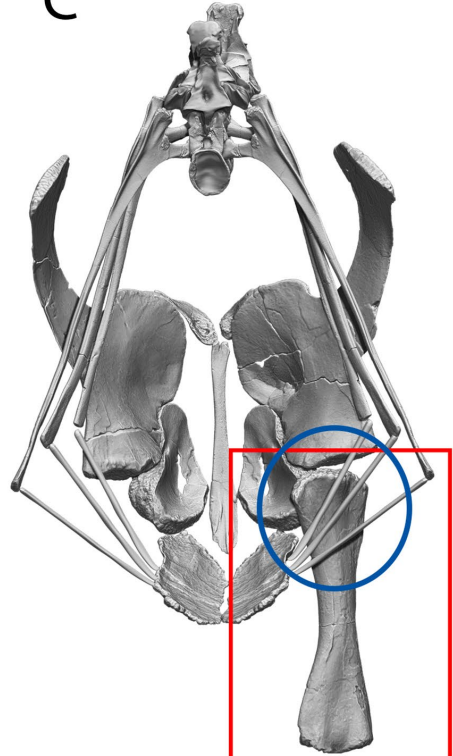
A



B



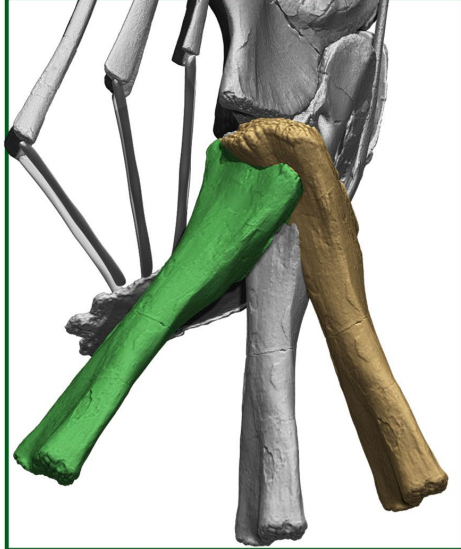
C



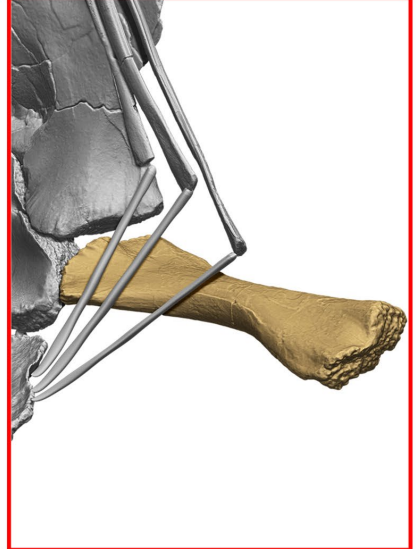
D



E



F



G

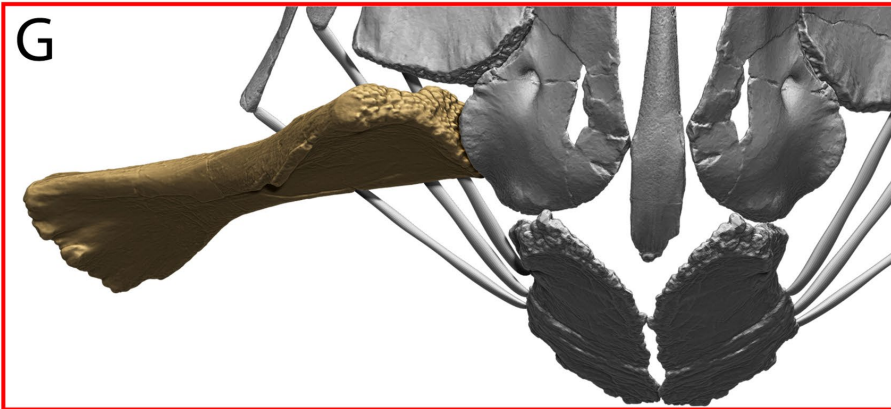


Figure 3.10 (previous page) - Range of motion in the shoulder of *Spinophorosaurus nigerensis*.

Humerus, pectoral girdle and ribcage in ONP in **A** - anterior, **B** - lateral, and **C** - posterior view. Notice the sternal ribs as an osteological stop for retraction in posterior view. **D** - Maximum abduction (purple) and adduction (yellow) in anterior view. **E** - Maximum protraction (yellow) and retraction (green) in lateral view. Retraction has an osteological limit due to the humerus colliding with the sternal ribs before disarticulation. **F** - Combined abduction and retraction allow posing the humerus sub-parallel to the ground in posterior and **G** - anterior view.

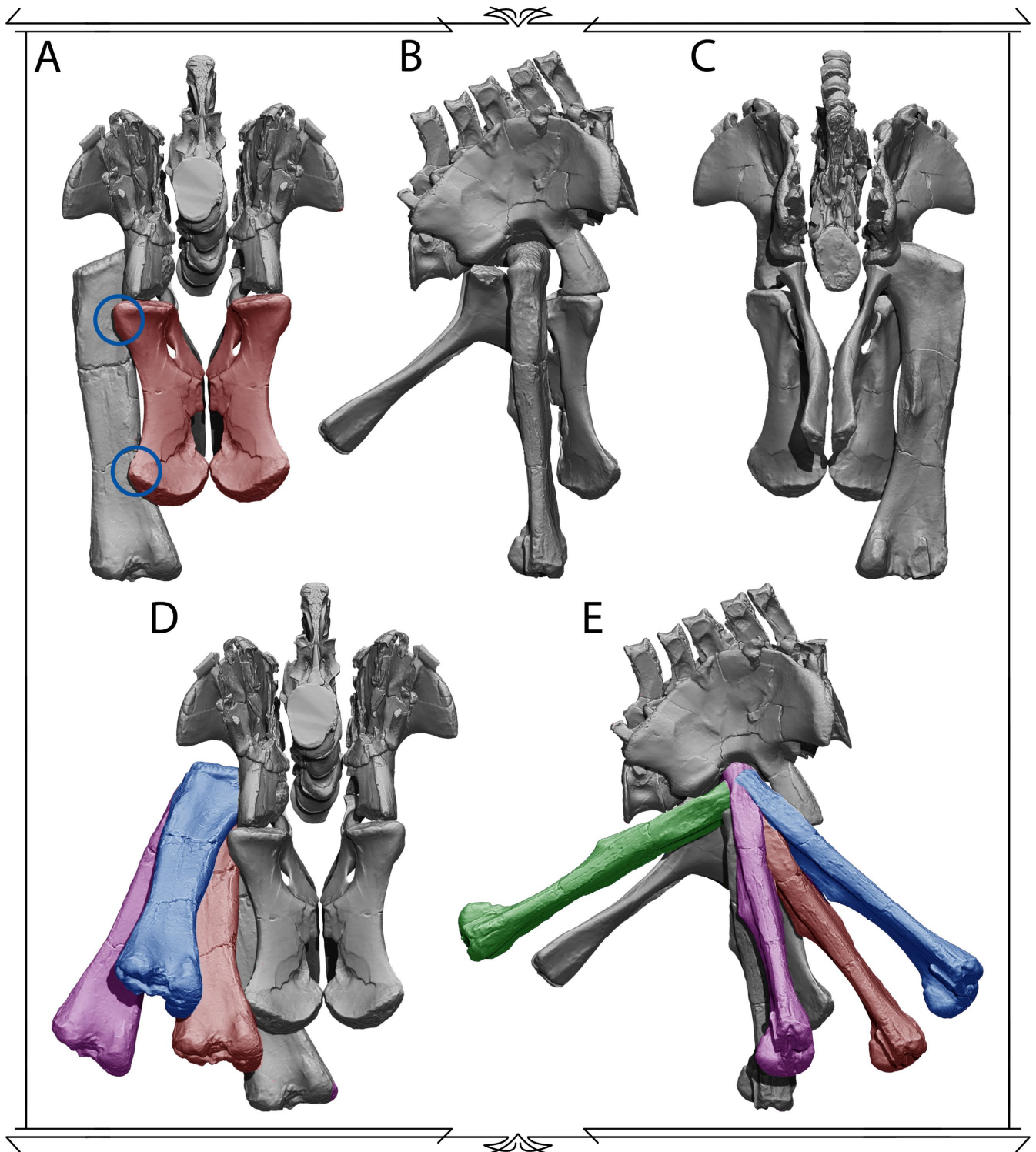


Figure 3.11 - Range of motion in the acetabulum of *Spinophorosaurus nigerensis*.

Femur, pelvic girdle and sacrum in osteologically neutral pose in **A** - anterior, **B** - lateral, and **C** - posterior view. Notice the pubes cause two osteological stops for femur protraction: the distal expansion and the proximo-lateral region. **D** - Maximum range of motion in anterior and **E** - lateral view. Green = maximum retraction (no osteological stop). Purple = maximum abduction. Gray = maximum adduction. Red = maximum protraction before osteological stop from the proximo-lateral pubis. Blue = maximum protraction before osteological stop from the proximal femur colliding with the acetabulum walls.

after deflecting 20° from ONP (Fig. 3.10 E). Retraction is limited by osteological stop from the sternal ribs after deflecting 18° from ONP. Combining abduction with retraction allows avoiding this osteological stop, allowing the humerus to become close to horizontal (75° from ONP) before disarticulating (Fig. 3.10 F, G).

The femur has some limits on its protraction due to the narrow pelvis, which makes the particular morphology of the pubes cause some osteological stops (Fig. 3.11 A). The first one is caused by the distal expansion of the pubis, which collides with the femur after 5° of protraction (Fig. 3.11 D). Abducting the femur 3° allows it to protract further, with an osteological stop from a lateral expansion of the proximal region pubis after 22° of protraction from ONP. The femur can protract further from this second osteological stop again with 24° of abduction. The pubic pedicle of the ilium is the final osteological stop for protraction, which cannot be avoided by abduction. Full protraction is 43° from ONP (Fig. 3.11 D, E) and it has an osteological limit. Retraction, on the other hand, is not limited by osteological stop or disarticulation (Fig. 3.11 C, E), with the femur able to retract until it is horizontal (90° from ONP). This implies soft tissues limited retraction *in vivo*. Abduction and adduction are both limited by an osteological stop (Fig. 3.11 D), with the femoral head colliding with the acetabulum walls after 10° (adduction) and 44° (abduction). This implies adduction would have likely had other limits on this motion (i. e. the counter-lateral hindlimb preventing further adduction) before osteological stop from the acetabulum.

The tibia-fibula can barely extend beyond being perpendicular to the femur, as the distal tibial and fibular condyles do not extend on the anterior face of the femur. These condyles allow for 67° degrees of flexion from ONP at this joint.

3.6 RECONSTRUCTION OF THE MUSCULAR SYSTEM

As stated in chapter 2, muscle reconstruction is a hypothetical inference process based on three main lines of evidence, in no particular order: muscle scars on the fossilized bones (osteological), presence or absence of the muscle and its electromyographic activation in extant relatives (phylogenetic) and lines of action and/or motion capabilities for said muscle (functional). The more lines of evidence supporting a particular muscle and its function, the more likely is for that muscle to have had been present and activated on those particular motions.

Cranio-cervical musculature

Cranio-cervical musculature includes all muscles with origins and insertions in the neck and back of the skull, which allow neck and head movement (Wedel & Sanders, 2002; Schwarz *et al.*, 2007b; Snively & Russell, 2007a,b). There have been previous studies reconstructing the myology on theropod necks using phylogenetic inference (EPB), particularly on tyrannosaurids (Snively & Russell, 2007b,c,a) and allosauroids (Snively *et al.*, 2013). On the other hand, sauropod muscular cranio-cervical reconstructions have been either based on birds (Wedel & Sanders, 2002) or crocodiles (Schwarz *et al.*, 2007b; Gascó, 2015).

In order to reconstruct the cranio-cervical musculature of *Spinophorosaurus*, the same EPB used by Snively & Russell (2007a) for reconstructing that of theropods was used. Considering that the even some coelurosaur theropods still retained cranio-cervical muscular osteological correlates more similar to those of crocodiles (Snively & Russell, 2007c) and that extant avian neck muscles which are absent in extant crocodile must have appeared already within Aves (Tsuihiji, 2005), the condition for sauropod musculature would have likely not been homologous to the avian condition. The origin and insertions for the different muscles are summarized in Table 3.6 and figures 3.12 and 3.13.

These muscles are divided in 3 different systems regarding the location of their origins on the neck (dorsally, laterally and ventrally), and are represented in 3 different color families: transversospinales (Purple), longissimus (Red) and Iliocostales and longus (Yellow).

Transversospinales: Most osteological correlates for insertions and origins these muscles are shared between the skull and neck of *Tyrannosaurus rex* and *Spinophorosaurus nigerensis*. Both have rugose scars on the nuchal crest for *M. transversospinalis capitis* insertion, making it a Level 2 inference (implying an ACCTRAN optimization for this muscle). The dorsal tips of the posterior cervical and anterior dorsal neural spines of *Tyrannosaurus* are flattened on the laterals, origin for that muscle. *Spinophorosaurus* has also flattened dorsal tips on the neural spines of DV1-CV5. This

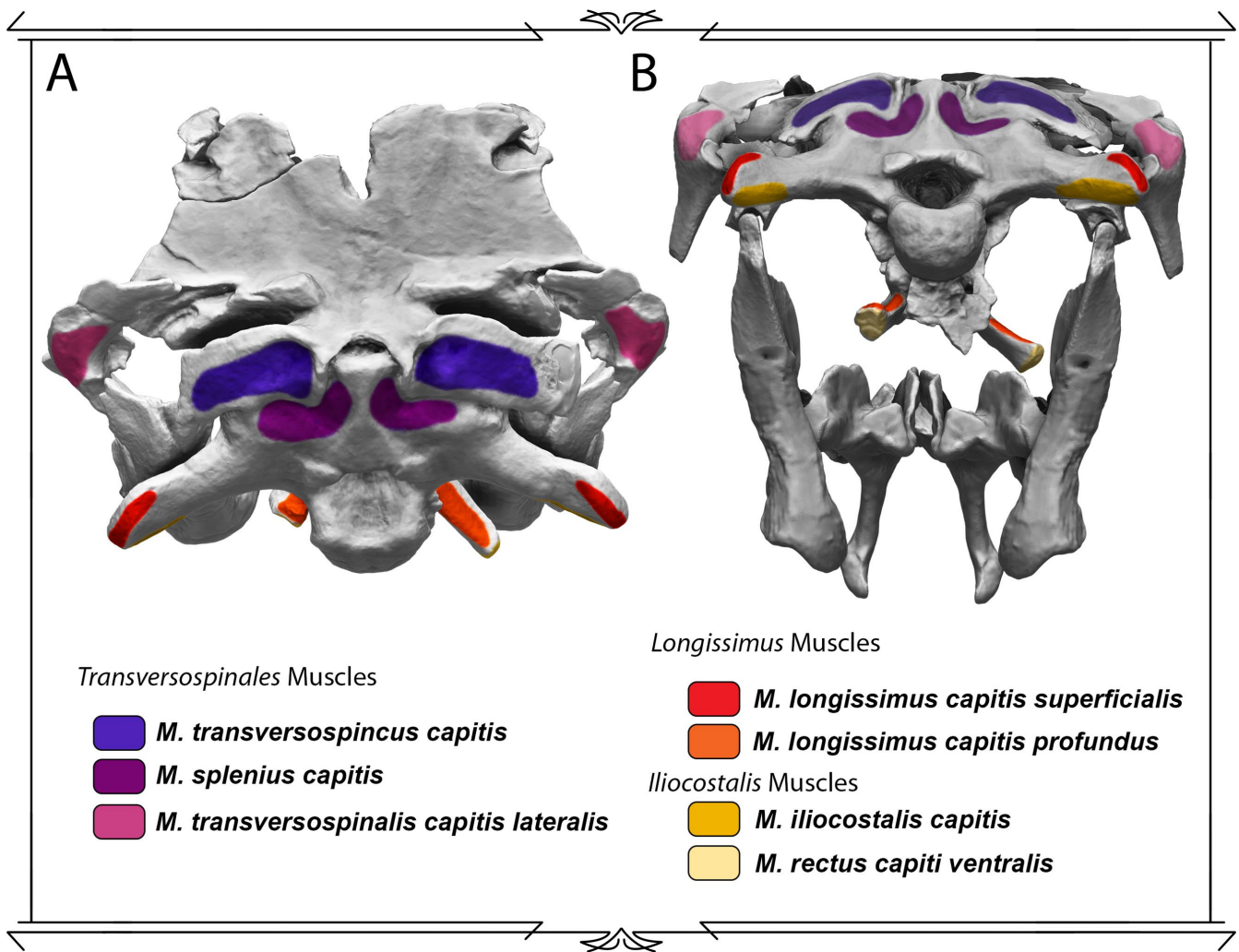


Figure 3.12 - Craniocervical musculature insertions in the braincase of *Spinophorosaurus nigerensis*.

Braincase in **A** - dorsal and **B** - posterior view with main muscle insertions highlighted and color-coded over their osteological correlates. List of osteological correlates in Table 3.6.

would make the origin for this muscle a Level 1 inference. *Spinophorosaurus* has a flat surface on the posterodorsal surface of the squamosal delimited by ridges. *T. rex* TMP 81.6.1 has a rugosity on the same position, interpreted as a possible insertion for *M. transversospinalis capitis lateralis* (Snively & Russell, 2007a). The flat surface on the squamosal of *Spinophorosaurus* might be the same insertion. The epiphyses on the cervical vertebrae CV4, CV3 and axis of *Spinophorosaurus* have dorsolateral ridges, absent from all other cervicals epiphyses. *Tyrannosaurus* also has ridges on CV4-Axis epiphyses, and this coincides with the origin for *M. transversospinalis capitis lateralis*

Both *Spinophorosaurus* and *Tyrannosaurus* share a depression on the parietals, lateral to the supraoccipital. This has been interpreted as the insertion of *M. splenius capitis*. All dinosaurs have teardrop shaped scar on the anterior face of the Axis neural spine (Snively & Russell, 2007a), which is the origin for *M. splenius capitis*. This teardrop shaped scar is not very developed in *Spinophorosaurus*, hinting at a smaller origin surface for this muscle. Regarding the cervical muscle *M. longus colli dorsalis*, in *Tyrannosaurus* the muscle only has insertions on epiphyses of CV6 to Axis. *Spinophorosaurus*, on the other hand, has epiphyses on all preserved cervical vertebrae, making likely that slips of this muscle complex inserted on all cervical vertebrae, in a fashion convergent to that of birds (Wedel & Sanders, 2002; Snively & Russell, 2007a), although whether it had two different origins or not as in birds is impossible to know from osteology alone.

Longissimus: The majority of these muscles do not have very clear osteological correlates, particularly regarding their origins. Both *M. longissimus capitis superficialis* and *profundus* originate from anterior dorsal and cervical diapophyses, but while some of these have left scars on the diapophyses of *Tyrannosaurus*, no scars could be observed on *Spinophorosaurus*. Therefore, the origins of these have inference confidence of Level 2' and 2, respectively. Their insertions, on the other hand, have

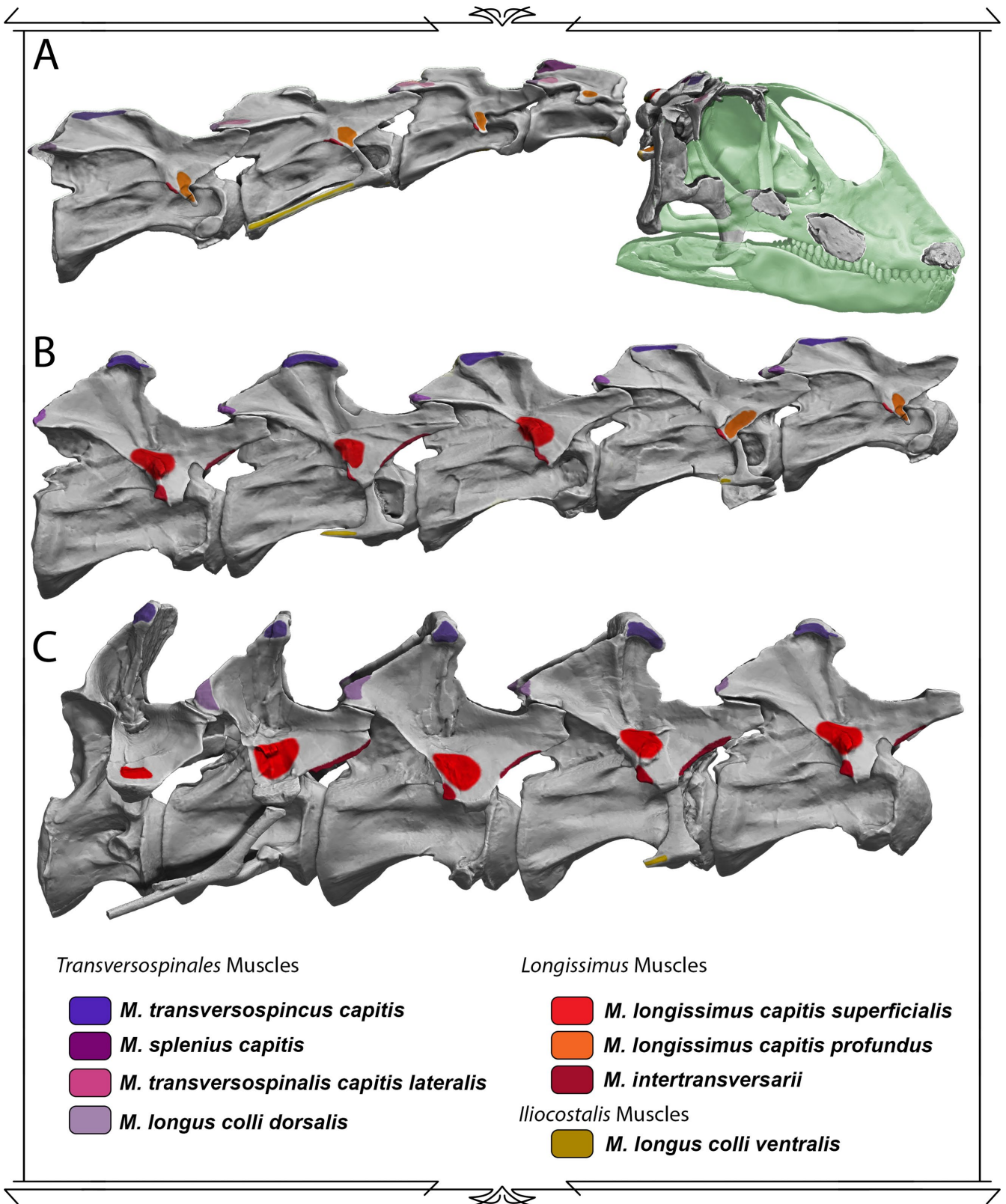


Figure 3.12 - Craniocervical musculature insertions in the braincase of *Spinophorosaurus nigerensis*.

Braincase in **A** - dorsal and **B** - posterior view with main muscle insertions highlighted and color-coded over their osteological correlates. List of osteological correlates in Table 3.6.

osteological correlates in *Spinophorosaurus*: A ridge on the laterals of the paraoccipital processes (*M. longissimus capitis superficialis*) and the dorsal surfaces of the Basioccipital tuberosities (*M. longissimus capitis profundus*).

M. intertransversarii is a segmented neck muscle which originates on the anterior diapophysis (posterior vertebra) and inserts on the posterior surface of the diapophysis (anterior vertebra), that is, connecting the posterior vertebra with the anterior vertebra. The insertion has a potential

Muscle	Crocodylia	Aves	<i>T.rex</i>	<i>S.nigerensis</i>
<i>M. transversospincus capitis</i>	<p>O: Neural spines of anterior dorsal vertebrae and CV9.</p> <p>I: Nuchal crest, supraoccipital.</p>	<p>O: Neural spines at base of the neck.</p> <p>I: Nuchal crest, parietals.</p>	<p>O: Posterior CV neural spines (dorsal and lateral surfaces).</p> <p>I: Nuchal crest, parietals (rugose scar).</p>	<p>O: DV1-CV5 Neural spines dorsolateral surface.</p> <p>I: Nuchal crest, parietals (rugose scar).</p>
<i>M. transversospinalis capitis lateralis</i>	<p>O: Ventrolateral portion of Axis-CV8 neural arches.</p> <p>I: Paraoccipital processes, dorsolateral portion.</p>	<p>O: Epiphyses of Axis-CV4 (CV6 in <i>Gallus</i>).</p> <p>I: Nuchal crest.</p>	<p>O: Epiphyses of Axis-CV4 (lateral rugosities).</p> <p>I: Squamosals (Ambiguous).</p>	<p>O: Epiphyses of Axis-CV4 (dorsolateral ridges).</p> <p>I: Squamosals.</p>
<i>M. splenius capitis</i>	<p>O: Axis neural spine (dorsal region), neural arch of atlas.</p> <p>I: Between squamosal and paraoccipital processes.</p>	<p>O: Axis neural spine, anterior face teardrop shaped scar.</p> <p>I: Nuchal crest, parietal (medial to <i>M. complexus</i>).</p>	<p>O: Axis neural spine, anterior face teardrop shaped scar.</p> <p>I: Parietals.</p>	<p>O: Axis neural spine, anterior face teardrop shaped scar.</p> <p>I: Parietals.</p>
<i>M. longus colli dorsalis</i>	<p>O: Neural spines of CV9-CV3, lateral surfaces anterior to postzygapophyses.</p> <p>I: posterodorsal portion of Atlas-CV4 postzygapophyses.</p>	<p>O pars caudalis: Aponeurosis notarii (arises from Ant. Dorsal and Post. cervical neural arches).</p> <p>O pars cranialis: Aponeurosis notarii.</p> <p>I pars caudalis: Axis, DV1-CV4 epiphyses</p> <p>I pars cranialis: CV3-Axis epiphyses.</p>	<p>O: Ambiguous.</p> <p>I: CV5-Axis Epiphyses.</p>	<p>O: Ambiguous.</p> <p>I: CV12-Axis Epiphyses.</p>
<i>M. longissimus capitis superficialis</i>	<p>O: CV9-CV4 proximal diapophyses and neural arches.</p> <p>I: Paraoccipital processes, lateral scar.</p>	Absent	<p>O: DV2-CV7 Diapophyses, proximal scar.</p> <p>I: Paraoccipital processes, lateral portion.</p>	<p>O: Ambiguous.</p> <p>I: Paraoccipital processes, lateral portion (lateral to ridge).</p>
<i>M. longissimus capitis profundus</i>	<p>O: CV7-CV3 Diapophyses.</p> <p>I: Basioccipital, ventrolateral to occipital condyle.</p>	<p>O: CV6-Axis Diapophyses, lateral surface of Atlas.</p> <p>I: Basioccipital, anteroventrolateral to occipital condyle.</p>	<p>O: CV7-Atlas Diapophyses.</p> <p>I: Basioccipital, ventrolaterally projected tuberosities.</p>	<p>O: CV6-Axis Diapophyses.</p> <p>I: Basioccipital, ventrolaterally projected tuberosities, dorsal surfaces.</p>
<i>M. intertransversarii</i>	<p>O: Diapophyses, anterior surface.</p> <p>I: Diapophyses, lateral surface (ant. vertebra).</p>	<p>O: Diapophyses, anterior surface.</p> <p>I: Diapophyses, lateral surface (ant. vertebra).</p>	<p>O: CV6-CV10 Diapophyses anterior surface (post. vertebra).</p> <p>I: Diapophyses, posterior surface (ant. vertebra).</p>	<p>O: CV12-Axis, Diapophyses, anterior edge (post. vertebra).</p> <p>I: Diapophyses, posterior flange (ant. vertebra).</p>

<i>M. iliocostalis capitis</i>	O: Axis-Atlas Hypapophyses.	O: CV5-Axis Hypapophyses.	O: Ambiguous.	O: CV5-Axis ventral keels.
	I: Paraoccipital processes, ventral edge.	I: Paraoccipital processes, ventral edge.	I: Paraoccipital processes, distinct ridge on ventral edge.	I: Paraoccipital processes, distinct ridge on ventral edge.
<i>M. rectus capiti ventralis / longus capiti / flexor colli</i>	O: Axis-Atlas, ventrolateral surfaces of centra (<i>rectus capiti</i>), CV7-CV3 Hypapophyses lateral surfaces (<i>longus capitis</i>).	O: CV3-Atlas Hypapophyses.	O: Ambiguous.	O: Ambiguous.
	I: Basioccipital tuberosities, posteroventral surface.	I: basitemporal plate (<i>rectus capiti</i>), Cervical ribs, posterior surface (<i>flexor colli</i>)	O: Ambiguous.	O: Ambiguous.
<i>M. longus colli ventralis</i>	O: Hypapophyses and ventral surfaces of centra.	O: Hypapophyses (post).	O: Ant. Dorsal and Post. Cervical centra, ventral surfaces.	O: Ant. Dorsal and Post. Cervical centra, ventral keels.
	I: Posterior processes of cervical rib.	I: Cervical Ribs.	I: Ant. Cervical ribs, posterior edges.	I: Cervical ribs, posterior edges.
<i>Mm. intercostales</i>	Absent	O: Neural spine transverse oblique crest (post. vertebra). I: Neural spine transverse oblique crest (ant. vertebra).	O: CV10-CV5, Neural spine transverse oblique crest (post. vertebra)? I: CV10-CV5, Neural spine transverse oblique crest (ant. vertebra)?	O: CV10-CV5, Neural spine transverse oblique crest (post. vertebra)? I: CV10-CV5, Neural spine transverse oblique crest (ant. vertebra)?
	Absent	O: Diapophyses, anterior surface ventral to prezygapophyses. I: Epipophyses at least two cervicals more anterior.	Absent	Absent

Table 3.6 - Osteological origins and insertions of cranio-cervical musculature.

The muscles are grouped in their respective functional systems with a color-coding: *Transversospinales* (purple), *Longissimus* (red), *Iliocostalis / M. longus* (yellow) and complex muscles (white). Origins and insertions for extant *Crocodylia*, *Aves* and *Tyrannosaurus rex* from Snively & Russell (2007a). *Spinophorosaurus* osteological correlates are discussed in Chapter 3.6. Non-osteological origins/insertions are not contemplated.

osteological correlate on the posterior flange in the diapophyses of *Spinophorosaurus* (originally regarded as an autapomorphy of *Spinophorosaurus*, now known to be a more spread feature).

Iliocostalis / M. longus: All muscles of this system originate on the hypapophyses of both extant birds and crocodiles (Snively & Russell, 2007a). When reconstructing the musculature in *Tyrannosaurus*, which does not have ventral keels or hypapophyses on its cervical vertebrae, a shift on the origins was proposed (Snively & Russell, 2007a). *Spinophorosaurus*, however, has very strong ventral keels on all its cervical vertebrae and on its anterior dorsal vertebrae, which may have served as origin for all these muscles. If considered to be homologous to the condition of crocodiles and birds (ventral keels = hypapophyses), the origin of those muscles would be Level 1 for *Spinophorosaurus*.

Regarding the insertions, *M iliocostalis capitis* may have inserted on the flattened ventral surface on the laterals of the paraoccipital processes, and *M rectus capiti ventralis* likely inserted on the basioccipital tuberosities as in *T. rex*. *M longus colli ventralis* inserted onto the anteroventral faces of the cervical ribs, as in extant birds and *T.rex*.

Regarding the complex muscles which are present only in extant birds, only *Mm. intercostales* may have been present in non-avian dinosaurs (Snively & Russell, 2007a), with *Mm. cervicales ascendentes* having arisen only in taxa more deeply nested than *Archaeopteryx* (Tsuihiji, 2005).

Snively & Russell (2007a) estimated the potential function/s of these muscles in *Tyrannosaurus* by comparing extant archosaur electromyographies (physiological evidence) and the kinematic evidence of estimated lines of action for the muscles. Those were:

- (i) Head dorsiflexion for *M. transversospinus capitis*, *M. transversospinalis capitis lateralis*, *M. splenius capitis* *M. longissimus capitis superficialis* in bilateral contraction.
- (ii) Lateral head flexion for *M. splenius capitis*, *M. longissimus capitis superficialis*, *M. rectus capitis dorsalis* in unilateral contraction.
- (iii) Head ventriflexion for *M. rectus capitis dorsalis* and *M. rectus capitis ventralis* in bilateral contraction.
- (iv) Neck dorsiflexion for *M. longus colli dorsalis* and *M. intercostales* in bilateral contraction.
- (v) Neck lateral flexion for *M. intertransversarii*, *M. intercostales* and *M. longus colli ventralis* in unilateral contraction.
- (vi) Neck ventriflexion for *M. longus colli ventralis* in bilateral contraction.

Also, a large number of antagonist muscles may act isometrically dampening or stabilizing the tension caused by the agonist muscle/s (i.e. *M longus colli ventralis* may dampen head dorsiflexion when *M. longus colli dorsalis* and *M. intercostales* contract).

Since the lever arms for the first three muscles are similar in *T. rex* and *S. nigerensis*, the kinematics were similar and the head movements may have been similar. The elongated neck of sauropods in general and *Spinophorosaurus* in particular imply longer moment arms for neck muscles, while the lines of action remain similar. This suggests faster and contraction in shorter necks (see Chapter 5).

Pectoral Girdle and Shoulder musculature

There has been extensive research concerning pectoral girdle muscles in dinosaurs, particularly regarding the origin of flight, but also in sauropod dinosaurs (Remes, 2007; Hohn-Schulte, 2010; Klinkhamer *et al.*, 2019). There is a strong consensus regarding the reconstruction of these muscles in Sauropoda, so their reconstruction in *Spinophorosaurus* follows that of previous analyses (Tables 3.7 and 3.8). The pectoral girdle and shoulder musculature can be divided into 4 groups regarding what bone is affected by their action: Cingulo-axial, Humeral, Antebrachial and Manual (Remes, 2007) and has been followed here (in the absence of preserved forearm and hand material only cingulo-axial and humeral muscles could be restored in *Spinophorosaurus*).

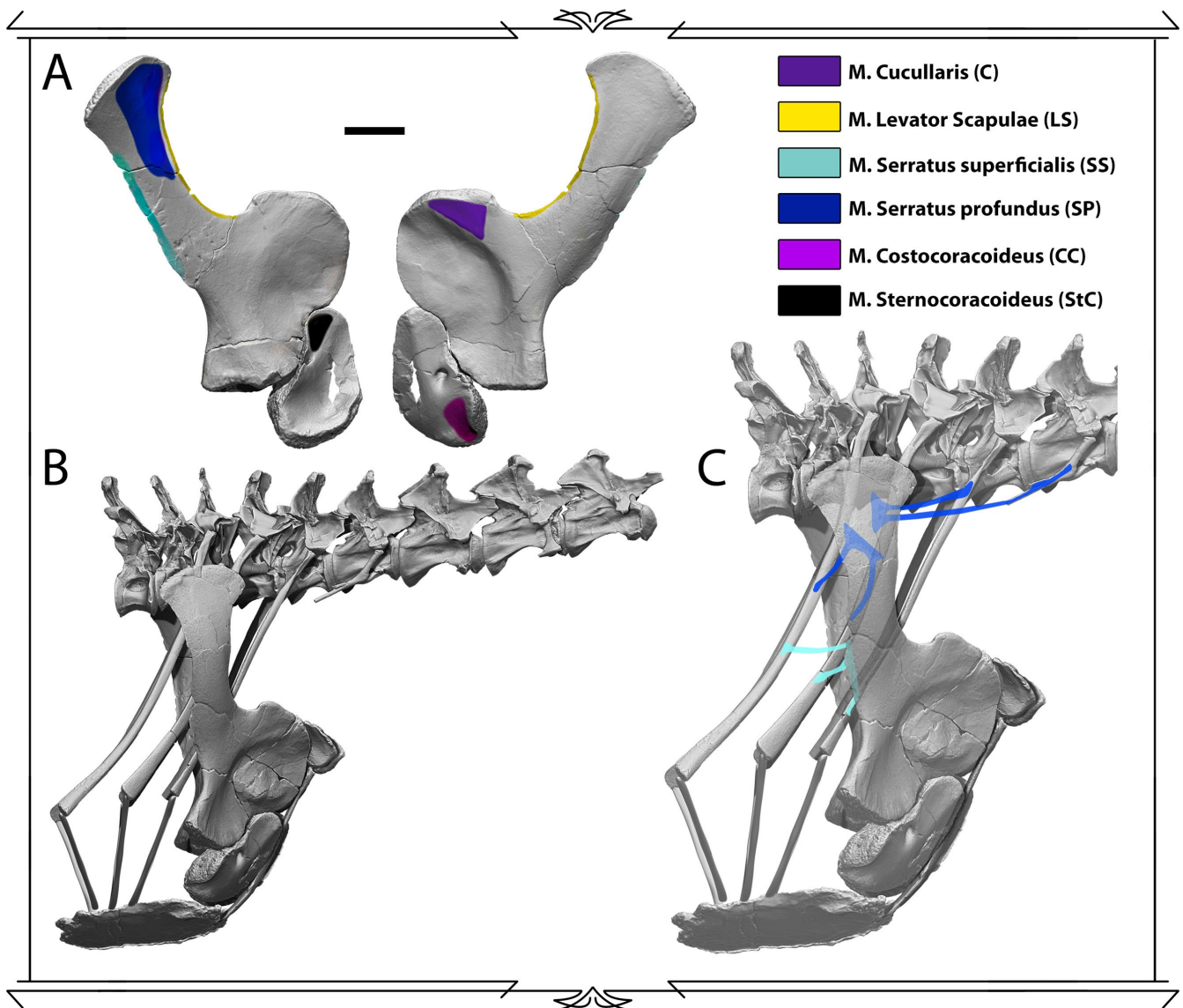


Figure 3.14 - Cingulo-axial musculature origins and insertions in the pectoral girdle and axial skeleton of *Spinophorosaurus nigerensis*.

A - Scapulocoracoid in lateral (left) and medial (right) view, with main muscle origins and insertions highlighted and color-coded over their osteological correlates. **B** - Pectoral girdle and anterior dorsal axial skeleton in lateral view. **C** - Closer view on pectoral girdle and anterior dorsal axial skeleton in lateral view, with lines of action for *M. serratus profundus* and *M. serratus superficialis* highlighted and color-coded. List of osteological correlates in Table 3.7.

Cingulo Axial Musculature: These muscles connect the pectoral girdle to the ribcage and vertebrae, as well as help to move the scapulae during locomotion (Remes, 2007). Both scapulae and the single preserved coracoid of *Spinophorosaurus* are extremely well-preserved, with osteological correlates for the insertions of many cingulo-axial muscles (Figs. 3.14).

M. cucullaris (C) originates from the occiput and the dorsal tips of the neural spines, inserting onto the acromial region of the scapula on both extant birds and crocodiles. There is a well-marked triangular depression in the acromial region of *Spinophorosaurus*, on its lateral side, making this muscle a Level I inference.

M. rhomboideus (R) originates on the laterals of the dorsalmost part of the dorsal spines and inserts on the suprascapula. The suprascapula is not preserved in *Spinophorosaurus*, so no osteological correlates are available, but it would have likely inserted there.

M. levator scapulae (LS) originates on cervical ribs and diapophyses and inserts on the anterior edge of the scapula only in extant crocodiles (and other non-avian amniotes). It is absent in extant birds, but it was present likely in sauropodomorph dinosaurs (Remes, 2007). In *Spinophorosaurus* it would have had the same insertion and origin.

Muscle	Crocodylia	Aves	Plateosaurus	<i>S.nigerensis</i>
<i>M. cucullaris</i> (C)	O: Occiput, cervical vertebrae dorsal midline.	O: Occiput, cervical vertebrae dorsal midline.	O: Occiput, cervical vertebrae dorsal midline. ?	O: Occiput, cervical vertebrae dorsal midline. ?
	I: Acromion and scapular blade, anterior edge.	I: Acromion and dorsal coracoid.	I: Scapula, acromial region.	I: Scapula, acromial region (triangular depression).
<i>M. rhomboideus</i> (R)	O: Dorsal fascia (posterior to <i>M. cucullaris</i>).	O: Dorsal neural spines, dorsolateral sides.	O: Dorsal neural spines, dorsolateral sides?	O: Dorsal neural spines, dorsolateral sides?
	I: Suprascapular cartilage, medial side.	I: Scapular blade, dorsomedial rim.	I: Suprascapular cartilage?	I: Suprascapular cartilage?
<i>M. Levator scapulae</i> (LS)	O: Cervical ribs and diapophyses.	Absent	O: Cervical ribs and diapophyses.	O: Cervical ribs and diapophyses.
	I: Scapular blade, anterior edge.		I: Scapular blade, anterior edge.	I: Scapular blade, sharp anterior edge.
<i>M. serratus superficialis</i> (SS)	O: Last cervical rib and DV3-DV1 ribs, uncinat processes.	O: Last cervical rib and DV6-DV1 ribs.	O: Last cervical rib and DV3-DV1 ribs, uncinat processes.	O: Last cervical rib and DV3-DV1 ribs, uncinat processes.
	I: Scapula and suprascapula, posterior edge.	I: Scapular blade, distal third of ventral edge.	I: Scapular blade, posterior edge, internal side.	I: Scapular blade, posterior flange, internal side (facet).
<i>M.serratus profundus</i> (SP)	O: DV2-CV5 ribs and diapophyses.	O: Six posterior cervical and anterior dorsal ribs.	O: DV2-CV5 ribs and diapophyses.	O: DV2-CV8 ribs and diapophyses.
	I: Suprascapula and distal scapula, medial.	I: Scapular blade, medial surface of the distalmost part.	I: Scapular blade, distalmost medial side.	I: Scapular blade, distalmost medial side.
<i>M. costocoracoideus</i> (CC)	O: Last cervical rib and first sternal rib, anterior edges.	Absent	O: Last cervical rib and first sternal rib, anterior edges.	O: Last cervical rib and first sternal rib, anterior edges.
	I: Coracoid, posterior and medial sides.		I: Coracoid, posterior and medial sides.	I: Coracoid, internal side, depression between glenoid and biceps tuberculum.
<i>M. sternocoracoideus</i> (StC)	O: Sternum, internal side.	O: Sternocoracoideal process, lateral side.	O: Sternum, internal side.	O: Sternum.
	I: Coracoid, medial side.	I: Coracoid, dorso-medial side.	I: Coracoid, medial side.	I: Coracoid, medial side, dorsal to a ridge, on triangular depression.

Table 3.7 - Origins and insertions of cingulo-axial muscles on the pectoral girdle.

Origins and insertions for extant Crocodylia, Aves and *Plateosaurus engelhardti* from Remes, (2007) and Hohn-Schulte (2010). *Spinophorosaurus* osteological correlates are discussed in Chapter 3.6.

Both *M. serratus superficialis* (SS) and *M. serratus profundus* (SP) originate on the posterior cervical ribs and insert on the internal side of the scapula. The scapula of *Spinophorosaurus* has a posterior flange on the blade, which would likely be the insertion area for SS. The distal part of the scapular blade is flat on its internal side, and while SP inserts here in both extant birds and crocodiles, the boundaries of the insertion area cannot be determined for *Spinophorosaurus*.

M. costocoracoideus (CC) originates on the last cervical rib and the first sternal rib and inserts on the coracoid. While *Spinophorosaurus* has not preserved any identifiable sternal rib, they were likely present (Tschopp & Mateus, 2013). There is a depression on the internal side of the coracoid between the glenoid and the biceps tubercle where this muscle likely inserted. *M. sternocoracoideus* (StC) originates on the sternum and inserts on the internal side of the coracoid. While the sternum of *Spinophorosaurus* was not preserved, it was likely present and the muscle originated there. It would insert on a triangular depression dorsal to a ridge on the coracoid internal side.

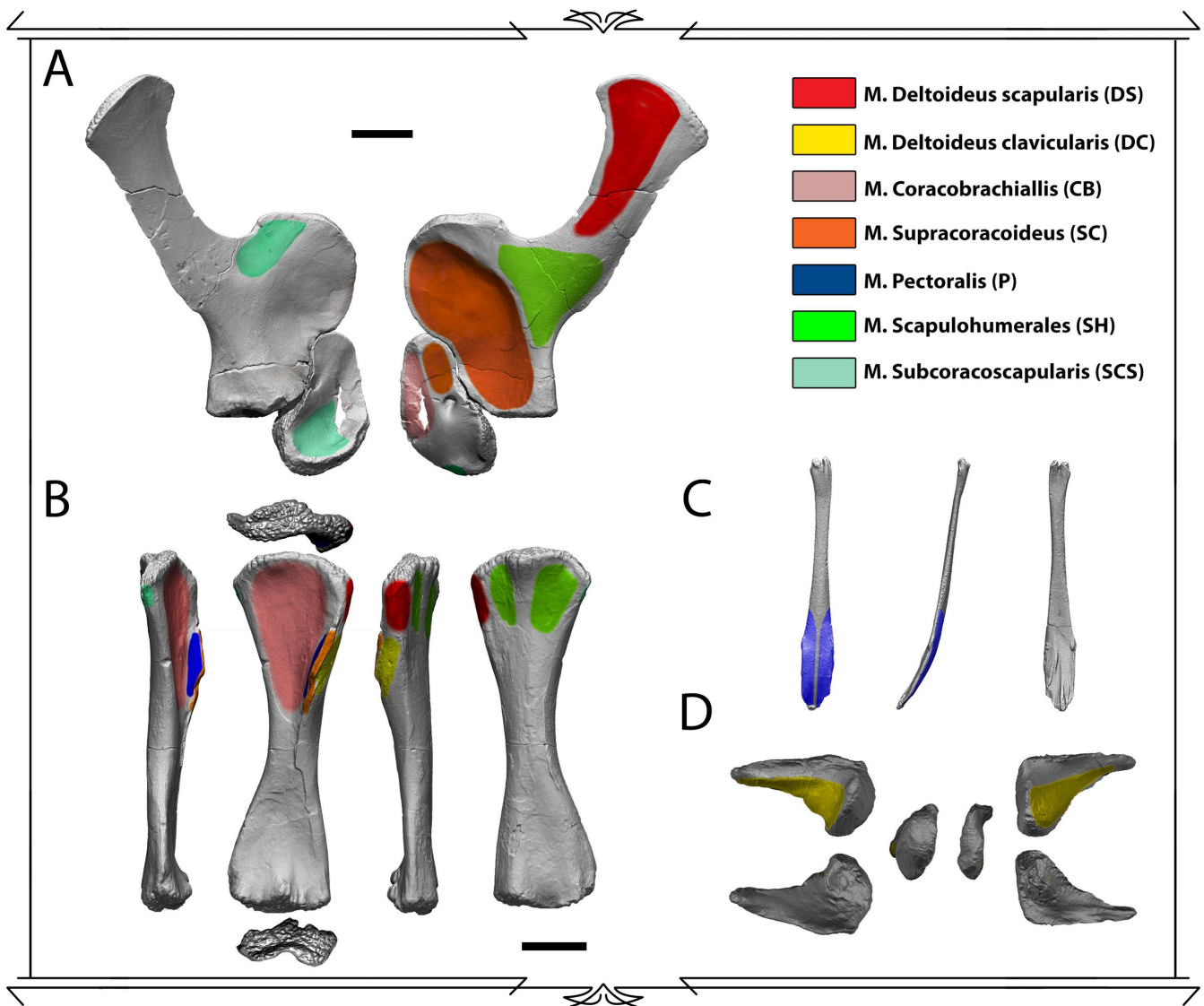


Figure 3.15 - Humeral musculature origins and insertions in the pectoral girdle and humerus of *Spinophorosaurus nigerensis*.

A - Scapulocoracoid in lateral (left) and medial (right) view, with main muscle origins and insertions highlighted and color-coded over their osteological correlates. **B** - Humerus in medial (left), anterior, lateral and posterior (left) view, with main muscle origins and insertions highlighted and color-coded over their osteological correlates. **C** - Interclavicle in external (left) lateral (middle) and internal (right) view, with main muscle origins and insertions highlighted and color-coded over their osteological correlates. **D** - Clavicles in external (top), internal (bottom) and medial (middle) view with main muscle origins and insertions highlighted and color-coded over their osteological correlates. List of osteological correlates in Table 3.8.

Humeral musculature: These muscles are mainly related to all motions concerning the shoulder articulation, as well as isometrically stabilizing the joint during antagonical motions.

M. deltoideus scapularis (DS) originates on the suprascapula in extant crocodiles and part of the distal scapular blade in both extant crocodiles and birds, inserting in the anterodorsal, proximal humerus. There is a well-marked distal expansion on the scapula of many sauropods, including *Spinophorosaurus*, which creates a larger surface for the origin of this muscle. It inserts on the lateral tubercle of the humerus, with a ridge marking its insertion.

M. deltoideus clavicularis (DC) originates acromion region of the scapula in crocodiles (which lack clavicles) and on the acromion and region of the furcula of birds where it articulates with the acromion. In *Spinophorosaurus*, the clavicles are ossified, and they bear a concave surface on one of its sides, where DC might have originated. It inserts on the anterior face of the deltopectoral crest.

M. coracobrachialis (CO) originates on the dorsolateral side of the coracoid and inserts on the anterior side of the humerus, on its proximal side. In *Spinophorosaurus*, there is a fossa anterior to the coracoid foramen where the muscle might have originated. It inserted on the anterior fossa of the humerus.

	Crocodylia	Aves	Plateosaurus	<i>S.nigerensis</i>
<i>M. deltoideus scapularis</i> (DS)	O: Scapular blade, lateral side, anterodistal end.	O: Lateral side of scapular head.	O: Scapular blade, lateral side, distal expansion.	O: Scapular blade, lateral side, distal expansion.
	I: Humerus, anterodorsal side.	I: Humerus, deltopectoral crest.	I: Humerus, lateral tubercle (distally limited by ridge).	I: Humerus, lateral tubercle (distally limited by ridge).
<i>M. deltoideus clavicularis</i> (DC)	O: Scapula, acromial region.	O: Furcula, proximal region. Scapula acromial region.	O: Clavicles (external side) and acromial region.	O: Clavicles, external side, on depression.
	I: Humerus, deltopectoral crest, anterior side.	I: Humerus, deltopectoral crest, proximal end.	I: Humerus, deltopectoral crest.	I: Humerus, deltopectoral crest, ventral to DS.
<i>M. coracobrachialis</i> (CB)	O: Coracoid, external side, posterior side.	O: Coracoid, dorsolateral edge.	O: Coracoid, lateral side.	O: Coracoid, lateral side.
	I: Humerus, proximo-ventral third.	I: Humerus, antero-proximal side.	I: Humerus, proximo-ventral third.	I: Humerus, anterior depression of humeral epiphysis.
<i>M. supracoracoideus</i> (SC)	O: Coracoid, lateral side, anterior half, Scapula, lateral side, ventral third.	O: Coracoid, lateral side, Sternum, ventral surface.	O: Coracoid, lateral side, anterior half, Scapula, lateral side, ventral third.	O: Scapular head, lateral side, ventrolateral fossa. Coracoid, lateral side, fossa dorsal to coracoid foramen.
	I: Humerus, deltopectoral crest apex.	I: Humerus, lateral tuberosity.	I: Humerus, deltopectoral crest apex.	I: Humerus, deltopectoral crest apex.
<i>M. pectoralis</i> (P)	O: Interclavicle, Sternum, Sternal ribs 1 to 8.	O: Furcula, lateral sides. Sternum.	O: Interclavicle? Sternum.	O: Interclavicle, lateral sides with striations. Sternal plates?
	I: Humerus, deltopectoral crest, posterior side.	I: Humerus, deltopectoral crest, posterior side.	I: Humerus, deltopectoral crest, medial side.	I: Humerus, deltopectoral crest, medial side.
<i>M. latissimus dorsi</i> (LD)	O: Dorsal neural spines 1 to 5.	O: Dorsal Neural spines, Ilium, anterior edge.	O: Anterior dorsal neural spines.	O: Anterior dorsal neural spines.
	I: Humerus, proximodorsal side (fused with Teres).	I: Posterior side of humerus.	I: Humerus, proximoposterior side.	I: Humerus, proximoposterior side.
<i>M. Teres major</i> (TM)	O: Scapula, lateral side, posterodorsal region.	Absent	Absent	Absent
<i>M. scapulohumerales</i> (SH)	I: Same for LD.			
	O: Coracoid, dorsal region. Scapula, ventral region.	O: Scapular blade, lateral surface.	O: Scapular blade, lateral side.	O: Scapular blade, lateral side.
<i>M. subcoracoscapularis</i> (SCS)	I: Humerus, distally to medial tuberosity.	I: Humerus, medial tuberosity.	I: Humerus, distally to medial tuberosity.	I: Humerus, posterior face, oval fossae to the sides of humeral head.
	O: Scapula, medial side.	O: Scapula, medial side, proximal half.	O: Ambiguous.	O: Scapular head, medial side, depression on acromial region. Coracoid, medial side, fossa ventral to coracoid foramen.
	I: Humerus, medial tuberosity and base.	I: Humerus, medial tuberosity.	I: Humerus, medial tubercle.	I: Humerus, medial tubercle.

Table 3.8 - Origins and insertions of humeral muscles of the pectoral girdle.

Origins and insertions for extant Crocodylia, Aves and *Plateosaurus engelhardti* from Remes (2007) and Hohn-Schulte (2010). *Spinophorosaurus* osteological correlates are discussed in Chapter 3.6.

M. supracoracoideus (SC) originates on the coracoid and scapula in extant crocodiles and in the coracoid and sternum in extant birds, always inserting on the medial apex of the deltopectoral crest. In non-avian theropods, the configuration of this muscle was likely the primitive condition of crocodiles, as evidenced by the large depression on the scapular head of most sauropods where the scapular portion originated.

M. pectoralis (P) originates on the sternal plates and inserts onto the medial side of the deltopectoral crest on both extant crocodiles and birds and, in crocodiles, it also originates on the lateral sides of the interclavicle. Given that *Spinophorosaurus* has an ossified interclavicle (retrieved on both the holotype and paratype specimens), which has one of its ends laterally expanded and with longitudinal scars, it is likely that P had its origin on the expansion of the interclavicle. The sternals were not retrieved (or did not ossify) in *Spinophorosaurus*, but they likely served as origin for P as well.

M. scapulohumerales (SH) originates on the lateral of the scapula in extant birds and crocodiles, and in the coracoid of extant crocodiles as well, and it inserts on distally to the medial tuberosity of the humerus. In *Spinophorosaurus* it originated on the convex surface of the scapular blade on its lateral side, and inserted on the posterior face of the humerus, on two fossae surrounding the posterior projection of the humeral head.

M. subcoracoscapularis (SCS) originates in the internal side of the scapula and coracoid in extant crocodiles, only on the internal side of the scapula in extant birds, inserting onto the proximo-medial side of the humerus, on the medial tubercle/tuberosity. In *Spinophorosaurus*, the *pars coracoidalis* of SCS originates on a fossa ventral to the coracoid foramen, and the *pars scapularis* of SCS originates on the medial side of the scapular head (Remes, 2007; Hohn-Schulte, 2010).

Pelvic, Hindlimb and Caudal musculature

Pelvic, hindlimb and caudal muscles must be among the most reconstructed muscle groups in non-avian dinosaurs, with multiple examples in Ornithischia (Romer, 1927), Theropoda (Romer, 1923; Carrano & Hutchinson, 2002; Hutchinson *et al.*, 2005, 2011; Persons & Currie, 2010, 2011, 2012; Grillo & Azevedo, 2011) and Sauropoda (Fechner, 2009; Klinkhamer *et al.*, 2018).

The muscle attachment scars are almost identical between theropod and sauropod pelvis, hindlimbs and tails, so their origins and insertions (Table 3.9) are fairly similar (compare Carrano & Hutchinson, 2002 with Fechner, 2009). The most interesting insights from reconstructing these muscles in *Spinophorosaurus* are those regarding the size of origins (Fig. 3.16).

Mm. iliobiales 1, 2 et 3 (IT) their origins are in the dorsal rim of the ilium and insert in the medial side of the cnemial crest of the tibia. Separating all 3 IT muscles is not always possible to do with certainty in the absence of clear muscle scars. In *Spinophorosaurus*, more or less abrupt changes in dorsal ilium rim width were used to separate all three groups, with IT2 having its origin in the thinnest portion and IT1 and IT3 on the wider anterior and posterior portions, respectively.

M. flexor tibiales externus (FTE) originates in the lateral aspect of the ilium posterior to the ILFIB. In *Spinophorosaurus*, there is a flat surface, dorsally and posteriorly to the ILFIB rugosities where the muscle would have originated. FTE inserts on the tibia, but it has no osteological correlates in sauropod dinosaurs (Fechner, 2009).

M. iliofibularis (ILFIB) originates on the posterior region of the iliac blade, anterior to FTE and posterior to IFE. There is a fossa in the preserved ilium of *Spinophorosaurus* with a distinct ornamentation pattern, which delimits the insertion area for this muscle dorsally and anteriorly. It inserts in the fibula, on the tuberculum iliofemorale, at midshaft height.

M. iliofemoralis externus (IFE) originates anteriorly to ILFIB on the iliac blade, dorsal to the acetabulum. In *Spinophorosaurus* there is an inverted triangle shaped region dorsal to the acetabulum with faint rugosities, which may indicate its origin area. Since in crocodiles and other non-avian extant amniotes it inserts on the lesser trochanter, and *Spinophorosaurus* has a faint lesser trochanter, IFE likely inserted there.

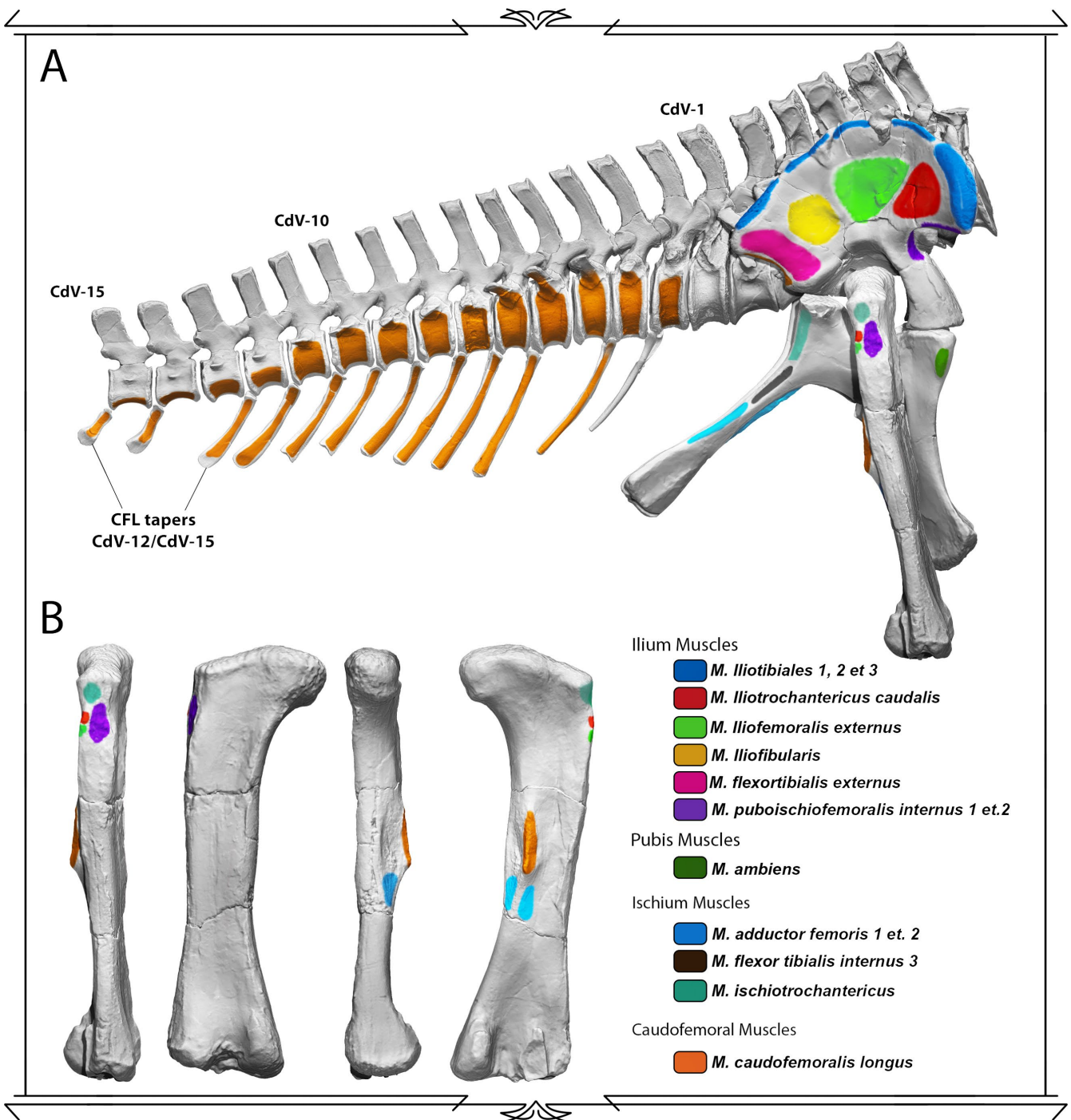


Figure 3.16 - Femoral musculature origins and insertions in the pelvic girdle and femur of *Spinophorosaurus nigerensis*.

A - Femur, pelvic girdle, sacrum and anterior tail in lateral view with main muscle origins and insertions highlighted and color-coded over their osteological correlates. **B** - Femur in lateral (left), anterior, medial and posterior (left) view, with main muscle origins and insertions highlighted and color-coded over their osteological correlates. List of osteological correlates in Table 3.9.

M. ilioprochantericus caudalis (ITC) originates on the iliac blade surface, more anterior to IFE and more posterior than FTE. In *Spinophorosaurus* there are no clear rugosities or ornamentation on this region of the ilium, but it is likely that it was present in all dinosaurs (Fechner, 2009). In extant crocodiles and other sauropsids, it inserts on the lesser trochanter. In *Spinophorosaurus*, there is a shelf dorsal to the lesser trochanter where ITC likely inserted.

M. caudofemoralis brevis (CFB) originates on a shelf on the posterior margin of the ilium in extant archosaurs (Gatesy, 1990; Gatesy & Middleton, 1997; Fechner, 2009), and on the centra of the anteriormost caudal vertebrae (Mallison *et al.*, 2015). In *Spinophorosaurus*, the shelf on the posterior margin of the ilium has some striations, which may indicate the origin of this muscle. It inserts on the fourth trochanter of the femur.

M. caudofemoralis longus (CFL) is the main retractor of the femur in non-avian archosaurs (Gatesy, 1990; Stephen M. Gatesy, 1997), although it also has an important role in femoral adduction and rotation (Gatesy, 1990; Mallison *et al.*, 2015) and tail lateral stabilization (Mallison *et al.*, 2015). It inserts via tendon in the fourth trochanter, and originates on the lateral surfaces of the caudal centra and chevrons (Persons & Currie, 2010; Ibiricu *et al.*, 2014; Mallison *et al.*, 2015; Klinkhamer *et al.*, 2017). It is the deepest hypaxial muscle, surrounded by the *Mm. ilio-ischiocaudalis* group. As the CFL tapers toward its posterior end before disappearing, the *ilio-ischiocaudalis* intrudes on the surface of the chevrons and centrum, (Persons & Currie, 2010). Since there is a strong skeletogenous septum separating both muscles (Persons & Currie, 2010), the final tapering of the CFL may leave a dorsal scar on the caudal vertebrae centra as a longitudinally lateral ridge separating a primary and secondary lateral surfaces (Ibiricu *et al.*, 2014) and a ventral scar on the chevrons as a longitudinally lateral ridge as well (Persons & Currie, 2010). As *Spinophorosaurus* preserves an almost continuous caudal axial skeleton (including vertebrae and chevrons), the exact extent of the CFL can be accurately established, as well as its tapering. The first caudal with a longitudinal ridge on the centrum is CdV-12, and the last caudal with longitudinal ridge is CdV-15 (Fig. 3.16 A). The first chevron with a longitudinal ridge is that articulating with CdV-11 and the last chevron with a longitudinal ridge is that articulating with CdV-15. The CFL therefore originated from CdV-2 and disappeared by CdV-15, beginning to taper by CdV-12.

M. flexor tibialis internus (FTI) originates on the lateral surface of the ischium. There is a strong osteological correlate on the ischia of *Spinophorosaurus*, a shallow fossa on the posterolateral surface of the ischium where the muscle originated. It inserts on the proximal region of the tibia, but there are no osteological correlates for *Spinophorosaurus*.

M. ischiotrochantericus (ISTR) originates on the posterior lateral margin of the ischium. In *Spinophorosaurus*, there is a distinct rugose ornamentation in the right ischium, where it may have originated. It inserts between the lesser and greater trochanter in extant crocodiles, theropods and non-sauropod sauropodomorphs. In *Spinophorosaurus*, there is a rugose depression posterolateral between the lesser and greater trochanters where it inserted.

M. adductor femoris (ADD 1 et 2) inserts close to the fourth trochanter. In *Spinophorosaurus*, there is a sulcus medial to the fourth trochanter indicating the separation for the origin of these two muscles.

M. ambiens (AMB) originates on the proximal region of the pubis, close to the pubic pedicle. In many dinosaurs, including *Spinophorosaurus*, there is a process in this region called “ambiens process”, referencing the origin of this muscle. It inserts on the cnemial crest of the tibia.

M. puboischiofemorales (PIFE 1, 2, et 3) has two origins on the pubis (PIFE 1 et 2) and one on the ischium (PIFE 3). PIFE 1 et 2 originate on the internal surface of the pubis, and PIFE 3 originates close to the foramen obturator. They all insert on the greater trochanter of the femur.

The caudal musculature of archosaurs includes segmented epaxial and hypaxial musculature in addition to both *caudofemorales* (Persons & Currie, 2010; Mallison *et al.*, 2015), which unlike CFL, run for the complete length of the tail. The epaxial muscles consist of *Mm. spinalis*, which originates on the lateral surfaces of the neural spines and insert onto the tip of the neural spines. *Mm. longissimus* originates on the lateral surfaces of the neural arches and inserts on the dorsal surface of the caudal ribs. *Mm. ilio-ischiocaudalis* (which can only be differentiated on some taxa) originate on the ilium and ischium and inserts on the lateral and ventral surfaces of the caudal ribs and the dorsal tip of the chevrons. As CFL disappears posteriorly, the *ilio-ischiocaudalis* also inserts on the lateral faces of the vertebral centra.

	Crocodylia	Aves	Plateosaurus	<i>S.nigerensis</i>
<i>Mm. Iliotibiales 1,2 et 3 (IT)</i>	O: Ilium, dorsal rim. I: Tibia, cnemial crest.	O: Ilium, dorsal rim. I: Tibia, cnemial crest.	O: Ilium, dorsal rim. I: Tibia, cnemial crest.	O: Ilium, dorsal rim.. I: Tibia, cnemial crest.
<i>M. flexor tibiales externus (FTE)</i>	O: Ilium, posterior part of the blade. I: Tibia, posteromedial surface.	O: Ilium, posterior part of the blade. I: Tibia, posteromedial surface.	O: Ilium, postacetabular blade. I: Tibia, proximomedial diaphysis.	O: Ilium, postacetabular blade. I: Tibia, posteromedial surface with PIT and FTI 1 et 3.
<i>M. iliofibularis (ILFIB)</i>	O: Ilium, posterolateral surface of blade. I: Fibular tubercle.	O: Ilium, posterolateral surface of blade. I: Fibula, <i>Tuberculum iliofibularis fibulae</i> .	O: Ilium, postacetabular blade, between FTE and IFE. I: Fibula, <i>Tuberculum iliofibularis fibulae</i> .	O: Ilium, postacetabular blade, between FTE and IFE. I: Fibula, <i>Tuberculum iliofibularis fibulae</i> .
<i>M. iliofemoralis externus (IFE)</i>	O: Ilium, posterolateral surface of blade, anterior to ILFIB. I: Femur, trochanteric shelf.	O: Ilium, supraacetabular blade, between ILFIB and ITC. I: Femur, proximo-lateral surface.	O: Ilium, supraacetabular blade, between ILFIB and ITC I: Femur, third trochanter.	O: Ilium, supraacetabular blade, between ILFIB and ITC I: Femur, third trochanter.
<i>M. iliiochantericus caudalis (ITC)</i>	O: Ilium, posterolateral surface of blade (same muscle as IFE, <i>iliofemoralis</i>). I: Femur, trochanteric shelf.	O: Ilium, preacetabular process blade, anterior to IFE. I: Femur, proximo-lateral surface.	O: Ilium, preacetabular process blade, anterior to IFE, ventral to IT1. I: Femur, third trochanter.	O: Ilium, preacetabular process blade, anterior to IFE, ventral to IT1. I: Femur, third trochanter.
<i>M. puboischiofemoralis internus (PIFI)</i>	O: Ilium, medial surface, proximal ischium. I: Femur, proximo antero-lateral surface.	O: Ilium, preacetabular fossa. I: Femur, proximo antero-lateral surface.	O: Ilium, preacetabular fossa. I: Femur, proximomedial to third trochanter.	O: Ilium, preacetabular fossa. I: Femur, proximomedial to third trochanter.
<i>M. ischiotrochantericus (ISTR)</i>	O: Ischium, medial surface. I: Proximal femur, latero-posterior surface.	O: Ischium, lateral surface. I: Proximal femur, latero-posterior surface.	O: Proximal ischium, lateral and medial region dorsal to FTI. I: Proximal femur, latero-posterior surface.	O: Proximal ischium, lateral and medial region dorsal to FTI. I: Proximal femur, latero-posterior surface.
<i>M. flexor tibialis internus 3 (FTI)</i>	O: Ischium, ischial tuberosity. I: Tibia, proximo-posterior surface.	O: Ischium, ischial tuberosity. I: Tibia, proximo-posterior surface.	O: Ischium, ischial tuberosity. I: Tibia, proximo-posterior surface.	O: Ischium, ischial tuberosity. I: Tibia, proximo-posterior surface.
<i>M. adductor femoris 1 et. 2 (ADD)</i>	O: Ischium, obturator blade and lateral shaft. I: Femur, posterior surface.	O: Ischium, anteroventrally placed in lateral surface. I: Femur, posterior surface.	O: Ischium, obturator blade and lateral shaft. I: Femur, posterior surface, distal to 4th trochanter.	O: Ischium, obturator blade and lateral shaft. I: Femur, posterior face, lateral and medial to the ridge distal to 4th trochanter.
<i>M. ambiens (AMB)</i>	O: Proximal pubis. I: Tibia, anteroproximal surface.	O: Pubis, ambiens process. I: Tibia, cnemial crest.	O: Pubis, ambiens process. I: Tibia, cnemial crest.	O: Pubis, ambiens process. I: Tibia, cnemial crest.
<i>M. caudofemoralis longus (CLF)</i>	O: Lateral sides of caudal vertebrae and chevrons. I: Femur, fourth trochanter.	O: Lateral sides of anterior caudal vertebrae. I: Femur, posterior surface.	O: Lateral sides of caudal vertebrae and chevrons. I: Femur, fourth trochanter.	O: Lateral sides of caudal vertebrae and chevrons. I: Femur, fourth trochanter.

Table 3.9 - Origins and insertions of muscles acting on the acetabular joint of the pelvic girdle.

Origins and insertions for extant Crocodylia and Aves from Carrano & Hutchinson (2002), Plateosaurus engelhardti from Fechner (2009). Spinophorosaurus osteological correlates are discussed in Chapter 3.6.

3.7 VOLUMETRIC RECONSTRUCTIONS AND MASS ESTIMATES

Given the relative absence of studies on muscle volumes on the neck and forelimbs of extant archosaurs, volumetric reconstruction on those regions on extant archosaurs would carry on many assumptions resulting in larger error for estimates. Therefore, they have only been performed on tail muscles, where readily available published data on cross-sections exists (Mallison, 2011a; Mallison *et al.*, 2015).

These studies have particularly focused on estimating the size of *M. caudofemoralis longus*, the main leg retractor (Persons & Currie, 2010, 2011, 2012; Mallison, 2011a; Hutchinson *et al.*, 2011; Ibiricu *et al.*, 2014; Mallison *et al.*, 2015). The majority of those studies have focused on theropod dinosaurs and their locomotion capabilities, and the most thorough study on the size of this muscle in sauropods is restricted to Titanosauria (Ibiricu *et al.*, 2014), with little to no information on earlier branching sauropods.

The volumetric reconstruction of the tail musculature of *Spinophorosaurus* (Fig. 3.17 A, B), using the osteological correlates from 3.6, reveals an estimated caudofemoral musculature volume of 149057 cm³ for each CFL. Assuming a 1.06 g/cm³ density for muscle tissue (Méndez & Keys, 1960), the estimated mass for this muscle would be 158 kg, with a total combined mass of 316 kg of caudofemoral musculature (left and right).

The complete volumetric reconstruction of *Spinophorosaurus* reveals a body volume of 8400000 cm³, which translates to an estimated mass ranging from 6700 kg (assuming 0.9 g/cm³ density) to 8400 kg (assuming 1 g/cm³ density). In this scenario, the caudofemoral musculature would make up from 4% to 5% of the whole-body mass (Table 3.10).

The center of mass of *Spinophorosaurus* is located in front of the pelvis (Fig. 3.17 H) when in ONP. If the neck is raised to the alert posture proposed by Taylor *et al.* (2009), the center of mass barely moves a little dorsally and posteriorly.

3.8 DISCUSSION

Body plan and feeding capabilities of Spinophorosaurus.

Although there has been a thorough debate on the feeding capabilities of the different Sauropoda taxa, most analyses have focused on skull, teeth and neck functional morphology. Previous studies hinted at the fact that pectoral girdle and forelimb position created a dorsal sloping of the presacral vertebrae (Schwarz *et al.*, 2007a; Stevens, 2013), suggesting that studying only cranial and cervical anatomy might be insufficient to understand the sauropod body plans and feeding capabilities (Stevens, 2013). Mounting the virtual skeleton of *Spinophorosaurus* has revealed that the morphology of sacrum and posterior dorsal vertebrae also have a crucial role on the overall body plan by deflecting the presacral series from the caudal series in osteologically neutral pose (Fig. 3.5). Given the general position of the pelvis in Sauropoda, with an antero-posteriorly projected ilium and a mesopubic and opisthopubic condition (Rasskin-Gutman & Buscalioni, 2001), the coalesced sacrum is situated so that the posterior face of the last sacral centrum is sub-vertical. This makes the presacral series to slope dorsally and the tail to be subhorizontal (Fig. 3.2, Fig. 3.5). A subhorizontal tail has been known to be present in the majority of known sauropods (Gilmore, 1932; Bakker, 1968; Coombs, 1975), and the OIC of the tail of *Spinophorosaurus* is therefore compatible with this condition.

The dorsal sloping of presacral vertebrae in sauropod dinosaurs was noticed by Gilmore when assembling *Diplodocus* sp. USNM 10865, in which the posteriormost dorsal vertebrae would dorsally deflect from the

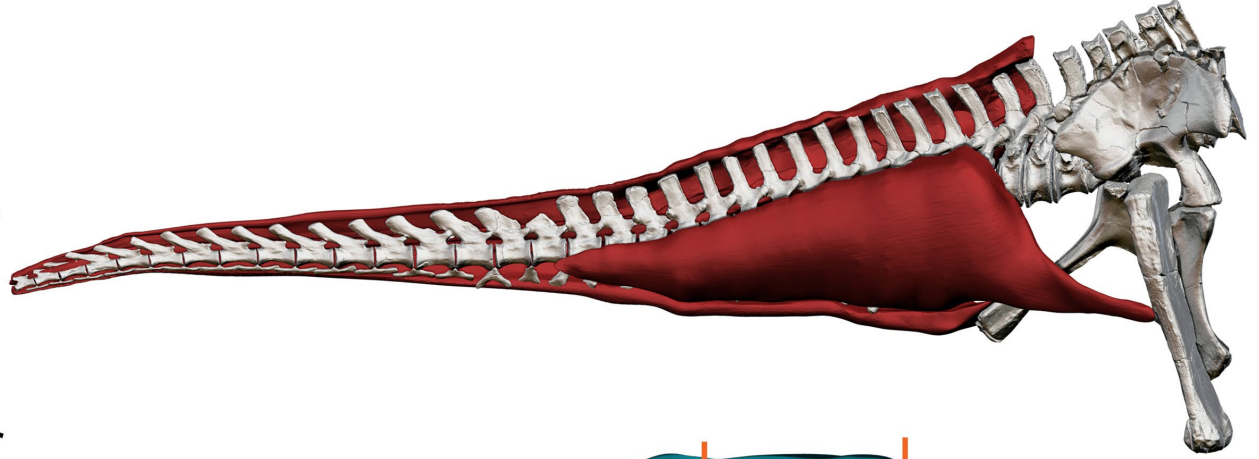
Figure 3.17 (next page) - Volumetric reconstruction of caudal musculature and full body of *Spinophorosaurus nigerensis*.

A - Volumetric reconstruction of caudal musculature in dorsal view. **B** - Volumetric reconstruction of caudal musculature in lateral view, with emphasis on *M. caudofemoralis longus*. **C** - Full body volumetric reconstruction in dorsal view, with different cross-sections highlighted. **D** - Cross-section of the volumetric reconstruction at caudal vertebra 4. **E** - Cross-section of the volumetric reconstruction at dorsal vertebra 9. **F** - Cross-section of the volumetric reconstruction at dorsal vertebra 1. **G** - Cross-section of the volumetric reconstruction at cervical vertebra 6. **H** - Full body volumetric reconstruction in lateral view, with different cross-sections highlighted. Computed position of center of mass marked as a white dot.

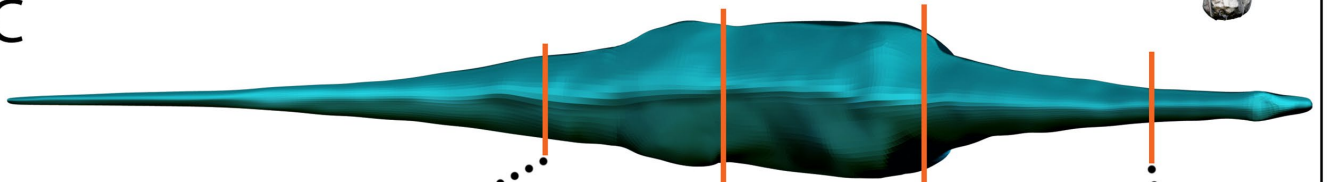
A



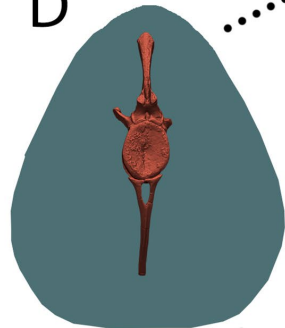
B



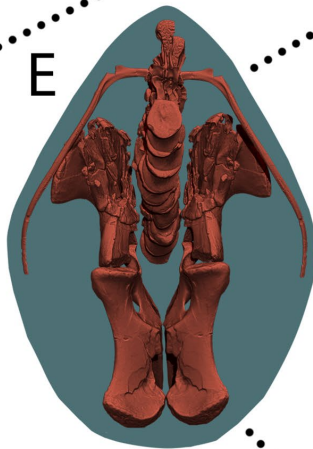
C



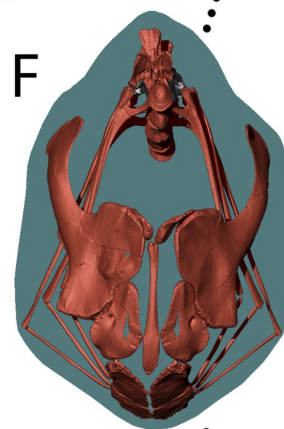
D



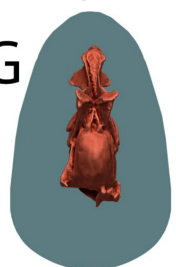
E



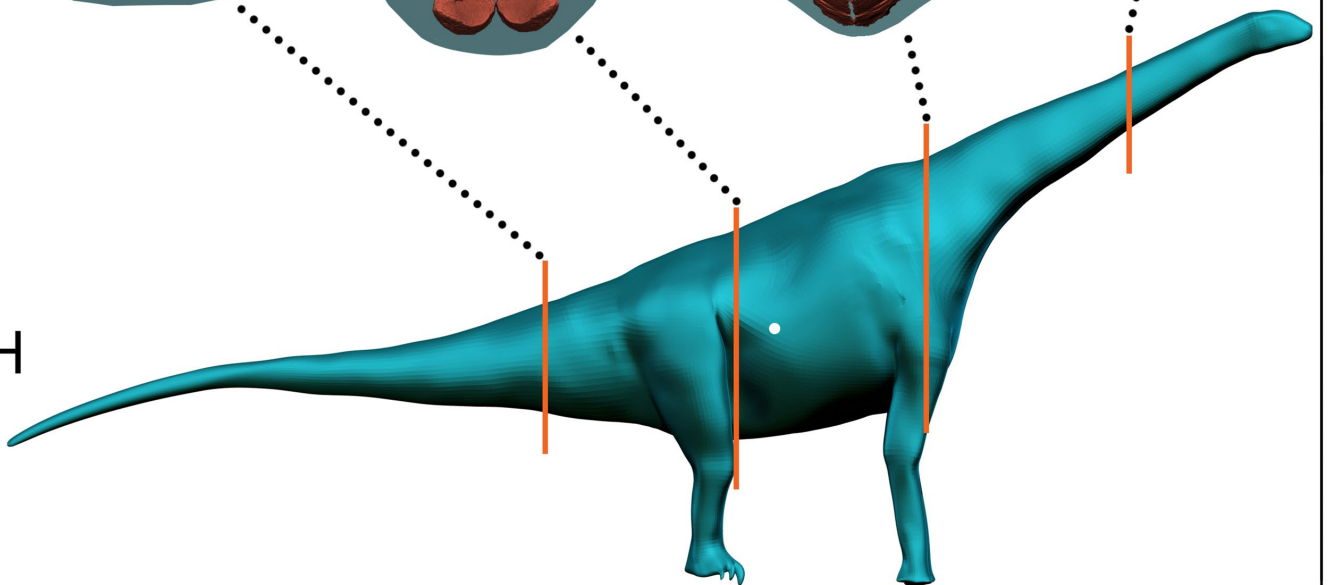
F



G



H



sacrum when in articulation (Gilmore, 1932). Gilmore also noticed that the posteriormost dorsal vertebrae of USNM 10865 had an anteriorly pointed neural spine which was perpendicular to the ground when vertebrae were in articulation with one-another and with the sacrum (Gilmore, 1932). The neural spines of posterior dorsal vertebrae DV12-DV9 are also anteriorly directed in the holotype of *Spinophorosaurus* (Fig. 3.5 B). However, Gilmore remarked that around mid-thoracic region, the dorsal spine of USNM 10865 reversed its curvature, deflecting ventrally, making an arched torso (Gilmore, 1932).

This arching of the torso is not present in *Spinophorosaurus* in osteologically neutral pose, nor is any mid or anterior dorsal vertebra wedged to create a ventral deflection (Fig. 3.2). Instead, the presacral column of *Spinophorosaurus* is very straight, with only a slight dorsal deflection of 10° from the last dorsal to the axis. This configuration of a dorsally sloping presacral column in *Spinophorosaurus* is compatible with the sub-vertical, more antero-ventrally placed scapula proposed by independent osteological (Schwarz *et al.*, 2007a; Tschopp & Mateus, 2013), myological (Remes, 2007), biomechanical (Hohn-Schulte, 2010) and phylogenetical bracketing (Schwarz *et al.*, 2007a) studies (see Fig. 3.4 and section 3.6 above), as well as with an elongated scapula and humerus.

Forelimb length and shoulder height are important factors for estimating the feeding capabilities of sauropod dinosaurs. Those with longer forelimbs relative to their hindlimbs are interpreted as having high browsing capabilities (Stevens & Parrish, 2005; Stevens, 2013). *Camarasaurus* is a genus typically interpreted as a capable medium to high browser based on its shoulder height (Stevens, 2013; Paul, 2017), with a humerus to scapula ratio around 0.74 and a femur to humerus ratio around 1.37. Both the humerus to scapula ratio (0.816) and the estimated femur to humerus ratio (1.21) of *Spinophorosaurus* indicate a relatively larger humerus than that of *Camarasaurus*.

The scapula of *Spinophorosaurus* is also slightly longer than its femur, whereas that of *Camarasaurus* is slightly shorter than its femur (Table 3.1). Therefore, the preserved forelimb and pectoral girdle elements of *Spinophorosaurus* are relatively longer than those of *Camarasaurus*. All in all, *Spinophorosaurus* had a humerus and scapula relatively longer, making its shoulders relatively taller than those of most known sauropods, with the exception of at least *Atlasaurus* (Monbaron, Russell, & Taquet, 1999) brachiosaurids (Janensch, 1950; Christian, 2002; Paul, 2017) and some titanosaurs (Table 3.1, Fig. 3.7 B).

Regarding the missing forearm and hand bones in *Spinophorosaurus*, if they were as long relative to the humerus as in other non-neosauropod Eusauropoda (Table 3.2, Fig. 3.4), they would be compatible with the virtual mount. Shorter or taller shoulder would require, respectively, shorter or longer hypothetical forearm and hand relative to the humerus. This implies that any hypothesis regarding much shorter or much taller shoulders for *Spinophorosaurus* than those proposed in this reconstruction requires additional evolutionary steps (to acquire relatively shorter or longer missing elements) and are, therefore, less parsimonious.

This shows that the overall body plan of this sauropod has a clear tendency toward verticalization due to its sacral wedging as well as humerus and scapula to femur proportions, especially when compared with its earlier branching relatives (Table 3.1). This tendency to verticalization, coupled with the increased dorso-ventral neck flexibility granted by the elongated prezygapophyseal facets, and coordinated by its relatively large and slender inner ear (Knoll *et al.*, 2012), reveals a feeding envelope with a large vertical component. This feeding envelope is greater than those calculated for *Diplodocus carnegii* (Stevens & Parrish, 1999), *Apatosaurus louisae* (Stevens & Parrish, 1999) or *Mamenchisaurus youngii* (Christian *et al.*, 2013), and possibly greater than those of *Camarasaurus* or *Haplocanthosaurus* (Fig. 3.18).

The muscle reconstruction for *Spinophorosaurus* also shows a higher development of muscles *M. longus colli dorsalis* (stout, pillar-like epiphyses), *M. longus colli ventralis* or *M. flexor colli* (very developed ventral keels, suggesting a large insertion and origin for said muscles). Although *M. intertransversarii* is also developed, but the neck of *Spinophorosaurus* is generally taller than wider, making the lever arm for lateral flexion smaller. All this suggests motion on the dorso-ventral plane as very active in this sauropod.

Summing up, *Spinophorosaurus* can be interpreted as adept at high browsing, like modern giraffes are (Young & Isbell, 1991): its skeleton conferred *Spinophorosaurus* the capability to browse on vegetation at nearly three times the height of its shoulders, and hence it might have been part of its feeding strategy.

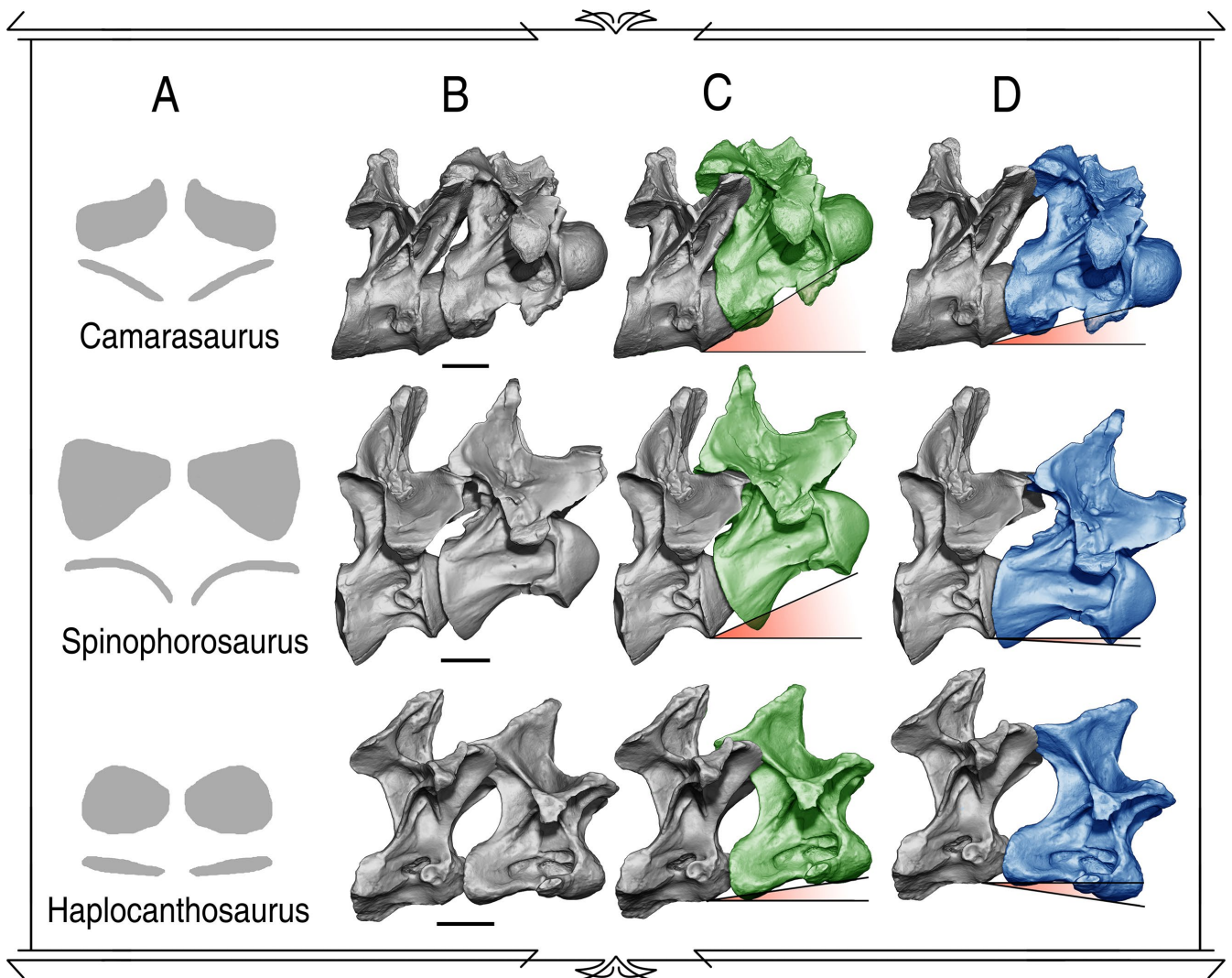


Figure 3.18 - Range of motion on the cervico-dorsal transition in selected eusauropod sauropods.

A - Outlines of the prezygapophyseal facets of *Camarasaurus* sp. (CM 584), *Spinophorosaurus nigerensis* (GCP-CV-4229) and *Haplocanthosaurus priscus* (CM 572) in dorsal view. **B** - First dorsal and last cervical vertebrae of *Camarasaurus* sp. (CM 584), *Spinophorosaurus nigerensis* (GCP-CV-4229) and *Haplocanthosaurus priscus* (CM 572) in Osteological Neutral Pose and right view. **C** - Maximum dorsiflexion for that joint. **D** - Maximum ventriflextion at that joint. Scales under B = 100 mm.

The specialized tail of Spinophorosaurus

Despite nearly complete sauropod tails being more common in the fossil record than nearly complete sauropod necks, there is far less published studies on them than on necks. Recently, there has been an increased interest in studying theropod tails, as the size of *M. caudofemoralis longus* is likely to have an important role their locomotion capabilities (Gatesy, 1990; Stephen M. Gatesy, 1997; Persons & Currie, 2010, 2011; Hutchinson *et al.*, 2011), as well as on the specialized functions the tail may have evolved in some taxa (Persons, Currie, & Norell, 2013).

The tails of sauropods also evolved some specialized features, such as tail clubs in *Shunosaurus* and some Mamenchisauria (Dong, Peng, & Huang, 1989) or whiplashes in diplodocoid sauropods (Holland, 1906; Gilmore, 1932; Myhrvold & Currie, 1999) and perhaps on some titanosaurs (Wilson, Martinez, & Alcober, 1999). Tail clubs had been proposed to work in a way similar to those of ankylosaurs, as active defense. However, finite element analyses on the tail club of *Mamenchisaurus* sp. revealed it would not withstand stresses as high as those reported for ankylosaurs (Xing *et al.*, 2009), and while other functions were proposed, they have not been thoroughly tested.

Whiplashes, on the other hand, have been more thoroughly studied than tail clubs. The first proposed function of whiplashes was also as an active defense, for lashing predators. However, Myhrvold & Currie (1999)

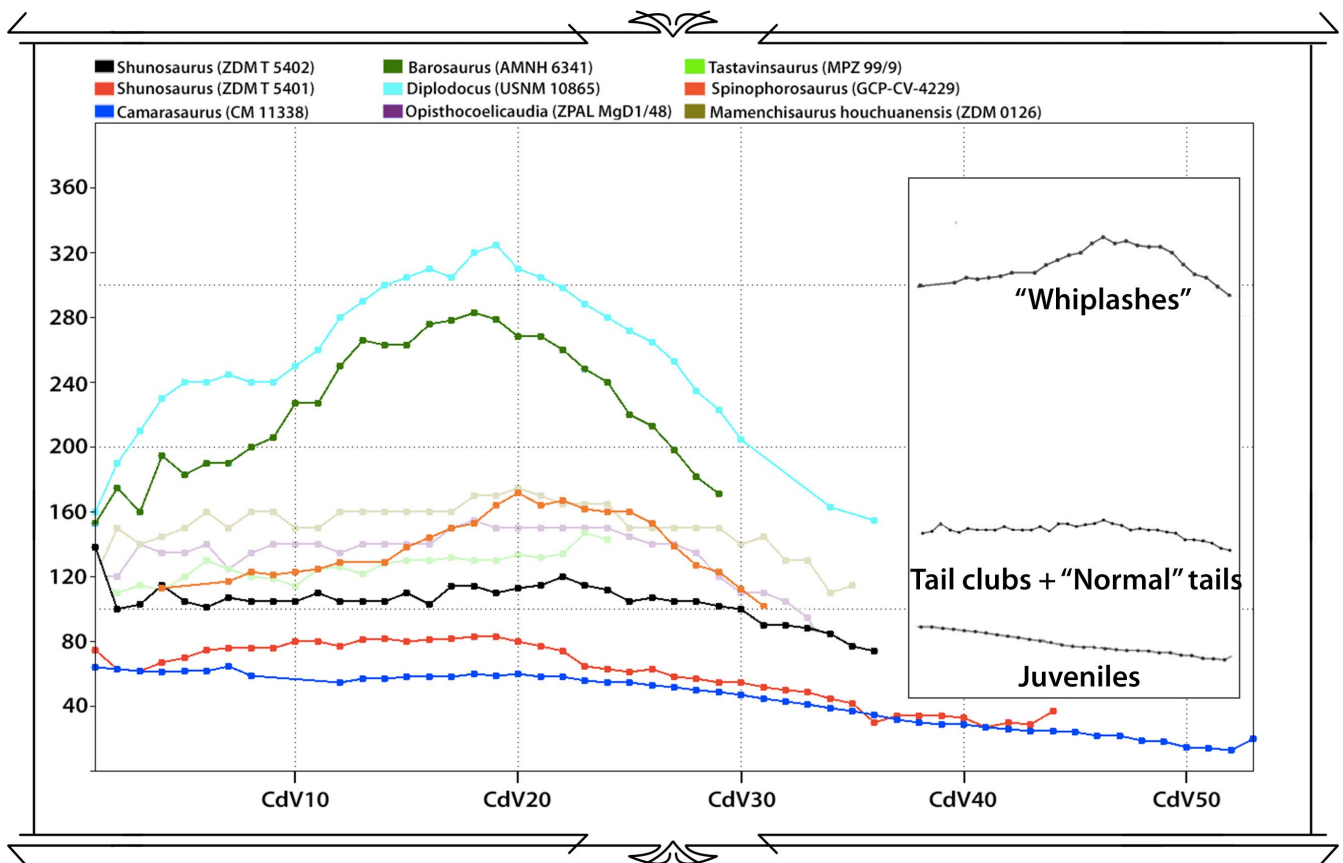


Figure 3.19 - Length of caudal vertebral centra throughout the tail of sauropod dinosaurs.

On the Y-axis, centrum length in mm. On the X-axis, caudal vertebra number. Notice how there are two main patterns of centrum length variation throughout the series: constant but slight decrease in length (in sauropods without specialized tails and those with tail clubs), and a steady increase in length until caudal vertebra 20, and an abrupt decrease in length from that point on (sauropods with a whiplash and *Spinophorosaurus*).

showed that a small twist at the anteriormost tail may have caused the tip of the tail to reach supersonic speeds, at which impact may have shattered the small distal caudal vertebrae. In absence of a high number of distal tail pathologies in diplodocoids, they ruled out the lashing hypothesis. However, they proposed that supersonic speed may have caused the tail to produce sonic booms like those produced by cracking whips. Furthermore, they proposed that the elongation of mid-caudals vertebrae and the high prevalence of mid-caudals fusion in diplodocoids may have been related to the ability to produce sonic booms (Myhrvold & Currie, 1999).

While *Spinophorosaurus* does not preserve the complete caudal vertebral sequence (the caudalmost vertebrae have not been retrieved), what is preserved shows some specialized characters worth noticing. On one hand, the overlapping forked chevrons prevent dorso-ventral motion and only allow lateral flexion with some degree of torsion (Fig. 3.9 B). On the other, the last 10 preserved caudal vertebrae have extremely reduced prezygapophyses, which allow the torsion needed to flex the tail (Fig. 3.9 D). The anteriormost caudal ribs are posterodorsally oriented, creating more room for *M. ilio-ischiocaudalis* and especially *M. caudofemoralis* longus. Also, just as in diplodocid sauropods with whiplashes, the mid caudal vertebrae are elongated (Fig. 3.19). Finally, *Spinophorosaurus* shares many basal traits with other non-neosauropod sauropods, such as dorso-ventrally elongated chevrons and long neural spines, implying more developed hypaxial and epaxial musculature than in more deeply nested taxa (see below). This shows *Spinophorosaurus* had a very muscular tail with restricted motion in the dorso-ventral plane in the mid-distal region due to the overlapping chevrons and the elongated vertebral centra.

Interestingly, while the elongation of the centra of the middle caudal vertebrae (Fig. 3.19) has been related to the capability to generate a sonic boom in sauropods with a whiplash (Myhrvold & Currie, 1999), the overlapping chevrons of the posterior region of ankylosaur tails seem to have an important role in the function of the tail club for impacting (Arbour, 2009). In both cases, the stiffening of bounded regions of the tail in diplodocids and ankylosaurs have been compared to handles (that of a bullwhip and a mace, respectively) and to serve the same purpose: to reinforce that region against the stresses of higher forces in the distalmost tail (Myhrvold & Currie, 1999).

It is therefore possible that the specializations of the tail of *Spinophorosaurus* are part of a functional complex

of which some elements in the distalmost tail have not yet been recovered. Although a whiplash is possible (since they may have also evolved convergently in titanosaurs, not only in diplodocids), the phylogenetic position of *Spinophorosaurus* as more deeply nested than *Shunosaurus* and probably closely related to mamenchisaurs (Mocho *et al.*, 2013) would suggest a tail club to be a more likely possibility. However, the hypothesis of the specializations as part of an incomplete functional complex will not be possible to test until distal tail remains of *Spinophorosaurus* are retrieved.

Also, different hypotheses may be regarded for the tail of *Spinophorosaurus* as complete specialized structure. Since the distal tail would be stiffened in the dorso-ventral plane, it may have acted as a somewhat stiff rod. A stiffened mid-tail has been proposed as helpful in rearing in a tripod pose. However, a rearing *Spinophorosaurus* would not support itself on this particular segment of the tail, so that hypothesis can be refuted at least for this taxon. Stiffening in the mid-distal tail may also be regarded as evidence against the hypothesis of dinosaurs dragging their tails, supporting instead a horizontal tail in *Spinophorosaurus*.

All in all, while the tail of *Spinophorosaurus* shares some basal and probably autapomorphic, specialized traits, its precise function is hard to understand under our current understanding of sauropod tails in general, and the tail of *Spinophorosaurus* in particular.

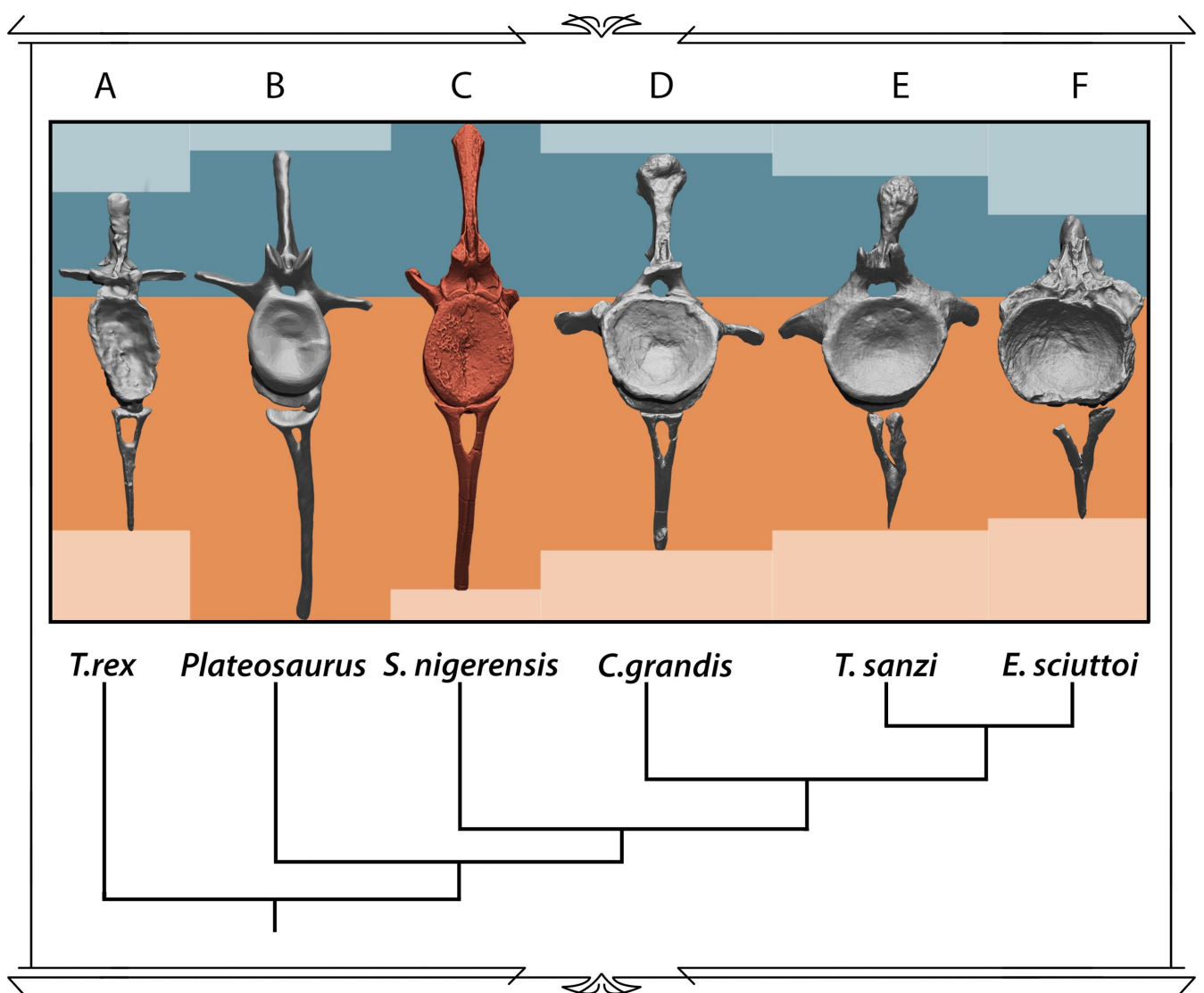


Figure 3.20 - Relative size of caudal musculature osteological correlates in Saurischia.

A - Caudal vertebra 3 and chevron of *Tyrannosaurus rex* (MOR-555) in anterior view. **B** - Caudal vertebra 4 and chevron of *Plateosaurus engelhardti* (GPIT 1) in anterior view. **C** - Caudal vertebra 4 and chevron of *Spinophorosaurus nigerensis* (GCP-CV-4229) in anterior view. **D** - Caudal vertebra 4 and chevron of *Camarasaurus grandis* (YPM-1901) in anterior view. **E** - Caudal vertebra 4 and chevron of *Tastavinsaurus sanzi* (MPZ 99/9) in anterior view. **F** - Caudal vertebra 4 and chevron of *Epachthosaurus sciuttoii* (UNPSJB-PV-920) in anterior view. All vertebrae have been scaled to same centrum height, in order to compare the proportions of their epaxial (blue) and hypaxial (orange) regions. The dendrogram depicts their phylogenetic relationships.

M. caudofemoralis longus and locomotor capabilities of *Spinophorosaurus*

Caudal and pelvic musculature are key in understanding dinosaur locomotion, and a great number of studies have been published regarding this subject in bipedal theropod dinosaurs (Gatesy, 1990; Carrano & Hutchinson, 2002; Hutchinson & Garcia, 2002; Hutchinson *et al.*, 2005, 2011; Persons & Currie, 2010, 2011; Grillo & Azevedo, 2011) and ornithopods (Maidment & Barrett, 2011; Bates *et al.*, 2012; Maidment *et al.*, 2012, 2014; Słowiak, Tereshchenko, & Fostowicz-Frelik, 2019). In sauropods, studies are scarcer and more recent (Carrano, 2005; Fechner, 2009; Sellers *et al.*, 2013; Klinkhamer *et al.*, 2018), with a particular lack of published mass estimates on isolated muscle groups.

Full body mass estimates for sauropods, however, have been published for decades using many different approaches, from regression models extrapolating from extant taxa long bone measurements and masses (Anderson, Hall-Martin, & Russell, 1985) to physical models submerged in a fluid using Archimede's principle (Colbert, 1962; Alexander, 1989) and virtual 3D models, obtained either by hand modelling or using scanned mounts and/or modelled skeletons (Sellers *et al.*, 2013; Bates *et al.*, 2016).

Caudofemoral musculature in particular has been the focus of recent studies focusing on the locomotion capabilities of large theropod dinosaurs (Persons & Currie, 2010, 2011; Hutchinson *et al.*, 2011). Since this muscle is the main retractor of the hindlimb and the most important force in forward propulsion in reptiles (Stephen M. Gatesy, 1997; Mallison *et al.*, 2015), estimating its mass and its proportion to the full body mass estimation of the animal is prime data for understanding the locomotion of dinosaurs. As summarized in Table 3.9, the origin and insertion of this muscle is a Level I inference for dinosaurs using EPB (Witmer, 1995), so reconstructing its volume should be relatively accurate.

However, there is a large caveat on estimating caudal muscle volume: their lateral extent cannot be accurately estimated at present (Mallison *et al.*, 2015). In any case, muscle mass is not a constant during the life of an individual, as famine during droughts or dry seasons and processes associated with ageing such as sarcopenia (Cruz-Jentoft, Baeyens, & Bauer, 2010), so it is reasonable to think that estimated values may correspond with the value at some point in the life of a fossil individual. Moreover, by applying the same lateral muscle extent ratio to all taxa, the dorso-ventral and antero-posterior osteological correlates make the most difference among taxa, since the proportions of sauropod tails to pelvis vary considerably. Therefore, for the sake of comparative analyses, neural spine and chevron length can be used as proxies for caudal muscle mass comparison (Fig. 3.20).

The caudal musculature of *Spinophorosaurus* would therefore be very developed due the large size of its neural spines and chevrons. Particularly, *M. caudofemoralis* may have a greater development in *Spinophorosaurus nigerensis* than in the bipedal theropod *Tyrannosaurus rex*. For both taxa, *M. caudofemoralis* spans from the second or third caudal vertebra until CdV 15 (Persons & Currie, 2010), however, the chevrons in *Spinophorosaurus* are almost twice as long respect to the vertebral centrum than in *T. rex*. Therefore, although estimated mass for a single CFL in *Spinophorosaurus* is a little bit smaller in absolute terms than for *T. rex*, the % of whole tail muscle mass and % of total body mass is surprisingly slightly larger for *Spinophorosaurus* than for *T. rex* (Table 3.10).

Taxon	Estimated CFL mass	Estimated body mass	CFL/BM ratio
<i>Crocodylus johnstoni</i>	0.311 kg	19.43 kg	3.2 %
<i>Tyrannosaurus rex</i>	167 kg	5777-10768 kg	3-4 %
<i>Spinophorosaurus nigerensis</i>	158 kg	8400-6700 kg	4-5 %

Table 3.10 - CFL mass relative to body mass.

Data from *C. johnstoni* (measured) and *T. rex* (estimated for specimen MOR-555) from Hutchinson *et al.* (2011). The mass estimations for *T. rex* were obtained using the same NURBS methodology employed for *Spinophorosaurus* in this thesis.

The main functions of CFL in extant archosaurs are femoral retraction, femoral adduction and stabilization in other motions (Gatesy, 1990; Mallison *et al.*, 2015). Lines of action expressed as the sum of two vectors is a way to estimate the roles of a muscle in an extinct animal (Remes, 2007), although additional lines of evidence are needed to completely assess the function of a muscle (Snively & Russell, 2007a). By comparing the vectors for 100% adduction (0°) and 100% retraction (90°) for *Spinophorosaurus* in dorsal view with the actual projected line of action of CFL (73°), the dominant vector would be retraction (Fig. 3.21). *Spinophorosaurus* has a narrow pelvis, as do the large majority of non-neosauropod eusauropods, sauropodomorphs and theropods. The

fourth trochanter is situated closer to midshaft height than to the femoral head, indicating a larger moment arm than in *Plateosaurus* or *Tyrannosaurus*.

Klinkhamer *et al.* (2018) found that *Diplodocus* and *Giraffatitan* (both Neosauropoda) had a larger moment arm than *Plateosaurus* (Klinkhamer *et al.*, 2018). Since smaller moment arms with a similar relative muscle mass imply faster and stronger contraction, while larger moment arms imply the contrary (Nagano & Komura, 2003), this suggests faster locomotion for the bipedal *Plateosaurus* (Klinkhamer *et al.*, 2018). On the other hand, the titanosaur *Diamantinasaurus* also had a smaller moment arm for CFL (Klinkhamer *et al.*, 2018), but its CFL estimated mass is relatively much smaller than in *Plateosaurus*. This has been interpreted as a progressive reduction of CLF role in forward propulsion, with a larger role of the forelimb evolving in sauropod locomotion (Klinkhamer *et al.*, 2018). The condition in *Spinophorosaurus* resembles more that of *Diplodocus* or

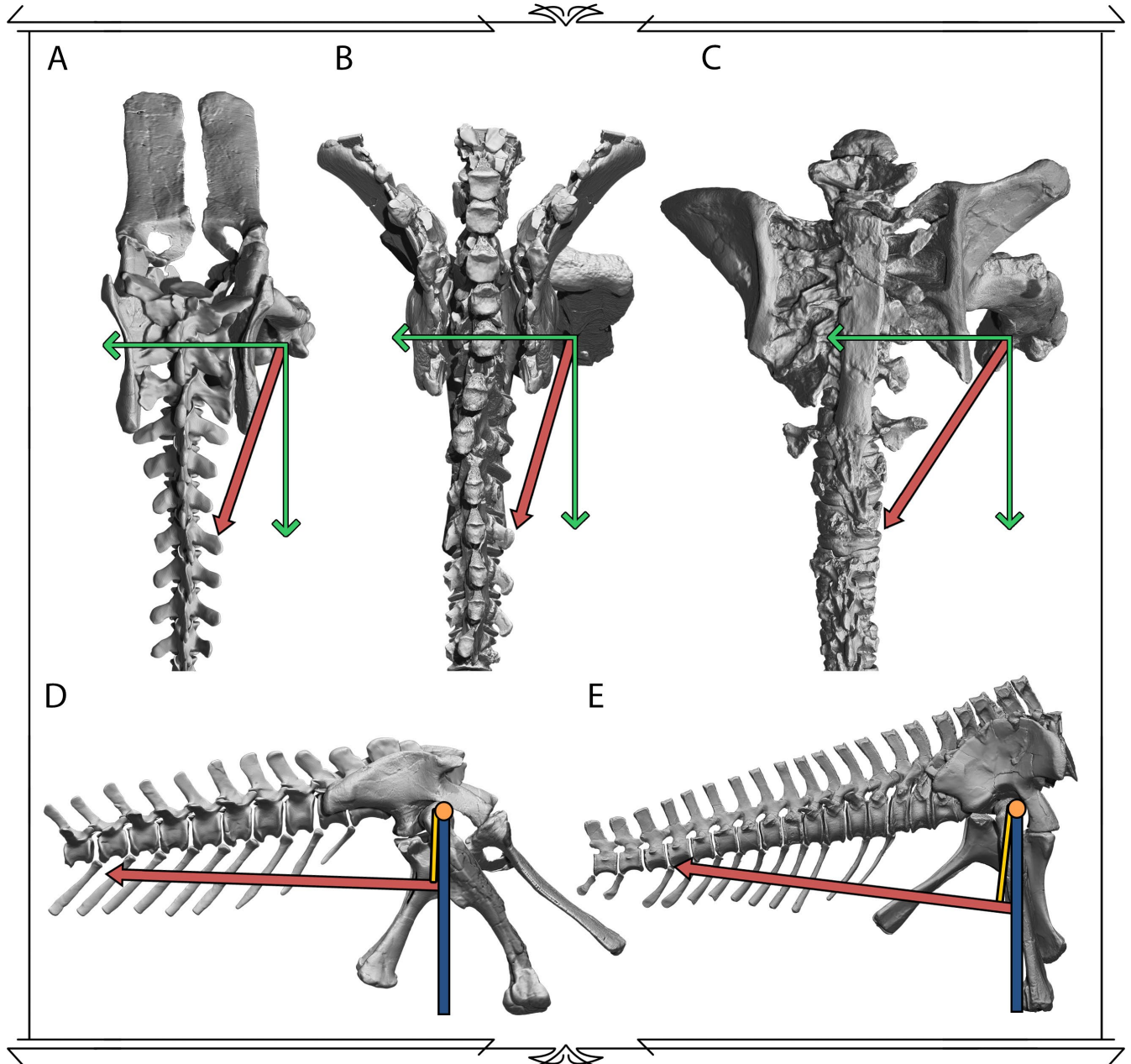


Figure 3.21 - Lines of action, lever arms and moment arms for *M. caudofemoralis longus* in sauropodomorpha.

A - Sacrum, anterior tail, ilia and femur of *Plateosaurus engelhardti* (GPIT 1) in dorsal view. **B** - Sacrum, anterior tail, ilia and femur of *Spinophorosaurus nigerensis* (GCP-CV-4229) in dorsal view. **C** - Sacrum, anterior tail, ilia and femur of *Epachthosaurus sciuttoii* (UNPSJB-PV-920) in dorsal view. In green, the two components for CFL line of action: femoral retraction (down) and adduction (left). In red, the actual inferred line of action, which in A and B is closer to retraction than to adduction while in C both components contribute equally to the line of action. **D** - Sacrum, anterior tail, ilia and femur of *Plateosaurus engelhardti* (GPIT 1) in lateral view. **E** - Sacrum, anterior tail, ilia and femur of *Spinophorosaurus nigerensis* (GCP-CV-4229) in lateral view. Orange circle = center of rotation. Blue bar = lever arm. Red arrow = CFL line of action. Yellow bar = moment arm (vector perpendicular to the line of action and the center of rotation). Notice the moment arm of D is smaller than in E (both skeletons scaled to the same Lever arm (femur) length).

Brachiosaurus, but while the moment arm is similar, the osteological correlates for CFL origin are much larger in *Spinophorosaurus* (Fig. 3.20). This suggests that *Spinophorosaurus* could not retract its femur at a much faster pace than Neosauropods, but could do so with exerting larger forces.

Locomotion on most non-neosauropod sauropods does not appear to be radically different from Neosauropoda such as *Camarasaurus*, *Diplodocus* or *Apatosaurus*, and neither do ilia or pubes go through great proportional changes (see Chapter 5). However, ischia and chevrons diminish their relative size on Neosauropoda next to non-Neosauropoda. This suggests that the extremely large caudofemoral musculature of many non-Neosauropoda Eusauropoda is more likely a plesiomorphic condition inherited from their bipedal ancestors, since even some lineages of Eusauropoda such as genus *Mamenchisaurus* reduced the relative size of its chevrons (Young & Zhao, 1972; Ouyang & Ye, 2002).

Spinophorosaurus paleobiology inferred from virtual paleontology

Drinking: Giraffes are typically considered to have “long necks”, despite them being extremely short for a fundamental behavior: drinking. Giraffes are not able to reach ground level just with neck ventriflexion (see Chapter 4), and they need to splay their forelimbs by abducting the humerus and flexing the elbow to the extreme to reach the ground. Some sauropods have been noted to have the same issue, particularly taxa such as *Atlasaurus* or *Camarasaurus* with relatively tall shoulders and relatively shorter necks (Paul, 1998; Hallett & Wedel, 2016), and the same happens with *Spinophorosaurus* (Fig. 3.7).

In order to test whether osteological range of motion alone would allow the nout of *Spinophorosaurus* to reach past ground level (feet/hand ventralmost point), the same conditions for all other ROM analyses applied: joints could not go past disarticulation or reach an osteological stop.

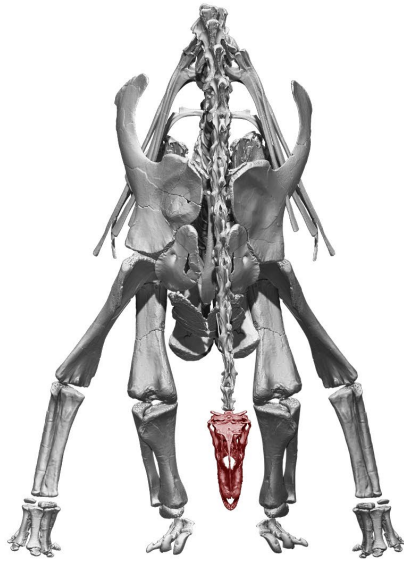
A first pose was attempted by ventriflexing the neck to reach the lowest point (by fully ventriflexing CV12-CV6, while CV5-Axis remained in ONP) and abducting the forelimbs to the limit, mimicking the splaying posture of giraffes (see Chapter 4). In this posture, however, the snout could not pass beyond the ground (Fig. 3.22 A). A second, more complex pose was attempted by moving additional joints: the femur was protracted, the knee and elbow were flexed and the first two dorsal vertebrae were ventriflexed to their limit (Fig. 3.8). In this posture, the head could pass beyond the ground (Fig. 3.22 B,C).

To evaluate this pose, when taking into consideration the elements unknown for *Spinophorosaurus*, such as the forearm, the degree of flexion needed to adopt the pose is far from what could be considered extreme (Fig. 3.22 C3). The knee is also far from its full flexion to achieve the pose (Fig. 3.22 C2). Finally, both femur and humerus are within their osteological range of motion capabilities. It is well known that nonavian dinosaurs in general and sauropods in particular had extensive soft tissue epiphyses in their long bones which may have increased the range of motion in some joints (Schwarz, Wings, & Meyer, 2007c; Holliday *et al.*, 2010) and limited it in others (such as the olecranon process of the ulna in *Kentrosaurus*, which would block hyperextension (Mallison, 2010c)). However, the fact that this pose can be achieved well within the limits of osteological range of motion implies that, unless a very unusual non preserved soft tissue really limited range of motion on the joints, the pose could be attained.

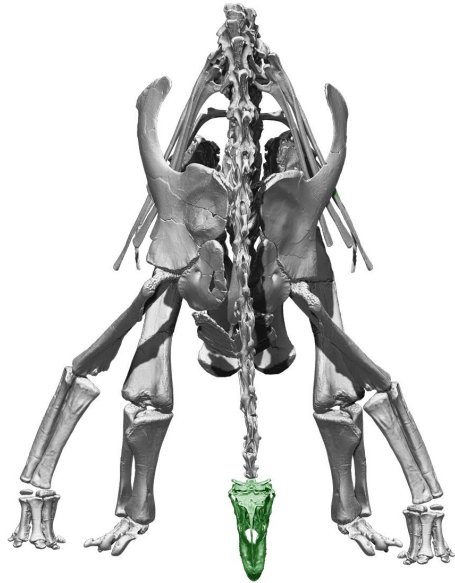
Some humeral muscles in *Spinophorosaurus* have ossified anchor sites which in other sauropods may have not ossified, particularly those with active participation in abduction (ossified clavicles, *M. deltoideus clavicularis*) as well as adduction (ossified interclavicle, *M. pectoralis*). The fact that muscles performing these motions have stronger anchors in *Spinophorosaurus* than other sauropods does not allow to refute the pose either. Knee flexors and extensors are less developed in sauropods than in other dinosaurs (Fechner, 2009; Klinkhamer *et al.*, 2018), but the flexion at the knees in this posture is far from extreme, and likely within the habitual range of motion of walking gait (Sellers *et al.*, 2013). Although little can be said about the osteological correlates of forearm musculature, the amount of elbow flexion in the pose is also little.

Regarding the dorsal vertebrae (Fig. 3.22 C1), the anterior dorsal vertebrae were more flexible than middle or posterior vertebrae (Table 3.5), as they had opisthocoelous centrum articulations and relatively developed ventral keels. Extant giraffes have a first dorsal vertebra partially cervicalized, which also has more range of motion capability than the second dorsal, although less than the last cervical vertebra (Table 3.5). In fact, some studies hypothesize that the long neck of giraffes and the cervicalization of their first dorsal vertebra might be an adaptation to cope with the extreme elongation of the forelimbs that increase the difficulty of drinking water. Whatever the ultimate reason for neck elongation and cervicalization of dorsal vertebra in both giraffes

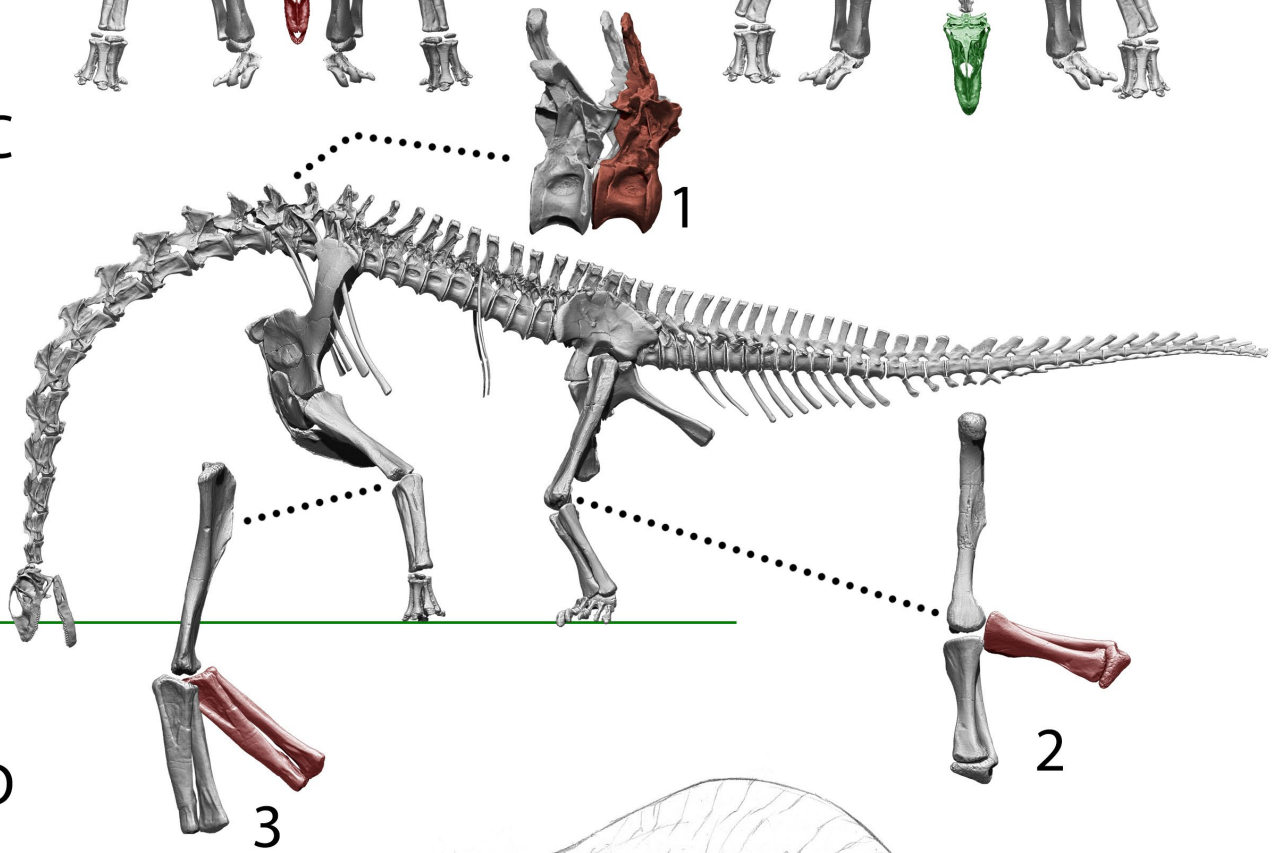
A



B



C



D



Figure 3.22 (previous page)- Testing the capability of the virtual *Spinophorosaurus nigerensis* skeleton to “drink”.

A - Anterior view of the virtual *Spinophorosaurus* with its neck ventriflexed as seen in Fig. 3.7.5 and its humerus abducted. The snout is unable to reach beyond the ground in this posture. **B** - Anterior and **C** - lateral view of the virtual *Spinophorosaurus* with its neck ventriflexed and its humerus abducted as in A, but also with the anteriormost two dorsal vertebrae fully ventriflexed (1), and the knees and elbows slightly flexed, far from their inferred limits (limits to flexion respectively 2 and 3). In this position, the snout is able to reach beyond the ground. **D** - Paleoartistic reconstruction of *Spinophorosaurus* drinking with the hypothetical posture. Drawn by Diego Cobo on top of a 3D render of the skeleton posed as in B and C in a three-quarter view.

and sauropods, it is clear that both taxa ultimately benefited from the increased range of motion to help them lower their heads toward the ground.

To summarize, whether this was a pose actually adopted for drinking in life or not is beyond what present evidence can refute. However, several lines of evidence support that there were no osteological or myological reasons to prevent the animal from adopting the pose, had it needed or wanted to.

Mating capabilities: The study of mating among extinct dinosaurs is still an obscure subject, despite being of great academic and popular interest (Isles, 2009; Sopelana, 2011). Among the gigantic sauropod dinosaurs, mating is one of the most intriguing aspects of their biology. While it is known they mated, for they had a great evolutionary success for 120 million years, the specific aspects of their mating are still largely unknown. An interesting hypothesis which can be tested with virtual paleontology is whether sauropods could physically perform a “cloacal kiss” that is, to mate without the need of an intromittent male organ. Hence, all mating hypotheses proposed for sauropods (Isles, 2009) were tested by means of virtual paleontology to show whether they were possible in the first place, and whether or not a “cloacal kiss” was possible.

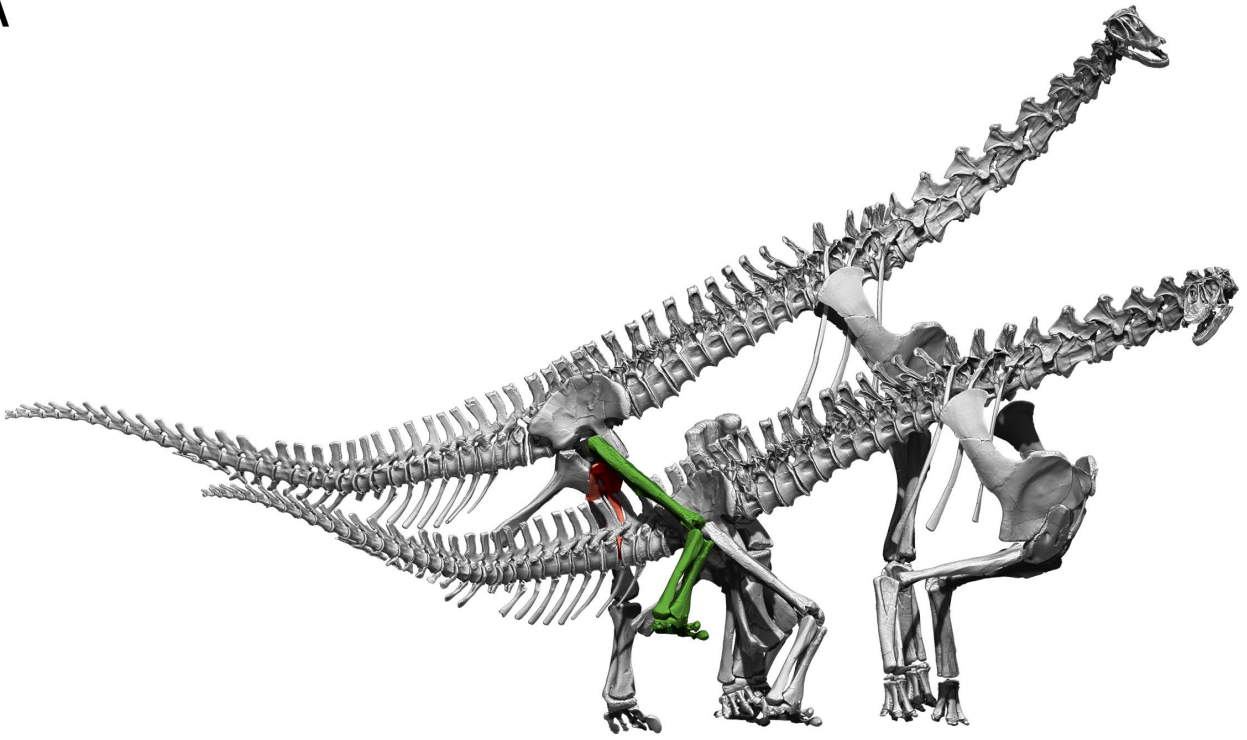
To test this hypothesis, the skeleton was posed in different mating posture hypotheses taken from Isles (2009): (i) Leg over back, (ii) male mounting female from behind; and (iii) “backwards mating”. If any of the mating postures produced either disarticulation and/or osteological stops, it was deemed not feasible.

Leg over back, a posture consisting in the male wrapping the leg over the tail or pelvis of the female, is very common among extant nonavian sauropsids (Isles, 2009) one of the most typically depicted positions for dinosaur mating behavior, and is regarded as a likely possibility for the majority of nonavian dinosaurs (Isles, 2009). The range of motion analysis proves that *Spinophorosaurus* would not be able to perform the “leg over back” posture, due to its distally expanded pubes, well-developed *ambiens* process and narrow hips, which pose osteological limits to femoral protraction and abduction (Fig. 3.11). In an attempt to pose two virtual skeletons of *Spinophorosaurus* in a “leg over back” mating position, the anatomical impossibilities of this posture become evident (Fig. 3.23 A, B). Accounting for two equally sized virtual skeletons, the greatest problem stems from the large antero-ventrally pointed pubes. In a standing virtual skeleton of *Spinophorosaurus* with the limbs in ONP, the pubis to floor distance is 1.28 m, while the tip of the sacrum to floor distance is 2.77 m. Also, abduction of the femur is restricted due to the ~90° angulation of the femoral head and the femoral diaphysis, making the head collide with the acetabulum wall (as was determined for *Diplodocus* a century ago (Holland, 1910)), preventing further abduction (Fig. 3.11). Both factors make impossible that a standing *Spinophorosaurus* would fit under the leg of a second, equally sized individual.

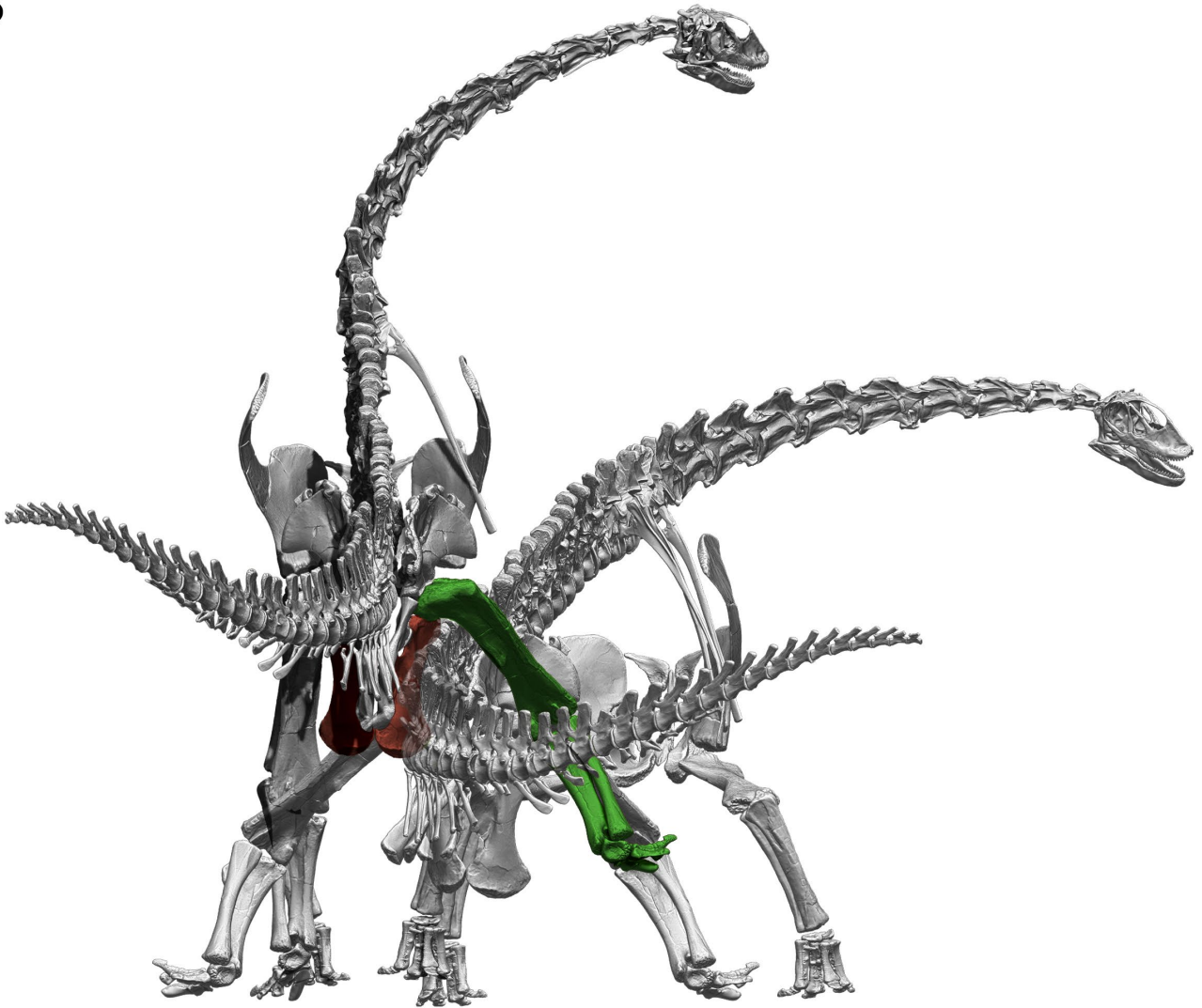
In an attempt to try to stretch the test, it was decided to make the female crouch, flexing and abducting its fore and hindlimbs. The femora were both abducted and protracted at their maximum capacity, and the tibia and fibula flexed at their maximum flexion capability. The non-preserved radius and ulna were assumed to have been capable of the same flexion than their hindlimb counterparts. However, even at this extreme, the pubes of the male still collide with the axial skeleton of the female, as the crouching female sacrum is at 2.06 m high, 70 cm higher than the pubes of the male (Fig. 3.23 A, B). Since there is no possibility of further abducting the femur of either the male or female due to an osteological stop, “leg over back” has to be considered impossible to perform, and the hypothesis refuted. Curiously, when mounting the mating *Tyrannosaurus rex* cast specimens at the Museo del Jurásico de Asturias in the early 2000s, the leg over back pose was attempted and rejected due to similar impossibilities as found for *Spinophorosaurus* (JL Sanz, F Ortega, pers. comm. 2018).

A possibility could be that there was a strong sexual dimorphism concerning size. Sexual dimorphism in sauropods has been only superficially studied, given that most species are known from single specimens or, when more specimens are present, they are fragmentary (Isles, 2009). *Camarasaurus* is the only sauropod for which sexual dimorphism has been proposed, but the putative male and female morphotypes were about equal size (Ikejiri, 2004). Given there is no current evidence of extreme sex-related size differences reported in sauropods, no evidence supports these animals could physically perform a “leg over back”.

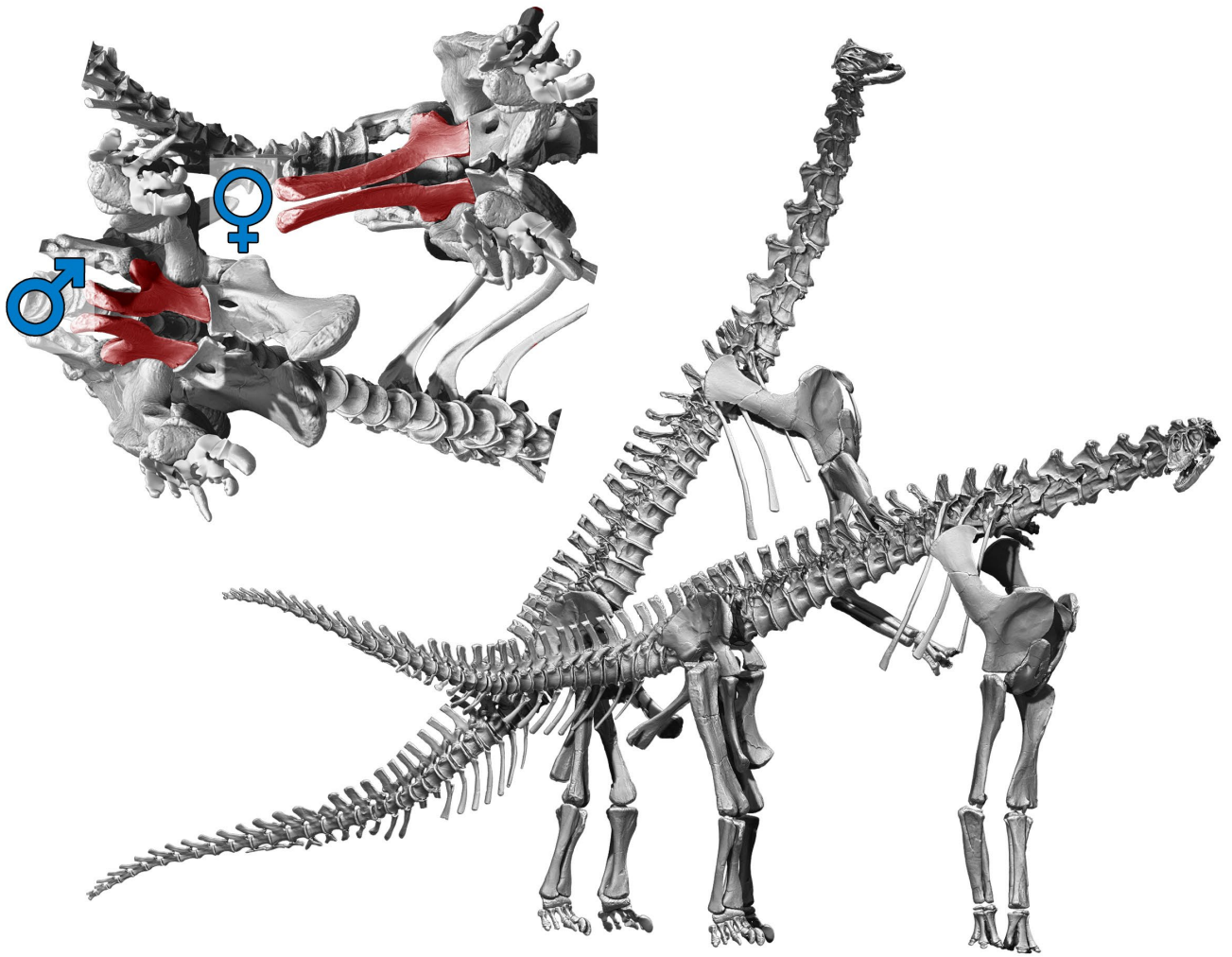
A



B



C



D

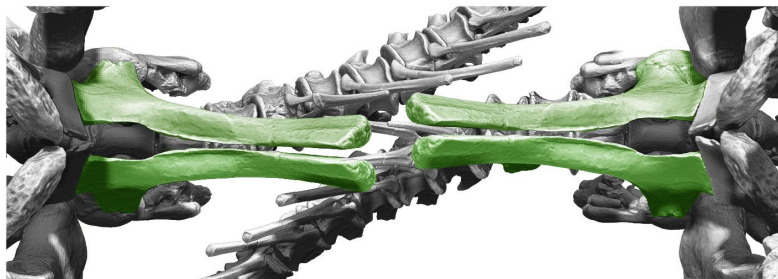
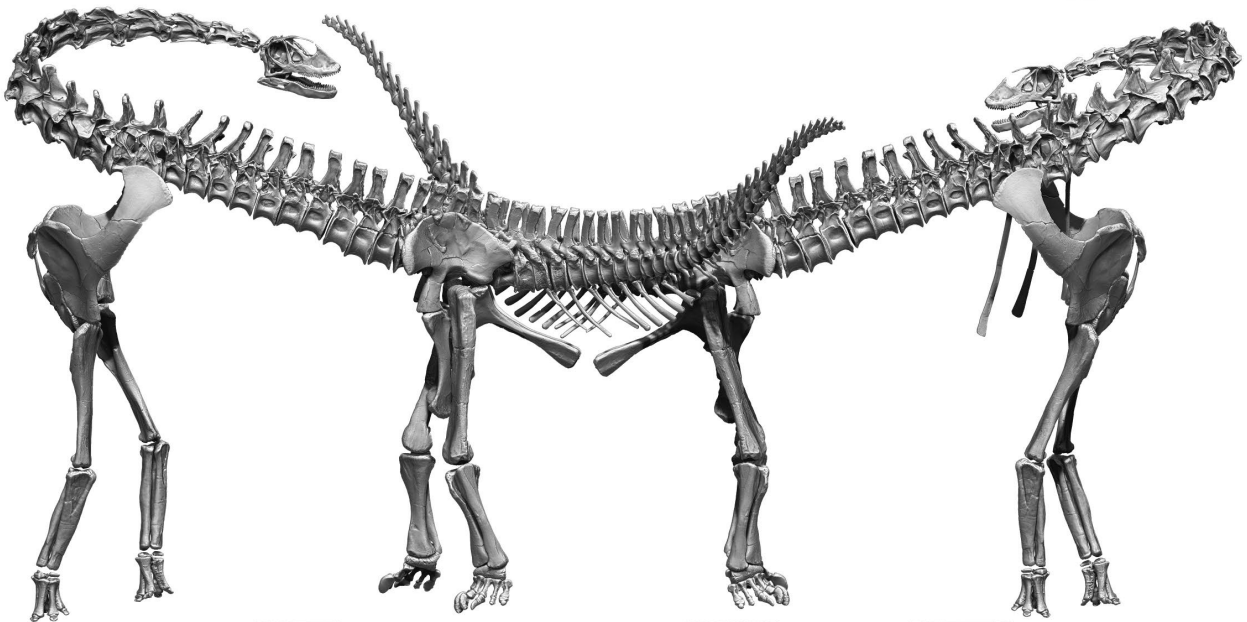


Figure 3.23 (previous page) - Testing possible mating capabilities on the virtual *Spinophorosaurus nigerensis* skeleton.

A - “Leg over back” posture in lateral view. **B** - “Leg over back” posture in posterior view. Notice how the “female” skeleton has to abduct and flex to the extreme both its femora and humeri and flex to the extreme the knees and elbows as well. Despite this, the pubis of the “male” skeleton is too large for the back of the female to fit between the leg of the male and its body, rendering the posture impossible due to the osteological stop. **C** - Mounting posture as seen in large extant large land mammals depicted in lateral view, with a close up of the posture in ventral view, showing the cloacae are well-separated in this posture. While the virtual skeleton can perform the posture without osteological stops or disarticulation, a “cloacal kiss” is impossible in this posture. **D** - “Backwards mating” posture as shown by Isles (2009) depicted in lateral view, with a close up of the posture in ventral view, showing the cloacae close to one another. The virtual skeleton can perform the posture without osteological stops or disarticulation, and the “cloacal kiss” appears to be possible. However, the likely large amount of muscle and fat in the anteriormost region of the tail may have impeded to perform the “cloacal kiss”.

Concerning the possibility of performing a “cloacal kiss”, the only posture which would allow sauropods to do so within their osteological range of motion capabilities would be the “backwards mating” pose (Fig. 3.23 D). This pose allows the dorsal region of the ischia of two individuals (where *cloacae* are found in all non-mammalian amniotes) to come very close. This kind of pose is common in many arthropods and part of the “tied/lock” phase of mating in some *Carnivora (Mammalia)*, such as *Canis sp.* (Carlson, 2008). Other poses, such as a mount of the male from behind precludes situating the cloacae close, and would require an intromittent organ (Fig. 3.23 C).

Summing up, the virtual *Spinophorosaurus* model refutes the “leg over back” posture as a feasible way for most sauropods to mate and implies that, with the exception of the “backwards mating” model, all the achievable postures require an intromittent organ.

Sauropod sacra as an evolutionary innovation.

Given the high disparity of hindlimb/forelimb length proportions among Sauropoda (McIntosh, 1990; Upchurch *et al.*, 2004), the evidence of different feeding capabilities in different sauropods (Christian & Dzemski, 2007; Sereno *et al.*, 2007; Stevens, 2013) and the role of the wedged sacrum on the high browsing capabilities in *Spinophorosaurus* (due its high impact on vertebral column OIC), a hypothesis can be formulated: only sauropod dinosaurs with moderately to extremely elongated forelimbs would have strongly acute wedged sacra and dorsal vertebrae.

Interestingly, a comparison of sacral wedging with the relative lengths of humeri and femora reveals a correlation: higher humerus maximum length/femur maximum length ratios are associated with a higher wedging angle of the sacrum and vice versa (Fig. 3.7 B). However, all eusauropod sauropods have wedged sacra, even those with shorter humeri (Figs. 3.7 B, Fig.). Sauropods with extremely short humeri (dicraeosaurids and some titanosaurs) have sacrum wedging angles of around 10° or a little higher, whereas extremely tall-shouldered sauropods with humeri longer than femora (Brachiosauridae) have sacrum angles of up to 30° (Table 3.1). This sacrum wedging to humerus relative length correlation, however, is only found in Eusauropoda. There are few known non-eusauropod sauropods preserving sacral and limb material, but those which preserve complete sacra have very little to no wedging (i.e. *Kotasaurus* (Yadagiri, 2001) or *Barapasaurus* (Jain *et al.*, 1979)) despite having columnar fore and hindlimbs (Fig. 3.24) and being obligatory quadrupeds. The sacrum in non-sauropod sauropodomorphs is also hardly wedged even in large, quadrupedal species (i.e. *Melanorosaurus* (Bonnar & Yates, 2007)). Some of these quadrupedal non-sauropod sauropodomorphs have relatively larger humeri than some eusauropods, that also were obligatory quadrupeds but had wedged sacra (i.e. *Shunosaurus* (Zhang, 1988)). Therefore, a rectangular or barely wedged sacrum would be the basal condition in Sauropodomorpha, which eventually derived to a more strongly wedged one in Eusauropoda, 10° or more (Fig. 3.24). From this point on, the relative length of the humeri correlates with the amount of wedging in the sacrum, which does not happen in non-Eusauropoda (Fig. 3.7 B).

This correlation between the sacrum and forelimbs appears to have worked as a functional module during sauropod evolution, with evolutionary changes in limb proportions happening in a reciprocal way (Fig. 3.7 B.): changes in limb proportions resulted in modifications on the angulation of the sacrum wedging. In those sauropods with extremely short forelimbs and low/ground level browsing capabilities, the sacral wedging diminishes, making the presacral series deflect dorsally with a lesser angle. The sacrum, however, never returned to the basal condition of a more rectangular sacrum (Fig. 3.7 B, Table 3.5). The acute sacrum wedging

in sauropods with extremely short forelimbs, i.e. *Dicraeosaurus*, is also counteracted by an obtuse wedging in the dorsal vertebrae, which makes the dorsal spine deflect ventrally (Fig. 3.24, see Fig. 6.5C in Stevens & Parrish, 2005). Some of these sauropods had proportionately shorter necks than other sauropods (Taylor & Wedel, 2013b), and medium-height browsing (Whitlock, 2011a; Carabajal *et al.*, 2014) or ground level browsing (Sereno *et al.*, 2007; Whitlock, 2011a) has been proposed for them. Some titanosaurs with relatively shorter necks and forelimbs might also have been medium to ground level browsers, and they also have wedged sacra and obtuse wedging in the dorsal vertebrae (Fig. 3.24, Saltasaurini), although more functional analyses are necessary. Sauropods with shorter forelimbs arose separately in at least two different clades according to phylogenetic analyses (Wilson, 2002; Upchurch *et al.*, 2004; Bates *et al.*, 2016; Xu *et al.*, 2018) (Fig. 3.24, Diplodocoidea and Titanosauria) and all of them had close relatives with longer forelimbs and more wedged sacra. This implies that the acute wedged sacrum became irreversible for Eusauropoda, thus fixed in their body plan, likely a constraint for sauropods that evolved lower browsing feeding strategies.

The evolution of an acute wedged sacrum in sauropods appears to have been abrupt (Fig. 3), turning the non-wedged sacrum of basally branching Early to Middle Jurassic sauropods such as *Barapasaurus* and *Kotasaurus*, into a quite acute wedged one in Middle Jurassic sauropods such as *Shunosaurus* (Zhang, 1988) or *Patagosaurus* (Bonaparte, 1986). This derived sacrum evolved well after sauropods had already become obligate quadrupeds, earlier in their evolution (Wilson, 2002), implying it was not linked to the evolution of quadrupedality. Neck elongation has typically been regarded as the most important key innovation in sauropod evolution (Bates *et al.*, 2016), directly affecting the size of the feeding envelope (Sander *et al.*, 2011). Its size, and with it, the feeding efficiency, increased primarily from neck elongation (Sander, 2013). However, the appearance of strongly wedged sacral and dorsal vertebrae and changes in limb proportions might also have been important factors on feeding envelope size. As evidenced for the first time in the almost complete skeleton of *Spinophorosaurus*, further increase in the vertical component of feeding envelopes could have been achieved by relative forelimb elongation, longer prezygapophyseal facets in cervical vertebrae, cervicalization of anterior dorsals, and an acute wedged sacrum, the latter of which occurred in sauropods more deeply nested than *Kotasaurus* and *Barapasaurus* (Fig. 3.24).

The fact that an acute wedged sacrum of more than 10° remained present in all eusauropods, supports the trait as a synapomorphy rather than a convergent character. Moreover, it may represent a new factor in the evolutionary cascade proposed for sauropod gigantism (Sander *et al.*, 2011; Sander, 2013), directly affecting the energy-efficient feeding selective advantage proposed in that evolutionary cascade.

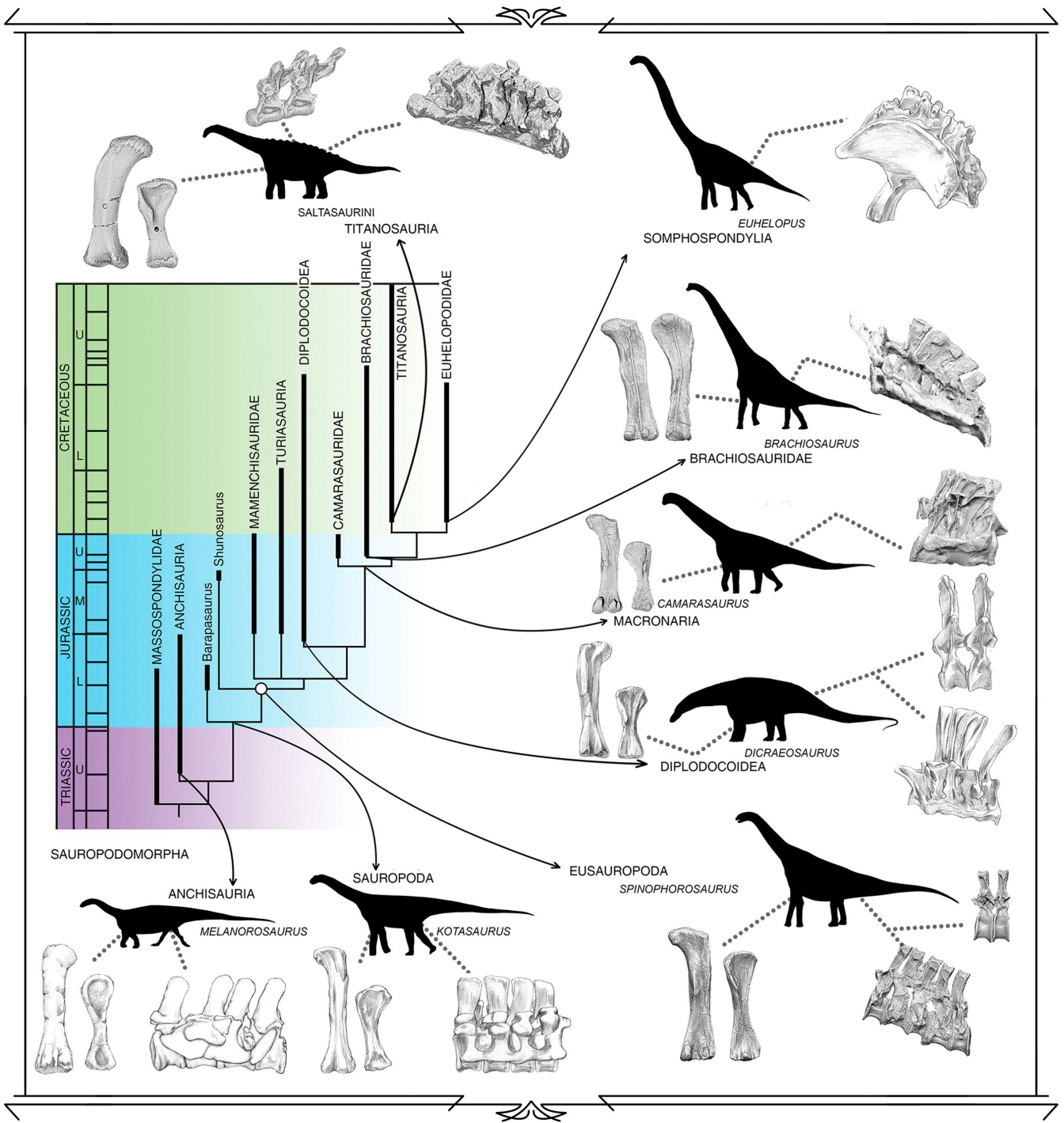


Figure 3.24 - Time calibrated sauropodomorph phylogenetic relationships with emphasis on different body proportioned taxa.

Different body proportions for sauropodomorph dinosaurs include (1) facultative quadrupedalism and medium height browsing in derived sauropodomorphs with non-wedged sacrum; (2) obligatory quadrupedalism and medium height browsing in basally branching sauropods with longer limbs but no wedged sacrum; (3) medium-high browsing in non-neosauropod eusauropods, with longer necks and forelimbs and an acute wedged sacrum; (4) medium-ground level browsing in dicraeosaurid and rebbachisaurid diplocooid sauropods, with short legs, shorter forelimbs than non-neosauropod sauropodomorphs but with acute wedged sacrum and obtuse wedge dorsal vertebrae; (5) medium-height browsing in macronarian sauropods, with a wedge shaped sacrum and retroverted pelvis; (6) extreme high browsing in brachiosaurid sauropods, with extremely elongated necks, humeri longer than femora and extremely wedged sacra; (7) extreme high browsing in euhelopodid titanosauriforms, with extremely long necks and extremely wedged sacra; and (8) medium-low browsing in some lithostrotian titanosaurs, with shorter forelimbs than other titanosaurs and titanosauriforms but still retaining a wedged sacrum. A wedged sacrum is only found in Eusauropoda, and albeit the degree of wedging varies among sauropods, it never returns to the basal condition. *Melanorosaurus* bones redrawn from Galton, Van Heerden, & Yates (2005). *Kotasaurus* bones redrawn from Yadagiri (2001). *Dicraeosaurus* bones redrawn from Janensch (1929, 1961). *Euhelopus* bones redrawn from Wiman (1929). Femora and humeri are in proportion to each other following measurements on Table 3.1. Time calibration of nodes after Xu *et al.* (2018).

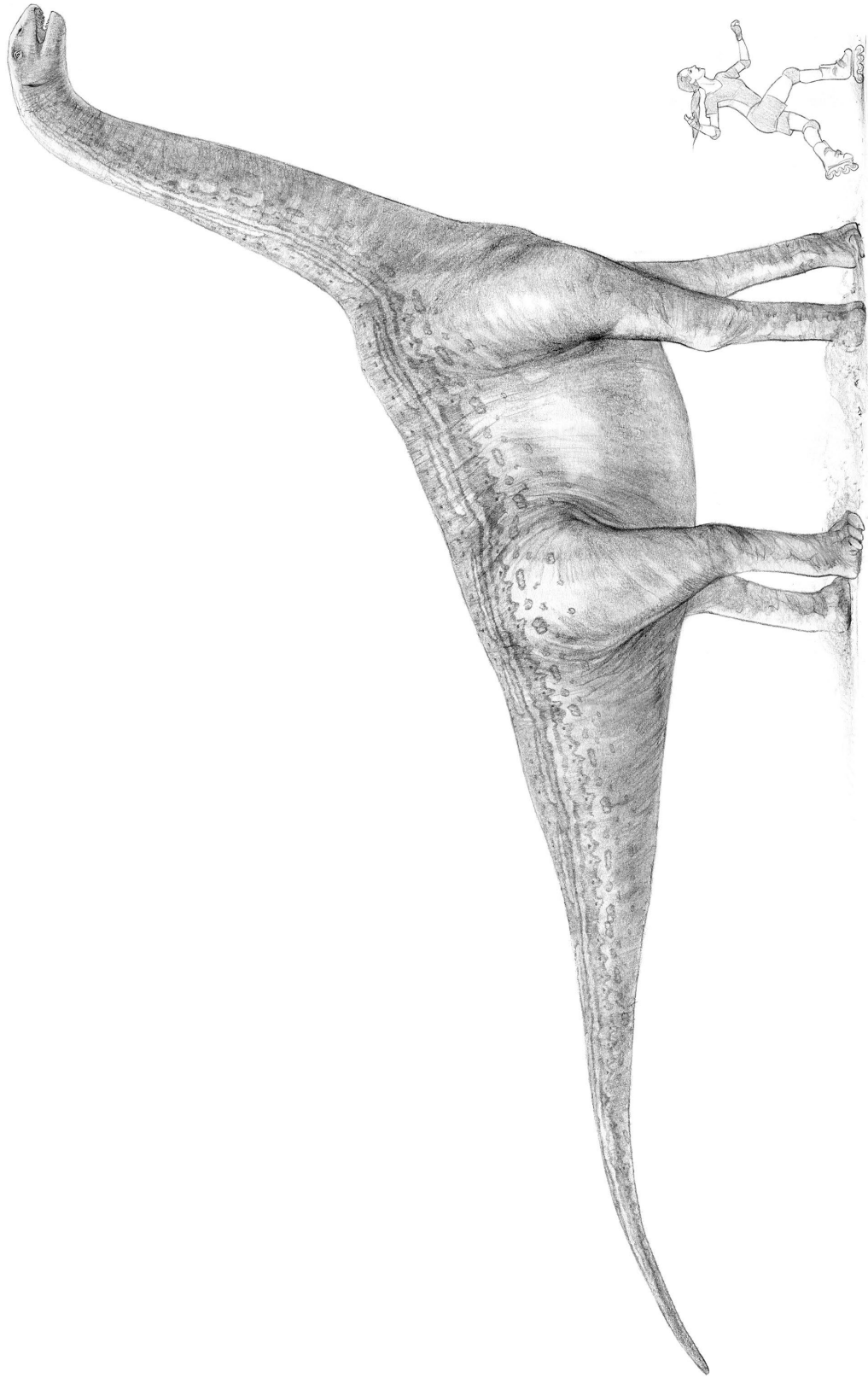
3.8 CONCLUSIONS

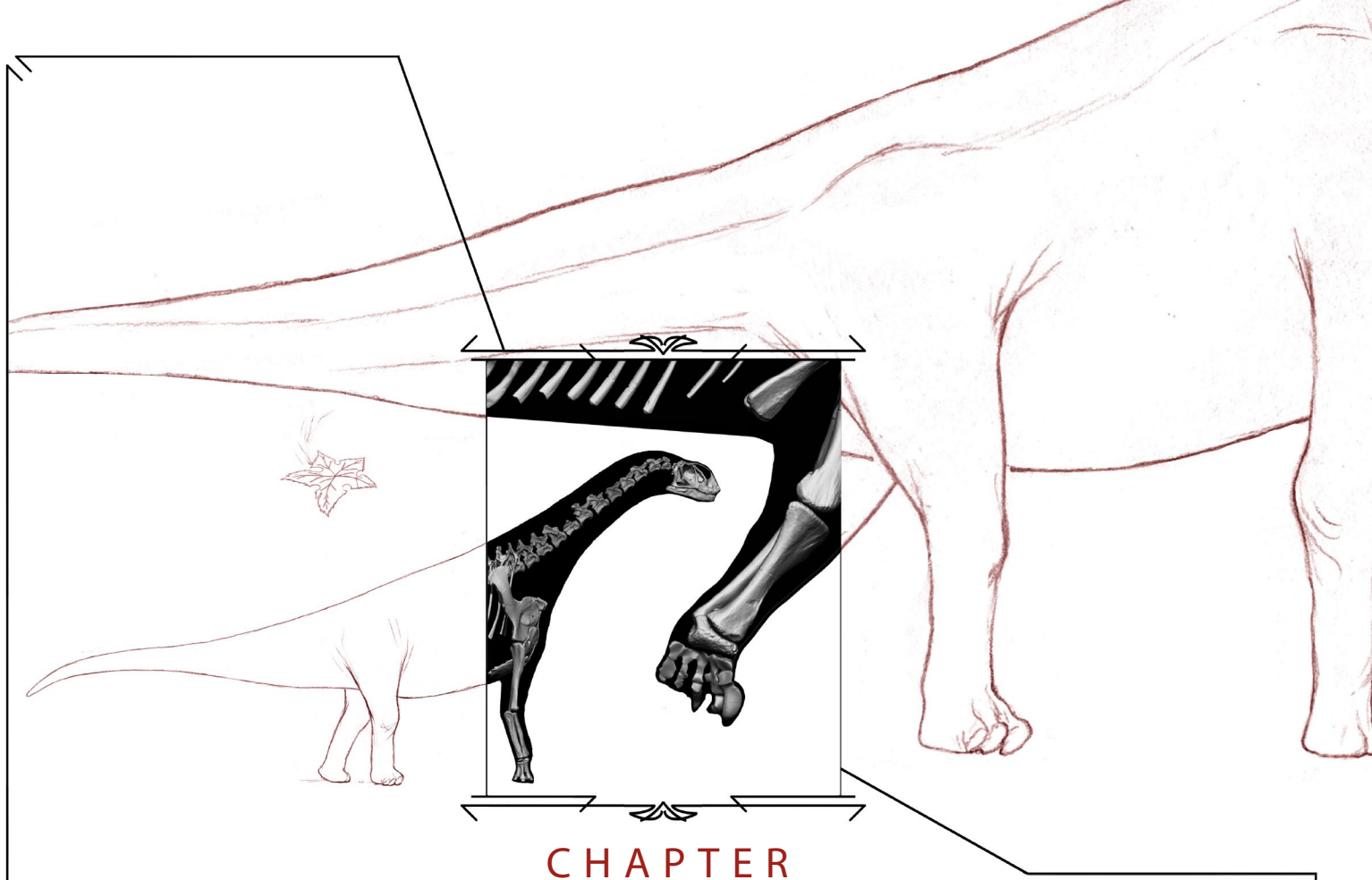
The virtual skeleton of *Spinophorosaurus nigerensis*, the first digital mount using a single specimen from a sauropod dinosaur so complete, reveals a body plan very different from previous reconstructions of this animal, with the presacral column antero-dorsally deflected and relatively tall shoulders (Fig. 3.25). The following conclusions support this reconstruction, as well as several morphofunctional hypotheses:

1. *Spinophorosaurus* shows an important tendency toward verticalization: A 20° wedged sacrum, together with slightly wedged dorsal vertebrae cause most of antero-dorsal sloping of the presacral column. The humerus is relatively more elongated respect to both femur and scapula than in most sauropods. Elongated pre and postzygapophyses and a partially cervicalized first dorsal vertebra enabled a greater dorso-ventral range of motion in *Spinophorosaurus* than in all previously studied sauropods. This enlarged vertical component of the feeding envelope, together with the dorsal sloping and well-developed epaxial and hypaxial musculature, show *Spinophorosaurus* had high browsing capabilities. Thus, the first evident skeletal adaptations to high browsing in sauropods were present as early as the Early-Middle Jurassic
2. The wedged sacrum condition is not exclusive of *Spinophorosaurus*: it appears to be present in all eusauropods. This evolved in correlation with humerus/femur proportions in what could be part of a functional module: the greater the sacral wedging, the longer the humerus relative to the femur. This skeletal adaptation was likely a synapomorphy and a key factor on the evolutionary cascade proposed for sauropod gigantism and for the evolution of their body plan, as it remained present in all known eusauropods until their extinction at the K-Pg boundary.
3. The tail of *Spinophorosaurus* appears to be specialized: the distalmost preserved region of the tail has all dorso-ventral motion blocked due to the overlapping chevrons at the end of the tail (lateral flexion is possible with slight intervertebral torsion, which is possible due to the reduced prezygapophyses) as happens in dinosaur taxa with tail clubs. On the other hand, middle caudal vertebrae increase their absolute length next to more anterior caudal vertebrae, as happens in taxa with a whiplash at the distalmost tail. These peculiarities, however, are difficult to interpret functionally (or if they were functionally coupled to begin with) and may or may not be part of a functional complex which still has not been completely retrieved, since the distalmost tail of *Spinophorosaurus* is unknown so far.
4. The osteological correlates of caudal musculature are extremely developed in *Spinophorosaurus* next to more deeply nested members of Neosauropoda. However, this extreme development of caudal musculature, particularly *M. caudofemoralis longus*, does not seem to respond a need for a larger capability of femoral retraction, since the osteological correlates for humeral muscles in the forelimb and pectoral girdle are well developed. Considering earlier branching sauropodomorphs such as *Plateosaurus* had a developed caudal musculature as well, the condition of *Spinophorosaurus* is likely retention of the basal condition rather than an adaptation.
5. The virtual skeleton of *Spinophorosaurus* allows testing hypothetical positions for drinking and mating. Some poses can be refuted, since osteological stop or disarticulation prevent the skeleton to adopt them. Drinking at ground level is only possible combining abduction (femur and humerus) and flexion (knee and elbow) of both limbs, combined with posterior cervical and anterior dorsal vertebrae ventriflexion. Regarding mating, "Leg over back" is impossible to perform for *Spinophorosaurus*, and only "backwards mating" would allow bringing the cloacae close enough to perform a "cloacal kiss".

Figure 3.25 (next page) - Paleoartistic reconstruction of *Spinophorosaurus nigerensis* by Diego Cobo.

The reconstruction has been carried out with a 3D render of the virtual skeleton in lateral view underneath to nail down the proportions. The neck has been posed in the alert pose proposed by Taylor *et al.* (2009) depicted in Fig. 3.7.3. Volumes are based on the full body volumetric reconstruction shown in Fig. 3.17. Human scale = 1700 mm.





CHAPTER
• 4 •

**ONTOGENETIC SIMILARITIES BETWEEN GIRAFFE
AND SAUROPOD NECK OSTEOLOGICAL MOBILITY**

Introduction.....	119
Material.....	120
Methods.....	121
Results.....	126
Discussion.....	133
Conclusions.....	141

4.1 INTRODUCTION

The elongated neck of sauropod dinosaurs is one of their more notable and trademark features. These necks vary tremendously in length, both in relative and absolute terms: from the short-necked *Brachytrachelopan mesai*, with a one meter neck long representing less than a quarter of the length of the axial skeleton (Rauhut *et al.*, 2005) to the up to nine meter long neck of *Mamenchisaurus sp.*, accounting for around half the total length of its whole vertebral column (Young & Zhao, 1972; Ouyang & Ye, 2002). The number of cervical vertebrae also varies in sauropods, with a basal condition of likely 12 cervical vertebrae (Wilson & Sereno, 1998) to a derived condition of up to 19 cervical vertebrae in *Mamenchisaurus hochuanensis* (Young & Zhao, 1972).

There has been a keen interest in understanding their functional capabilities, particularly their mobility: While early works described sauropod necks as extremely mobile, with even “avian-like flexibility” (Marsh, 1883; Hatcher, 1901), sauropod neck mobility would not be rigorously analyzed until the late 1980s, when Martin published his analyses on the mobility of the Leicester “*Cetiosaurus*” specimen (LCM G468.1968). Using the actual fossils when assembling the skeleton, Martin revealed this Middle Jurassic sauropod had a very limited range of motion, both in dorso-ventral and lateral planes (Martin, 1987). *Cetiosaurus* was found barely able to lift the skull 3.5 meter from the ground and make an arc of 4.5 meters in the lateral plane before disarticulation (Martin, 1987). Later works of Stevens and Parrish, with their computerized DinoMorph models, also found diplodocid sauropods *Diplodocus* and *Apatosaurus* to have also not very flexible necks (Stevens & Parrish, 1999, 2005; Stevens, 2002), with *Diplodocus* in particular barely able to lift its head above its shoulder-height (Stevens & Parrish, 1999).

However, some researchers have questioned particularly the DinoMorph results, on the grounds of (i) an arbitrary 50% zygapophyseal safety limit for disarticulation, by which the pre- and postzygapophyseal facets would always retain at least a 50% overlap for any given posture (Dzemeski & Christian, 2007), and (ii) an underestimation of the amount of intervertebral and zygapophyseal soft tissue/cartilage (Taylor & Wedel, 2013a), which would make the necks to have more range of motion in the vertical component (Paul, 2000). Dzemeski and Christian conducted range of motion analyses on three long-necked extant animals (*Struthio camelus*, *Camelus bactrianus* and *Giraffa camelopardalis*) by manipulating their bones manually, noticing that *in vivo* flexibility was attainable with the bare bones, although with less zygapophyseal overlap than 50% (Dzemeski & Christian, 2007), which had been proposed by Stevens and Parrish as the limit for range of motion (Stevens & Parrish, 1999).

Mallison’s work with the non-sauropod sauropodomorph *Plateosaurus* (Mallison, 2010a,b) were crucial in establishing high fidelity 3D-scanned skeletons as one of the optimal ways to build skeletal mounts, with several advantages over using real fossil bones (Mallison, 2010b). Among them, the ability to operate more than one element at one time without external supports, hence minimizing damage to the original fossils (Mallison, 2010b). However, few sauropod taxa account for a completely known neck, and fewer are known by a complete neck from a single individual (Taylor, 2015). All in all, there are roughly above a dozen taxa with complete necks known from a single specimen, and, among those, few are well preserved or easily accessible (due the original fossils are exhibited as a mounted skeleton). Therefore, very few range of motion analyses have been carried out on actual full known, well-preserved sauropod necks, and the osteological neck motion capabilities of most sauropods remain largely unknown.

Spinophorosaurus nigerensis, an early branching Eusauropod sauropod from the Middle? Jurassic of Niger (Remes *et al.*, 2009; Mocho *et al.*, 2013), is one of the few sauropods known with a virtually complete and well-preserved neck (only missing the atlas). Also, a putative juvenile *Spinophorosaurus* specimen was retrieved few meters away from the holotype (Páramo & Ortega, 2012), consisting of an almost complete, articulated cervical series and some dorsal vertebrae and rib remains. Since almost two complete necks of two individuals at two markedly different ontogenetic stages are known for *Spinophorosaurus nigerensis* (Fig. 1A,B), neck mobility can be tested minimizing reconstructive speculation in two specimens which likely belong to the same sauropod taxon for the first time.

The following hypotheses have been evaluated: (i) osteology alone does not allow to estimate the amount of intervertebral space (Taylor, 2014; Paul, 2017), (ii) some neck postures attained in life require disarticulating vertebrae (Stevens & Parrish, 2005; Taylor & Wedel, 2013a), (iii) the amount of intervertebral space diminishes with ontogenetic development (Taylor & Wedel, 2013a), and (iv) the neck range of motion increases with ontogenetic development.

Given the size and fragility of the adult skeleton and all the potential dangers of working with real fossils, a virtual paleontology approach was taken. Since both range of motion and intervertebral space is known to vary with ontogeny in the extant *Giraffa camelopardalis*, we also analyzed two giraffe specimens at two different ontogenetic stages (adult and newborn, Fig. 1), following the same methodology to assess whether the analyses with digital skeletons would render results compatible with *in vivo* observations and if that compatibility can help to interpret the obtained results from the analyses of the two necks referred to *Spinophorosaurus*.

4.2 - MATERIAL

Three specimens of a sauropod dinosaur and two specimens of extant artiodactyl mammal are the subject of this study (Fig. 4.1). The extant sample consisted of two specimens of *Giraffa camelopardalis* of different ontogenetic stages. Both specimens were digitized via CT-scan. The juvenile specimen (TMM M-16050) is a dead newborn from the Gladys Porter Zoo, scanned post necropsis (Fig. 4.2), then skeletonized after the scan and donated to the University of Texas Vertebrate Paleontology collections. The scan files are deposited at the online repository MorphoSource by Duke University. The adult specimen consists of 7 cervical vertebrae (CV) and 1 thoracic (T) vertebra deposited at the American Museum of Natural History. It was CT-scanned for an exhibition in the early 2000s (Kent Stevens, pers.comm. 2018) and has been used in previous studies regarding giraffe osteological range of motion (Stevens, 2013). The 3D files were loaned generously by the AMNH and Kent Stevens. The actual specimen number or scanning specifications were not available.

The extinct sample studied were three specimens of *Spinophorosaurus nigerensis* of different ontogenetic stages (Fig. 1). All specimens were collected in an area north of the Rural Community of Aderbissinat (Thirozerine Dept., Agadez Region, Republic of Niger), stratigraphically below the outcrops of the Tegama Group in the "Falaise de Tiguidit". Holotype and paratype were found in the same level of this layer, about 15 meters laterally apart from each other on the upper unit (Remes *et al.*, 2009).

The holotype specimen (GCP-CV-4229 and NMB-1699-R) preserves most of the skeleton, only missing most of the preorbital region of the skull, the atlas and distalmost caudal vertebrae, one coracoid, both sternal plates (if they were ossified), forelimbs, distal left ischium, both feet and left hindlimb. It is possibly a subadult specimen, as it has unfused arches and centra in most vertebrae and sutures still visible in those vertebrae with fused centra and arches and is smaller than the paratype (which has ossified vertebrae and is histologically an adult, see below) (Fronimos & Wilson, 2017). However, since neurocentral suture fusion may not be the most reliable indicative of ontogenetic state (Brochu, 1996; Irmis, 2007), its subadult status must be considered tentative and to be tested by histological sampling in the future. However, thorough this paper both "subadult" and "holotype" will refer to this specimen.

The paratype specimen (NMB-1698-R) preserves fewer elements than the holotype, among them six cervical vertebrae, four with remarkably well-preserved pre- and postzygapophyses. It is not a fully grown adult, but appears to be in a more advanced stage in its ontogeny than the holotype, since most bones are larger than the same bones on the holotype, the neurocentral sutures are closed and not visible, but the cervical ribs and scapula and coracoid are unfused. Recent histological analyses have found it not only to be an adult, but also to have survived an osteological tumor-like pathology which caused radial fibrolamellar bone (Jentgen-Ceschino *et al.*, 2019).

A third, likely juvenile specimen (GCP-CV-BB-15) preserves an almost complete neck from the axis to the first dorsal vertebra, with one cervical vertebra (CV6) very damaged. These vertebrae share most (but not all) of the diagnostic characters of *Spinophorosaurus* (Páramo & Ortega, 2012) (Under description by AP). The neurocentral sutures are open, the centra are less elongated than on the holotype and paratype and the vertebrae are a quarter the size of the holotype. The third specimen was found *ex-situ* in the surface, but with most elements articulated and no duplicity in vertebrae, so it can be considered a single specimen. The lithology of the matrix containing this specimen is identical to both holotype and paratype, and the absence of relief and being found near the upper unit close to both specimens likely means that it stems from the same horizon.

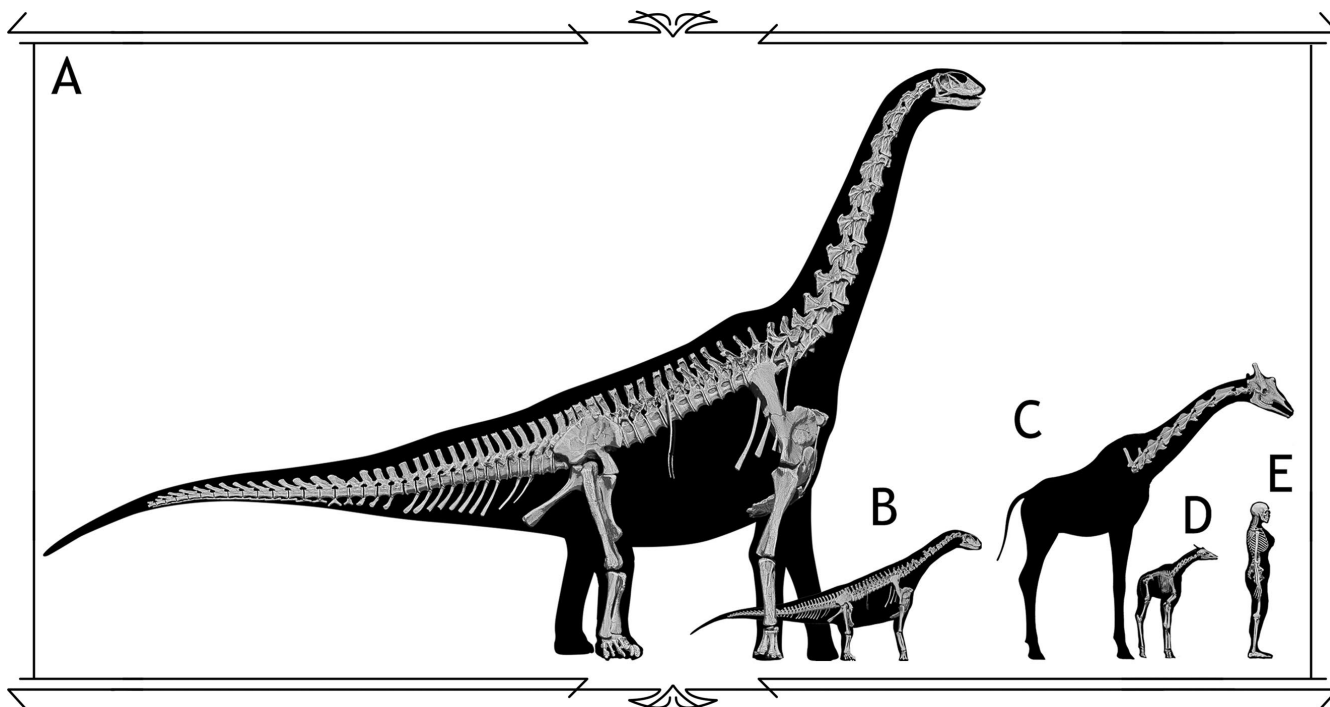


Figure 4.1 - Extant and extinct analyzed specimens size comparison.

A - *Spinosaurus nigerensis* adult composite specimen. **B** - *Spinosaurus nigerensis* juvenile composite specimen. **C** - *Giraffa camelopardalis* adult specimen. **D** - *Giraffa camelopardalis* newborn specimen (TMM M-16050). **E** - 1700 mm. *Homo sapiens* for scale.

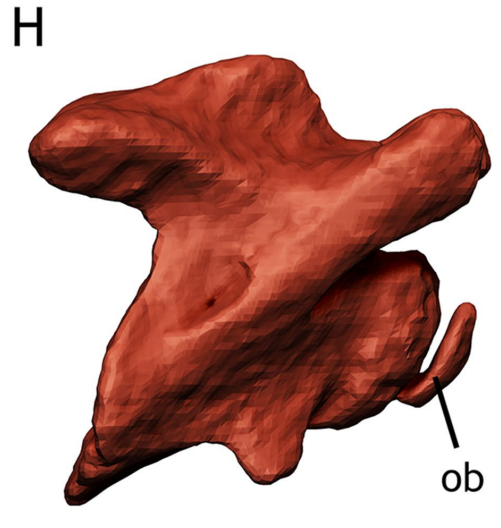
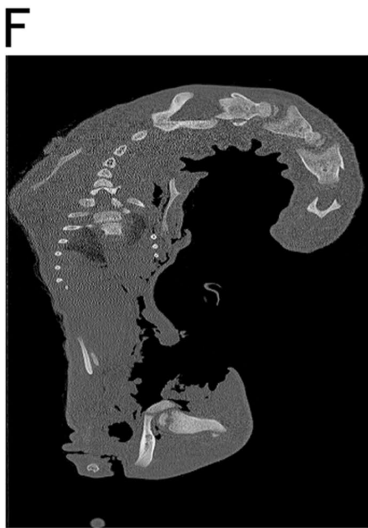
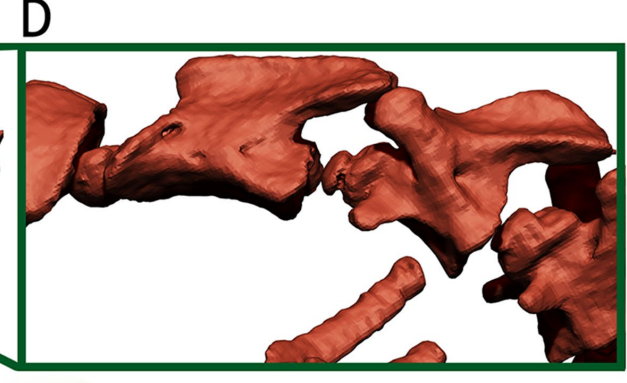
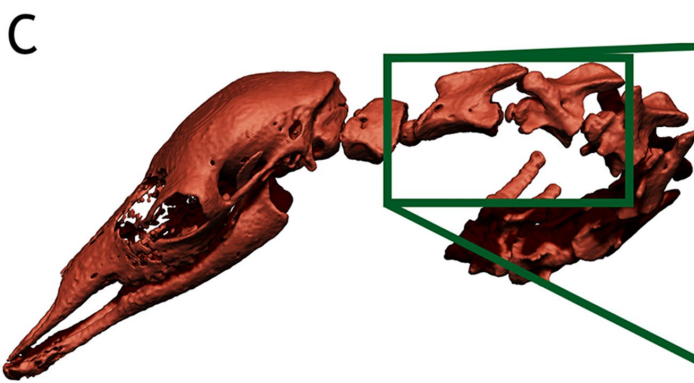
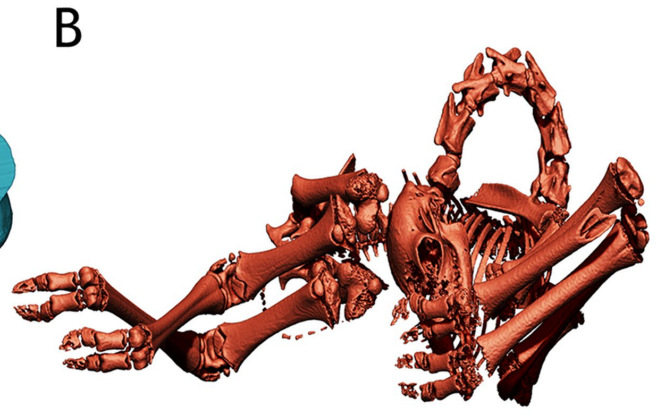
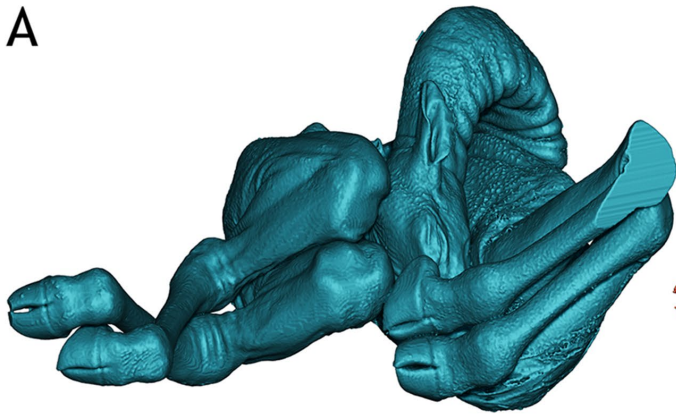
4.3 - METHODS

Preparing the virtual skeletons

For the juvenile specimen of *Giraffa camelopardalis* (TMM M-16050), the CT-Scan data was first imported to ImageJ 1.49b (National Institutes of Health, USA, 2014) for artifact removal and optimizing contrast. Then, it was imported into Avizo 7.1.0 (VSG, Burlington, MA, USA, 2013) for segmentation and 3D reconstruction. The soft tissues were reconstructed as a whole mesh and exported in Wavefront OBJ format (Fig. 4.2 A). Each cervical vertebra and the first two dorsal vertebrae were reconstructed individually, slice per slice, and exported as a high-resolution Wavefront OBJ model in their original position (Fig. 4.2 C). The remaining dorsal vertebrae and ribs were reconstructed as a whole, single structure, and exported as a high resolution Wavefront OBJ. The same was done with the sacrum and pelvis, each limb and the skull. Overall we reconstructed as individual models: seven cervical vertebrae, two dorsal vertebrae, one mesh of dorsal vertebrae + ribs, one mesh with the sacrum + pelvic girdle + caudal vertebrae, two meshes of pectoral girdle + forelimbs, two meshes of hindlimbs.

The fossil *Spinosaurus* specimens were surface-scanned by photogrammetry, following the protocol of Mallison and Wings (Mallison & Wings, 2014) in Photoscan 1.3 (Agisoft LLC11 Degtyarniy per., St. Petersburg, Russia, 191144). The juvenile specimen GCP-CV-BB-15 was digitized following the exact same protocol as the holotype. Unlike the holotype, most cervical vertebrae were easily separated physically from each other during preparation, with the exception of vertebrae CV11 and CV10, which had to be digitally separated in ZBrush 4R6. (Pixologic, USA, 2013). The mesh was duplicated as two separate sub-tools. Using the mask-lasso brush each vertebra was masked (a different one in each of the models) and then the trim-lasso brush was used to eliminate the unmasked vertebra. The missing portions (prezygapophysis medial side, anterior centrum cotyle and pedicels in CV11, postzygapophyses, posterior centrum condyle and pedicels in CV10) were digitally sculpted based upon preceding and following vertebrae. CV12 right prezygapophysis was broken, physically attached to CV11. It was digitally separated following the same procedure to separate CV11 and CV10. The articular facet was visible and needed no restoration, unlike the medial side, which was not visible, and was sculpted based upon that of DV-1.

The subadult skeleton was assembled from the holotype specimen, with missing elements stemming from the paratype (humerus, scaled to have the same humerus/scapula ratio as in the paratype) and closely related sauropods (with forelimb and feet proportions close to those from *Shunosaurus* (Zhang, 1988), *Mamenchisaurus*



(Ouyang & Ye, 2002) or *Jobaria* (Sereno *et al.*, 1999)). Since many cervical vertebrae could not be separated from the preceding vertebra during preparation, the medial portion of many prezygapophyseal facets is obscured. To estimate the medial side of the prezygapophyses, the visible lateral portion was used as the posteriormost limit for the prezygapophyseal facet, with the rest of the facet reconstructed by digitally sculpting the missing medio-dorsal part of the facet (area between visible dorsal side of the facet and the ventro-medial, non-facet side of the prezygapophyses). This was done following the same protocol described above for the juvenile specimen.

Assembling the virtual skeletons

Each skeleton was imported into ZBrush 4R6 bone by bone and articulated following the protocol of Mallison (Mallison, 2010a,b). Overall, the axial skeleton was articulated in pairs, with only two elements visible at once in order to minimize preconceived notions: one remained static while the other was articulated in Osteologically Neutral Pose (ONP). A majority of authors have defined ONP as the maximum alignment of the zygapophyses (Stevens & Parrish, 1999; Stevens, 2002, 2013; Dzemeski & Christian, 2007; Taylor *et al.*, 2009; Mallison, 2010a,b). On the other hand, in addition to the maximum overlap of the zygapophyses, some authors implemented that anterior and posterior facets of vertebral centra had to be parallel in their definitions of ONP (Stevens & Parrish, 2005; Christian *et al.*, 2013; Carabajal *et al.*, 2014). While intervertebral soft tissue might vary in relative size to the vertebral centra and it may change the geometry of the axial skeleton, the zygapophyseal capsules are not thicker than a flat sheet covering which does not affect the shape of the zygapophyseal articulations (Taylor & Wedel, 2013a). Our usage of the term ONP refers only to the zygapophyseal joints, given i) the discrepancy between zygapophyseal and zygapophyseal + centra alignments, ii) the more widespread use of the maximal zygapophyseal overlap criterion alone without the parallel centra criterion, and iii) the fact that intervertebral soft tissue thickness is more variable than zygapophyseal capsule thickness. So, ONP is the full articulation of the zygapophyseal facets, with complete overlap of the facet outlines in all three anatomical planes (antero-posterior, lateral-medial, dorso-ventral). Paul coined Neutral Bone Only Posture (NBOP *sensu* Paul (Paul, 2017)) for including not only the best possible fit of pre- and postzygapophyseal facets, but also the rims of the vertebral centra parallel (Fig. 4.3; see discussion).

If both skeletal assemblages (anterior to posterior and vice-versa) had the same Osteologically Induced Curvature (OIC, *sensu* Stevens (Stevens, 2013); “the curvature of a vertebral column in ONP, as distinguished from curvature induced by joint deflection”) the virtual mount was considered positive. The appendicular skeleton was articulated following Reiss and Mallison (Reiss & Mallison, 2014), in ONP (long axes of two bones articulating with each other were placed approximately parallel to each other in lateral view) by pairs. Since the juvenile *Spinophorosaurus* fossil specimen is small and stable, it was also articulated in pairs manually and the results compared with those obtained in the virtual workspace.

All measurements relative to neck and head heights and angles were taken relative to the ground: set as 0° for measuring angles and as 0 meters for measuring heights. In the case of the adult giraffe, for which we do not have a complete skeleton, we used a 3D full body flesh model of a giraffe, scaled to have the same neck length. In the case of the juvenile *Spinophorosaurus*, for which we have a less complete skeleton, we used an isometrically scaled-down virtual skeleton of the adult (Fig. 1), assuming limbs grew isometrically (Ikejiri, 2004). To measure the angles between two individual vertebrae, we used the angulation between the same landmark of two consecutive vertebrae (see “Measuring inter-vertebral range of motion” below for a more detailed explanation).

Figure 4-2 (previous page) - *Giraffa camelopardalis* newborn TMM M-16050.

A - 3D render of the newborn giraffe body as it was CT-scanned in approximate ventral view. **B** - 3D render of the newborn giraffe skeleton from CT data, same view as A. **C** - Cervical vertebrae and skull of the newborn giraffe as it was CT-scanned, showing the intervertebral space. **D** - Close up on Axis-CV3 of the newborn giraffe, showing the intervertebral space and the ossification body anterior to the condyle. **E** - Dissected neck from a different newborn giraffe, showing the separation between vertebrae is similar to that of TMM M-16050, modified from Taylor & Wedel (2013). **F** - CT-scan slide of TMM M-16050. **G** - Highlight of CV5 on the CT-scan slide from F, showing the ossification body anterior to the vertebral centrum. **H** - 3D render of CV5 from CT data, showing the ossification body (ob). Scale for E= 200 mm.

Specimen	Greatest	Lowest	Average (whole neck)
Newborn <i>Giraffa</i> (articulated)	52 %	11.6 %	27.27 %
Newborn <i>Giraffa</i> (ONP)	45 %	12.3 %	27.03%
Adult <i>Giraffa</i> (ONP)	6 %	4 %	4.8 %
Juvenile <i>Spinophorosaurus</i> (ONP)	16 %	11.1 %	13.5 %
Adult <i>Spinophorosaurus</i> (ONP)	7 %	3 %	4.5 %

Table 4.1 - Amount of neck intervertebral space.

Percentages measure the amount of the segment length corresponding to intervertebral space.

Measuring the inter-vertebral space

Intervertebral space was measured using two different ways with the virtual bones in ONP in ZBrush 4R6 (Pixologic, USA, 2013). First, a direct measurement of the gap separating two vertebrae was measured, as the maximum distance between the deepest region of the cotyle of the anterior vertebra and the anteriormost part on the condyle of the posterior vertebra. An indirect measurement was also made by measuring the complete length of the segment (as the distance between the deepest region of the cotyle of the posterior vertebra and the anteriormost part on the condyle of the anterior vertebra) and the individual length of both vertebrae in the segment (also deepest cotyle to anteriormost condyle, “functional length”, Fig. 9 in Taylor and Wedel (Taylor & Wedel, 2013a)). The difference between the complete length of the segment and the addition of both vertebrae would correspond to the intervertebral space:

$$\text{Complete Segment Length} - (\text{Anterior Vert. Length} + \text{Posterior Vert. Length}) = \text{Intervertebral space}$$

The difference between the direct measurement and the indirect measurement turned out to be minimal. The percentage of the intervertebral space is the percentage of the length of the corresponding measured segment (Table 4.1).

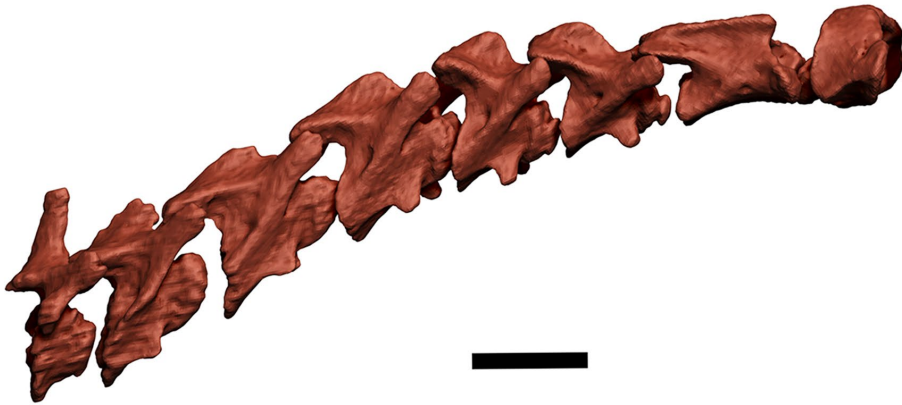
Measuring the inter-vertebral range of motion

The osteological range of motion (ROM) was calculated by deflecting each vertebra one pair at a time, with the posteriormost one remaining static while the anteriormost one was deflected. There has been some discrepancies on how much pre- and postzygapophyseal articular facets may deflect before disarticulation. Early on, the zygapophyseal safety factor, the minimal overlap of the facets before there is too much strain on the zygapophyseal articular capsules *sensu* Stevens (Stevens, 2013), was set to be at around 50% of overlap (Stevens & Parrish, 1999). However, observations on extant crocodiles (Stevens & Parrish, 2005) or birds (Mallison, 2010b) show that alive extant animals can attain postures with little overlap between their zygapophyseal facets.

For this study, we decided to follow the protocols of Mallison (Taylor & Wedel, 2013b), in which all vertebrae, in the absence of an osteological stop, were deflected until only a minimum overlap of the facets was retained. Beyond that point, they were considered disarticulated. That way, accounting a larger facet *in vivo* with a fresh zygapophyseal capsule (Taylor & Wedel, 2013a), the range of motion is underestimated rather than overestimated, in accordance with what happens in present day archosaurs. In lateral flexion, zygapophyseal overlap was retained in three different ways: (i) maintaining one zygapophyseal pair in full articulation and deflecting the other pair anteriorly, (ii) maintaining one zygapophyseal pair in full articulation and deflecting the other pair posteriorly, and (iii) deflecting one zygapophyseal pair posteriorly and the other pair anteriorly (as seen in Mallison (Mallison, 2010b) figure 3A), which would be the maximum range of motion before disarticulation. Both (i) and (ii) rendered similar range of motion at all intervertebral joints, so all figures depicting lateral range of motion of the neck depict (i) and (iii).

To measure the angles between two individual vertebrae, we used the angulation between the same landmark of two consecutive vertebrae: the posteriormost and ventralmost point of the vertebral centrum in lateral view for dorso-ventral ROM, and the right prezygapophyses in dorsal view for lateral ROM. These were

A



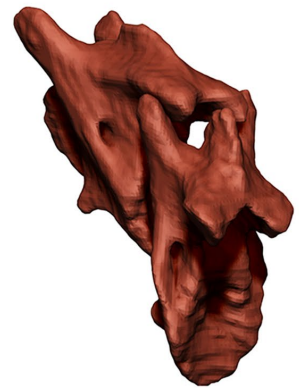
B



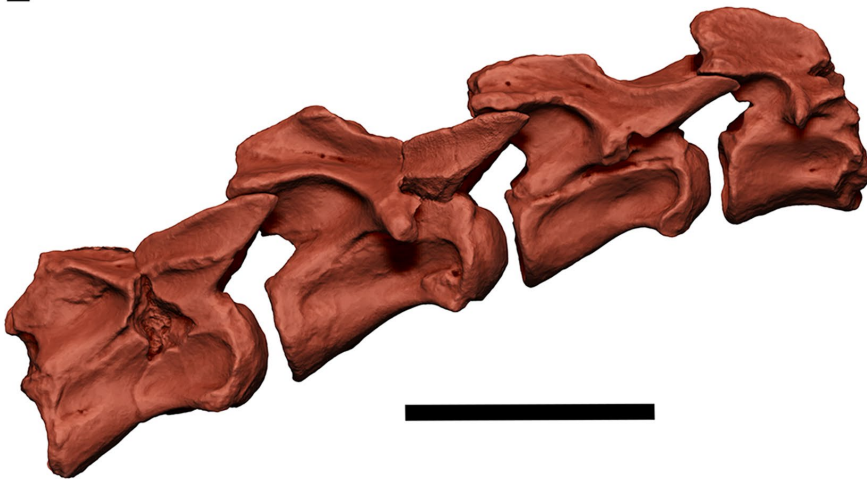
C



D



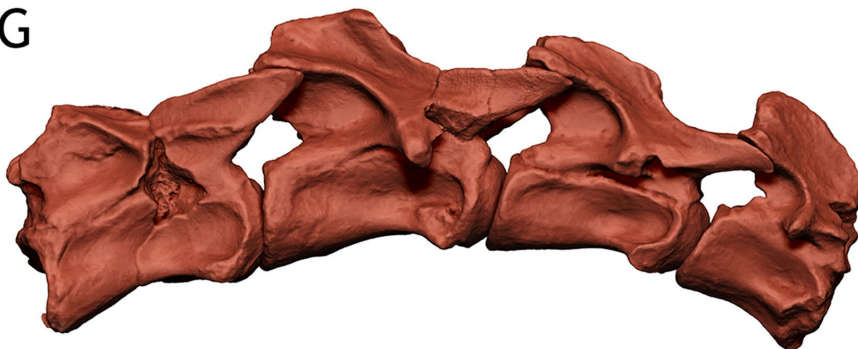
E



F



G



H

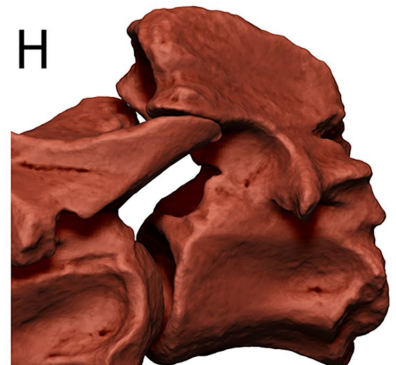


Figure 4.3 (previous page) - Comparing osteologically neutral pose (ONP) and neutral bone only posture (NBOP).

Notice the vast difference between in the osteologically induced curvature (OIC) and amount of intervertebral space rendered by ONP and that rendered by NBOP. **A** - Newborn *Giraffa* neck in ONP **B** - CV7 and CV6 in postero-lateral view in ONP, notice the full zygapophyseal overlap. **C** - Newborn *Giraffa* neck in NBOP. **D** - CV7 and CV6 in postero-lateral view in NBOP, notice how the zygapophyses are not fully overlapped, and have to be angled in order to have the centra rims parallel. **E** - Juvenile *Spinophorosaurus* CV5 to Axis in ONP. **F** - CV3 and Axis in postero-lateral view in ONP, notice the full zygapophyseal overlap. **G** - Juvenile *Spinophorosaurus* CV5 to Axis in NBOP. **H** - CV3 and Axis in postero-lateral view in NBOP, how the zygapophyses are not fully overlapped, and have to be angled in order to have the centra rims parallel. Scales for A, C, E and G = 50 mm.

later contrasted against a different method: drawing straight lines parallel to the main axis of the vertebral centrum in lateral (dorso-ventral ROM) or the neural spines in dorsal view (lateral ROM) and measuring the angle they make, which was the same measured between landmarks in all cases. As with the OIC, the juvenile *Spinophorosaurus* specimen range of motion was manually measured with the original fossils and the results compared favorably with those obtained in the virtual workspace.

4.4 - RESULTS

Giraffa camelopardalis newborn

Since the scanned skeleton of the newborn giraffe comes from an articulated dead newborn (Fig. 4.2 A-B), we made the following remarkable observations of the scan before digitally separating the bones: (i) the intervertebral space between cervical vertebrae and caudal vertebrae pairs (Fig. 4.2 B-D) is much greater than the one between dorsal and sacral pairs (ii) There is an ossification body in the anterior centrum of most cervical vertebrae which may be slightly separated from the actual condyle but are joint together by an ossified constriction in most vertebrae (Fig. 4.2 F-H). (iii) The mineralized bone matrix of some cervical vertebrae is asymmetrical, that is, one of the sides (left or right) is more ossified than the other. (iv) The pose of the neck, flexed ventrally and laterally to the right with some torsion, makes the head reach the torso and required the left pre- and postzygapophyseal facets to be completely disarticulated from Axis-CV3 to CV6-CV7 joints (Fig. 4.2 C). The ribs of the right side are misaligned from their proximal diaphysis, where they were apparently cut when necropsy was performed. The ossified epiphyses and diaphyses of long bones are well separated and unfused.

We measured the intervertebral space on the cervical and anterior dorsal vertebrae on the virtual skeleton as it was scanned in order to have some measurements without any manipulation of the bones. The intervertebral space accounted for about 27.27% the length of the Axis-T2 segment, with the amount of intervertebral space ranging between 18.2 mm. and 8.7 mm (Table 4.1).

After articulating the neck in osteologically neutral pose (ONP), that is, fully articulating the pre- and postzygapophyseal facets, the intervertebral space in all vertebrae present, albeit with some differences in the exact intervertebral space amount from the non-manipulated pose (Table 4.1). The intervertebral space accounted for 27.03% of the length of the Axis-T2 segment in ONP, ranging between 17.9 mm. and 8.9 mm (Table 4.1).

Figure 4.4 (next page) - *Giraffa camelopardalis* neck postures.

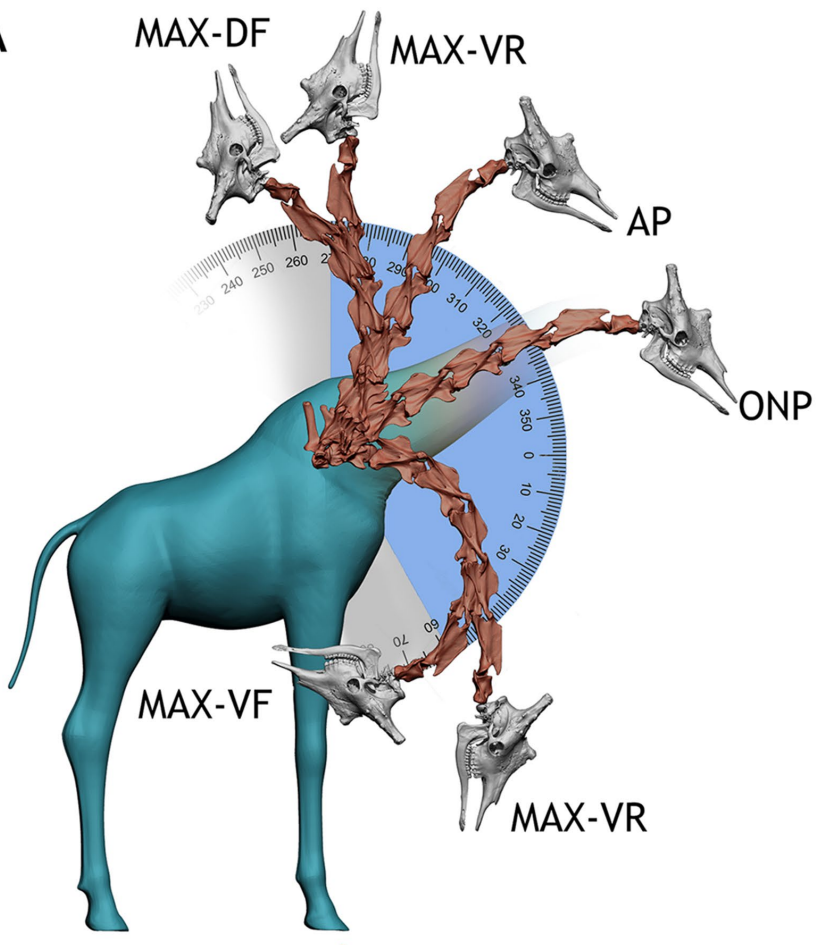
A - Several postures within the dorso-ventral osteological range of motion of the adult *Giraffa* in lateral view. Yellow indicates the arc described between maximum and minimum head heights. Grey indicates the arc described between maximum dorsiflexion and ventriflexion. **B** - Adult *Giraffa* in posterior view, with the neck folded against the body, achieved with full lateral flexion (III) of T1-CV7, CV7-CV6, and CV6-CV5 joints. **C** - Several postures within the dorso-ventral osteological range of motion of the newborn *Giraffa* in lateral view. Yellow indicates the arc described between maximum and minimum head heights. Grey indicates the arc described between maximum dorsiflexion and ventriflexion. **D** - Newborn *Giraffa* in posterior view, with the neck folded against the body, achieved with full lateral flexion (III) of T1-CV7, CV7-CV6, and CV6-CV5.

Max-DF = maximum dorsiflexion. Max-DR = maximum dorsal reach. AP = alert posture. ONP = osteologically neutral pose. Max-VR = maximum ventral reach. Max-VF = maximum ventriflexion.

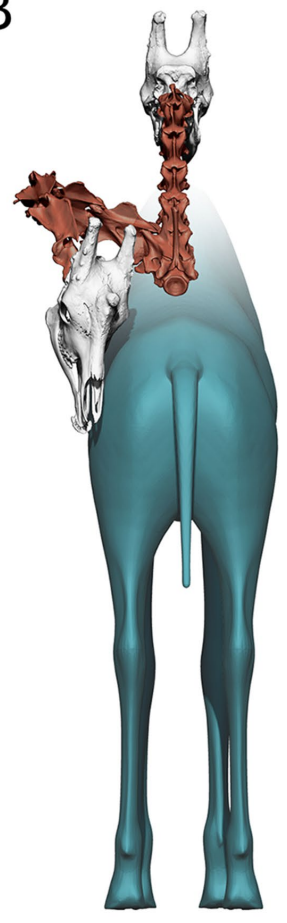
Red bones = main specimen. White bones = extrapolated elements (see methods). Blue = flesh model.

Angles in degrees.

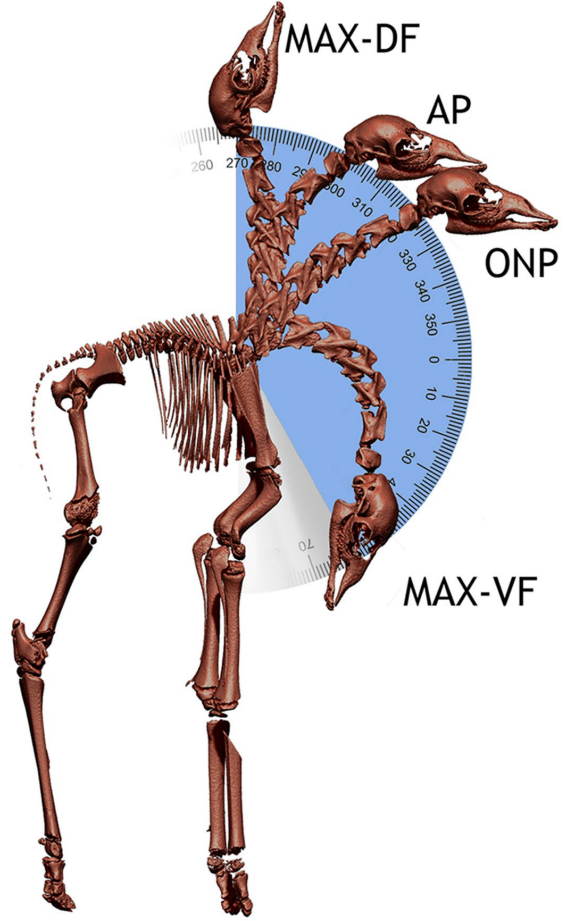
A



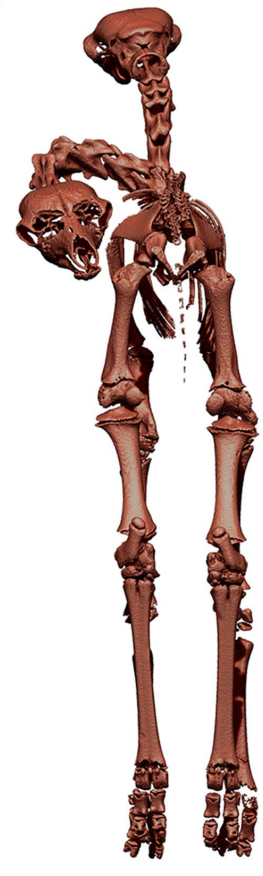
B



C

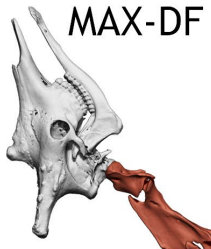


D



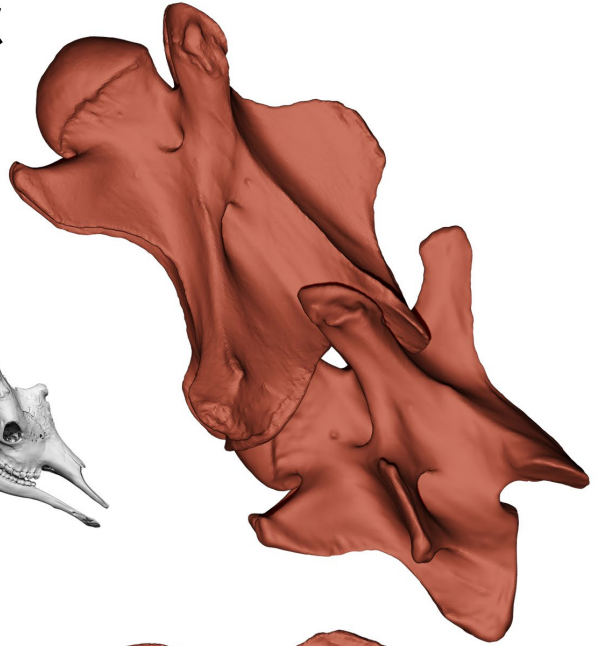


A



MAX-DF

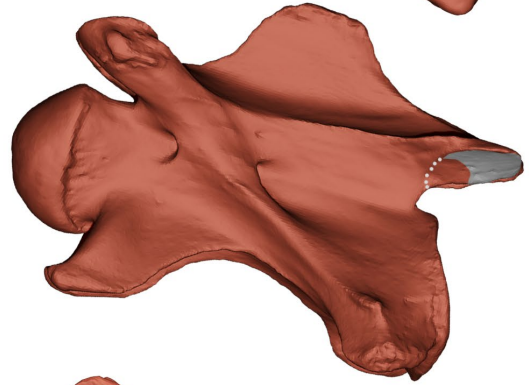
C



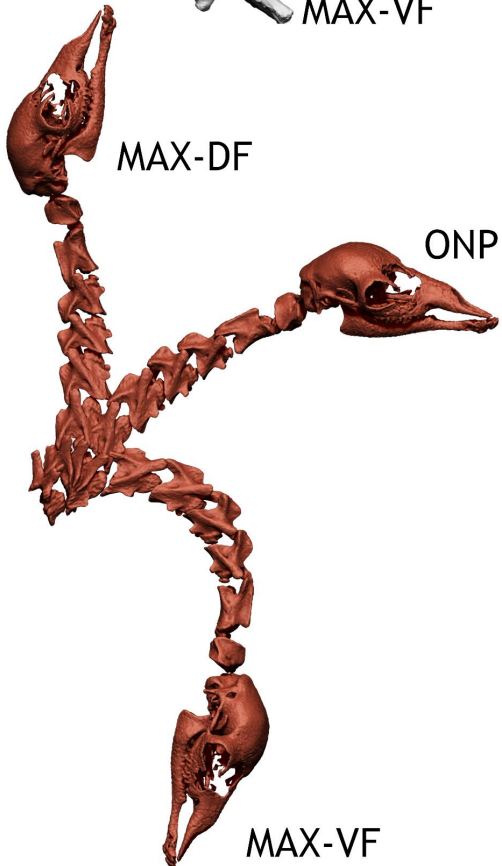
ONP



D



B



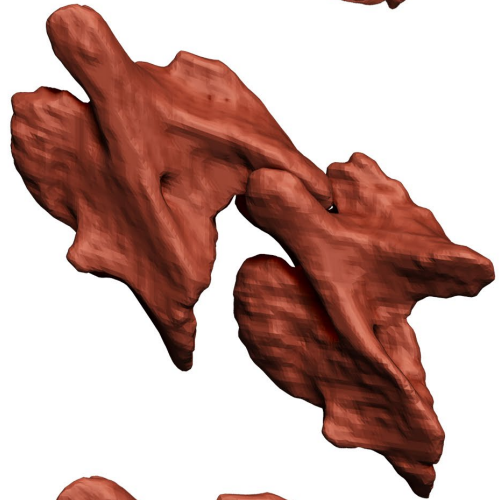
MAX-DF

ONP

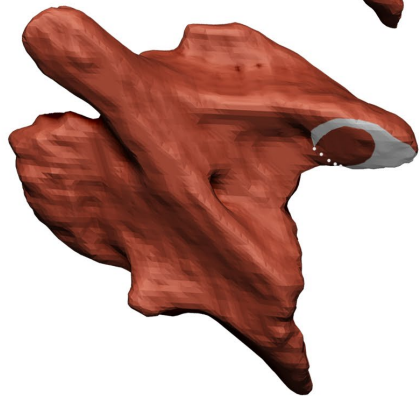
MAX-VF

MAX-VF

E



F

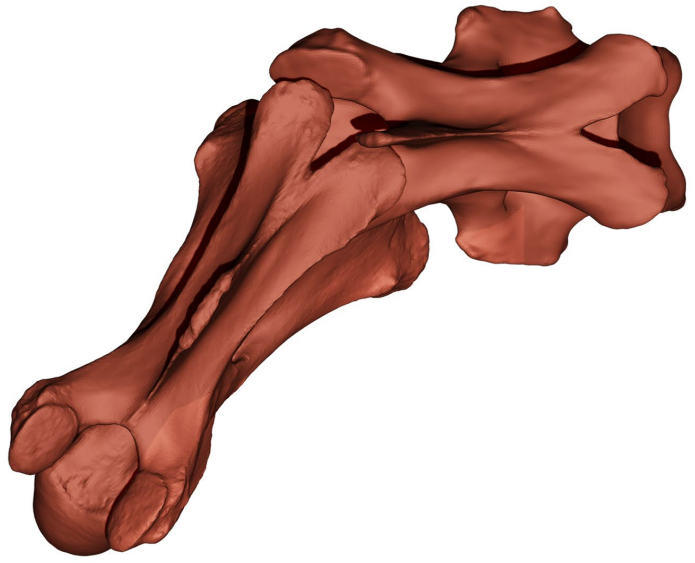


G

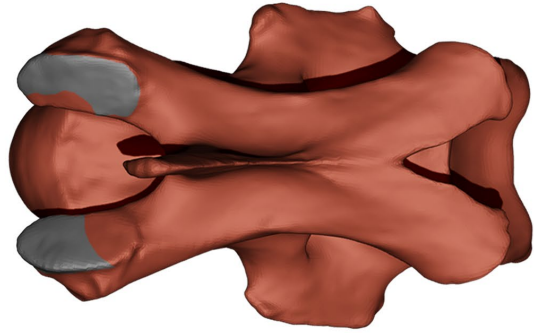
ONP



I

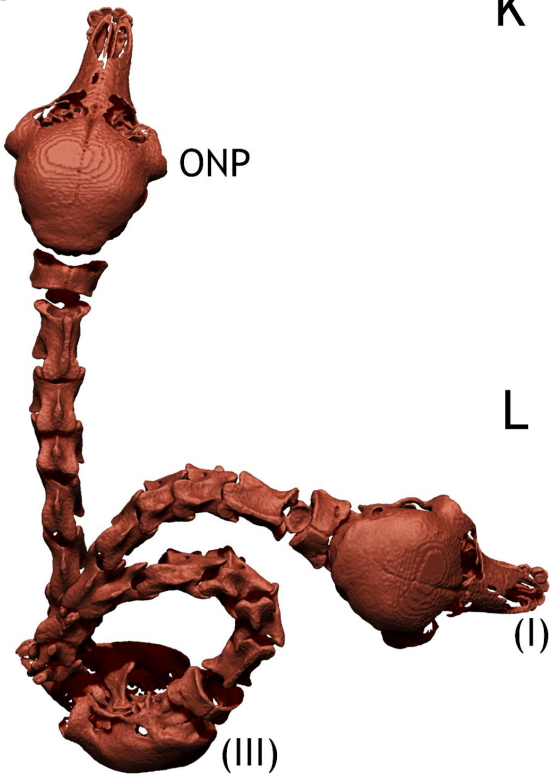


J



H

ONP



K



L



Figure 4.5 (previous page) - *Giraffa camelopardalis* osteological neck range of motion.

A - Dorso-ventral osteological range of motion of the adult *Giraffa* in lateral view. **B** - Dorso-ventral osteological range of motion of the newborn *Giraffa* in lateral view. **C** - CV7-CV6 joint of the adult *Giraffa* in maximum dorsiflexion (Max-DF) in lateral view. **D** - CV6 of the adult in lateral view *Giraffa* showing how much of the postzygapophysis overlaps with the prezygapophysis of CV7 in maximum dorsiflexion (in red, zygapophyseal overlap, in gray non overlapped area of the facet). **E** - CV7-CV6 joint of the newborn *Giraffa* in maximum dorsiflexion (Max-DF) in lateral view. **F** - CV6 of the newborn *Giraffa* in lateral view showing how much of the postzygapophysis overlaps with the prezygapophysis of CV7 in maximum dorsiflexion (in red, zygapophyseal overlap, in gray non overlapped area of the facet). **G** - Lateral osteological range of motion of the adult *Giraffa* in dorsal view. **H** - Lateral osteological range of motion of the newborn *Giraffa*. **I** - CV7-CV6 joint of the adult *Giraffa* in maximum lateral flexion (III) in dorsal view. **J** - CV7 of the adult *Giraffa* in dorsal view showing how much of the prezygapophysis overlaps with the postzygapophysis of CV6 in maximum dorsiflexion (in red, zygapophyseal overlap, in gray non overlapped area of the facet). **K** - CV7-CV6 joint of the newborn *Giraffa* in maximum lateral flexion (III) in dorsal view. **L** - CV6 of the newborn *Giraffa* in dorsal view showing how much of the prezygapophysis overlaps with the postzygapophysis of CV6 in maximum dorsiflexion (in red, zygapophyseal overlap, in gray non overlapped area of the facet).

Red bones = main specimen. White bones = extrapolated elements (see methods).

Max-DF = maximum dorsiflexion. ONP = osteologically neutral pose. Max-VF = maximum ventriflexion. I = lateral flexion attained when maintaining one zygapophyseal pair in full articulation and deflecting the other pair anteriorly. III = maximum lateral flexion.

The osteologically induced curvature (OIC) of the newborn giraffe dorsal vertebrae shows a slightly bowed spine, with an angle of only 5° between the first sacral centrum and the first dorsal (T1). The neck, on the other hand, has a steeper angle (Fig. 4C), forming a 39° angle between T1 and the atlas. This is caused by greatly wedge-shaped T2, T1 and CV7 vertebrae, which account for most of the verticalization of the neck (the angle between the centra of T2-CV6 is already 40°). From CV5 to Atlas, the OIC is slightly ventriflexed, with a -1° angle between CV5 and the atlas. The muzzle of the newborn giraffe is at a height of 1.12 meters from the ground when in ONP (with T1 at 0.91 meters and the shoulder joint at 0.72 meters).

The osteological range of motion (ROM) of the neck in dorsiflexion allows the neck to be placed vertical and a little beyond, with the atlas forming a 91° angle with T1 at full dorsiflexion. This dorsiflexion allows the muzzle to reach a maximum height of 1.47 meters. Maximum ventriflexion makes the atlas form an angle of -46° with T1. This allows placing the muzzle at 0.49 meters from the ground (Fig. 4C). The range of motion in lateral flexion allows the head to touch the body without disarticulating, with the head colliding with the body at full range of motion. (Fig. 4D) However, it is necessary to deflect both zygapophyseal articulations to allow the head to reach the body (Fig. 4.5 H-L). When only one pair of pre- and postzygapophyseal facets are deflected before disarticulation (ii, see methods), the arc described by the neck is of around 90°, but it does not allow pointing the muzzle posteriorly (that is, 180° from ONP, Fig. 4.5 H).

Giraffa camelopardalis adult

The intervertebral space is significantly smaller in the adult specimen than in the newborn, at least on the 7 cervical vertebrae, in ONP. The condyles fit deeply in the cotyles. The intervertebral space accounted for about 4.8 % the length of the Axis-T1 segment (Table 4.1).

The OIC of the adult giraffe neck has a steep angle (Fig. 4A), forming a 26° angle between T1 and the atlas (Fig. 4.4 A, Fig. 4.5 A). Most of this deflection occurs at the T1-CV7 and CV7-CV6 joints, since the centra of T1 and CV7 are wedge-shaped, and therefore dorsally deflect the vertebrae anterior to them in ONP. The remaining cervical vertebral centra are not wedged, and therefore articulate almost straight, although very slightly dorsally deflected (about 2° between CV6 and the atlas).

The osteological ROM of the adult giraffe neck is greater in all respects compared with that of the newborn (Fig.4). In maximum dorsiflexion, the atlas can deflect up to 103° from T1 vertebra before disarticulation. In maximum ventriflexion, the atlas can deflect up to -73° from T1 before disarticulation. The muzzle can therefore be situated at 90° respective to the ground before disarticulation occurs, at 4.1 meters. It is, however, impossible for the muzzle to reach the ground by ventriflexion of the neck alone, reaching a minimum height of 0.45 meters. In lateral flexion, the neck can describe a curve of more than 180°, with the head reaching the body well before disarticulating any of the cervical vertebrae joints (Figs. 4B, 5G).

Joint	N. Giraffa	A. Giraffa	J. <i>Spinophorosaurus</i>	A. <i>Spinophorosaurus</i>
CV2-CV3	31	34	25	35
CV3-CV4	24	48	15	28
CV4-CV5	38	46	17	25
CV5-CV6	32	39	15	21
CV6-CV7	40	44	13*	22
CV7-CV8/T1	34	30	12	23
CV8-CV9	-	-	13*	18
CV9-CV10	-	-	14*	21
CV10-CV11	-	-	15	28
CV11-CV12	-	-	16	27
CV12-DV1	-	-	7	17

Table 4.2 - Osteological dorso-ventral neck range of motion.

Angles are measured in degrees, and represent the range between maximum dorsiflexion and maximum ventriflexion. An asterisk (*) indicates that joint could not be measured and therefore was estimated based on the arithmetic mean of ROM at preceding and following joint. N = newborn; A = adult; J = juvenile. CV = Cervical Vertebra. T = Thoracic Vertebra (for giraffe only). DV = Dorsal Vertebra (for *Spinophorosaurus* only).

Spinophorosaurus nigerensis juvenile

The best-preserved cervical vertebrae of the juvenile *Spinophorosaurus* are the axis, CV3, CV4, CV12 and DV1. The remaining vertebrae either lack pre-postzygapophyses or are too distorted for the virtual or manual articulation to be completely reliable. However, the fossil was found in articulation and photographed before preparation (Fig. 4.6 A), so intervertebral space can be roughly assessed and compared with that obtained in the virtual mount.

The OIC reveals a significant amount of intervertebral space among the best-preserved vertebrae. The amount of intervertebral space in the Axis-CV5 segment is 12.4% of its length, with a maximum of 17.96 mm and a minimum of 11.28 mm. Between the CV7-CV8 joint there is 18.77 mm of intervertebral space, and 18.87 mm between CV12-D1, which accounts for 12.6% and 15.86% respectively of those segments length. The pictures of the fossils before preparation all show some intervertebral space, since the condyles barely fit into the cotyles (Fig.6A).

The osteological range of motion of the juvenile *Spinophorosaurus* can only be accurately estimated in the axis-CV5 segment and the CV7-CV8 and DV1-CV12 joints, since those preserve pre- and postzygapophyses. In order to obtain an approximation of the complete neck range of motion, the missing joints have been estimated to have as deflection the arithmetic mean of the closest preceding and following joints angles (Table 4.2). In full dorsiflexion, the curve described by the neck allows the head to be situated vertically, at 90° (at an angle of 79° with DV1). This dorsiflexion allows the muzzle to reach a maximum height of 1.83 meters. Maximum ventriflexion makes the axis form an angle of -53° with DV1. This allows placing the muzzle at 0.35 m from the ground (Fig. 4.7 C). The range of motion in lateral flexion allows the head to touch the

Figure 4.6 (next page) - *Spinophorosaurus nigerensis* neck fossils.

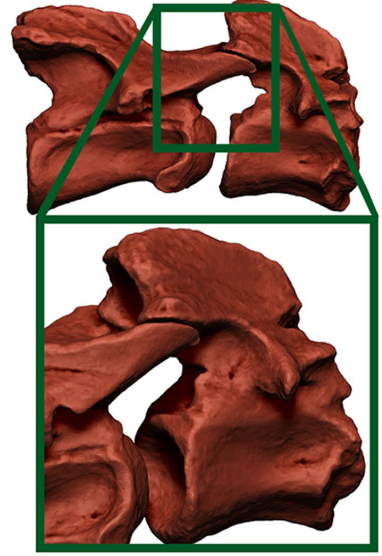
A - Articulated anterior segment of the neck (CV5-Axis) from the juvenile *Spinophorosaurus* before preparation (picture and 3D model articulated mimicking the field pose. Notice the condyles barely fit inside the cotyles). **B** - CV3-Axis joint from the juvenile *Spinophorosaurus* in ONP (zygapophyses in full overlap). Notice the intervertebral space. **C** - Articulated segment of the neck (CV7-CV5) from the subadult holotype *Spinophorosaurus* (Notice the condyles are more deeply nested inside the cotyles than in the juvenile). **D** - CV6-CV5 joint from the subadult *Spinophorosaurus* in ONP (zygapophyses in full overlap). Notice there is barely any intervertebral space, and the condyles are nested within cotyles. **E** - Antarticulated anterior segment of the neck (CV5-Axis) from a subadult specimen of *Camelus bactrianus* pictured in the Sahara dessert, showing the presence of intervertebral space (still filled with the intervertebral disc) remains despite desiccation in an arid environment.

Scale bars = 50 mm. dt = desiccated tissue. id = intervertebral disc

A



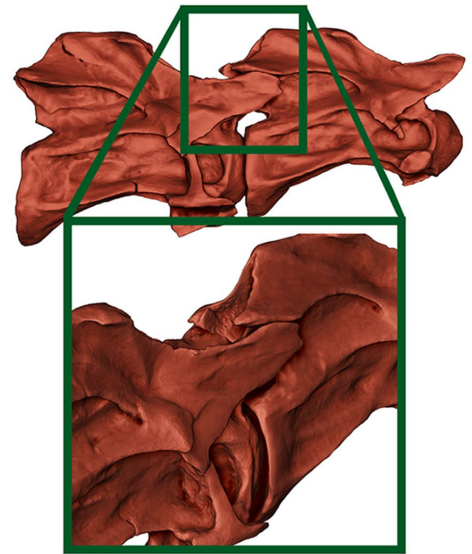
B



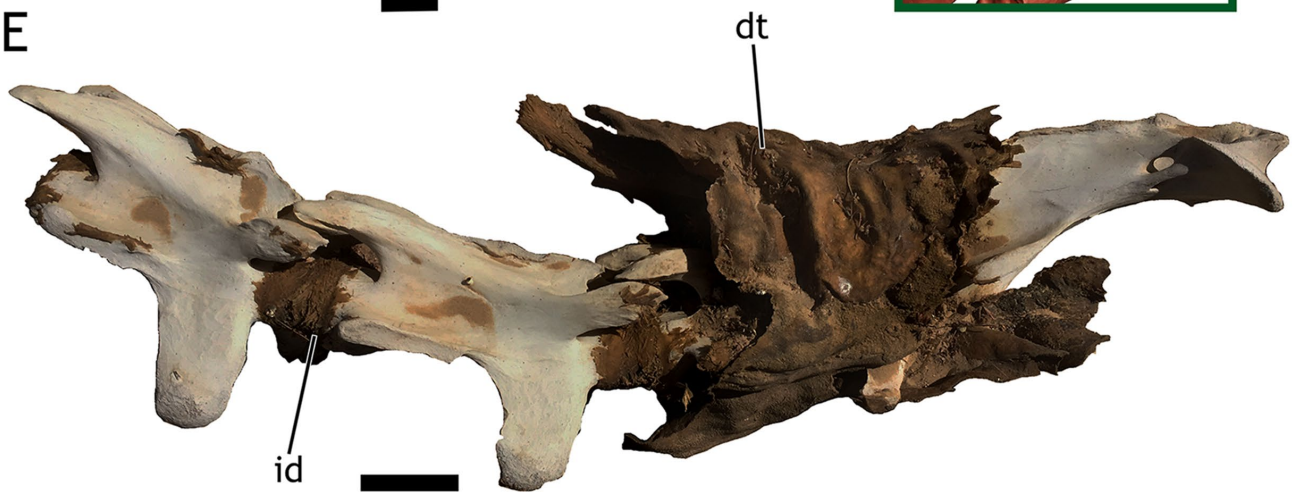
C



D



E



body without disarticulating (Fig. 4.8 H,K,L), with the head actually colliding with the body before reaching the maximum lateral flexion (Fig. 4.7 D). When only one pair of pre- and postzygapophyseal facets are deflected before disarticulation, the arc described by the neck is of around 80°, so it does not allow pointing the muzzle posteriorly (Fig. 4.8 H).

Spinophorosaurus nigerensis subadult

In the holotype of *Spinophorosaurus*, the intervertebral space in ONP is significantly lower than in the juvenile specimen. The condyles fit deeply in the cotyles, and the intervertebral space ranges from 6-2.5% in the joints it could be accurately measured, in the absence of CT scan (Table 4.1). The amount of intervertebral space for the whole neck length is around 4.5%. The pictures of those vertebrae still in articulation show the condyles are deeply nested in the cotyles (Fig. 4.6 C). As with the juvenile specimen, the fossil was found in opisthotonic posture (Remes *et al.*, 2009), so the amount of intervertebral space might have varied. When articulating the complete axial sequence of the holotype of *Spinophorosaurus nigerensis*, the presacral and caudal sections of the vertebral column deflect 20°. This, in addition with the slightly wedged dorsal vertebrae and the articulation of the cervical vertebrae in ONP, makes the axis deflect 31° from the last sacral vertebra (Fig. 4.7 A, ONP).

The osteological ROM of the subadult *Spinophorosaurus* can be better estimated in the antero-posterior axis in all joints, since the medial portions of the prezygapophyses are obscured in most vertebrae, as they could not be separated from the preceding vertebra during preparation. The lateral range of motion is more dubious, so the only considered postures were those in which the portion of the prezygapophyses overlapped was not extrapolated, and was visible in the actual fossil. Despite those caveats, the postures in Figs. 6 and 7 could be attained with the visible portions of the prezygapophyseal facets.

In full dorsiflexion, the curve described by the neck allows the head to be situated beyond vertical, at around 120° from DV1. At maximum verticality (90°) the muzzle can reach a maximum height of 7.16 meters from the ground. Maximum ventriflexion makes the skull form an angle of -70° with DV1. This allows placing the muzzle at 0.72 m from the ground (Fig. 4.7 A). The range of motion in lateral flexion allows the head to touch the body without disarticulating (Fig. 4.8 A), with the head actually colliding with the body before reaching the maximum lateral flexion (Fig. 4.7 B). When only one pair of pre- and postzygapophyseal facets are deflected before disarticulation, the arc described by the neck is of around 100°, allowing to point the muzzle toward posterior (Fig. 4.8 H).

4.5 - DISCUSSION

Intervertebral Space estimation

The amount of soft tissue in archosaur joints has been shown recently to potentially affect the amount of motion (Holliday *et al.*, 2010; Mallison, 2010c; Taylor & Wedel, 2013a). Estimating the amount of soft tissue in joints therefore is an important step in assessing more accurately the motion capabilities of extinct vertebrates. Unfortunately, although some long bone epiphyses show a different texture in juveniles in which the amount of articular soft tissue is greater than in the adults (Holliday *et al.*, 2010), there are no yet identifiable osteological correlates which can help estimate the exact amount of separation between adjacent bones. The same is true for estimating intervertebral space, since the bone texture of tetrapods with opisthocoelus vertebrae with different amounts of intervertebral space is indistinguishable (Taylor & Wedel, 2013a).

Our approach of estimating intervertebral space with the osteologically neutral pose in the newborn giraffe TMM M-16050 shows two things: (i) that in the newborn specimen, only the ONP rendered an intervertebral space which came close to the intervertebral space observed in the articulated CT-Scan of the specimen and, (ii) neutral bone only posture (NBOP), in which the rims of the vertebral centra are situated parallel (Paul, 2017), greatly underestimates the amount of intervertebral space as observed in the articulated CT-Scan of the specimen (Fig. 4.2 C vs. Fig. 4.3 C). Also, the amount of intervertebral space measured in this newborn, both in the scan of the corpse and the virtual articulated model in ONP, is very similar to the baby giraffe physically dissected and skeletonized by Taylor and Wedel (Taylor & Wedel, 2013a) (24% intervertebral space in their specimen versus around 27% in TMM M-16050).

Different criteria have been applied in the definition of ONP for vertebrae since the concept was coined. The most widespread criterion is the maximum overlap between pre- and postzygapophyseal facets (Stevens &

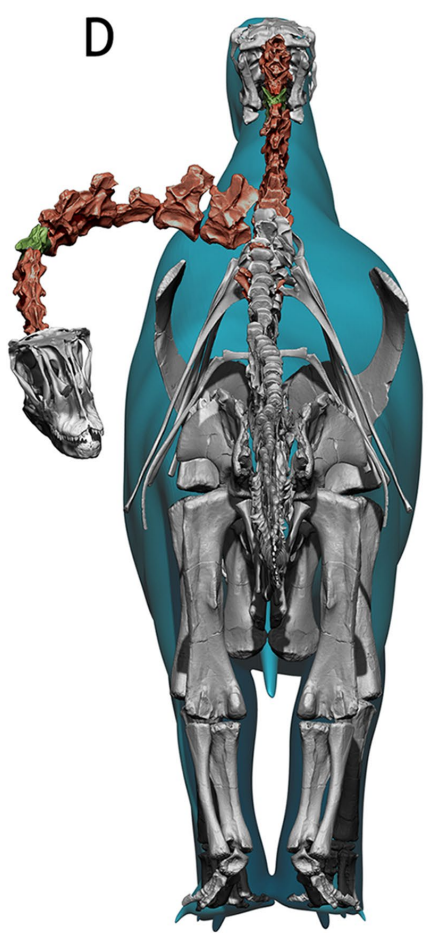
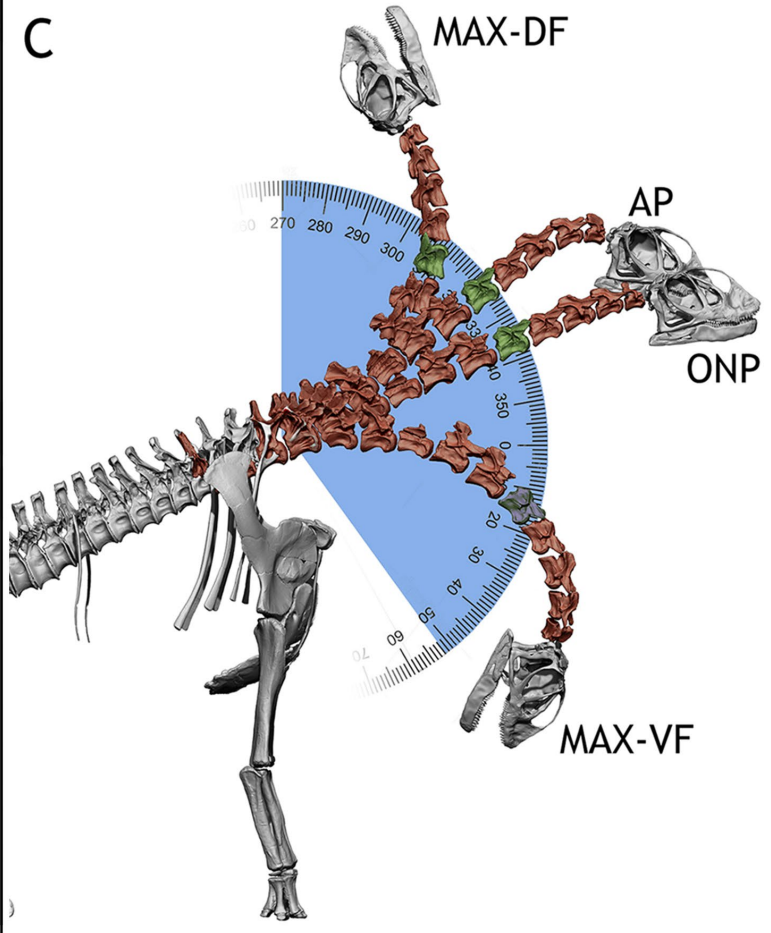
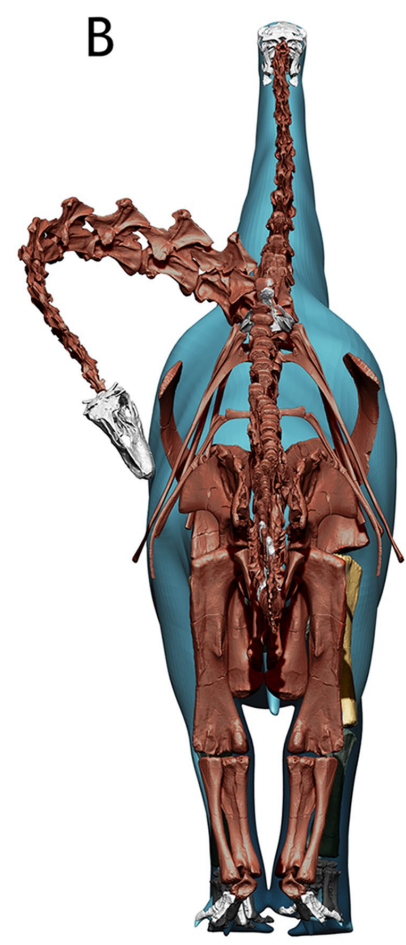
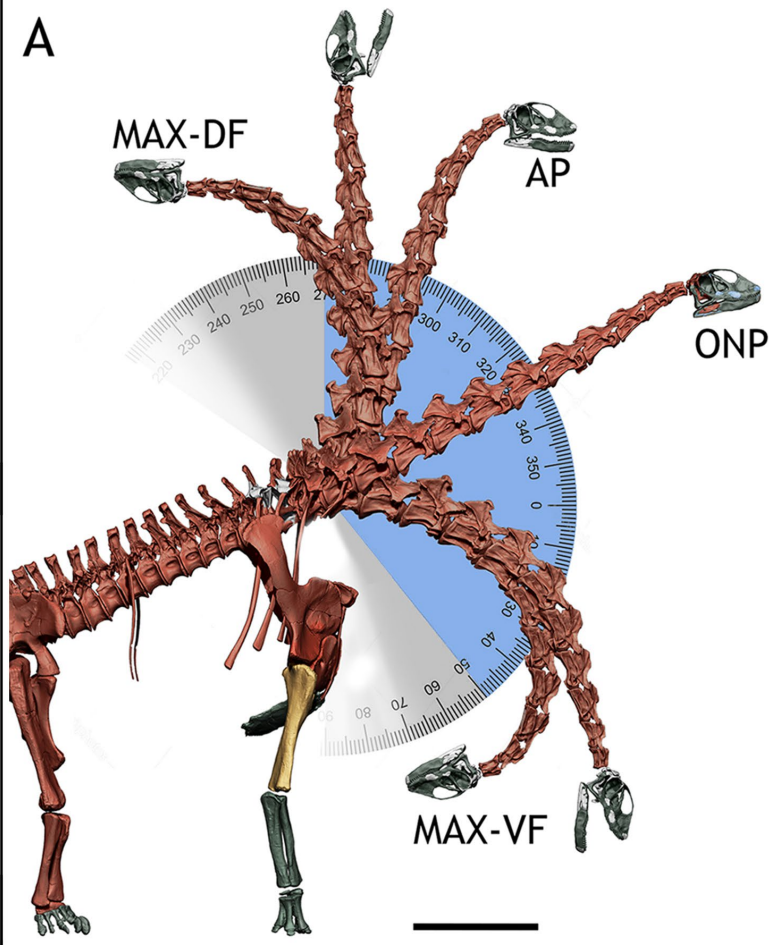


Figure 4.7 (previous page) - *Spinophorosaurus nigerensis* neck postures.

A - Several postures within the dorso-ventral osteological range of motion of the subadult *Spinophorosaurus*. Yellow indicates the arc described between maximum and minimum head heights. Grey indicates the arc described between maximum dorsiflexion and ventriflexion. **B** - Subadult *Spinophorosaurus* in posterior view, with the neck folded against the body. **C** - Several postures within the dorso-ventral osteological range of motion of the juvenile *Spinophorosaurus*. Yellow indicates the arc described between maximum and minimum head heights. Grey indicates the arc described between maximum dorsiflexion and ventriflexion. **D** - Juvenile *Spinophorosaurus* in posterior view, with the neck folded against the body. Max-DF = maximum dorsiflexion. Max-DR = maximum dorsal reach. AP = alert posture. ONP = osteologically neutral pose. Max-VR = maximum ventral reach. Max-VF = maximum ventriflexion.

Red bones = main specimen. White bones = hypothetical scaled elements (see methods). Green Bones = vertebrae modeled after the closest complete element. Yellow Bones = bones modeled after different sized specimens (see methods). Blue = flesh model.

Angles in degrees.

Parrish, 1999; Stevens, 2002, 2013; Dzemski & Christian, 2007; Taylor *et al.*, 2009; Mallison, 2010b). Some authors introduced as a criterion that the centra must also be in articulation (Christian, 2002; Stevens & Parrish, 2005; Carabajal *et al.*, 2014), but since the original definition of the concept did not include the centra in its criterion (Stevens & Parrish, 1999), a new term, NBOP, has been recently proposed (Paul, 2017) and since ONP and NBOP can render very different postures for the same neck (Fig. 4.3) we choose to consider them different criteria for assessing osteologically induced curvatures (OIC).

The usefulness of OIC (obtained by either ONP or NBOP) as something beyond establishing a standard for comparing different axial skeletons has been called into question (Dzemski & Christian, 2007; Taylor *et al.*, 2009; Mallison, 2010b). Our findings, however, show that ONP of the neck TMM M-16050 rendered an OIC in which the amount of intervertebral space is very similar to the one in the CT-Scan of that very specimen (27.03% in ONP vs. 27.27% in the CT-Scan of the articulated specimen). NBOP, however, rendered almost no intervertebral space (Fig. 4.3).

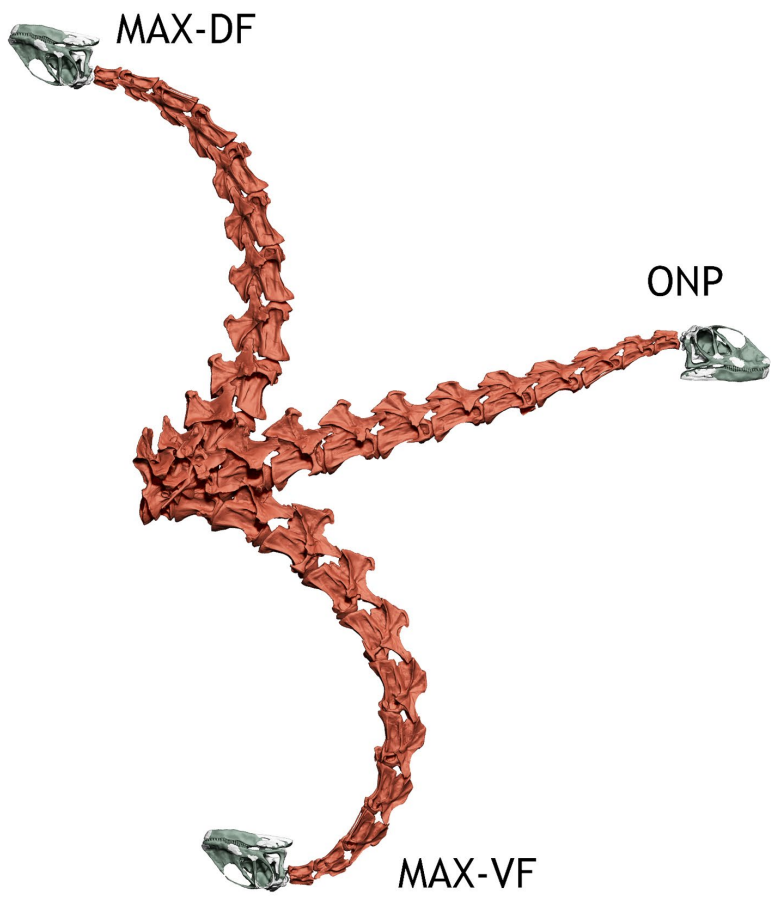
In the fossil specimens of *Spinophorosaurus*, ONP also has been able to predict the presence of intervertebral space in the articulated fossils: the juvenile specimen GCP-CV-BB-15 showed intervertebral space before being disarticulated for preparation, with the condyles barely around the outer rim of the cotyles (Fig. 4.6 A) This is similar to what can be seen in dromedary camel radiographs (Taylor & Wedel, 2013a) and skeletonizing corpses found in the Sahara desert (Fig. 4.6 E). ONP revealed the juvenile had around 12-16% out of the complete neck length intervertebral space, which is a relatively large amount. The articulated adult specimen of *Spinophorosaurus* showed the condyles nested inside the cotyles in all vertebrae (Fig. 4.6 C), and ONP revealed that, although there was up to 6% intervertebral space, the condyles are still nested inside the cotyles (Fig. 4.6 D).

However, the opisthotonic posture does not represent necessarily a habitual posture and is thought to be reached either by peri-mortem contractions [27] or by post-mortem events (Reisdorf & Wuttke, 2012). This, together with the desiccation of vertebrate remains during decay (Cambra-Moo, 2006) makes the intervertebral space observed in fossils likely smaller than *in vivo*. However, since both ONP and the articulated fossils opisthotonic pose reveal the juvenile *Spinophorosaurus* had greater intervertebral space than the adult specimen we can claim ONP is a good criterion to estimate the relative amount of intervertebral space. All in all, ONP is a close proxy to the cartilaginous neutral pose (CNP) proposed by Taylor (Taylor, 2014), since it can roughly predict the amount of intervertebral space.

Intervertebral Space and Range of Motion ontogenetic changes

As both extant giraffes and *Spinophorosaurus* have ontogenetic differences between the amount of intervertebral space and the range of motion in cervical vertebrae, heterochrony may explain both. Peramorphosis processes have been linked to the elongation of the neck in giraffes, particularly hypermorphosis (Hillis, 2011). Both acceleration and hypermorphosis have been proposed as an explanation for overall size increases in many dinosaurs as well as many of their positive allometries (McNamara, 2012). Hypermorphosis has been determined also as the main cause for cervical vertebrae elongation in prolacertiform reptiles (Tschanz, 1988). The amount of intervertebral space and the ossification body observed anterior to the vertebral body condyles

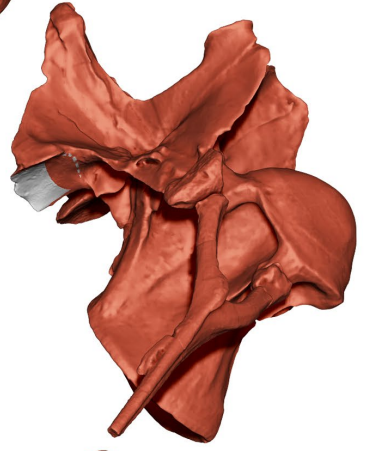
A



C



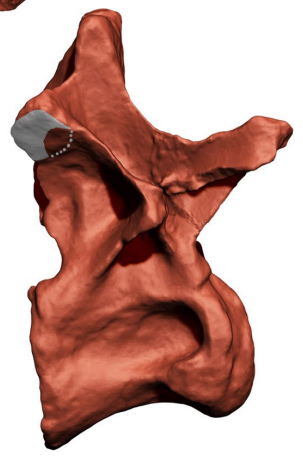
D



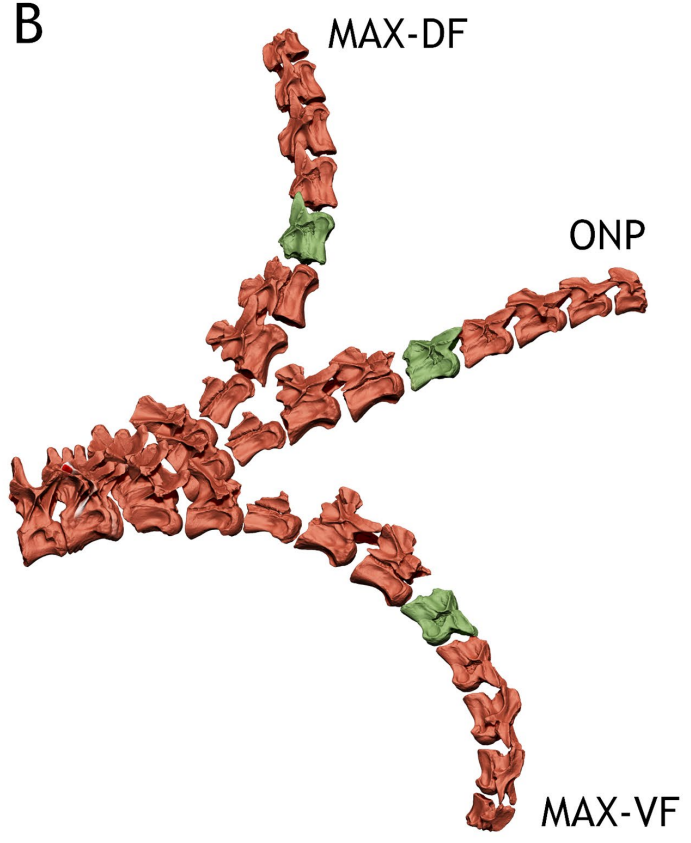
E



F

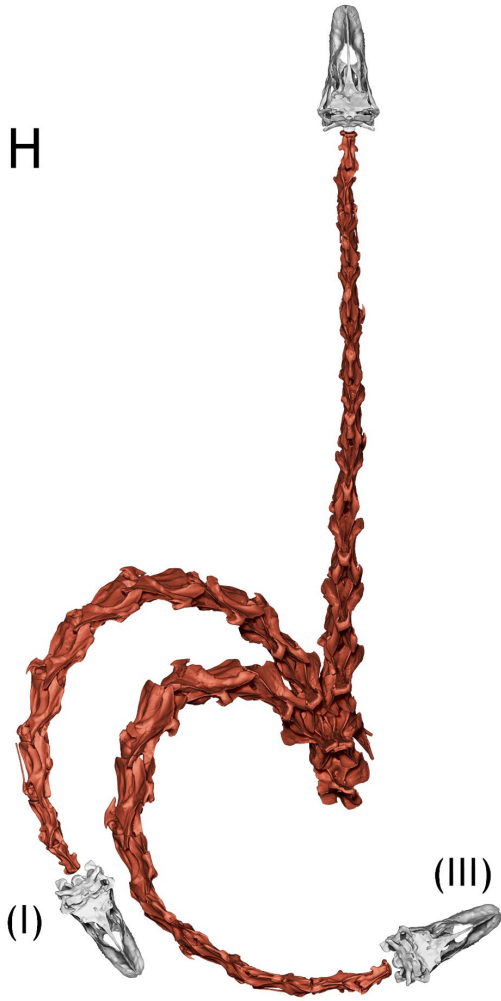


B



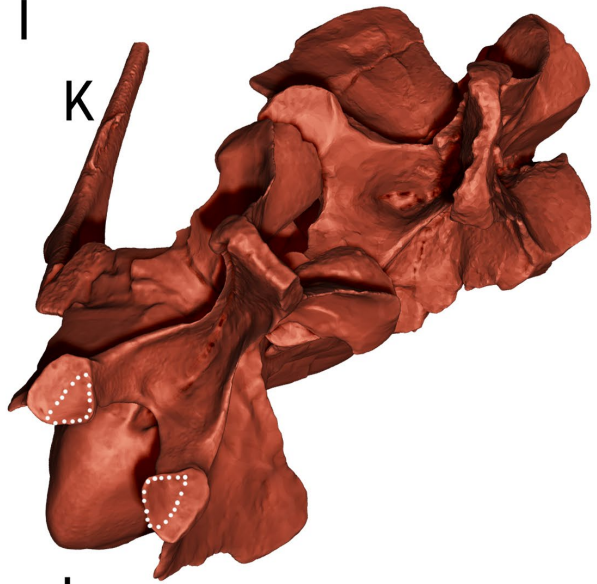
G

H

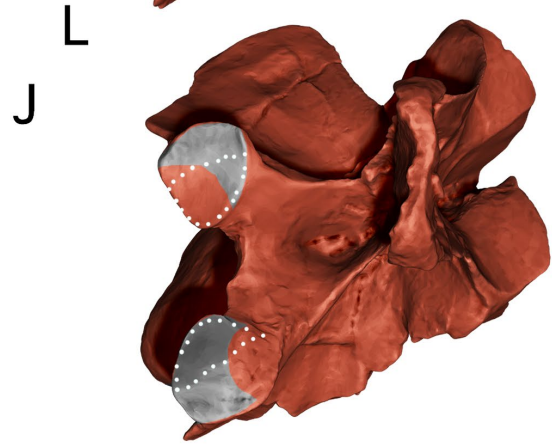


I

K

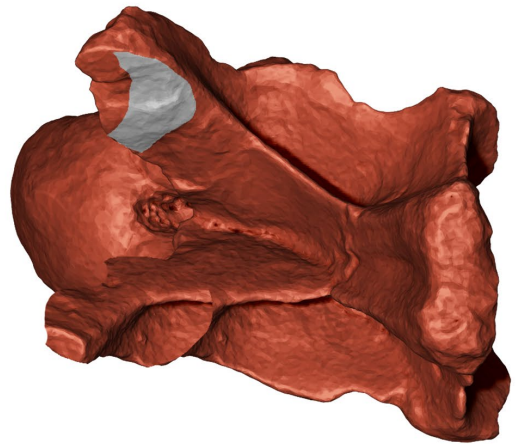
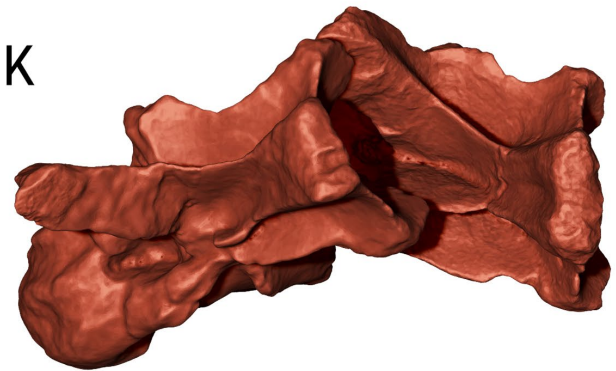


L



K

L



H

ONP



Figure 4.8 (previous page) - *Spinophorosaurus nigerensis* neck osteological range of motion.

A - Dorso-ventral osteological range of motion of the subadult *Spinophorosaurus* in lateral view. **B** - Dorso-ventral osteological range of motion of the juvenile *Spinophorosaurus* in lateral view. **C** - DV1-CV12 joint of the subadult *Spinophorosaurus* in maximum dorsiflexion (Max-DF) in lateral view. **D** - CV12 of the subadult *Spinophorosaurus* in lateral view showing how much of the postzygapophysis overlaps with the prezygapophysis of DV1 in maximum dorsiflexion (in red, zygapophyseal overlap, in gray non overlapped area of the facet). **E** - DV1-CV12 joint of the juvenile *Spinophorosaurus* in maximum dorsiflexion (Max-DF) in lateral view. **F** - CV12 of the juvenile *Spinophorosaurus* in lateral view showing how much of the postzygapophysis overlaps with the prezygapophysis of DV1 in maximum dorsiflexion (in red, zygapophyseal overlap, in gray non overlapped area of the facet). **G** - Lateral osteological range of motion of the subadult *Spinophorosaurus* in dorsal view. **H** - Lateral osteological range of motion of the juvenile *Spinophorosaurus*. **I** - D1-CV12 joint of the subadult *Spinophorosaurus* in maximum lateral flexion (III) in dorsal view (dots indicate estimated region of the prezygapophyseal facet). **J** - DV1 of the subadult *Spinophorosaurus* in dorsal view showing how much of the prezygapophysis overlaps with the postzygapophysis of CV12 in maximum dorsiflexion (in red, zygapophyseal overlap, in gray non overlapped area of the facet, dots indicate estimated region of the prezygapophyseal facet). **K** - DV1-CV12 joint of the juvenile *Spinophorosaurus* in maximum lateral flexion (III) in dorsal view. **L** - DV1 of the juvenile *Spinophorosaurus* in dorsal view showing how much of the prezygapophysis overlaps with the postzygapophysis of CV12 in maximum dorsiflexion (in red, zygapophyseal overlap, in gray non overlapped area of the facet).

Max-DF = maximum dorsiflexion. ONP = osteologically neutral pose. Max-VF = maximum ventriflexion. I = lateral flexion attained when maintaining one zygapophyseal pair in full articulation and deflecting the other pair anteriorly. III = maximum lateral flexion.

Red bones = main specimen. White bones = extrapolated elements (see methods). Green Bones = vertebrae modeled after the closest complete element.

of the newborn giraffe (Fig. 4.2 F-H) appears to be part of the process of hypermorphosis for vertebral elongation in this taxon. Moreover, it would be possible that dromedary camels, which retain large intervertebral spaces in adulthood (Taylor & Wedel, 2013a), might have them due a pedomorphic process. Regarding *Spinophorosaurus*, the small sample and therefore not knowing accurately the ontogeny of this taxon is a caveat when testing this hypothesis. However, the elongation index in the subadult *Spinophorosaurus* is slightly larger than other non-Neosauropoda Eusauropoda (Remes *et al.*, 2009) (with the exception of Mamenchisauridae), that it is also greater than in the juvenile specimen and that the biggest difference on the sizes of the individual bones between the holotype and the paratype are found among the cervical vertebrae (while the cervicals in the paratype are larger, the ilium and preserved caudal vertebrae of the paratype are about the same size as in the holotype). This suggests hypermorphosis as the most likely explanation, although more specimens in different ontogenetic stages would be needed to further test the hypothesis.

However, the size and shape of the prezygapophyseal facets, which also determine the amount of range of motion in the neck, does not fit into the heterochronic hypothesis in both giraffes and *Spinophorosaurus*. The more elongated a prezygapophyseal facet, the more deflection can be attained before there is no pre-postzygapophyseal overlap. Given this, sauropods with more elongated prezygapophyseal facets have been shown to have greater ranges of motion per joint than those with shorter and wider than long prezygapophyseal facets (Stevens & Parrish, 1999; Taylor & Wedel, 2016). The giraffe and *Spinophorosaurus* have longer than wide prezygapophyseal facets, and this reflects on a relatively large range of motion per joint (Figs. 5 and 8). Although the range of motion is greater in grown than in juvenile specimens, the proportions on the prezygapophyseal facets do not drastically change during ontogeny in *Giraffa* or *Spinophorosaurus*. This implies that other factors, such as the distance between the center of rotation of the vertebra and the zygapophyseal facets (Stevens, 2013), have a bigger impact in the differences observed between juveniles and adults of both species. Since that relative distance decreases with vertebral elongation in both species (the prezygapophyses are relatively closer to the center of rotation due to vertebral elongation), vertebrate elongation has a direct impact in the increase in range of motion during ontogeny for these taxa.

Potential implications for sauropod dinosaurs paleobiology

From a functional morphology point of view, the observed differences in posture and range of motion between newborn and adult giraffes are compatible with ethological differences observed in wild populations. Giraffes exhibit a wide range of behaviors regarding their necks in the wild (Dagg, 1962). By comparing giraffe wild behavior and postures obtained with the osteological range of motion analyses, we can assess whether disarticulating vertebrae, the limits set for most osteological ROM analyses, is or not necessary to achieve certain extreme live postures. Whether range of motion may have been greater than the actual bone geometry suggests (Taylor *et al.*, 2009) has tremendous implications for range of motion analyses in extinct taxa. If the

proposed ROM limits would not allow positioning a skeleton of an extant vertebrate in postures adopted *in vivo*, they would be refuted and new limits for osteological ROM analyses would need to be proposed.

On the contrary, if even the most extreme postures fall within the limits of bone-bone articulation in live extant taxa, current limits of such analyses can still be used as a first approximation of motion capabilities for fossil vertebrates (which can be then contrasted against further analyses or fossil evidence). Also, it allows setting a comparative framework with standards for ONP and ROM limits, which help when comparing different taxa.

We have analyzed the following behaviors in giraffes:

(1) Alert Posture. Giraffes are known for their steep necks: adult giraffes (male and female) usually hold their necks in 50°-60° angles when standing alert, while newborns hold them at 70° (Dagg, 1962). Curiously, the 50-60° angles attained by the adults are a combination of a 20° dorsally sloping dorsal vertebrae series (Dagg, 1962), a dorsally deflected neck in ONP (Christian & Dzemski, 2007; Stevens, 2013; Paul, 2017) (Fig. 4.4 A, ONP) and a slight dorsiflexion at the posterior end of the neck (Christian & Dzemski, 2007; Taylor *et al.*, 2009) (Fig. 4.4 A, AP). Juvenile giraffes, however, show barely no sloping on their dorsal vertebrae (Dagg, 1962) (Fig 4C), and they attain the 70° angle by a combination of OIC (Fig. 4.4 C, ONP) and dorsiflexion of their necks (Dagg, 1962). Since the ONPs of other long-necked vertebrates have been proven to be lower than their resting, alert poses (Christian & Dzemski, 2007; Taylor *et al.*, 2009) it is conceivable that the same was true for sauropods (Christian, 2002, 2010; Taylor *et al.*, 2009; Mallison, 2010b; Paul, 2017). For both *Spinophorosaurus* specimens, the reconstructed alert pose (Fig. 4.7, AP) was obtained by maximum dorsiflexion at the posteriormost cervical vertebrae CV12-CV10 and ventriflexion at CV4-CV3-axis and the skull, with the CV9-CV5 portion of the neck in ONP. This follows what has been documented for extant tetrapods, in which the base of the neck is fully dorsiflexed, anteriormost vertebrae and skull dorsiflexed and middle neck in ONP (Taylor *et al.*, 2009).

With the same configuration for the presacral vertebral deflection described above, the alert pose has a higher angle in the subadult *Spinophorosaurus* (Fig 7). This is due the adult has a larger range of motion in the posteriormost cervical vertebrae (Table 4.2) and a more dorsally deflected neck in ONP than the juvenile. However, most of the post-cervical skeleton used as a proxy for the juvenile specimen is just an isometrically scaled down version of the subadult skeleton. This means the sloping of the dorsal vertebrae and the forelimb might have been different than those from the subadult, and therefore the alert pose of the juvenile might have been somewhat, but not remarkably, higher or lower. Nevertheless, the amount of dorsiflexion at the base of the neck of the juvenile is smaller than that of the adult. Therefore, a hypothetical scenario with a higher alert pose for the juvenile would require either (i) dorsiflexion on more cervical vertebrae or (ii) more sloping of the dorsal vertebrae and forelimbs relatively longer than in the adult, a less likely scenario since no drastic ontogenetic allometry has been reported for sauropod anatomy beyond neck elongation (Sander *et al.*, 2011).

(2) Feeding height capabilities. In the wild, adult male and female giraffes tend to feed at the most optimum feeding rate, at around 60% of their top feeding height (Young & Isbell, 1991). Nevertheless, different feeding behaviors are reported: grazing at ground level (adopting the same splaying pose as for drinking) or browsing lower than shoulder-height is reported from females with calves in more open areas (Young & Isbell, 1991), and extreme high browsing, with the neck and head almost vertical, is reported from males in open areas (Young & Isbell, 1991). The long neck of the giraffe therefore enables them to have versatile feeding behaviors, which account for a great deal of the amount of dorso-ventral osteological range of motion. All feeding postures reported in wild giraffes fall within the osteological range of motion for both the adult and newborn specimen (Figs. 4-5).

While there is little information regarding the feeding ecology of sauropod dinosaurs, the range of motion of *Spinophorosaurus* potentially enabled them to browse at the same positions as giraffes (Fig. 4.7). Previous studies have reported lower ranges of motion and/or low/ground browsing in several taxa from multiple lines of evidence (*Cetiosaurus* (Martin, 1987), *Apatosaurus* (Stevens & Parrish, 1999; Whitlock, 2011a), *Diplodocus* (Stevens & Parrish, 1999; Whitlock, 2011a), *Nigersaurus* (Serenó *et al.*, 2007; Whitlock, 2011a)). Basal sauropodomorph *Plateosaurus*, while not interpreted as a low browser, has also a smaller range of motion in the cervical vertebrae than *Spinophorosaurus* (Mallison, 2010b). Few sauropods have been interpreted as high browsers (Brachiosauridae (Christian, 2002; Stevens & Parrish, 2005; Christian & Dzemski, 2007; Paul, 2017), *Euhelopus* (Christian, 2010)). *Spinophorosaurus* shares more similarities with the taxa interpreted as high browsers, such as broad teeth crowns (Remes *et al.*, 2009), a narrow snout or a relatively

long humerus in relation to the scapula (Remes *et al.*, 2009). While a more detailed analysis on teeth wear will shed more light into the feeding ecology of *Spinophorosaurus*, its postcranial anatomy is compatible with high browsing, being the earliest basally branching sauropod known to have such capability. It must be noted, however, that despite having an overall range of motion similar to the giraffe, the inter-vertebral flexibility of the sauropod is much lower. *Spinophorosaurus* achieves the same overall range of motion of the whole neck by having almost twice the cervical vertebrae the giraffe has (Table 4.2).

- (3) Drinking. While the neck length of the adult giraffe does not allow the muzzle to reach the ground just by ventriflexion, it allows the head to reach a little past the wrist (Fig. 4.4 A). On the other hand, the neck of the newborn has a length and range of motion that barely allow the muzzle to pass beyond the elbow (Fig. 4.4 C). It is known that giraffes engage in complex splaying or flexing behaviors while drinking or grazing (Seeber *et al.*, 2012b; Seeber, Ciofolo, & Ganswindt, 2012a) in order to reach the ground due their necks are shorter than their forelimbs (Dagg, 1971; Solounias, 1999). Newborn giraffes, however, do not drink water in the wild (Horwich *et al.*, 1983), likely due to the fact their neck is too short to reach the ground, even splaying the legs and flexing the carpus, and that they are breastfeeding.

Both specimens of *Spinophorosaurus* cannot reach the ground just by ventriflexion of the neck (Fig. 4.7), and if they needed to actively drink water at or lower than ground level, they would have needed to either flex their elbows or to abduct the shoulders in a fashion similar to giraffe splaying. Since *Spinophorosaurus* did not preserve forearm elements, it is impossible to test whether elbow flexion, shoulder abduction or a combination of both would be a more likely way to help the head reach the ground. However, the ossified dermal elements of the pectoral girdle have been proposed as providing more stability during certain movements (Tschopp & Mateus, 2013), and the distal expansion of the scapula indicate a larger insertion area for the deltoids (Remes, 2007), which would actively participate in shoulder abduction. The ossified clavicles are also an origin for the deltoid muscles (Remes, 2007), and the ossified interclavicle is partially the origin of the pectoral musculature (Remes, 2007) (which also originates at the sternal plates, not recovered for any preserved *Spinophorosaurus* specimen yet). All this suggests that abduction-adduction may have been carried out with more stability by this taxon than in sauropods without distal expansion of the scapula and/or ossified dermal elements of the pectoral girdle. However, a detailed analysis of the pectoral muscles and forelimb functional morphology is beyond the scope of this paper.

- (4) Lateral movement of the neck. Giraffes are known to sleep with their neck folded against the body and can also be observed scratching and cleaning their torsos with their mouths by folding the neck against the body. This type of movement had been claimed to disarticulate some cervical vertebrae due to the extreme lateral flexion of the posteriormost cervical vertebrae (Stevens & Parrish, 2005; Taylor & Wedel, 2013a). However, the range of motion analyses shows the postures are attainable in both the adult and juvenile specimens (Fig. 4.4) without completely disarticulating the neck, although with little zygapophyseal overlap left (Fig. 4.5). This implies that, at least in giraffes, it is not necessary to disarticulate cervical vertebrae in order to achieve their most extreme postures.

Both the adult and juvenile *Spinophorosaurus* can also attain the same extreme neck posture without disarticulating the cervical vertebrae (Figs. 7-8). However, unlike giraffes, many sauropods, including *Spinophorosaurus*, had long ossified and overlapping cervical ribs (Klein, Christian, & Sander, 2012). While the elongated cervical ribs have been claimed as a reason for highly immobile necks in sauropods and other tetrapods (Tschanz, 1988; Martin *et al.*, 1998), the elongated, overlapping chevrons, postzygapophyses and ossified tendons of dromaeosaur theropod tails seem to allow considerable motion of the tail (Persons & Currie, 2012). Nevertheless, it is likely that the ossified and overlapping cervical ribs had an impact on the motion capabilities of sauropod necks. Albeit how much impact on motion they would pose is still unknown and beyond the scope of this paper, the case of dromaeosaur tails suggests it would be less than previous studies proposed. In *Spinophorosaurus*, the only cervical vertebrae not affected by cervical rib overlap would be CV12, which has an extremely short cervical rib and, to a lesser extent, CV11 whose cervical rib does not really overlap with that of CV12.

Whether folding the neck against the body was possible or not for *Spinophorosaurus* due the cervical ribs, the zygapophyseal overlap in the posteriormost cervicals is comparable to that of a giraffe (Figs. 5,8), and the posture would be attainable under the same criteria. The study of the effect of the cervical ribs in the range of motion in sauropod necks is still needed in order to assess whether neck folding was possible in *Spinophorosaurus*, and consequently in other sauropods with elongated cervical ribs.

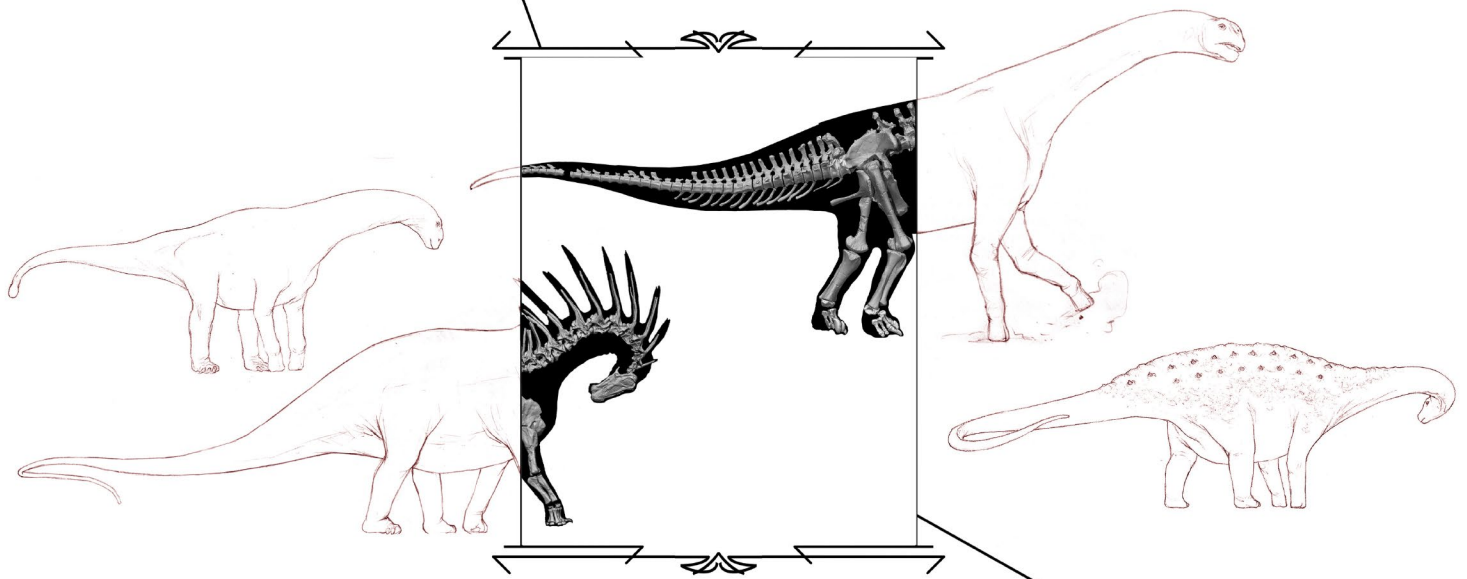
4.6 - CONCLUSIONS

1. Applying the ONP criterion for articulating cervical series predicts the amount of intervertebral space in the newborn *Giraffa* with 0.24% difference from the actual bones articulated with tissue, as well as the presence of large intervertebral space in the juvenile *Spinophorosaurus* and smaller spaces in the subadult (both observable in the articulated skeletons before preparation). Therefore ONP appears to be a reliable method to grossly estimate the amount of intervertebral space in *Spinophorosaurus* and possibly other extinct taxa. However, a more extensive sample is needed both to confirm the last statement and to make finer, more precise estimations of intervertebral space. Hypothesis (i), "osteology alone does not allow to estimate the amount of intervertebral space," can be refuted, at least for giraffes and *Spinophorosaurus*. Hypothesis (iii), "the amount of intervertebral space diminishes with ontogenetic development," is compatible with the data from this study, so it could not be refuted.
2. All reported neck postures attained by live giraffes in the wild can be replicated with the virtual skeleton range of motion without disarticulating the cervical vertebrae, therefore the cervical range of motion of extinct vertebrates should follow the same criteria until evidence suggests otherwise. Hypothesis (ii) "some neck postures attained in life require disarticulating vertebrae", can be refuted.
3. Both *Giraffa* and *Spinophorosaurus* increase the amount of osteological range of motion of their necks throughout ontogeny due to the elongation of the neck, which causes the relative distance between pre-postzygapophyses and vertebral centra to reduce. Hypothesis (iv), "the neck range of motion increases with ontogenetic development", is compatible with the data from this study, so it could not be refuted.
4. *Giraffa* have generally more flexibility per vertebra pair than *Spinophorosaurus* in all specimens.
5. The differences in osteological range of motion observed between grown and juveniles of both *Giraffa* and *Spinophorosaurus* are a product of neck elongation and the morphological changes suffered by elongating the cervical vertebrae.
6. The osteological range of motion of the subadult *Spinophorosaurus* is larger than the sauropodomorph *Plateosaurus*, as well as that of previously analyzed sauropods, enabling its neck to engage in many different postures unattainable by other sauropods.
7. *Spinophorosaurus* is the most basally branching sauropod to date to have evidence of capabilities for high browsing

Figure 4.9 (next page) - Paleoartistic reconstruction of juvenile *Spinophorosaurus nigerensis* by Diego Cobo.

The reconstruction has been carried out with a 3D render of the virtual skeleton in lateral view underneath to nail down the proportions. The neck has been posed in the alert pose proposed by Taylor *et al.* (2009) depicted in Fig. 4.7. Volumes are based on the full body volumetric reconstruction shown in the adult specimen (Fig. 3.17). Human scale = 1700 mm.





CHAPTER
• 5 •

**THE EVOLUTION OF BIOMECHANICAL
CAPABILITIES IN SAUROPODA**

Introduction.....	147
Morphological characters with functional implications.....	147
Systematic paleontology of personally reviewed taxa.....	163
Phylogenetic analysis and character optimization.....	202
Discussion.....	205
Conclusions.....	208

5.1 INTRODUCTION

Sauropod classification and systematics were problematic for a long time until the advent of phylogenetic systematics in paleontology. Since the publication of the first cladistic analysis focused on sauropod dinosaur evolution (Russell & Zheng, 1993) plenty of analyses have been carried out using a multitude of datasets (i.e. Upchurch, 1995; Wilson & Sereno, 1998; Wilson, 2002; Upchurch *et al.*, 2004; Mannion *et al.*, 2013). Although some analyses have focused on particular clades of Sauropoda, such as Diplodocidae (Tschopp *et al.*, 2015) or Titanosauria (Curry Rogers, 2005), the majority have included a taxon sample consisting of an outgroup Sauropoda and representatives of all major sauropod clades.

Despite all these advances, sauropod phylogenies still suffer from unstable tree topologies for the large majority of analyses, with low supports for the majority of nodes, particularly in those less inclusive. Nevertheless, a relatively high number of clades are commonly retrieved by independent analyses using different datasets.

Although a large number of morphology-based characters used in phylogenies have been described and their variability among different taxa has been discussed (i.e. Upchurch, 1995; Wilson & Sereno, 1998; Wilson, 2002; Tschopp *et al.*, 2015), their potential functional implications regarding motion capabilities, myology or biomechanical capabilities have yet to be discussed in depth. This analysis can be interesting, since using characters with potential functional implications (which in turn may have been under selective pressure) may have two potential effects: (i) if the number of characters with morphofunctional implications is high, some nodes may constitute convergence-based aggrupations, not actual clades, and (ii) if those aggrupations are true clades (supported by additional synapomorphies, without strong functional implications), synapomorphies with strong functional implications may be potential key innovations if they coincide with cladogenesis events.

Here, the postcranial characters in the matrix of Carballido *et al.* (2017) with potential functional implications have been reviewed attending to establishing what functional differences may exist between the existing character states. A selection of sauropod taxa (some represented by several specimens) representing the majority of well-established clades have been digitized and some of the analyses performed in *Spinophorosaurus* have been replicated to some extent to compare what differences may render different character states on the same motion, muscle size or lever. Finally, a modified version of Carballido *et al.* (2017) matrix has been analyzed, and the characters with potential functional implications mapped on the strict consensus to evaluate potential functional modules, key innovations and whether their evolution may have occurred in a stepwise manner or not.

5.2 MORPHOLOGICAL CHARACTERS WITH FUNCTIONAL IMPLICATIONS

The following characters of the Carballido *et al.* (2017) data matrix have been found linked to potential differences in range of motion, muscle inferred cross-sections or lines of action. The characters follow the same numeration than on their character list. Although characters related to pneumaticity may have had very relevant mechanical implications in the sauropod body plan (Wedel, 2003a,b) they are beyond the scope of this analysis. Some new characters, based on what has been learned in the functional analysis of *Spinophorosaurus* in chapters 3 and 4 are proposed and included in the matrix. The original characters have been quoted literally, so there may be slight differences in anatomical nomenclature (i.e. cranio-caudal instead of antero-posterior).

Cervical Vertebrae

119 - Cervical vertebrae, number: 10 or fewer (0); 12 (1); 13-14 (2); 15 (3); 16 or more (4)

A larger amount of joints will increase the range of motion by adding any number of given degrees per added joint. How the range of motion increases, however, cannot be only explained by the number of cervical vertebrae, as other factors come into account (zygapophyseal facets shape, size, orientation, neural spine height...) as will be discussed below.

123 - Cervical centra, articulations: amphicoelous (0); opisthocoelous (1).

A ball and socket type of centrum (either procoelous or opisthocoelous) renders a greater amount of range of motion per joint than a platycoelous or amphicoelous centrum joint, particularly in lateral

flexion and ventriflexion. This is due no centra-centra osteological stops can happen in these joints.

125 - Cervical centra, midline keels on ventral surface: prominent and plate-like (0); reduced to low ridges or absent (1).

Midline keels on the ventral surface of cervical vertebrae are likely both origins and insertions of craniocervical musculature of the Iliocostalis/*M. longus* group. The presence of prominent keels indicates greater surface area for these origins and insertions, suggesting larger cross-sections and anchor points. Also, developed keels also provide a larger moment arm for neck ventriflexion. The absence of keels, on the other hand, may either mean a migration of several muscle groups as suggested for theropods (Snively & Russell, 2007a) or less developed muscles. One of the caveats of this character as it is written is that keels may be present on a sector or sectors of the neck (anteriormost vertebrae only, for example).

128 - Cervical vertebrae, well developed epiphyses: absent (0); present (1).

Epiphyses (Fig. 5.1 B, D) are insertion for *M. longus colli dorsalis*, as well as origin for *M. transversospinalis capitis lateralis*, both muscles with an important role in neck dorsiflexion and stabilization (Snively & Russell, 2007a). The absence of epiphyses (Fig. 5.1 C) implies those muscles might have been less developed, and it may be correlated with less developed insertions/origins (i.e. less developed scars on the squamosal for the insertion of *M. transversospinalis capitis lateralis*).

129 - Cervical vertebrae, epiphyses shape: stout, pillar like expansions above postzygapophyses (0); posteriorly projecting prongs (1).

The morphology of the epiphyses may be well related with the preferential vector of forces exerted by *M. longus colli dorsalis*. Given that the orientation and length of processes of the vertebrae are determined by the resultant force acting upon the vertebral centrum (Kardong, 2012), the stout pillar like epiphyses may indicate a resultant force with a dominant dorso-ventral component, while posteriorly projecting prongs may imply a dominant antero-posteriorly force.

The morphology, size, orientation and even presence of epiphyses changes thorough the neck of a single individual. This may be used to determine whether a neck had regions that experienced different movements regarding *M. longus colli dorsalis* contraction.

130 - Prezygapophyses, anterior process (pre-epiphyses) suited ventrolaterally to the articular surface: absent (0); present (1).

Pre-epiphyses are only present in some sauropods (Fig. 5.1 B, D); at one point, they were even thought to be an autapomorphy for the sauropod *Jobaria* (Sereno *et al.*, 1999). Since they are anterior projections of the PRDL, they may increase the area of origin for *M. intertransversarii*, implying a greater development of this muscle.

137 - Anterior cervical vertebrae, prespinal lamina: absent (0); present (1).

Prespinal laminae may be an osteological correlate for interspinous ligaments, with the most potential correlates the interspinous septum or the elastic ligament (Tsuihiji, 2005; Schwarz *et al.*, 2007b). The ossification of the proximal parts of the ligaments may indicate a greater role of these in supporting the axial skeleton due to a reduction of epaxial musculature.

138 - Anterior cervical vertebrae, neural spine shape: single (0); bifid (1).

Although known to be a homoplastic characteristic, the appearance of a bifid neural spine in cervical vertebrae has very interesting functional implications regarding the ligamentous system of the neck, as well as the muscles with origins and insertions on the neural spine. The nuchal ligament is known not to bifurcate and remain attached to each metapophysis, but to remain in the midline, sometimes leaving an ossified notch between both metapophyses (Schwarz *et al.*, 2007b). Regarding the musculature, *M. transversospinus capitis* originates on the sides and top of the neural spines, inserting onto the nuchal crest. The more separated the metapophyses are from the midline, the greater the angulation between the muscle and the nuchal crest. This creates a more efficient line of action for lateral flexion of the head on unilateral flexion of said muscle.

139 - Mid and posterior cervical vertebrae, prespinal lamina: absent (0); present (1).

As for 137.

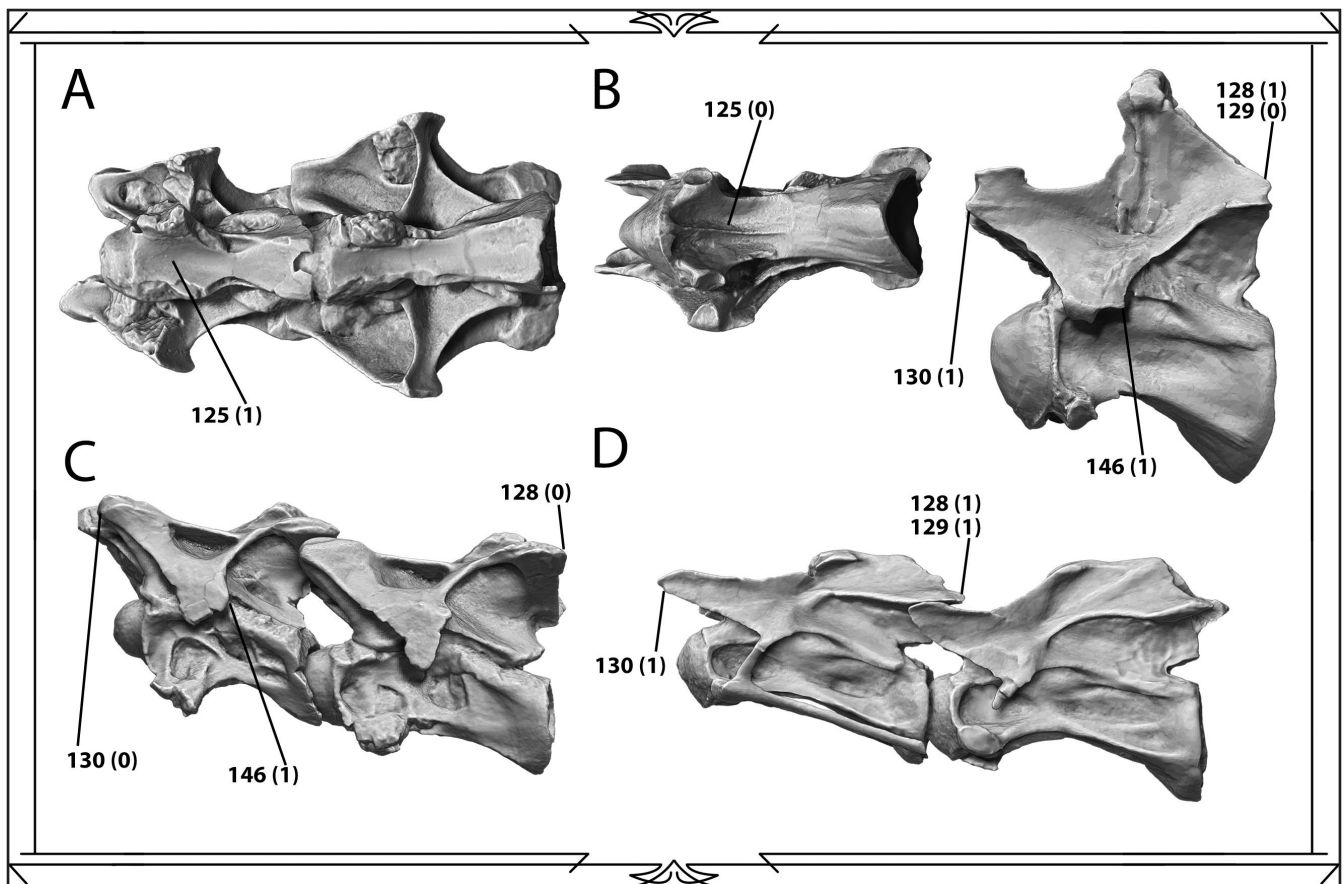


Figure 5.1 - Character states for sauropod cervical vertebrae.

A - Articulated cervical vertebrae 5 and 6 of *Camarasaurus grandis* (YPM 1905) in ventral view. **B** - Cervical vertebra 10 of *Spinophorosaurus nigerensis* (GCP-CV-4229) in ventral (left) and lateral (right) view. **C** - Articulated cervical vertebrae 5 and 6 of *Camarasaurus grandis* (YPM 1905) in lateral view. **D** - Articulated cervical vertebrae 4 and 5 of *Spinophorosaurus nigerensis* (GCP-CV-4229) in lateral view. Arrows point at anatomical features (character) with the character state between parentheses.

141 - Middle, cervical vertebrae, height of the neural arch: less than the height of the posterior articular surface (0); higher than the height of the posterior articular surface (1).

Higher neural arches have several implications regarding osteological range of motion and/or leverage for muscle contraction. However, neural arch height can vary depending on different ways, and therefore have different functional implications. If the neural arch becomes higher due the pedicels are dorso-ventrally elongated, the distance between the vertebral centrum and the pre-postzygapophyseal articulation increases. The further the zygapophyses are from the centrum (center of rotation), the smaller the range of motion. If the neural spine is elongated and thus increases neural arch overall height, it implies a larger leverage for muscles inserting or originating on the neural spine. It also implies also larger attachment for interspinal ligaments (Schwarz *et al.*, 2007b). Splitting the character (elongated pedicels and elongated neural spines) may provide additional resolution to phylogenetic analyses.

142 - Middle cervical centrum, anteroposterior length divided the height of the posterior articular surface: less than 4 (0); more than 4 (1).

This character measures vertebral centrum elongation. As commented on character 121, the length of cervical centra on the one hand makes overall neck length greater, with the advantage and disadvantages associated (i.e. reaching further from the body vs. pumping blood to the brain). However, additional characters may derive from elongating the centrum, such as larger insertions for craniocervical muscles originating or inserting onto the ventral surface of the centrum or keel.

145 - Middle and posterior cervical vertebrae, articular surface of zygapophyses: flat (0); transversally convex (1).

The shape of the zygapophyseal facets in anterior view may have important range of motion consequences, particularly regarding torsion. It is known that in extant crocodiles, the vertically oriented pre-postzygapophyseal articulations in the transverse plane does not affect dorso-ventral or lateral flexion, but has an important role in blocking torsion (Mallison *et al.*, 2015). The same effect can be

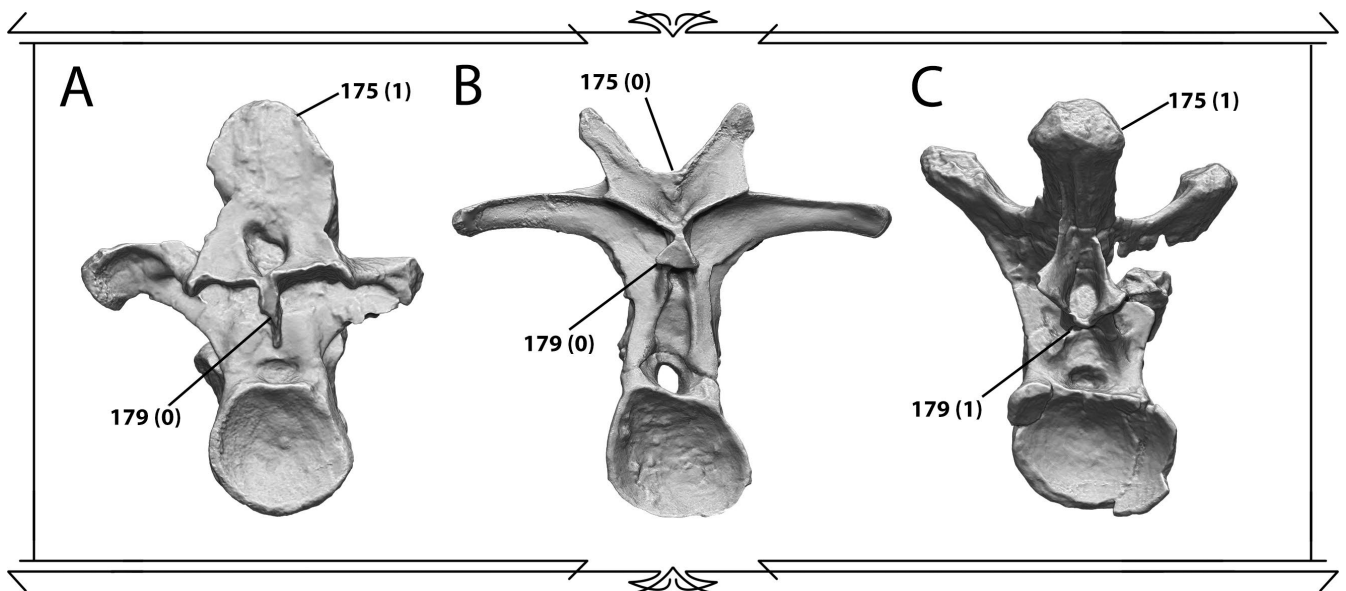


Figure 5.2 - Character states for sauropod dorsal vertebrae.

A - Middle dorsal vertebra of *Patagosaurus fariasi* (MACN-CH-436) in posterior view. **B** - Middle dorsal vertebra of *Camarasaurus grandis* (YPM-1901) in posterior view. **C** - Middle dorsal vertebra of *Neuquensaurus australis* (MCS-5) in posterior view. Arrows point at anatomical features (character) with the character state between parentheses. Vertebrae scaled to same overall height.

replicated with transversally convex zygapophyseal facets in the neck of sauropod dinosaurs: those with flat zygapophyses have no osteological restrictions to torsion, while those with convex zygapophyses have an osteological stop.

146 - Middle and posterior cervical vertebrae, prominent triangular flange on posterior edge of the diapophyseal process (in the PODL): absent (0); present (1).

This triangular posterior flange in the PODL had been proposed to be a synapomorphy of *Spinophorosaurus nigerensis* but is currently known to be more widespread among sauropods. Since *M. intertransversarii* inserts on the PODL, the triangular flange may indicate on the one hand an osteological correlate, and on the other an indication of a strong activity of this muscle.

147 - Middle cervical vertebrae, prezygapophyses position: do not extend beyond the anterior margin of the centrum (0); extends beyond the anterior margin of the centrum (1).

As commented on character 141, the distance between the zygapophyses and has an impact on the amount of range of motion given the same zygapophyseal facet shape. Extending the prezygapophyses beyond the anterior margin of the centrum also increases this distance, therefore, the further the prezygapophyses are from the centrum, the less range of motion on that joint.

150 - Posterior cervical vertebrae, neural spine shape: not expanded distally (0); expanded but not as much as the width of the centrum (1); laterally expanded, being equal or wider than the vertebral centrum (2).

The expansion of the neural spine in the latero-medial plane can have a role similar to that of the metapophyses on bifurcated vertebrae by separating the origin of *M. transversospinus capitis* from the midline, creating more angulation between the muscle origin and its insertion on the nuchal crest. In addition, this expansion creates more area for origin and/or insertion for the *Mm. intercostales*, suggesting a larger size for this muscle. It may be possible that sauropods with large, distally expanded neural spines may have had reduced epipophyses, implying that *Mm. intercostales* contraction had a larger role on neck dorsiflexion in some sauropods while in others *M. longus colli dorsalis* may have had a more important role in dorsiflexion.

153 - Posterior cervical vertebrae, proportions – ratio total height / centrum length: less than 1.5 (0); more than 1.5 (1).

As for 141 and 142, neural arch height (which can contribute to a greater vertebra height, which this ratio measures) can have strong impact on the range of motion. The same can be said about centrum elongation (which is also measured in this ratio). This ratio may be better split in characters referencing centrum elongation, pedicle elongation and neural spine elongation.

Dorsal Vertebrae

168 - Anterior dorsal centra, articular face shape: amphicoelous (0); opisthocoelous (1).

As for character 123 in cervical vertebrae, a ball and socket type of joint is more mobile than an amphiplatian or amphicoelous joint. Range of motion in dorsal vertebrae is generally more restricted than on cervical vertebrae in most sauropods, both due osteological and soft tissues. However, anterior dorsal vertebrae transition from cervical vertebrae, and in some taxa they don't have hyposphene/hypantrum articulations and the pre-postzygapophyseal articulations are closer to the centrum than in more posterior dorsal vertebrae. Therefore, since the majority of Eusauropoda have opisthocoelous anterior dorsal vertebrae it is likely they were more mobile than posteriormost dorsal vertebrae.

171 - Anterior and middle dorsal vertebrae, zygapophyseal articulation angle: horizontal or slightly posteroventrally oriented (0); posteroventrally oriented (around 30°) (1); strongly posteroventrally oriented (more than 40°) (2).

A posterior inclination of the zygapophyseal articulation may cause the zygapophyseal facets to collide against each other when attempting to ventriflex, generating an osteological stop for ventriflexion.

172 - Anterior dorsal vertebrae, neural spine orientation: vertical, or slightly inclined (less than 20°) (0); posterodorsally, more than 20° (1); anteriorly directed (2).

As mentioned in character 129 regarding the orientation and shape of epiphyses, the size and orientation of neural spines is a direct product of the resultant force acting upon them (Kardong, 2012). This implies that anteriorly pointed neural spines are caused due the forces exerted posterior the neural spine in question, suggesting the need to cantilever a weight anterior to that vertebra (i.e. the neck). This may imply that sauropods with anterior dorsal vertebrae with anteriorly pointed spines may have had heavier necks or more movement in the dorso-ventral plane.

However, the orientation of the neural spine can change drastically in the cervico-dorsal transition of some sauropods. *Spinophorosaurus* (Fig. 3.1), *Overosaurus* (Fig. 5.20), *Trigonosaurus* or *Bonitasaura* (Gallina, 2011) have the spines of their fourth dorsal vertebra inclined posteriorly, their second and third dorsal vertebrae subvertical, and the neural spine of their first dorsal vertebra is inclined anteriorly. In other sauropods, however, such as *Camarasaurus* or *Diplodocus* that transition in neural spine orientation is not present, indicating a shift in the forces acting upon the anterior dorsal spines in sauropods displaying the transition, possibly related to dorso-ventral vs. lateral motion of the neck.

175 - Anterior dorsal vertebrae, neural spine length (from TPRL to top; Fig. 5.2): less than the height of the centrum (0); slightly higher than the centrum (1); twice or more the height of the centrum (2).

As mentioned in character 141 in cervical vertebrae, the height of the neural spine implies larger leverage for the epaxial muscles inserting and the ligaments attaching onto them. In addition, enlarged neural spines imply also greater forces acting upon the vertebra in most vertebrates (with sailed backs being, perhaps, an exception).

179 - Middle dorsal vertebrae, hyposphene-hypantrum system: present (0); absent (1).

Hyposphene and hypantra have much variability within Sauropoda, with different laminae forming them in different taxa (Apesteguia, 2005). Their function, however, is analogous to the zygosphene-zygantra of lepidosaurs: to stabilize the dorsal vertebrae against torsion (Romer, 1956), but also against lateral flexion in laminar hyposphenes (see Fig. 3.8) and possibly supporting part of the weight of the viscerae in rhomboid hyposphenes, particularly those with nearly horizontal articular facets (Fig. 5.2 B).

Hyposphene and hypantra may also vary within the dorsal series of the same individual (i.e. *Haplocanthosaurus priscus*, CM-572, in which there are dorsal vertebrae without the articulation, with rhomboid and with laminar hyposphene in the same individual). This implies that functional hypotheses only may be proposed for sauropods with consistent hyposphene-hypantrum articulations throughout their dorsal series.

180 - Posterior dorsal vertebrae, hyposphene-hypantrum system: present and well developed, usually with a rhomboid shape (0); present and weakly developed, mainly as a laminar articulation (1); absent or only present in posteriormost dorsal vertebrae (2).

As for character 179.

185 - Middle and posterior dorsal neural spines orientation: vertical (0); slightly inclined, with an angle of around 70 degrees (1); strongly inclined, with an angle not bigger than 40 degrees (2).

As for character 172.

Sacral Vertebrae

214 - Sacral vertebrae, number: 3 or fewer (0); 4 (1); 5 (2); 6 (3).

Sacral vertebrae (considered as those physically coalesced to the ilia, independently on whether they were dorsal or caudal vertebrae in earlier evolutionary stages) provide stability to the pelvis and limb via the sacroiliac joint. The more sacral vertebrae, therefore, imply more sacroiliac joints and therefore a more stable pelvis

215 - Sacrum, sacricostal yoke: absent (0); present (1).

The sacricostal yoke, the fusion of the sacral ribs distally to form a single articulation surface for the ventral part of the sacroiliac joint, provides a larger surface of articulation. The presence of a sacricostal yoke, therefore, generates a more stable articulation between the sacrum and pelvis.

218 - Sacral ribs, dorsoventral length: low, not projecting beyond dorsal margin of ilium (0); high extending beyond dorsal margin of ilium (1).

As for character 217, if the amount of surface articulation between the ilium and the sacrum is larger, the sacro-iliac joint will have greater stability.

408 (New) - Sacrum morphology, acute wedging in lateral view: less than 10° or even not wedged, rectangular (0); wedged more than 10° (1).

All Eusauropoda have sacra wedged more than 10° (Fig. 3.24). This causes the caudal and dorsal series to deflect said amount of degrees, making the sacrum one of the main keystones of the dorsal spine osteologically induced curvature. Since sacrum wedging can have a huge impact in the body plan of a sauropod, the inclusion of this character in a data matrix may help evaluate whether it is phylogenetically informative. Although it may be possible to further subdivide the character, those sacra wedged more than 10° appear to be a continuum (Fig. 3.7 B) and any subdivisions may be too arbitrary.

409 (New) - Sacrum morphology, neural spines constriction: absent, their anteroposterior length at the apices are as long as the centra (0); present, the neural spines are constricted and the anteroposterior length of their apices is 3/4 the length of the centra or less (1).

Just as the wedged morphology of the sacrum, the constriction of the neural spines can cause the sacrum to become a keystone in the osteologically induced curvature of the axial skeleton. The inclusion of this character in a data matrix may help evaluate whether it is phylogenetically informative.

Caudal Vertebrae

220 - Caudal vertebrae, number: 35 or fewer (0); 40 to 55 (1); increased to 70-80 (2).

The number of caudal vertebrae is increased by the addition of distal caudal vertebrae (more discussed below, on character 223). Previous studies have suggested that the extremely long tails of some sauropods (diplodocids and, perhaps, some titanosaurs) had the capability of breaking the sound barrier and creating a sonic boom in a way similar to a cracking whip (Myhrvold & Currie, 1999). Shorter tails may have been or not used as whips, but they would not have enough length to reach supersonic speeds at their tips.

223 - Caudal transverse processes (caudal ribs): persist through caudal 20 or more posteriorly (0); disappear by caudal 15 (1); disappear by caudal 10 (2).

Caudal ribs serve as attachment for some of the caudal muscle groups, more notably the *M. ilioischio-caudalis* and the *Mm. longissimus* both insert into the transverse processes in the vertebrae they are present. The presence of caudal ribs implies a stronger insertion anchor for the muscles, so the further the caudal ribs persist the potentially stronger contractions.

224 - First caudal centrum anterior articular surface: flat (0); concave (1); convex (2).

As for characters 123 or 168 in presacral vertebrae, a procoelous (1) or opisthocoelous (2) anterior joint for the first caudal vertebra implies potentially more mobility than an amphiplatian or amphicoelous joint.

225 - First caudal centrum, posterior articular surface: flat (0); concave (1); convex (2).

As for characters 123, 168 or 224 in presacral vertebrae, a procoelous (1) or opisthocoelous anterior joint for the first caudal vertebra implies potentially more mobility than an amphiplatian or amphicoelous joint.

227 - Anterior caudal vertebrae (mainly the first and second): ventral bulge on transverse process: absent (0); present (1).

M. caudofemoralis longus is surrounded by *M. ilio-ischiocaudalis* both dorso-ventrally and laterally. Given that as CFL shrinks to disappear posteriorly on the tail, the *M. ilio-ischiocaudalis* engulfs it, leaving scars on the chevrons and caudal centra (Persons & Currie, 2010; Mallison *et al.*, 2015). It is likely that this ventral bulge on the anterior caudal ribs represents the limit of CFL and *M. ilio-ischiocaudalis*.

229 - Posteriormost anterior and middle caudal vertebrae, transverse processes orientation: perpendicular (0); swept backwards, reaching the posterior margin of the centrum (1).

As for characters 129 or 172, the orientation of caudal ribs is also determined by the sum of all the forces acting upon them (Kardong, 2012).

230 - Anterior caudal vertebrae, transverse processes: ventral surface directed laterally or slightly ventrally (0); directed dorsally (1).

Caudal ribs are the dorsal limit to *M. caudofemoralis longus*. It is known that some theropod dinosaurs with extremely dorsalized caudal ribs had larger CFL cross-sections on those vertebrae than theropods with laterally directed caudal ribs (Persons & Currie, 2010). The same is true for some sauropods such as *Jobaria*, *Patagosaurus* or *Spinophorosaurus* that have extremely large and dorsalized caudal ribs.

234 - Anterior and middle caudal vertebrae, ventrolateral ridges: absent (0); present (1).

Some taxa such as *Camarasaurus* are known to have ventrolateral ridges that persist for most of the tail, always at around the same height of the centrum. However, all surveyed sauropods show a different kind of ventrolateral ridges, which is coincident with the region of the tail in which *M. caudofemoralis longus* tapers as it disappears, engulfed by *M. ilio-ischiocaudalis*. This ridge usually is present on two to four vertebrae, and always migrates from dorsal to ventral the more posterior the vertebra gets (Fig. 5.3 A). The ridge likely represents the scar left by the septum separating both muscle groups, as in the same ridge that occurs in chevrons (Persons & Currie, 2010, 2011), as they appear at the same position. Since two different types of ventrolateral ridges may occur at once in the same taxon (i.e. *Camarasaurus*, Fig. 5.3 A), it would be necessary to split this character to differentiate the different types of ridges that may appear on the centra of caudal vertebrae.

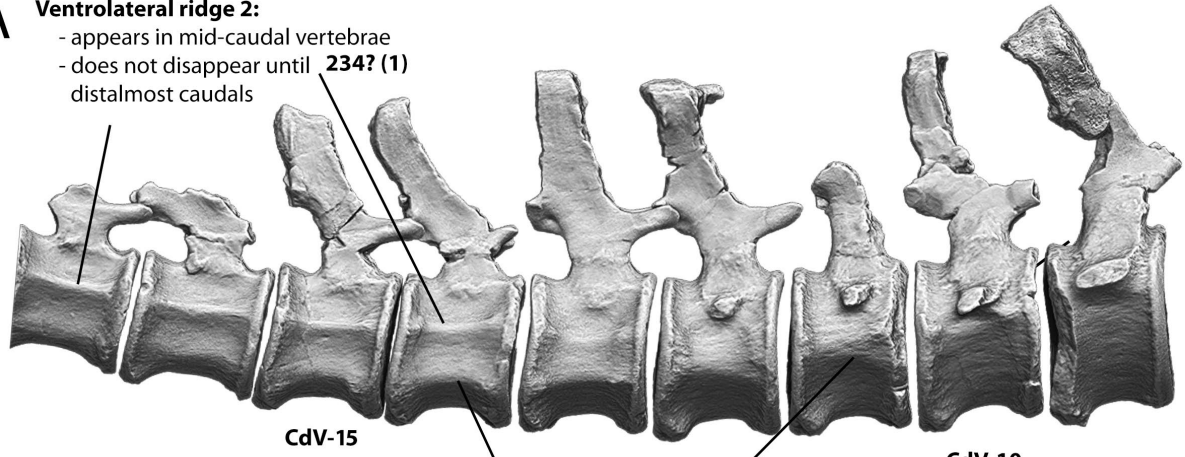
241 - Anterior caudal vertebrae, hyposphene ridge: absent (0); present (1).

Although they may not represent a structure homologous to the dorsal vertebrae hyposphene, some anterior caudal vertebrae of titanosaur sauropods have a ridge and sometimes a rhomboid structure (stated to be an autapomorphy of some taxa, such as *Epachthosaurus* (Martínez *et al.*, 2004)), similar to the hyposphene which would be functionally analogous to what is described in character 179 for dorsal vertebrae. Sauropods with "hyposphene" in caudal vertebrae (Fig. 5.3 C, E) would have lateral flexion and torsion more limited than sauropods without them.

242 - Anterior caudal centra, length: approximately the same (0); or doubling over the first 20 vertebrae (1).

The progressive elongation of the first 20 caudal vertebrae has been associated with the extremely elongation of tails in diplodocids and their whiplashes, to the point of being associated with the capacity of generating the sonic boom (Myhrvold & Currie, 1999). However, some sauropods such as *Spinophorosaurus* increase the length of their anterior caudal vertebrae (Fig. 3.19) with no evidence as of yet of an extremely elongated tail or the presence of a specialized distal caudal structure (whiplash or tail club). The functional implication of this character is, therefore, tentative.

A **Ventrolateral ridge 2:**
 - appears in mid-caudal vertebrae
 - does not disappear until **234? (1)**
 distalmost caudals



Ventrolateral ridge 1:
 - migrates ventrally
234? (1) - disappears in 2 to 4 caudal vertebrae
 - marks CFL/IIC separation?

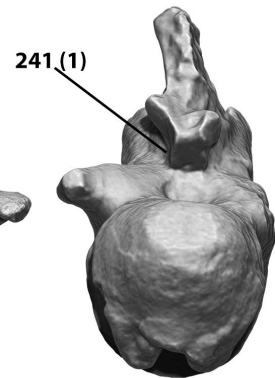
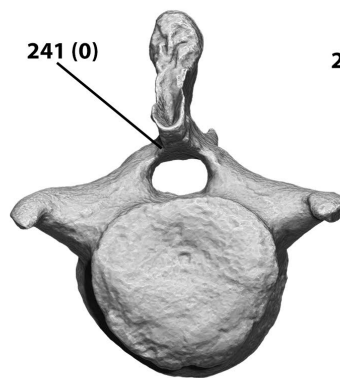
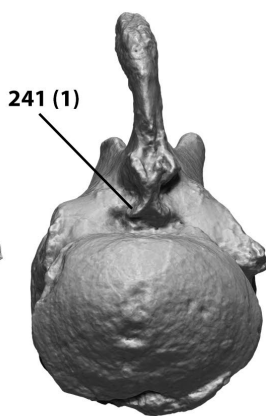
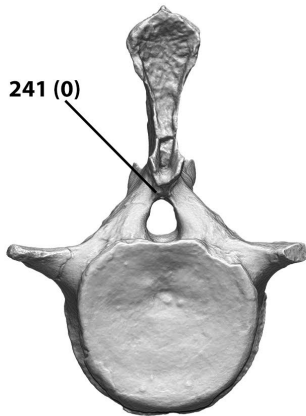
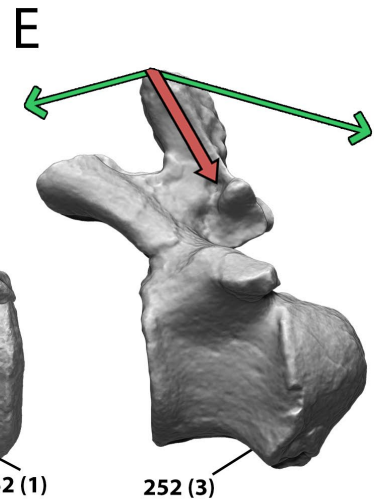
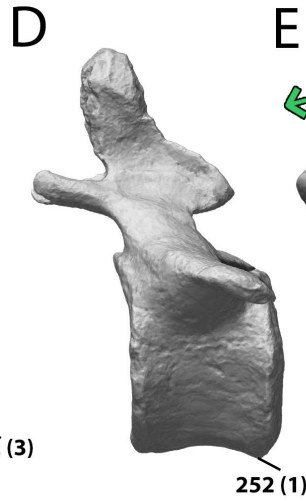
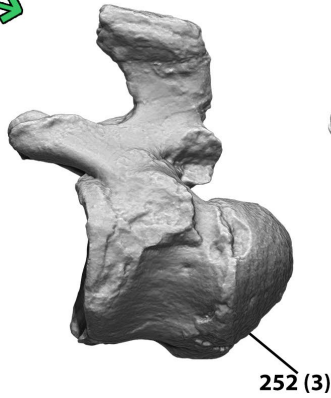
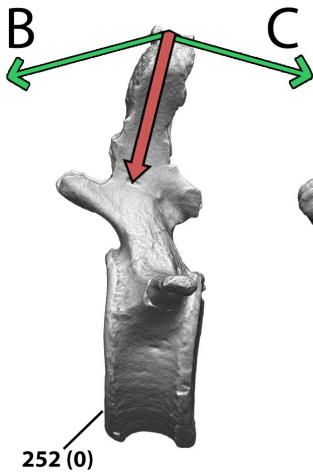


Figure 5.3 - Character states for sauropod caudal vertebrae.

A - Caudal sequence of *Camarasaurus* sp. (CM-572) in lateral view, showing the two different ridges that may appear in the lateral surface of the centra at once in the same caudal vertebrae sequence. The anteriormost one is likely an osteological correlate the boundary between *M. caudofemoralis longus* and *M. ilio-ischiocaudalis*. The posteriormost ridge is perhaps an osteological correlate for the boundary between *M. ilio-ischiocaudalis* and *M. longissimus*, after *M. caudofemoralis longus* has tapered completely. **B** - Caudal vertebra 5 of *Camarasaurus grandis* (YPM-1901) in lateral (top) and posterior (bottom) views. **C** - Caudal vertebra 8 *Epachthosaurus sciuttoii* (UNPSJB-PV-920) in lateral (top) and posterior (bottom) views. **D** - Caudal vertebra 7 *Tastavinsaurus sanzi* (MCZ-99/9) in lateral (top) and posterior (bottom) views. **E** - Middle caudal vertebra of *Aeolosaurus* sp. (MPCA 27174) in lateral (top) and posterior (bottom) views. Arrows point at anatomical features (character) with the character state between parentheses.

252 - Middle caudal centra, articular face shape: amphiplatyan or amphicoelous (0); procoelous/distoplatyan (1); slightly procoelous (2); procoelous (3).

As for characters 123, 168, 224 or 225.

254 - Anterior caudal vertebrae, anterior face of the centrum strongly inclined anteriorly: absent (0); present (1).

Much like what happens on the first dorsal vertebra of many sauropods or the first thoracic vertebra of giraffes, having the anterior centrum face inclined relative to the posterior face can cause a vertebral series to deviate from the horizontal in ONP. This character, which is typical in Aeolosaurine titanosaurs (but not restricted to them, see *Tastavinsaurus* below), causes the caudal vertebrae to deflect ventrally in ONP. This kind of osteologically induced curvature has a direct impact in the disposition of the caudal musculature, including CFL.

255 - Middle caudal vertebrae, with the anterior face strongly inclined anteriorly: absent (0); present (1).

As for character 254.

257 - Middle caudal vertebrae, orientation of the neural spines: anteriorly (0); vertical (1); slightly directed posteriorly (2); strongly directed posteriorly (3).

As for character 172, the orientation of the neural spines is the sum of the forces acting upon the vertebral centra. In the case of middle caudal vertebrae, the orientation of the tail in space, and therefore gravity, may be the strongest force being counteracted by ligaments and muscles (Fig. 5.3 E *contra* B). The orientation of the tail in space, particularly its ventral deflection, is related to characters 254 and 255, so there possibly may be a correlation between neural spine orientation and the inclination of the anterior face of the centrum.

260 - Anterior-posterior caudal vertebrae (those with still well-developed neural spine), neural spine orientation: vertical (0); slightly directed posteriorly (1); strongly directed posteriorly (2).

As for character 257.

261 - Posterior caudal centra, articular face shape: anphyplatic (0); procoelous (1); opisthocelous (2).

As for characters 123, 168, 224 or 225, 252.

267 - Forked chevrons with anterior and posterior projections: absent (0); present (1).

Forked chevrons, whether they completely overlap or they are close to overlapping, may represent osteological stops to tail ventriflexion and dorsiflexion (Mallison, 2010c).

268 - Forked chevrons, distribution: distal tail only (0); throughout middle and posterior caudal vertebrae (1).

As stated in character 267, forked chevrons may cause osteological stops in caudal vertebrae. The more inter-vertebral joints have a forked chevron, the greater the potential osteological impediment to range of motion.

270 - Chevron haemal canal, depth: short, approximately 25% (0); or long, approximately 50% chevron length (1).

The proportion of the haemal canal relative to chevron length may vary depending on two different ways: if the haemal canal increases its overall size, or if the overall chevron length diminishes while the size of the haemal canal length remains similar relative to other variables (centrum height for example). Since there is a very evident trend in the Titanosauriform lineage of sauropods to reduce the size of the caudal vertebrae and chevrons (see Discussion below), whether this character measures haemal canal enlargement or chevron will depend on each taxon.

271 - Chevrons: persisting throughout at least 80% of tail (0); disappearing by caudal 30 (1).

Middle and distal chevrons are an insertion for the *M. ilio-ischiocaudalis*. Their persistence on the distalmost part of the tail suggests, with an equal number of vertebrae, a more muscular tip of the tail.

273 - Posture: bipedal (0); columnar, obligatory quadrupedal posture (1).

The change from a bipedal to an obligatory quadrupedal posture is a key change in sauropodomorph evolution with important functional consequences regarding many areas of sauropod biology (Sander *et al.*, 2011; Sander, 2013). The change to an obligatory quadrupedal stance also resulted in a series of

modifications of more discrete characters (i.e. columnar limbs, hypertrophy of preacetabular lobe of the ilium, retroversion of the pubis...) as has been discussed in previous research concerning the evolution of sauropod locomotion (Wilson & Carrano, 1999; Carrano, 2005). The independence of this character from others it has a direct relation with (i.e. characters referring to appendicular skeleton shape, proportions or orientations) should be explored.

Scapular Girdle

275 - Scapular blade, orientation respect to coracoid articulation: perpendicular (0); forming a 45° angle (1).

The angle between the scapular blade and the coracoid (and glenoid/humerus) has important consequences regarding its position on the ribcage (due the disposition of the cingulo-axial muscles with the ribs) and the moment arms of the humeral muscles with an origin on the scapular blade, as an angulation change of 45° can drastically alter the lines of action and therefore functions of a given muscle. It may also have an impact in the orientation of the coracoid relative to the sternal plates and ribcage, as the sternal plates in titanosaurs also have a characteristic shape, which may have resulted in rearrangements on the pectoral girdle configuration (Schwarz *et al.*, 2007a)

276 - Scapular blade, distal expansion: absent (0); present (1).

The distal expansion of the scapula (Fig. 5.4 B) is a larger osteological origin area for the *M. deltoideus scapularis*, which is one of the main muscles contracting in humerus abduction. A larger osteological insertion area implies more stability for muscle contraction than the cartilaginous suprascapula.

280 - Scapula, development of the acromion process: undeveloped (0); well developed (1).

The acromion process is the articulation for the clavicles (Remes, 2007). It could be hypotesyzed that a development of this process (Fig. 5.4 A) may be related to the presence of ossified clavicles or to its absence, as an extra anchorage point for muscles such as *M. deltoideus clavicularis*. The presence of ossified clavicles and interclavicles, however, has been assessed in only a minority of sauropods (Tschopp & Mateus, 2013), so it is still difficult to establish whether the development of the acromion process is a consequence of ossified, non-ossified or absent clavicles or if such a potential association is non-existent.

285 - Glenoid scapular orientation: relatively flat or laterally facing (0); strongly beveled medially (1).

Sauropod glenoids usually favor a protraction-retraction motion of the humerus within a parasagittal plane, with little abduction/adduction before disarticulation. However, the presence of a laterally beveled glenoid implies a greater range of motion for humeral abduction before disarticulation.

287 - Coracoid, proximodistal length: less than the length of scapular articulation (0); approximately twice the length of scapular articulation (1).

The coracoid is the origin an insertion of plenty of cingulo-axial, humeral and some antebrachial muscles. A larger coracoid in proximo-distal length implies larger origins for muscles such as *M. coracobrachialis*, *M. subcoracoscapularis* or *M. supracoracoideus*.

291 - Coracoid, infraglenoid lip: absent (0); present (1).

The infraglenoid lip corresponds to the biceps tubercle according to Remes (2007), and its presence may indicate a stronger anchor for the coracoid origin of this muscle.

296 - Ridge on the ventral surface of the sternal plate: absent (0); present (1).

The ventral surface of the sternal plates is the area of origin for *M. pectoralis*, one of the main humeral adductors. The presence of a well-marked ridge in the ventral side of the sternal plates may indicate a stronger anchor and/or more intense *M. pectoralis* activity thorough the life of the animal.

Forelimbs

298 - Humerus, strong posterolateral bulge around the level of the deltopectoral crest: absent (0); present (1).

The posterolateral edge of the deltopectoral crest is the site of insertion for both *M. deltoideus scapularis* and *M. deltoideus clavicularis*. The posterolateral bulge (Fig. 5.4 D) may indicate an osteological correlate

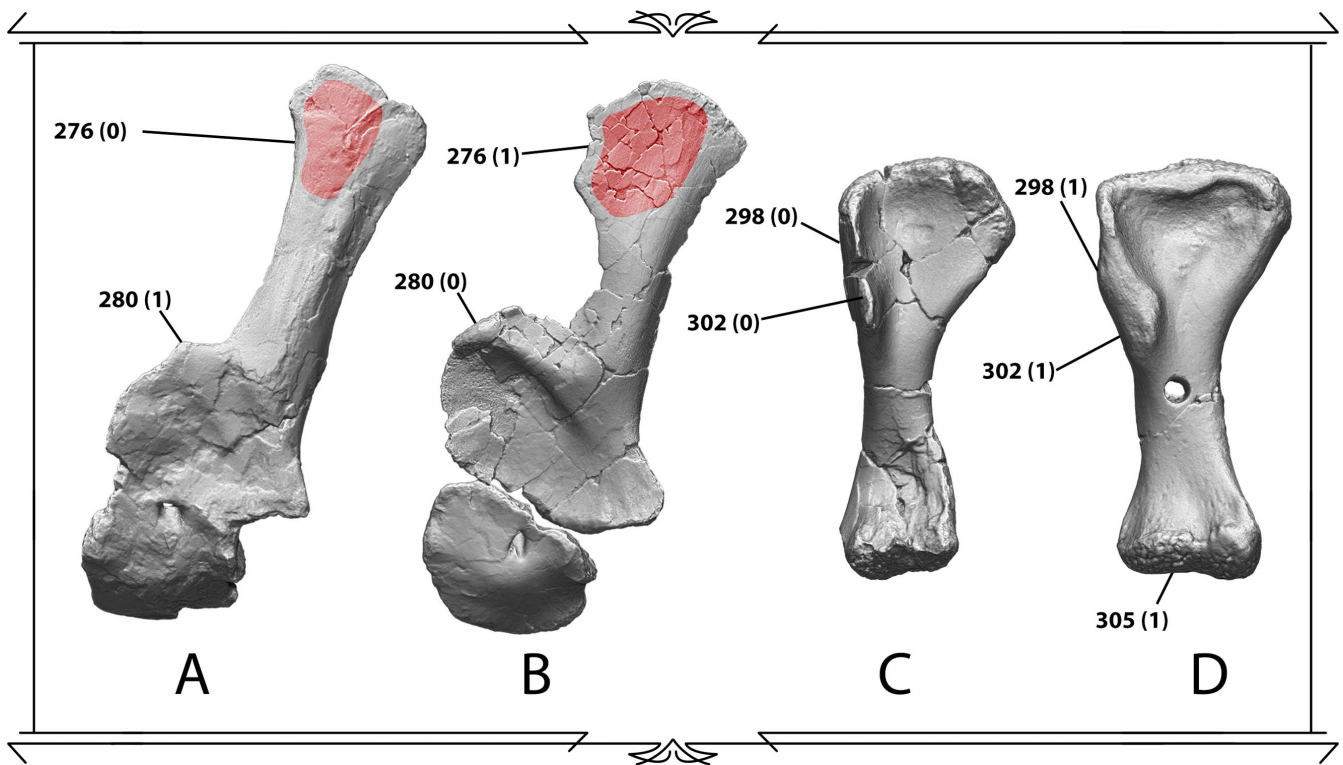


Figure 5.4 - Character states for sauropod pectoral girdle and humeri.

A - Scapulocoracoid of *Amargasaurus cazau* (MACN-N-15) in lateral view. **B** - Scapulocoracoid of *Camarasaurus grandis* (YPM-1901) in lateral view. **C** - Humerus of *Camarasaurus grandis* (YPM-1901) in anterior view. **D** - Humerus of *Neuquensaurus australis* (MCS-8) in anterior view. Red indicates origin for *M. deltoideus scapularis* in A and B. Arrows point at anatomical features (character) with the character state between parentheses.

for the insertion of one of the deltoids. Having a strong bulge implies a stronger anchor for one of these muscles or a very intense activity of this muscle during the life of the animal. Its appearance may indicate locomotor or postural differences in the forelimb.

300 - Humerus-to-femur ratio: less than 0.60 (0); 0.60 to 0.90 (1); greater than 0.90 (2).

The humerus-to-femur ratio is a good proxy for estimating the proportions of a sauropod, since each bone is the longest in their respective limbs. Sauropods with shoulders taller than the acetabulum usually have a H/F ratio greater than 0.90, such as *Brachiosaurus*. This ratio correlates well with the amount of sacral wedging (see Chapter 3.8, Fig. 3.7 B). This suggests that, in absence of sacral material, the H/F ratio may be a good predictor for sacral wedging and *viceversa*.

301 - Humeral deltopectoral attachment, development: prominent (0); reduced to a low crest or ridge (1).

The apex of the deltopectoral crest is the insertion area for *M. supracoracoideus*. The more prominent the deltopectoral crest apex is, the stronger the insertion and/or the more intense the activity of this muscle was during the life of the animal.

302 - Humeral deltopectoral crest, shape: relatively narrow throughout length (0); markedly expanded distally (1).

A narrower deltopectoral crest (Fig. 5.4 C) is a weaker anchor point for a muscle insertion than a more expanded, thicker "crest" (Fig. 5.4 D). Sauropods with a thickened deltopectoral crest were able to exert more force during contraction of the muscles inserting onto the deltopectoral crest with more stability, particularly *M. supracoracoideus*.

304 - Humerus, RI (*sensu* Wilson and Upchurch, 2003): Gracile (less than 0,27) (0); medium (0,28-0,32) (1); Robust (more than 0,33) (2).

The gracile or robust component of an appendicular element may or not be related to its capability to bear a larger weight. Since sauropod limbs are columnar and the main bearers of the weight of the animal, there may be a correlation between long bone gracility and overall weight.

305 - Humeral distal condyles, articular surface shape: restricted to distal portion of humerus (0); exposed on anterior portion of humeral shaft (1).

The actual shape of the articular surfaces of non-ossified sauropod long bone epiphyses may have been very different than what actual bone shows (Holliday *et al.*, 2010). However, the fact that some sauropods exposed part of the articular surface of the distal condyles anteriorly (Fig. 5.4 D) suggests a greater range of motion for elbow flexion in the taxa showing this trait.

311 - Ulnar olecranon process, development: prominent, projecting above proximal articulation (0); rudimentary, level with proximal articulation (1).

The olecranon is the insertion area for *M. triceps*, which is the main extensor of the forelimb. Although a cartilaginous, non-ossified may have been present in most sauropods (as happens in the stegosaur *Kentrosaurus* (Mallison, 2010c) or in some sauropod bones with ossified cartilage caps (Schwarz *et al.*, 2007c), an ossified olecranon is a stronger anchor for muscle contraction than a cartilaginous one. Therefore, taxa with prominent, ossified olecranon may have been able to exert stronger forces when contracting the triceps for forelimb extension.

312 - Ulna, length-to-proximal breadth ratio: gracile (0); stout (1).

As for character 304.

320 - Longest metacarpal-to-radius ratio: close to 0.3 (0); 0.45 or more (1).

As for character 300, forelimb elongation appears to correlate with sacral wedging. However, whether metacarpal elongation correlates with sacral wedging or not is unknown, although it may be possible, since sauropods with more elongated humeri tend to have elongated metacarpals (Table 3.2).

Pelvic Girdle

327 - Pelvis, anterior breadth: narrow, ilia longer anteroposteriorly than distance separating preacetabular processes (0); broad, distance between preacetabular processes exceeds anteroposterior length of ilia (1).

The widening of the sauropod pelvis during titanosauriform evolution has been well documented, and is linked to features such as wide-gauge trackways, which implies numerous modifications in the locomotor apparatus of those sauropods. Since the anterior breadth of the ilia may be coupled with other pelvic and even appendicular and tail modifications, this character may as well have derived as part of a functional module.

329 - Ilium, dorsal margin shape: flat (0); semicircular (1).

The shape of the dorsal margin of the ilium has two different effects: a semicircular dorsal rim separates further all three *M. iliotibiales* generating a larger lever arm for their contraction, rendering a stronger femoral abduction and leg protraction. It also generates a taller iliac blade, which in turn implies a larger area for the origin of ITC, IFE, ILFIB and FTE, implying potentially larger cross-sections for these muscles.

330 - Ilium, preacetabular process, kink on ventral margin: absent (0); present (1).

The ventral margin of the preacetabular process of the ilium is the origin area for both *M. puboischiofemoralis 1 et. 2*. This kink may indicate a stronger anchor point for one of the two PIFI.

333 - Highest point on the dorsal margin of the ilium: lies caudal to the base of the pubic process (0); lies cranial to the base of the pubic process (1).

The highest point on the dorsal margin of the ilium marks the longest lever arm for a particular set of muscles originating on the rim of the ilium or the lateral surface of the iliac blade. An ilium with its highest point posterior to the base of the pubic process (or with subequal height of the iliac blade; Fig. 5.5 A, B) will have similar lever arms and surface for retraction, abduction and protraction. An ilium with a more dorso-ventrally developed preacetabular process (Fig. 5.5 C) implies greater insertion areas for *M. iliotrochantericus caudalis* (ITC), *M. iliotibialis 1* (IT1) and *M. iliofemoralis externus* (IFE) and somewhat longer lever arms for these muscles (Fig. 5.5 G *contra* F).

334 - Pubis length respect to ischium: pubis slightly smaller or subequal to ischium (0); pubis larger (120% +) than ischium (1).

This character measures the relative size of the ischium, which in most sauropods tends to be shorter than the pubis, except in some early branching taxa such as *Spinophorosaurus*. The ischium is the pelvic bone experiencing the most reduction during sauropodomorph evolution, with some taxa such as *Rapetosaurus* having an extremely reduced ischium opposed to a relatively elongated pubis. The derived

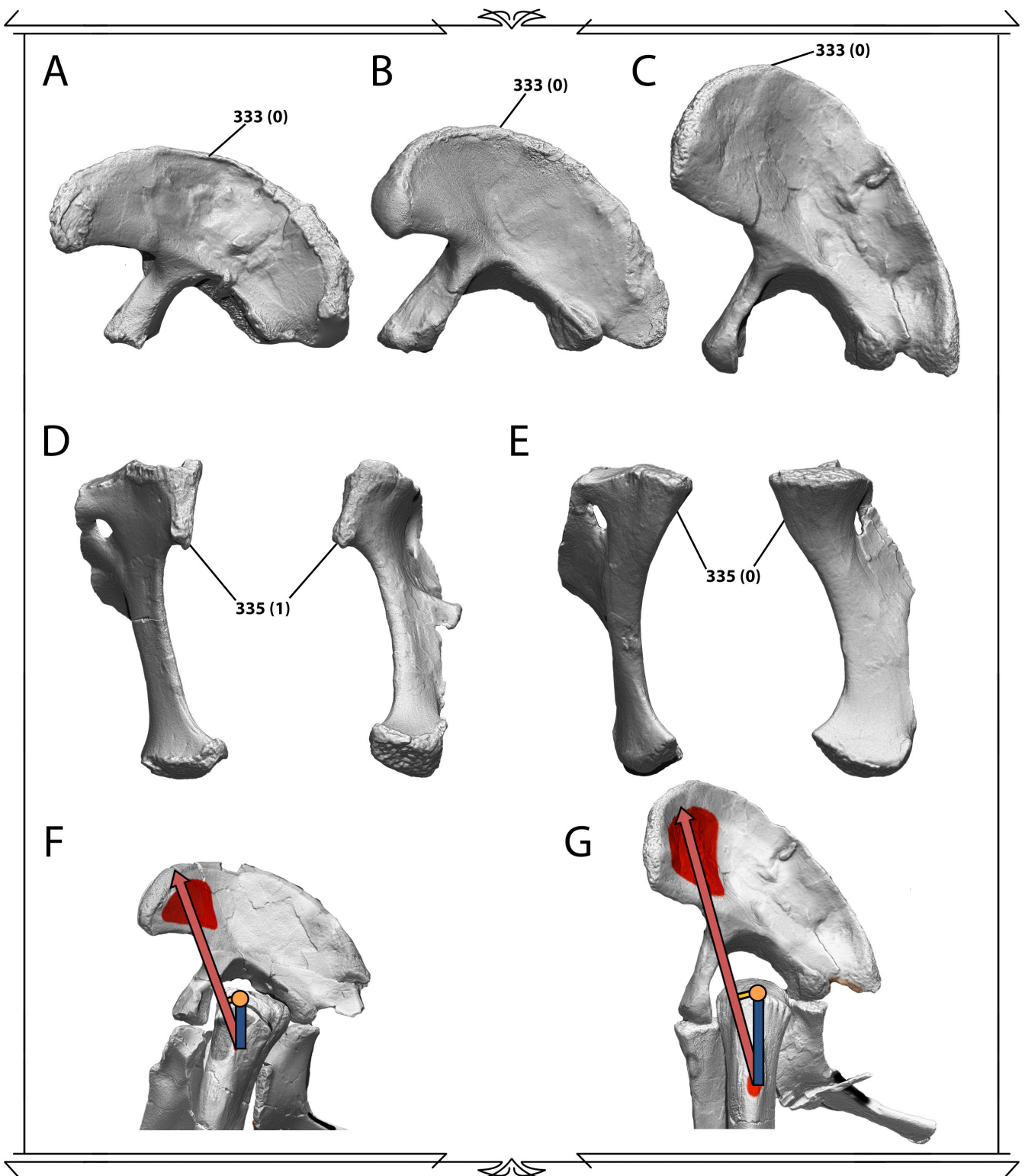


Figure 5.5 - Character states for sauropod pelvic girdle.

A - Ilium of *Diplodocus carnegie* (CM-94) in lateral view. **B** - Ilium of *Camarasaurus supremus* (AMNH-5761) in lateral view. **C** - Ilium of *Tastavisaurus sanzi* (MCZ-99/9) in lateral view. **D** - Pubis of *Diplodocus carnegie* (CM-94) in lateral (left) anterior (right) views. **E** - Pubis of *Tastavisaurus sanzi* (MCZ-99/9) in lateral (left) anterior (right) views. **F** - Pelvis of *Camarasaurus grandis* (YPM-1901) in lateral view, with line of action (red), lever arm (blue) and moment arm (yellow) for *M. iliotochantericus caudalis*. **G** - Pelvis of *Tastavisaurus sanzi* (MCZ-99/9) in lateral view, with line of action (red), lever arm (blue) and moment arm (yellow) for *M. iliotochantericus caudalis*. Arrows point at anatomical features (character) with the character state between parentheses. F and G scaled to same acetabulum length.

character state implies a reduction of the musculature originating in the ischium (Table 3.9), which in turn may be correlated with the reduction in the size of caudal vertebrae and chevrons. This may be related with the appearance of wide-gauge trackways and the change in sauropod locomotor apparatus.

335 - Pubis, ambiens process development: small, confluent with anterior margin of pubis prominent, (0); projects anteriorly from anterior margin of pubis (1).

Ambiens process marks the origin area for the muscle of the same name. A well-marked, prominent ambiens process suggests either a stronger anchor for this muscle or a very intense activity of of this muscle during the life of the animal.

340 - Ischium, elongate muscle scar on proximal end: absent (0); present (1).

The specific muscle scar should be explicitly named for this character, just as is the case of character 335. It is likely referring to a scar more proximal than the ischial tuberosity, which is the origin for *M. flexor tibialis internus 3* (FTI 3). The only muscle more proximal on the ischium than FTI 3 is *M. ischiotrochantericus*, so the presence or absence of this scar may indicate use that is more pronounced during the life of the animal.

345 - Ischial distal shafts, cross-sectional shape: V-shaped, forming an angle of nearly 50° with each other (0); flat, nearly coplanar (1).

Given the surface of articulation in coplanar ischia is much smaller than in non-coplanar ischia, coplanar ischia are weaker articulations than non-coplanar ischia. This may or may not be related with the presence of larger tails in sauropods with non-coplanar ischia.

346 - Ischia, distal end: is only slightly expanded (0); is strongly expanded dorsoventrally (1).

The distal end of the ischia is the origin points for *M. ischiocaudalis*. A strongly expanded distal ischial end suggests a stronger anchor for the contraction of that muscle.

348 - Ischial tuberosity: absent (0); present (1).

The ischial tuberosity may represent an osteological correlate for the origin of *M. flexor tibialis internus 3* (Wilson & Carrano, 1999; Carrano, 2005; Fechner, 2009), and its absence may indicate an overall reduction of the muscle.

Hindlimb

349 - Femur, longitudinal ridge on the anterior face: absent (0); present (1).

Absent in a majority of sauropods, the longitudinal ridge on the anterior face of the femur of some sauropods, particularly the titanosaur *Neuquensaurus australis* has been interpreted as the *linea intermuscularis cranialis*, which indicates the separation of *M. femorotibialis lateralis*, *medius* and *intermedius* (Romer, 1923; Fechner, 2009). Although it has been proposed it may not be homologous to the condition seen in other dinosaurs and archosauromorphs (it is a ridge/crest, not a line), no compelling arguments have been made to argue this.

352 - Femur, fourth trochanter position: almost at the half of the femur (0); in the proximal third of the femur (1).

The fourth trochanter is the insertion point for both *M. caudofemoralis longus* and *M. caudofemoralis brevis*. The height of this insertion on the femur has important implications regarding the moment arm for this muscle: the distance from the center of rotation (femoral head) and the insertion for CFL is the lever arm. At an identical angle between the CFL line of action and the lever arm, the moment arm increases. This implies that if two sauropods had similar CFL physiological cross-sections, the one with the basal condition (Fig. 5.6 B, C) would have more efficient capability to retract the femur in slower motions, while the one with the derived condition (Fig. 5.6 D, E) would have better capability to generate retraction in fast motions (Fechner, 2009; Otero, 2010).

353 - Femur, fourth trochanter development: prominent (0); reduced to crest or ridge (1); extremely reduced (2).

As has been discussed for previous osteological marks of muscle insertions and origins, the reduction in size may be a potential indicator of muscle reduction (Nagano & Komura, 2003). As sauropods evolved

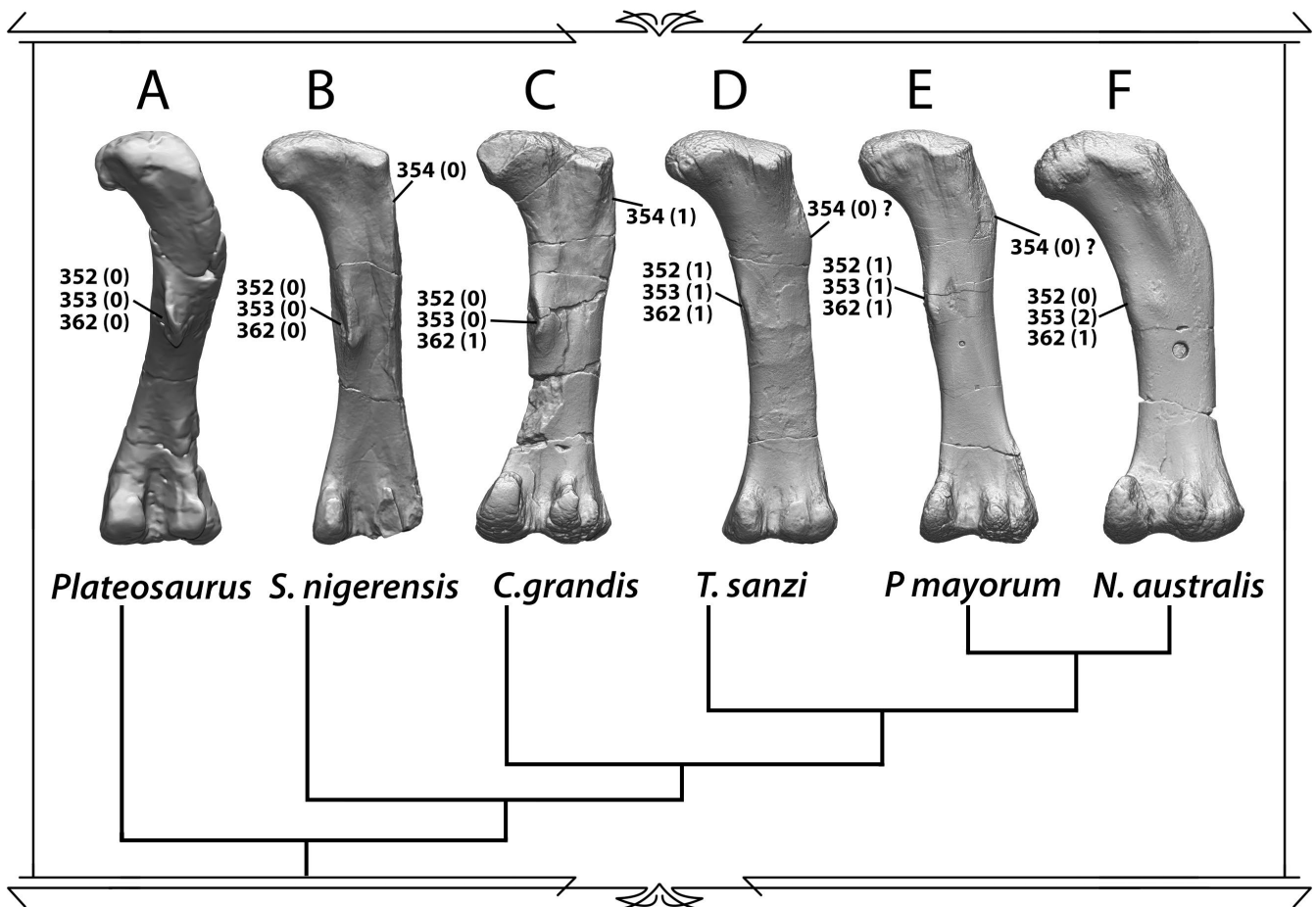


Figure 5.6 - Character states for sauropod femora.

A - Femur of *Plateosaurus engelhardti* (GPIT-1) in posterior view. **B** - Femur of *Spinophorosaurus nigerensis* (GCP-CV-4229) in posterior view. **C** - Femur of *Camarasaurus grandis* (YPM-1901) in posterior view. **D** - Femur of *Tastavisaurus sanzi* (MCZ-99/9) in posterior view. **E** - Femur of *Patagotitan mayorum* (MPEF-PV-3400) in posterior view. **G** - Femur of *Neuquensaurus australis* (MCS-9) in posterior view. Arrows point at anatomical features (character) with the character state between parentheses. The dendrogram represents the phylogenetic relationships between taxa.

from bipedal ancestors, a reduction in CFL could be explained from the transition to an obligatory quadrupedal locomotor strategy (Gatesy, 1990). Further reduction of the CFL during sauropod evolution may be related with the development of different locomotory styles (Carrano, 2005), particularly the evolution of wide-gauge locomotion (Carrano, 2005). A reduction in the fourth trochanter (Fig. 5.6 F) should correlate with a reduction in the osteological correlates for CFL origin (tail vertebrae and chevrons).

354 - Femur, lesser trochanter: present (0); absent (1).

The lesser trochanter (Fig. 5.6 B) is the insertion for *M. iliotrochantericus caudalis* (ITC) and *M. iliofemoralis externus* (IFE). The reduction of the lesser trochanter (Fig. 5.6 C) may also indicate a reduction in the mass of these muscles and their capacity to generate torque. The origins of these two muscles on the iliac blade may also be smaller in taxa without a clear lesser trochanter.

356 - Femur, lateral bulge (marked by the lateral expansion and a dorsomedial orientation of the laterodorsal margin of the femur, which starts below the femur head ventral margin): absent (0); present (1).

The lateral bulge coincides with the area where ITC and IFE insert. Actually, the lateralmost tip of the lateral bulge is located in the same region where the third trochanter was in earlier branching eusauropods, perhaps being homologous (Carrano, 2005). This bulge sometimes has ornamentation, perhaps related to the insertion of one or both of these muscles. The lateralmost tip of the bulge being more distal than lesser trochanter of earlier branching sauropod implies larger lever arms for muscles inserting there (Fig. 5.5 G *contra* F).

358 - Femur head position: perpendicular to the shaft, rises at the same level than the greater trochanter (0); dorsally directed, rises well above the level of the greater trochanter (1).

The angulation of the femoral head and its position relative to the shaft is one of the best known factors

related with wide-gauge in sauropods (Wilson & Carrano, 1999). This is potentially related also with rearrangements of the lines of action of the main muscles inserting on the femur, particularly with the extreme development of the lateral bulge and the extreme lateral flaring of the preacetabular region of the ilia (Carrano, 2005).

362 - Situation of the femoral fourth trochanter: on the caudal surface of the shaft, near the midline (0); on the caudomedial margin of the shaft (1).

Much like the height of the fourth trochanter on the femoral shaft, the medio-lateral situation also may have an important impact in the angulation between the lever arm and the line of action of the muscle: the more medially situated the fourth trochanter, the greater the angle between the line of action of CFL and the lever arm (Fig. 3.21). This is likely a compensation for separating the legs from the body due to the derived state in character 358, to help maintain a similar moment arm. However, a medially placed trochanter (Fig. 5.6 C-F) is usually also reduced and appears in taxa with smaller correlates for the caudofemoral musculature.

364 - Tibial cnemial crest, orientation: projecting anteriorly (0); or laterally (1).

The cnemial crest is a site of attachment for femoral extensors and ankle flexors (Carrano & Hutchinson, 2002; Fechner, 2009). Among the first are the *M. iliotibialis* (IT), which originate in the dorsal rim of the ilium. Changes in the orientation of the iliac blade, from parasagittal to deflect laterally occur early on in sauropod evolution (Wilson & Carrano, 1999; Carrano, 2005), so it is likely that changes in cnemial crest orientation also occur associated with changes in the lines of action of these muscles.

367 - Fibula, proximal tibial scar, development: not well-marked (0); well-marked and deepening anteriorly (1).

The proximal tibial scar marks the contact area between tibia and fibula. A well-marked and deepened scar implies the partial ossification of tissue connecting both bones, suggesting a stronger connection, which might be related with size/weight increase and/or greater rotational forces acting in the shank in those sauropods in which it is present.

368 - Fibula, lateral trochanter: absent (0); present (1).

The lateral trochanter of the fibula is an insertion site for *M. iliofibularis*. Its absence may indicate a reduction in the capacity of this muscle to generate torque, as the forces exerted during the life of the animal would not have left mark on the bone.

5.3 SYSTEMATIC PALEONTOLOGY OF PERSONALLY REVIEWED TAXA

Some of the characters reviewed above are discussed within the context of the virtual skeleton of a selection of sauropod taxa representing the majority of currently well-established clades.

Specimens marked with a single asterisk (*) were inspected firsthand and photographed. Specimens marked with two asterisks (**) were inspected firsthand and digitized. All figured specimens are digital models unless were specified.

Dinosauria Owen 1842 *sensu* Baron, Norman, & Barrett (2017)

Sauropodomorpha Huene 1932 *sensu* Sereno (2005)

Sauropoda Marsh 1878 *sensu* Sereno (2005)

Eusauropoda Upchurch 1995 *sensu* Sereno (2005)

Patagosaurus fariasi **Bonaparte, 1979**

Holotype. **PVL-4170 Partial skeleton of a large individual with fused neurocentral sutures consisting of 4 anterior cervical vertebrae, 3 posterior dorsal vertebrae, anteriormost 3 dorsal vertebrae, 5 middle and posterior dorsal vertebrae, sacrum, 6 anterior caudal vertebrae, 12 middle caudal vertebrae, many incomplete ribs, some chevrons, right ilium, partial fused ischia missing proximal region, right pubis, proximal right scapula and broken coracoid, proximal right humerus and right femur.

Referred specimens. **MACN-CH-935 Similar in size to the holotype, but without fused neurocentral sutures, it consists of four middle dorsal neural arches, three dorsal centra, four sacral centra with the sacricostal yoke preserved, one sacral centrum without ribs, two fused sacral neural arches, one anterior caudal vertebra centrum, six middle caudal vertebrae, three chevrons. **MACN-CH-936 six cervical vertebrae, six dorsal vertebrae. **MACN-CH-1299 nine proximal caudal vertebrae in sequence, left ilium, left femur and incomplete left tibia.

Locality and horizon. North of Cerro C ndor, Toarcian/Bajocian wet floodplain tuff/sandstone. Ca nad n Asfalto Formation, Chubut (Argentina).

Personal description/remarks. Although several specimens were referred to the taxon and figure as such in both PVL and MACN, there may be more diversity than a single species on the referred material, so only the material personally reviewed has been taken into account. All cervical vertebrae from the holotype and those referred to the taxon share a similar morphology, but none of the digitized could be arranged into a continuous sequence. All of them have prezygapophyseal facets longer anteroposteriorly than wide latero-medially (Fig. 5.7 D), similar to the condition seen in *Spinophorosaurus*. Since the neck of *Patagosaurus* is slightly less elongated than that of *Spinophorosaurus*, maybe *Patagosaurus* may have had an overall smaller range of motion (since the distance between the center of rotation and zygapophyseal facets is a little larger in *Patagosaurus* than in *Spinophorosaurus*).

The dorsal vertebrae have hyposphene-hypantrum complex (Fig. 5.2 A). However, in some of the surveyed dorsal vertebrae, these are a thickened lamina, whereas in others they have a ventral expansion, similar to that of more deeply nested sauropods. Since this variability regarding the hyposphene-hypantrum may or may not respond to a taxonomic scenario, its functional implications should only be discussed regarding the holotype, which has ventrally expanded hyposphene, and therefore more restricted range of motion in the dorsal vertebrae than *Spinophorosaurus*. Both reviewed sacra (that of the holotype and MACN-CH-935) are acute wedged around 20  (Fig. 5.7 B), and both are very similar to that of *Spinophorosaurus*. Since none of the examined dorsal vertebrae had obtuse wedging or had keystone shaped centra, there is no doubt to think that the presacral column articulated at least relatively straight. The ilium is not coalesced to the pelvis in the holotype as in *Spinophorosaurus*, but manually articulating them makes the overall sacrum orientation respect to the pelvis coincide with that of *Spinophorosaurus*. This implies, in accordance with the available fossil evidence, that the osteologically induced curvature of *Patagosaurus* likely was similar to that of *Spinophorosaurus*.

The ilium of the holotype has a very small preacetabular lobe next to other Eusauropoda, more similar to

that of non-sauropod sauropodomorphs. This implies that *M. iliotibialis 1* (IT1) and *M. ischiotrochantericus* (ITC) were less developed than in other sauropods (Fig. 5.7 A). However, the preacetabular lobe is already oriented slightly bowed laterally and anterior to the acetabulum, more similar to the sauropod condition, so the line of action for ITC was similar to those of other sauropods. This implies ITC may have been acted more during protraction than in abduction (Carrano, 2000). All in all, the development of this muscle on *Patagosaurus* is much smaller than in the majority of eusauropods. The posterior region of the iliac blade, on the other hand, is very developed dorso-ventrally, as in *Spinophorosaurus* and other early eusauropods, suggesting larger origin sites for *M. flexor tibialis externus* (FTE) and *M. iliofibularis* (ILFIB) and a larger lever arm for IT3. This condition seems to be present in many eusauropods, and, given that the posterior half of the ilium is also very developed in non-sauropod sauropodomorphs, it may represent the retention of this basal trait. A similar situation would be that of the correlates for caudal musculature. The neural spines on the caudal vertebrae of *Patagosaurus* are even longer respect to the centrum than in *Spinophorosaurus*, implying very large epaxial muscles. As has been discussed in chapter 3, this condition likely represents the retention of the basal condition.

Jobaria tigidensis **Sereno et al. 1999**

Holotype. MNN-TIG-3 (cast at University of Chicago)* Axis, 33 caudal vertebrae (some in sequence), 20 chevrons including the anteriormost (first), complete forelimb, fused pubes.

Referred specimens. MNN-TIG-4* Adult specimen including posteriormost three dorsal vertebrae, sacrum and left ilium, anteriormost caudal vertebrae, femur, several ribs. **MNN-TIG-6*** Almost complete neck from Axis to CV-11. **MNN-TIG-9*** Subadult with neck missing atlas, an almost complete dorsal series missing posteriormost 3 dorsal vertebrae, partial tail missing the proximal and distalmost parts, ulna and radius, femur, tibia and fibula.

Locality and horizon. Támerat, L'Irhazer plain close to the "Falaise de Tiguidit" (Agadez, Niger), Tiourarén Formation (Niger), Late? Jurassic.

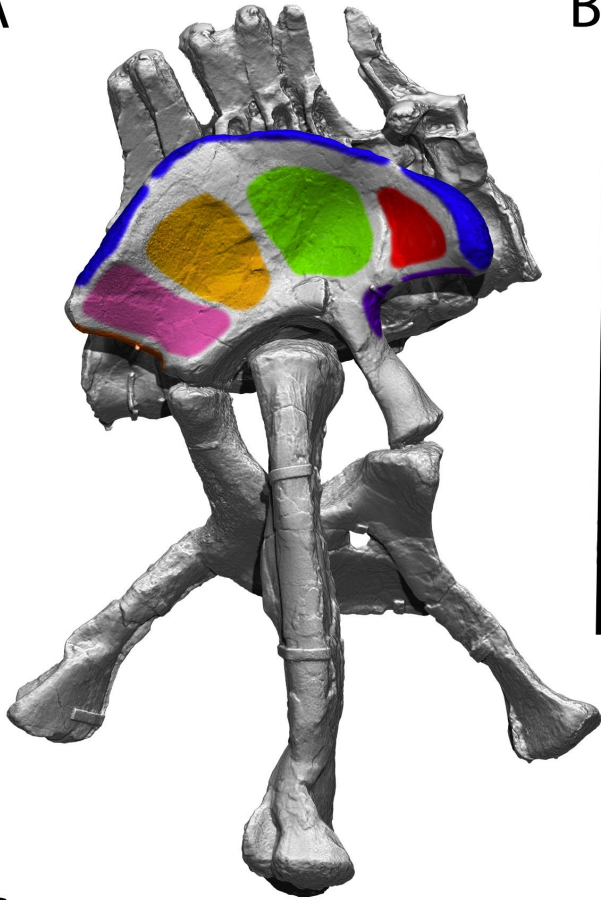
Personal description/remarks. *Jobaria* is one of the better represented sauropods of the Jurassic of Africa. Known from multiple skeletons with lots preserved and overlapping bones, its phylogenetic position is still controversial, as it is retrieved by analyses as a non-neosauropod Eusauropoda close to Neosauropoda, as an early branching Neosauropoda, an early branching Macronaria or an early branching Diplodocoidea.

Some characteristics regarding morphofunctional capabilities present in the holotype and referred specimens are more similar to those of *Spinophorosaurus* or *Patagosaurus* than to any Neosauropod. The osteological correlates of caudal musculature, neural arches and chevrons, are very developed respect to the height of the centrum, suggesting both epaxial and hypaxial musculature was very developed in *Jobaria*. A close examination of the tail of MNN-TIG-3 cast revealed CdV-13 to CdV-15 had ridges on the lateral surfaces of their centra, migrating ventrally the more posterior the vertebra. Also, three chevrons of slightly descending length, with a ridge on their lateral surfaces, articulated perfectly with those caudals, likely belonging in those positions or very close. These ridges mark the tapering of *M. caudofemoralis longus*, as seen in other sauropod and theropod dinosaurs. The tapering of CFL in *Jobaria* occurs in the same position as it does in *Spinophorosaurus*, more posterior than in all surveyed neosauropods. While other tails referred to *Jobaria* are not as complete as the holotypic tail, they also share extremely developed neural spines.

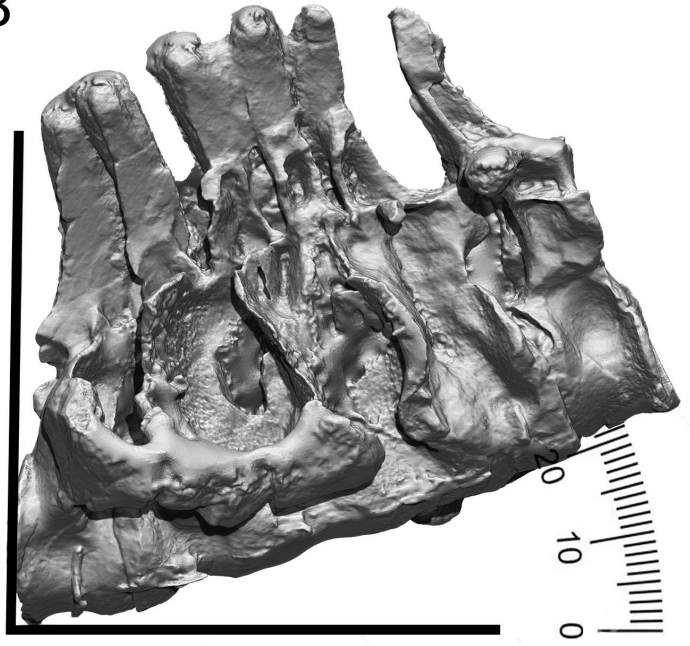
Figure 5.7 (next page) - *Patagosaurus fariasi*.

A - Pelvis, sacrum and femur of the holotypic specimen of *Patagosaurus fariasi* (PVL-4170) with muscular origins and insertions highlighted and colored (see Fig. 3.16 for color legend). **B** - Sacrum of the holotypic specimen of *Patagosaurus fariasi* (PVL-4170) showing a 20° wedging. **C** - Middle cervical vertebra of specimen MACN-CH-936 referred to *Patagosaurus fariasi* in lateral view. **D** - Middle cervical vertebra of specimen MACN-CH-936 referred to *Patagosaurus fariasi* in dorsal view, with the longer than wide prezygapophyseal facets highlighted in red. Femur = 1320 mm.

A



B



C



D



Haplocanthosaurus priscus **Hatcher, 1903**

Haplocanthus priscus **Hatcher, 1903a**

Haplocanthosaurus utterbackii **Hatcher, 1903b**

Holotype. **CM 572 relatively complete skeleton of a single adult individual, preserving posteriormost two cervical vertebrae, 11 dorsal vertebrae (DV1,4-13), five sacral vertebrae, 20 caudal vertebrae in sequence, several ribs, a right scapulocoracoid, both ilia, both ischia, both pubes, right femur.

Referred specimens. **CM 879 relatively complete skeleton of a single, subadult individual, preserving at least eight cervical vertebrae, 13 dorsal vertebrae, five sacral vertebrae (missing anteriormost three centra), seven caudal vertebrae, right coracoid.

Locality and horizon. Felch Quarry 1, Garden Park (Colorado, USA). Middle levels of the Morrison Formation (USA), Brushy Basin Member, Kimmeridgian.

Personal description/remarks. Despite Hatcher's original claim of *Haplocanthosaurus* having 14 dorsal vertebrae and 15 cervical vertebrae (Hatcher, 1903), the uninterrupted dorsal series of CM 879 clearly shows only 13 true dorsal vertebrae, making the number of cervical vertebrae likely 12 as in most sauropods with 25 presacral vertebrae (the basal condition). The cervical vertebrae are moderately elongated, with flat and rounded (as long as wide) prezygapophyseal facets. Overall, the range of motion in the joints it can be measured is smaller than in *Spinophorosaurus*, but is greater than in sauropods such as *Camarasaurus*.

One of the most interesting features of *Haplocanthosaurus* (shared with some diplodocoids and titanosaurs) is the osteologically induced curvature of the axial skeleton: despite having an acute wedged sacrum like all eusauropods (Fig. 5.8 B), the dorsal series have an OIC with a ventrally deflected spine due to the obtuse wedging of some middle dorsal vertebrae (Fig. 5.8 C). This condition can be seen in both CM 572 and CM 879. Also, the hyposphene-hypantrum complex shows a lot of variation on the dorsal vertebrae sequences of both specimens (Fig. 5.8 D), with some vertebrae having just a thickened tpol, some having a ventrally expanded hyposphene and some vertebrae completely lacking a hyposphene. This suggests a dorsal sector of the presacral spine with irregular stability *a priori*. Given the unstable phylogenetic position of this taxon (it has been considered an early branching Neosauropoda (Mocho, Royo-Torres, & Ortega, 2014; Carballido *et al.*, 2017), an early branching Macronarian (Wilson & Sereno, 1998; Royo-Torres *et al.*, 2006) or an early branching Diplodocoidea (Wilson, 2002; Whitlock, 2011b; Tschopp *et al.*, 2015) the significance of this variability on the hyposphene-hypantrum complex may have phylogenetic implications for the loss of the complex in some diplodocoids, or it may just be an autapomorphic feature. The extremely tall pedicels in the middle and posterior dorsals of this taxon separate the center of rotation from the zygapophyseal facets, indicating smaller dorso-ventral ranges of motion in these vertebrae than in comparable positions of other sauropods with smaller pedicels.

The caudal vertebrae centra of both specimens are shorter than those of most sauropods, with centra taller than long even in middle caudal vertebrae, indicating an overall short tail was likely. The osteological correlates for caudal musculature, particularly for *M. caudofemoralis longus* are almost as developed in the antero-posterior axis as in *Spinophorosaurus nigerensis*, with a lateral ridge appearing on caudal centrum 12, which is also present (each time more ventrally located) on caudal centra 13 and 14 (Fig. 5.8 A). The preserved chevrons of *Haplocanthosaurus priscus* (figured by Hatcher, 1903b) are apparently shorter respective to the caudal vertebrae than those of *Spinophorosaurus* or *Jobaria*, suggesting a smaller surface of insertion for CFL in the dorso-ventral plane than in earlier branching eusauropods. The sacrum is wider in latero-medial plane than those of *Spinophorosaurus*, *Jobaria* or *Patagosaurus*, implying femora more separated from the midline and therefore an action line for CFL with a greater adduction component than those taxa. The fourth trochanter is hard to interpret, as the femur is badly damaged from taphonomic processes, so its exact position cannot be determined with precision, it appears more medially placed than in the aforementioned eusauropods as well.

The iliac blade is not particularly tall at any point, with a relatively constant height from its preacetabular lobe until the postacetabular ischial pedicle. This implies none of the IT muscles from the iliac dorsal rim has a longer lever arm, and neither of the muscles originating at the iliac blade have origin surfaces particularly larger respect to each other.

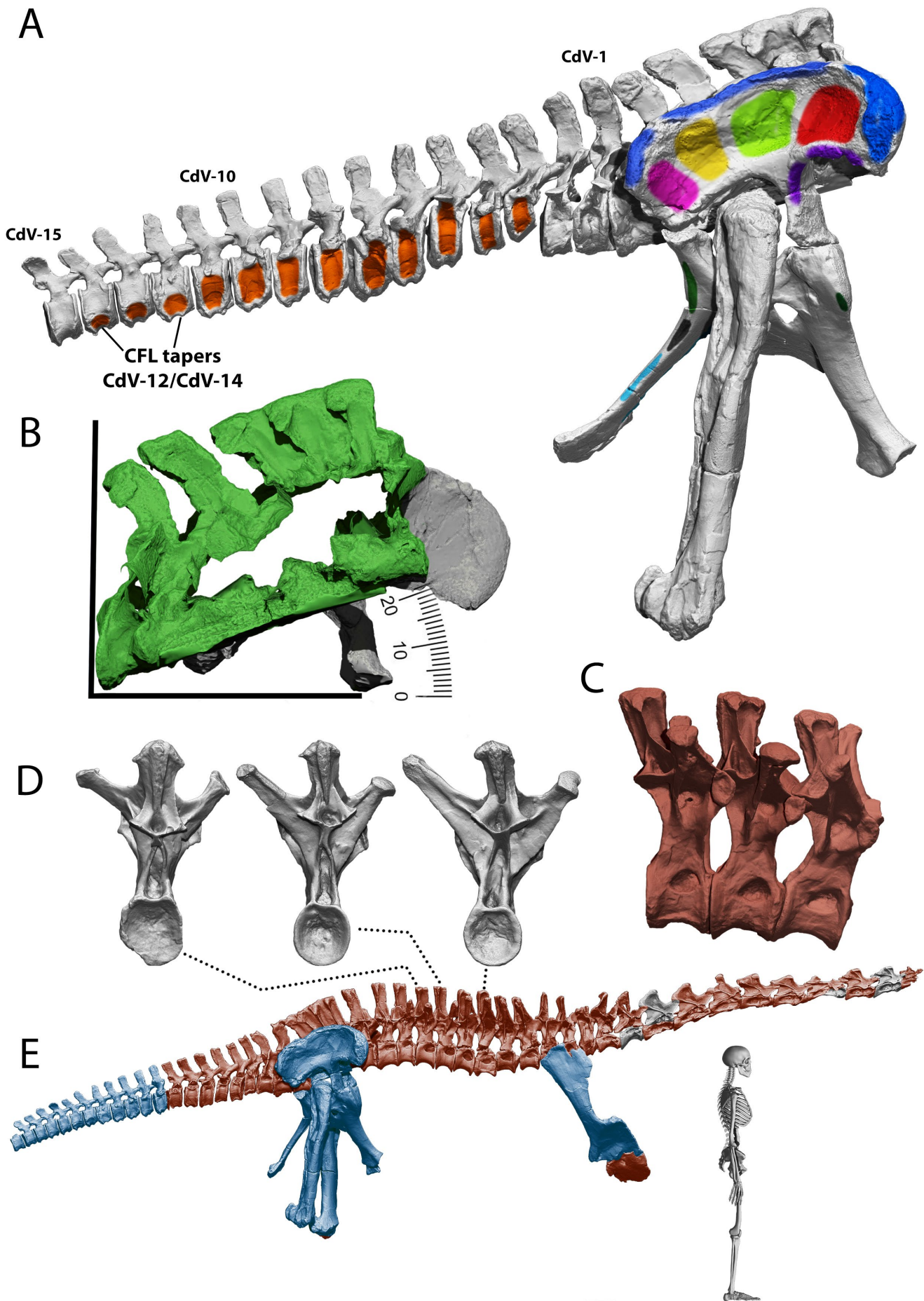


Figure 5.8 (previous page) - *Haplocanthosaurus priscus*.

A - Pelvis, sacrum, femur and tail of the holotypic specimen of *Haplocanthosaurus priscus* (CM-572) with muscular origins and insertions highlighted and colored (see Fig. 3.16 for color legend). **B** - Sacrum of the holotypic specimen of *Haplocanthosaurus priscus* (CM-572) showing a 20° wedging. **C** - Middle dorsal vertebrae of the holotypic specimen of *Haplocanthosaurus priscus* (CM-572) in lateral view, showing slight obtuse wedging (middle vertebra), which makes the anterior vertebra deflect ventrally. **D** - Middle dorsal vertebrae of the holotypic specimen of *Haplocanthosaurus priscus* (CM-572) in posterior view, showing different types of hyposphene within the same dorsal sequence (from left to right, rhomboid, thickened lamina, no actual hyposphene). Their position on the sequence is highlighted. **E** - Composite skeleton of *Haplocanthosaurus priscus* composed from elements stemming from the holotype CM-572 (blue) and referred specimen CM-879 (red), with elements interpolated from the anteriormost and posteriormost least damaged elements in gray. Human skeleton = 1700 mm.

Haplocanthosaurus delfsi McIntosh & Williams, 1988

Holotype. *CMNH 10380 relatively complete skeleton of a single adult individual, preserving anteriormost 4 cervical vertebrae, posteriormost 9 dorsal vertebrae, 5 sacral vertebrae, 14 caudal vertebrae in sequence, several ribs, partial left scapula, right sternal plate, both ilia, left pubis, left ischium, left femur.

Referred specimens. N/A

Locality and horizon. Delfs Quarry, Garden Park (Colorado, USA). Salt Wash Member, Upper Morrison Formation (USA), Kimmeridgian.

Personal description/remarks. This specimen has been mounted since the 1950s, so many observations regarding the osteologically neutral pose and analyses which would be performed in other specimens can only be roughly estimated for *H. delfsi*. As mentioned in chapter 1, the mount has several disarticulated vertebrae on the caudal series and the presacral column. Although the morphology of the sacrum cannot be as precisely assessed as in digitized specimens, it is definitely wedged as in other eusauropods. The disarticulated dorsal sequence, mounted to emerge slightly ventrally deflected from the sacrum, if articulated, would be anterodorsally deflected as in other sauropods. Also, some of the fossil dorsal vertebrae were mounted disarticulated, such as the posterior sector, enhancing this ventrally curved dorsal spine (Fig. 4.8 in McIntosh & Williams, 1988). However, since the original vertebrae are hard to study due to the mounted ribcage, it is hard to determine whether there is obtuse wedging on any of the preserved dorsal vertebrae. This is not evident on the figures from McIntosh & Williams (1988), as the slight ventral deflection seen in Fig. 9 of that paper may be due ventriflexion.

Regarding the caudal vertebrae, the posture would have likely resembled the horizontal OIC seen in other sauropods. Only the antero-posterior limit of *M. caudofemoralis longus* could be assessed in this specimen. The lateral surfaces of the caudal centra are concave, until caudal vertebra 12, where a ridge appears below the caudal rib. The ridge is present also in caudal vertebrae 13 and 14, the more posterior, the more ventral, as in other surveyed specimens. This implies CFL was tapering by CdV12, and reached at least CdV14, but whether it was already totally gone by CdV15 cannot be assessed at present. One of the retrieved chevrons has a lateral ridge on its lateral surfaces much like those present in *Spinophorosaurus*. Interestingly, this scar is asymmetric, suggesting the tapering of CFL, as other biological features, was not 100% symmetric.

Neosauropoda Bonaparte 1986

Diplodocoidea Marsh 1884

Rebbachisauridae Bonaparte 1996 *sensu* Tschopp *et al.* 2015

“Holotype”. **MMCh-PV-49 Partially articulated skeleton, with posteriormost 7 cervical vertebrae, anteriormost 4 vertebrae, 7 disarticulated middle to posterior dorsal vertebrae, several fragmentary ribs (some associated with the dorsal vertebrae), nearly complete right scapulocoracoid and right humerus.

Referred specimens. N/A

Locality and horizon. Las Campanas creek, 25 km southwest of Villa El Chocón (Neuquén, Argentina). Huincul Formation of the Neuquén Group (Argentina), upper Cenomanian.

Personal description/remarks. This remarkably complete specimen was found partially in articulation, and is one of the most complete Rebbachisauridae individuals known from Argentina. It preserves the last 6 cervical vertebrae and the first 4 dorsal vertebrae in connection, with additional 9 dorsal vertebrae that can be assembled in sequence, despite their variable states of preservation. In ONP, the posterior region of the neck articulates straight as in other eusauropods (Fig. 5.9 F). There are large gaps between the condyle and cotyle of the cervical vertebrae. However, given the poor state of preservation of this particular region in most cervical vertebrae, it is impossible to assess whether the condyles would fit inside the cotyles when complete or this specimen had large intervertebral spaces.

The range of motion on the neck of MMCh-PV-49 is relatively high, comparable to that of *Spinophorosaurus* (Fig. 5.9 A, B), as these vertebrae have relatively elongated and flat prezygapophyseal facets (Fig. 5.9 G, H), very large relative to their centrum size (although not as enlarged as in *Amargasaurus*). This renders a highly mobile neck in the dorso-ventral plane.

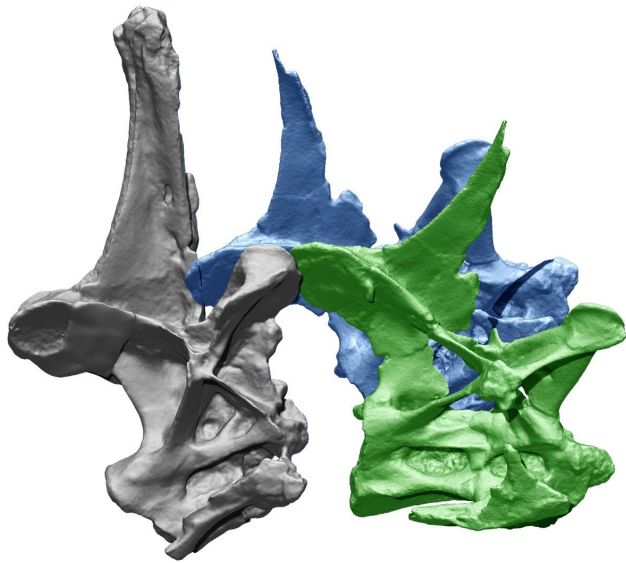
The dorsal vertebrae of the majority of known Rebbachisaurids lack hyposphene-hypantrum complex. Also the zygapophyseal facets of their middle and posterior dorsal vertebrae are one single zygapophyseal facet, conjoined in their medial side. Also, the angulation of this zygapophyseal facet has positional variability: some vertebrae have steeply angled zygapophyses (with an angle close to 60°) and some have an obtuse angle (around 140°). The highly complete series of MMCh-PV-49 allows exploring the transformation of this angulation along the series and to test the potential range of motion of these vertebrae. The anteriormost dorsal vertebrae have the steeper angled zygapophyses (Fig. 5.9 E), with DV-4 being the first dorsal with conjoined prezygapophyses (but not postzygapophyses). At midback, the zygapophyses reach an obtuse angle (Fig. 5.9 D) and the posteriormost vertebrae reach the most obtuse angle (Fig. 5.9 C). The zygapophyses of anteriormost dorsal vertebrae being so medio-laterally angled imply torsion is blocked (Mallison *et al.*, 2015). Given the anteriormost dorsal vertebrae bear the ribs which support the pectoral girdle, blocking torsion is likely to occur in this region, as it renders the region stable. However, in the absence of a rhomboid hyposphene-hypantrum, there is not a resistance as strong against ventral forces (i.e. the weight of viscerae). In anteriormost dorsal vertebrae it is not a large caveat, since the sternal plates and sternal ribs bear the load as well. In middle and posterior dorsal vertebrae (those which do not contact with the sternal plates), dorso-ventral bracing may be more necessary for stability, and hence the conjoined, subhorizontal prezygapophyses.

Apesteguía, Gallina, & Haluza (2010) proposed these obtuse zygapophyseal facets were one of three characters part of an adaptation for torsional motion in the middle and posterior dorsal vertebrae of rebbachisaurids, in which the centra would pivot against each other. Wilson & Allain (2015) found the characters proposed were a combination of plesiomorphies and anatomical impossibilities. While torsion is possible in posteriormost dorsal vertebrae in MMCh-PV-49, it appears more to be a secondary capability rather than an adaptation.

Figure 5.9 (next page) - Rebbachisauridae indet. (MMCh-PV-49) from El Chocón.

A - Maximum dorso-ventral range of motion between dorsal vertebra 1 and last cervical vertebra of MMCh-PV-49, with maximum dorsiflexion (blue) and ventriflexion (green) highlighted. **B** - Maximum dorso-ventral range of motion of the preserved neck of MMCh-PV-49. **C** - Posterior dorsal vertebra of MMCh-PV-49 in anterior view, showing conjoined, almost horizontal prezygapophyses. **D** - Middle dorsal vertebra of MMCh-PV-49 in anterior view, showing conjoined, slightly angled prezygapophyses. **E** - Dorsal vertebra 4 of MMCh-PV-49 in anterior view, showing conjoined prezygapophyses with a very steep angle. **F** - Reconstructed skeleton of MMCh-PV-49 (red) with hypothetical ulnae and radii (gray). Positions of C-E and G-H highlighted. Human skeleton = 1700 mm. **G** - Dorsal vertebra 1 in dorsal view, with the extremely large prezygapophyseal facet highlighted in red. **H** - Middle cervical vertebra in dorsal view, with the large, elongated prezygapophyseal facet highlighted in red.

A



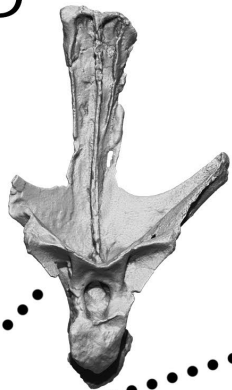
B



C



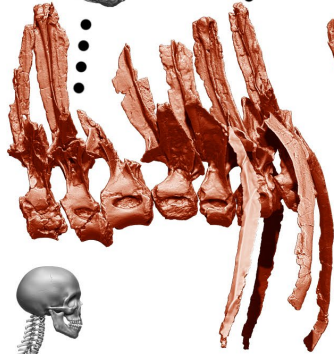
D



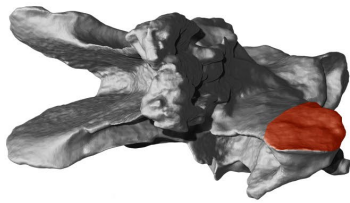
E



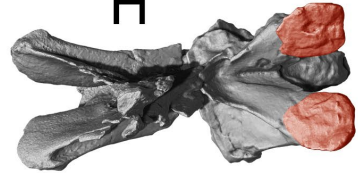
F



G



H



Flagellicaudata. Harris & Dodson 2004

Dicraeosauridae Janensch 1929 *sensu* Tschopp *et al.* 2015

Amargasaurus cazauui **Salgado & Bonaparte, 1991**

Holotype. **MACN-N-15 relatively complete skeleton of a single individual, preserving the braincase, 12 cervical vertebrae, 11 dorsal vertebrae, 5 sacral vertebrae, some proximal and middle caudal vertebrae, a right scapulocoracoid, humerus, radius and ulna, a partial right ilium, femur, tibia, fibula, astragalus and right metatarsals.

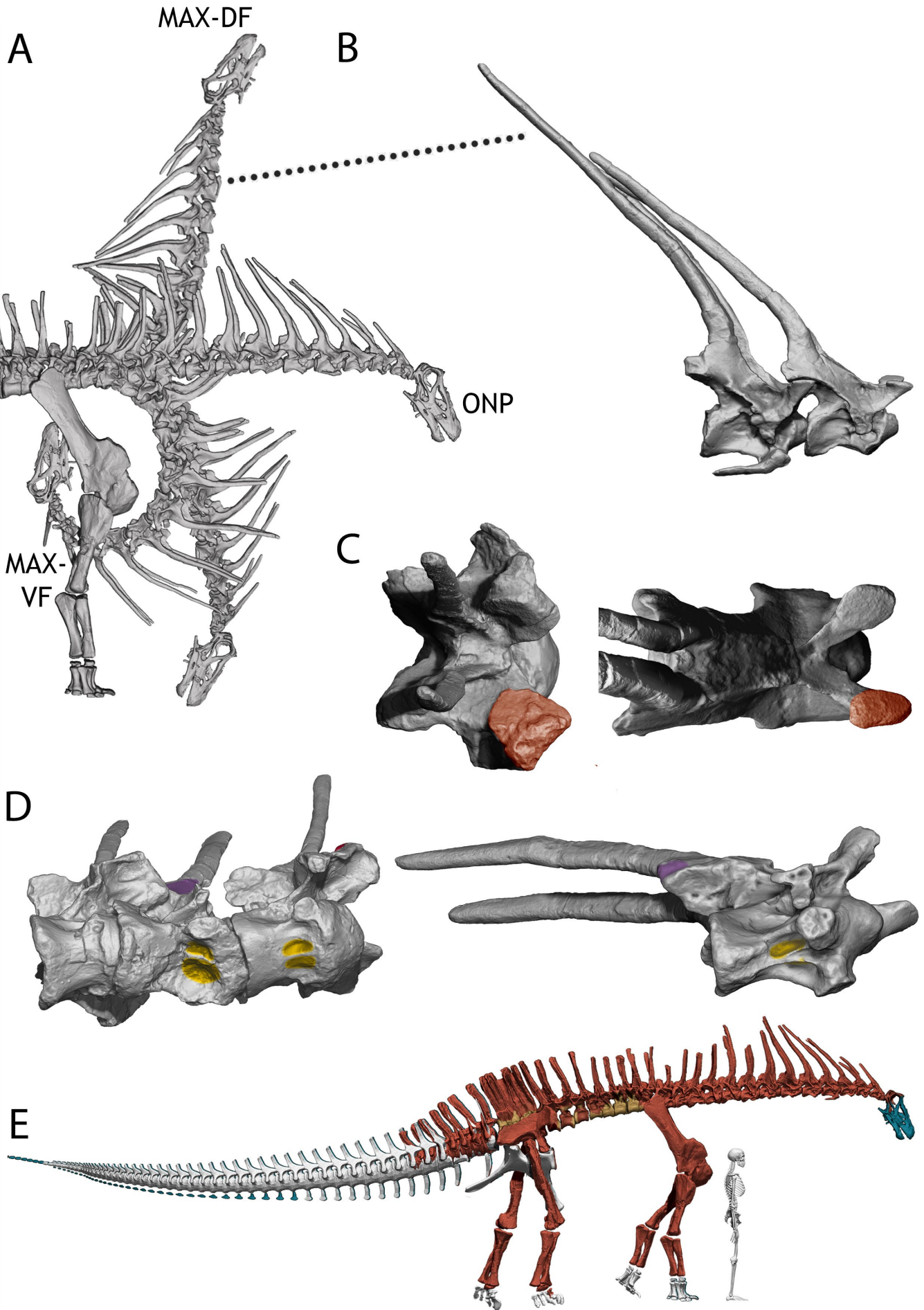
Referred specimens. N/A

Locality and horizon. 2.5 km southeast of La Amarga Arroyo bridge on Route nº 40 (Neuquén, Argentina). Lower Amarga Formation (Neuquén, Argentina), Barremian.

Personal description/remarks. Considering the poor preservation state of most dorsal vertebrae (particularly the middle and posterior ones), the fact that the very poorly preserved “sacrum” includes 6 neural spines and the complete dorsal series known from *Brachytrachelopan* and *Dicraeosaurus*, there is a good chance that there is a missing dorsal vertebra and the first “sacral” spine is actually a dorsal spine. The preservation of the dorsal vertebrae precluded creating a good ONP, as most of the pre and postzygapophyses have not been preserved. In order to have a proxy for ONP, most of the dorsal vertebrae were “articulated” by situating the neural spines parallel. This rendered an OIC of an almost straight, slightly dorsally bowed dorsal sector (Fig. 5.10 E). This is different from the condition seen in *Dicraeosaurus* (Stevens & Parrish, 2005), but more similar to the condition from *Brachytrachelopan* (see below). The neck, although distorted from taphonomical processes, is much better preserved than the dorsal vertebrae, which allow articulating the cervical vertebrae in ONP. The OIC is, like that of most sauropods, nearly straight with a little ventral deflection at the anteriormost part of the neck (Fig. 5.10 A).

One of the most notable features of this taxon are its extremely elongated and forked neural spines. This peculiar combination of extremely elongated neural spines with an orientation ranging from slightly anteriorly oriented in the posteriormost cervical vertebrae to a quite posteriorly inclined mid to anterior ones (unique in Dicraeosauridae, in which all other members have anteriorly pointed neural spines) imply a specialization in an already specialized lineage. Although difficult to test, both active and passive defence hypotheses have been proposed for these spines, as well as a potential role in sexual selection. Although none of these are actually testable, a range of motion analysis could refute the display hypothesis (if the range of motion was very limited).

However, the prezygapophyseal facets are extremely large and elongated in all cervical vertebrae up to the cervico-dorsal transition, substantially more than in *Brachytrachelopan* or any other surveyed diplodocoid species. However, dorsiflexion is limited due to the elongated, posteriorly directed neural spines collide creating an osteological stop (Fig. 5.10 A). Ventriflexion is not limited by osteological stop, and the head reaches the body before achieving the complete curvature allowed by the osteological range of motion. Ventriflexion allows the snout to reach the ground without dislocation or flexing/ abducting the forelimbs (Fig. 5.10 A), while maximum dorsiflexion allowed a maximum height of 4.5 m. This implies *Amargasaurus* was a medium to low browser, as previous studies proposed. The greater intervertebral flexibility than in other diplodocoids, many of which have also been interpreted as low browsers (i.e. *Nigersaurus*), support the absence of a double sail in the neck of *Amargasaurus*. It also supports the ability to perform potential display and/or agonistic behaviors in this taxon (Fig. 5.10 F), given the extensive range of motion capabilities for dorsi- and ventriflexion. Also, having flat prezygapophyses, torsion is not as restricted as in sauropods with transversely convex prezygapophyses.



F

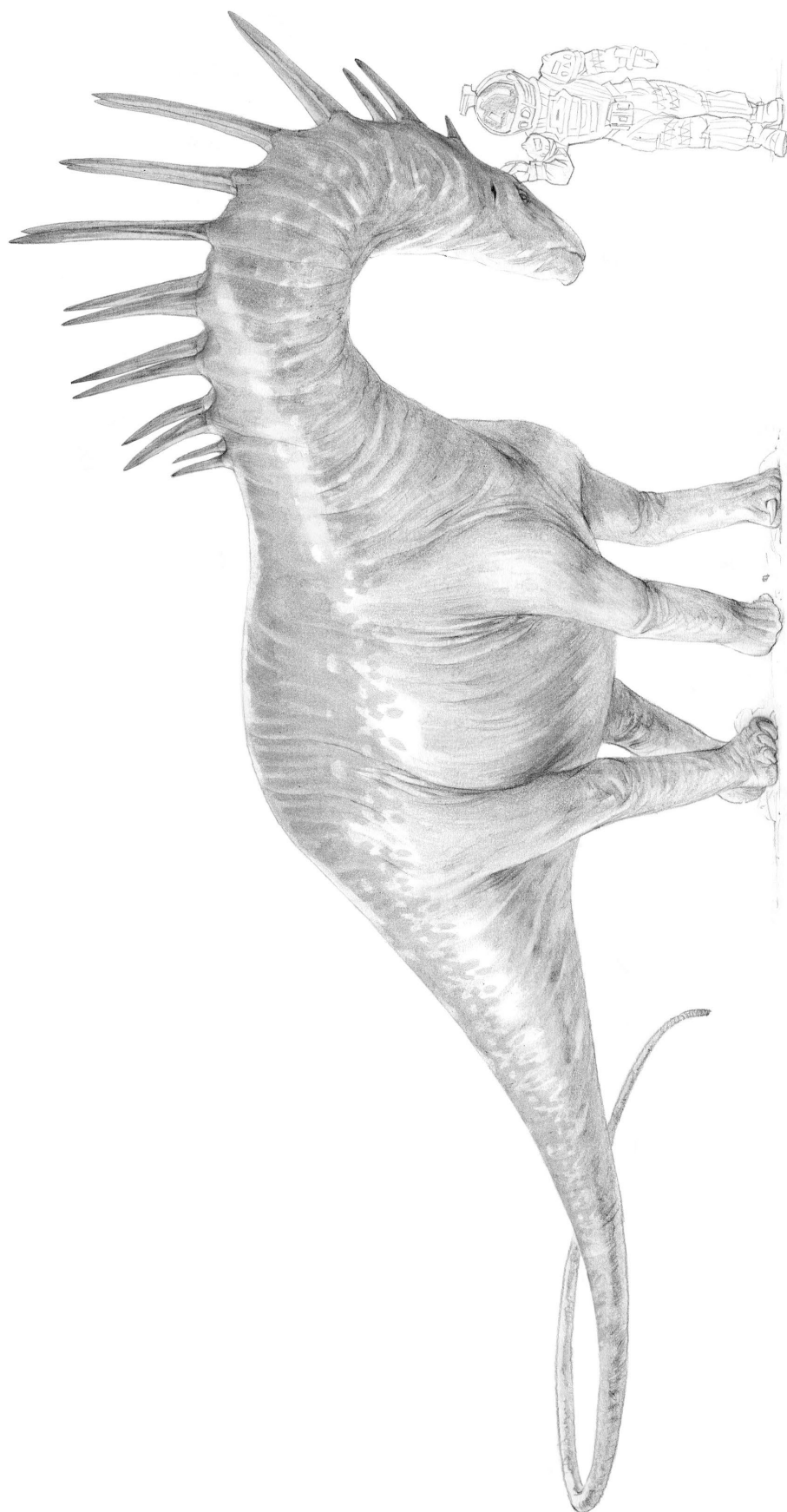


Figure 5.10 (previous page)- *Amargasaurus cazai*.

A - Maximum dorso-ventral range of motion of the neck of *Amargasaurus cazai*. **B** - Maximum dorsiflexion in cervical vertebrae 4 and 5 of *Amargasaurus cazai*, showing the osteological stop caused by the extremely elongated neural spines. **C** - Dorsal vertebra 1 (left) and cervical vertebra 4 (right) in dorsal view, with the elongated zygapophyseal facets highlighted in red. **D** - Articulated dorsal vertebrae 1 and 2 and cervical vertebra 12 (left) and cervical vertebra 3 (right) in ventro-lateral view, with origin for *M longus colli ventralis* on the well-developed ventral keels highlighted in yellow. **E** - Reconstructed skeleton of *Amargasaurus cazai* from elements of the holotypic specimen (red) with plaster restoration on the actual fossils (yellow), *Diplodocus sp.* skull (blue) and hypothetical modeled elements (gray). Human skeleton = 1700 mm. **F** - Paleoartistic restoration of *Amargasaurus cazai* using its neck spines for hypothetical display behavior. Size of human = 1700 mm. Drawing by Diego Cobo.

Brachyrachelopan mesai Rauhut et al. 2005

Holotype. **MPEF-PV 1716 partial skeleton of a single individual, preserving posteriormost 6 cervical vertebrae, 13 dorsal vertebrae, a partial sacrum, 12 proximal right side ribs, a partial right ilium, and a distal femur epiphysis.

Referred specimens. N/A

Locality and horizon. Cerro Cóndor NE sauropod site. Cañadón Calcáreo Formation, most probably Oxfordian-Tithonian, Chubut (Argentina).

Personal description/remarks. *Brachyrachelopan* is the sauropod with the shortest neck known to date. Although only the posteriormost 6 cervical vertebrae have been preserved, there are no signs on this specimen (or any other sauropod for that matter) that the anteriormost part of the neck would have more elongated vertebrae. As in all other Dicraeosauridae with the exception of *Amargasaurus*, the cervical neural spines are pointed anteriorly, and they are much more reduced in this taxon than in *Dicraeosaurus* or *Amargasaurus*.

The osteologically induced curvature of the dorsal spine can be assessed better than in *Amargasaurus*, as the preservation of the dorsal vertebrae in *Brachyrachelopan* is extremely good. In ONP, the dorsal series of *Brachyrachelopan* is slightly antero-dorsally deflected in the posteriormost four dorsal vertebrae. Then, there is a slight ventral deflection at dorsal vertebrae 10-9-8, due to the slight obtuse wedging in the centra, particularly on DV10. The rest of the dorsal spine from DV8 until the first dorsal vertebra articulates more or less horizontal without any apparent deflection. The overall result is similar to what appears to happen in *Dicraeosaurus* with a less abrupt ventriflexion in the curvature, and similar to what happens in *Neuquensaurus* MCS-5.

The sacrum of *Brachyrachelopan* is incomplete, so whether it was wedged or not cannot be directly observed. However, the wedged sacra of *Lingwulong* and *Dicraeosaurus* and the ventral deflection of the dorsal sector of the axial skeleton in *Brachyrachelopan* suggest its sacrum might have been wedged.

As of the digitization of the neck, preparation had not been completely carried out, so the only accessible pre-postzygapophyses were those of the first dorsal vertebra and last cervical vertebrae respectively. The relative size is surprisingly smaller, next to those of *Amargasaurus*, but also next to those of many other sauropods, whose largest zygapophyseal facets are found in the cervico-dorsal transition. The size of the prezygapophyseal rami in lateral view does not suggest the other prezygapophyses from the cervical vertebrae were particularly elongated as is the case of *Amargasaurus*, suggesting a less flexible neck on this taxon, which might have been functionally more similar to those of long necked stegosaurs (i.e. *Stegosaurus* or *Miragaia*).

Overall, present evidence suggests that, in order to fill the ecological niche more similar to those of phytophagous Ornithischian dinosaurs as proposed by Rauhut et al. (2005), *Brachyrachelopan* still had to cope with the same wedged sacrum inherited from earlier branching ancestors, and the solution to lower its neck toward the ground was also to modify the middle dorsal vertebrae. We cannot presently assess the humerus to femur proportions in *Brachyrachelopan*, but it is likely that it had a relatively shorter humerus, much like *Dicraeosaurus*.

Diplodocidae Marsh 1884 *sensu* Tschopp et al. 2015

Holotype. CM 84* Partial skeleton consisting of an almost complete presacral series (14 cervical and 10 dorsal vertebrae), five sacral vertebrae, the first 12 caudal vertebrae, 18 dorsal ribs, left scapulocoracoid, two sternals, interclavicle, right ilium, both pubes, both ischia and right femur.

Paratype. CM 94* Partial skeleton consisting of nine cervical vertebrae, nine dorsal vertebrae, five sacral vertebrae**, 39 caudal vertebrae, five chevrons, ribs, both scapulocoracoids**, sternal plates, both ilia**, both pubes**, both ischia**, left femur, right tibia, right fibula, complete right pes.

Referred specimens. CM 33985* Left fibula, left metatarsals III, IV, V from the same quarry as type and paratype but not belonging to either.

Locality and horizon. Sheep Creek Quarry D (Wyoming, USA). Middle Morrison Formation (USA), Kimmeridgian.

Personal description/remarks. *Diplodocus* has been one of the most widely studied sauropods in the last century. However, despite this, the majority of mounted skeletons, even those assembled in recent years (both in private and public institutions), have incorrectly articulated presacral vertebrae and pectoral girdles, likely due to preconceived notions (chapter 1). As mentioned, several preserved sacra of *Diplodocus carnegii* and other species within the same genus are markedly wedged. The wedged sacrum (Fig. 5.11 B) makes the presacral column deflect anterodorsally in the mounted specimen at the Seckenberg Museum of Natural History (Frankfurt, Germany; Fig. 5.11 C). However, Gilmore (1932) noted that while the posteriormost vertebrae of *Diplodocus* sp. USNM 10865 deflected anterodorsally, around the mid back of this specimen a ventral deflection occurred (which is not evident in the Seckenberg Museum mount). Unfortunately, no complete dorsal series of *Diplodocus* could be digitized and assembled to settle down whether the presacral spine of *Diplodocus* slopes anterodorsally as in *Spinophorosaurus*, *Camarasaurus* or *Brachiosaurus* or it is arched, as in *Haplocanthosaurus*, *Dicraeosaurus* or *Neuquensaurus*.

The long neck of *Diplodocus carnegii* has elongated cervical vertebrae with short, wide and convex zygapophyseal facets (Fig. 5.11 A). Previous studies have found this to cause the neck of *Diplodocus* to be less flexible than those of other sauropods with more elongated zygapophyseal facets, such as *Apatosaurus* (Stevens & Parrish, 1999). The convex zygapophyseal facets would brace against torsional forces, as happens with the medially inclined zygapophyses of *Alligator* caudal vertebrae (Mallison *et al.*, 2015). Stevens & Parrish (1999) found *Diplodocus* able to ventriflex its neck to its head was well below ground level, to the point to suggest an aquatic plant diet. However, considering the wedged sacrum and the still unclear orientation of presacral vertebrae, it is uncertain whether *Diplodocus* would reach ground level just ventriflexing the neck.

Diplodocus carnegii is one of the few species of sauropods with confirmed ossified interclavicles (Tschopp & Mateus, 2013), suggesting a stronger anchor for *M. pectoralis*. However, when comparing this taxon with other sauropod species with ossified interclavicle such as *Spinophorosaurus* or *Jobaria* there is one big difference in the anchor for *M. Deltoideus scapularis* one of the agonist muscles (adduction (P) vs. abduction (DS)): the former taxa have distally expanded scapulae, whereas the scapulae of *Diplodocus* lack such an expansion, suggesting a smaller origin for DS. Tschopp & Mateus (2013) proposed the ossification of dermal pectoral girdle elements in diplodocids, *Shunosaurus* or mamenchisaurids may be related with stabilizing the body against lateral motion of the specialized tails. However, the study of Myhrvold & Currie (1999) reported that the energy necessary to create a sonic boom by the whiplash of a diplodocid would be less than that needed for walking. This would not strongly support (but neither refutes) the hypothesis of Tschopp & Mateus.

Overall, with the availability of postcranial material of *Diplodocus*, building a digital model from digitized fossils in the future will be key in settling in the abundant evidence from previous studies into the framework of a rigorous skeletal mount.

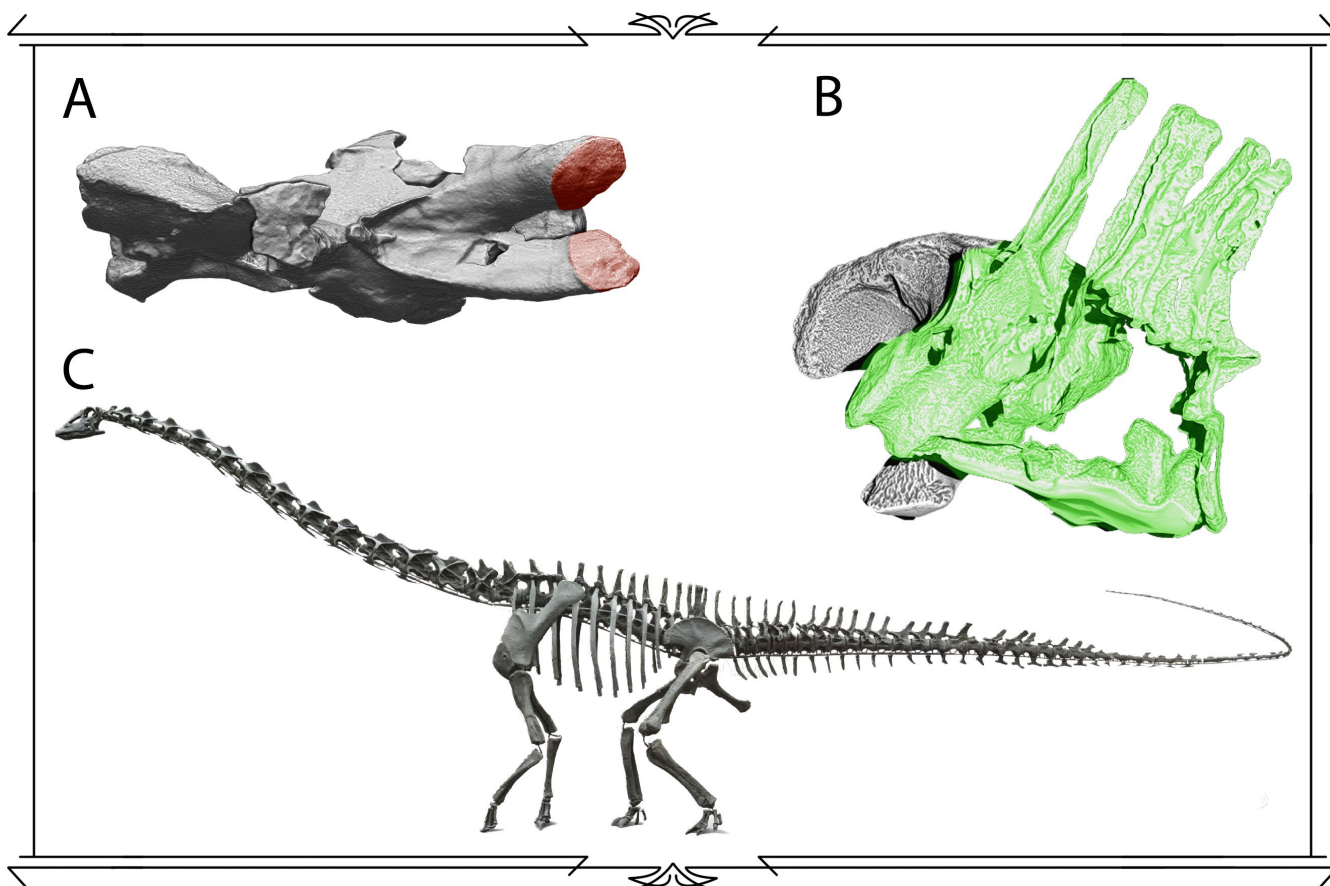


Figure 5.11 - *Diplodocus carnegie*.

A - Middle cervical vertebra of *Diplodocus carnegie* (CM-94) in dorsal view, with wider than long prezygapophyseal facets highlighted in red. **B** - Sacrum and coalesced ilium of *Diplodocus carnegie* (CM-94) in lateral view, showing a 16° wedging. **C** - Mounted skeleton of *Diplodocus* at the Naturmuseum Senckenber (Frankfurt, Germany), showing the effect on the sacrum on the osteologically induced curvature, making the presacral series slope anterodorsally.

Barosaurus lentus **Marsh 1890**

Holotype. YPM 429* Partial skeleton consisting of 3 cervical vertebrae**, 6 dorsal vertebrae, fragmentary sacrum, 13 caudal vertebrae, 7 left and 2 right ribs, 3 chevrons, sternal plate, right pubis.

Referred specimens. AMNH 6341 Partial skeleton consisting of an uninterrupted axial sequence of posteriormost six cervical vertebrae, nine dorsal vertebrae, five sacral vertebrae and 29 caudal vertebrae, six ribs and fragments, one chevron, left scapulocoracoid, partial right scapula, left humerus, both ilia, both pubes, both ischia, right hindlimb and partial right pes. **CM 11984*** Articulated series of presacral vertebrae from the anterior part of the neck to mid dorsal region, several ribs. Under preparation as of 2017. **CM 1198** Four cervical vertebrae. **CM 21744** Articulated distal half of humerus, radius, ulna and most of the manus. **ROM 3670** Partial skeleton consisting of nine dorsal vertebrae, sacrum, 14 caudal vertebrae, both femora. Likely, the same individual as CM 1198.

Locality and horizon. Hatch Ranch, Piedmont Butte, eastern Black Hills (South Dakota, USA). Morrison Formation (USA), Kimmeridgian.

Personal description/remarks. Although the similarities between *Diplodocus* and *Barosaurus* have been mentioned numerous times, one of the more neglected differences between both genera are the cervical vertebrae (Taylor & Wedel, 2016). The cervical vertebrae of *Barosaurus* are more elongated than in *Diplodocus* or *Kaatedocus*, and the zygapophyseal facets are even less antero-posteriorly elongated than in *Diplodocus* (Fig. 5.12 B). This renders a smaller range of motion in the dorso-ventral plane than in other sauropods with antero-posteriorly shorter zygapophyseal facets (Fig. 5.12 C), such as *Camarasaurus* or *Diplodocus* as proposed by Taylor & Wedel (2016). However, their proposal of a greater lateral range of motion could not be evaluated with the digitized specimens (as not two of them preserve both the pre- and postzygapophyses at once). It is true, however, that cervical vertebrae of *Barosaurus* are wider than those of *Diplodocus* or *Kaatedocus*, making the lever arms for lateral flexion longer. The cervical ribs and diapophyses, were many of these muscles origin

and insert (such as *M. intercostales*) are more posteriorly placed than in other diplodocids, making the moment arm shorter, and conferring them mechanical advantage for muscle contraction in the lateral plane.

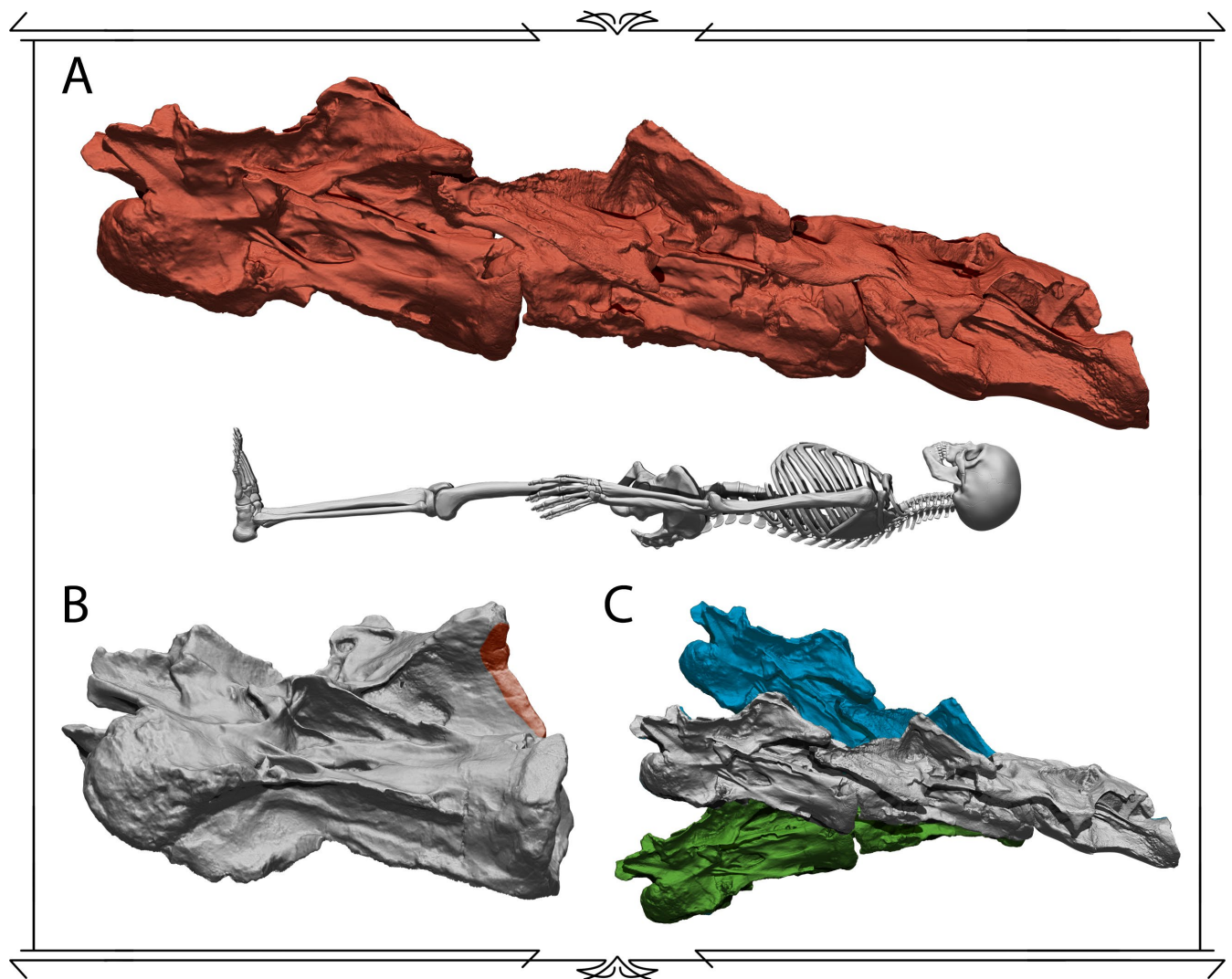


Figure 5.12 - *Barosaurus lentus*.

A - Middle and posterior cervical vertebrae of the holotypic skeleton of *Barosaurus lentus* (YPM-429) articulated in osteologically neutral pose, lateral view. Human skeleton = 1700 mm. **B** - Cervical vertebra S of the holotypic skeleton of *Barosaurus lentus* (YPM-429) in ventro-lateral view, with the extremely short and wide postzygapophyseal facet highlighted in red. **C** - Maximum dorso-ventral range of motion of the three holotypic cervical vertebrae of *Barosaurus lentus* (YPM-429), with maximum dorsiflexion (blue) and ventriflextion (green) limited by disarticulation, not osteological stops.

Macronaria Wilson & Sereno 1998 *sensu* Sereno 2005

Camarasauridae Cope 1877 *sensu* Mocho *et al.* 2014

Camarasaurus supremus Cope, 1877

Amphicoelias latus Cope, 1877b:4.

Caulodon diversidense Cope, 1877c:193.

Caulodon leptoganus Cope, 1877c:193.

Camarasaurus leptodirus Cope, 1879:404.

Camarasaurus supremus: Osborn and Mook 1921:262.

Holotype. *AMNH 5760 remains of at least two different individuals consisting of 2 cervical vertebrae, 18 dorsal vertebrae, 55 caudal vertebrae, 17 left ribs, 8 chevrons, a right scapula and coracoid, a partial left ilium, a left and right pubis (of different individuals), 2 left and 2 right ischia, a left femur, a right tibia and a right fibula (McIntosh, 1998).

Referred specimens. **AMNH 5761 (topotype) remains of two, maybe up to three different individuals, including DMNH 27228 2 cervical, 1 dorsal and 2 caudal vertebrae, 1 pubis.

Locality and horizon. Near Cope's Nipple, Garden Park Colorado (USA). Uppermost levels of Morrison Formation, Late Kimmeridgian-Tithonian.

Personal description/remarks. *C. supremus* is the largest known species of *Camarasaurus* and the first to be described. Since all its remains stem from several quarries in the area of Garden Park, there are no quarry maps and field photographs show associated but disarticulated bones. The digitized specimen number (AMNH 5761) has remains of up to three individuals stemming apparently from a single quarry. Some bones of compatible sizes articulate perfectly and appear to stem from the same individuals, others are of radically different sizes and can be ruled out as belonging to different individuals, but others are of compatible sizes but do not articulate due to taphonomical deformation. In the majority of cases, retrodeformation would allow a seamless articulation, suggesting the bones stemmed from the same individual. However, an in-depth study of what has survived of E.D. Cope's and O.W. Lucas' correspondence and the shipment manifests are key to solve the number of specimens under the number AMNH 5761 (McIntosh, 1998).

Overall, the reconstructed skeleton of AMNH 5761 (Fig. 5.13 D) bears a lot of similarity with the reconstructed composite skeleton of *Camarasaurus grandis* (from the bones of individuals YPM 1901 and 1905) and the preserved portions of CM 584. The sacrum is wedged around 16° (Fig. 5.13 C), making the presacral and caudal series to deflect from each other. The tail describes a sigmoidal curvature, although less pronounced than that of *C. grandis* and more similar to that of CM 584. There are no dorsal vertebrae with obtuse wedging, so the presacral column is dorsally deflected from the sacrum. The dorsal vertebrae articulate slightly dorsally deflected. Most of them articulated without retrodeformation, with the exception of dorsal vertebrae DV8, DV7 and DV4. One of the particularities found in the cervical vertebrae of AMNH 5761 is two fused cervico-dorsals (interpreted here to be the first dorsal vertebra and the last cervical vertebra, due to the shape of the cervical rib articulating with the latter). The cervical vertebra is around 10° deflected from the dorsal in lateral view (Paul, 2017) and the pathology which may have caused the fusion appears to have altered the posture to some extent (Guerrero & Vidal, 2018). However, the first dorsal and last cervical vertebrae of CM 584 articulate also with a similar deflection in ONP (Fig. 5.15 C), suggesting this condition may be characteristic of *Camarasaurus*. The anterior sector of the neck (from CV6 to axis) has a somewhat bowed OIC, with CV6-CV4 dorsally deflected and CV4-axis strongly ventrally deflected (Fig. 5.13 B). This posture is very similar to that of *C. grandis* (Fig. 5.13 A), hinting that it may also be characteristic of the genus.

The pelvis of AMNH 5761 is one of the set of bones which more likely belongs to the same single specimen (they all articulate perfectly among them and with the sacrum without needing retrodeformation at all). It is particularly retroverted when articulated (although not as extreme as in the holotype of *Cathetosaurus lewisii* (Jensen, 1988; McIntosh *et al.*, 1996)), with both pubes and ischia rotated posteriorly (counterclockwise in left lateral view). The implication suggested by Paul (2017), who argued a retroverted pelvis implied a wedged sacrum has been refuted in chapter 2.3. Jensen (1988) proposed the retroverted pelvis as giving mechanical advantage when rearing in *Cathetosaurus*. While *C. supremus* does not have as much retroversion as *Cathetosaurus*, so the functional implications may differ. A more in-depth functional analysis on the pelvis of *Cathetosaurus* should be carried out to fully understand the precise functional differences of the pelvis.

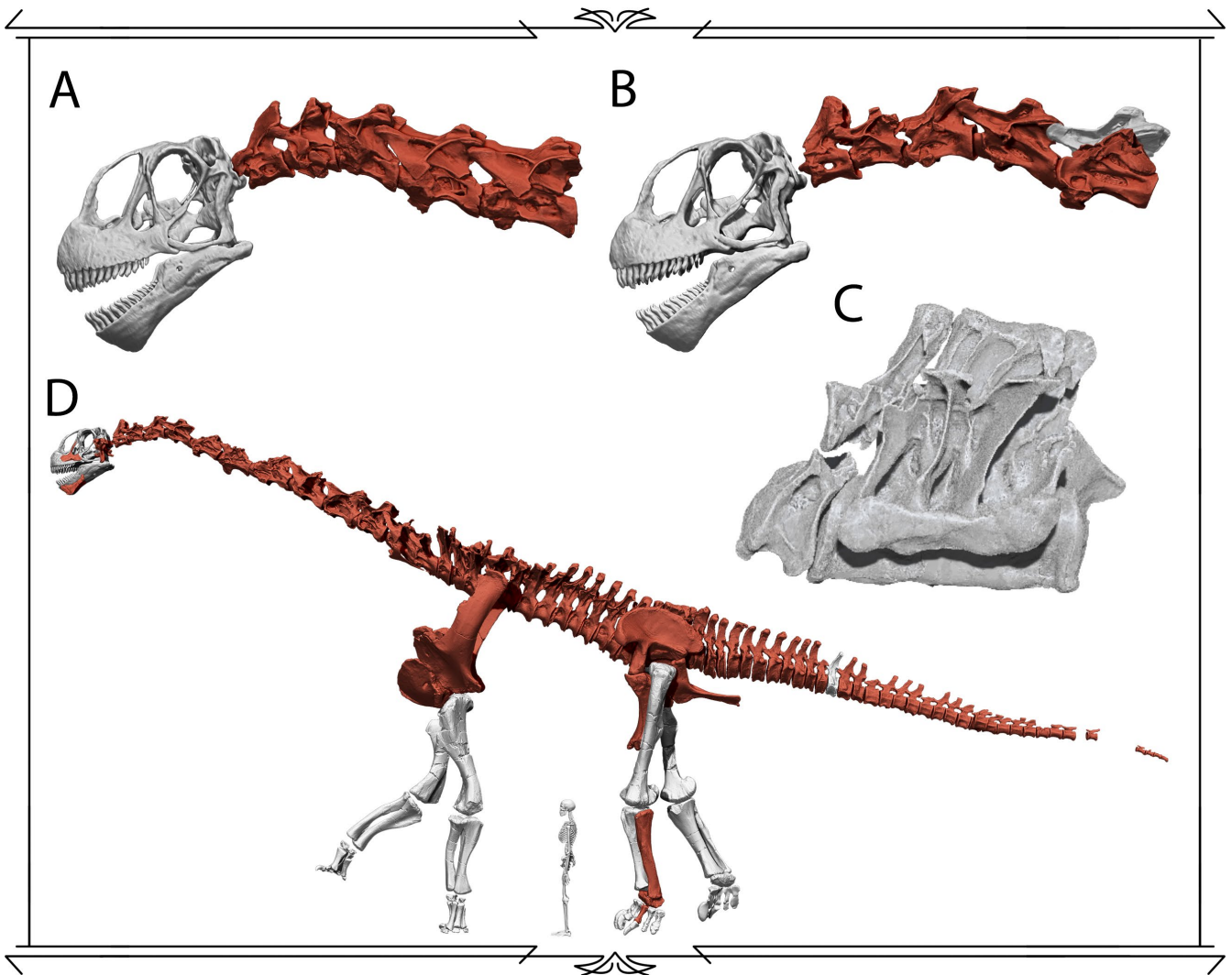


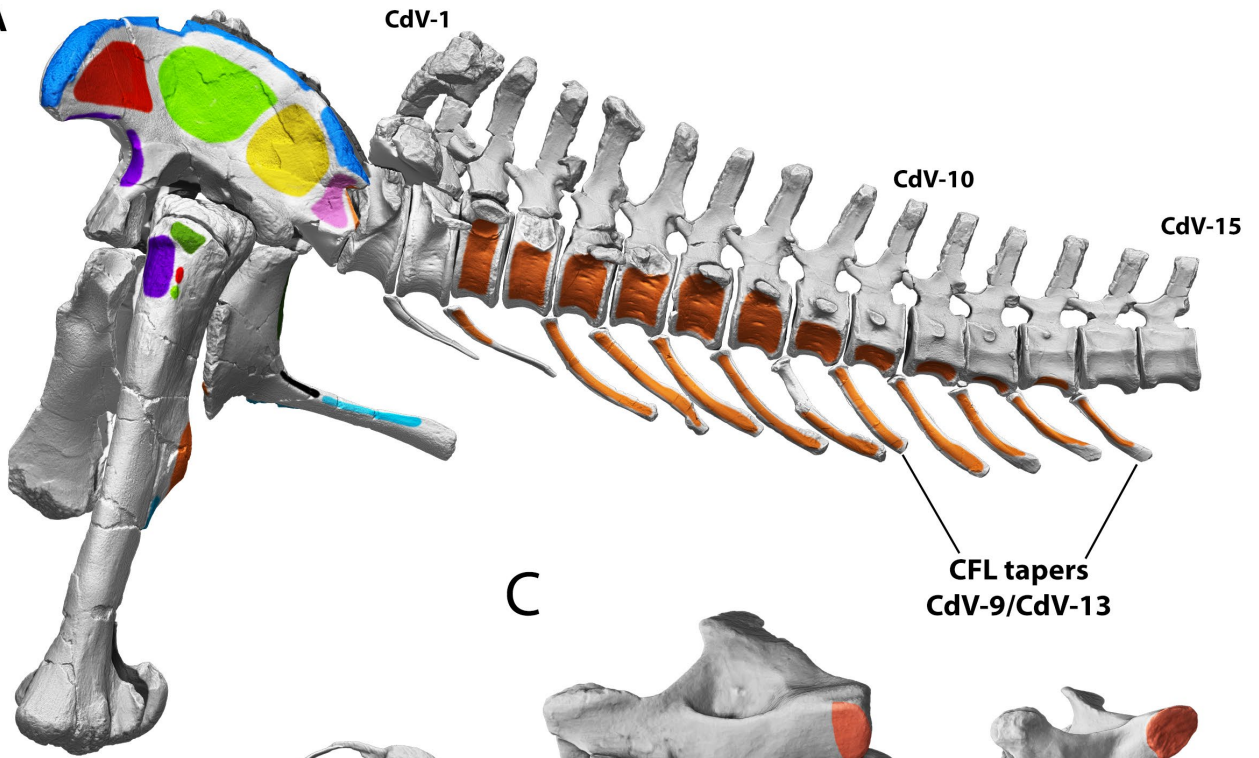
Figure 5.13 - *Camarasaurus supremus*.

A - Anteriormost six cervical vertebrae of *Camarasaurus grandis* (YPM-1905) in osteologically neutral pose. Note these vertebrae stem from the same individual. **B** - Anteriormost six cervical vertebrae of *Camarasaurus supremus* (AMNH-5761) in osteologically neutral pose. Note these vertebrae likely come from different individuals (McIntosh, 1998), yet the osteologically induced curvature is very similar to that of *C. grandis*. **C** - Sacrum of *Camarasaurus supremus* (AMNH-5761) in lateral view, showing wedging as well as a ventrally rotated sacricostal yoke, likely the origin of pelvic retroversion. **D** - Reconstructed skeleton of *Camarasaurus supremus* (AMNH-5761) from elements of the holotypic specimen (red) with elements from the reconstruction of *Camarasaurus grandis* (gray) in Fig. 5.14 . Human skeleton = 1700 mm.

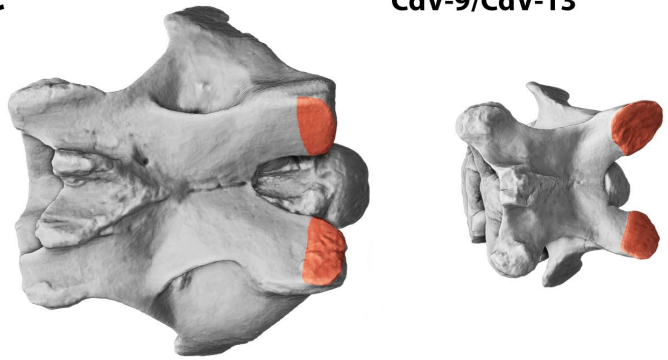
Figure 5.14 (next page) - *Camarasaurus grandis*.

A - Pelvis, sacrum, femur and tail of the holotypic specimen of *Camarasaurus grandis* (YPM-1901) with muscular origins and insertions highlighted and colored (see Fig. 3.16 for color legend) **B** - Maximum dorso-ventral range of motion in the anteriormost 6 cervical vertebrae of *Camarasaurus grandis* (YPM-1905) in lateral view. **C** - Cervical vertebra 6 (right) and 3 (left) in dorsal view, with the prezygapophyseal facets highlighted in red. **D** - Maximum latero-medial range of motion in the anteriormost 6 cervical vertebrae of *Camarasaurus grandis* (YPM-1905) in lateral view. **E** - Reconstructed skeleton of *Camarasaurus grandis* from elements of the holotypic specimen YPM-1901 (red), paratype YPM-1905 (blue) and elements from other *Camarasaurus* specimens (gray). Human skeleton = 1700 mm. **F** - Paleoartistic restoration of *Camarasaurus supremus*. Size of human = 1700 mm. Drawing by Diego Cobo.

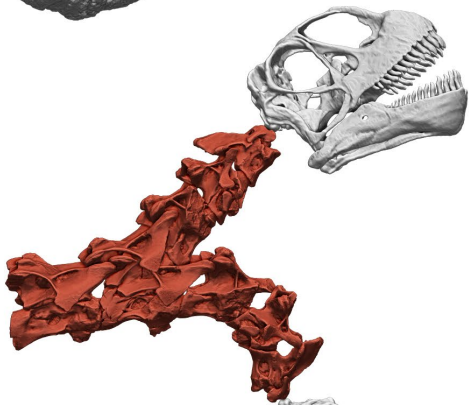
A



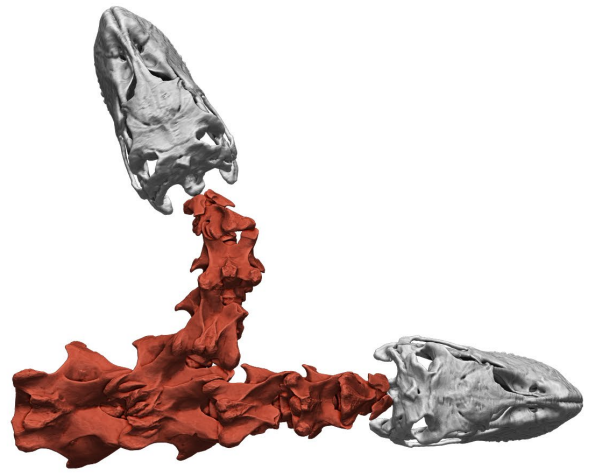
C



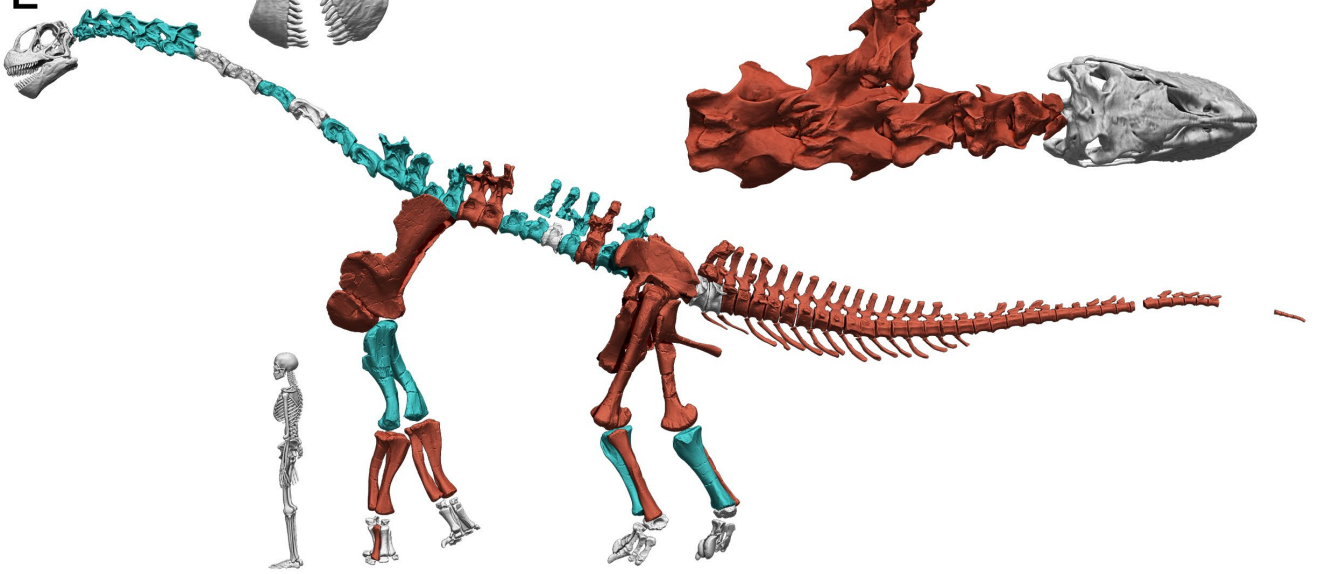
B



D



E



F



Camarasaurus grandis Marsh 1877

Apatosaurus Marsh, 1877:515 (in part).

Amphicoelias Cope, 1877b:2 (in part).

Morosaurus impar Marsh, 1878a:242.

Morosaurus robustus Marsh, 1878b:414.

Pleurocoelus montanus Marsh, 1896:184.

Camarasaurus grandis Gilmore, 1925:352.

Holotype. **YPM 1901 partial skeleton consisting of a basioccipital, at least 3 complete dorsal vertebrae, 27 caudal vertebrae in sequence (from CdV1 to CdV27) and possibly the distalmost part of the tail, right scapula and coracoid, left sternal plate, 2 femora, left tibia and fibula, rib fragments and a set of chevrons (which may contain chevrons of other individuals).

Paratypes. **YPM 1905 (including formerly YPM 1900) fairly complete skeleton, including a fairly complete skull, 10 cervical vertebrae (anteriormost six complete, posteriormost four missing the arches), most, or possibly all dorsal vertebrae (see remarks), a partial sacrum (formerly YPM 1900, holotype of *Morosaurus impar*) 12 anterior and mid caudal vertebrae, both scapulae, both coracoids, left humerus, right ulna, right ischium, both femora, both tibiae, both fibulae, some pes elements. *YPM 1903 both coracoids, right scapula, left pubis, both ischia, left femur.

Referred specimens. DMNH 2850, 3 middle dorsal vertebrae. **FMNH-P-25118, 10 dorsal vertebrae (2 on loan to Mesa County Junior College in Grand Junction, Colorado, USA), 4 sacral vertebrae (4 centra, 3 arches) right scapulocoracoid. GMNH-PV-101 nearly complete adult skeleton. KUVF 1354 four dorsal vertebrae.

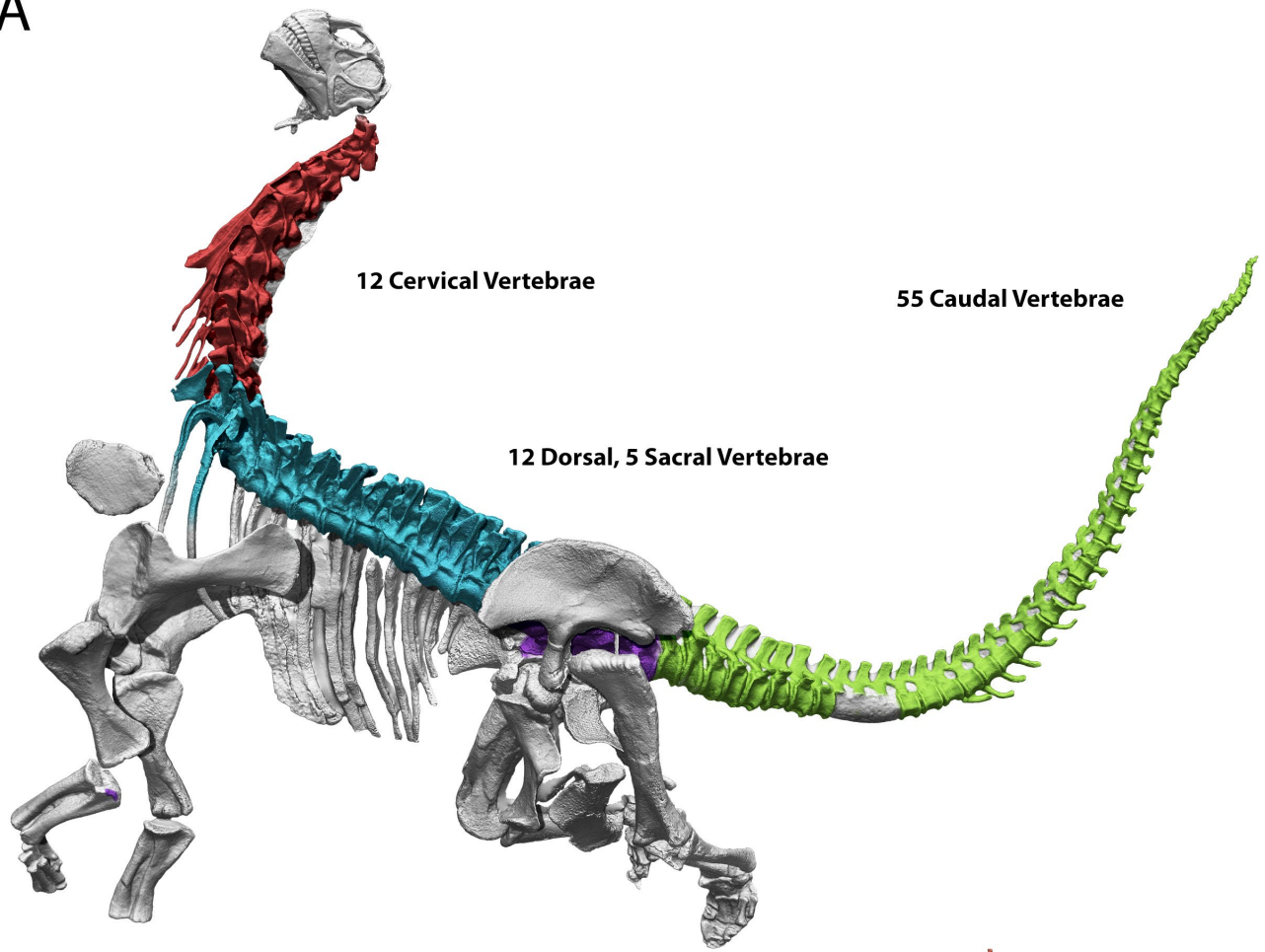
Locality and horizon. Middle and Upper lower levels of Morrison Formation, Late Kimmeridgian, Late Jurassic of south-central Wyoming, Colorado and New Mexico (USA)

Personal description/remarks. The holotype and cotypes from Como Bluff Quarry 1 originally excavated by Marsh's crew were subadult individuals, so full-grown size is uncertain. The most conspicuous characters separating this species from other *Camarasaurus* species are a well-marked process on the anterior side of the scapula and anterior-middle dorsal vertebrae with relatively high pedicels. These characters are absent from some referred specimens, which in absence of diagnosable characters, should be reassigned to *Camarasaurus* sp. until a better diagnosis for the species is established.

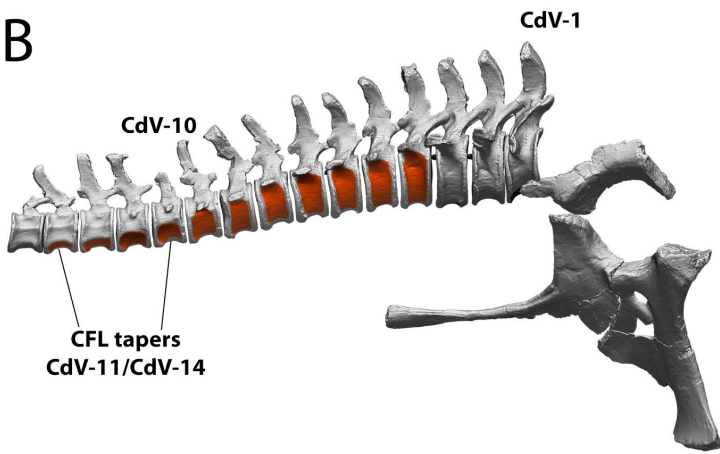
The assembled skeleton of *C. grandis* is a composite of mainly YPM 1901 and YPM1905, with some interpolated bones and hand and feet modified from *Camarasaurus lentus* CM 11338 scaled to match the size of the few preserved bones preserved from the YPM specimens. Overall, the virtual skeleton is missing a great deal of the posterior half of the neck (some vertebrae and all neural arches), some dorsal centra and neural arches and the sacral arches. The sacrum of YPM 1905 (formerly YPM 1900) is wedged 16° in lateral view. Assuming the same condition as in *C. supremus* (the dorsal series articulated without strong dorsal or ventral deflection among its elements), the presacral vertebrae would deflect 16° from the first caudal vertebra (Fig. 5.14 E). The anterior sector of the neck has a slightly bowed OIC, with CV6-CV4 deflecting dorsally and CV4-axis strongly ventrally deflected (Fig. 5.13 A), due the centra of CV4 and CV3 have obtuse wedging. This condition is also present in the composite virtual skeleton of *C. supremus*, suggesting it is characteristic of the genus. The tail articulates in a sigmoid curvature, stronger than the OIC of other sauropods in general and other studied *Camarasaurus* in particular (Fig. 5.14 E), but overall it is similar.

The anteriormost cervical vertebrae have prezygapophyses wider latero-medially than antero-posteriorly (Fig. 5.14 C), with the exception of CV3, which has more or less rounded (subequally as long as wide). This renders an overall smaller range of motion per joint in the anterior sector of the neck, with the exception of the CV3-axis joint, which can deflect more degrees than other cervical vertebrae pairs. On the other hand, the anterior and middle cervical vertebrae are wider than tall (Fig. 5.14 C), including particularly wide diapophyses, similar to the condition of *Barosaurus* or *Ligabuesaurus* (which also have wider than long prezygapophyses). The more lateral the diapophyses (and therefore, the tuberculum of the cervical rib) are from the sagittal plane and center of rotation, the larger the lever arm for lateral flexion (particularly of *M. intercostales*). This indicates a more efficient lateral flexion (Fig. 5.14 D), at the expense of longer contractions. The reduction of sites of insertion of

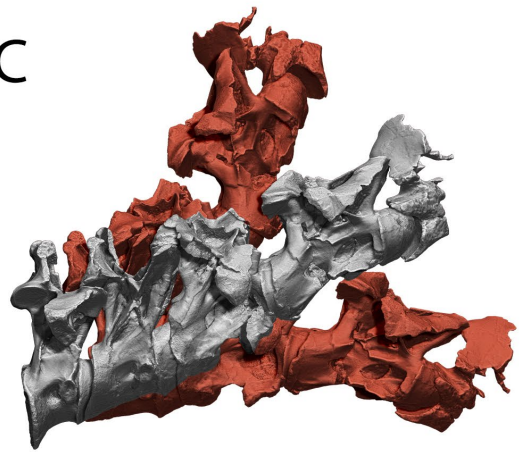
A



B



C



D

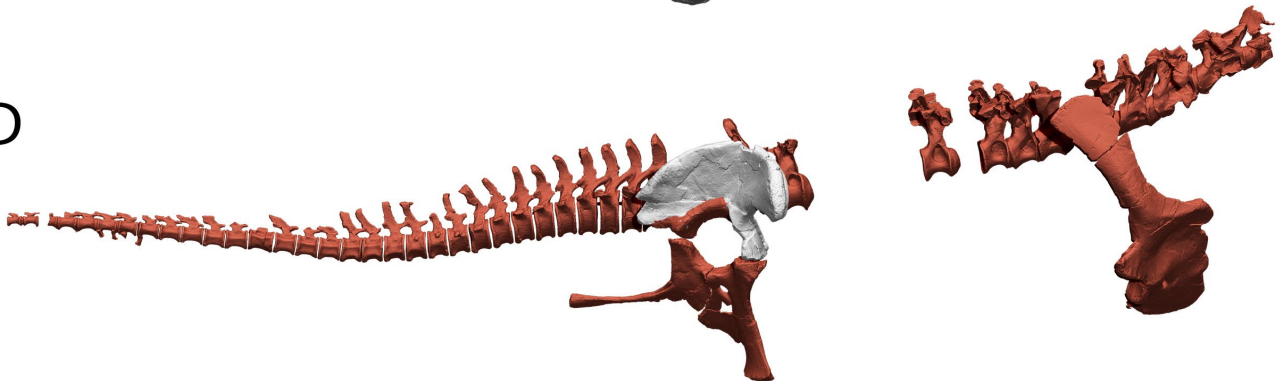


Figure 5.15 (previous page)- *Camarasaurus lentus* and *Camarasaurus* sp.

A - Referred *Camarasaurus lentus* specimen (CM-11338), the most complete skeleton known of a sauropod dinosaur, with different sectors of the axial skeleton highlighted. **B** - Pelvis, femur and tail of the specimen CM-584 referred to *Camarasaurus* sp. with muscular origins and insertions for *M. caudofemoralis longus* highlighted and colored (see Fig. 3.16 for color legend). **C** - Maximum dorso-ventral range of motion of the posteriormost region of the neck of CM-584. **D** - Reconstructed skeleton of *Camarasaurus* sp. (CM-584) from elements from this specimen (red) and *Camarasaurus grandis* (gray). Human skeleton = 1700 mm.

muscles for dorsal (shorter neural spines, reduced epiphyses...) and ventral flexion (absence of ventral keels) suggests *Camarasaurus* could exert stronger contractions for lateral flexion of the neck than for flexion in the dorso-ventral plane.

The ilium has a more developed preacetabular lobe in the antero-posterior axis than early branching eusauropods such as *Patagosaurus* or *Spinophorosaurus*. This implies a more developed origin surface for *M. iliotrochantericus* (ITC). The preacetabular lobe is also more laterally oriented, which overall suggest an even more efficient line of action for protraction, rather than for abduction. The height of the iliac blade is sub-equal, suggesting none of the muscles originating in the ilium was particularly more developed respect to each other.

Regarding caudal musculature, *M. caudofemoralis longus* shows a decrease both in antero-posterior and dorso-ventral axes for the first time in surveyed sauropods in *Camarasaurus* (Fig. 5.14 A). Not only does CFL taper at a more anterior position than in earlier branching eusauropods (starting at CdV-9 and disappearing by CdV-13), but the chevrons are smaller relative to centrum height (Fig. 3.20). All this implies a relatively smaller CFL muscle mass, but still very large compared with deeper nested taxa.

Camarasaurus lentus **Marsh 1889**

Uintasaurus douglassi **Holland 1919**

Camarasaurus annae **Ellinger 1950**

Holotype. *YPM 1910 partial juvenile skeleton consisting of the jaws, partial braincase, 11 cervical vertebrae, 12 dorsal vertebrae, five sacral vertebrae, 14 anterior and middle caudal vertebrae, distalmost caudal vertebrae, several chevrons left scapula, right coracoid, humeri, left ulna, ilia, right pubis, left ischium, left femur, tibiae, left fibula, left pes.

Referred specimens. **CM 11338 almost complete juvenile skeleton including a complete skull, a nearly complete axial skeleton (only missing caudal vertebrae centra 10-12 and come left side ribs), complete left and right pectoral girdles and forelimbs.

Locality and horizon. Morrison formation,

Personal description/remarks. The juvenile specimen CM 11338 is the only known *Camarasaurus* individual with a completely preserved axial skeleton, allowing therefore to assess its vertebral formula. Ever since the description of this specimen in 1925, vertebral formula for *Camarasaurus* had been established as 13 cervical, 12 dorsal, five sacral and 53+/- caudal vertebrae. However, a close inspection of the skeleton CM 11338 shows no evidence for 13 cervical vertebrae, since both the parapophysis has migrated by presacral 13 and the matching rib is clearly a dorsal rib, not a cervical rib (Fig. 5.15 A). This shows *Camarasaurus* had the plesiomorphic vertebral formula (12/13/5/44+). This, together with the condition seen in *Rebbachisaurus* and *Haplocanthosaurus*, implies Neosauropoda, Diplodocoidea and Macronaria retained the basal vertebral formula in their basalmost members.

The neck of this specimen has been used to discuss most of the paleobiology of *Camarasaurus* due its completeness. However, the largest caveat when studying this specimen is that it was not completely prepared out of the matrix and has remained in exhibit since the 1920s, so studying certain areas of the bones is difficult as in many specimens in exhibition. The neck is in opisthotonic posture, with cervicals CV3-CV7 completely disarticulated and CV8-CV12 are very dorsiflexed. Given that the amount of flexion of the neck is much smaller than that seen in the opisthotonic posture of *Spinophorosaurus* (Fig. 3.1), *Mamenchisaurus youngi* (Ouyang & Ye, 2002) or *Jobaria* (Paul Sereno, *pers. comm.* 2017) and many vertebrae are disarticulated or close to disarticulation, it suggests the amount of dorsoventral range of motion for CM 11338, as in other *Camarasaurus*, was reduced

relative to other sauropods.

The tail is remarkably complete, from the first caudal to its tip. Unfortunately, the anterior chevrons and the centra of CdV10-12 were not preserved. This is crucial, as the actual extent of *M. caudofemoralis longus* cannot be estimated ventrally for this taxon, as the first preserved chevron is that articulating with CdV-14. Luckily, the preserved centrum of CdV-13 has two ridges: the dorsalmost which is a characteristic of mid-distal caudal vertebrae in *Camarasaurus* and which is present until past CdV-30, and a more ventral ridge, which delimits a ventro-lateral concavity which is not present in CdV-14. This might indicate that the postero-dorsal limit for CFL was at around CdV-13, which is roughly the same position as on *Camarasaurus grandis* YPM 1901 and one position more anterior than *Camarasaurus* sp. CM 584.

Titanosauriformes Salgado 1997 *sensu* Sereno 2005

Brachiosauridae Riggs 1904 *sensu* Sereno 2005

Brachiosaurus altithorax Riggs, 1903b

Holotype. **FMNH-P-25107 partial skeleton consisting of posteriormost 6 dorsal vertebrae, 5 sacral vertebrae, anteriormost 2 caudal vertebrae, several ribs, right coracoid, right humerus, right ilium and right femur.

Referred specimens. **USNM 21903 left humerus. **BYU 4744** a dorsal vertebra, a partial left ilium, a left radius and a metacarpal. **SMA 0009** highly complete juvenile skeleton

Locality and horizon. Middle and Upper lower levels of Morrison Formation, Late Kimmeridgian, Late Jurassic of central and western Colorado and eastern Utah (USA)

Personal description/remarks. There are many remains referred to *Brachiosaurus* sp. Found in the Morrison Formation, but since the possibility of more than a single brachiosaurid in the formation exists and that most of that referred material consists of elements which do not overlap with the holotype, they are not being considered as referable. The holotype of *Brachiosaurus altithorax* preserves one of the few remarkably complete brachiosaurid sacra (*Giraffatitan* sacrum was figured by Janensch but could not be located in the collections after WWII). This sacrum (Fig. 5.16 D) is one of the most extremely wedged sacra known in sauropods, making the presacral column slope dorsally more than 30°. This, together with its extremely elongated humerus respect to the femur (Fig. 5.16 A, B), made the presacral region of *Brachiosaurus* to be extremely verticalized, rendering Brachiosauridae the more verticalized of all known sauropods.

Despite claims of *Brachiosaurus* (and other members of Brachiosauridae) having a retroverted pelvis (Paul, 1998, 2017), the articulation of the virtual skeleton did not show retroversion as that of *Cathetosaurus lewisi* or *Camarasaurus supremus*. The preserved anteriormost two caudal vertebrae are noticeably smaller than the dorsal vertebrae (Fig. 5. 16 C), which suggested the tail was much reduced respect to the presacral column. While originally this was thought to be a feature exclusive of this taxon (autapomorphy in phylogenetic conception), and later a synapomorphy of Brachiosauridae, this character appears to be actually a plesiomorphy for Brachiosauridae, as tail reduction occurs in the majority of known titanosauriforms (Fig. 3.20). The main repercussion of a reduced tail is a heavier presacral region of the body, resulting in a more anteriorly located center of mass (Mallison, 2011b) and the reduction of the caudal musculature, particularly of *M. caudofemoralis longus*. However, since the tail of *Brachiosaurus* is not complete, it is not possible to estimate the extent of the muscle, but the more complete tails of *Giraffatitan brancai* or *Tastavinsaurus sanzi* suggest the extent of the muscle may have been similar in *Brachiosaurus*. The wide sacrum of *Brachiosaurus* and the more medially located fourth trochanter in the femur indicate a condition similar to *Tastavinsaurus*, in which the adductor component of CFL is larger than in earlier branching sauropods.

The coracoid has a characteristic laterally deflected glenoid, absent in other brachiosaurids but also present in *Ligabuesaurus*. A laterally deflected glenoid suggest more range of motion for the humerus in the lateral plane, implying more abduction before osteological disarticulation. Brachiosaurids have marked distal expansions in their scapulae, suggesting large *M. deltoideus scapularis* (implied in humeral abduction). However, there is no preserved scapula for *Brachiosaurus*, so its laterally deflected glenoid cannot be explained within its context at present.



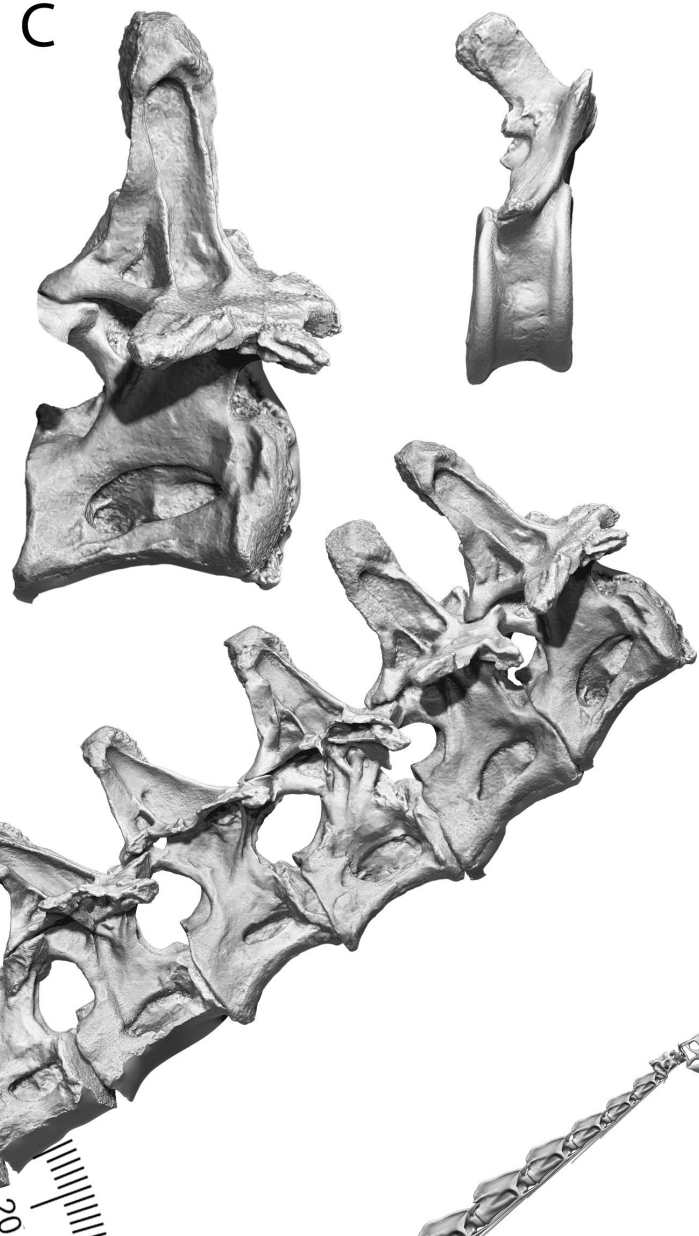
A



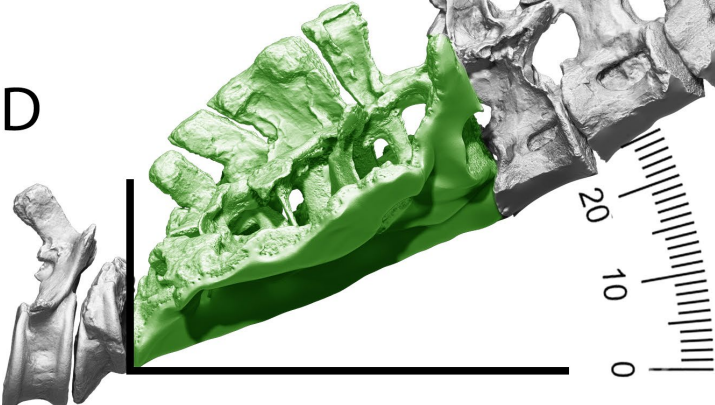
B



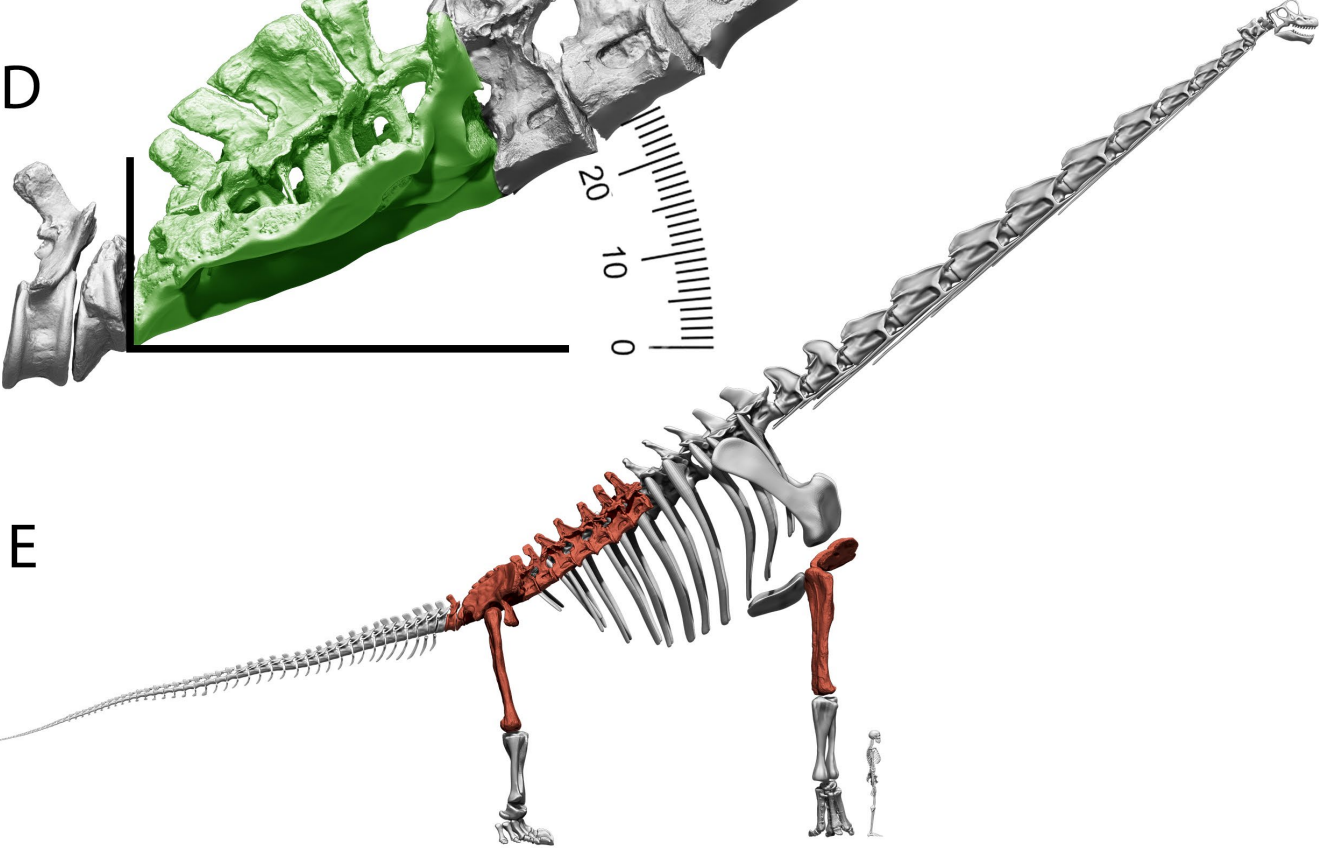
C



D



E



F

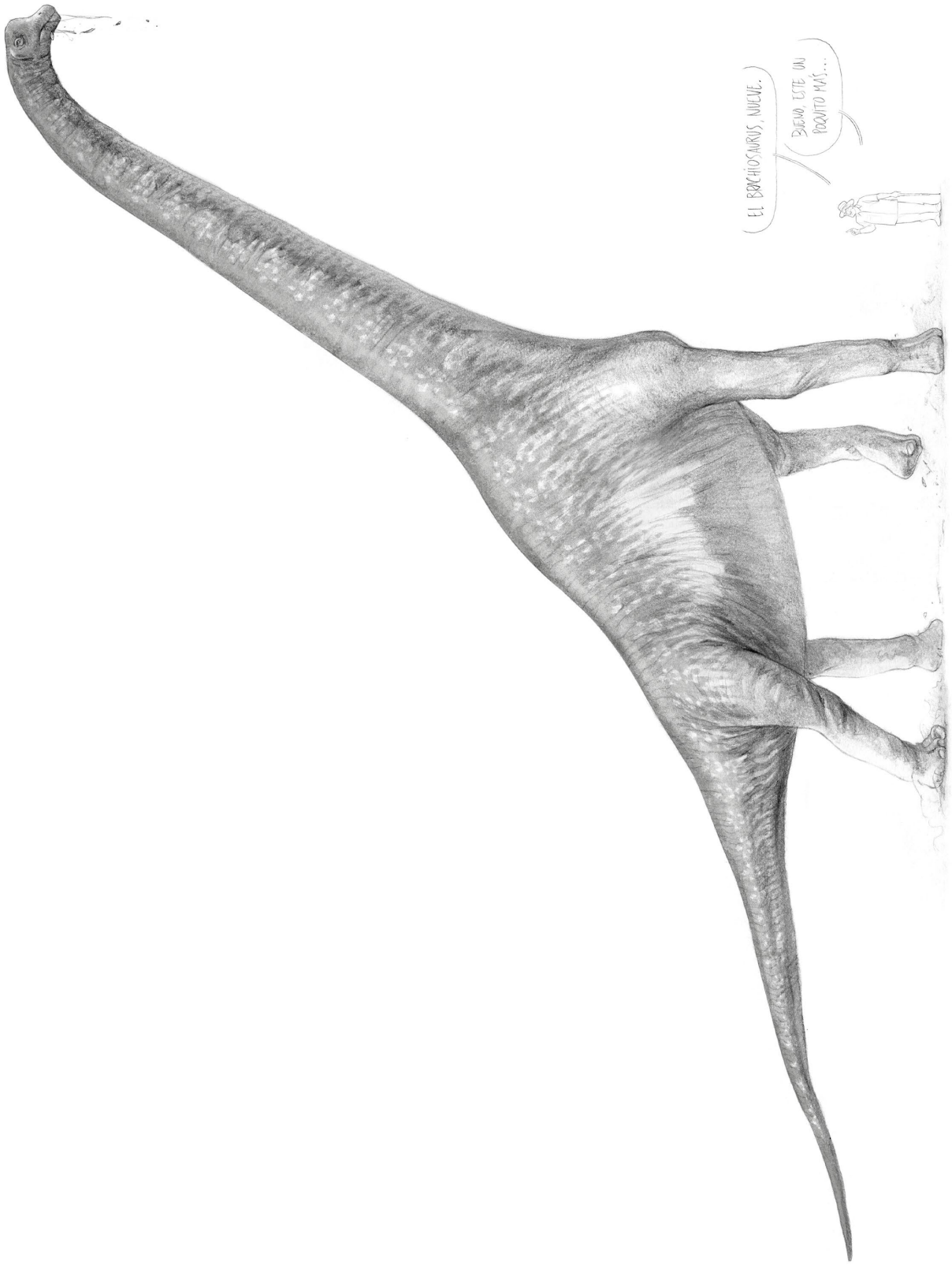


Figure 5.16 (previous page) - *Brachiosaurus altithorax*.

A - Femur and **B** - humerus of the holotypic specimen of *Brachiosaurus altithorax* (FMNH-P-25107) in posterior view to scale, showing the humerus is slightly longer than the femur. **C** - Antermost preserved dorsal vertebra (left) and caudal vertebra 2 (right) of the holotypic specimen of *Brachiosaurus altithorax* (FMNH-P-25107) in lateral view to scale. **D** - Preserved axial skeleton of the holotypic specimen of *Brachiosaurus altithorax* (FMNH-P-25107) in lateral view, showing the extremely wedged sacrum (green). **E** - Reconstructed skeleton of *Brachiosaurus altithorax* (FMNH-P-25107) from elements of the holotypic specimen (red) and elements modeled after *Giraffatitan brancai* (gray). Human skeleton = 1700 mm. **F** - Paleoartistic reconstruction of *Brachiosaurus altithorax*. Size of human = 1700 mm. Drawing by Diego Cobo.

Tastavinsaurus sanzi **Canudo, Cuenca-Bescós, Royo 2009**

Holotype. **FCPT-D-MPZ-99/9 partial skeleton consisting of posteriormost three dorsal vertebrae, five sacral vertebrae, 25 caudal vertebrae, several rib fragments, right and left ilia, pubes and ischia, right and left femora, right tibia, right fibula and almost complete right foot missing some phalanges.

Referred specimens. FCPT-D-CT-19 partial skeleton consisting of fragments of up to 16 ribs, a fragmentary caudal vertebra, left radius, two proximal metacarpus fragments, fragmentary ilium (distal pubic and ischial pedicles), left pubis and fragmentary right pubis, both ischia, left femur, left tibia, left fibula, left astragalus, left calcaneum, five fragmentary metatarsals and ten pedal phalanges.

Locality and horizon. Arsis 1 site, Peñarroya de Tastavins (Teruel, Spain). Xert Formation (Maestrazgo Basin, Spain), early Aptian.

Personal description/remarks. *Tastavinsaurus* is one of the most complete published titanosauriform individuals from the Early Cretaceous of Europe, despite lacking the anterior half of the body. It is a medium-sized titanosauriform, with a particularly short shank bones reaching only 55% length of the femur, an autapomorphy of the taxon (Royo-Torres, Alcalá, & Cobos, 2012). Several osteological features of this titanosauriform indicate further steps in a major transition occurring in the locomotion mechanics of this lineage.

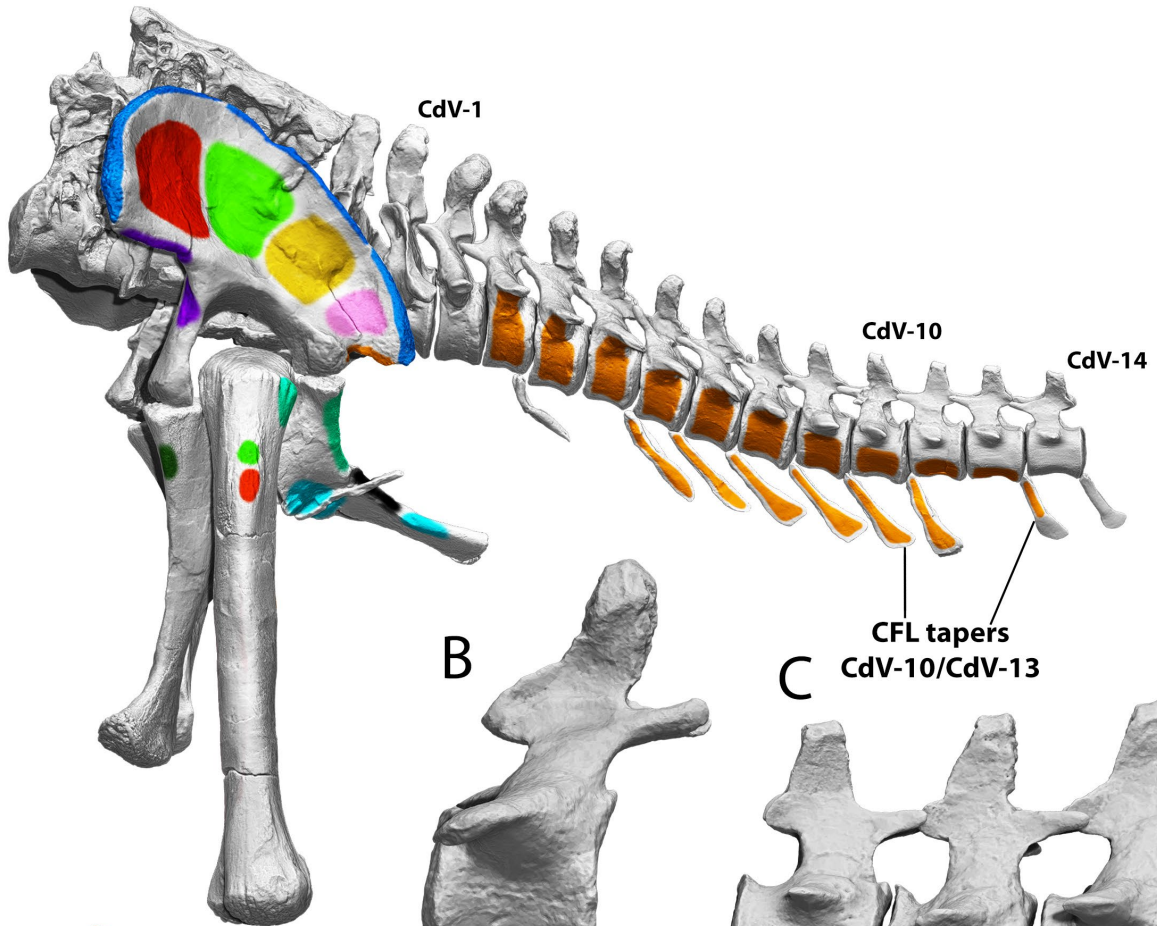
The sacrum is wedged as in other eusauropods (Fig. 5.17 E), making the preserved dorsal vertebrae deflect anterodorsally from the caudal vertebrae. The tail articulates in a sigmoidal curvature as in all previously surveyed sauropods, but is particularly ventrally deflected in its anteriormost region, from CdV-2 to CdV-9 (Fig. 5.17 A, D). This is likely related to the neural arch being anteriorly inclined (Fig. 5.17 B), instead of perpendicular to the centrum as in earlier branching sauropods. Interestingly, the ventral deflection changes to a more horizontal articulation around CdV-9 to CdV-11, in which the neural arch shifts its orientation from anteriorly pointed in CdV-9 to perpendicular in CdV-11 (Fig. 5.17 C).

The tail is more reduced in size than in Diplodocidae, non-neosauropod Eusauropoda and earlier branching Macronaria such as *Camarasaurus*. This reduction in size can be appreciated in the sacrum, as the last sacral centrum is around 30% shorter in dorso-ventral height than than first sacral centrum. The caudal neural spines and chevrons are also smaller relative to the centrum than in earlier branching Macronaria (Fig. 3.20). Absolutely smaller caudal vertebrae, with neural spines and chevrons also relatively smaller respect to the centrum imply much reduced caudal muscle mass. The anteriormost preserved dorsal vertebra is also quite elongated, with a longer than tall centrum, suggesting a longer torso, and a more anteriorly located center of mass.

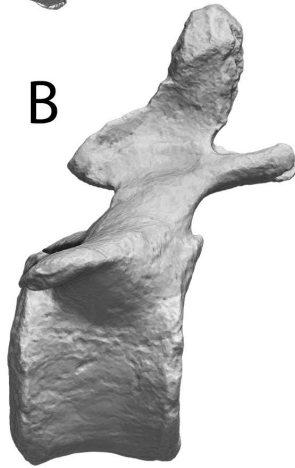
This reduction in post-sacral musculature is also patent in the muscles originating in the posterior region of the ilium and the ischium (Fig. 5.17 A). The iliac blade is particularly tall at the preacetabular process, which is also very developed in the antero-posterior axis (a little more than a third of ilium length is the preacetabular process). The iliac blade above the ischial pedicle is close to half the height of the preacetabular lobe. All this implies the anterior muscles originating in the ilium (ITC and IFE, implied in protraction and abduction respectively) were more developed and had larger lever arms than the posterior ones (ILFIB and FTE, both implied in leg retraction). Also, the reduced ischium implies smaller origins for ADD and FTI muscles, which are implied in leg adduction.

This has its implications regarding *M. caudofemoralis longus*. This muscle is also reduced, given the reduction in absolute tail size and relative chevron size. CFL tapers from CdV-10 to CdV-13, at the same position than in *Camarasaurus*, but with smaller osteological correlates for its origin. Regarding the function of CFL, the wider pelvis of *Tastavinsaurus* (next to those of non-neosauropod Eusauropoda or even *Camarasaurus*) and the more medially located fourth trochanter indicates the line of action for CFL was more similar to that in *Epachthosaurus* (Fig. 3.21), with a stronger contribution from adduction than in earlier branching sauropods, although less than in titanosaurs.

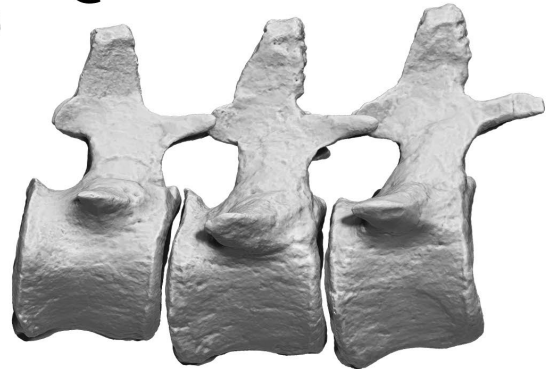
A



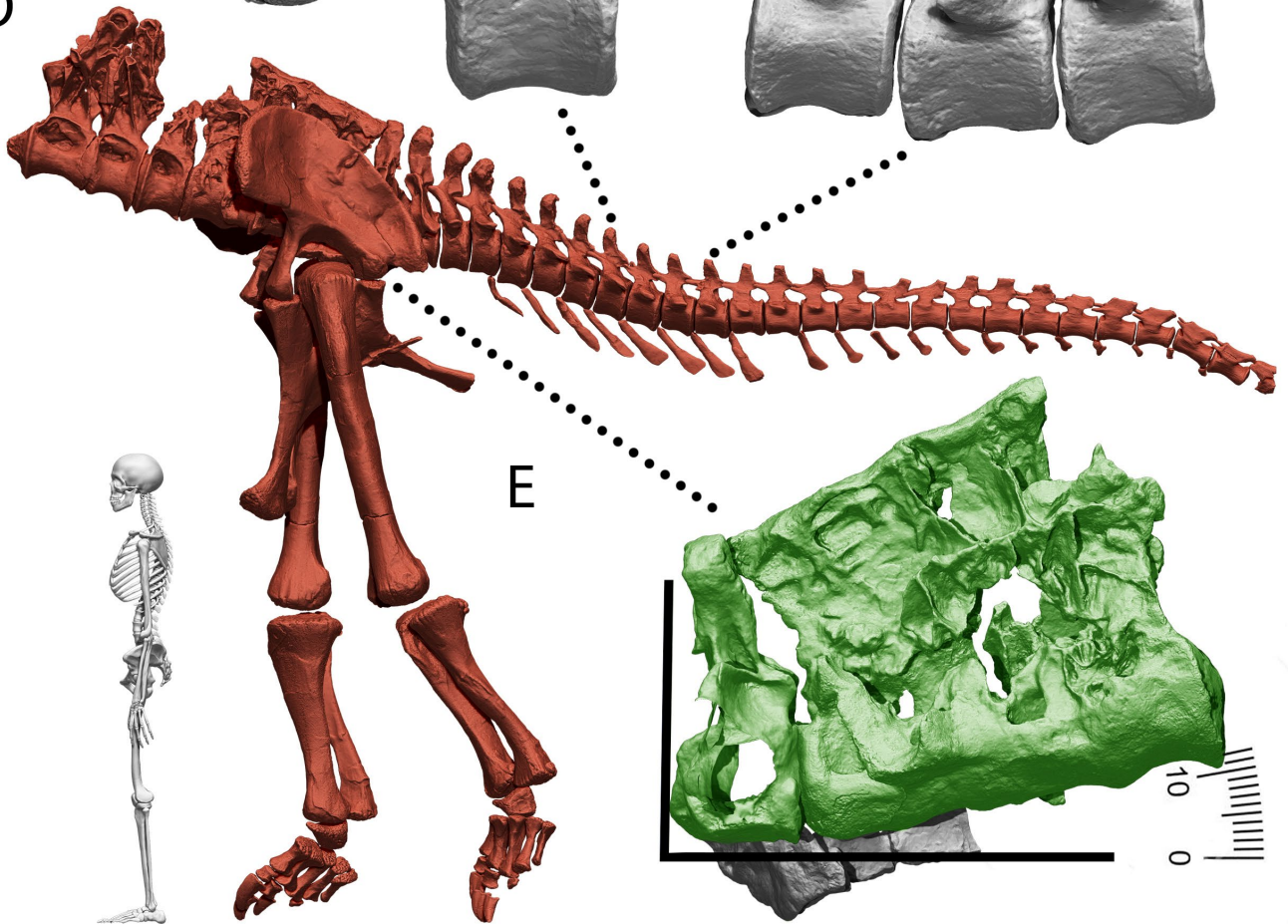
B



C



D



E

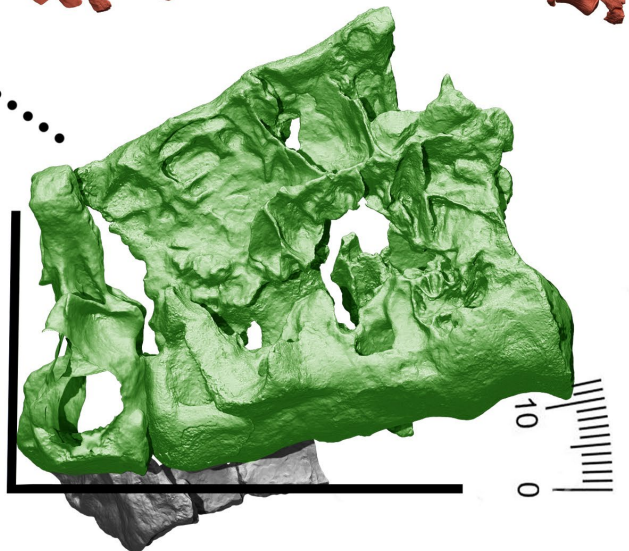


Figure 5.17 (previous page) - *Tastavinsaurus sanzi*.

A - Pelvis, sacrum, femur and tail of the holotypic specimen of *Tastavinsaurus sanzi* (MPZ-99/9) with muscular origins and insertions highlighted and colored (see Fig. 3.16 for color legend) **B** - Caudal vertebra 7 of *Tastavinsaurus sanzi* (MPZ-99/9) in lateral view, showing the anteriorly inclined neural arch. **C** - Caudal vertebrae 9 to 11 of *Tastavinsaurus sanzi* (MPZ-99/9) in lateral view, showing the anteriorly inclined neural arch in CdV-9 and its transition to a neural arch perpendicular to the centrum in CdV-11. **D** - Reconstructed skeleton of *Tastavinsaurus sanzi* (MPZ-99/9) from elements of the holotypic specimen (red). Human skeleton = 1700 mm. **E** - Sacrum of *Tastavinsaurus sanzi* (MPZ-99/9) in lateral view, showing a more than 10° wedging.

Somphospondyli Wilson & Sereno 1998 *sensu* Sereno 2005

Ligabuesaurus leanzai **Bonaparte, González Riga, & Apesteguía 2006**

Holotype. ** MCF-PVPH-233 partial skeleton consisting of an incomplete maxilla with ten teeth, six cervical and dorsal vertebrae, incomplete ribs, left and right scapulae, left humerus and proximal and distal parts of the right one, four left metacarpals and a right hind limb made of an incomplete femur, tibia, fibula, astragalus, five metatarsals and phalanges.

Referred specimens. **MCF-PVPH-261 partial skeleton.

Locality and horizon. Cerro León, 10 km to the north-west of Picún Leufú (Neuquén, Argentina). Upper section (Cullín Grande Member) of the Lohan Cura Formation, late Aptian-Albian.

Personal description/remarks. *Ligabuesaurus* is a taxon of uncertain phylogenetic position within Somphospondylia, close to Titanosauria but possibly branching earlier than that clade. Although it is also likely more deeply nested than *Tastavinsaurus*, they share some characteristics regarding their overall proportions and each complement missing portions of the other, a reconstruction can be attempted. The reconstructed skeleton incorporates the tail of *Tastavinsaurus*, scaled to match the single caudal vertebra centrum yet known for *Ligabuesaurus*. The overall body plan (Fig. 5.18 E) is that of a sauropod with reduced caudal axial skeleton, long torso (given the antero-posteriorly elongated middle and posterior dorsal centra) and long and wide neck, with shoulders as tall or taller than the acetabulum, and extremely slender limbs (Fig. 5.18 C).

The most ambiguous feature of this sauropod would be its neck length, since it is unknown whether it had the basal condition of 12 or 13 cervical vertebrae or whether the number had increased as is the case in Euhelopodidae, which were closely related. What is evident is that posterior and middle cervical vertebrae were extremely wide, similar to the condition in *Camarasaurus* or *Barosaurus*. The prezygapophyseal facets (Fig. 5.18 A) are also similar to those of *Camarasaurus*, flat and wider latero-medially than long antero-posteriorly (but not as short antero-posteriorly as those from *Barosaurus*). Since the cervical vertebrae preserved do not articulate with each other, it is difficult to make anything but an educated estimation of the motion capabilities, but overall they appear similar to those of *Camarasaurus*. Only posteriormost cervical vertebrae preserve complete neural arches with neural spines, which are relatively tall and wide (Fig. 5.18 B). None of the cervical vertebrae have ventral keels, suggesting either weaker anchor points for ventriflexion or a shift of these muscles to the cervical ribs as proposed for *Tyrannosaurus rex* (Snively & Russell, 2007a). Since no cervical rib heads have been yet retrieved for *Ligabuesaurus* neither hypothesis can be confidently tested. The extremely wide diapophyses, however, suggest long lever arms for *M. intercostales* as in *Camarasaurus*, suggesting more efficient lateral flexion, but longer contraction times.

Several features of the pectoral girdle and forelimb, such as the distal expansion of the scapula, the laterally deflected glenoid (Fig. 5.18 D) or a humeral head expanded into the posterior face of the humerus suggest a highly mobile shoulder articulation. This may have aided *Ligabuesaurus* in reaching the ground with the head for drinking or other purposes, given its relatively inflexible neck in the dorso-ventral plane. However, this hypothesis cannot be confidently tested without a better estimation of *Ligabuesaurus* neck length.

The ilium of *Ligabuesaurus* resembles that of other Titanosauriformes, with a proximo-distally longer pubic process than earlier branching sauropods such as *Camarasaurus*. This suggests the ischium might have been reduced as in *Tastavinsaurus* and more deeply nested titanosaurs.

Overall, *Ligabuesaurus* shows that extremely wide cervical vertebrae with wide zygapophyseal facets, suggesting better capabilities for lateral flexion than dorso-ventral flexion converge in sauropods with radically different limb proportions and likely different trophic preferences.

Epachthosaurus sciuttoi Powell 1990

Holotype. MACN-CH 1317 a single middle dorsal vertebra.

Referred specimens. UNPSJB-PV-920**, relatively complete skeleton, including a continuous axial skeleton including 6 dorsal vertebrae, the sacrum and 31 caudal vertebrae, complete left and right forelimbs, fragmentary coracoids, both ilia, fragmentary pubes and ischia and complete hindlimbs.

Locality and horizon. 6 km north of Estancia “Ocho Hermanos” (Chubut, Argentina). Bajo Barreal Formation (Argentina), Cenomanian/Turonian.

Personal description/remarks. *Epachthosaurus* is likely an early branching titanosaur known from a highly complete individual only missing the anteriormost dorsal vertebrae and neck. A large majority of phylogenetic analyses recover it in a more deeply nested position than *Andesaurus delgadoi* (which roots the node Titanosauria), but its precise position is still subject of debate.

The closely related *Choconsaurus baileywillisii* (Simón, Salgado, & Calvo, 2017) which preserves cervical and anterior dorsal material suggest *Epachthosaurus* had a very elongated neck like most known non-saltosaurine titanosaurs. The fact that UNPSJB-PV-920 was found articulated with no scattering of elements (Martínez *et al.*, 2004) suggests it did not possess any osteoderms. The preserved dorsal vertebrae have extremely elongated hyposphenes, with the ventral region being as medio-laterally long as the postzygapophyses, implying a strong ventral bracing.

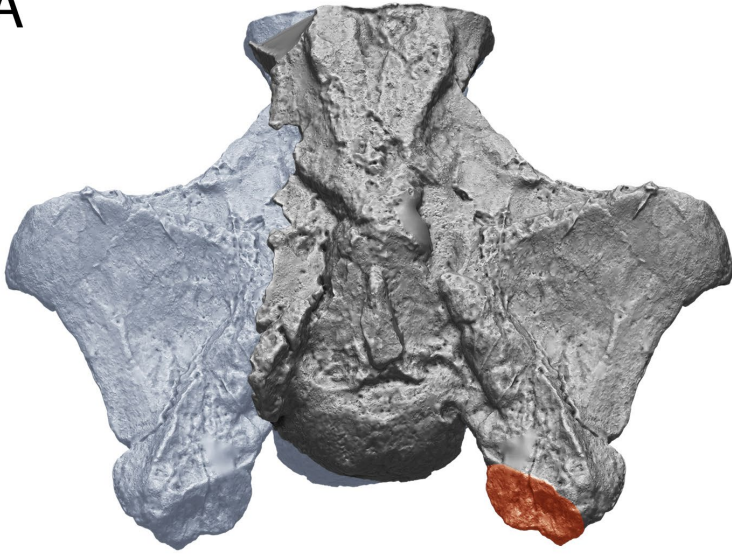
The assembled virtual skeleton reveals it had a fairly long tail next to other titanosaurs (Fig. 5.19 E), which tend to maintain the reduced tail inherited from earlier branching Titanosauriformes. The caudal vertebrae are relatively larger relative to the posteriormost dorsal vertebrae, so the tail is overall bigger than in other earlier branching titanosauriforms. However, the neural spines and chevrons are smaller relative to the size of the centrum, implying the caudal musculature is overall more reduced than in earlier branching titanosauriforms, despite the overall size of the vertebrae being larger.

Previous estimations on the extension of *M. caudofemoralis longus* have used the disappearance of caudal ribs to mark the posterior limit for CFL (Ibiricu *et al.*, 2014), placing it in CdV-17, which would be the longest CFL in any known sauropod. However, given that dissections of extant sauropsida have shown that caudal ribs are not an origin site for CFL (Persons & Currie, 2010) and that scarring on the centrum and chevrons is a much more likely indicator of CFL tapering. The chevrons in UNPSJB-PV-920 are not very well preserved, but the lateral surfaces of the caudal centra are. As in all other surveyed sauropods, a ridge appears on the lateral face of CdV-8, it is present in CdV-9 as well (more ventrally placed) and in CdV-10 (very ventral). CdV-11 does not have the ridge, and the lateral face of the centrum is not as concave as in vertebrae anterior to CdV-8. This marks CFL as disappearing by CdV-10 (Fig. 5.19 A). It is more posterior than in more deeply nested titanosaurs such as *Neuquensaurus*, and more posterior than earlier branching titanosauriforms such as *Tastavinsaurus*. *Epachthosaurus* therefore lies in an interesting phylogenetic position regarding the reduction of caudofemoral musculature, as complete enough tails are unknown in earlier branching titanosaurs.

Figure 5.18 (next page) - *Ligabuesaurus leanzai*.

A - Middle cervical vertebra of *Ligabuesaurus leanzai* (MCF-PVPH-261) in dorsal view, with the wider than long prezygapophyseal facet highlighted in red. **B** - Posterior dorsal vertebra of the holotypic specimen of *Ligabuesaurus leanzai* (MCF-PVPH-233) in anterior view. **C** - Femur (left) and humerus (right) of *Ligabuesaurus leanzai* (MCF-PVPH-233) in anterior view, to scale. Notice the humerus is slender and long, but not longer than the femur. **D** - Coracoid of *Ligabuesaurus leanzai* (MCF-PVPH-261) in lateral (left) and anterior (right) view, with the glenoid highlighted in green. Notice the glenoid is laterally deflected. **E** - Reconstructed skeleton of *Ligabuesaurus leanzai* from elements of the both specimens (red) and elements from *Tastavinsaurus sanzi* (tail, sacra and feet, in gray) and modeled elements (gray). Human skeleton = 1700 mm. **F** - Paleoartistic reconstruction of *Ligabuesaurus leanzai*, highlighting the extreme wide neck at its base. Size of human = 1700 mm. Drawing by Diego Cobo.

A



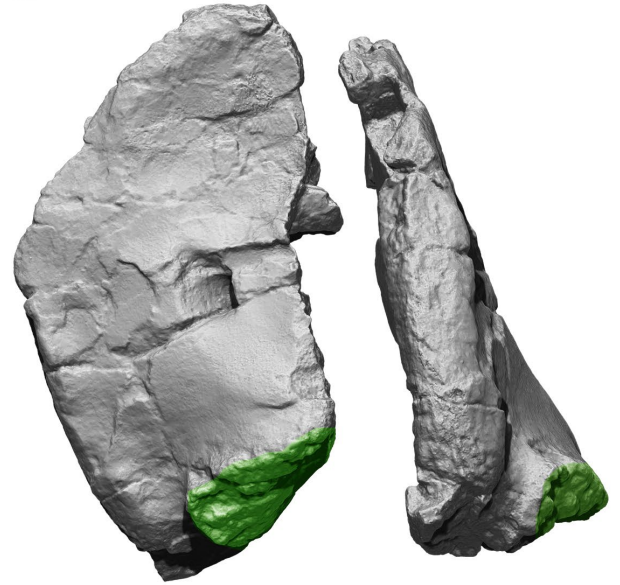
B



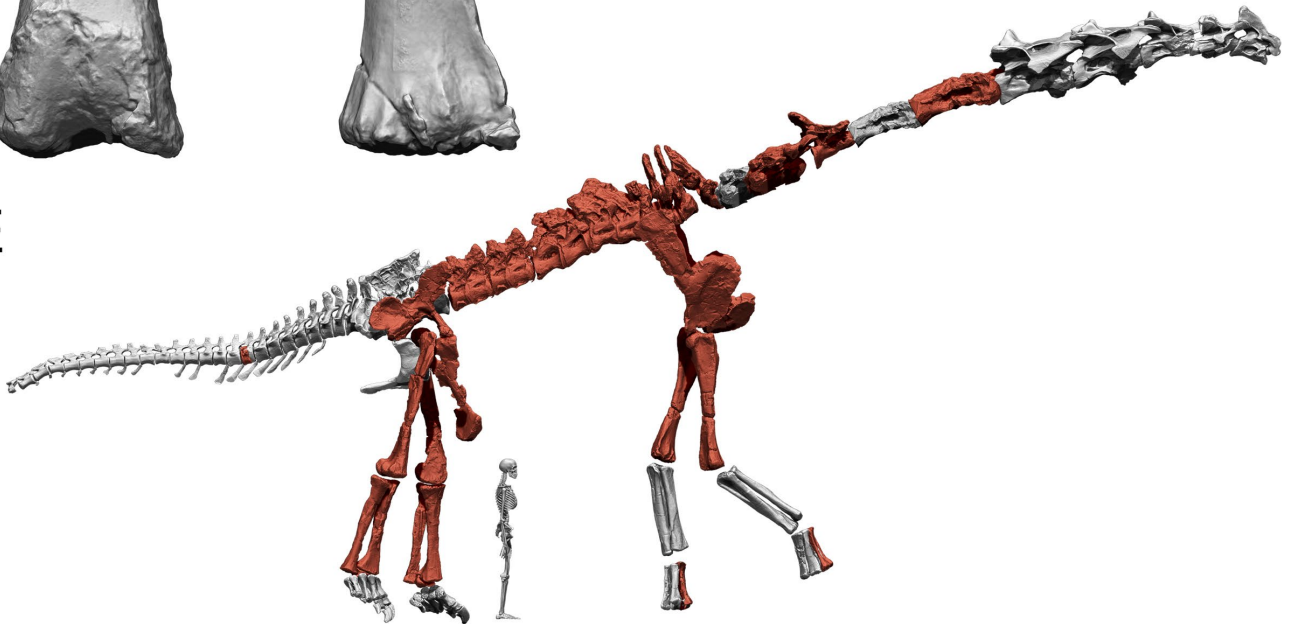
C



D

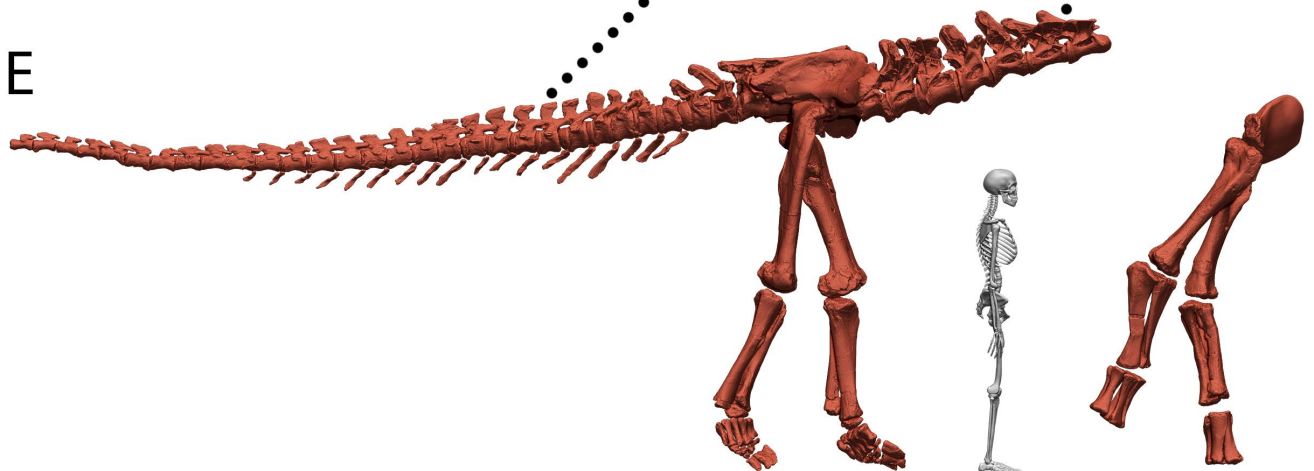
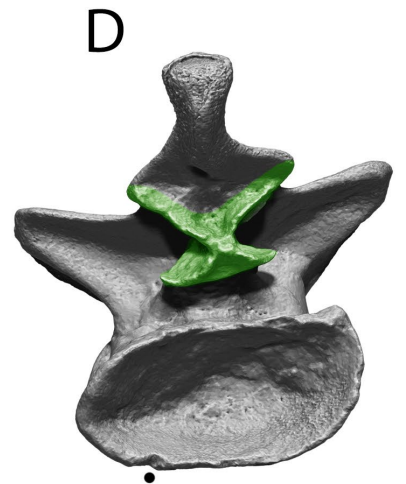
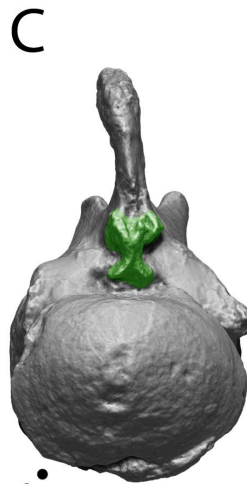
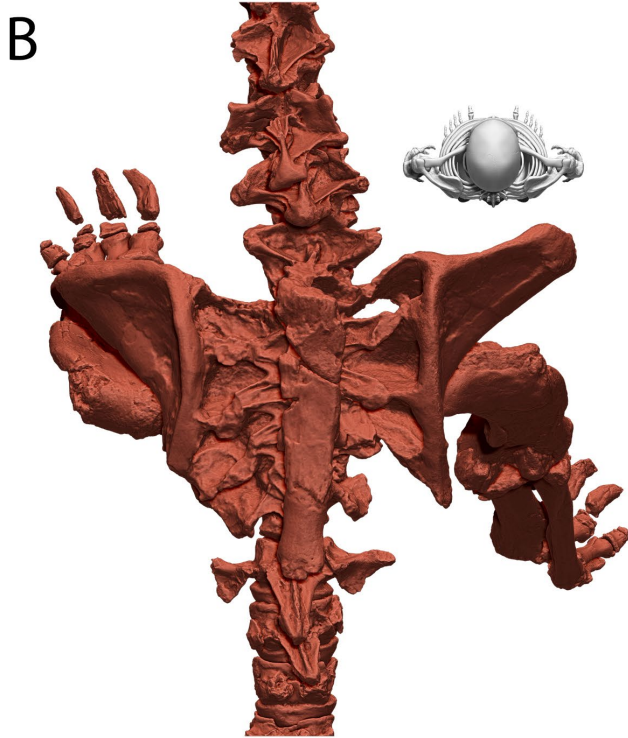
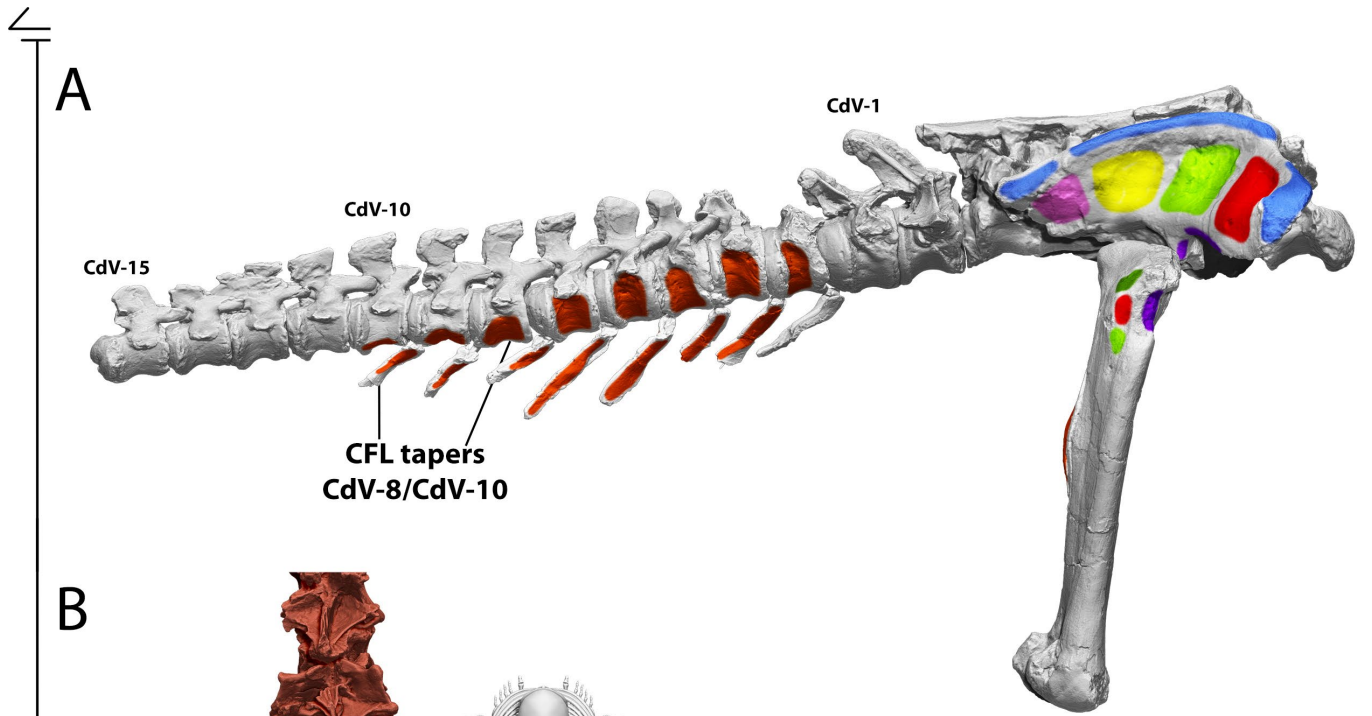


E



F





F



Figure 5.19 (previous page) - *Epachthosaurus sciuttoui*.

A - Pelvis, sacrum, femur and tail of the specimen UNPSJB-PV-920 referred to *Epachthosaurus sciuttoi* with muscular origins and insertions highlighted and colored (see Fig. 3.16 for color legend). **B** - Pelvis, sacrum, hindlimbs of UNPSJB-PV-920 in dorsal view. Notice the lateral flaring of the ilia. **C** - Caudal vertebra 8 of UNPSJB-PV-920 in posterior view, with “hyposphene” highlighted in green. **D** - Dorsal vertebra 5 of UNPSJB-PV-920 in posterior view, with hyposphene highlighted in green. **E** - Reconstructed skeleton of *Epachthosaurus sciuttoi* from elements UNPSJB-PV-920 (red). Human skeleton = 1700 mm. **F** - Paleoartistic reconstruction of *Epachthosaurus sciuttoui*, highlighting the wide hindquarters and reduced tail, with hypothetical neck after *Choconsaurus*. Size of human = 1700 mm. Drawing by Diego Cobo.

Overosaurus paradasorum **Coria et al. 2013**

Holotype. MAU-Pv-CO-439 partial skeleton consisting of an uninterrupted axial skeleton (posteriormost four cervical vertebrae, 10 dorsal vertebrae, 6 sacral vertebrae, 20 caudal vertebrae), seven right and five left ribs, and both ilia (right one complete).

Referred specimens. N/A

Locality and horizon. Cerro Overo, 40 km southwest of Rincón de los Sauces (Neuquén Argentina), Lowermost Anacleto Formation (Argentina), Campanian.

Personal description/remarks. *Overosaurus* is one of the most complete specimens of Rinconsauria and Aeolosaurini yet known, key in understanding the body-plan of this clade and to interpret more fragmentary remains which share similar characteristics. The uninterrupted axial sequence of *Overosaurus* has an OIC similar to other eusauropods, with the presacral vertebrae deflecting antero-dorsally from the sacrum, forming a steep angle. However, the tail has an OIC different from other sauropodomorphs. It has a strong ventral deflection from the sacrum (Fig. 5.20 D, E). This is due two different characters present in anterior and middle caudal vertebrae: the neural arches are anteriorly inclined as in *Tastavinsaurus*, making the vertebrae deflect ventrally when articulating. However, the preserved prezygapophyses are also dorsally inclined, making ventral deflection increase further. This ventrally deflected tail is also extremely reduced, with the first caudal centrum being half the size of the last dorsal centrum, being one of the most extreme reductions in the tail of a sauropod known as of present (the length of the articulated 20 preserved caudal vertebrae is almost as long as the posteriormost four preserved cervical vertebrae).

It is difficult to assess how much caudal musculature would be reduced, as the chevrons and neural spines of anterior and anteriormost caudal vertebrae have not been preserved. However, the antero-posterior length of *M. caudofemoralis longus* can be assessed, as the centra are well enough preserved. The first caudal vertebra with a ridge on the centrum is CdV-7, and the last to have one is CdV-9 (Fig. 5.20 D). This implies CFL disappeared in *Overosaurus* one vertebra more anterior than in *Epachthosaurus*. While this is in agreement with the overall trend of reduction of hindlimb retractor musculature in Titanosauriformes, the extreme size reduction of the tail of *Overosaurus* is likely more an autapomorphic feature than part of this general trend.

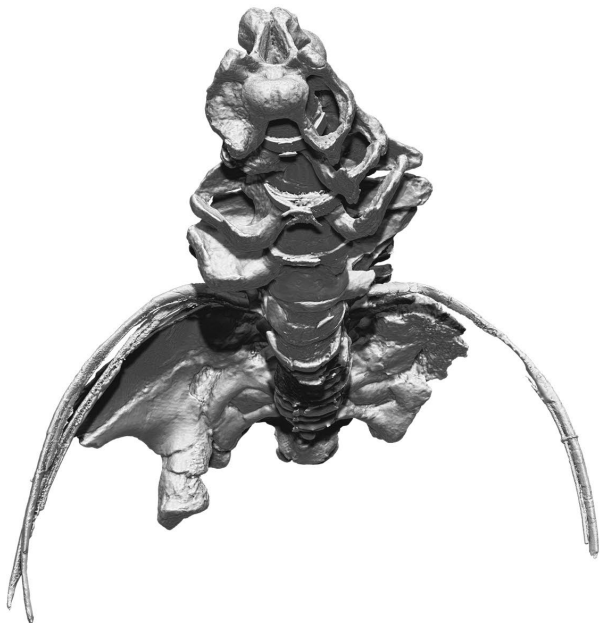
One of the most interesting features preserved in *Overosaurus* is a large number of complete dorsal ribs associated with their corresponding vertebrae. This allows comparing the cross-sections of the ribcage from *Spinophorosaurus*, and interestingly they share more similitudes than differences. While the ribs are overall more robust in *Overosaurus*, the anteriormost three ribs are also very straight (Fig. 5.20 B), with barely any curvature. This is likely due to the fact that the non-preserved scapulae articulated with these three ribs in *Overosaurus* as it did in *Spinophorosaurus*. The ribcage section at mid-thorax of both sauropods has more slender ribs, with more pronounced curvatures (although the curvature is much more pronounced in *Overosaurus*, Fig. 5.20 A).

Another feature shared between *Overosaurus* and *Spinophorosaurus* (and other sauropods) is the orientation of the neural spines on anteriormost dorsal vertebrae, in which the neural spine of DV-1 is anteriorly directed, that of DV-2 is perpendicular to the centrum and that of DV-3 is posteriorly directed (Fig. 5.20 C).

Figure 5.20 (next page) - *Overosaurus paradasorum*.

A - Ribcage, dorsal vertebrae and ilia of the holotypic specimen of *Overosaurus paradasorum* (MAU-Pv-CO-439) in anterior view, at dorsal vertebra 7 level. **B** - Ribcage, dorsal vertebrae and ilia of *Overosaurus paradasorum* (MAU-Pv-CO-439) in anterior view, at dorsal vertebra 1 level. **C** - Dorsal vertebrae 3 (red), 2 (blue) and 1 (green) and last cervical vertebra (gray) of *Overosaurus paradasorum* (MAU-Pv-CO-439) in lateral view. Notice the shift in neural spine orientation. **D** - Pelvis, sacrum, femur and tail of *Overosaurus paradasorum* (MAU-Pv-CO-439) with muscular origins and insertions highlighted and colored (see Fig. 3.16 for color legend). **E** - Reconstructed skeleton of *Overosaurus paradasorum* (MAU-Pv-CO-439). Human skeleton = 1700 mm.

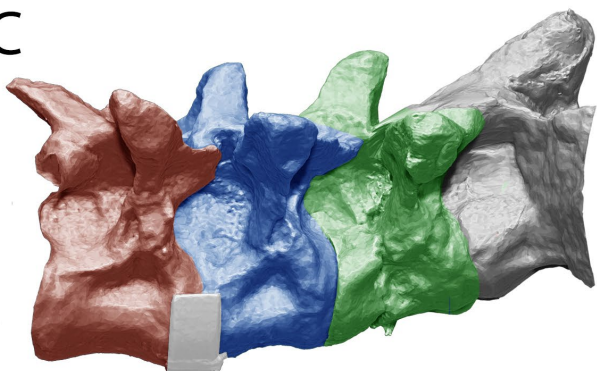
A



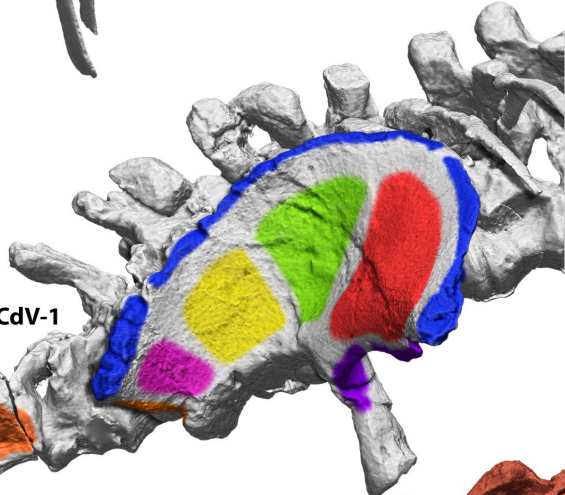
B



C



CdV-1

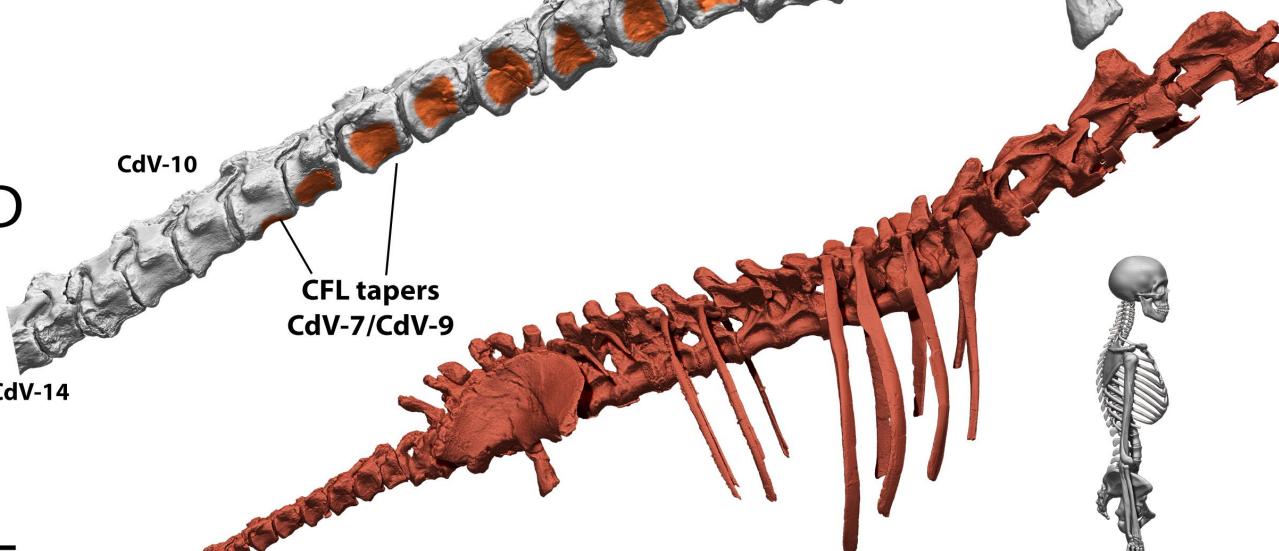


D

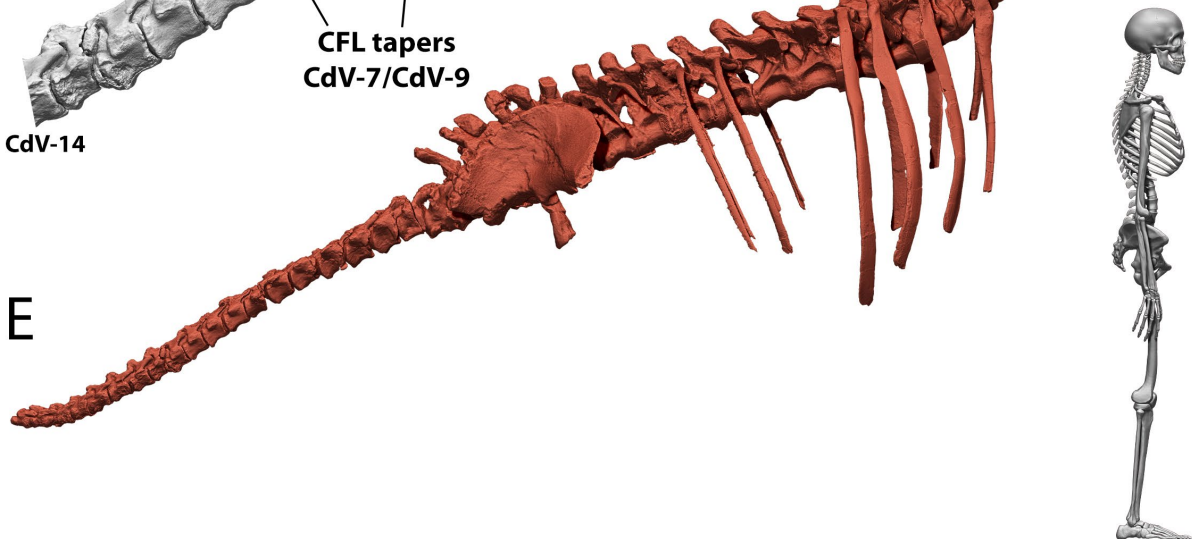
CdV-10

CFL tapers
CdV-7/CdV-9

CdV-14



E



Neuquensaurus australis Huene, 1929

Holotype. MLP Ly 1-7 Partial sacrum consisting of six coossified sacral vertebrae, one unfused seventh sacral vertebra and six partial anterior caudal vertebrae.

Referred specimens. MCS-5** partial skeleton including one cervical vertebra, six dorsal vertebrae, 1 partial sacrum and coalesced ilia, 15 caudal vertebrae in sequence, three chevrons, one ischium, two femora, right tibia, fibula and astragalus, 3 osteoderms. PVL-4017-18* Partial sacrum

Locality and horizon. Elevated right bank of Neuquén river (Neuquén, Argentina), 2 to 4 km from the railway bridge and confluence before Neuquén. Anacleto Formation (Argentina), Santonian-Campanian.

Personal description/remarks. MCS-5 is the most complete skeleton of a single individual of a Saltasaurine titanosaur known as of 2019. The virtual skeleton assembled, completed with additional bones from *Saltasaurus* and *Rocasaurus*, reveals the majority of previous hypotheses regarding the body plan of these sauropods were fairly accurate. Comparing this body plan with those of *Overosaurus*, *Epachthosaurus* or *Rapetosaurus* shows that Titanosauria was a morphologically disparate clade in terms of body proportions and their functional morphology.

The sacrum of *Neuquensaurus*, although not complete, appears to have a wedging similar to that of the holotypic sacrum of *Saltasaurus* and other referred specimens. The wedging is around 13°-14°, making the dorsal and caudal vertebral series to deflect. The uninterrupted 15 caudal vertebrae sequence of *Neuquensaurus* articulate with a slight ventral deflection, but far from the ventral deflection observed in *Overosaurus* and other Aeolosaurines, more similar to the condition from *Alamosaurus*, suggesting vertebrae posterior to CdV-15 may have followed a similar OIC to that of the north-American titanosaur. The dorsal series, however, has pretty extensive modifications on the middle dorsal vertebrae, with the prezygapophyses and anterior centrum face ventrally displaced from the postzygapophyses and posterior centrum face of the same vertebra, making the immediately anterior vertebra to articulate deflecting ventrally. Also, the dorsal centrum of these dorsals has obtuse wedging, further ventrally deflecting the anterior vertebra. This results in an extremely bowed dorsal series, more so than in *Haplocanthosaurus* or Dicraeosauridae.

Although MCS-5 does not preserve humeri, a femur and a humerus from different individuals (likely belonging to the same genus) were found in the same quarry. The humerus is short and robust, as are the humeri from *Saltasaurus*. Although the exact femur to humerus proportions cannot be established for any Saltasaurine as of present, it is likely that the forelimb of *Neuquensaurus* would have been much shorter than the hindlimb, as suggested by the ventral deflection of the presacral column and the overall proportions from retrieved appendicular material.

Neuquensaurus is remarkable among sauropods for having the most reduced *M. caudofemoralis longus* known so far in this clade of dinosaurs. Although the caudal vertebrae are not as reduced in size relative to the dorsal and cervical vertebrae as in other Titanosauriformes (in which anterior caudal vertebrae usually are one third to half the size of the posteriormost dorsal vertebrae), the only complete anterior chevron is very short relative to anterior caudal centra height. Also, the lateral ridge on the caudal vertebrae which marks the tapering of CFL before disappearing engulfed by *M. ilio-ischiocaudalis* appears on CdV-5 and has disappeared by CdV-7 (Fig. 5.21 A), with the centra lateral surface becoming flat instead of concave after the ridge has disappeared. The fourth trochanter of the femur is extremely medially deflected and is also extremely faint, suggesting the force exerted by CFL during the life of the animal was smaller than in other sauropods. The pelvis of *Neuquensaurus* is also extremely wide and the distal end of the femora particularly laterally deflected next to the femoral head, making the line of action of CFL have a greater contribution from adduction than retraction.

Neuquensaurus has also been associated with osteoderms similar to those from *Saltasaurus* (scutes, different from the bulb and root osteoderms found in non-saltasaurine titanosaurs).

Saltasaurus loricatus Bonaparte & Powell, 1980

Holotype. PVL-4017-92** Sacrum and coalesced ilia.

Referred specimens. PVL-4017-1 to PVL-4017-140 skeletal remains of at least six individuals including at least 14 cervical vertebrae, 20 dorsal vertebrae, two sacra, 26 caudal vertebrae, four scapulae, three coracoids, four sternal plates, 10 humeri, five ulnae, four radii, five metacarpals, five ilia, four pubes, two ischia, five femora, five tibiae, four fibulae, seven metatarsals, six osteoderms, four patches with ossicles.

Locality and horizon. Estancia "El Brete" (Salta, Argentina), Formación Lecho de El Brete (Argentina), Maastrichtian.

Personal description/remarks. Although the majority of fossils referred to *Saltasaurus* stem from a single quarry from El Brete, it is a bonebed, and the potential presence of *Neuquensaurus* in the same quarry (D'Emic & Wilson, 2011) could complicate referring all the remaining material to a single taxon. However, all retrieved bones clearly share similarities with all material referred to *Neuquensaurus* and *Rocasaurus*, suggesting they all belong to the same clade (although not all phylogenetic analyses retrieve it). For the intent and purposes of this thesis, all material from El Brete will be tentatively considered to be *Saltasaurus*.

Saltasaurus has more referred cervical vertebrae than any other saltosaurine. Their morphology is very characteristic and different from those of most other sauropods, since the prezygapophyses are posterior to the anterior condyle of the centrum, and the postzygapophyses are posterior to the posterior cotyle of the centrum (Fig. 5.21 C). The position of the zygapophyses relative to the centrum is therefore the opposite from that of the majority of sauropods. The same condition is found in cervical vertebrae referred to *Rocasaurus* and *Neuquensaurus*, likely a synapomorphy of Saltosaurinae, and a convergent feature with many ornithischians, such as ornithopods and thyreophorans. This zygapophyseal disposition allows having the center of rotation and the facets much closer than in other sauropods. Also, the zygapophyseal facets are quite elongated in most vertebrae. These characteristics result in a large amount of dorso-ventral range of motion (Fig. 5.21 C).

The osteoderms of *Saltasaurus* are part of the "scute" morphotype: rounded, with internal and external keels and roughly the length of a dorsal or caudal vertebra. *Saltasaurus* is also the only sauropod to have also densely packed dermal ossicles, which would cover continuously large portions of the back of the animal. The presence of such a thick covering of dermal ossicles would likely stiffen the mobility of the area they covered in the torso of the animal. Since their actual extension and precise location is still unknown, which regions of *Saltasaurus* were more stiffened cannot be ascertained at present. However, the size of preserved patches with dermal ossicles is greater than one dorsal or caudal vertebra. Had they been situated in the torso or tail of the animal and they would have affected the mobility of the axial skeleton.

Rocasaurus muniozii Salgado & Azpilicueta 2000

Holotype. MPCA-Pv 46 Partial skeleton of a subadult, consisting of a cervical neural arch and a cervical centrum, three dorsal neural arches and two dorsal centra, two sacral neural arches, a mid caudal vertebra, a distal caudal vertebra, both ilia, left pubis, both ischia, left femur.

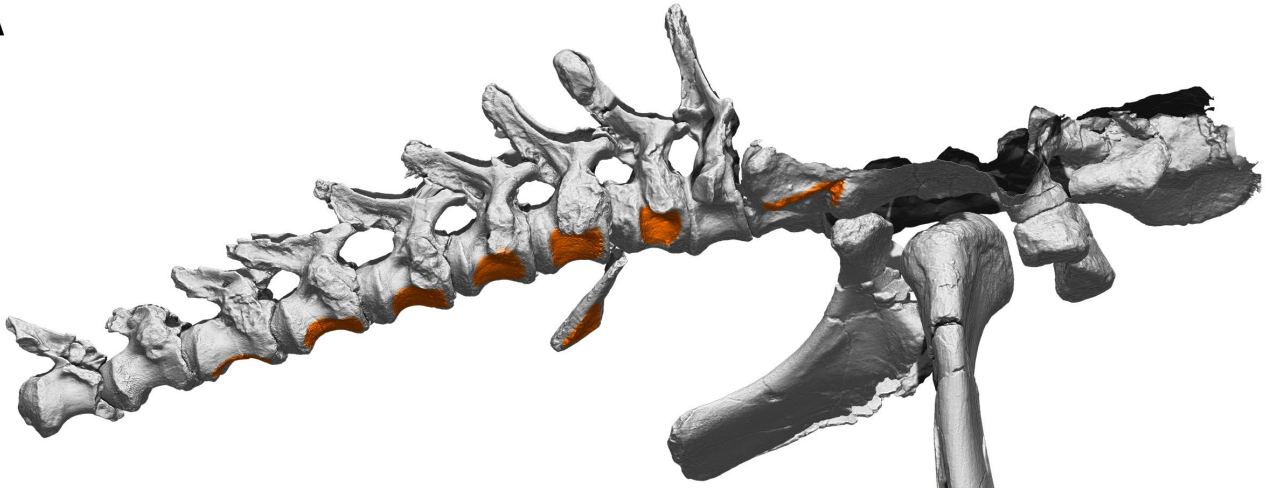
Referred specimens. MPCA-Pv 47,48 and 60 three anterior caudal centra. MPCA-Pv 49 mid caudal centrum. MPCA-Pv 51-56 six distal caudal centra. MPCA-Pv 57 anterior caudal vertebra. MPCA-Pv 59 posterior caudal vertebra.

Locality and horizon. Salitral Moreno, 25 km south of General Roca (Río Negro, Argentina). Inferior member of Allen Formation

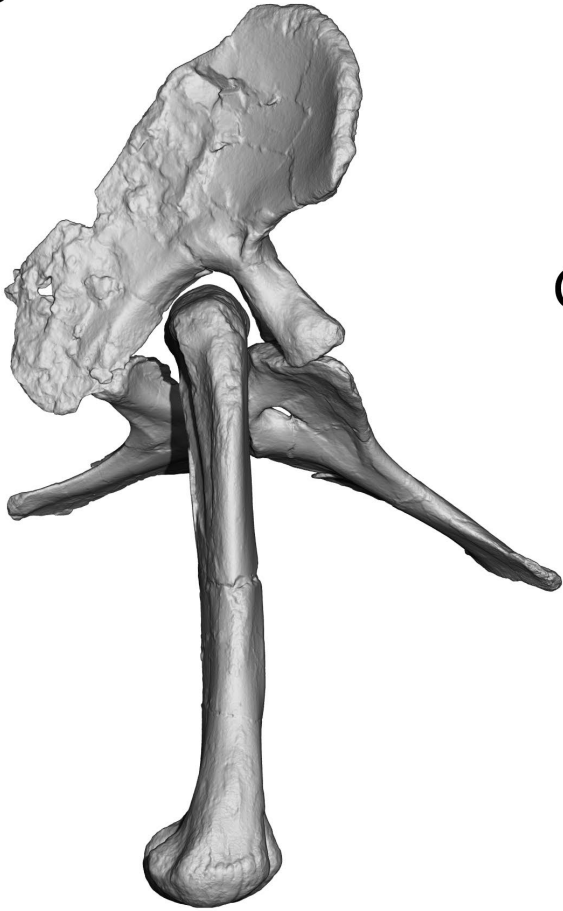
Personal description/remarks. The holotype specimen of *Rocasaurus* is far from the relative completeness of other Saltosaurinae, but it preserves the only complete pelvis from a single individual from this clade (Fig. 5.21 B). The pubis is larger than the ischium as in other Titanosauriformes, but the ischium is not as reduced as in titanosaurs such as *Rapetosaurus*. The ilium, unlike those of *Neuquensaurus* or *Saltasaurus* is complete, and is overall similar to that of its sister taxa, with a preacetabular lobe not as dorso-ventrally tall as in other titanosauriformes.

The open neurocentral sutures suggest the holotypic individual had not yet completed its growth.

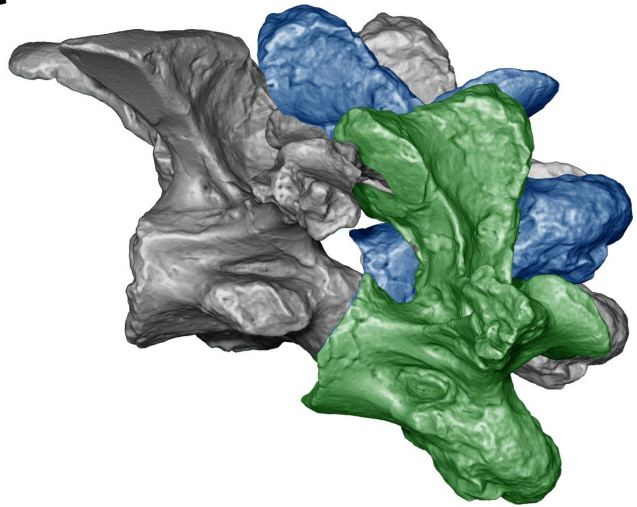
A



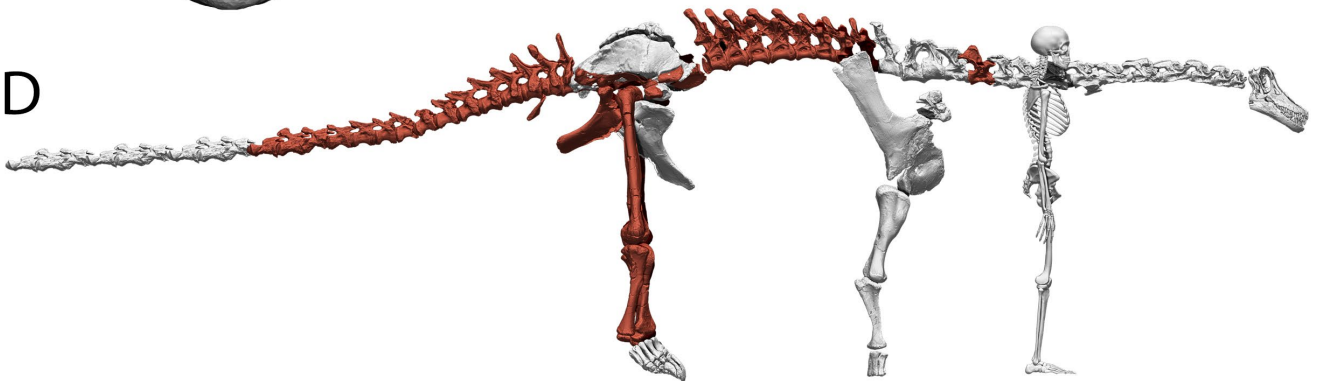
B



C



D



E



Figure 5.21 (previous page) - Saltosaurini.

A - Pelvis, sacrum, femur and tail of *Neuquensaurus australis* with *M. caudofemoralis longus* origins and insertions highlighted and colored (see Fig. 3.16 for color legend). **B** - Pelvic girdle and femur of the holotypic specimen of *Rocasaurus muniozi* (MPCA-PV- 46) in lateral view. Notice the wide angle between pubis and ischium. **C** - Maximum range of motion between two consecutive cervical vertebrae of *Saltasaurus loricatus* (PVL-4017). **D** - Reconstructed skeleton of *Neuquensaurus australis*, with elements from MCS-5 (red), *Saltasaurus loricatus* and *Alamosaurus sanjuanensis* (gray). Human skeleton = 1700 mm. **E** - Paleoartistic reconstruction of a Saltosaurini indet., highlighting the wide torso and pelvis, as well as the osteoderm covering. Size of human = 1700 mm. Drawing by Diego Cobo.

5.4 PHYLOGENETIC ANALYSIS AND CHARACTER OPTIMIZATION

The phylogenetic analyses retrieved 68 most parsimonious trees, with a consistency index of 0.378 and a retention index of 0.727. The MPTs have a length of 1316 steps. A strict consensus of the MPTs reveals a topology very consistent with that obtained by Carballido *et al.* (2017), despite the modifications of new characters and two additional taxa.

The most common synapomorphies retrieved by the analyses were mapped onto the strict consensus topology and, those among the characters evaluated in chapter 5.2 were identified and tracked in the phylogenetic hypothesis (Fig. 5.22, 5.23 and 5.24). These are the major changes, from the earlier branching nodes to the most deeply nested nodes, with character states and numbers noted between parentheses:

[[[Sauropoda]+Lessemsaurus]+[Antetonitrus]

The distal expansion of the scapula (character 275) appears on this clade.

[[Sauropoda]+Lessemsaurus]

The proportions of the humerus relative to the femur (character 300) changes in this node, with all sauropodomorphs nested within this node having humerus to femur ratios larger than 0.60 (1), and some sauropods with extremely elongated forelimbs (Brachiosauridae, *Ligabuesaurus*) with a ratio larger than 0.90 (2), but never reverting to a ratio smaller than 0.60 (0). Also, the deltopectoral crest size (character 301) is reduced to a low ridge (1), making the anchor for the muscles inserting there less prominent, suggesting reduced musculature of the humerus. This character does not revert to being prominent (1). These changes are likely related to the adoption of an obligatory quadrupedal posture.

[[Eusauropoda]+Barapasaurus]

The tibia and fibula experience changes around these earlier branching nodes, in relation with the lines of action of muscles implied in swinging in the antero-posterior axis in a parasagittal manner. The orientation of the cnemial crest (character 364) shifts from projecting anteriorly (0) to projecting laterally (1) for the first time on this node, although it will revert to the basal condition on some clades. Also, a proximal tibial scar (character 367) becomes well-marked (1).

Eusauropoda

A sacrum wedged (character 408) more than 10° (1) appears for the first time in this node, not associated with changes in locomotor capabilities.

Cetiosauridae

The orientation of the cnemial crest of the tibia (character 364) reverts on this node to the primitive condition of an anterior orientation (0).

[[Neosauropoda]+[Turiasauria]]+[Mamenchisauridae]

This clade has the derived condition on the orientation of the cnemial crest of the tibia (character 364), suggesting its reversion in Cetiosauridae is likely a synapomorphy of that lineage.

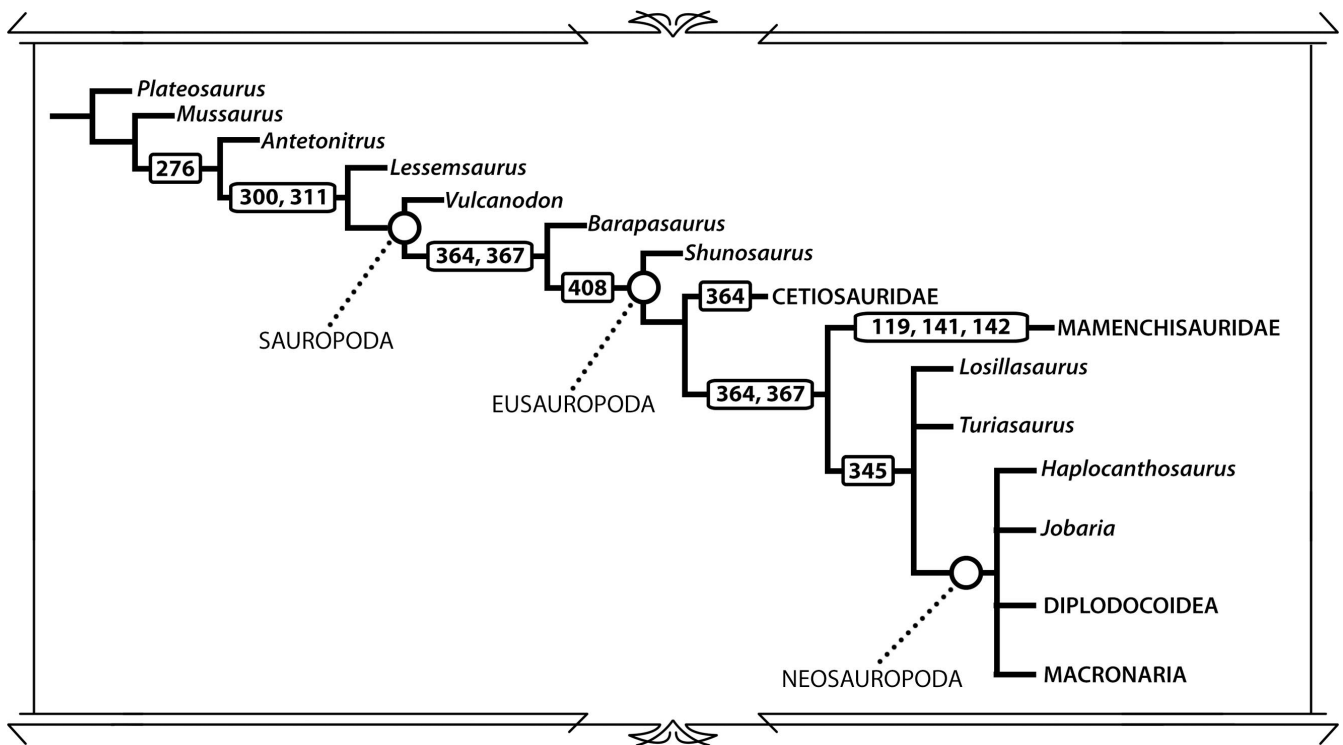


Figure 5.22 - Phylogenetic relationships of non-neosauropod Sauropodomorpha.

Simplified cladogram obtained after the strict consensus of 68 most parsimonious trees. Each node marked with changes of character states represents a common synapomorphy with potential functional implications.

Mamenchisauridae

This clade has four changes in character states with functional implications. The number of cervical vertebrae (character 119) increases greatly in this clade, with up to 19 cervical vertebrae (4). This increase in cervical vertebrae count is due neof ormation, as the number of dorsal vertebrae remains in the basal condition of 13 elements. The height of the neural spines in middle cervical vertebrae (character 141) is less than the posterior surface of the centrum (0), a reversion to the basal condition. The necks of mamenchisaurids are extremely elongated also due vertebral elongation (character 142), with middle cervical vertebrae more than four times longer than the posterior centrum height (1).

[Neosauropoda]+[Turiasauria]

The evolution of coplanar ischia, in which the distal shaft of these bones (character 345) becomes flat and articulates forming an angle close to 180° with each other (1), occurs in this node. Since it implies a smaller articulation surface, it may be related to a reduction in the relative size of tail musculature (Fig. 3.20) starting in nodes close to Neosauropoda. This character only reverts in Flagellicaudata.

Rebbachisauridae

The hyposphene ridge in caudal vertebrae (character 241) disappears in Rebbachisauridae, a clade that also has a tendency to lose the hyposphene and hypantra in the dorsal vertebrae. Characters 175 and 180 also derive to the absence of hyposphene (1) in middle and posterior dorsal vertebrae in many taxa within this clade, although since most earlier branching members of this dataset lack information on dorsal vertebrae. The height of the neural spines in middle cervical vertebrae (character 141) is less than the posterior surface of the centrum

Flagellicaudata

This clade has common synapomorphies in four characters among those evaluated. The orientation of the neural spines on caudal vertebrae (character 260) derives from a basal subvertical orientation (0) to being strongly posteriorly directed (2). The ambiens process of the pubis (character 335), origin of *M. ambiens*, derives from being a small process (0) to a larger projection. The distal shaft of the ischia (character 345) revert to the basal condition of articulating with a large surface making a 50°, V-like angle. Also, the distal ischia have a distal expansion (character 346), which is absent in other sauropods.

Dicraosauridae

The presence of keels on the ventral surface of cervical vertebrae (character 125) occurred in earlier branching Eusauropoda, but they tend to disappear to become faint ridges or completely flat ventral surfaces (1) in sauropods more deeply nested than Mamenchisauridae. In Dicraosauridae, however, the character reverts to the basal condition. Some taxa within this clade, such as *Amargasaurus* may even have double keels in some cervical vertebrae. Ventral keels are anchor sites for origin and insertion of muscles involved in neck and head ventriflexion.

Diplodocidae

The number of cervical vertebrae (character 119) in all known diplodocids with complete necks is more than 15 (3). Unlike in Mamenchisauridae, which increase their cervical count by adding new vertebrae to the neck, diplodocids increase their number of cervical vertebrae by incorporating anterior dorsal vertebrae to the neck (cervicalization of dorsal vertebrae), without modifying the basal condition of 25 presacral vertebrae.

[[Titanosauriformes]+[Galveosaurus+Euhelopus]]

The orientation of the caudal ribs from the posteriormost anterior and middle caudal vertebrae (character 229), shifts in this clade from being perpendicular (0) to being swept backwards (1), reaching the posterior end of the centrum. Also, the highest point on the dorsal margin of the ilium (character 333) derives from being posterior to the base of the pubic process (0) to being anterior to this process (1) in this clade. Both changes of these characters may be related, as the relative size of the caudal vertebrae starts to drastically diminish close to the radiation of Titanosauriformes, implying a relatively smaller *M. caudofemoralis longus* and a change in the locomotion, probably with musculature rearrangements.

Titanosauriformes

The length of the pubis relative to the ischium (character 334) shifts from the basal condition of a pubis longer or subequal in length (0) to a pubis more than 120% larger than the ischium (2). This occurs due to both a relative growth of the pubes and specially a reduction in the size of ischia. This reduction may well be coupled with the overall reduction in caudal vertebrae size (and associated musculature) in all Titanosauriformes.

Titanosauria

The orientation of the scapular blade relative to the coracoid (character 275) shifts from the primitive condition of being perpendicular (0) to forming an angle of around 45°. This may be related with a rearrangement of the disposition of the pectoral girdle elements (Schwarz *et al.*, 2007a) and with the extreme wide-gauge trackways linked to titanosaur sauropods (Wilson & Carrano, 1999).

[[Eutitanosauria]+[Epachthosaurus]]

The orientation of the neural spines in middle and posterior dorsal spines (character 185) in the majority of titanosaurs is strongly posteriorly inclined, forming an angle smaller than 40° with the dorso-ventral axis of the vertebra (2). This inclination occurs mainly in middle dorsal vertebrae (around DV-4 to DV-7), while posteriormost dorsal vertebrae tend to have vertical neural spines.

Eutitanosauria

The hyposphene-hypantrum complex in middle (character 179) and posterior dorsal vertebrae (character 180) is present (0) in the majority of sauropodomorphs, only disappearing (1) in members of Rebbachisauridae for which dorsal vertebrae are known and in Eutitanosauria. The disappearance of the hyposphene-hypantrum implies torsion and lateral flexion are possible in dorsal vertebrae.

Colossosauria

Epiphyses are present on cervical vertebrae (character 128) as the basal condition for the majority of dinosaurs (1), and they are lost or extremely reduced in Colossosauria. Also, the orientation of middle caudal vertebrae (character 257) is strongly directed posteriorly (3).

Rinconsauria

The anterior face of anterior caudal vertebrae is strongly inclined anteriorly (character 254), making

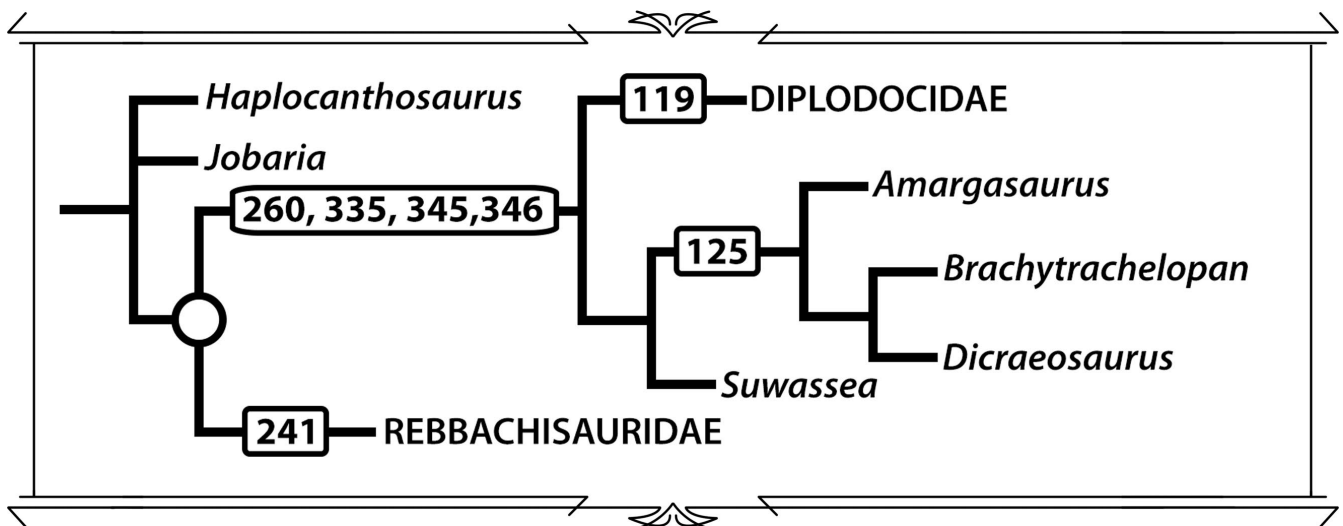


Figure 5.23 - Phylogenetic relationships of Diplodocoidea.

Simplified cladogram obtained after the strict consensus of 68 most parsimonious trees. Each node marked with changes of character states represents a common synapomorphy with potential functional implications.

the centrum have obtuse wedging only in Rinconsauria among sauropod dinosaurs. This inclination has an impact in the ONP further enhanced by the anterior inclination of the neural arches (including prezygapophyses, making the caudal vertebrae deflect ventrally when in full articulation. *Overosaurus* is the best example of the condition.

[[Longkosauria] + [Bonitasaura]]

Longkosauria and the taxa closer to them than to other titanosaurs share some modifications on posterior cervical vertebrae, such as an extremely latero-medially expanded neural spine (character 150, state 2) or an extremely dorso-ventrally tall neural spine (character 153, state 1). Also, the orientation of anterior dorsal neural spines (character 172) reverts to the basal condition of being nearly vertical or very slightly posteriorly inclined (0). However, this character is coded as such in *Futalongkosaurus*, which has the same condition in the first four dorsal vertebrae as *Overosaurus* (Fig. 5.20), so although the inclination of anterior neural spines is likely to have functional implications, the way it is coded in morphological matrices should be revised. Finally, the orientation of posterior and middle dorsal neural spines (character 185) reverts to the condition of being slightly posteriorly inclined (1).

5.5 DISCUSSION

The amount of postcranial characters with motion or myological functional implications is of 88. This implies 88/290 postcranial characters (around 30%) and 88/409 overall characters (around 21.5%) being analyzed in this phylogenetic analysis had morphofunctional implications. While the number is not excessive, it surely is greater than what was expected. However, when mapping common synapomorphies, most well-supported nodes did have additional synapomorphies also supporting them. Therefore, it can be considered that those nodes represent actual clades, and that those common synapomorphies with functional implications represent changes with functional significance that may have been under selective pressure. These are considered below.

Trends in feeding envelope characters

As proposed in chapter 3, some characters may have been coupled in a functional module related with the enlargement of the feeding envelope. The main evidence for this was the abrupt change in sacrum wedging in Eusauropoda (Fig. 3.24). Also, in all sauropods within this node, a correlation between the amount of wedging in the sacrum and the humerus/femur proportions was identified (Fig. 3.7 B). This coupling meant that further modifications could be expected in other skeletal regions related with the vertical lengthening of the presacral vertebrae (such as increased vertebral count, increased elongation of cervical vertebrae, increased elongation of zygapophyseal facets...).

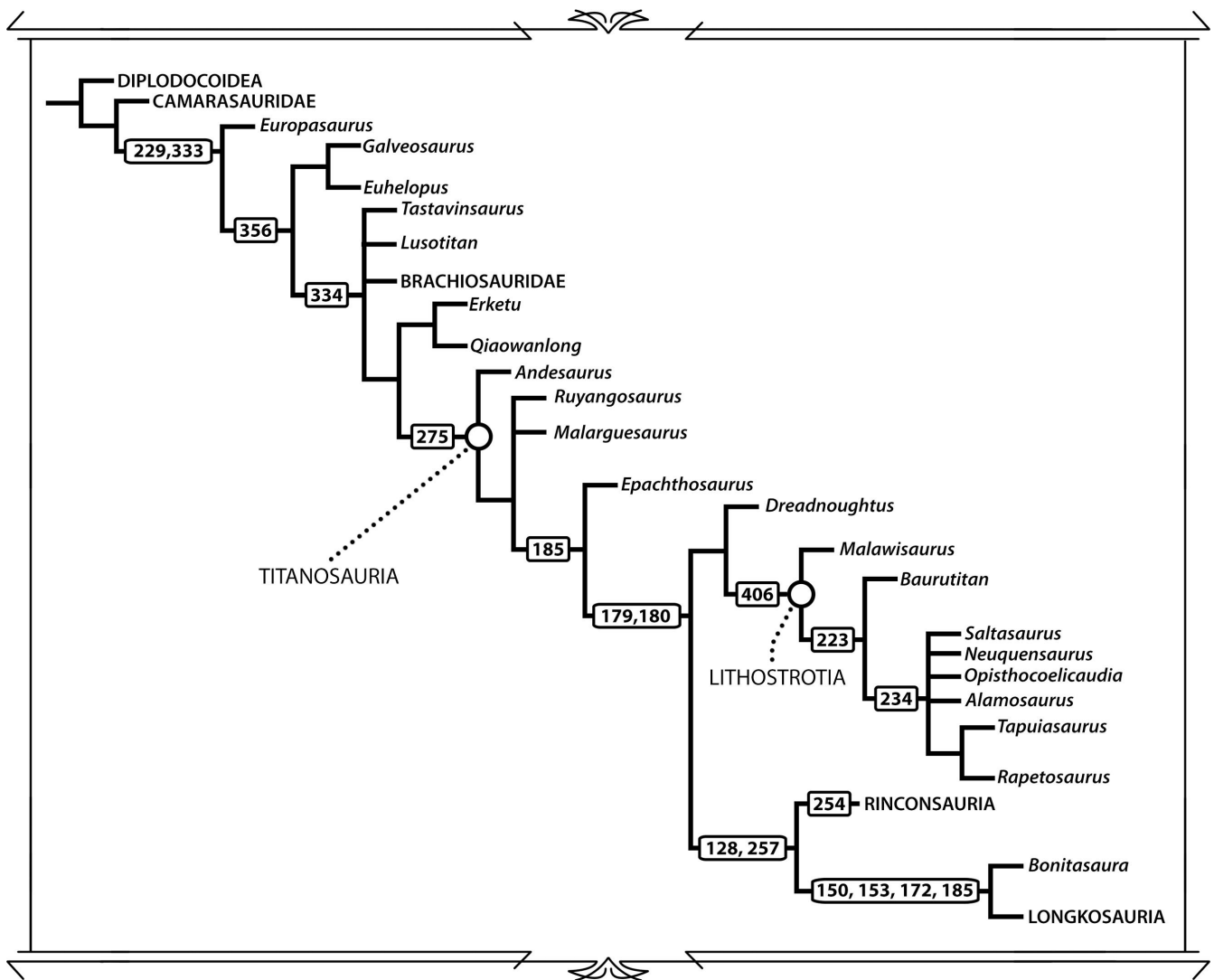


Figure 5.23 - Phylogenetic relationships of Macronaria.

Simplified cladogram obtained after the strict consensus of 68 most parsimonious trees. Each node marked with changes of character states represents a common synapomorphy with potential functional implications.

However, both mapping common synapomorphies and optimization of characters on the different most parsimonious trees show that those characters evolved in more inclusive nodes, sometimes as convergent features and sometimes with one or two reversions to the basal condition. The number of cervical vertebrae (character 119) derived from the basal condition of 12 at least three independent times in Mamenchisauridae, Diplodocidae and Somphospondylia. A similar situation occurs with the extreme elongation of middle cervical vertebrae (character 142), which derived three independent times within the same clades, with a reversion in *Abydosaurus*.

The presence of well-developed ventral keels in cervical vertebrae (character 125) is a basal feature for Sauropoda. Strong ventral keels suggest a stronger anchor for muscles related with neck and head ventriflexion. Ventral keels become faint or disappear in Eusauropoda more deeply nested than Mamenchisauridae. However, Dicraeosauridae revert to the basal condition, having relatively well-developed ventral keels in their cervical and anterior dorsal vertebrae. The fact that this reversion occurs in a very specialized clade suggests this reversion may have been under a different selective pressure.

Also, some features not coded in the modified dataset from Carballido *et al.* 2017, such as the obtuse wedging in middle dorsal vertebrae which is present in sauropods such as *Haplocanthosaurus*, Dicraeosauridae (*Dicraeosaurus*, *Brachytrachelopan*) or Saltasaurini (*Neuquensaurus*, *Saltasaurus*) also appears to have appeared in said clades in a convergent way. This wedging of the dorsal vertebrae, together with shortening the forelimbs, enabled these sauropods to reach the ground just by neck ventriflexion, which was impossible for sauropods such as *Spinophorosaurus* or *Camarasaurus*.

The shape of zygapophyseal facets, also not coded into the dataset, appears to be a highly homoplastic feature. Zygapophyses wider latero-medially than long antero-posteriorly appear in many non-related taxa,

such as *Jobaria*, *Camarasaurus*, Diplodocidae (*Diplodocus* and *Barosaurus*), *Ligabuesaurus* or *Neuquensaurus*. The relative width of the vertebra (measured as the distance between both diapophyses respect to centrum length) appears to be larger in some of these taxa, but not all of them have particularly wide cervical vertebrae.

While the wedged sacrum is a character state that never reverts to its basal condition throughout sauropod evolutions, nor does it appear to decouple from correlating with forelimb/hindlimb proportions, no other identifiable character related to the vertical component of the feeding envelope appeared at the same node and remained present in all Eusauropoda. Some characters, either implying increases or decreases in the vertical component of the feeding envelope evolved multiple times, independently in multiple clades. Increases in neck length would further increase vertical reach caused by the antero-dorsal deflection of presacral vertebrae caused by the wedging of the sacrum. These modifications in neck length in different clades, without modifications in sacral or dorsal wedging, suggest a selective pressure toward vertical lengthening in these clades (Mamenchisauridae, Diplodocidae, Brachiosauridae, Euhelopodidae, Titanosauria?). However, even within some of these clades additional features modifying neck function (i.e. bifid spines, wider than long prezygapophyses...) may arise in less inclusive nodes within these clades, even as autapomorphies of a single taxon (i.e. *Barosaurus*). This implies that, at present, the best interpretation for the sacrum wedging can be both an exaptation for some sauropod clades (those developing high browsing or extreme high browsing) and as a functional constraint (those which evolved towards low browsing or ground-level browsing).

This implies all characters belonging to this potential functional module, with the exception of forelimb relative length and a wedged sacrum, evolved responding to selective pressures independently in different clades, some of which appear to have radiated successfully with additional increases in vertical lengthening.

Trends in locomotion characters

Although some changes are known to have occurred at the forelimb throughout sauropod evolution regarding modifications in stance and locomotion (Wilson & Carrano, 1999; Carrano, 2005), only characters related to the evolution of the hindlimb and pelvic girdle have been identified from common synapomorphies. The majority of the propulsion force in dinosaurs is due to leg retraction from *M. caudofemoralis longus* (CFL) contraction (Gatesy, 1990; Persons & Currie, 2010; Ibiricu *et al.*, 2014; Mallison *et al.*, 2015; Klinkhamer *et al.*, 2018) and several modifications occurred regarding the osteological correlates of this muscle throughout sauropod evolution.

CFL is highly developed in earlier branching sauropodomorphs and sauropods (Fig. 3.20 B,C), with chevrons extremely long relative to centrum height and reaching as far back as caudal vertebra 15. At some stage in Neosauropoda evolution, evidenced for the first time in *Camarasaurus*, the chevrons become shorter relative to vertebral centrum height and CFL reaches a slightly more anterior position in the tail before disappearing (caudal vertebrae 13 or 14). This reduction is further carried out in Titanosauriformes by a reduction in absolute size of caudal vertebrae size (anteriormost caudal vertebrae may become one third to half the size of the posteriormost dorsal vertebra) and additional reduction in chevron relative length. Titanosauria sees further reduction of CFL correlates, with even shorter chevrons and the muscle reaching an even more anterior position in the tail, disappearing by caudal vertebra 10 in *Epachthosaurus* and in caudal vertebra 6 or 7 in *Neuquensaurus*. Reduction of CFL was relatively stepwise during the evolution of Macronaria, without abrupt changes in its size.

Reduction of CFL implied smaller torque generation capability for leg retraction. It is not surprising that further modifications regarding the pelvic girdle can be linked to the reduction of CFL. Among these, the highest point of the ilium (character 333) becomes the preacetabular process in the clade [[Titanosauriformes]+[*Galveosaurus*+*Euhelopus*]]. This is due a dorso-ventral development of the preacetabular process, which implies greater origin areas for *M. iliotrochantericus caudalis* (ITC) and *M. iliofemoralis* (IFE), as well as larger lever arms for *M. iliotibialis 1* (IT1). Also, in Titanosauriformes the size of the pubis relative to the ischium (character 334) becomes more than 120% the length of the latter, implying a reduction in ischium size and a consequently a reduction of the size of the origin areas of the adductor muscles in this bone. This may have been hampered or caused by the widening of the pelvis in Titanosauriformes (Carrano, 2005), which came with a medial deflection of the fourth trochanter in the femur and a change in the line of action of CFL, whose adduction component grew (Fig. 3.21).

In Titanosauria, the orientation of the scapular blade relative to the coracoid (character 275) shifted from being relatively straight to having a 45° angle. However, the mechanical implications of this change cannot be assessed at present (since a complete pectoral girdle and an anterior ribcage from the same titanosaur

individual or taxon could not be assembled). It may indicate a change in the position of the scapular blade and the lines of actions of its muscles (assuming the coracoids and sternals remained in the same position relative to the ribcage as in other titanosaurs) or a way for the scapular blade to preserve the same orientation and lines of action of its muscles relative to the humerus and ribcage (assuming the position of coracoids and sternals shifted, being the lines of action of the muscles muscles originating there the ones changing). This suggests that an increase in propulsion from the forelimb may have developed in this clade to counteract the reduction of CFL mass and its line of action changes.

The lateral flaring of the preacetabular ilium (the lateral deflection of the preacetabular process) becomes progressively more pronounced throughout Macronaria, Titanosauriformes and Titanosauria, to the extremes seen in Saltasaurini, *Futalognkosaurus* or *Lohuecotitan*. This flaring places the origins of IT1 and ITC even more laterally, implying a greater mechanical advantage for protraction and a smaller mechanical advantage for abduction (Carrano, 2005).

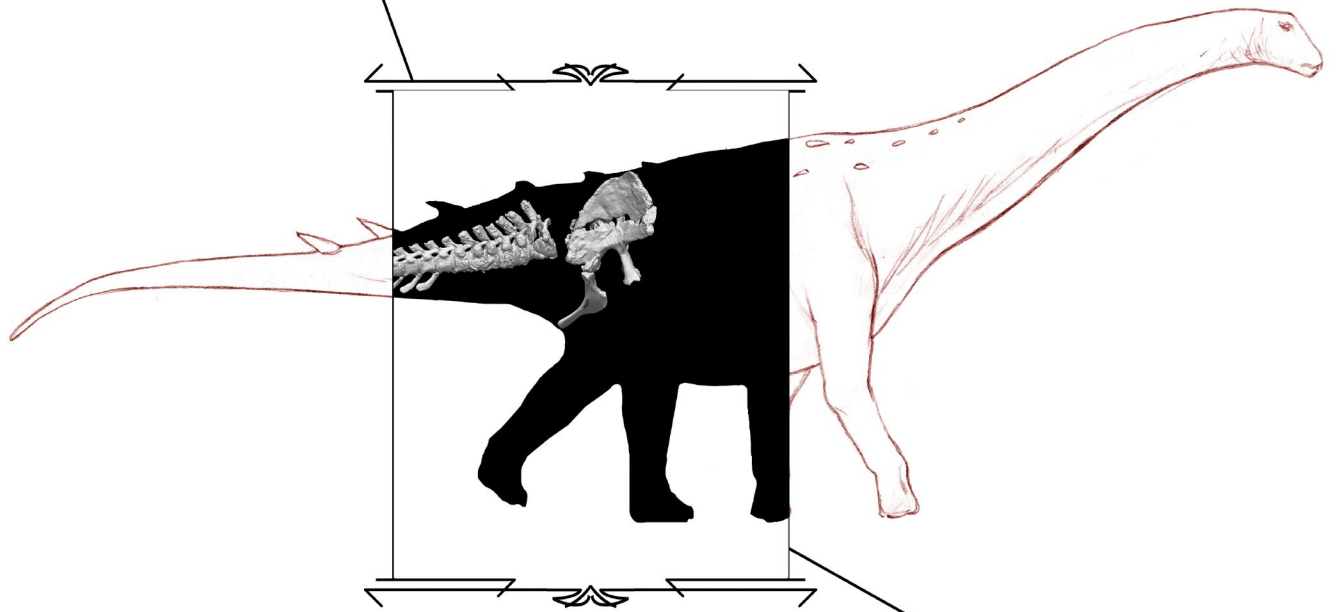
All these character state changes imply a remarkable change in locomotion dynamics of Macronaria throughout their evolution. These changes clearly evolved stepwise, suggesting a mosaic evolution for sauropod locomotion, as occurred with the evolution of avian flight module (Clarke & Middleton, 2008).

5.7 CONCLUSIONS

A large percentage of postcranial characters with motion and/or myological implications constitute Carballido *et al.* (2017) data set, but the recovered clades are not based only in synapomorphies regarding characters with functional implications.

Characters regarding verticalization of the presacral column and the enlargement of the vertical component of the feeding envelope show more homoplasy than those regarding locomotion. Only the wedging of the sacrum and its coupling to forelimb/hindlimb proportions appear at once and never revert to the basal condition. Other characters regarding neck elongation appear multiple times in several clades but appear to respond to different selective pressures.

Characters regarding locomotion are common synapomorphies, suggesting that changes in locomotion may have been phylogenetically constrained, particularly in Macronaria, the lineage toward Titanosauria and within Titanosauria as well. These changes consist in a progressive reduction of femoral retraction as the main thrust for propulsion in walking (reduction of caudofemoral musculature, changes in caudofemoral musculature to a greater role in adduction, reduction of ischium and its adductor muscles...). These changes occurred stepwise throughout the phylogeny, suggesting mosaic evolution.



CHAPTER
• 6 •

PRELIMINARY VIRTUAL PALEONTOLOGY APPROACH TO LO
HUECO TITANOSAURS

Introduction.....	213
Material.....	215
Results.....	215
Discussion.....	220
Conclusions.....	225

6.1 INTRODUCTION

Multi-specimen and multi-taxic dinosaur bonebeds, although known from several dinosaur-bearing Formations, are relatively uncommon next to sites including a single specimen with scarcer remains of other taxa. In the particular case of sauropod dinosaurs, cases of multi-specimen monotaxic bonebeds and multitaxic bonebeds are known. The best-known examples probably are in the Morrison Formation from the Upper Jurassic of the United States. Sites such as Como Bluff, Howe Quarry, Howe-Stephens Quarry or Dinosaur National Monument are assemblages in which several specimens of different sauropod (and other dinosaur, crocodile, turtle and mammal remains) are found together in single depositional events. Dinosaur National Monument particularly is remarkable not only for the large number of specimens but also for the high number of articulated and complete individuals present, belonging to at least four sauropod genera: *Camarasaurus*, *Apatosaurus*, *Diplodocus* and *Barosaurus*. This site has been interpreted as a product of non-catastrophic mass mortality during extreme droughts (Carpenter, 2013), suggesting many of the sauropods in similar degrees of preservation may have coexisted in the same ecosystem.

A high number of phylogenetic studies find the sauropods from Dinosaur National Monument belong to two different clades: *Camarasaurus* is an early branching Macronaria, *Apatosaurus*, *Diplodocus* and *Barosaurus* are Diplodocidae, the latter two sister taxa in plenty of analyses (Wilson, 2002; Upchurch *et al.*, 2004; Tschopp & Mateus, 2012; Mocho *et al.*, 2014). Despite being closely related, the functional morphology of *Diplodocus* and *Barosaurus* regarding their feeding strategy may have been different, particularly regarding their cervical vertebrae: *Barosaurus* is extremely specialized in sideways sweeping of the neck (Taylor & Wedel, 2016), supporting a vacuum-cleaner model similar but not identical to that proposed for *Nigersaurus* (Sereno *et al.*, 2007; Taylor & Wedel, 2016), while the neck of *Diplodocus* is not as specialized (Stevens & Parrish, 1999). *Diplodocus* and *Apatosaurus*, a bit more distantly but also closely related, also had very different neck motion capabilities, with *Apatosaurus* having a more mobile neck (Stevens & Parrish, 1999), among other differences between them. These differences in postcranial motion capabilities, together with other lines of evidence, suggest potential niche partitioning in the adults of these sauropods (Stevens & Parrish, 1999, 2005; Whitlock, 2011a; Paul, 2017), which may explain the coexistence of several large phytophagous dinosaurs in the same ecosystem.

Lo Hueco fossil site was discovered in 2007 close to the town of Fuentes, Cuenca (Spain). To date, Lo Hueco has yielded a large collection of well-preserved Cretaceous macrofossils. The recovered fossil assemblage is mainly composed of plants, mollusks (bivalves and gastropods), actinopterygians and teleostean fishes, amphibians, panpleurodiran (bothremydids) and pancryptodiran turtles, squamate lizards, eusuchian crocodyliforms, rhabdodontid ornithopods, theropods (mainly dromaeosaurids), and titanosaur sauropods (Ortega *et al.*, 2008, 2015; Barroso-Barcenilla *et al.*, 2009). These titanosaurs have been found in various degrees of articulation and completeness, being the most common tetrapods in the assemblage.

The first preliminary analyses indicated the presence of, at least, two titanosaur taxa in Lo Hueco based upon two distinct types of cranial morphologies, appendicular bones and teeth. Up to now, there is no clear relationship between the remains, and therefore it is not possible to correlate the distinct types of teeth with the postcranial sets of bones and the isolated braincases at the moment. Some cranial elements present affinities with the French titanosaur *Ampelosaurus* (Knoll *et al.*, 2012) and others with the Indian *Jainosaurus* (Knoll *et al.*, 2015). The recognized tooth morphotypes can be respectively correlated with the robust spatulated teeth of the titanosaur from Masecaps and the teeth of *Atsinganosaurus* (Díez Díaz, Ortega, & Sanz, 2014). The first articulated skeleton found was recently described as a new taxon, *Lohuecotitan pandaflandi* (Díez Díaz *et al.*, 2016) based on axial, girdle and appendicular elements from a single individual.

An approximation based on the more than seventy femora collected states that the minimum number of titanosaur individuals represented in the association is above forty. However, the number of partially articulated individuals is twenty. The majority of the articulated specimens come from the same bed, G1 quarry, which has been interpreted preliminarily as a single depositional event (Cambra-Moo *et al.*, 2012; Domingo, Barroso-Barcenilla, & Cambra-Moo, 2015; Vidal *et al.*, 2017), suggesting the dinosaurs may have coexisted in the same environment. Among the skeletons retrieved from G1 quarry (Fig. 6.1), about eight are currently in different stages of preparation and study (among them the holotype of *Lohuecotitan*). Preliminary analyses have shown that disparity in the axial skeleton is greater than expected, with up to four different morphotypes in articulated caudal vertebrae. This raises an issue on the potential diversity of titanosaurs at the end of the Cretaceous in the Ibero-Armorican island. With up to four different taxa coexisting in Lo Hueco, understanding

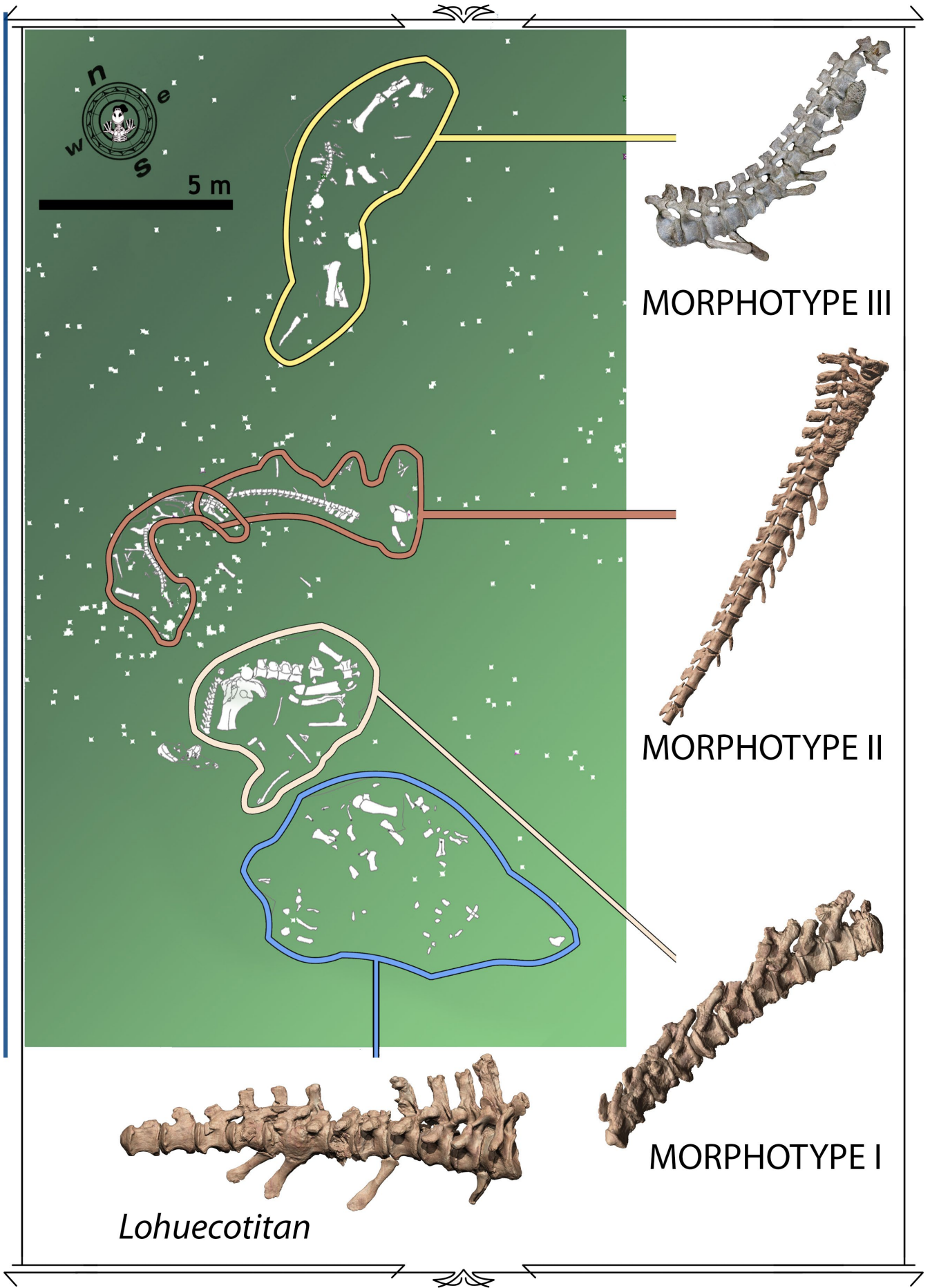


Figure 6.1 - Titanosaur saupod association at Lo Hueco G1 Quarry.

Quarry map for the west sector of Lo Hueco G1 quarry, which yielded the most articulated titanosaur skeletons from the locality. The highlighted skeletons have caudal vertebrae belonging to at least four different morphotypes, and were found closely associated in similar degrees of articulation.

their functional morphology may help to test a niche partitioning general hypothesis, which may also help in the discussion on whether evolutionary history of European titanosaurs is better explained by: an endemic cladogenesis event or the product of dispersal events.

Here, the virtual paleontology techniques are applied to the titanosaur skeletons from Lo Hueco, comparing with results obtained in the previous chapters to establish a preliminary framework in which to study the different morphotypes as more material is prepared and becomes available for digitization. This framework will allow future analyses to understand the disparity of Lo Hueco titanosaurs from a functional point of view, which will aid in determining whether this disparity is a product of taxonomic, sexual or ontogenetic variability. The following hypotheses are evaluated: (i) Lo Hueco fossil site includes at least 3 titanosaur sauropod morphotypes with a great degree of neck/trunk/tail and forelimb/hindlimb proportions. (ii) The adult specimens of Lo Hueco titanosaurs would have non-overlapping feeding envelopes, implying a niche partition among them. (iii) The different morphotypes of Lo Hueco titanosaurs have marked differences in their locomotor dynamics. (iv) Morphotypes of Lo Hueco titanosaurs with dermal armor have osteological characteristics setting them apart from unarmored morphotypes. (v) Given the dorsal armor acts as a limit to range of motion, morphotypes of Lo Hueco titanosaurs with dermal armor would have a greater range of motion (without the armor) than unarmored morphotypes.

6.2 MATERIAL

Table 6.1 lists all available material from Lo Hueco and the anatomical regions that were available to be analyzed. Only completely prepared specimens were possible to digitize in order to perform the analyses under the same conditions as for other sauropods in this thesis. While this renders the results preliminary, the better-represented regions (caudal series and pelvic girdles) allow drawing some tentative conclusions for the taxa in which they are present. The division of morphotypes employed is based almost exclusively on the caudal series (vertebrae and chevrons), as it represents the highest level of disparity found (Fig. 6.2).

Specimen	Morphotype	Neck	Dorsal	Sacral	Caudal	A. Girdle	Forelimb	P. Girdle	Hindlimb	Dermal
HUE-EC-1	<i>Lohuecotitan</i>	Y**	Y**	P**	Y**	N	Y	Y**	Y**	N
HUE-EC-2	II	Y*	Y*	P**	Y**	N	Y?	Y**	?	N
HUE-EC-3	II	N	N	N	Y**	N	N	P	N	N
HUE-EC-4	I	N	Y*	Y**	Y**	N	N	Y**	P	N
HUE-EC-5	?	Y*	Y*	?	?	N	Y	?	Y	N
HUE-EC-6	III	N	?	P	Y*	N	N	Y*	Y*	Y*
HUE-EC-11	III?	?	Y*	P	Y**	N	N	Y	Y*	Y**
HUE-EC-13	III	?	Y*	P	Y**	N	?	Y	?	N

Table 6.1 - Titanosaur specimens from Lo Hueco G1 Quarry.

Specimens of titanosaurs from Lo Hueco of which some material has been prepared to date. Y (green) indicates elements pertaining to that anatomical region have been identified for that specimen. N (red) indicates no elements from that anatomical region have yet been identified for that specimen. P indicates elements are partially preserved (fragmentary) Question mark indicates elements from that anatomical region which may belong to the specimen have been identified. * Studied. ** Digitized and studied.

6.3 RESULTS

While few prepared skeletal regions overlap in the titanosaurs from Lo Hueco, the caudal series and pelvic girdles overlap in a relatively large number of individuals. Since the morphotypes are characterized based on the caudal vertebrae and chevron morphology, characters from different bones are yet to be assessed as shared features or differences. Each morphotype will be described in detail as in chapter 5.

Lohuecotitan pandaflandi **Díez Díaz et al. 2016**

Holotype. MUPA-HUE-EC-1 Partial skeleton consisting of three cervical vertebrae, four almost complete anterior-middle dorsal vertebrae and two fragmentar dorsal vertebrae, sacral ribs, at least the anteriormost 14

caudal vertebrae, four chevrons, several rib fragments, left ulna, both ischia, left pubis, right femur, right fibula, right tibia, some indeterminate remains.

Referred specimens. N/A

Locality and horizon. Lo Hueco fossil site (Cuenca, central Spain), Villalba de la Sierra Formation (Spain), upper Campanian-lower Maastrichtian.

Personal description/remarks. *Lohuecotitan* is a fairly complete skeleton. However, with the majority of the sacrum, posterior dorsal vertebrae and most cervical vertebrae missing, to assess the osteologically induced curvature is difficult until more remains referable to this taxon are found. The tail, pelvis and hindlimb, however, are fairly informative.

The anteriormost 14 caudal vertebrae were found articulated or very closely articulated. There is a sequence of another eight middle to posterior caudal vertebrae found in very close association and was referred to the holotype. However, the anteriormost of this set of middle-distal caudals has a centrum larger than the posteriormost of the 14 caudal vertebrae of *Lohuecotitan*, making referring the second set of caudals to the holotype specimen doubtful, although it may belong to the taxon.

The anteriormost 14 caudal vertebrae articulate in ONP as in the majority of surveyed sauropods, with a slight ventral deflection in the anteriormost caudals, deflecting to become subhorizontal by CdV-7 and CdV-8 (which became fused due to a spondyloarthropathy while the animal was alive). The chevrons are remarkable for their extremely anteroposteriorly developed proximal ends, with autapomorphic double articulation facets. The lateral faces of the anterior caudal centra, with the exception of the aforementioned pathological vertebrae, are fairly concave, with a ridge present in CdV-9 marking the end of the lateral concave surface of the centra (which may have started in CdV-8). There is no lateral concavity in the centrum of CdV-10, and the ridge is extremely ventral, so it is likely that CFL barely reached CdV-10 (Fig. 6.3 A). The chevrons of *Lohuecotitan* are particularly robust and relatively elongated next to the centrum, implying a CFL more developed dorso-ventrally than in titanosaurs such as *Epachthosaurus* or *Neuquensaurus*.

The pelvic girdle is highly complete, although the pubis is somewhat damaged. The ilium does not have a particularly developed blade in the dorso-ventral plane. However, the preacetabular lobe is extremely developed antero-posteriorly, and extremely laterally flared, making an almost 90° angle with the sagittal plane (Fig. 6.3 A; Fig. 6.4 A).. While this deflection is typical in other titanosaurs, it is particularly deflected in *Lohuecotitan*, closer to the condition observed in saltasaurids (but even more flared) than that in *Epachthosaurus* or *Trigonosaurus*. It is the most laterally flared preacetabular process from the ilia found in other articulated specimens from Lo Hueco thus far. This deflection further enhances the role of *M. ilioprochantericus caudalis* (ITC) as a femoral protractor rather than an abductor (the basal condition). *M. iliotibialis 1* (IT1) also has an efficient line of action to act as a protractor, but such a lateral deflection may have conferred some role in abductor, although more exhaustive tests should be performed. The other pelvic muscles are as much developed relative to ITC similarly to *Epachthosaurus*.

MORPHOTYPE I

Referred specimens. MUPA-HUE-EC-04 partial skeleton consisting of four to six dorsal vertebrae, rib fragments, six sacral vertebrae, 11 first caudal vertebrae in sequence, complete left ilium, fragmentary right ilium, both pubes and ischia, partial femur?

Locality and horizon. Lo Hueco fossil site (Cuenca, central Spain), Villalba de la Sierra Formation (Spain), upper Campanian-lower Maastrichtian.

Personal description/remarks. This morphotype has (i) short and anteriorly directed neural spines in middle caudal vertebrae, (ii) long pedicels and (iii) robust, dorsally inclined and robust prezygapophyses in all preserved caudal vertebrae, with anteroposteriorly elongated articular facets. These caudal vertebrae are similar to those from aeolosaurine titanosaurs, and have the exact same type of osteologically induced curvature in ONP: a strong ventral deflection. The pelvis is remarkable regarding the proportion of the ischia relative to the pubes, as the former are extremely reduced and the latter extremely elongated (as long as the antero-posterior length of the ilium). The ilium, while not particularly dorso-ventrally developed, has a shorter posterior region, with the preacetabular lobe extremely antero-posteriorly developed, being as long as the acetabular and postacetabular regions together (Fig. 6.3 C).

This implies an extremely reduced posterior pelvic musculature (*M. flexor tibialis internus*, *M. iliotibialis 3* and *M.*

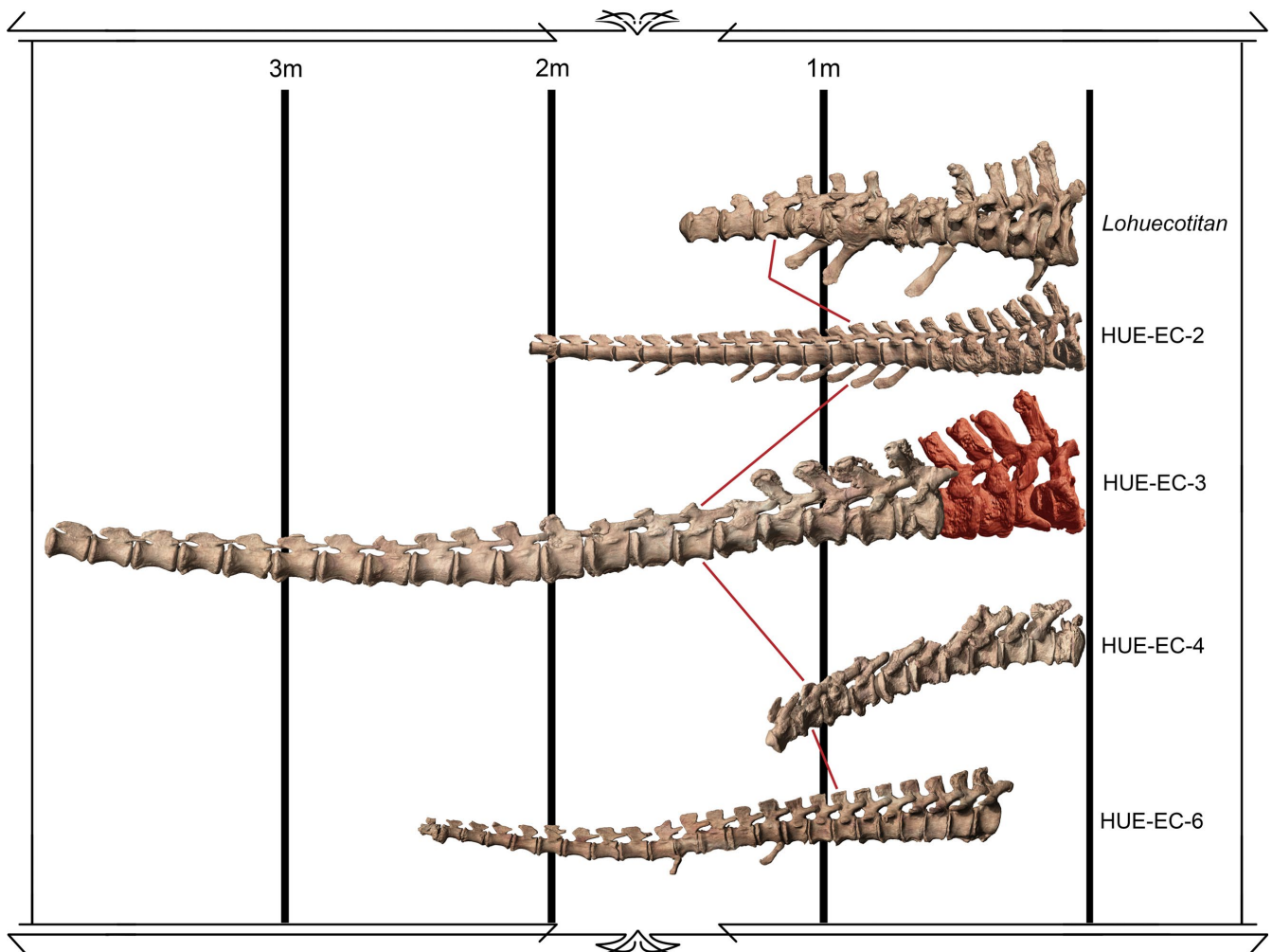


Figure 6.2 - Titanosaur sauropod caudal morphotypes from Lo Hueco.

Articulated virtual models of caudal sequences of five different titanosaurs from Lo Hueco, to scale. Each morphotype is designated. Lines point to caudal vertebra 10 on each specimen.

iliofibularis) and relatively developed anterior pelvic musculature (*M. iliotrochanterichus caudalis*, *M. iliotibialis 1* and *M. iliofemoralis externus*). *M. caudofemoralis longus* is as reduced as in other studied non-saltosaurine titanosaurs, disappearing by CdV-10 (Fig. 6.3 C), as in *Epachthosaurus*. On the other hand, the *ambiens* process of the pubis is not marked, suggesting a smaller anchor for *M. ambiens*. Unfortunately, the putative femur is poorly preserved and not yet completely prepared, so the insertions and origins cannot be accurately assessed.

All in all, this morphotype has a lot of similarities with *Overosaurus paradasorum*, the most complete Aeolosaurini currently known. While these similarities do not necessarily imply phylogenetic proximity, they imply similar or even identical functional capabilities.

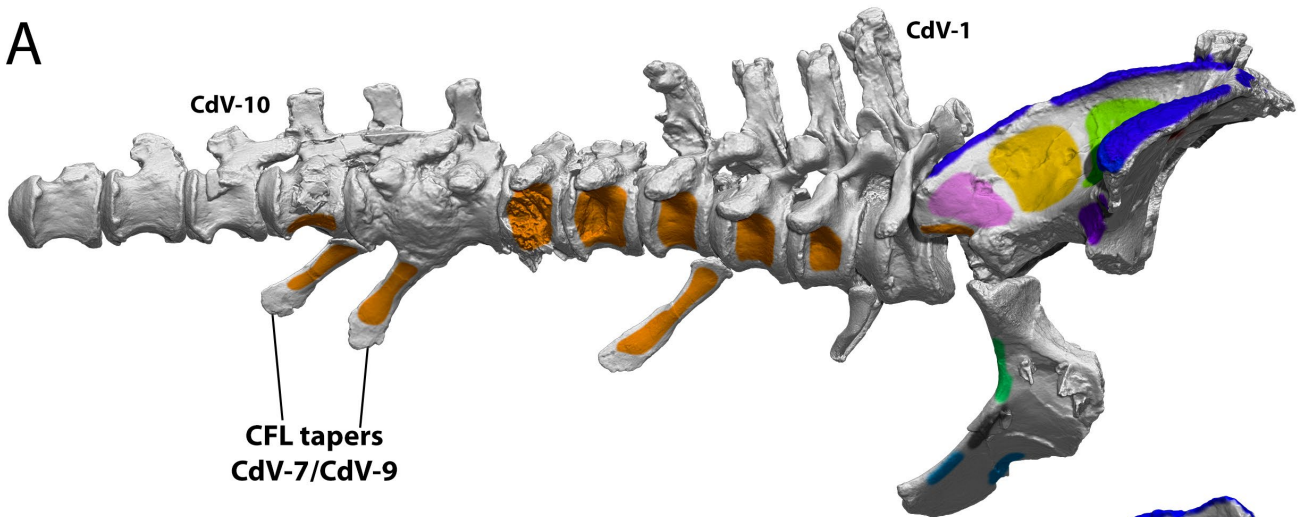
MORPHOTYPE II

Referred specimens. **MUPA-HUE-EC-02** partial skeleton consisting of up to eight cervical vertebrae, seven dorsal vertebrae, sacrum fragments, the first 22 caudal vertebrae, several fragmentary ribs, 10 chevrons, right ilium and both ischia. **MUPA-HUE-EC-03** articulated tail consisting of 26 vertebrae (from CdV-4 until CdV-30), eight chevrons and some pelvic girdle fragments.

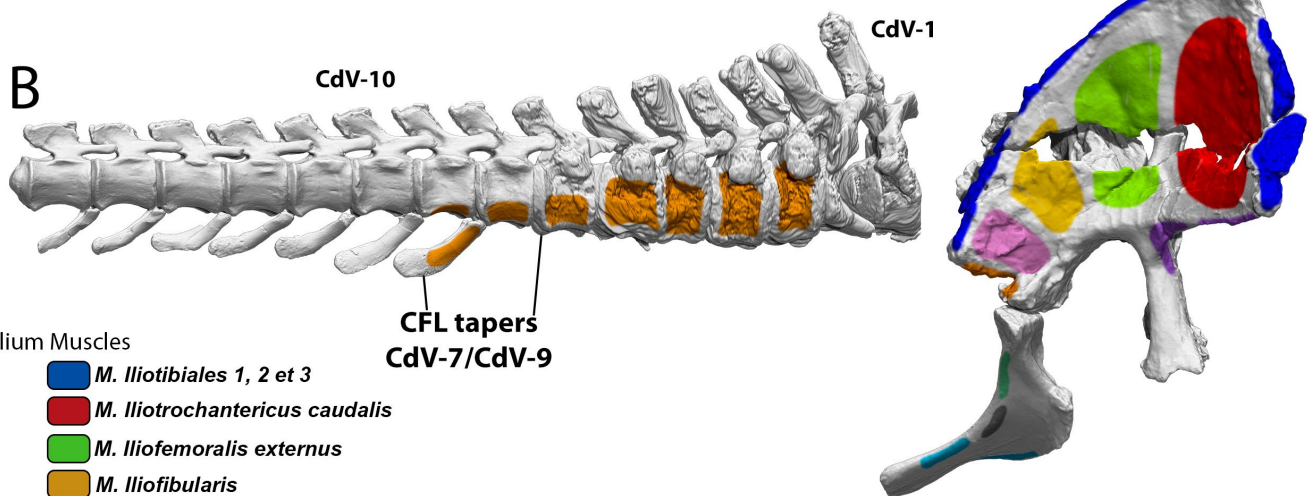
Locality and horizon. Lo Hueco fossil site (Cuenca, central Spain), Villalba de la Sierra Formation (Spain), upper Campanian-lower Maastrichtian.

Personal description/remarks. HUE-EC-02 is probably the most complete and best-preserved titanosaur individual retrieved from Lo Hueco. It is also one of the smallest individuals retrieved, but its neurocentral sutures are completely fused in all examined vertebrae. The tail of HUE-EC-03, on the other hand, is twice the size of that of HUE-EC-02. Preliminary histological analyses on dorsal ribs of HUE-EC-02 have shown it is likely a juvenile/subadult individual (Gascó *et al.*, 2018), suggesting it may still have grown to double its size.

A



B



Ilium Muscles

- *M. Iliotibiales 1, 2 et 3*
- *M. Iliotrochantericus caudalis*
- *M. Iliofemoralis externus*
- *M. Iliofibularis*
- *M. flexortibialis externus*
- *M. puboischiofemoralis internus 1 et.2*

Pubis Muscles

- *M. ambiens*

Ischium Muscles

- *M. adductor femoris 1 et. 2*
- *M. flexor tibialis internus 3*
- *M. ischiotrochantericus*

Caudofemoral Muscles

- *M. caudofemoralis longus*

C

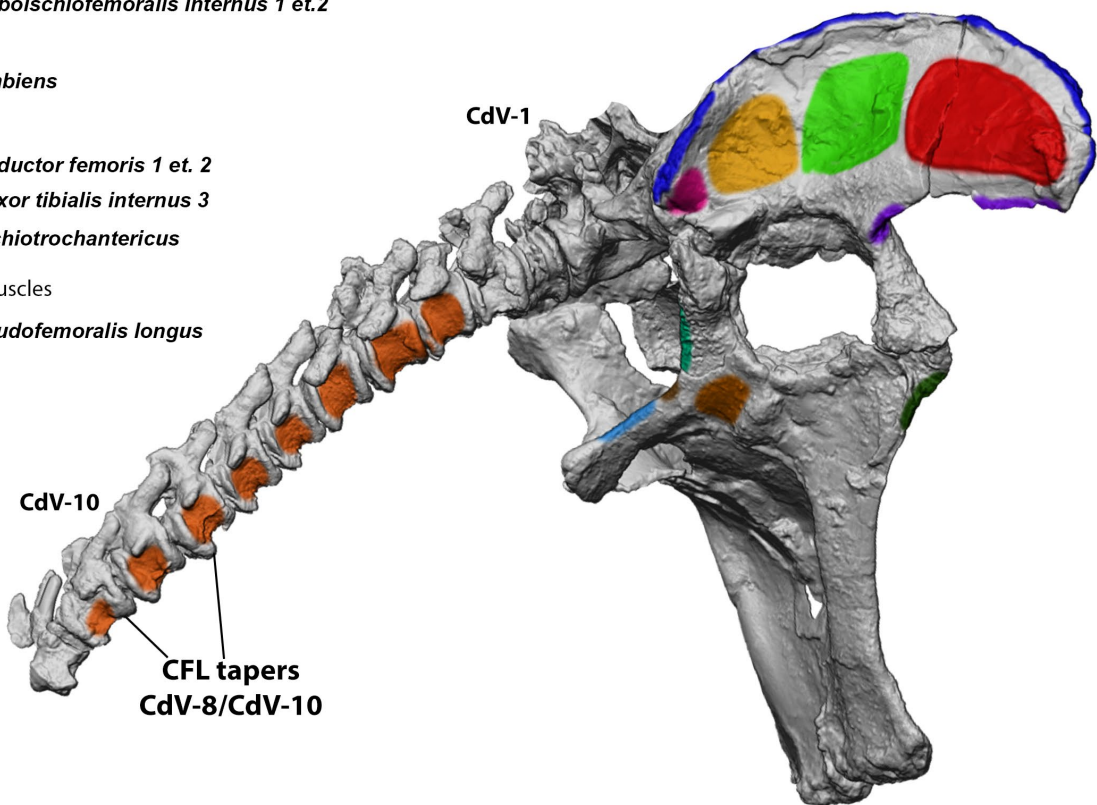


Figure 6.3 (previous page) - Lo Hueco titanosaur caudal and pelvic muscle reconstruction.

A - Ilium, ischium, sacrum and tail of the holotypic specimen of *Lohuecotitan pandafileandi* (HUE-EC-01) in lateral view, with muscular origins and insertions highlighted and colored. **B** - Ilium, ischium, sacrum and tail of specimen HUE-EC-02 (Morphotype II) in lateral view, with muscular origins and insertions highlighted and colored. **C** - Pelvis, sacrum and tail of specimen HUE-EC-04 (Morphotype I) in lateral view, with muscular origins and insertions highlighted and colored.

This morphotype has (i) long and posteriorly inclined neural spines in anterior caudal vertebrae, (ii) extremely dorso-ventrally short pedicels in middle and posterior caudal vertebrae (iii) slender, long and horizontally oriented prezygapophyses in middle and posterior caudal vertebrae and (iv) postero-distally curved anterior and middle chevrons.

The examined posterior cervical vertebrae and anterior dorsal vertebrae have extremely large and antero-posteriorly elongated prezygapophyseal facets, and both centra and pedicels are not particularly tall. This suggests great dorso-ventral flexibility in the dorso-ventral plane, although it will have to be tested after preparation is finished and digitization of the elements is possible.

Both tails of this morphotype have an almost identical OIC (Fig. 6.2), with a very smooth sigmoid curvature, less pronounced than in other sauropods, with an almost straight anterior region of the tail, with a dorsal deflection starting at around CdV-14. Although the dorsal deflection is not reverted in the preserved length of both tails, it is likely that it would have deflected ventrally at some point, as in the majority of sauropods. The lateral surfaces of the caudal centra from HUE-EC-03 are extremely concave, with a faint lateral ridge appearing on CdV-8, and disappearing by CdV-10, suggesting a *M. caudofemoralis longus* disappearing at the same region in other studied titanosaur. Caudal vertebrae 1 to 7 in HUE-EC-02 are covered in a thick iron crust that impedes assessing whether these centra lateral faces are as concave as in HUE-EC-03. However, there is a lateral ridge on CdV-8 and CdV-9 of HUE-EC-02, suggesting the tapering of CLF might have started at the same region in both specimens.

The ilium of HUE-EC-02 has a remarkably tall preacetabular process (Fig. 6.3 B), and its anterior end is not complete, but still appears to be remarkably developed as well. The pubic pedicle is also retroverted, making an acute angle with the ischial pedicle, unlike in the majority of known sauropods. Actually, proportionately, the dorso-ventral development of the iliac blade at the preacetabular lobe is greater than that of *Brontomerus mcintoshi*, which has one of the most dorso-ventrally tall ilia (Taylor, Wedel, & Cifelli, 2011). This implies the anterior ilium musculature (*M. iliotibialis 1 et 2*, *M. iliotrochantericus caudalis* and *M. iliofemoralis externus*) has both greater origin areas and longer lever arms than in other Lo Hueco titanosaur. Protraction and abduction in this morphotype were possibly more efficient than in other sauropods from the site. Unfortunately, no hindlimb elements referable to this morphotype have been presently recognized, so it is not possible to further assess its locomotor capabilities.

MORPHOTYPE III

Referred specimens. **MUPA-HUE-EC-06** partial skeleton consisting of an articulated sequence of 24 caudal vertebrae, a partial pelvis with both ilia and parts of the sacrum, two femora, one tibia, one fibula, a relatively complete foot, an osteoderm in direct association with the caudal vertebrae. **MUPA-HUE-EC-013** partial skeleton consisting of at least eight dorsal vertebrae, at least 15 caudal vertebrae in sequence, some chevrons, ribs, both pubes, an ischium.

Locality and horizon. Lo Hueco fossil site (Cuenca, central Spain), Villalba de la Sierra Formation (Spain), upper Campanian-lower Maastrichtian.

Personal description/remarks. Remains of this morphotype are still in earlier stages of preparation than those of other morphotypes, so the information regarding their anatomy is scarcer. The morphotype has (i) short, distally expanded neural spines in middle caudal vertebrae, (ii) long pedicels in all the caudal vertebrae, (iii) horizontal and short prezygapophyses in middle and distal caudal vertebrae, and (iv) straight chevrons without a double articulation facet as in *Lohuecotitan*.

The tail of HUE-EC-06 has its anteriormost caudal centra with concave lateral faces as other titanosaur from Lo Hueco. A lateral ridge appears by the fifth preserved vertebra in the sequence and disappears in the seventh (marking the dorsal tapering of *M. caudofemoralis longus*). While CFL may have tapered in a more anterior or position than other titanosaur, this tapering region is tentatively assigned to be CdV-8 to CdV-10, suggesting only the anteriormost three caudal vertebrae would be missing in HUE-EC-06. The osteologically induced

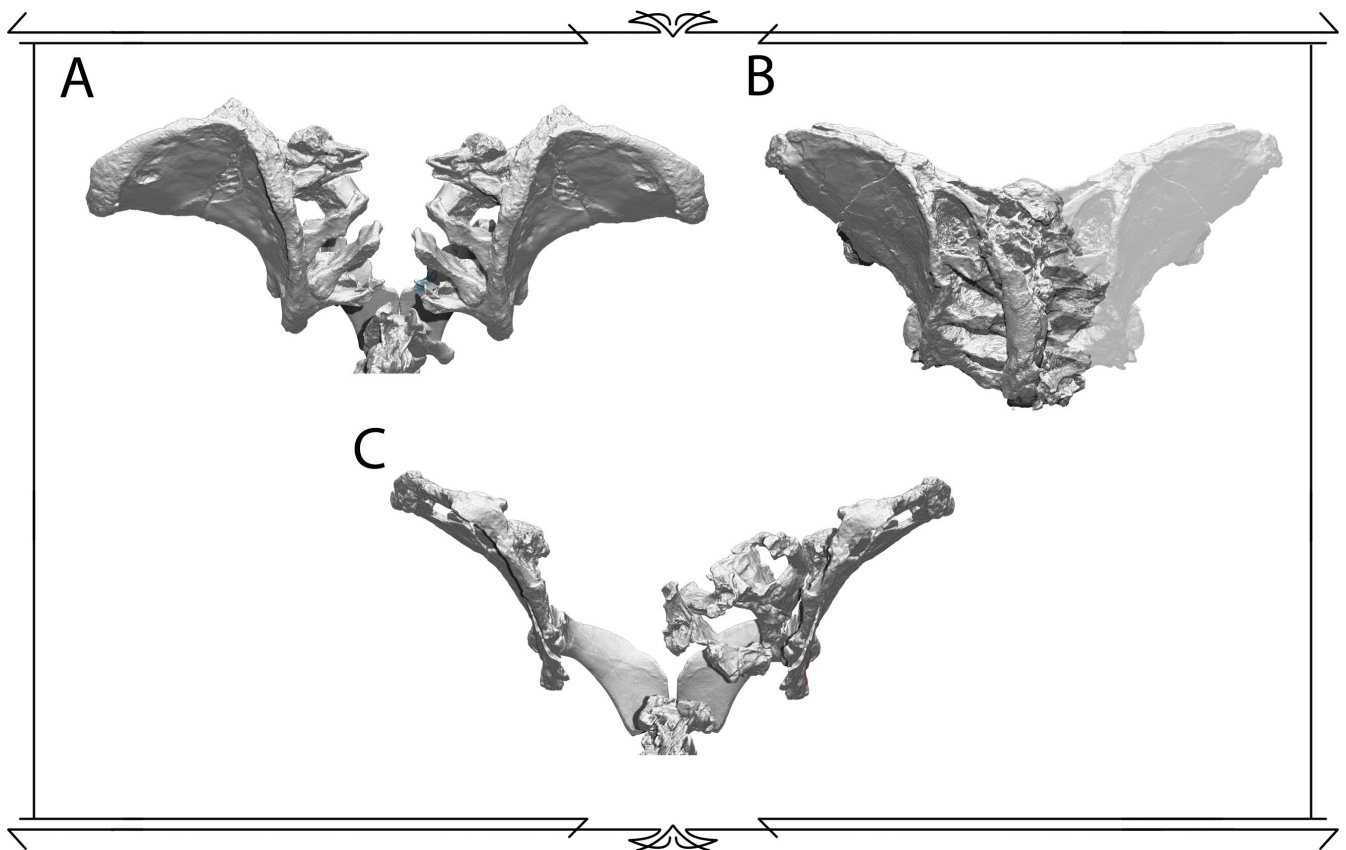


Figure 6.4 - Lo Hueco titanosaur pelvises.

A - Pelvis of the holotypic specimen of *Lohuecotitan pandafileandi* (HUE-EC-01) in dorsal view. **B** - Pelvis of specimen HUE-EC-02 (Morphotype II) in dorsal view. **C** - Pelvis of specimen HUE-EC-04 (Morphotype I) in dorsal view. Notice the differences in overall pelvis width and lateral flaring of preacetabular processes in the sacrum.

curvature of the tail is, as in other sauropods, a sigmoidal curvature with a ventrally deflected anterior region, dorsally deflecting from CdV-16 on. This sigmoidal curvature is more pronounced than in morphotype 2 or *Lohuecotitan*.

The accessible region of the preserved ilia of HUE-EC-06 shows a preacetabular lobe different from all other morphotypes, with a dorsal and ventral rims converging in a more acute angle. The preacetabular lobe is not particularly tall, being shorter than the pubic pedicles. This suggests this morphotype probably had smaller leg protractors and abductors (*M. iliotibialis 1 et 2*, *M. iliotrochantericus caudalis* and *M. iliofemoralis externus*) than other titanosaurs from Lo Hueco. However, the inability to see the lateral surfaces or the complete ilia at present impedes testing this hypothesis.

This morphotype is the only one with confidently associated osteoderms. HUE-EC-06 has a single osteoderm located in the underside of the tail, over the chevrons, displacing one of them laterally. This implies this was not its original position, as all the other chevrons are perfectly articulated and undisturbed. The fact that titanosaur osteoderms are asymmetric makes them likely parasagittal structures located over the neural spines, as in most armored archosaurs (Vidal, Ortega, & Sanz, 2014). Given this, and that the length of the osteoderm associated with this tail is equivalent of two caudal vertebrae, it implies a dorsal bracing, making the tail less flexible than that of non-armored titanosaurs or other armored titanosaurs such as *Neuquensaurus* or *Saltasaurus*, whose osteoderms are as long as one vertebra.

6.4 DISCUSSION

Caudal neural arches and forces acting upon the spine

The variability of anterior and middle caudal vertebrae of the titanosaurs from Lo Hueco is extremely high (Fig. 6.5). As has been evaluated throughout Chapter 5, the osteologically induced curvature of sauropod caudal vertebrae is usually a subhorizontal tail with a slight sigmoidal curvature: ventral deflection in anteriormost

caudals, a shift to a dorsal deflection in middle caudals and another shift to ventriflexion again in distal caudals. These shifts in curvature do not occur at the same position in all sauropods, nor are always as pronounced.

Also, it is not a universal rule, as some sauropods have different OICs on their caudal vertebrae series. Two examples are *Tastavinsaurus sanzi* and *Overosaurus paradasorum*. These sauropods have ventrally and extremely ventrally deflected tails respectively. This is due (or, rather, as a result of this OIC) to the orientation of the neural arch and neural spine relative to the centrum. Both taxa have anteriorly directed neural arches and neural spines, with the second sauropod having dorsally inclined prezygapophyses as well. A similar situation happens with HUE-EC-04 (Morphotype I). This titanosaur has dorsally deflected prezygapophyses (albeit not a lot) and preserved neural spines are anteriorly directed. Both *Tastavinsaurus* and *Overosaurus* are sauropods with dorsal vertebrae larger than the anteriormost caudal vertebrae, at least twice their size. This suggests the same may have been true for HUE-EC-04, although further preparation of the specimen may help solve the question in the near future. Gravity is the main force acting on the tails of dinosaurs (Galton, 1970; Coombs, 1975). With a ventral deflection of the tail in neutral pose, the direction of the vector of gravity acting on the vertebrae is different from a subhorizontal horizontal tail. The anterior direction of the neural spine is likely a consequence of this, as the ligament and muscular system has to counteract the effect of gravity in this plane. The direction of the neural spine is likely to be opposite or close to opposite to the main vector of forces acting against the vertebra (Kardong, 2012).

Considering this, all other morphotypes from Lo Hueco have subhorizontal tails. However, none of these morphotypes has preserved a complete sacrum, so it is difficult to assess the actual inclination of the tails respect to the body. However, the chevrons may provide additional clues. The tail of HUE-EC-02 and HUE-EC-03 (Morphotype II) are the least sigmoidal, with a pronounced dorsal deflection at the middle caudals. The caudal vertebrae of this morphotype have posteriorly inclined spines (the opposite of Morphotype I). Also, chevrons are deflected posteriorly at midshaft, creating an osteological stop for ventriflexion in some caudal vertebrae (although allowing far more motion than sauropods with overlapping chevrons such as *Spinophorosaurus*). The prezygapophyseal facets of Morphotype II are among the smallest in Lo Hueco titanosaurs, granting less range of motion per joint. Overall, Morphotype II appears to have had a stiffer tail held more or less horizontally.

Lohuecotitan and Morphotype III have neural spines perpendicular to the vertebral centrum and subhorizontal prezygapophyses. The largest difference between them is the size of the neural spines, with them being as tall as the centrum in *Lohuecotitan* anterior caudals and smaller than half the centrum height in Morphotype III. This implies the lever arms for the epaxial muscles of *Lohuecotitan* were much larger than for Morphotype III. Also, Morphotype III was likely armored titanosaur, with osteoderms providing a dorsal bracing system for suspending the axial skeleton (see below), which may also explain the short caudal neural spines.

Overall, the differences in the caudal vertebrae of Lo Hueco titanosaurs show remarkable differences in the forces acting upon the tails, suggesting differences in the body plan of these sauropods. However, this hypothesis will remain untested until more remains from these skeletons are prepared.

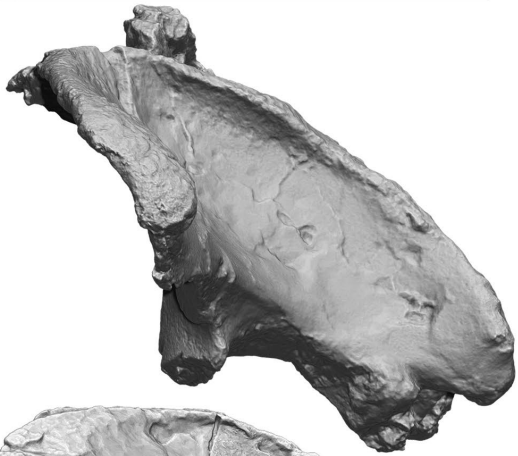
Locomotion differences between Lo Hueco titanosaurs?

Despite not having a large set of bones ready to be compared between the titanosaur individuals from Lo Hueco, ilia are the only non-caudal vertebral element which can be compared between them (Fig. 6.5). As happens with the caudal vertebrae, the ilia have morphological differences with relatively important implications regarding the locomotion capabilities of the titanosaurs from Lo Hueco.

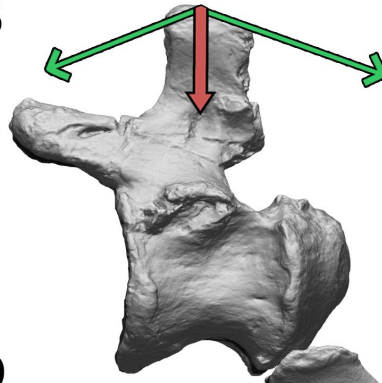
As seen in Chapter 5, sauropod ilia vary a lot in the proportions of its different parts throughout their evolution, with some changes in iliac proportions changing associated with different moments of cladogenesis. Titanosauriformes have a preacetabular process more developed antero-posteriorly in earlier branching taxa. While the preacetabular ilium is flared laterally in most Neosauropoda, this trend increases greatly in Titanosauria, with the preacetabular process flaring laterally in a condition convergent with that of ankylosaur dinosaurs (Carrano, 2005). While interpretations of these changes in iliac proportions have been attempted from a phylogenetic perspective, trying to identify trends in the evolution of sauropod locomotion (Wilson & Carrano, 1999; Carrano, 2005; Klinkhamer *et al.*, 2018), no studies regarding locomotion in the sauropod dinosaurs from the same fossil locality has been attempted.

The differences in the ilium of the titanosaurs from Lo Hueco are enough to suggest differences between the lines of actions of the same muscles. *Lohuecotitan* has an extremely laterally flared preacetabular process. The differences implied for *M. iliotibialis 1* (IT1), *M. iliotrochantericus caudalis* (ITC) and probable *M. iliofemoralis externus* (IFE) muscles would have likely been reduced mediolateral actions (abduction) relative to their

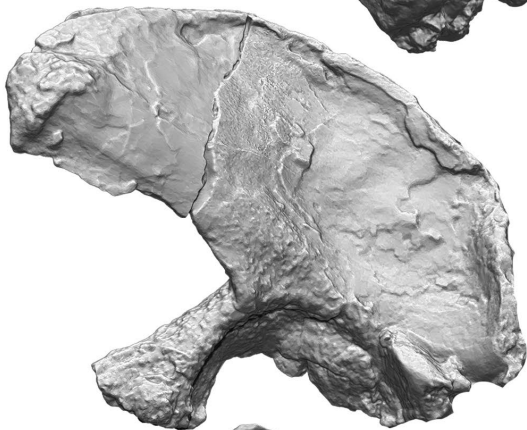
A



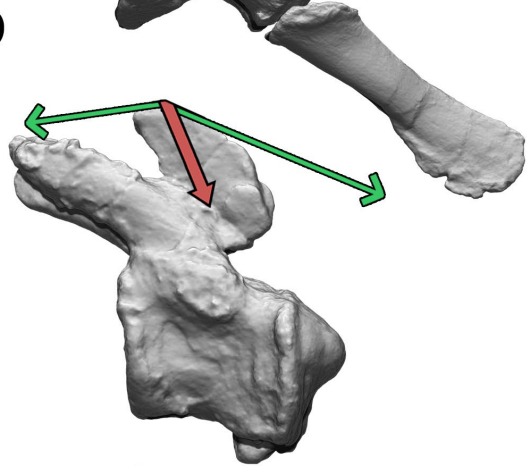
B



C



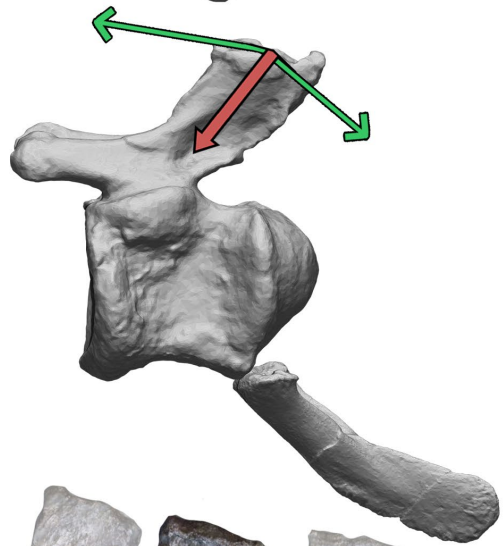
D



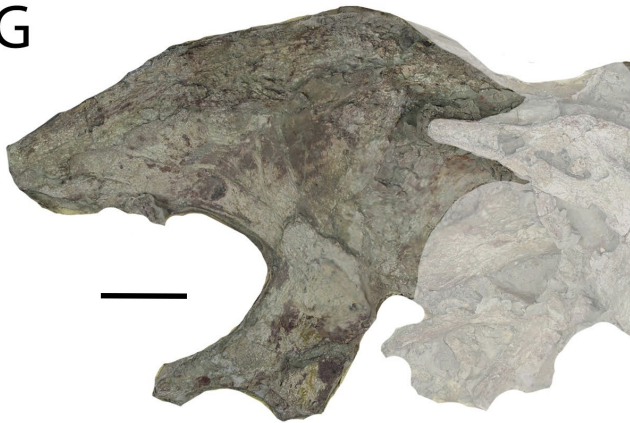
E



F



G



H



Figure 6.5 (previous page) - Variability of Lo Hueco titanosaurs.

A - Ilium of the holotypic specimen of *Lohuecotitan pandaflandi* (HUE-EC-01) in lateral view. **B** - Caudal vertebra 9 of the holotypic specimen of *Lohuecotitan pandaflandi* (HUE-EC-01) in lateral view. **C** - Ilium of specimen HUE-EC-02 (Morphotype II) in lateral view. **D** - Caudal vertebra 9 of specimen HUE-EC-02 (Morphotype II) in lateral view. **E** - Ilium of specimen HUE-EC-04 (Morphotype I) in lateral view. **F** - Caudal vertebra 11 of specimen HUE-EC-04 (Morphotype I) in lateral view. **G** - Ilium of specimen HUE-EC-06 (Morphotype III) in lateral view. **H** - Caudal vertebra 9? of specimen HUE-EC-06 (Morphotype III) in lateral view. B, D and F show the resultant vector of the main forces acting upon the neural spines.

anteroposterior and/or dorso-ventral (protraction, extension) as stated by Carrano (2005). *Lohuecotitan* had these changes in the lines of action of said muscles to the extreme, given its extreme flaring of the preacetabular ilium. This sauropod had a remarkably slender femur, with a subcircular cross-section at its midshaft. While there are other femora from Lo Hueco similar to that of *Lohuecotitan*, the majority of femora of comparable sizes have more eccentric cross-sections (Adrián Páramo, pers. comm. 2019). This implies the particular configuration of the ilium of *Lohuecotitan* may have had implications on the femur morphology as well. However, since only the femora of HUE-EC-06 can be confidently referred to one of the other morphotypes at present, this hypothesis cannot be tested.

The other morphotypes from Lo Hueco have also laterally flared ilia, but not as radically flared as *Lohuecotitan* (Fig. 6.4). The lateral flaring of both Morphotype I (HUE-EC-04) and Morphotype II (HUE-EC-02) is of a similar degree. However, the biggest difference between them is the extreme dorso-ventral development of the preacetabular process from Morphotype II (Fig. 6.3 B). This kind of dorso-ventral development is present in other sauropods, such as *Tastavinsaurus sanzi* (Fig. 5.17). However, the development seen in the ilium of HUE-EC-02 is comparable to that of *Brontomerus mcintoshii*, the sauropod with the largest reported preacetabular process in dorso-ventral and antero-posterior terms (Taylor *et al.*, 2011). *Brontomerus* has been interpreted as having hypertrophied femoral protractor and abductor musculature, and the same would have been true for the titanosaurs from Lo Hueco. The greatest difference resides in the lever arm for IT1, which increases with a longer ilium in the dorso-ventral plane, making protraction more efficient (Taylor *et al.*, 2011). However, since complete femora and tibiae of HUE-EC-02 and HUE-EC-04 have not yet been retrieved, it is difficult to evaluate the exact impact of this difference in dorso-ventral development of the ilium in the moment arm for this muscle.

Finally, the only currently accessible ilium belonging Morphotype 3 (HUE-EC-06) is crushed and not completely prepared, so only the preacetabular process, pubic process and part of the acetabulum are accessible (Fig. 6.5 G). The shape of the preacetabular process is different from all other morphotypes, particularly regarding its proportions, its highest point being the region immediately anterior to the acetabulum. Therefore, the dorso-ventral development of the preacetabular ilium is smaller than in the other morphotypes, and even other titanosaurs. This implies a smaller moment arm and area for the origin of ITC. All in all, the ilia of the different morphotypes from Lo Hueco have remarkable differences with functional implications.

Given the sauropod faunal assemblages of the Morrison Formation were deposited in different types of paleoenvironments (Dodson *et al.*, 1980) and that the taxa associated with the different quarries vary, paleoecological interpretations regarding these associations and the habitats the different dinosaurs would frequent have been proposed (Dodson *et al.*, 1980; Bakker, 1996). These hypotheses regarding different habitats may have been reflected in the functional capabilities of these animals, as is evidenced by the proposed different trophic habits between *Apatosaurus*, *Diplodocus*, *Brachiosaurus* (Stevens & Parrish, 2005), *Barosaurus* (Taylor & Wedel, 2016) and the putatively more generalist *Camarasaurus* (Stevens, 2013). Similarly, different habitat preferences may have also been reflected in differences in locomotor capabilities.

In the case of Lo Hueco titanosaurs, while there were differences in locomotor capabilities revealed by the different ilium morphologies, it is not possible to assess whether this may have actually implied different ecomorphotypes. Further analyses on extant large vertebrates and potential locomotor modifications due to habitat constraints, other sauropods from different assemblages and Lo Hueco titanosaurs as preparation advances will create a better framework to evaluate the hypothesis.

Dermal armor motion restrictions in Morphotype III

Titanosaur osteoderms are fairly common in Lo Hueco, being the largest collection in Europe, and one of the largest worldwide (Vidal *et al.*, 2014). These osteoderms are exclusively of the “bulb and root” morphotype, since no scutes (the morphotype associated with saltasaurine titanosaurs; keeled *sensu* D’Emic *et al.*, 2009) or dermal ossicles have been retrieved. Although primarily thought of as passive defensive structures, osteoderms

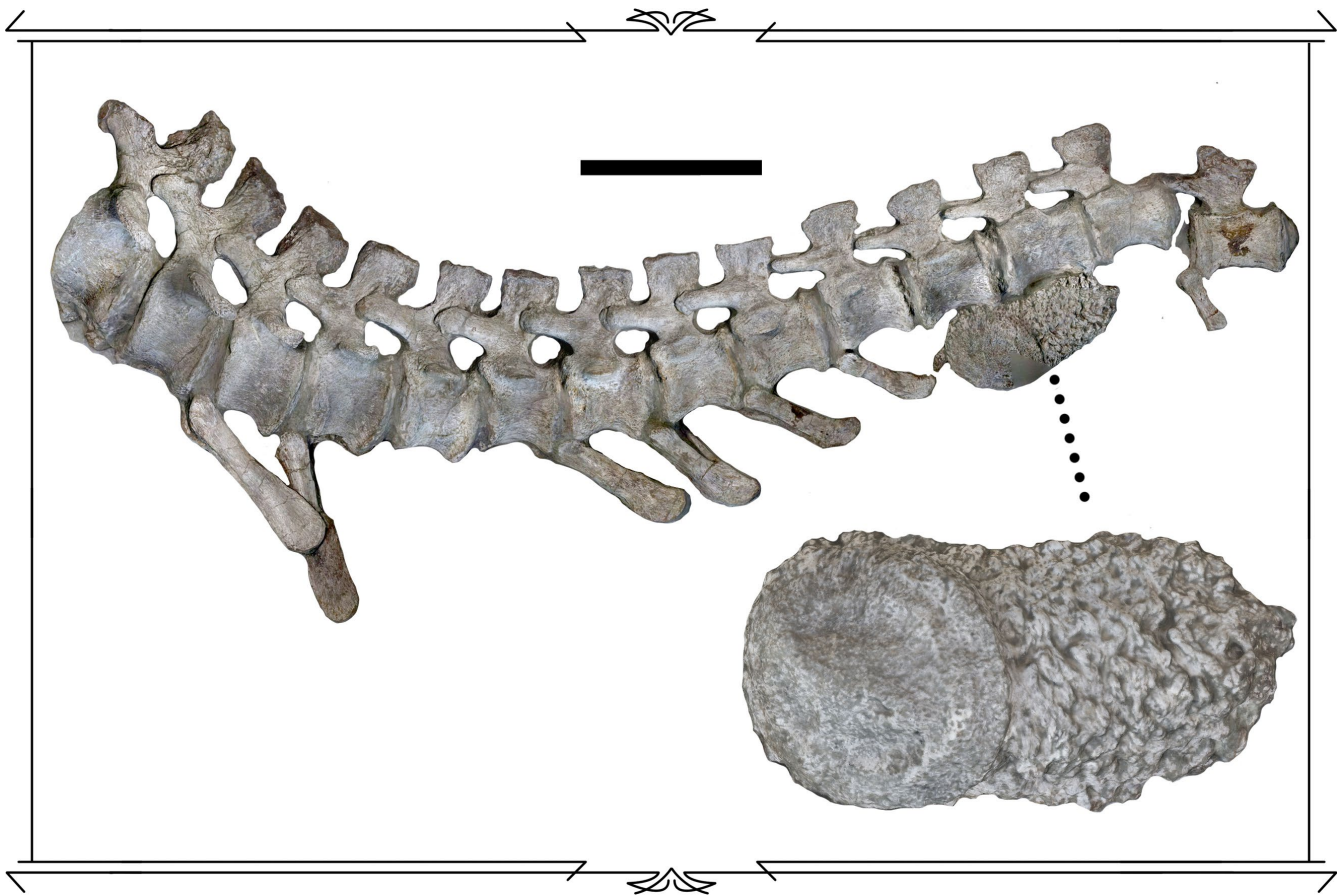


Figure 6.6 - Armored titanosaur from Lo Hueco.

Articated tail of HUE-EC-06 with associated bulb and root osteoderm in the ventrolateral side, displacing the chevron between those vertebrae. Notice the osteoderm is as long as two caudal vertebrae. Scale = 200 mm.

may have served multiple functions beyond defense. An important physiological role has been attributed to these bones in Lo Hueco titanosaur (Vidal *et al.*, 2017) and in *Rapetosaurus* (Curry Rogers *et al.*, 2011). However, a structural role in dorsally bracing the axial skeleton, as happens in extant crocodiles (Frey, 1988), may have been possible, since most titanosaur osteoderms from Lo Hueco have very pronounced internal keels. These keels likely were insertion sites for ligaments connecting the neural spine tips to the osteoderms, as happens in extant crocodiles (Seidel, 1979).

Morphotype III is the only one with a clear association with osteoderms (Fig. 6.6), the osteoderm being as long as two consecutive vertebrae. While longer osteoderms are known to be associated with putative Morphotype III individuals at Lo Hueco (Vidal *et al.*, 2014), their position in the body cannot be determined. Nevertheless, it is possible that some osteoderms may have been as long as three consecutive vertebrae in some regions of the body in titanosaur from Lo Hueco. Given the most likely orientation of the osteoderms would have been parasagittal, in rows dorsal to the neural spines (Vidal *et al.*, 2014). The internal keels would likely have been connected to the neural spine tips via ligaments, as one of the osteoderms has what appears to be ossified ligament in its internal keels (Vidal *et al.*, 2017). This implies that the mobility of two coadjacent vertebrae would have been extremely reduced by an osteoderm.

6.5 CONCLUSIONS

The main conclusion is that preliminary results from virtual paleontology techniques applied to the prepared remains from the titanosaurs of Lo Hueco have shown morphological differences with important implications regarding their functional capabilities. Virtual paleontology can therefore yield evidence that, in addition to different lines of evidence, can be applied in multidisciplinary analyses to help to reconstruct the paleoecology from multi-taxic sauropod assemblages.

The highest amount of disparity so far is shown by the caudal vertebrae series, which allows separating at least four different morphotypes. These differences have great mechanical implications, particularly those related with the direction of the neural spine, which indicate radically different orientations for the tails relative to the pelvis, with Morphotype I having a ventrally deflected tail (and anteriorly pointed neural spines), while Morphotype II would have had more horizontal tail and Morphotype 3 and *Lohuecotitan* a more sigmoid tail.

The ilia associated with each of the articulated specimens from the different morphotypes have remarkably different morphologies, even accounting for taphonomic deformation. This implies differences in the lines of actions, lever arms and relative size of origin areas of some muscles (particularly femoral protractors). While all morphotypes have a relatively well-developed preacetabular process in the antero-posterior axis, Morphotype II has one of the tallest preacetabular processes in Sauropoda, indicating large moment arms for abduction and protraction. This implies the titanosaurs of Lo Hueco had different locomotion capabilities.

The osteoderms retrieved from Lo Hueco are among the longest osteoderms in the fossil record. These may measure up to three times the length of a single dorsal or anterior caudal vertebra. All evidence from their internal sides suggests a parasagittal position over the neural spines in rows. Given this, the only morphotype with a clear association with osteoderms (morphotype III) would have had its motion reduced in all vertebrae pairs over which there was an associated osteoderm pair.



CHAPTER
.7.

CONCLUSIONS

The results obtained during the development of this PhD thesis have allowed to reach the main objective: to generate a virtual model for the early branching sauropod *Spinophorosaurus nigerensis* and to use it as a foundation to evaluate the evolution of the postcranial biomechanical capabilities of Sauropoda .

The main conclusions are detailed below, with hypotheses proposed in chapter 1 evaluated:

BLOCK 1: Body plan and biomechanical capabilities in Sauropoda

1.1 The assemblage of a virtual skeleton of *Spinophorosaurus* using osteologically neutral pose (ONP) as an objective criterion rendered an osteologically induced curvature (OIC) different from what had been proposed in earlier works. This OIC is mainly caused by a wedged sacrum, which makes the presacral column deflect anterodorsally and the tail to be subhorizontal. The inspection of other sauropod skeletal mounts and the virtual assemblage of several sauropod skeletons shows previous skeletal reconstructions were due disarticulated or deflected vertebrae. **This supports hypothesis 1.1.**

1.2 The virtual articulation in ONP of the necks of adult and newborn specimens of extant giraffes rendered large intervertebral spaces in the juvenile and barely any in the adult. This is congruent with what is known in this extant taxon, as they reduce their intervertebral spaces from around 24% neck length in juveniles to barely any intervertebral space in adults. The same protocol was applied to necks of a juvenile and subadult of the fossil sauropod *Spinophorosaurus*, both found articulated with and without intervertebral spaces respectively. The result was a juvenile with intervertebral spaces and an adult without them. **Hypothesis 1.2 is refuted, as ONP was able to accurately reconstruct the amount of intervertebral space.**

1.3 The range of motion (ROM) analyses on virtual neck skeletons of extant giraffes showed that even the most extreme postures attained by live giraffes could be replicated by the virtual skeletons. This was done without disarticulating the zygapophyseal facets, which is an arbitrary limit established in the majority of ROM analyses. **Hypothesis 1.3 is refuted, as the ROM analysis of a virtual skeleton could replicate any pose achieved by a live giraffe.**

1.4 The amount of osteological ROM of the necks of the adult and juvenile *Spinophorosaurus* increases throughout ontogeny due to the elongation of the neck. This elongation causes the relative distance between pre-postzygapophyseal joints and vertebral centra joint to become smaller. While the juvenile individual has a larger ROM in the cervical vertebrae than an earlier branching sauropodomorph such as *Plateosaurus*, in part due to its opisthocoelous centra, ROM increases throughout its ontogeny. **Hypothesis 1.4 is partially refuted, since the range of motion of a juvenile sauropod is not closer to that of earlier branching sauropodomorphs.**

1.5 The size of the feeding envelope of a long-necked vertebrate depends on its overall amount of ROM. This may vary depending on several factors, mainly prezygapophyseal facet elongation and the distance between zygapophyseal facets and center of rotation (intercentral articulation of that vertebra pair). While elongation of cervical vertebrae can reduce that distance, it has no effect on zygapophyseal facet elongation, as evidenced by *Barosaurus*, whose zygapophyseal facets are extremely short and extremely wide. **Hypothesis 5 is refuted, as prezygapophyseal facet shape, one of the main factors related to greater ROM, is independent from vertebral elongation.**

1.6 Sauropod dinosaurs with antero-posteriorly elongated zygapophyseal facets (i.e. *Spinophorosaurus*, *Amargasaurus*) have greater ROM in their cervical vertebrae, being able to achieve more deflection per joint in absence of an osteological stop than sauropods with latero-medially wider than long zygapophyseal facets (i.e. *Camarasaurus*, *Barosaurus*) in the same joints. **This supports hypothesis 1.6, as for the same position in the cervical series, more elongated prezygapophyses enable more deflection per joint.**

1.7 A sacrum wedged more than 10° is present in all surveyed specimens of Eusauropoda, whereas earlier branching sauropods and sauropodomorphs have barely wedged sacrum, if at all. This wedging causes the presacral vertebrae series to deflect dorsally from the caudal series in ONP. This evolved in correlation with humerus/femur proportions: the greater the sacral wedging, the longer the humerus relative to the femur. **This supports hypothesis 1.7, as sacra are the main keystone in axial skeleton geometry and their wedging correlates with humerus/femur proportions.**

BLOCK 2: Evolution of Sauropoda body plan and biomechanics

2.1 The sacra with a higher amount of wedging belong to eusauropods with the longest forelimbs relative to their hindlimbs. However, despite the extremely short forelimbs relative to the hindlimbs in some eusauropods, the sacrum is always wedged more than 10°. **Hypothesis 2.1 is refuted.**

2.2 There is a strong correlation between sacrum wedging and forelimb/hindlimb proportions in Eusauropoda. However, the identification of additional characters which may have been part of a functional module regarding the enlargement of the vertical component of the feeding envelope for all Eusauropoda cannot be assessed at present. Some clades increased their neck length by adding more vertebrae and/or elongating their vertebrae in convergent evolution, while others do the opposite by reducing the length of their necks, forelimbs and modify their dorsal vertebrae to revert the deflection caused by the sacrum. This implies the modified sacrum, which never reverted to the non-wedged basal condition, was an exaptation and a functional constraint depending on the clade considered. **This partially supports hypothesis 2.2, as some axial and appendicular characters evolved as a functional module.**

2.3 The pelves of earlier branching sauropods were narrow (longer anteroposteriorly than wider lateromedially), and they became progressively wider throughout their evolution, particularly in the lineage of Macronaria. The widening of the pelvis implied separating the femora from the midline and a medial migration of the fourth trochanter (insertion site for caudofemoral muscles). All this implied the angle of the line of action for *M. caudofemoralis longus* (CFL) shifted its direction progressively from the basal condition as subparallel with the tail to form a 45° angle with the tail. **This supports hypothesis 2.3, as adduction became a greater component in CFL action in sauropods with wide gauge stance.**

2.4 Caudal neural spines and chevrons (these correlates of caudofemoral musculature), become progressively reduced relative to the centrum height throughout sauropod evolution. The posterior limit for CFL is delimited by ridges on these surfaces, which migrate ventrally and dorsally (respectively) for two to three caudal vertebrae, indicating the tapering of this muscle. This posterior limit shifts its position toward more anterior caudal vertebrae throughout sauropod evolution, from caudal vertebra 14 in earlier branching eusauropods to caudal vertebra 13 in titanosauriforms and caudal vertebra 6 in deeply nested titanosaurs. **This supports hypothesis 2.4, as a massive reduction of the osteological correlates of CFL occurs in the titanosauriforms, which developed wide gauge stance.**

2.5 Only characters related with the locomotor module, particularly those regarding the hindlimb and pelvic girdle, appear to have followed a phylogenetic trend. Changes in characters implied in the orientation of locomotor muscles lines of action, size and mechanical advantage of these muscles were stepwise throughout the phylogeny, suggesting mosaic evolution. **This supports hypothesis 5, as characters with strong functional implications on the same functional module derived at different rates.**

BLOCK 3: Ecology of “Lo Hueco” titanosaurs from biomechanical evidence

3.1 The highest amount of disparity so far is shown by the titanosaurs from Lo Hueco are the caudal vertebrae series, which allow separating at least four different morphotypes. Each of these morphotypes also has a distinctive morphology on the ilium. **Hypothesis 3.1 is partially refuted, as the presently assessed disparity of Lo Hueco titanosaur is greater than 3 morphotypes, although their proportions cannot be evaluated at present.**

3.2 The ilia associated with each of the articulated titanosaurs from Lo Hueco have remarkably different morphologies. This implies differences in lines of actions, lever arms and relative size of origin areas of some muscles (particularly femoral protractors and abductors). Also, the radically different orientations for the tails relative to the pelvis and the different proportions of their hypaxial and epaxial musculature suggest differences in the lines of actions and sizes of the caudofemoral musculature. **This supports hypothesis 3.2, as both tails and ilia imply the titanosaurs of Lo Hueco had different locomotion capabilities.**

3.3 Only one morphotype of Lo Hueco titanosaurs can be confidently associated with osteoderms. This morphotype has some mechanical characteristics separating them from other morphotypes, particularly the extremely short and anteroposteriorly expanded neural spines. Shorter spines have less mechanical advantage in supporting the tail than longer spines. Also, the prezygapophyses in middle caudal vertebrae are shorter, and do not contact the previous vertebra. Anteroposteriorly expanded neural spines imply a potentially larger supraspinal ligament attached to the internal keels of the osteoderms. This supports a dorsal bracing function for the osteoderms. **This supports hypothesis 3.3, as the only armored Lo Hueco titanosaur morphotype has different osteological characteristics.**

3.4 The osteoderms retrieved from Lo Hueco are among the relatively longer sauropod osteoderms in the fossil record, up to three times the length of a single dorsal or anterior caudal vertebra. All evidence from their internal sides suggests a parasagittal position over the neural spines in rows. The only caudal morphotype with a clear association with osteoderms (Morphotype III) would have had its motion reduced in all vertebrae pairs over which there was an associated osteoderm pair. **This partially supports hypothesis 3.4, as osteoderms act as a ROM limit and have been found associated with regions with more mobility than in other Lo Hueco titanosaurs, although whether osteoderms were actually located within this region cannot be evaluated at present.**



REFERENCES

- Alexander RM. 1989. *Dynamics of Dinosaurs & Other Extinct Giants*. New York: Columbia University Press.
- Alifanov V, Averianov AO. 2003. *Ferganasaurus verzilini*, gen. et sp. nov., a new neosauropod (Dinosauria, Saurichia, Sauropoda) from the Middle Jurassic of Fergana Valley, Kirghizia. *Journal of Vertebrate Paleontology* 23: 358–372.
- Anderson JF, Hall-Martin A, Russell DA. 1985. Long-bone circumference and weight in mammals, birds and dinosaurs. *Journal of Zoology* 207: 53–61.
- Ansón M, Hernández Fernández M. 2013. Artistic reconstruction of the appearance of *Prosantorhinus* Heissig, 1974, the teleoceratine rhinoceros from the Middle Miocene of Somosaguas. *Spanish Journal of Paleontology* 28: 43–54.
- Ansón M, Hernández Fernández M, Saura Ramos PA. 2015. Paleoart: term and conditions (a survey among paleontologists). In: Domingo L, Domingo S, Fesharaki O, García Yelo B, Gómez Cano AR, Hernández-Ballarín V, Hontecillas D, Cantalapiedra JL, López Guerrero P, Oliver A, Pelegrín J, Pérez de los Ríos M, Ríos M, Sanisidro O, Valenciano A, eds. *Current Trends in Paleontology and Evolution. XIII Encuentro de Jóvenes Investigadores en Paleontología*, 28–34.
- Antón M, Sanchez IM. 2004. Art and science: the methodology and relevance of the reconstruction of fossil vertebrates. In: Baquedano Pérez E, Rubio Jara S, eds. *Miscelanea en homenaje a Emiliano Aguirre, Paleontología*. Alcalá de Henares: Museo Arqueológico Regional, 74–94.
- Apesteguía S. 2005. Evolution of hyposphene-hypantrum complex within Sauropoda. In: Tidwell V, Carpenter K, eds. *Thunder-lizards: The Sauropodomorph Dinosaurs*. Indiana University Press, 248–267.
- Apesteguía S, Gallina PA, Haluza A. 2010. Not just a pretty face: Anatomical peculiarities in the postcranium of Rebbachisaurids (Sauropoda: Diplodocoidea). *Historical Biology* 22: 165–174.
- Arbour VM. 2009. Estimating impact forces of tail club strikes by ankylosaurid dinosaurs. *PLoS ONE* 4: e6738.
- Arbour VM, Currie PJ. 2012. Analyzing taphonomic deformation of ankylosaur skulls using retrodeformation and finite element analysis. *PLoS ONE* 7: e39323.
- Bakker RT. 1968. The Superiority of Dinosaurs. *Discovery* 3: 11–22.
- Bakker RT. 1971. Ecology of the brontosaurus. *Nature* 229: 172–174.
- Bakker RT. 1975. Dinosaur Renaissance. *Scientific American* 232: 58–79.
- Bakker RT. 1986. *The Dinosaur Heresies: New Theories Unlocking the Mystery of the Dinosaurs and Their Extinction*. Citadel Press.
- Bakker RT. 1996. The real Jurassic Park: Dinosaurs and Habitats at Como Bluff, Wyoming. *Museum of Northern Arizona Bulletin* 60: 35–40.
- Ballou WH. 1897. Strange Creatures of the Past: Giant Saurians of the Reptilian Age. *Century Magazine* 55:1.
- Baron MG, Norman DB, Barrett PM. 2017. A new hypothesis of dinosaur relationships and early dinosaur evolution. *Nature* 543: 501–506.
- Barroso-Barcenilla F, Cambra-Moo O, Escaso F, Ortega F, Pascual A, Pérez-García A, Rodríguez-Lázaro J, Sanz JL, Segura M, Torices A. 2009. New and exceptional discovery in the Upper Cretaceous of the Iberian Peninsula: the palaeontological site of 'Lo Hueco', Cuenca, Spain. *Cretaceous Research* 30: 1268–1278.
- Bates KT, Maidment SCR, Allen V, Barrett PM. 2012. Computational modelling of locomotor muscle moment arms in the basal dinosaur *Lesothosaurus diagnosticus*: Assessing convergence between birds and basal ornithischians. *Journal of Anatomy* 220: 212–232.
- Bates KT, Manning PL, Hodgetts D, Sellers WI. 2009. Estimating mass properties of dinosaurs using laser imaging and 3D computer modelling. *PLoS ONE* 4: e4532.
- Bates KT, Mannion PD, Falkingham PL, Brusatte SL, Hutchinson JR, Otero A, Sellers WI, Sullivan C, Stevens KA, Allen V. 2016. Temporal and phylogenetic evolution of the sauropod dinosaur body plan. *Royal Society Open Science* 3: 1–17.
- Bonaparte JF. 1979. Dinosaurs: A jurassic assemblage from Patagonia. *Science* 205: 1377–1379.
- Bonaparte JF. 1986. Les dinosaures (Carnosaures, Allosauridés, Sauropodes, Cétiosauridés) du Jurassique moyen de Cerro Condor (Chubut, Argentine). *Annales de Paléontologie* 72: 325–386.
- Bonaparte JF, González Riga BJ, Apesteguía S. 2006. *Ligabuesaurus leanzai* gen. et sp. nov. (Dinosauria, Sauropoda), a new titanosaur from the Lohan Cura Formation (Aptian, Lower Cretaceous) of Neuquén, Patagonia, Argentina. *Cretaceous Research* 27: 364–376.

- Bonaparte JF, Powell JE. 1980. A continental assemblage of tetrapods from the Upper Cretaceous bed of El Brete, northwestern Argentina (Sauropoda-Coelurosauria-Carnosauria-Aves). *Memoires de la Société Géologique de la France Nouvelle Série* 139: 19–28.
- Bonnan MF, Yates AM. 2007. A new description of the forelimb of the basal sauropodomorph *Melanorosaurus*: Implications for the evolution of pronation, manus shape and quadrupedalism in sauropod dinosaurs. *Evolution and Palaeobiology* 77: 157–168.
- Borsuk-bialynicka M. 1977. A New Camarasaurid Sauropod *Opisthoceolicaudia skarzynskii* gen. n., sp. n. from the Upper Cretaceous of Mongolia. *Paleontologia Polonica* 37: 5–64.
- Boyd JP. 1958. The *Megalonyx*, the *Megatherium*, and Thomas Jefferson's Lapse of Memory. *Proceedings of the American Philosophical Society* 102: 420–435.
- Breithaupt BH, Matthews NA, Noble TA. 2003. An integrated approach to three-dimensional data collection at dinosaur tracksites in the Rocky Mountain West. *Ichnos* 11: 11–26.
- Brochu CA. 1996. Closure of neurocentral sutures during crocodylian ontogeny: Implications for maturity assessment in fossil archosaurs. *Journal of Vertebrate Paleontology* 16: 49–62.
- Bru JB. 1796. Descripción del esqueleto en particular, según las observaciones hechas al tiempo de armarle y colocarle en este Real Gabinete. *Descripción del esqueleto de un cuadrupedo muy corpulento y raro, que se conserva en el Real Gabinete de Historia Natural de Madrid*, 1–16.
- Bryant HN, Russell AP. 1992. The Role of Phylogenetic Analysis in the Inference of Unpreserved Attributes of Extinct Taxa. *Philosophical Transactions of the Royal Society B: Biological Sciences* 337: 405–418.
- Cambra-Moo O. 2006. Bioestratimología y fosildiagénesis de arcosaurios aplicación de la actuotafonomía al estudio de la influencia paleobiológica en el proceso tafonómico. Unpublished thesis, Universidad Autónoma de Madrid.
- Cambra-Moo O, Barroso-Barcenilla F, Berreteaga A, Carenas B, Coruña F, Domingo L, Domingo MS, Elvira A, Escaso F, Ortega F, Pérez-García A, Peyrot D, Sanz JL, Segura M, Soplana A, Torices A. 2012. Preliminary taphonomic approach to 'Lo Hueco' palaeontological site (Upper Cretaceous, Cuenca, Spain). *Geobios* 45: 157–166.
- Carabajal AP, Carballido JL, Currie PJ. 2014. Braincase, neuroanatomy, and neck posture of *Amargasaurus cazaui* (Sauropoda, Dicraeosauridae) and its implications for understanding head posture in sauropods. *Journal of Vertebrate Paleontology* 34: 870–882.
- Carballido JL, Pol D, Otero A, Cerda IA, Salgado L, Garrido AC, Ramezani J, Cúneo NR, Krause JM. 2017. A new giant titanosaur sheds light on body mass evolution among sauropod dinosaurs. *Proceedings of the Royal Society B: Biological Sciences* 284: 1–10.
- Carlson DA. 2008. Reproductive biology of the coyote (*Canis latrans*): Integration of behavior and physiology. Unpublished thesis, Utah State University.
- Carpenter K. 2013. History, Sedimentology, and Taphonomy of the Carnegie Quarry, Dinosaur National Monument, Utah. *Annals of Carnegie Museum* 81: 153–232.
- Carpenter K, Madsen J, Lewis A. 1994. Mounting of fossil vertebrate skeletons. In: Leiggi P, May P, eds. *Vertebrate Paleontological Techniques vol. 1*. NY: Cambridge University Press, 285–322.
- Carrano MT. 2000. Homoplasy and the evolution of dinosaur locomotion. *Paleobiology* 26: 489–512.
- Carrano MT. 2005. The Evolution of Sauropod Locomotion: Morphological Diversity of a Secondarily Quadrupedal Radiation. In: Curry Rogers K, Wilson JA, eds. *The Sauropods: Evolution and Paleobiology*. Berkeley: University of California Press, 229–249.
- Carrano MT, Hutchinson JR. 2002. Pelvic and hindlimb musculature of *Tyrannosaurus rex* (Dinosauria: Theropoda). *Journal of Morphology* 253: 207–228.
- Chapman RE, Andersen AF, Sabo SJ. 1999. Construction of the virtual *Triceratops*: procedures, results, and potentials. *Journal of Vertebrate Paleontology* 19: 37A.
- Christian A. 2002. Neck posture and overall body design in sauropods. *Fossil Record* 5: 271–281.
- Christian A. 2010. Some sauropods raised their necks—evidence for high browsing in *Euhelopus zdanskyi*. *Biology Letters* 6: 823–825.
- Christian A, Dzemplski G. 2007. Reconstruction of the cervical skeleton posture of *Brachiosaurus brancai* Janensch, 1914 by

- an analysis of the intervertebral stress along the neck and a comparison with the results of different approaches. *Fossil Record – Mitteilungen aus dem Museum für Naturkunde* 10: 38–49.
- Christian A, Peng G, Sekiya T, Ye Y, Wulf MG, Steuer T. 2013. Biomechanical reconstructions and selective advantages of neck poses and feeding strategies of Sauropods with the example of *Mamenchisaurus youngi*. *PloS one* 8: e71172.
- Chure D, Britt BB, Whitlock JA, Wilson JA. 2010. First complete sauropod dinosaur skull from the Cretaceous of the Americas and the evolution of sauropod dentition. *Naturwissenschaften* 97: 379–391.
- Clarke JA, Middleton KM. 2008. Mosaicism, modules, and the evolution of birds: Results from a bayesian approach to the study of morphological evolution using discrete character data. *Systematic Biology* 57: 185–201.
- Cohen KM, Finney SC, Gibbard PL, Fan JX. 2013. The ICS International Chronostratigraphic Chart. *Episodes* 36: 199–204.
- Colbert E. 1962. The weights of dinosaurs. *American Museum Novitates* 2076: 1–16.
- Conniff R. 2016. *House of Lost Worlds: Dinosaurs, Dynasties & the story of Life on Earth*. New Haven: Yale University Press.
- Coombs WP. 1975. Sauropod habits and habitats. *Palaeogeography, Palaeoclimatology, Palaeoecology* 17: 1–33.
- Cope ED. 1877a. On a Gigantic Saurian form the Dakota Epoch of Colorado. *Paleontological Bulletin* 26: 5–10.
- Cope ED. 1877b. On *Amphicoelias*, a genus of Saurians from the Dakota epoch of Colorado. *Proceedings of the American Philosophical Society* 17: 242–246.
- Cope ED. 1877c. On reptilian remains from the Dakota Beds of Colorado. *Proceedings of the American Philosophical Society* 17(100): 193–196.
- Cope ED. 1878a. On the vertebrata of the Dakota Epoch of Colorado. *Proceedings of American Philosophical Society* 17: 233–247.
- Cope ED. 1878b. A new species of *Amphicoelias*. *American Naturalist* 13: 563–564.
- Cope ED. 1879. New Jurassic Dinosauria. *American Naturalist* 13: 402–404.
- Coria R a, Filippi L, Chiappe LM, Garcia R, Arcucci AB. 2013. *Overosaurus paradasorum* gen. et sp. nov., a new sauropod dinosaur (Titanosauria: Lithostrotia) from the Late Cretaceous of Neuquén, Patagonia, Argentina. *Zootaxa* 3683: 357–376.
- Cruz-Jentoft AJ, Baeyens JP, Bauer JM. 2010. Sarcopenia: European consensus on definition and diagnosis: Report of the European Working Group on Sarcopenia in Older People. *Age Ageing* 39: 412–23.
- Curry Rogers K. 2005. Titanosauria: a phylogenetic overview. *The Sauropods: Evolution and Paleobiology*. University of California Press, 50–103.
- Curry Rogers K, D’Emic M, Rogers R, Vickaryous M, Cagan A. 2011. Sauropod dinosaur osteoderms from the Late Cretaceous of Madagascar. *Nature Communications* 2: 564.
- Cuvier G. 1804. Sur le *Megatherium*. *Annales du Museum National d’Histoire Naturelle*.
- D’Emic MD, Wilson JA. 2011. New remains attributable to the holotype of the Sauropod Dinosaur *Neuquensaurus australis*, with implications for saltosaurine systematics. *Acta Palaeontologica Polonica* 56: 61–73.
- D’Emic MD, Wilson J a., Chatterjee S. 2009. The titanosaur (Dinosauria: Sauropoda) osteoderm record: review and first definitive specimen from India. *Journal of Vertebrate Paleontology* 29: 165–177.
- Dagg AI. 1962. The Role of the Neck in the Movements of the Giraffe. *Journal of Mammalogy* 43: 88–97.
- Dagg AI. 1971. *Giraffa camelopardalis*. *Mammalian Species* 5: 1–8.
- Díez Díaz V, Mocho P, Páramo A, Escaso F, Marcos-Fernández F, Sanz JL, Ortega F. 2016. A new titanosaur (Dinosauria, Sauropoda) from the Upper Cretaceous of Lo Hueco (Cuenca, Spain). *Cretaceous Research* 68: 49–60.
- Díez Díaz V, Ortega F, Sanz JL. 2014. Titanosaurian teeth from the Upper Cretaceous of ‘Lo Hueco’ (Cuenca, Spain). *Cretaceous Research* 51: 285–291.
- Dingus L. 1995. *Next of Kin: Great Fossils at the American Museum of Natural History*. Rizzoli International Publications.
- Dodson P, Behrensmeyer AK, Bakker RT, McIntosh JS. 1980. Taphonomy and Paleocology of the Dinosaur Beds of the Jurassic Morrison Formation. *Paleobiology* 6: 208–232.

- Domingo L, Barroso-Barcenilla F, Cambra-Moo O. 2015. Seasonality and paleoecology of the late cretaceous multi-taxa vertebrate assemblage of 'Lo Hueco' (Central Eastern Spain). *PLoS ONE* 10: e0119968.
- Dong ZM, Peng G, Huang D. 1989. The discovery of the bony tail club of sauropods. *Vertebrata Palasiatica* 27: 219–224.
- Dzemeski G, Christian A. 2007. Flexibility Along the Neck of the Ostrich (*Struthio camelus*) and Consequences for the Reconstruction of Dinosaurs With Extreme Neck Length. *Journal of Morphology* 268: 701–714.
- Ellinger TUH. 1950. *Camarasaurus annae*. A new American sauropod dinosaur. *The American Naturalist* 84: 225–228.
- Erwin DH. 2015. Novelty and innovation in the history of life. *Current Biology* 25: 930–940.
- Erwin DH. 2017. The topology of evolutionary novelty and innovation in macroevolution. *Philosophical Transactions of the Royal Society B: Biological Sciences* 372: 1–8.
- Evers SW, Rauhut OWM, Milner AC, McFeeters B, Allain R. 2015. A reappraisal of the morphology and systematic position of the theropod dinosaur *Sigilmassasaurus* from the "middle" Cretaceous of Morocco. *PeerJ* 3: e1323.
- Falkingham PL. 2012. Acquisition of high resolution three-dimensional models using free, open-source, photogrammetric software. *Palaeontologia Electronica* 15: 1-15.
- Faux CM, Padian K. 2007. The opisthotonic posture of vertebrate skeletons: postmortem contraction or death throes? *Paleobiology* 33: 201-226.
- Fechner R. 2009. Morphofunctional Evolution of the Pelvic Girdle and Hindlimb of Dinosauromorpha on the Lineage to Sauropoda. Unpublished thesis, Ludwigs Maximilians Universität.
- Filla JA, Redman PD. 1994. *Apatosaurus yahnahpin*: a preliminary description of a new species of diplodocid dinosaur from the Late Jurassic Morrison Formation (Kimmeridgian-Portlandian) and Cloverly Formation (Aptian-Albian) of the western United States. *Mémoires de la Société Géologique de France (Nouvelle Série)* 139: 87–93.
- Frey E. 1988. Das Tragsystem der Krokodile - eine biomechanische und phylogeneitische Analyse (The carrying system of crocodilian: a biomechanical and phylogenetic analysis). *Stuttgarter Beiträge zur Naturkunde, Serie A (Biologie)* 426: 1–60.
- Fronimos JA, Wilson JA. 2017. Neurocentral Suture Complexity and Stress Distribution in the Vertebral Column of a Sauropod Dinosaur. *Ameghiniana* 54: 36-49.
- Gallina PA. 2011. Notes on the axial skeleton of the titanosaur *Bonitasaura salgadoi* (Dinosauria-Sauropoda). *Anais da Academia Brasileira de Ciências* 83: 235–246.
- Galton PM. 1970. The posture of hadrosaurian dinosaurs. *Journal of Paleontology* 4: 464–476.
- Galton PM, Van Heerden J, Yates AM. 2005. Postcranial Anatomy of Referred Specimens of *Melanorosaurus*. In: Carpenter K, Tidwell V, eds. *Thunder-lizards: The Sauropodomorph Dinosaurs*. Indiana University Press, 1–37.
- García-Martínez D, Vidal D, Ortega F. 2018. Using 3D geometric morphometrics to estimate missing vertebrae in a *Spinophorosaurus* dorsal spine (Middle Jurassic, Niger). *Abstract book of the XVI Annual Meeting of the European Association of Vertebrate Palaeontology*.75.
- Garriga J. 1796. *Descripción del esqueleto de un cuadrupedo muy corpulento y raro, que se conserva en el Real Gabinete de Historia Natural de Madrid*.
- Gascó F. 2015. Anatomía funcional de *Turiasaurus riodevensis* (Dinosauria, Sauropoda). Unpublished thesis, Universidad Autónoma de Madrid.
- Gascó F, Vidal D, Páramo A, Mocho P, Ortega F. 2018. New insights into the palaeohistology of the titanosaur sauropods from the Upper Cretaceous of Lo Hueco (Cuenca, Spain). *XVI EAVP Program and abstracts*.76.
- Gatesy SM. 1990. Caudofemoral musculature and the evolution of theropod locomotion. *Paleobiology* 16: 170–186.
- Gatesy SM, Middleton KM. 1997. Bipedalism, flight, and the evolution of theropod locomotor diversity. *Journal of Vertebrate Paleontology* 17: 308–329.
- Gilmore CW. 1925. A nearly complete articulated skeleton of *Camarasaurus*, a saurischian dinosaur from the Dinosaur National Monument, Utah. *Memoirs of the Carnegie Museum* 10: 347–384.
- Gilmore CW. 1932. On a newly mounted skeleton of *Diplodocus* in the United States National Museum. *Proceedings of the United States National Museum* 81: 1–21.

- Gilmore CW. 1946. Reptilian fauna of the North Horn Formation of central Utah. *U.S. Geological Survey Professional Paper* 210: 29–53.
- Goloboff PA, Farris JS, Nixon KC. 2008. TNT, a free program for phylogenetic analysis. *Cladistics* 24: 774–786.
- Gomani EM. 2005. Sauropod Dinosaurs From the Early Cretaceous of Malawi, Africa. *Palaeontologia Electronica* 8: 1–37.
- Grillo ON, Azevedo SAK. 2011. Pelvic and hind limb musculature of *Staurikosaurus pricei* (Dinosauria: Saurischia). *Anais da Academia Brasileira de Ciências* 83: 73–98.
- Guerrero A, Vidal D. 2018. El cuello de *Camarasaurus*: ¿pueden dos vértebras cervicales fusionadas revelar su postura habitual? In: Amayuelas E, Bilbao-Lasa P, Bonilla O, del Val M, Errandonea-Martin J, Garate-Olave I, García-Sagastibelza A, Intxauspe-Zubiaurre B, Martínez-Braceras N, Perales-Gogenola L, Ponsoda-Carreres M, Portillo H, Serrano H, Silva-Casal R, Suárez-Bilbao A, Suarez-Hernando O, eds. *Life Finds a Way*. Gasteiz, 71–74.
- Gunji M, Endo H. 2016. Functional cervicothoracic boundary modified by anatomical shifts in the neck of giraffes. *Royal Society Open Science* 3: 150604.
- Hallett M, Wedel MJ. 2016. *The Sauropod Dinosaurs*. Johns Hopkins University Press.
- Hatcher JB. 1901. *Diplodocus* (Marsh): Its osteology, taxonomy and probable habits, with a restoration of the skeleton. *Memoirs of the Carnegie Museum* 1: 1–63.
- Hatcher JB. 1903a. A new sauropod dinosaur from the Jurassic of Colorado. *Proceedings of the Biological Society of Washington* 16: 1–2.
- Hatcher JB. 1903b. Osteology of *Haplocanthosaurus*, with description of a new species. *Memoirs of the Carnegie Museum* 2: 1–72.
- Hay OP. 1908. On the Habits and Pose of the Sauropod Dinosaurs, especially of *Diplodocus*. *The American Naturalist* 42: 672–681.
- Hay OP. 1909. On the restoration of skeletons of fossil vertebrates. *Science* 30: 93–95.
- Hay OP. 1910. On the Manner of Locomotion of the Dinosaurs, Especially *Diplodocus*, With Remarks on the Origin of the Birds. *Proceedings of the Washington Academy of Sciences* 12: 1–25.
- Hillis DM. 2011. *Principles of Life*. Palgrave Macmillan.
- Hohn-Schulte B. 2010. Form and Function of the Shoulder Girdle in Sauropod Dinosaurs: A Biomechanical Investigation with the Aid of Finite Elements. Unpublished thesis, Ruhr-Universität Bochum.
- Holland WJ. 1905. The presentation of a reproduction of *Diplodocus carnegii* to the trustees of the British Museum. *Annals of the Carnegie Museum* 3: 442–452.
- Holland WJ. 1906. The Osteology of *Diplodocus* Marsh. *Memoirs of the Carnegie Museum* 2: 223–278.
- Holland WJ. 1910. A Review of Some Recent Criticisms of the Restorations of Sauropod Dinosaurs Existing in the Museums of the United States, with Special Reference to that of *Diplodocus carnegii* in the Carnegie Museum. *The American Naturalist* 44: 259–283.
- Holland WJ. 1919. *Report on the section of paleontology: Annual Report of the Carnegie Museum*.
- Holliday CM, Ridgely RC, Sedlmayr JC, Witmer LM. 2010. Cartilaginous epiphyses in extant archosaurs and their implications for reconstructing limb function in dinosaurs. *PLoS ONE* 5: e13120.
- Horner JR, Lessem D. 1993. *The Complete T. rex*. Simon & Schuster.
- Horwich RH, Kitchen C, Wangel M, Ruthe R. 1983. Behavioral development in okapis and giraffes. *Zoo Biology* 2: 105–125.
- Hutchinson J, Anderson F, Blemker S, Delp SL. 2005. Analysis of hindlimb muscle moment arms in *Tyrannosaurus rex* using a three-dimensional musculoskeletal computer model: implications for stance, gait, and speed. *Paleobiology* 31: 373–701.
- Hutchinson JR, Bates KT, Molnar J, Allen V, Makovicky PJ. 2011. A computational analysis of limb and body dimensions in *Tyrannosaurus rex* with implications for locomotion, ontogeny, and growth. *PLoS one* 6: e26037.
- Hutchinson JR, Garcia M. 2002. *Tyrannosaurus* was not a fast runner. *Nature* 415: 1018–1021.
- Ibiricu LM, Lamanna MC, Lacovara KJ. 2014. The influence of caudofemoral musculature on the titanosaurian (Saurischia:

- Sauropoda) tail skeleton: morphological and phylogenetic implications. *Historical Biology* 26: 454–471.
- Ibiricu LM, Martínez RD, Casal GA. 2018. The pelvic and hindlimb myology of the basal titanosaur *Epachthosaurus sciuttoii* (Sauropoda: Titanosauria). *Historical Biology*, 1-6.
- Ibrahim N, Sereno PC, Sasso CD, Maganuco S, Fabbri M, Martill DM, Zouhri S, Myhrvold N, Iurino DA. 2014. Semiaquatic adaptations in a giant predatory dinosaur. *Science* 345: 1613–1616.
- Ikejiri T. 2004. Anatomy of *Camarasaurus lentus* (Dinosauria: Sauropoda) from the Morrison formation (Late Jurassic), Thermopolis, Central Wyoming, with determination and interpretation of ontogenetic, sexual dimorphic and individual variation in the genus. Unpublished thesis, Fort Hays State University.
- Irmis RB. 2007. Axial skeleton ontogeny in the Parasuchia (Archosauria: Pseudosuchia) and its implications for ontogenetic determination in archosaurs. *Journal of Vertebrate Paleontology* 27: 350–361.
- Isles TE. 2009. The socio-sexual behaviour of extant archosaurs: Implications for understanding dinosaur behaviour. *Historical Biology* 21: 139–214.
- Jain SL, Kutty TS, RoyChowdhury TKR, Chatterjee S. 1979. Some characteristics of *Barapasaurus tagorei*, a sauropod dinosaur from the Lower Jurassic of Deccan, India. *Forth International Gondwana Symposium: Calcutta, India, 1977 - papers (Vol 1)*. 204–216.
- Janensch W. 1950. Die Skelettrekonstruktion von *Brachiosaurus brancai*. *Palaeontographica Supplement*: 95 – 103.
- Jensen JA. 1985. Three new sauropod dinosaurs from the Upper Jurassic of Colorado. *Great Basin Naturalist* 45: 697–709.
- Jensen JA. 1988. A fourth new sauropod dinosaur from the Upper Jurassic of the Colorado Plateau and sauropod bipedalism. *Great Basin Naturalist* 48: 121–145.
- Jentgen-Ceschino B, Stein K, Fisher V. 2019. Cases of pathological bone growth in *Isanosaurus* and *Spinophorosaurus* (Sauropoda): periosteal reactions and tumor-like conditions in dinosaurs. *XVII EAVP Program and abstracts*.51.
- Kardong K V. 2012. *Vertebrates : Comparative, Function, Evolution*.
- Kellner W, Campos D, Trotta MNF. 2005. Description of a titanosaurid caudal series from the Bauru Group, Late Cretaceous of Brazil. *Arquivos do Museu Nacional, Rio de Janeiro* 63: 529–564.
- Klein N, Christian A, Sander PM. 2012. Histology shows that elongated neck ribs in sauropod dinosaurs are ossified tendons. *Biology Letters* 8: 1032–1035.
- Klinkhamer AJ, Mallison H, Poropat SF, Sinapius GHK, Wroe S. 2018. Three-Dimensional Musculoskeletal Modeling of the Sauropodomorph Hind Limb: The Effect of Postural Change on Muscle Leverage. *Anatomical Record* 301: 2145–2163.
- Klinkhamer AJ, Mallison H, Poropat SF, Sloan T, Wroe S. 2019. Comparative Three-Dimensional Moment Arm Analysis of the Sauropod Forelimb: Implications for the Transition to a Wide-Gauge Stance in Titanosaurs. *Anatomical Record* 302: 794–817.
- Klinkhamer AJ, Wilhite DR, White MA, Wroe S. 2017. Digital dissection and three-dimensional interactive models of limb musculature in the Australian estuarine crocodile (*Crocodylus porosus*). *PLoS ONE* 12: e0175079.
- Knoll F, Witmer LM, Ortega F, Ridgely RC, Schwarz-Wings D. 2012. The braincase of the basal sauropod dinosaur *Spinophorosaurus* and 3D reconstructions of the cranial endocast and inner ear. *PLoS ONE* 7: e30060.
- Knoll F, Witmer LM, Ridgely RC, Ortega F, Sanz JL. 2015. A new titanosaurian braincase from the cretaceous 'Lo Hueco' locality in Spain sheds light on neuroanatomical evolution within titanosauria. *PLoS ONE* 10: 1–24.
- Lacovara KJ, Lamanna MC, Ibiricu LM, Poole JC, Schroeter ER, Ullmann P V., Voegelé KK, Boles ZM, Carter AM, Fowler EK, Egerton VM, Moyer AE, Coughenour CL, Schein JP, Harris JD, Martínez RD, Novas FE. 2014. A Gigantic, Exceptionally Complete Titanosaurian Sauropod Dinosaur from Southern Patagonia, Argentina. *Scientific Reports* 4: 6196.
- Langer MC, Abdala F, Richter M, Benton MJ. 1999. A sauropodomorph dinosaur from the Upper Triassic (Carnian) of southern Brazil. *Comptes Rendus de l'Academie de Sciences - Serie IIa: Sciences de la Terre et des Planetes* 329: 511–517.
- Lautenschlager S. 2016. Reconstructing the past: methods and techniques for the digital restoration of fossils. *Royal Society Open Science* 3: 160342.
- Leidy J. 1865. Cretaceous reptiles of the United States. *Smithsonian Contribution to Knowledge* 14 (6): 1-212.
- López Piñero JM. 1988. Juan Bautista Bru (1740-1799) and the description of the genus *Megatherium*. *Journal of the History of Biology* 21: 147–163.

- Maidment SCR, Barrett PM. 2011. The locomotor musculature of basal ornithischian dinosaurs. *Journal of Vertebrate Paleontology* 31: 1265–1291.
- Maidment SCR, Bates KT, Falkingham PL, VanBuren C, Arbour V, Barrett PM. 2014. Locomotion in ornithischian dinosaurs: An assessment using three-dimensional computational modelling. *Biological Reviews* 89: 588–617.
- Maidment SCR, Linton DH, Upchurch P, Barrett PM. 2012. Limb-bone scaling indicates diverse stance and gait in quadrupedal ornithischian dinosaurs. *PLoS ONE* 7: e36904.
- Mallison H. 2007. Virtual Dinosaurs: Developing Computer Aided Design and Computer Aided Engineering Modeling Methods for Vertebrate Paleontology. Unpublished thesis, Eberhard-Karls-Universität Tübingen.
- Mallison H. 2010a. The Digital *Plateosaurus* I : Body Mass , Mass Distribution and Posture Assessed Using Cad and Cae on a Digitally Mounted Complete Skeleton. *Palaeontologia Electronica* 2: 1–26.
- Mallison H. 2010b. The Digital *Plateosaurus* II: An Assessment of the Range of Motion of the Limbs and Vertebral Column and of Previous Reconstructions using a Digital Skeletal Mount. *Acta Palaeontologica Polonica* 55: 433–458.
- Mallison H. 2010c. CAD assessment of the posture and range of motion of *Kentrosaurus aethiopicus* Hennig 1915. *Swiss Journal of Geosciences* 103: 211–233.
- Mallison H. 2011a. Defense capabilities of *Kentrosaurus aethiopicus* Hennig, 1915. *Palaeontologia Electronica* 14: 1-25.
- Mallison H. 2011b. Rearing Giants – kinetic-dynamic modeling of sauropod bipedal and tripodal poses. In: Klein N, Remes K, Gee C, Sander PM, eds. *Biology of the Sauropod Dinosaurs: Understanding the life of giants*. Indiana University Press, 237–250.
- Mallison H, Pittman M, Schwarz D. 2015. Using crocodylian tails as models for dinosaur tails. *PeerJ Preprints*. 3: e1339v1.
- Mallison H, Wings O. 2014. Photogrammetry in paleontology - A practical guide. *Journal of Paleontological Techniques* 12: 1–31.
- Mannion PD, Allain R, Moine O. 2017. The earliest known titanosauriform sauropod dinosaur and the evolution of Brachiosauridae. *PeerJ* 5: e3217.
- Mannion PD, Calvo JO. 2011. Anatomy of the basal titanosaur (Dinosauria, Sauropoda) *Andesaurus delgadoi* from the mid-Cretaceous (Albian-early Cenomanian) Río Limay Formation, Neuquén Province, Argentina: Implications for titanosaur systematics. *Zoological Journal of the Linnean Society* 163: 155–181.
- Mannion PD, Upchurch P, Barnes RN, Mateus O. 2013. Osteology of the Late Jurassic Portuguese sauropod dinosaur *Lusotitan atalaiensis* (Macronaria) and the evolutionary history of basal titanosauriforms. *Zoological Journal of the Linnean Society* 168: 98–206.
- Marsh OC. 1877. Notice of new dinosaurian reptiles from the Jurassic formation. *American Journal of Science and Arts* 14: 514-516.
- Marsh OC. 1878a. Principal characters of American Jurassic dinosaurs. Part I. *American Journal of Science and Arts* 16: 411-416.
- Marsh OC. 1878b. Notice of new dinosaurian reptiles. *American Journal of Science and Arts* 15: 241-244.
- Marsh OC. 1883. Principal characters of American Jurassic dinosaurs; Part VI, Restoration of *Brontosaurus*. *American Journal of Science* 26: 81–85.
- Marsh OC. 1889. Notice of new American Dinosauria. *American Journal of Science* s3-37: 331–336.
- Marsh OC. 1890. Description of new dinosaurian reptiles. *American Journal of Science* 39: 81–86.
- Marsh OC. 1896. The dinosaurs of North America. *United States Geological Survey, 16th Annual Report, 1894-95* 55: 133-244.
- Martin J. 1987. Mobility and feeding of *Cetiosaurus* (Saurischia, Sauropoda): why the long neck? In: Currie PJ, Koster EH, eds. *4th Symp. Mesozoic Terrestrial Ecosystems*, 154–159.
- Martin J, Martin-Rolland V, Frey E. 1998. Not cranes or masts, but beams: the biomechanics of sauropod necks. *Oryctos* 1: 113–120.
- Martínez RD, Giménez O, Rodríguez J, Luna M, Lamanna MC. 2004. An articulated specimen of the basal titanosaurian (Dinosauria: Sauropoda) *Epachthosaurus sciuttoi* from the early Late Cretaceous Bajo Barreal Formation of Chubut Province, Argentina. *Journal of Vertebrate Paleontology* 24: 107–120.

- Mateus O, Maidment SCR, Christiansen NA. 2009. A new long-necked 'sauropod-mimic' stegosaur and the evolution of the plated dinosaurs. *Proceedings of the Royal Society B: Biological Sciences* 276: 1815–1821.
- Matthew WD. 1915. *Dinosaurs, with special reference to the American Museum collections*. New York: American Museum of Natural History.
- Matthews NA, Noble TA, Breithaupt BH. 2006. The application of photogrammetry, remote sensing and geographic information systems (GIS) to fossil resource management. *Bulletin New Mexico Museum of Natural History and Science* 34: 119–131.
- McIntosh JS. 1990. Sauropoda. In: Weishampel DB, Dodson P, Osmólska H, eds. *The Dinosauria*. Berkeley: University of California Press, 345–401.
- McIntosh JS. 1998. New information about the Cope collection of sauropods from Garden Park, Colorado. *Modern Geology* 23: 481–506.
- McIntosh JS, Miller WE, Stadtman KL, Gillette DD. 1996. The Osteology of *Camarasaurus lewisi* (Jensen, 1988). *BYU Geology Studies* 41: 73–116.
- McIntosh JS, Williams ME. 1988. A new species of sauropod dinosaur, *Haplocanthosaurus delfsi* sp. nov., from the Upper Jurassic Morrison Fm. of Colorado. *Kirtlandia* 43: 3–26.
- McNamara KJ. 2012. Heterochrony: the Evolution of Development. *Evolution: Education and Outreach* 5: 203–218.
- Méndez J, Keys A. 1960. Density and composition of mammalian muscle. *Metabolism* 9: 184–188.
- Mocho P, Ortega F, Aberasturi A, Escaso F. 2013. *Spinophorosaurus* (Sauropoda), a new look inside eusauropod evolution. *VI Jornadas Internacionales sobre Paleontología de dinosaurios Abstract Book*. 89–90.
- Mocho P, Royo-Torres R, Ortega F. 2014. Phylogenetic reassessment of *Lourinhasaurus alenquerensis*, a basal Macronaria (Sauropoda) from the Upper Jurassic of Portugal. *Zoological Journal of the Linnean Society* 170: 875–916.
- Monbaron M, Russell DA, Taquet P. 1999. *Atlasaurus imelakei* n.g., n.sp., a brachiosaurid-like sauropod from the Middle Jurassic of Morocco. *Comptes Rendus de l'Academie de Sciences - Serie IIa: Sciences de la Terre et des Planetes* 329: 519–526.
- Myhrvold NP, Currie PJ. 1999. Supersonic sauropods? Tail dynamics in the diplodocids. *Paleobiology* 23: 393–409.
- Nagano A, Komura T. 2003. Longer moment arm results in smaller joint moment development, power and work outputs in fast motions. *Journal of Biomechanics* 36: 1675–1681.
- Norman DB. 1980. On the ornithischian dinosaur *Iguanodon bernissartensis* from the Lower Cretaceous of Bernissart (Belgium). *Institut Royal des Sciences Naturelles de Belgique Memoire* 178: 1–103.
- Ortega F, Bardet N, Barroso-Barcenilla F, Callapez PM, Cambra-Moo O, Daviero-Gómez V, Díez Díaz V, Domingo L, Elvira A, Escaso F, García-Oliva M, Gómez B, Houssaye A, Knoll F, Marcos-Fernández F, Martín M, Mocho P, Narváez I, Pérez-García A, Peyrot D, Segura M, Serrano H, Torices A, Vidal D, Sanz JL. 2015. The biota of the upper cretaceous site of Lo Hueco (Cuenca, Spain). *Journal of Iberian Geology* 41: 83–99.
- Ortega F, Sanz JL, Barroso-Barcenilla F, Fernández FM. 2008. El yacimiento de macrovertebrados fósiles del Cretácico Superior de "Lo Hueco" (Fuentes , Cuenca). *Sierra* 2008: 119–131.
- Osborn HF. 1899. A skeleton of *Diplodocus*, recently mounted in the American Museum. *Science* 10: 870–874.
- Otero A. 2010. The appendicular skeleton of *Neuquensaurus*, a Late Cretaceous saltasaurine sauropod from Patagonia, Argentina. *Acta Palaeontologica Polonica* 55: 399–426.
- Ouyang H, Ye Y. 2002. *The first Mamenchisaurian skeleton with complete skull Mamenchisaurus youngi*. Chengdu: Sichuan Science Technology Press 1: 111.
- Owen R. 1842. *Report on British fossil reptiles. Part II*. London.
- Páramo A, Ortega F. 2012. A probable juvenile *Spinophorosaurus nigerensis* (Sauropoda) from the Middle Jurassic of Niger. In: Royo-Torres R, Gascó F, Alcalá L, eds. *Fundamental* 20: 177–178.
- Paul GS. 1998. Terramegathermy and Cope's Rule in the Land of Titans. *Modern Geology* 23: 179–217.
- Paul GS. 2000. Restoring the life appearances of dinosaurs. *The Scientific American book of dinosaurs*. New York: St Martin's Press, 78–106.
- Paul GS. 2017. Restoring Maximum Vertical Browsing Reach in Sauropod Dinosaurs. *Anatomical Record* 300: 1802–1825.

- Paul GS, Chase TL. 1989. Reconstructing extinct vertebrates. *The guild handbook of scientific illustration*, 239–256.
- Pérez García A, Sánchez Chillón B. 2009. Historia de *Diplodocus carnegii* del MNCN: Primer Esqueleto de dinosaurio Montado en la Península ibérica. *Revista Espanola de Paleontologia* 24: 133–148.
- Persons WS, Currie PJ. 2010. The Tail of Tyrannosaurus: Reassessing the Size and Locomotive Importance of the M. caudofemoralis in Non-Avian Theropods. *The Anatomical Record* 294: 119–131.
- Persons WS, Currie PJ. 2011. Dinosaur speed demon: the caudal musculature of *Carnotaurus sastrei* and implications for the evolution of South American abelisaurids. *PLoS one* 6: e25763.
- Persons WS, Currie PJ. 2012. Dragon Tails: Convergent Caudal Morphology in Winged Archosaurs. *Acta Geologica Sinica* 86: 1402–1412.
- Persons WS, Currie PJ, Norell M a. 2013. Oviraptorosaur tail forms and functions. *Acta Palaeontologica Polonica* 59: 553–567.
- Phillips J. 1871. *Geology of Oxford and the Valley of the Thames*. Oxford: Clarendon Press.
- Powell JE. 1990. *Epachthosaurus sciuttoi* (gen. et sp. nov.) un dinosaurio sauropodo del Cretácico de Patagonia (provincia de Chubut, Argentina). *Actas del Congreso Argentino de Paleontología y Bioestratigrafía*, 125–128.
- Rasskin-Gutman D, Buscalioni AD. 2001. Theoretical morphology of the Archosaur (Reptilia: Diapsida) pelvic girdle. *Paleobiology* 27: 59–78.
- Rauhut OWM, López-Arbarello A. 2009. Considerations on the age of the Tiouaren Formation (Iullemeden Basin, Niger, Africa): Implications for Gondwanan Mesozoic terrestrial vertebrate faunas. *Palaeogeography, Palaeoclimatology, Palaeoecology* 271: 259–267.
- Rauhut OWM, Remes K, Fechner R, Cladera G, Puerta P. 2005. Discovery of a short-necked sauropod dinosaur from the Late Jurassic period of Patagonia. *Nature* 435: 670–672.
- Rea T. 2004. *Bone wars: the excavation and celebrity of Andrew Carnegie's dinosaur*. Pittsburgh: University of Pittsburgh Press.
- Reisdorf AG, Wuttke M. 2012. Re-evaluating Moodie's opisthotonic-posture hypothesis in fossil vertebrates part I: Reptiles—the taphonomy of the bipedal dinosaurs *Compsognathus longipes* and *Juravenator starki* from the Solnhofen Archipelago (Jurassic, Germany). *Palaeobiodiversity and Palaeoenvironments* 92: 119–168.
- Reiss S, Mallison H. 2014. Motion range of the manus of *Plateosaurus engelhardti* von Meyer, 1837. *Paleontologica Electronica* 17: 1–19.
- Remes K. 2007. Evolution of the Pectoral girdle and Forelimb in Sauropodomorpha (Dinosauria, Saurischia): Osteology, Myology and Fuction. Unpublished thesis, Ludwig-Maximilians-Universität München.
- Remes K, Ortega F, Fierro I, Joger U, Kosma R, Ferrer JMM, Ide OA, Maga A. 2009. A new basal sauropod dinosaur from the middle Jurassic of Niger and the early evolution of sauropoda. *PLoS one* 4: e6924.
- Rich TH, Vickers-Rich P, Giménez O del V, Cúneo R, Puerta P, Vacca R. 1999. A new sauropod dinosaur from Chubut Province, Argentina. *National Science Museum Monographs* 15: 61–84.
- Riesco A, García-Martínez D, Bastir M. 2018. Reconstrucción del segmento torácico de la columna vertebral en paleoantropología. In: Amayuelas E, Bilbao-Lasa P, Bonilla O, del Val M, Errandonea-Martin J, Garate-Olave I, García-Sagastibelza A, Intxauspe-Zubiaurre B, Martínez-Braceras N, Perales-Gogenola L, Ponsoda-Carreres M, Portillo H, Serrano H, Silva-Casal R, Suárez-Bilbao A, Suarez-Hernando O, eds. *Life Finds a Way*. Gasteiz, 241–244.
- Riggs ES. 1903a. *Brachiosaurus altithorax*, the largest known dinosaur. *American Journal of Science* 15: 299–306.
- Riggs ES. 1903b. The largest known dinosaur. *Science* 13: 549–550.
- Riggs ES. 1904. Structure and relationships of opisthocoelian dinosaurs. Part II. The Brachiosauridae. *Publications of the Field Columbian Museum, Geology* 2 (6): 229–247.
- Romer AS. 1923. The pelvic musculature of saurischian dinosaurs. *Bulletin of the American Museum of Natural History*: 48, 605–617.
- Romer AS. 1927. The pelvic musculature of ornithischian dinosaurs. *Acta Zoologica* 8: 225–275.
- Romer AS. 1956. *Osteology of the Reptiles*. University of Chicago Press.
- Royo-Torres R, Alcalá L, Cobos A. 2012. A new specimen of the Cretaceous sauropod *Tastavinsaurus sanzi* from El Castellar (Teruel, Spain), and a phylogenetic analysis of the Laurasiformes. *Cretaceous Research* 34: 61–83.

- Royo-Torres R, Cobos A, Alcalá L. 2006. A Giant European Dinosaur and a New Sauropod Clade. *Science* 314: 1925–1927.
- Russell DA, Zheng Z. 1993. A large mamenchisaurid from the Junggar basin, Xinjiang, People's Republic of China. *Canadian Journal of Earth Sciences* 30: 2082–2095.
- Salgado L, Azpilicueta C. 2000. Un nuevo saltasaurino (Sauropoda, Titanosauridae) de la provincia de Rio Negro (Formacion Allen, Cretacico Superior), Patagonia, Argentina. *Ameghiniana* 37: 259–264.
- Sander PM. 2013. An evolutionary cascade model for sauropod dinosaur gigantism—overview, update and tests. *PLoS one* 8: e78573.
- Sander PM, Christian A, Clauss M, Fechner R, Gee CT, Griebeler EM, Gunga HC, Hummel J, Mallison H, Perry SF, Preuschoft H, Rauhut OWM, Remes K, Tütken T, Wings O, Witzel U. 2011. Biology of the sauropod dinosaurs: The evolution of gigantism. *Biological Reviews* 86: 117–155.
- Schwarz-Wings D. 2009. Reconstruction of the thoracic epaxial musculature of diplodocid and dicraeosaurid sauropods. *Journal of Vertebrate Paleontology* 29: 517–534.
- Schwarz D, Frey E, Meyer CA. 2007a. Novel reconstruction of the orientation of the pectoral girdle in sauropods. *Anatomical Record* 290: 32–47.
- Schwarz D, Frey E, Meyer CA. 2007b. Pneumaticity and soft-tissue reconstructions in the neck of diplodocid and dicraeosaurid sauropods. *Acta Palaeontologica Polonica* 52: 167–188.
- Schwarz D, Wings O, Meyer CA. 2007c. Super sizing the giants: First cartilage preservation at a sauropod dinosaur limb joint. *Journal of the Geological Society* 164: 61–65.
- Seeber PA, Ciofolo I, Ganswindt A. 2012a. Behavioural inventory of the giraffe (*Giraffa camelopardalis*). *BMC Research Notes* 5: 650.
- Seeber PA, Ndlovu HT, Duncan P, Ganswindt A. 2012b. Grazing behaviour of the giraffe in Hwange National Park, Zimbabwe. *African Journal of Ecology* 50: 247–250.
- Seidel MR. 1979. The Osteoderms of the American *Alligator* and Their Functional Significance. *Herpetologica* 35: 375–380.
- Sellers WI, Margetts L, Ébal Coria RA, Manning PL. 2013. March of the titans: The locomotor capabilities of sauropod dinosaurs. *PLoS ONE* 8: e78733.
- Sereno PC. 1999. The Evolution of Dinosaurs. *Science* 284: 2137–2147.
- Sereno PC. 2005. TaxonSearch.
- Sereno PC, Beck AL, Dutheil DB, Larsson HCE, Lyon GH, Moussa B, Sadleir RW, Sidor CA, Varricchio DJ, Wilson GP, Wilson JA. 1999. Cretaceous sauropods from the Sahara and the uneven rate of skeletal evolution among dinosaurs. *Science* 265: 267–271.
- Sereno PC, Wilson JA, Witmer LM, Whitlock JA, Maga A, Ide O, Rowe TA. 2007. Structural extremes in a Cretaceous dinosaur. *PLoS ONE* 2: 1230.
- Serrano-Martínez A, Vidal D, Sciscio L, Ortega F, Knoll F. 2016. Isolated theropod teeth from the Middle Jurassic of Niger and the early dental evolution of Spinosauridae. *Acta Paleontologica Polonica* 61: 403–415.
- Simpson GG. 1942. The Beginnings of Vertebrate Paleontology in North America. *Proceedings of the American Philosophical Society* 86: 130–188.
- Słowiak J, Tereshchenko VS, Fostowicz-Freluk Ł. 2019. Appendicular skeleton of *Protoceratops andrewsi* (Dinosauria, Ornithischia): comparative morphology, ontogenetic changes, and the implications for non-ceratopsid ceratopsian locomotion. *PeerJ* 7: e7324.
- Snively E, Cotton JR, Ridgely R, Witmer LM. 2013. Multibody dynamics model of head and neck function in *Allosaurus* (Dinosauria, Theropoda). *Palaeontologia Electronica* 16: 29.
- Snively E, Russell AP. 2007a. Functional morphology of neck musculature in the Tyrannosauridae (Dinosauria, Theropoda) as determined via a hierarchical inferential approach. *Zoological Journal of the Linnean Society* 151: 759–808.
- Snively E, Russell AP. 2007b. Craniocervical feeding dynamics of *Tyrannosaurus rex*. *Paleobiology* 33: 610–638.
- Snively E, Russell AP. 2007c. Functional variation of neck muscles and their relation to feeding style in Tyrannosauridae and other large Theropod dinosaurs. *Anatomical Record* 290: 934–957.

- Solounias N. 1999. The remarkable anatomy of the giraffe's neck. *Journal of Zoology* 247: 257–268.
- Sopelana A. 2011. Estado de conocimiento sobre el sexo en los dinosaurios no avianos. In: Pérez-García A, Gascó F, Gasulla JM, Escaso F, eds. *Viajando a mundos pretéritos*. Morella: Ayuntamiento de Morella, 379–388.
- Stephen M. Gatesy. 1997. An electromyographic analysis of hindlimb function in *Alligator* during terrestrial locomotion. *Journal of Morphology* 324: 197–212.
- Stevens KA. 2002. DinoMorph: Parametric modeling of skeletal structures. *Senckenbergiana Lethaea* 82: 23–34.
- Stevens KA. 2013. The articulation of sauropod necks: methodology and mythology. *PLoS one* 8: e78572.
- Stevens KA, Parrish MJ. 1999. Neck Posture and Feeding Habits of Two Jurassic Sauropod Dinosaurs. *Science* 284: 798–800.
- Stevens KA, Parrish MJ. 2005. Neck posture, dentition, and feeding strategies in Jurassic sauropod dinosaurs. In: Tidwell V, Carpenter K, eds. *Thunder-lizards: The Sauropodomorph Dinosaurs*. Bloomington: Indiana University Press, 212–232.
- Taylor MP. 2010. Sauropod Dinosaur Research: a historical review. *Geological Society London Special Publications* 343: 361–386.
- Taylor MP. 2014. Quantifying the effect of intervertebral cartilage on neutral posture in the necks of sauropod dinosaurs. *PeerJ* 2: e588v2.
- Taylor MP. 2015. Almost all known sauropod necks are incomplete and distorted. *PeerJ* 3: e1418v1.
- Taylor MP, Wedel MJ. 2013a. The effect of intervertebral cartilage on neutral posture and range of motion in the necks of sauropod dinosaurs. *PLoS ONE* 8: e78214.
- Taylor MP, Wedel MJ. 2013b. Why sauropods had long necks; and why giraffes have short necks. *PeerJ* 1: e36.
- Taylor MP, Wedel MJ. 2016. The neck of *Barosaurus*: longer , wider and weirder than those of *Diplodocus* and other diplodocines. *PeerJ preprints* 4: e67v2.
- Taylor MP, Wedel MJ, Cifelli RL. 2011. A new sauropod dinosaur from the Lower Cretaceous Cedar mountain formation, Utah, USA. *Acta Palaeontologica Polonica* 56: 75–98.
- Taylor MP, Wedel MJ, Naish D. 2009. Head and Neck Posture in Sauropod Dinosaurs Inferred from Extant Animals. *Acta Palaeontologica Polonica* 54: 213–220.
- Tornier G. 1909. Wie war der *Diplodocus carnegii* wirklich gebaut? *Sitzungsberichte der Gesellschaft Naturforschender Freunde zu Berlin* 4: 193–209.
- Tschanz K. 1988. Allometry and heterochrony in the growth of the neck of prolacertiform reptiles. *Palaeontology* 31: 997–1011.
- Tschopp E, Mateus O. 2012. A sternal plate of a large-sized sauropod dinosaur from the Late Jurassic of Portugal. *Fundamental* 20: 263–266.
- Tschopp E, Mateus O. 2013. Clavicles, interclavicles, gastralia, and sternal ribs in sauropod dinosaurs: New reports from Diplodocidae and their morphological, functional and evolutionary implications. *Journal of Anatomy* 222: 321–340.
- Tschopp E, Mateus O, Benson RBJ. 2015. A specimen-level phylogenetic analysis and taxonomic revision of Diplodocidae (Dinosauria, Sauropoda). *PeerJ* 3: e857.
- Tschopp E, Russo J, Dzemski G. 2013. Retrodeformation as a test for the validity of phylogenetic characters: an example from diplodocid sauropod vertebrae. *Paleontologia Electronica* 16: 1–23.
- Tsuihiji T. 2005. Homologies of the transversospinalis muscles in the anterior presacral region of Sauria (crown Diapsida). *Journal of Morphology* 263: 151–178.
- Upchurch P. 1995. The Evolutionary History of Sauropod Dinosaurs. *Philosophical Transactions of the Royal Society B: Biological Sciences* 349: 365–390.
- Upchurch P, Barrett PM, Dodson P. 2004. Sauropoda. In: Weishampel DB, Dodson P, Osmólska H, eds. *The Dinosauria, 2nd edition*. Berkeley and Los Angeles: University of California Press, 259–322.
- Vidal D, Ortega F, Gascó F, Serrano-Martínez A, Sanz JL. 2017. The internal anatomy of titanosaur osteoderms from the Upper Cretaceous of Spain is compatible with a role in oogenesis. *Scientific Reports* 7: 42035.
- Vidal D, Ortega F, Sanz JL. 2014. Titanosaur osteoderms from the Upper Cretaceous of Lo Hueco (Spain) and their



UNED